2. SITE CHARACTERISTICS

2.1 GEOGRAPHY AND DEMOGRAPHY

The data and information contained in Section 2.1 and referenced appendices are historical information developed during San Onofre's original design to address geography and demography. The information was used to determine the plant's design basis. Unless otherwise noted in the text, this information has not been updated to reflect data from later years (revisions of population data resulted from editorial and arithmetic corrections of the original data.)

2.1.1 SITE LOCATION AND DESCRIPTION

2.1.1.1 Specification of Location

The San Onofre site is located on the coast of Southern California in San Diego County, approximately 62 miles southeast of Los Angeles and 51 miles northwest of San Diego. The site is located entirely within the boundaries of the United States Marine Corps Base, Camp Pendleton, California, near the northeast end of the 18-mile shoreline.

The coordinates for Unit 2 are latitude 33°22'9" N and longitude 117°33'16" W or Universal Transverse Mercator Zone Number 11; N 3,692,150 meters and E 448,420 meters. Unit 3 coordinates are latitude 33° 22'7" N and longitude 117°33'13" W or Universal Transverse Mercator Zone Number 11; N 3,692,100 meters and E 488,500 meters.

2.1.1.2 Site Area Map

The plant easement boundary, which is also the site boundary, and the location of major structures of the facilities are delineated in Controlled Drawings 21000 and 17002 . The site, comprising 83.63 acres, is approximately 4500 feet long and 800 feet wide. The North Industrial Area (NIA), formerly referred to as the Unit 1 power block, is located northwest of Units 2 and 3 and occupies 11.7 acres. The Units 2 and 3 power block occupies 19.5 acres. A spur of the commercial railroad line extends into the site area.

The San Onofre Units 2 and 3 exclusion area is roughly formed by two semi-circles with radii of 1967.5 feet each, centered on the Unit 2 containment and a point 134 feet southeast of the Unit 3 containment, with a tangent connecting the landward arcs and the seaward arcs of the two semi-circles. The exclusion area boundary is delineated in Figure 2.1-5. At the northwest and southeast site boundaries, the exclusion area is tangent to, but does not exceed, the site boundary. There are no industrial, commercial, institutional, or residential structures within the exclusion area boundary.

The Pacific Ocean is located immediately west of the site and traverses the seaward side of the exclusion area. The San Onofre State Beach developed along the coast on both sides of the site, as shown in Figure 2.1-3. Access between open beach areas upcoast and downcoast from the exclusion area is provided by a walkway (the beach passage-way) adjacent to the NIA and Units

2&3 seawall. The passageway extends the 2200-foot length of the seawall and is bounded on the seaward side by a concrete wall extending approximately three (3) feet above the passageway surface.

A typical cross-section through the beach passageway is shown on Figure 2.1-4. The passageway is 15 feet in total width with a hard surface which can accommodate pedestrian traffic only. Two removable vehicle barriers are installed along the beach passageway (one at the northwest corner of Unit 2 boundary and another at the southwest corner of Unit 3 boundary) as part of SONGS security enhancements following NRC's order issued on April 29, 2003 to upgrade the plant's security. A 3-foot wide, 20-foot long removable pedestrian bridge is also installed along the passageway at the intake structure area of Units 2 and 3 to permit pedestrian access when the saltwater cooling system of Units 2 and 3 is discharging to the beach, during which the beach passageway will be flooded. The seaward side of the walkway is formed by a concrete retaining wall which is protected by riprap in the event of infrequent beach erosion caused by wave action.

Old Highway 101 is immediately adjacent to the east boundary line of the site. The highway is presently being used as an entrance to the south end of the State Beach. The commercial railroad right-of-way is east of Highway 101. Interstate Highway 5 is adjacent to the railroad right-of-way.

2.1.1.3 Boundaries for Establishing Effluent Release Limits

The site restricted area defined for the purpose of establishing effluent release limits coincides with the exclusion area boundary as defined in Figure 2.1-5. The procedures for control of individual access and a description of the boundary are provided in Subsection 2.1.2.

Figure 2.1-5 delineates the effluent release points and their distances to the restricted area boundary line.

2.1.2 EXCLUSION AREA AUTHORITY AND CONTROL

2.1.2.1 Authority

The applicant's authority to control all activities within the exclusion area was acquired by grant of easement from the United States of America made by the Secretary of the Navy pursuant to the authority of Public Law 88-82. This easement is recorded in the official records of the Recorder of San Diego County, California, on Page 85887, Series 5, Book 1964.

In order to remove any ambiguities contained in the original grant of easement with respect to the applicant's authority to control activities in the exclusion area, an amendment to the grant of easement was executed on September 18, 1975, and is reproduced below, in part:

> "In order to protect the public health and safety, and in accordance with the rules, regulations and requirements of the United States Nuclear Regulatory Commission, successor to the

United States Atomic Energy Commission, applicable to the Nuclear Station, the Grantees may determine all activities including exclusion or removal of personnel and property from such exclusion area as is established from time to time by or with the approval of the United States Nuclear Regulatory Commission and is located within the lands described in Exhibit B. Subject to the foregoing, such exclusion area may be used by the Government, its successor or assigns, for military operations (provided same do not endanger operation of the Nuclear Station), agricultural, recreational and such other uses as may be compatible with operation of the Nuclear Station, provided that any and all uses of the exclusion area shall be in accordance with and subject to the rules, regulations and requirements of the United States Nuclear Regulatory Commission applicable to the Nuclear Station, and further provided that no significant hazards to the public health and safety shall result from any such uses."

This amendment to the grant of easement expires on May 12, 2024.

All mineral rights in the land portion of the exclusion area are held by the United States Government.

The Pacific Ocean, Interstate Highway 5 (San Diego Freeway), old U.S. Highway 101, the commercial railroad right-of-way, and the beach passageway constitute traversals of the site exclusion area as allowed by 10CFR100.3[a].

2.1.2.2 Control of Activities Unrelated to Plant Operation

Recreational activities, such as sunbathing or picnicking, are not permitted within the landward portion of the exclusion area (the area landward of the contour of mean high tide). The seaward portion of the exclusion area (the area seaward of the contour of mean high tide) may be occupied by small numbers of people for passageway transit between the public beach areas upcoast and downcoast from the plant. Additional small numbers of people may be anticipated to occasionally be in the water.

Transient access to an approximately 5-acre area at the southwest corner of the site for the purposes of viewing the scenic bluffs and barrancas will be on an unimproved walkway. The improved walkway affords landward passage between the two beach areas.

The number and distribution of persons expected to be within the exclusion zone as a result of the nearby beaches have been estimated by the consulting firm of Wilbur Smith and Associates, Inc. These estimates were developed by:

A. Determination of the nature, size, and location of facilities planned in the development of the San Onofre State Beach

B. Application of the standard rates of persons per camp site and persons per parking space as used by the Department of Parks and Recreation

C. Distribution of persons from access points to the beach based upon a Poisson probability distribution function

Results are shown in Table 2.1-1.

Physical features and administrative controls are planned to control activities in the landward portion of the exclusion area. These features and controls will have the effect of minimizing use of the seaward portion so that it will be predominately passageway use.

Table 2.1-1
ESTIMATES OF THE NUMBER OF PERSONS PRESENT
IN THE BEACH ZONE OF THE EXCLUSION AREA[(a)]

	Maximum Use		Average Use
Exclusion Area	Full Development of Facilities	Current Facilities	Current Facilities
Walkway and barranca area	25	9	2
Beach (below mhw line) and adjacent water	75	26	5
Total	100	35	7

[(a)] Excludes highway, rail, and waterway traversals.

The following enforcement measures are planned in order to ensure that use of the beach exclusion area, not related to operation of the facility, will be minimized and will be predominantly passageway transit:

A. Beach areas within the exclusion area will be subject to periodic surveillance by direct means.

B. If use of beach areas within the exclusion area is observed to be other than for transient use, an announcement will be made over the public address system or other means to request the movement of persons out of the exclusion area.

C. Should actions described above prove to be unsuccessful, plant security personnel will request the assistance of the California State Park Rangers or Camp Pendleton Military Police.

2.1.2.3 Arrangements for Traffic Control

The environs of the Site are the Pacific Ocean and the beach passageway on the west, the San Diego Freeway (Interstate 5), old U.S. Highway 101, and the commercial railroad on the southeast and north. These environs of the plant are not a factor in decommissioning activities.

In the event of an emergency, all traffic within the roadways and waterways is subject to control by agencies of state and local governments. Surveillance measures discussed in Paragraph 2.1.2.2 will control the use of the beach passageway.

2.1.2.4 Abandonment or Relocation of Roads

There are no public roads subject to abandonment or relocation as a result of construction of San Onofre Units 2 and 3.

2.1.3 POPULATION DISTRIBUTION

Sections 2.1.3.1, 2.1.3.2, and 2.1.3.3 were updated to include data from the 1990 U.S. Decennial Population and Housing Census as part of Amendments 166 and 157 to the Unit 2 and Unit 3 Operating Licenses respectively.

2.1.3.1 Population Within 10 Miles

2.1.3.1.1 Population Growth

The population of the area within a 10-mile radius of the San Onofre Nuclear Generating Station is projected to increase from 59,024 in 1980 to 95,301 by 2020. [1][2][3][4][8] The population figures for selected years (from 1980 to 2020 by decade) by sector and distance from the plant are shown in Tables 2.1-2 through 2.1-6 and on Figures 2.1-6 through 2.1-12. The population within 10 miles is projected to expand by 61.5%, an annual increase of 1.2%, as shown in Table 2.1-7. The growth rate within the period is expected to fluctuate. The annual rate of growth between 1980 and 1990 was approximately 1.4%, and is projected to increase to 1.8% between 1990 and 2000, and then decrease to about 0.2% between 2010 and 2020.

Within the 10-mile radius, the majority of the population is projected to reside between 5 and 10 miles. In 1980, 37,670 or 63.8% of the 59,024 residents within 10 miles of the plant site lived at least 5 miles from the site. In 2020, 59,244 or 62.2% of the 95,301 projected residents would live between 5 and 10 miles from the plant site.

The remainder of the area within the 10-mile radius falls within the boundaries of the USMC Base at Camp Pendleton. Population estimates and projections are based on USMC data and are presented on Table 2.1-8.[5] Resident population at the base was 35,682 in 1990 and is forecast to increase only slightly, as shown on Tables 2.1-2 through 2.1-6.

2.1.3.1.2 Basis of Population Projections

Population projections were developed in the following manner. On census tract maps of suitable scale, concentric circles were drawn at distances of 1, 2, 3, 4, 5, and 10 miles from the station. The circles were divided into 22-1/2° sectors with each sector centered on one of the 16 compass points. Residential population for each sector was calculated from 1980 and 1990 census data, and for each census decade through the projected plant life based on the relative proportion of a city within a given sector.

The population within 10 miles of the plant either live on Camp Pendleton or within Orange County. To derive the non-USMC base projections, the population forecasts by the Center for Demographic Research, California State University of Fullerton, for Dana Point, San Clemente, and San Juan Capistrano were used for each decade.

2.1.3.2 Population Between 10 and 50 Miles

2.1.3.2.1 Population Growth

The population of the area between 10 and 50 miles of the plant site is projected to increase from 5,456,861 in 1980 to 6,515,287 by 2020[(1)(2)(3)(6)(4)(9)]. The population figures for selected years (from 1980 to 2020 by decade) by sector and distance from the plant are shown in Tables 2.1-9 to 2.1-13. As shown in Table 2.1-14, the projected annual rate of population growth was 1.66% between 1980 and 1990, and is expected to decrease to a rate of 1.02% between 1990 and 2000. The annual rate of growth is then expected to increase to 1.41% between 2000 and 2010 and to 1.44% between 2010 and 2020. The annual growth rate for the entire period, 1980 to 2020, is 1.39% with the population estimated to expand by a total of 74.27%.

Table 2.1-2
1980 POPULATION BY SECTOR AND DISTANCE
WITHIN 10 MILES OF THE SAN ONOFRE SITE

	0-1	1-2	2-3	3-4	4-5	5-10	Total
N	0	0	0	2564	0	193	2757
NNE	0	0	0	0	0	0	0
NE	0	0	4804	0	0	0	4804
ENE	0	0	0	0	0	0	0
E	0	0	0	0	2426	0	2426
ESE	0	0	0	0	0	1821	1821
SE	0	0	0	0	0	538	538
SSE	0	0	0	0	0	0	0
S	0	0	0	0	0	0	0
SSW	0	0	0	0	0	0	0
SW	0	0	0	0	0	0	0
WSW	0	0	0	0	0	0	0
W	0	0	0	0	0	0	0
WNW	0	0	0	0	0	0	0
NW	0	865	81	3517	4612	27626	36701
NNW	0	945	810	0	730	7492	9977
SUM	0	1810	5695	6081	7768	37670	59024

Sources: Southern California Association of Governments;
Williams-Kuebelbeck and Associates, Inc.; U.S. Marine Corps.

Table 2.1-3
1990 POPULATION BY SECTOR AND DISTANCE
WITHIN 10 MILES OF THE SAN ONOFRE SITE

	0-1	1-2	2-3	3-4	4-5	5-10	Total
N	0	0	0	2867	0	216	3083
NNE	0	0	0	0	0	0	0
NE	0	0	5372	0	0	0	5372
ENE	0	0	0	0	0	0	0
E	0	0	0	0	2713	0	2713
ESE	0	0	0	0	0	2036	2036
SE	0	0	0	0	0	652	652
SSE	0	0	0	0	0	0	0
S	0	0	0	0	0	0	0
SSW	0	0	0	0	0	0	0
SW	0	0	0	0	0	0	0
WSW	0	0	0	0	0	0	0
W	0	0	0	0	0	0	0
WNW	0	0	0	0	0	0	0
NW	0	650	650	5343	6987	28976	42607
NNW	0	1070	650	0	1233	8296	11249
SUM	0	1720	6673	8210	10933	40177	67713

Sources: Southern California Association of Governments; Center for Demographic Research, California State University, Fullerton: http://www.fullerton.edu/cdr/cities; U.S. Marine Corps.

Table 2.1-4
2000 POPULATION BY SECTOR AND DISTANCE
WITHIN 10 MILES OF THE SAN ONOFRE SITE

	0-1	1-2	2-3	3-4	4-5	5-10	Total
N	0	0	0	3231	0	243	3475
NNE	0	0	0	0	0	0	0
NE	0	0	6054	0	0	0	6054
ENE	0	0	0	0	0	0	0
E	0	0	0	0	3057	0	3057
ESE	0	0	0	0	0	2295	2295
SE	0	0	0	0	0	735	735
SSE	0	0	0	0	0	0	0
S	0	0	0	0	0	0	0
SSW	0	0	0	0	0	0	0
SW	0	0	0	0	0	0	0
WSW	0	0	0	0	0	0	0
W	0	0	0	0	0	0	0
WNW	0	0	0	0	0	0	0
NW	0	733	733	6539	8551	35450	52006
NNW	0	1205	733	0	1509	10176	13623
SUM	0	1938	7520	9770	13117	48899	81245

Sources: Southern California Association of Governments; Center for Demographic Research, California State University, Fullerton: http://www.fullerton.edu/cdr/cities; U.S. Marine Corps.

Table 2.1-5
2010 POPULATION BY SECTOR AND DISTANCE
WITHIN 10 MILES OF THE SAN ONOFRE SITE

	0-1	1-2	2-3	3-4	4-5	5-10	Total
N	0	0	0	3189	0	240	3429
NNE	0	0	0	0	0	0	0
NE	0	0	5975	0	0	0	5975
ENE	0	0	0	0	0	0	0
E	0	0	0	0	3017	0	3017
ESE	0	0	0	0	0	2265	2265
SE	0	0	0	0	0	725	725
SSE	0	0	0	0	0	0	0
S	0	0	0	0	0	0	0
SSW	0	0	0	0	0	0	0
SW	0	0	0	0	0	0	0
WSW	0	0	0	0	0	0	0
W	0	0	0	0	0	0	0
WNW	0	0	0	0	0	0	0
NW	0	723	723	7913	10348	42064	61772
NNW	0	1190	723	0	1826	12260	15999
SUM	0	1913	7421	11102	15191	57554	93182

Sources: Southern California Association of Governments; Center for Demographic Research, California State University, Fullerton: http://www.fullerton.edu/cdr/cities; U.S. Marine Corps.

Table 2.1-6
2020 POPULATION BY SECTOR AND DISTANCE
WITHIN 10 MILES OF THE SAN ONOFRE SITE

	0-1	1-2	2-3	3-4	4-5	5-10	Total
N	0	0	0	3184	0	240	3423
NNE	0	0	0	0	0	0	0
NE	0	0	5965	0	0	0	5965
ENE	0	0	0	0	0	0	0
E	0	0	0	0	3012	0	3012
ESE	0	0	0	0	0	2261	2261
SE	0	0	0	0	0	724	724
SSE	0	0	0	0	0	0	0
S	0	0	0	0	0	0	0
SSW	0	0	0	0	0	0	0
SW	0	0	0	0	0	0	0
WSW	0	0	0	0	0	0	0
W	0	0	0	0	0	0	0
WNW	0	0	0	0	0	0	0
NW	0	722	722	8092	10582	43417	63535
NNW	0	1188	722	0	1867	12602	16379
SUM	0	1910	7409	11276	15462	59244	95301

Sources: Southern California Association of Governments; Center for Demographic Research, California State University, Fullerton: http://www.fullerton.edu/cdr/cities; U.S. Marine Corps.

Table 2.1-7
PROJECTED POPULATION AND ANNUAL RATES
OF POPULATION GROWTH (EXPONENTIAL)
WITHIN 10 MILES DURING VARIOUS PERIODS BETWEEN 1980 AND 2020[(a)]

1980	59,024
Percent annual growth between 1980 and 1990	1.37%
1990	67,713
Percent annual growth between 1990 and 2000	1.82%
2000	81,245
Percent annual growth between 2000 and 2010	1.37%
2010	93,182
Percent annual growth between 2010 and 2020	0.22%
2020	95,301
Percent annual growth between 1980 and 2020	1.18%
Percent change between 1980 and 2020	61.5%

Source: Southern California Association of Governments (SCAG); San Diego Association of Governments (SANDAG); California State Fullerton, Center for Demographic Research; U.S. Marine Corps.

Table 2.1-8
U.S. MARINE CORPS CAMP PENDLETON POPULATION[a]
1981

Area	Name	Population	Direction	Distance (miles)
11	-	0	ESE	14-1/2
12	-	241	ESE	14-1/2
13	-	1,122	ESE	14-1/2
14	-	2,443	ESE	12-1/2
15	-	0	ESE	14-1/2
16	-	413	ESE	14-1/2
17	-	356	ESE	15-3/4
20	-	5,267	SE	14
21	Del Mar	2,516	SE	13-1/2
22	Chappo	1,326	ESE	13
24	-	537	ESE	13
25	-	5	ESE	12-1/2
27	-	1,115	E	13
31	Edison	887	SE	10-3/8
32	-	2	ESE	11-1/2
33	-	1,981	ESE	11-1/2
41	Las Flores	538	SE	8
43	Pulgas	1,821	ESE	8-1/4
51	Mobile Home Park	375	NNW	1-7/8
52	San Onofre	4,804	NE	2-1/2
53	Horno	2,426	E	4-1/2
62	San Mateo	2,564	N	3-1/2
63	Christianitos	0	N	4-1/4
64	Talega	193	N	5-1/2
51	Enlisted Family Housing	2,326	NNW & NW	1-3/4 - 2-1/4
	Total[b]	33,258	-	-

[a] Source: Camp Pendleton Joint Public Affairs Office; Williams-Kuebelbeck, Inc.

[b] Total reflects nighttime population excluding civilian population.

Table 2.1-9
1980 POPULATION BY SECTOR AND DISTANCE
BETWEEN 10 AND 50 MILES FROM THE SAN ONOFRE SITE[(a)]

Sector	10-20	20-30	30-40	40-50	Total 10-50
W	0	0	0	2,010	2,010
WNW	0	0	0	90,693	90,693
NW	40,495	258,382	692,236	1,089,641	2,080,754
NNW	106,327	120,568	443,801	513,889	1,184,585
N	2,080	4,752	151,747	365,084	523,663
NNE	5,624	12,338	67,590	183,102	268,654
NE	5,673	6,973	26,670	59,882	99,198
ENE	4,110	2,306	2,306	7,164	15,886
E	19,640	5,229	2,661	1,316	28,846
ESE	32,297	49,403	66,183	11,789	159,672
SE	78,668	89,035	116,015	196,729	480,447
SSE	0	10,343	70,354	441,756	522,453
Total	294,914	559,329	1,639,563	2,963,055	5,456,861

(a) Sources: 1980 Federal Census; Southern California Association of Governments; San Diego Association of Governments; Williams-Kuebelbeck and Associates, Inc.

Table 2.1-10
1990 POPULATION BY SECTOR AND DISTANCE
BETWEEN 10 AND 50 MILES FROM THE SAN ONOFRE SITE[a]

	10-20	20-30	30-40	40-50	10-50
W	0	0	0	2,918	2,918
WNW	0	0	0	63,877	63,877
NW	95,945	234,592	847,450	1,175,258	2,353,245
NNW	155,219	155,833	429,286	525,735	1,266,073
N	14,227	13,372	203,842	436,810	668,251
NNE	14,035	21,784	78,069	258,462	372,350
NE	9,067	33,852	56,385	128,761	228,064
ENE	6,726	23,065	11,246	15,955	56,991
E	24,200	10,452	11,454	2,579	48,685
ESE	34,044	67,340	105,652	29,445	236,480
SE	108,221	182,222	169,843	173,599	633,885
SSE	0	7,148	61,262	448,346	516,755
Total	461,683	749,659	1,974,487	3,261,745	6,447,574

[a] Sources: Bureau of the Census, U.S. Department of Commerce, 1990 Decennial Population and Housing Census, Land View III, Disc 10, issued December 1997

Table 2.1-11
2000 PROJECTED POPULATION BY SECTOR AND DISTANCE
BETWEEN 10 AND 50 MILES FROM THE SAN ONOFRE SITE[a]

Sector	10-20	20-30	30-40	40-50	Total 10-50
W	0	0	0	2,200	2,200
WNW	0	0	0	99,200	99,200
NW	77,800	402,800	811,400	1,190,700	2,482,700
NNW	218,200	164,800	597,800	567,300	1,548,100
N	4,400	8,500	237,200	476,700	726,800
NNE	8,500	17,700	104,700	270,100	401,000
NE	8,400	9,700	36,300	80,700	135,100
ENE	6,500	3,300	3,300	9,500	22,600
E	29,760	15,000	10,400	2,200	57,360
ESE	51,450	9,500	114,200	34,600	209,750
E	165,390	183,900	259,300	263,100	871,690
SSE	0	15,100	112,900	461,600	589,600
Total	570,400	830,300	2,287,500	3,457,900	7,146,100

[a] Sources: Southern California Association of Governments; San Diego Association of Governments; Williams-Kuebelbeck and Associates, Inc.

Table 2.1-12
2010 PROJECTED POPULATION BY SECTOR AND DISTANCE
BETWEEN 10 AND 50 MILES FROM THE SAN ONOFRE SITE[a]

Sector	10-20	20-30	30-40	Total 40-50	Total 10-50
W	0	0	0	2,300	2,300
WNW	0	0	0	104,500	104,500
NW	100,100	471,100	852,300	1,239,000	2,662,500
NNW	293,000	188,600	677,500	592,100	1,751,200
N	6,100	10,700	269,200	523,600	809,600
NE	10,400	20,900	119,300	304,400	455,000
NE	10,400	11,500	42,600	95,300	159,800
NE	8,500	3,900	3,900	11,000	27,300
E	39,760	26,500	19,600	2,800	88,660
ESE	71,350	115,800	159,100	61,200	407,450
SE	243,390	250,500	357,900	293,600	1,145,390
SSE	0	17,600	134,000	465,200	616,800
Total	783,000	1,117,100	2,635,400	3,695,000	8,230,500

[a] Source: Williams-Kuebelbeck and Associates, Inc.

Table 2.1-13
2020 PROJECTED POPULATION BY SECTOR AND DISTANCE
BETWEEN 10 AND 50 MILES FROM THE SAN ONOFRE SITE[a]

Sector	10-20	20-30	30-40	40-50	Total 10-50
W	0	0	0	2,400	2,400
WNW	0	0	0	110,000	110,000
NW	128,700	552,600	895,600	1,288,900	2,865,800
NNW	393,800	219,900	773,900	618,300	2,005,900
N	8,400	13,500	304,000	515,100	841,000
NNE	12,900	24,600	135,300	342,400	515,200
NE	13,000	13,700	50,000	112,600	189,300
ENE	11,200	4,700	4,700	12,900	33,500
E	54,160	41,000	38,000	3,500	136,660
ESE	92,950	160,500	247,700	109,100	610,250
SE	363,790	351,700	498,400	332,500	1,546,390
SSE	0	20,400	162,800	469,900	653,100
Total	1,078,900	1,402,600	3,110,400	3,917,600	9,509,500

[a] Source: Williams-Kuebelbeck and Associates, Inc.

Table 2.1-14
PROJECTED POPULATION AND ANNUAL RATES OF POPULATION GROWTH BETWEEN 10 AND 50 MILES DURING VARIOUS PERIODS BETWEEN 1980 AND 2020[a]
(EXPONENTIAL)

1980	5,456,861
1990	6,446,906
Percent annual growth between 1980 and 1990	1.66%
2000	7,146,100
Percent annual growth between 1990 and 2000	1.02%
2010	8,230,500
Percent annual growth between 2000 and 2010	1.41%
2020	9,509,500
Percent annual growth between 2010 and 2020	1.44%
Percent annual growth between 1980 and 2020	1.39%
Percent change between 1980 and 2020	74.27%

[a] Source: Williams-Kuebelbeck and Associates, Inc. Bureau of the Census, U.S. Department of Commerce, 1990 Decennial Population and Housing Census, Land View III, Disc 10, issued December 1997

Of the residents living between 10 and 50 miles of the plant site in 1980, 54.30% live between 40 and 50 miles, and 84.35% live between 30 and 50 miles from the subject area. Near the end of plant operation in 2020, 41.20% of the population between 10 and 50 miles from the plant site will live at a distance of at least 40 miles, and 73.91% will live at least 30 miles from the plant site.

2.1.3.2.2 Areas with Greatest Population Growth

The areas within the subject region in which population increases are expected to be greatest between 1980 and 2020 lie primarily in Orange and San Diego Counties. In Orange County, the northern (NW and NNW sectors, 30 to 40 miles) and central (NW and NNW sectors, 20 to 30 miles) portions should experience continuing population expansion. The rate of growth in the central portion, however, is estimated to be the highest in the county. In San Diego County, the City of San Diego, its immediate environs (SSE and SE sectors, 30 to 40 and 40 to 50 miles), and the communities along the coast and inland (SE and ESE sectors, 10 to 20 miles, 20 to 30 miles, and 30 to 40 miles) are projected to experience the highest population growth. Other areas of population growth include the Pomona-Whittier areas of Los Angeles County (NNW sector, 40 to 50 miles) and the Ontario-San Bernardino-Riverside areas (N and NNE sector, 40 to 50 miles).

2.1.3.2.3 Basis of Population Projection

Population projections were developed in the following manner. On census tract maps of suitable scale, concentric circles were drawn at distances of 10, 20, 30, 40 and 50 miles from the station. The circles were divided into 22-1/2° sectors with each sector centered on one of the 16 compass points. The residential population for each sector was calculated for 1980 (utilizing 1980 census data) and for each census decade through the projected plant life (2020). For the sectors lying within the region covered by the SCAG, including Los Angeles, Orange, Riverside, and San Bernardino Counties, the population forecasts were derived by updating SCAG's 1978 report to 1980 with the use of census data and then developing the population forecast with the SCAG 1978 population growth rates. The SCAG growth rates assume a future birth rate of 2.1 live births per woman and an average annual net in-migration to the SCAG region of 33,000 persons per year. SCAG assumed that governmental policies would not limit growth coming into the region.

The remainder of the area between 10 and 50 miles of the plant site is contained in San Diego County and the Pacific Ocean. Census tracts were allocated by sector and the population forecast growth rates through 2000 were obtained from the San Diego Association of Governments (SANDAG), the officially endorsed forecast for San Diego County. For the census decades 2010 and 2020, population forecasts were extrapolated from the SCAG and SANDAG (Series 5) forecast growth rates.

2.1.3.3 Transient Population

The transient population resulting from recreational and industrial land uses in the area within a 10-mile radius of the San Onofre Nuclear Generating Station has been evaluated to determine the seasonal and daily levels and variations. This area includes the City of San Clemente, parts of the City of San Juan Capistrano, and a portion of Camp Pendleton. This area is identified in this section as south coastal Orange County. Daily transient population at Camp Pendleton is approximately 11,000[5]. This comprises civilian and non-resident employment at the Base. The non-military personnel employed within 10 miles of the plant are assumed to be included in the traffic count along Interstate 5 or to be residents of Oceanside or other nearby communities, and therefore not part of the transient population. The sector location of their place of employment has not been included in the analysis to avoid double counting.

2.1.3.3.1 Industrial

The transient population resulting from industrial land use in south coastal Orange County is insignificant. No evidence is available that would alter this situation in the future. At present, there are few acres of light industrial land use in the City of San Clemente. The San Clemente Planning Department states that there is no projected expansion of light industrial land use or conversion to heavy industrial land use.

In addition, the San Clemente Planning Department reports that the city has not zoned nor will it rezone any land for heavy industrial use. While the subject area within 10 miles of the plant site will experience sizeable residential population growth, it is not forecast to become a location of industrial activity.

2.1.3.3.2 Recreational

At present, a substantial transient population results from recreational land uses which include tourist activities and highway traffic originating outside the 10-mile radius. There are four major sources of transient population within the 10-mile radius: public beaches and campgrounds, Mission San Juan Capistrano, Amtrak, and Interstate 5. The transient population from these activity sources, as indicated in Table 2.1-15, was approximately 99,831,903 (excluding SONGS Community Outreach Program activities) for the calendar year 2000.

Of this total, 4,970,121 attended the beaches and state campgrounds, about 540,000 toured Mission San Juan Capistrano, 999,114 rode Amtrak, and 94,207,857 traveled along Interstate 5. Total attendance at these activities was greater during the summer than the other seasons and greater during weekends than weekdays. The 2000 attendance figure for individuals participating in tours through the SONGS Community Outreach Program represents actual attendance for tours of the plant or simulator facilities at the Mesa. Attendance figures for Mission San Juan Capistrano, (10 miles north northwest of the plant), are averages that reflect the seasonal and monthly variation in southern California tourism in general and the historic peak attendance at the Mission in early summer. The beach and state campgrounds attendance, as noted in Table 2.1-16, consists of totals from five public beaches (all but one with camping facilities) and one additional campground within the subject area: San Onofre State Beach (0 to 3.5 miles southeast and 0.5 to 1.0 mile west northwest of the plant), Trestles (2.0 to 2.5 miles west northwest of the plant), San Clemente State Beach, (3 to 4.3 miles northwest of the plant), San Clemente City Beaches, (4.3 to 5.5 miles northwest of the plant), and Doheny State Beach (9.2 to 10.5 miles northwest of the plant). The additional State campground, San Mateo, is located 2.7 to 3 miles northwest of the plant. Beach attendance for the San Clemente City Beaches was provided by the San Clemente Lifeguard Department and for the four State beaches and additional campground by the California Department of Parks and Recreation. Amtrak figures were based on monthly passage figures prepared by their Public Relations Office and represent ridership, both northbound and southbound, between Oceanside and San Juan Capistrano.

2.1.3.3.3 Highway

The estimated highway passenger population along Interstate 5 (located generally northwest and southeast of the plant), as noted in Table 2.1-17, is estimated by actual vehicular counts taken once per quarter for a week and applied occupants per vehicle type. The estimated highway passenger population originated from telephone conversations with the Traffic Census Department (CalTrans San Diego) and Division of Traffic Engineering (CalTrans Los Angeles). Given the suburban, retirement, and military base characteristics of the subject area and the insignificant number of work trips by residents of Orange County to work places in San Diego County and vice versa, it is assumed that the majority of the traffic count at the intersection of Interstate 5 and the San Diego-Orange County line (2.75 miles northwest of the plant) is transient and does not originate within the subject area.

2.1.3.3.4 Forecasts

The transient population in south coastal Orange County should continue to increase in the future in response to growth in the population of the local area and tourism in southern California, as shown in Table 2.1-18. There are many factors that contribute to the demand by the public for beach use and to the volume of tourism including, but not limited to, personal income, transportation costs, available leisure time, costs of alternative vacations, and weather.

To project transient population from 1980 to 2020, the following four assumptions have been employed:

A. Beach attendance is related to the population of the local area which is defined to be Orange County.

B. Visitation of the subject points of interests by residents of southern California is a function of the population of the region.

C. The tourists visiting points of interest in the southern California region could also be visiting friends and relatives in the region so there exists a positive relation between tourism and the population of the 10-county southern California area.

D. Transient highway traffic is related to the population of southern California. On this basis, transient population within a 10-mile radius of the plant is forecast to be 51,331,000 in 1980 and 88,216,900 in 2020. The greatest proportion of transient population will continue to be on Interstate 5.

Table 2.1-15
TOTAL TRANSIENT POPULATION IN THOUSANDS AT MAJOR RECREATIONAL AND TOURIST ACTIVITIES AND ALONG INTERSTATE 5 WITHIN A 10-MILE RADIUS OF THE SAN ONOFRE STATION, 2000[a]

2000	Total Transient Population	Beach and Campground Attendance	SONGS Community Outreach Program	Mission San Juan Capistrano	Interstate 5[b]	Amtrak
January	7799.7	166.8	0.123	35	7531.2	66.6
February	7302.5	146.3	0.335	35	7052.3	68.5
March	7821.4	176.5	0.121	45	7523.6	76.2
April	7795.9	290.1	0.320	45	7370.5	90.0
May	8124.5	403.0	0.394	45	7593.1	83.0
June	8066.5	611.7	0.320	55	7314.6	84.9
July	9719.7	890.4	0.253	55	8674.1	99.9
August	9680.2	914.8	0.134	45	8609.2	111.0
September	9001.2	506.1	0.098	45	8365.7	84.3
October	8274.3	309.1	0.180	45	7845.7	74.3
November	7958.3	236.1	0.161	45	7594.6	82.5
December	8290.3	319.4	0.098	45	7847.9	78.0
TOTAL	99834.4	4970.1	2.537	540	93322.7	999.1

(a) Sources: California Department of Parks and Recreation; San Clemente Lifeguard Department, City of San Clemente; SONGS Community Outreach, Southern California Edison Company; Mission San Juan Capistrano; Office of Traffic, California Department of Transportation; and Amtrak Public Relations Office.

(b) Figures shown for Interstate 5 have been reduced to avoid double counting of individuals traveling to the San Onofre Nuclear Generating Station Information Center and the San Onofre State Beach.

Table 2.1-16
ATTENDANCE IN THOUSANDS AT PUBLIC BEACHES WITHIN A 10-MILE RADIUS OF SAN ONOFRE STATION, 2000

2000	Total	San Clemente City Beach	Doheny State Beach	San Clemente State Beach	San Onofre State Beach	Trestles State Beach	San Mateo State Campground
January	166.7	88.4	26.2	3.3	32.5	9.4	7.0
February	146.3	84.4	15.4	3.0	23.2	14.0	6.3
March	176.5	82.4	26.8	4.9	40.1	16.2	6.1
April	290.1	148.4	38.1	7.0	66.4	19.5	10.7
May	403.0	140.1	118.0	15.8	91.6	32.1	5.4
June	611.7	278.0	141.0	29.1	122.3	29.0	12.3
July	890.3	428.0	260.2	82.7	79.9	26.2	13.4
August	914.8	366.0	284.9	71.4	144.9	31.3	16.2
September	506.1	212.1	96.1	52.4	106.1	27.5	12.0
October	309.1	76.8	129.6	19.9	60.6	15.7	6.5
November	236.1	83.8	54.0	16.4	56.7	18.8	6.4
December	319.4	107.3	114.3	12.5	58.4	20.5	6.2
TOTAL	4970.1	2095.6	1304.7	318.4	882.6	260.2	108.5

Sources: California of Parks and Recreation; San Clemente Lifeguard Department, City of San Clemente

Table 2.1-17
TOTAL ANNUAL VEHICLE TRAFFIC AND ESTIMATED PASSENGER POPULATION IN THOUSANDS ALONG INTERSTATE 5, SAN DIEGO-ORANGE COUNTY LINE 2000[a]

2000	Average Monthly Traffic			Estimated Passenger Population		
	Total	Passenger Cars[b]	Truck[c]	Total	Passenger Cars[d]	Truck[e]
January	3725.1	3338.0	387.0	7563.8	7176.8	387.0
February	3484.8	3122.7	362.1	7075.8	6713.8	362.1
March	3725.1	3338.0	387.0	7563.8	7176.8	387.0
April	3662.7	3282.2	380.6	7437.2	7056.7	380.6
May	3784.8	3391.6	393.2	7685.1	7291.9	393.2
June	3662.7	3282.2	380.6	7437.2	7056.7	380.6
July	4311.4	3863.4	447.9	8754.3	8306.3	447.9
August	4311.4	3863.4	447.9	8754.3	8306.3	447.9
September	4172.3	3738.8	433.5	8471.9	8038.4	433.5
October	3893.8	3489.2	404.6	7906.5	7501.9	404.6
November	3768.2	3376.7	391.5	7651.4	7259.9	391.5
December	3893.8	3489.2	404.6	7906.5	7501.9	404.6
TOTAL	46396.0	41575.5	4820.5	94207.9	89387.3	4820.5

(a) Source: Office of Traffic, California Department of Transportation; Williams-Kuebelbeck and Associates, Inc.
(b) Includes pickups, campers, and panel trucks.
(c) Approximately 10.39% of average daily traffic by month is commercial truck traffic.
(d) Approximately 2.15 occupants per car.
(e) Approximately 1.0 occupants per commercial truck.

Table 2.1-18
PROJECTED TOTAL TRANSIENT POPULATION IN THOUSANDS AT MAJOR RECREATIONAL AND TOURIST ACTIVITIES AND ALONG INTERSTATE 5 WITHIN A 10-MILE RADIUS OF THE SAN ONOFRE STATION, 1980-2020[a]

1980-2020	Total Attendance	Beach Attendance	Mission San Juan Capistrano	Interstate 5[b]	Amtrak
1980	51,331.0	3,415.8	350.0	46,324.5	1240.7
1990	60,196.0	4,223.2	408.6	54,115.8	1448.4
2000	68,841.2	4,836.2	467.2	61,881.6	1656.2
2010	78,094.1	5,551.5	529.5	70,136.0	1877.1
2020	88,216.9	6,402.9	597.2	79,099.8	2117.0

(a) Source: Williams-Kuebelbeck and Associates, Inc.

(b) Figures shown for Interstate 5 have been reduced to avoid double counting of individuals traveling to the San Onofre State Beach.

2.1.3.3.5 Peak Seasonal and Daily Population

Based on the review of data used to compile Table 2.1-15, peak seasonal transient population typically occurs in the summer months of July and August; peak daily transient population typically occurs on Sundays in late July or early August.

The peak seasonal transient population is estimated to range from 9,991,500 to 17,296,400 in 2020 as shown in Table 2.1-19. The peak daily transient population is projected to increase from 513,300 in 1980 to 882,200 in 2020 as shown in Table 2.1-20. Tables 2.1-21 to 2.1-24 show the population distribution by sector and distance within a 10-mile radius of the plant for the peak seasonal and daily transient population.

2.1.3.4 Low Population Zone

The low population zone (LPZ) is the area contained within 1.95 miles of the plant site. This distance is established to ensure that the guidelines of 10CFR100 are met with respect to the LPZ and the population center, as discussed in Paragraph 2.1.3.5. The LPZ is shown on Figure 2.1-13. Transportation routes that may be used by Marine Corps personnel for evacuation purposes are shown on Figure 2.1-13. More details can be found in the Permanently Defueled Emergency Plan (PDEP).

Table 2.1-19
PROJECTED PEAK SEASONAL TRANSIENT POPULATION IN THOUSANDS AT MAJOR RECREATIONAL AND TOURIST ACTIVITIES AND ALONG INTERSTATE 5 WITHIN A 10-MILE RADIUS OF THE SAN ONOFRE STATION, 1980-2020[a][b]

1980-2020	Total Attendance	Beach Attendance	Mission San Juan Capistrano	Interstate 5	Amtrak
1980	9,991.5	1,423.7	79.4	8,209.1	279.3
1990	11,767.6	1,765.4	92.7	9,583.4	326.1
2000	13,459.3	2,021.8	106.0	10,958.7	372.8
2010	15,283.9	2,320.7	120.1	12,420.5	422.6
2020	17,296.4	2,676.4	135.5	14,007.9	476.6

[a] Sources: Southern California Edison Company, Urban and Regional Planning, Williams-Kuebelbeck and Associates, Inc.

[b] Peak seasonal transient population is 19.4% of annual transient population and occurs during the summer months of July and August. Attendance at each activity is distributed in accordance with its share of total transient population during the two summer months.

2.1.3.4.1 Population

The LPZ is contained entirely within the boundaries of Camp Pendleton. Residential population is located in the NW and NNW sectors and is estimated in 1976 to number 1127.[5][3] It is expected to increase to 1201 by 1980 and remain at that level.[5] An elementary school for the residents of this military housing development is also located within the LPZ.

2.1.3.4.2 Population in the Vicinity of the LPZ

Beyond the LPZ there are three Marine base camps within a distance of 5 miles from the plant site. Camp San Onofre has a population of 4,804 and is located 2.5 miles from the site in the northeast sector, Camp San Mateo has a population of 2,564 and is located 3.5 miles from the plant site in the north sector, Camp Horno has a population of 2,426 and is located 4.5 miles from the plant in the east sector.[5]

The transient population generators within the LPZ are the San Onofre State Beach and Interstate 5. Camp Pendleton is not considered a transient population generator within the LPZ in as much as the main centers of activity on the Base are between 10 and 20 miles from the plant. The population distributions for seasonal and peak daily transient population are presented in Tables 2.1-25 through 2.1-29.

Table 2.1-20
PROJECTED PEAK DAILY TRANSIENT POPULATION IN THOUSANDS AT MAJOR RECREATIONAL AND TOURIST ACTIVITIES AND ALONG INTERSTATE 5 WITHIN A 10-MILE RADIUS OF THE SAN ONOFRE STATION, 1980-2020[a][b]

1980-2020	Total Attendance	Beach Attendance	Mission San Juan Capistrano	Interstate 5	Amtrak
1980	513.3	34.2	3.5	463.2	12.4
1990	602.0	42.2	4.1	541.2	14.5
2000	688.5	48.4	4.7	618.8	6.6
2010	781.0	55.5	5.3	701.4	18.8
2020	882.2	64.0	6.0	791.0	21.2

(a) Sources: Southern California Edison Company, Urban and Regional Planning, Williams-Kuebelbeck and Associates, Inc.

(b) Peak daily transient population is assumed to be 1% of annual transient population and occurs on a Sunday in August. Attendance at each activity is distributed in accordance with its share of total transient population during the month of August.

The peak seasonal transient population is projected to increase from 1,813,000 in 1980 to 3,123,700 in 2020. The peak daily population is anticipated to expand from 95,100 in 1980 to 164,600 in 2020.

2.1.3.5 Population Center

In the initial year of plant operation in 1982, the nearest population center, as defined in 10CFR100, was the City of San Clemente. According to the San Clemente Planning Department, the population of San Clemente in 1980 was approximately 27,325 with a projected buildout population of from 55,000 to 60,000 by 2000. The political boundary of the City of San Clemente is in the NW quadrant, approximately 2.65 miles from the Unit 2 reactor. However, the nearest residence within the San Clemente city limits corresponds to the former home of former President Richard Nixon, which is located approximately 2.85 miles from the Unit 2 reactor. The San Clemente Planning Department states that there is no potential for future residential population south of the Nixon residence because the Nixon property abuts the U.S. Coast Guard Reservation, which straddles the common boundary of the City of San Clemente, Orange County, and San Diego County. Therefore, the former Nixon residence represents the nearest residential population within the population center.

Table 2.1-21
PROJECTED PEAK SEASONAL TRANSIENT POPULATIONS (IN THOUSANDS)
BY SECTOR AND DISTANCE IN MILES WITHIN A 10-MILE RADIUS OF SONGS
(1980)
Sheet 1 of 3

	Distance, miles						Total Population 0-10 Miles
Sector	0-1	1-2	2-3	3-4	4-5	5-10	
WNW	34.9	9.9	14.1	0	0	0	58.9
NW	182.1	408.5	403.8	644.9	862.2	2,655.7	5,157.2
NNW	168.9	0	0	0	0	0	248.3
N	49.7	0	0	0	0	0	49.7
NNE	33.1	0	0	0	0	0	33.1
NE	20.7	0	0	0	0	0	20.7
ENE	50.0	0	0	0	0	0	50.0
E	132.8	0	0	0	0	0	132.8
ESE	210.3	417.4	306.9	0	0	0	934.6
SE	70.0	70.0	181.2	452.4	417.4	2,127.6	3,318.6
TOTAL	952.5	905.8	906.0	1,097.3	1,279.6	4,783.3	10,003.9

[a] Sources: Southern California Edison Company, Urban and Regional Planning, Williams-Kuebelbeck and Associates, Inc.

Table 2.1-21
(2000)
Sheet 2 of 3

	Distance, miles						Total Population 0-10 Miles
Sector	0-1	1-2	2-3	3-4	4-5	5-10	
WNW	49.7	13.2	18.8	0	0	0	81.7
NW	243.2	545.3	539.0	880.1	1,188.8	1,585.4	6,981.8
NNW	225.6	0	0	0	0	106.0	331.6
N	66.3	0	0	0	0	0	66.3
NNE	44.2	0	0	0	0	0	44.2
NE	27.7	0	0	0	0	0	27.7
ENE	66.7	0	0	0	0	0	66.7
E	177.4	0	0	0	0	0	177.4
ESE	280.7	557.2	409.7	0	0	0	1,247.6
SE	99.4	99.4	247.8	606.9	557.3	2,840.3	4,450.9
TOTAL	1,280.9	1,215.1	1,215.3	1,487.0	1,746.1	6,531.7	13,475.9

(a) Sources: Southern California Edison Company, Urban and Regional Planning, Williams-Kuebelbeck and Associates, Inc.

Table 2.1-21
(2020)
Sheet 3 of 3

Distance, miles							Total Population 0-10 Miles
Sector	0-1	1-2	2-3	3-4	4-5	5-10	
WNW	65.7	16.9	24.1	0	0	0	106.7
NW	310.9	697.1	689.0	1,139.8	1,548.4	4,613.5	8,998.8
NNW	288.3	0	0	0	0	135.5	423.8
N	84.8	0	0	0	0	0	84.8
NNE	56.5	0	0	0	0	0	56.5
NE	35.4	0	0	0	0	0	35.4
ENE	85.3	0	0	0	0	0	85.3
E	226.8	0	0	0	0	0	226.8
ESE	358.8	712.1	523.7	0	0	0	1,594.6
SE	131.5	131.5	321.2	777.9	712.1	3,630.7	5,704.9
TOTAL	1,644.0	1,557.6	1,558.0	1,917.7	2,260.5	8,379.7	17,317.7

[(a)] Sources: Southern California Edison Company, Urban and Regional Planning, Williams-Kuebelbeck and Associates, Inc.

Table 2.1-22
PROJECTED PEAK DAILY TRANSIENT POPULATION IN THOUSANDS BY SECTOR AND DISTANCE IN MILES
WITHIN A 10-MILE RADIUS OF THE SAN ONOFRE SITE (1980, 1990)

Sector	0-1	1-2	2-3	3-4	4-5	5-10	Total	0-1	1-2	2-3	3-4	4-5	5-10	Total
	1980							1990						
WNW	0.0	0.4	0.6	0	0	0	1.0	1.1	0.5	0.7	0	0	0	2.3
NW	10.2	23.0	22.8	28.8	34.2	133.7	252.7	11.9	26.8	26.6	34.0	40.4	156.9	296.6
NNW	9.4	0	0	0	0	3.5	12.9	11.0	0	0	0	0	4.1	15.1
N	2.8	0	0	0	0	0	2.8	3.3	0	0	0	0	0	3.3
NNE	1.9	0	0	0	0	0	1.9	2.3	0	0	0	0	0	2.3
NE	1.2	0	0	0	0	0	1.2	1.3	0	0	0	0	0	1.3
ENE	2.8	0	0	0	0	0	2.8	3.3	0	0	0	0	0	3.3
E	7.3	0	0	0	0	0	7.3	8.7	0	0	0	0	0	8.7
ESE	11.8	23.4	17.3	0	0	0	52.5	13.7	27.3	20.2	0	0	0	61.2
SE	1.7	1.7	7.8	24.3	23.4	119.3	178.2	2.1	2.1	9.3	28.4	27.3	139.4	208.6
Total	49.10	48.5	48.5	53.1	57.6	256.5	513.3	58.7	56.7	56.8	62.4	67.7	300.4	602.7

[a] Sources: Southern California Edison Company, Urban and Regional Planning, Williams-Kuebelbeck and Associates, Inc.

Table 2.1-23
PROJECTED PEAK DAILY TRANSIENT POPULATION IN THOUSANDS BY SECTOR AND DISTANCE IN MILES WITHIN A 10-MILE RADIUS OF THE SAN ONOFRE SITE (2000,2010)

Sector	0-1	1-2	2-3	3-4	4-5	5-10	Total	0-1	1-2	2-3	3-4	4-5	5-10	Total
	1980							1990						
WNW	1.2	0.6	0.8	0	0	0	2.6	1.4	0.7	0.9	0	0	0	3.0
NW	13.6	30.7	30.4	38.9	46.4	179.6	339.6	15.4	34.8	34.5	44.3	52.7	203.7	385.4
NNW	12.5	0	0	0	0	4.7	17.2	14.1	0	0	0	0	5.3	19.4
N	3.8	0	0	0	0	0	3.8	4.3	0	0	0	0	0	4.3
NNE	2.6	0	0	0	0	0	2.6	2.9	0	0	0	0	0	2.9
NE	1.5	0	0	0	0	0	1.5	1.7	0	0	0	0	0	1.7
ENE	3.8	0	0	0	0	0	3.8	4.2	0	0	0	0	0	4.2
E	9.9	0	0	0	0	0	9.9	11.2	0	0	0	0	0	11.2
ESE	15.7	31.2	23.0	0	0	0	69.9	17.9	35.4	26.2	0	0	0	79.5
SE	2.4	2.4	10.6	32.4	31.2	159.3	238.3	2.7	2.7	12.0	36.8	35.4	180.6	270.2
Total	67.0	64.9	64.8	71.3	77.6	343.6	689.2	75.8	73.6	73.6	81.1	88.1	389.6	781.8

[a] Sources: Southern California Edison Company, Urban and Regional Planning, Williams-Kuebelbeck and Associates, Inc.

Table 2.1-24
2020 PROJECTED PEAK DAILY TRANSIENT POPULATION IN THOUSANDS
BY SECTOR AND DISTANCE IN MILES
WITHIN A 10-MILE RADIUS OF THE SAN ONOFRE SITE

Sector	0-1	1-2	2-3	3-4	4-5	5-10	Total
WNW	1.6	0.8	1.1	0	0	0	3.5
NW	7.4	39.3	38.9	50.2	59.9	230.2	435.9
NNW 1.0	16.0	0	0	0	0	6.0	22.0
N	4.8	0	0	0	0	0	4.8
NNE	3.2	0	0	0	0	0	3.2
NE	1.9	0	0	0	0	0	1.9
ENE	4.8	0	0	0	0	0	4.8
E	12.8	0	0	0	0	0	12.8
ESE	20.1	39.9	29.5	0	0	0	89.5
SE	3.1	3.1	13.6	41.5	39.9	207.6	308.8
TOTAL	85.7	83.1	83.1	91.7	99.8	443.8	887.2

[a] Sources: Southern California Edison Company, Urban and Regional Planning, Williams-Kuebelbeck and Associates, Inc.

The distance from the Unit 2 reactor to the population center boundary is, therefore, at least 2.65 miles and, in fact, is 2.85 miles when measured to the nearest residence. The distance of 2.85 miles is 1.46 times the LPZ of 1.95 miles, which is greater than the 10CFR100 guideline of 1.33.

Several small communities exist immediately north and northwest of San Clemente. These include the communities of Dana Point, Capistrano Beach, and the City of San Juan Capistrano. The population of these three combined areas in 1980 and 1990 (latest year for community area projections by Orange County) is projected to increase from 33,444 to 43,033. (7) Farther north are the incorporated communities of El Toro and Laguna Hills and the unincorporated community of Mission Viejo. The 1980 population and projected 1990 population for these communities is: El Toro, 1980 - 24,139, 1990 - 26,949; Laguna Hills, 1980 - 31,605, 1990 - 38,878; and Mission Viejo, 1980 - 63,217, 1990 - 84,525. These population estimates and projections are based on residential population and do not include seasonal fluctuations generated by the tourist-oriented transient population.

Table 2.1-25
PROJECTED PEAK SEASONAL TRANSIENT POPULATION (1980, 1990)
IN THOUSANDS BY SECTOR AND DISTANCE IN MILES
WITHIN THE LOW POPULATION ZONE[a][b]

Sector	1980			1990		
	0-1	1-1.95	Total	0-1	1-1.95	Total
WNW	34.9	9.4	44.3	43.3	11.0	54.3
NW	182.1	388.1	570.2	212.7	453.1	665.8
NNW	168.9	0	168.9	197.3	0	197.3
N	49.7	0	49.7	58.0	0	58.0
NNE	33.1	0	33.1	38.7	0	38.7
NE	20.7	0	20.7	24.2	0	24.2
ENE	50.0	0	50.0	58.3	0	58.3
E	132.8	0	132.8	155.1	0	155.1
ESE	210.3	396.5	606.8	245.2	462.8	708.0
SE	70.0	66.5	136.5	86.8	82.5	169.3
TOTAL	952.5	860.5	1,813.0	1,119.6	1,009.4	2,129.0

[a] Source: Williams-Kuebelbeck and Associates, Inc.

[b] Only those sectors with projected transient population are shown.

2.1.3.6 Population Density

Cumulative residential population for 1980, within a 30-mile radius, is 913,267, as shown in Table 2.1-30. This compares to a cumulative population of 1,413,500 for a uniform density of 500 persons per square mile.

For 2020, the projected population within a 30-mile radius is 2,637,850, as noted in Table 2.1-31. At a uniform density of 1,000 persons per square mile, the population within the same radius would be 2,827,000.

Table 2.1-26
PROJECTED PEAK SEASONAL TRANSIENT POPULATION (2000, 2010, 2020) IN THOUSANDS
BY SECTOR AND DISTANCE IN MILES WITHIN THE LOW POPULATION ZONE[a][b]

Sector	2000			2010			2020		
	0-1	1-1.95	Total	0-1	1-1.95	Total	0-1	1-1.95	Total
WNW	49.7	12.6	62.3	57.7	14.2	71.9	65.7	16.1	81.8
NW	243.2	518.0	761.2	275.6	587.2	862.8	310.9	662.2	973.1
NNW	225.6	0	225.6	255.7	0	255.7	288.3	0	288.3
N	66.3	0	66.3	75.2	0	75.2	84.8	0	84.8
NNE	44.2	0	44.2	50.1	0	50.1	56.5	0	56.5
NE	27.7	0	27.7	37.1	0	37.1	35.4	0	35.4
ENE	66.7	0	66.7	75.6	0	75.6	85.3	0	85.3
E	177.4	0	177.4	201.0	0	201.0	226.8	0	226.8
ESE	280.7	529.3	810.0	318.2	599.9	918.1	358.8	676.5	1,035.3
SE	99.4	94.4	193.8	114.1	108.4	222.5	131.5	124.9	256.4
Total	1,280.9	1,154.3	2,435.2	1,460.3	1,309.7	2,770.0	1,644.0	1,479.7	3,123.7

[a] Source: Williams-Kuebelbeck and Associates, Inc.

[b] Only those sectors with projected transient population are shown.

Table 2.1-27
PROJECTED PEAK DAILY TRANSIENT POPULATION (1980, 1990) IN THOUSANDS BY SECTOR AND DISTANCE IN MILES WITHIN THE LOW POPULATION ZONE[a][b]

Sector	1980			1990		
	0-1	1-1.95	Total	0-1	1-1.95	Total
WNN	0.0	0.4	0.4	1.1	0.5	1.6
NW	10.2	21.8	32.0	11.9	25.5	37.4
NNW	9.4	0	9.4	11.0	0	11.0
N	2.8	0	2.8	3.3	0	3.3
NNE	1.9	0	1.9	2.3	0	2.3
NE	1.2	0	1.2	1.3	0	1.3
ENE	2.8	0	2.8	3.3	0	3.3
E	7.3	0	7.3	8.7	0	8.7
ESE	11.8	22.2	34.0	13.7	25.9	39.6
SE	1.7	1.6	3.3	2.1	2.0	4.1
Total	49.1	46.0	95.1	58.7	53.9	112.6

[a] Source: Williams-Kuebelbeck and Associates, Inc.
[b] Only those sectors with projected transient population are shown.

Table 2.1-28
PROJECTED PEAK DAILY TRANSIENT POPULATION (2000, 2010) IN THOUSANDS BY SECTOR AND DISTANCE IN MILES WITHIN THE LOW POPULATION ZONE[a][b]

Sector	1980			1990		
	0-1	1-1.95	Total	0-1	1-1.95	Total
WNW	1.2	0.6	1.8	1.4	0.7	2.1
NW	13.6	29.2	42.8	15.4	33.1	48.5
NNW	12.5	0	12.5	14.1	0	14.1
N	3.8	0	3.8	4.3	0	4.3
NNE	2.6	0	2.6	2.9	0	2.9
NE	1.5	0	1.5	1.7	0	1.7
ENE	3.8	0	3.8	4.2	0	4.2
E	9.9	0	9.9	11.2	0	11.2
ESE	15.7	29.6	45.3	17.9	33.6	51.5
SE	2.4	2.3	4.7	2.7	2.6	5.3
Total	67.0	61.7	128.7	75.8	70.0	145.8

[a] Source: Williams-Kuebelbeck and Associates, Inc.
[b] Only those sectors with projected transient population are shown.

Table 2.1-29
PROJECTED PEAK DAILY TRANSIENT POPULATION (2020) IN THOUSANDS
BY SECTOR AND DISTANCE IN MILES WITHIN THE LOW POPULATION ZONES[a][b]

Sector	2020		
	0-1	1-1.9	Total
WNW	1.6	0.8	2.4
NW	17.4	37.3	54.7
NNW	16.0	0	16.0
N	4.8	0	4.8
NNE	3.2	0	3.2
NE	1.9	0	1.9
ENE	4.8	0	4.8
E	12.8	0	12.8
ESE	20.1	37.9	58.0
SE	3.1	2.9	6.0
Total	85.7	78.9	164.6

(a) Source: Williams-Kuebelbeck and Associates, Inc.
(b) Only those sectors with projected transient population are shown.

Table 2.1-30
COMPARISON OF POPULATION BASED ON A DENSITY OF
500 PEOPLE PER SQUARE MILE TO PROJECTED POPULATION
INITIAL YEAR 1980[a]

Distance in Miles from Plant Site	Population at 500 People Per mi^2		Projected Population	
	Total	Cumulative Total	Total	Cumulative Total
0-1	1,570	1,570	0	0
1-2	4,715	6,285	1,810	1,810
2-3	7,850	14,135	5,695	7,505
3-4	11,000	25,135	6,081	13,586
4-5	14,135	39,270	7,768	21,354
5-10	117,810	157,080	37,670	59,024
10-20	471,420	628,500	294,914	353,938
20-30	785,000	1,413,500	559,329	913,267

(a) Source: Williams-Kuebelbeck and Associates, Inc.

Table 2.1-31
COMPARISON OF POPULATION BASED ON A DENSITY OF 1000
PEOPLE PER SQUARE MILE TO PROJECTED POPULATION;
INITIAL YEAR 2020[a]

Distance in Miles from Plant Site	Population at 500 People Per mi^2		Projected Population	
	Total	Cumulative Total	Total	Cumulative Total
0-1	3,140	3,140	0	0
1-2	9,430	12,570	2,050	2,050
2-3	15,700	28 270	6,460	8,510
3-4	22,000	50,270	14,100	22,610
4-5	28,270	78,540	19,750	42,360
5-10	235,620	314,160	114,490	156,850
10-20	942,840	1,257,000	1,078,900	1,235,750
20-30	1,570,000	2,827,000	1,402,100	2,637,850

[a] Source: Williams-Kuebelbeck and Associates, Inc.

2.1.4 REFERENCES

1. Orange County Administrative Office, 1980 Census Population Counts, April 1981, Santa Ana, California.

2. San Diego Association of Governments, "1980 Census of Population and Housing", San Diego, California.

3. San Diego Association of Governments, "Final Series V Population Projections", San Diego, California.

4. Southern California Association of Governments, '78 Growth Forecast Policy, 1979, Los Angeles, California.

5. Joint Public Affairs Office, U.S. Marine Corps Base, Camp Pendleton.

6. Southern California Association of Governments, "1980 Census Tract Statistics", Los Angeles, California.

7. Orange County Administrative Office, "1981 Draft Forecast by Community Analysis Areas".

8. CSUF Center for Demographic Research, 1990 Decennial Census of Population, http://www.fullerton.edu/cdr/cities

9. Bureau of the Census, U.S. Department of Commerce, 1990 Decennial Population and Housing Census, Land View III, Disc 10, issued December 1997

2.1.5 BIBLIOGRAPHY

1. Darrieulat, Carlena, CalTrans San Diego, Traffic Census Department.

2. Pruitt, Nancy, State of California, Department of Parks.

3. Wheeler, Sandy, Mission San Juan Capistrano

4. Steffensen, Jason, AMTRAK, Public Relations, San Francisco.

5. Nelson, Marsha, City of San Clemente, Department of Lifeguards.

6. Southern California Association of Governments, "1980 Census Tract to RSA Conversions".

7. CSUF Center for Demographic Research, 1990 Decennial Census of Population, http://www.fullerton.edu/cdr/cities

8. Bureau of the Census, U.S. Department of Commerce, 1990 Decennial Population and Housing Census, Land View III, Disc 10, issued December 1997

9. Southern California Edison, 2000 Community Event Quarterly Reports, Nuclear Communications

2.2 NEARBY INDUSTRIAL, TRANSPORTATION, AND MILITARY FACILITIES

The information contained in this section was prepared in accordance with the original plant licensing requirements. Most of the information is considered historical and representative of site conditions at the time the plant was licensed. Unless otherwise noted in the text, this information has not been updated to reflect data from later years.

The remaining off-site hazards of primary concern are those with explosive potential. Other hazards (toxic gases, asphyxiants, and flammable materials) may be assessed in the future; but, are no longer critical to the safe operation of the site and are no longer inputs of the current design of licensing basis of the site.

2.2.1 LOCATION AND ROUTES

There are three pipelines, three transportation routes, a quarry operation, and firing ranges on the United States Marine Corps Base at Camp Pendleton within a 5-mile radius of the plant. These facilities are illustrated in Figure 2.2-1. Items illustrated on the map are described in Subsection 2.2.2.

2.2.2 DESCRIPTIONS

2.2.2.1 Description of Facilities

2.2.2.1.1 Storage Facilities

Fuel storage areas include the following gasoline facilities at Camp Pendleton Special Services gas stations: (1) the nearest is located 0.1 mile east of the San Onofre gate on Basilone Road 1.5 miles northwest of the plant; (2) Camp San Onofre on Basilone Road; (3) on the corner of Cristianitos and San Mateo Roads near Camp San Mateo; and (4) at Camp San Onofre at the intersection of Basilone and San Mateo Roads.(1)

Ammunition is stored by the U.S. Marine Corps in the Las Pulgas area of Camp Pendleton approximately 9 miles from San Onofre Nuclear Generating Station. The material is Class 7 explosive and is stored in underground bunkers. This facility is separated from the plant site by the San Onofre mountains.(2)

2.2.2.1.2 Quarrying Operations

The only facility involving the manufacture or processing of products and the employment of personnel within 5 miles of the plant is Camp Pendleton quarry located 4 miles north of the plant site as shown in Figure 2.2-1.(1) Quarry operations are to crush and sort aggregate material for maintenance and construction. Explosives are not used.(1)

2.2.2.1.3 Military Operations

Except for maneuvers that involve the use of beach areas, such as amphibious landings, most Marine Corps activities are conducted inland from Camp San Onofre and the range of coastal hills that parallels the coast near the plant. With regard to amphibious landings, the plant is located in a separate designated sector (Section C) of the beach, and in discussions with the Marine Corps they indicated no landings will be made in this sector.(3)(4)

No firing of live ammunition is permitted throughout a strip along the seacoast. This strip is approximately 2 miles wide at its narrowest point and extends from the northern reservation boundary to approximately 10 miles south of the plant.(3)(4)

Where firing or weapon impact is permitted, the training is conducted under very close supervision since populated areas, the highway, rail line, and infantry maneuvering areas are located along the seacoast of the reservation to a distance of approximately 5 miles inland.(3)(4)

Military firing ranges are shown on U.S. Geological Survey (1968), 7.5 minute quadrangle sheets: San Clemente, Margarita Peak, San Onofre Bluffs, and Las Pulgas Canyon.

The nearest firing range is a known-distance range over which infantrymen are able to fire small arms to gain proper sighting data. The maximum range of firing is about 100 feet, with rounds impacting into a steep hillside. This range is approximately 5,000 meters from the plant. All other firing ranges are generally inland from Camp San Onofre and are located so that the maximum range of the weapons would not permit an impact closer than approximately 2 miles from the plant, assuming firing was directed toward the plant rather than within the designated sectors. Firing is also directed into hillsides or valleys to avoid any danger of projectile skipping.(3)(4)(5)

Aircraft practice firing and artillery bombardment is controlled at all times and is directed into impact areas located further than 5 miles inland. Aircraft approaches and pullouts are within a 15,000-foot altitude airspace, also located further than 5 miles inland, and therefore do not pass near the plant.(3)(4)

There are two bombing and strafing ranges located approximately 6 miles from the plant. Various types of aircraft delivered ordnance of up to 500-pound bombs are employed on these ranges as dictated by visibility and fire danger.(6)(5)

No bombardment from the sea is ever permitted, and the shore landing maneuvers do not involve the use of live ammunition. Thus, Marine Corps activities which could otherwise conceivably constitute a hazard to the plant are all conducted well away from the coastline and do not constitute a credible hazard to plant safety.(3)(4)

The proximity of missile sites to the plant was discussed with the Marine Corps who indicated that there are no missile sites on Camp Pendleton and none within a radius of at least 10 miles from the plant.(3)(4)

2.2.2.1.4 Brush Fires at Camp Pendleton

During the 10 years prior to about 1975, the average per year grass/brush fire experience base-wide has been 410 fires. In the area of the base property of reasonable concern, there have been 58 fires over the 5 years prior to about 1975. This area is the Coastal San Onofre Mountains, bounded by Basilone Road, Interstate 5, and Horno Canyon Road. Of the 58 fires only 3 have exceeded 100 acres, and 41 fires were less than 10 acres.(7) The three that exceeded 100 acres were as follows:

Date	Acres
1980	5,442
1981	27,960
1982	7,275

In addition, fires occurred on January 20, 1976 and November 7, 1990 amounting to 1,595 and 4,815 acres, respectively. These two fires are not included in the 5-year figures.(7)

Most grass/brush fires are the result of Marine Base training. The probable causes include impact area fires extending beyond impact areas, and various other causes such as careless smoking by troops in the field, motorized equipment failures and other accidents.(7)

The Base-wide wildfire prevention program is covered by Base Order and includes, but is not limited to, controls over training regarding kinds of ordinance allowed and training areas utilized depending upon "Fire Danger Rating" as established by the Base Fire Chief. Also, programs of firebreak maintenance and controlled burning are implemented to limit the spread of fire when it does occur.(7)

The initial response to grass/brush fires by Camp Pendleton Fire Department men and equipment depends upon the nature of the report received and the total Fire Department strength at the time of the report. The Base Fire Department is not manned nor equipped to handle multiple or major wildland fires without assistance from mutual aid participants such as the U.S. Forest Service, California Division of Forestry, or others. There are mutual aid agreements in existence.(7)

The U.S. Forest Service has provided the following information concerning brush and grass fires in coastal areas such as Camp Pendleton:(8)

A. Tonnage of Fuel

Grasses - 2 tons/acre - maximum
Grasses - 1 ton/acre - normal
Coastal Sage Brush - 10 tons/acre - maximum
Coastal Sage Brush - 6 tons/acres - normal

B. Rate of Spread

The worst case Santa Ana fire will consume 3000-4000 acres/hr with the fire front moving as much as 300 ft/min. Prevailing weather conditions are: 10% humidity, 30-45 mi/hr offshore winds; 80-90°F ambient temperature; and fall brush and moisture conditions.

C. Flame Temperature

The normal flame temperature for coastal sage fire is 2000 to 2500°F. Plume temperature drops to 25°F above ambient air temperature about 200 feet above the fire. Santa Ana conditions usually create a low inversion ceiling, resulting in rapid horizontal movement of plume. This draft usually returns to ambient temperature approximately 400-500 feet from the fire.

D. Emission Rates(9)

Pollutant	Fuels	
	Grasses (lb/ton)	Coastal Sage Brush and Grasses (lb/ton)
Carbon Monoxide	50-70	150-200
Hydrocarbons	5-6	20-40
Particulates	10	45-50

2.2.2.1.5 Transportation Routes

The old Highway 101 is immediately east of the site. It does not carry north-south through traffic, but rather is the entrance road to the south end of San Onofre State Beach.

The San Diego Freeway (Interstate 5) is east of the site. It is the only public, coastal vehicular link between Orange County and San Diego County.

The railroad right-of-way is east of the site between old Highway 101 and Interstate 5. The railroad is part of the Los Angeles – San Diego corridor. The North County Transit District (NCTD) of San Diego owns the track passing to the east of the site since this is south of the Orange/San Diego county line. Prior to 1992, the railroad was owned and operated by Atchison, Topeka, and Santa Fe (AT&SF) Railway. This is an active line with Amtrak passenger service and cargo service.

Commercial vessel shipping lanes are greater than 5 miles southwest of the plant in the Pacific Ocean.

Aircraft activities in the vicinity of the plant are generally associated with the following Federal airways:

Airway	Distance (Statute Miles)
V-23	0.5
V-25-27	12
V-208-458	7
J-1	12

A description of aircraft activity is found in Paragraph 2.2.2.5.

2.2.2.1.6 Oil and Gas Pipelines

There are three pipelines in the vicinity of the plant:

A. San Diego Gas & Electric - 6-inch natural gas pipeline adjacent to Basilone Road.

B. Southern California Gas Co. - 12-inch natural gas pipeline adjacent to Interstate 5.

C. San Diego Pipeline Company - 10-inch refined petroleum products pipeline 2 to 5 miles northeast of the plant in Camp Pendleton.

A description of the pipelines is found in Paragraph 2.2.2.3.

2.2.2.2 Description of Products and Materials

2.2.2.2.1 Railway Line

The railway line passes within approximately 490 feet of the closest San Onofre Units 2 and 3 safety-related structure (fuel handling buildings). SCE was previously required to send a report to the NRC triennially regarding shipment of a wide range of hazardous cargo near the site. As part of this report, the railroad is contacted every three years regarding the shipment of such materials past San Onofre. As noted earlier, the scope of hazardous materials of concern has been reduced to those with significant explosive potential.

The materials shipped by rail, which pose a potentially explosive/flammable cloud hazard are: LPG, Propane, Propylene, Butane, and Ethanol. Their explosive hazard baseline annual shipments is 2329.[94]

From 1979 through 2010 (with the exception of 1992) there were no shipments of explosives or military ordnance on the railroad. In 1992 there was one shipment of military Class B explosives.

2.2.2.2.2 Interstate Highway 5 (San Diego Freeway)

Interstate Highway 5 (I-5), the major transportation thoroughfare linking Los Angeles and San Diego, California, passes within approximately 585 feet of the closest San Onofre Units 2 and 3 safety-related structure. SCE is required to send an update to the Offsite Hazards Analysis to the NRC triennially. A highway survey of hazardous material shipments on I-5 is performed at the truck weigh station located three miles south of the plant every three years for the Offsite Hazards Analysis Update. Hazardous materials and their description, number of shipments, and maximum shipment size information is provided in Table 2.2-1. The required survey scope is limited to explosive hazards although additional data may be compiled.

The hazardous material transportation survey may identify several chemicals which were not considered in the original analysis. Each chemical is individually assessed. Chemicals with similar properties to those chemicals previously identified are grouped together in a chemical bin. The total number of shipments for the chemical bin is the sum of the shipments for all chemicals included in that bin. Any chemical determined not to be a hazard is eliminated from further consideration.

The hazardous material survey also identifies shipping container size. A comparison is made with the baseline shipment size to determine if there have been changes or to see if it is bounded by the previous analysis.

The explosive and flammable hazards are Acetylene, Compressed Hydrogen, Liquid Hydrogen, LPG, Liquefied Natural Gas (LNG), and military ordnance.

TABLE 2.2-1
HAZARDOUS CARGO WITH EXPLOSIVE POTENTIAL TRAFFIC ESTIMATES

Chemical[f]	Description	Baseline Annual Shipments[i]	2015 Annual Shipments[c]	Baseline Shipment Size[i]	2015 Shipment Size[a]
Acetylene	Gas	52[g]	979	3300 ft^3	6772 ft^3
Butane	Liquefied gas	2200[h] 210[g][j]	---	8485 gal[h] 11,000 gal[g][j]	---
Hydrogen	Liquefied gas Gas	210[j][g] 180[j][g]	75 979	10,120 lbs[j] 2,600 lbs[j]	3894 lbs 176 lbs
Liquefied Natural Gas (LNG)	Liquefied gas	420		9200 gal[g]	
Liquefied Petroleum Gas (LPG)	Liquefied gas	3577[j]	1657	11,000 gal[j]	9800 gal
Propane	Liquefied gas	3367[j][g]	4029	11,000 gal[j]	10,408 gal

TABLE 2.2-1
HAZARDOUS CARGO WITH EXPLOSIVE POTENTIAL TRAFFIC ESTIMATES

Notes:
(a) Maximum size based on actual observed shipments.
(b) Deleted.
(c) Annual shipments are equal to the observed shipments multiplied by a shipment adjustment factor.
(d) Deleted.
(e) Deleted.
(f) May include chemicals judged to have similar properties to those previously evaluated.
(g) For explosive/flammable cloud hazard analysis.
(h) For toxic hazard analysis.
(i) 1977 Baseline values given unless otherwise noted.
(j) Revised Baseline from 1996 OHA.[96]
--- Indicates no shipments observed during the survey

2.2.2.3 Pipelines

The San Diego Pipeline Company, Southern California Gas Company, and San Diego Gas and Electric each own a pipeline that passes within 5 miles of the plant, as shown on Figure 2.2-1.

2.2.2.3.1 San Diego Pipeline Company[14][15]

A. Size: 10-inch diameter

B. Age: Constructed in 1962

C. Operating pressure: 1440 lb/in.^{2} (maximum)

D. Depth of burial: 30-inches average

E. Location: See Figure 2.2-1

F. Valves: Manually-operated gate valve at milepost 58.24 (see Figure 2.2-1)

G. Material: Gasoline, diesel fuel, turbine fuel, Navy jet fuel (JP-5)

H. Storage: The pipeline is not used for gas storage

I. Future plans: No immediate plans to expand. Future demand could necessitate construction of a parallel pipeline.

J. Leaks: None within 5 miles

K. Flow direction: South

L. Release event: Product initially released at flowrate. Within 20 seconds the pressure drop would be detected and the pipeline shut down by automatic warning devices. The nearest main line valves upstream and downstream of the break would be closed.

2.2.2.3.2 Southern California Gas Company[16][17]

A. Size: 12-inch diameter

B. Age: It was constructed in several phases. The section from 0.4 mile northwest to 1.6 miles northwest of the plant was built in 1932. The section from 1.6 to 1.9 miles northwest was constructed in 1960. The section from 1.9 to 2.8 miles northwest was built in 1966. The section from 2.8 to 5.0 miles northwest was built in 1929. And the section from 0.4 mile northwest to 5.0 miles south-east of the plant was built in 1966.

C. Operating pressure: 400 lb/in.^{2}g (maximum allowable).

D. Depth of burial: 30 inches average

E. Location: See Figure 2.2-1. The pipeline is located 585 feet northeasterly from the centerline of Unit 3 containment. The pipeline is located within the right-of-way of U.S. Highway 101, approximately 5 feet southwesterly of the northeast edge of the right-of-way.

F. Valves: There are three plug valves located 1.3 and 2.8 miles northwest of the plant and 2.1 miles southeast (see Figure 2.2-1).

G. Material: Natural gas (91% methane, 5% ethane, 4% miscellaneous).

H. Storage: The pipeline is not used for gas storage.

I. Future plans: There are no present plans for expansion. Southern California Gas Company has no plans to use the pipeline for a product other than natural gas.

J. Leaks: There have been two leaks on the 12-inch pipeline within 5 miles of the plant. One, in 1967, was approximately 3.5 miles north of the plant, a small corrosion leak with no fire or explosion. The other, in 1963, was approximately 3.3 miles north of the plant, a break in the pipeline due to exterior stress, with no fire or explosion. Repair was made by replacing 449 feet of pipe.

K. Flow direction: South

L. Release event: Southern California Gas is unable to determine release rate versus time for hypothetical double-ended guillotine break. A pressure drop created by a major break would be detected almost immediately. The flow of gas would stop in 45 to 90 minutes.

2.2.2.3.3 San Diego Gas & Electric Company[18][19]

A. Size: 6-inch diameter, 12,058 feet long, 4-inch diameter, 3634 feet long

B. Age: 1968

C. Operating pressure: 200 lb/in.^{2}g

D. Depth of burial: 36 inches average

E. Location: Adjacent to Basilone Road

F. Valves: Plug type, manual

G. Material: Natural gas

H. Storage: The pipeline is not used for gas storage

I. Future plans: No plans to expand

J. Leaks: None

K. Flow direction: Northeast

L. Release event: Gas would be lost at a rate of 875 x 106 ft^3/h for about 1 hour. Release would be noticed prior to 1 hour because of drop at U.S. Marine Corps control house, or by regular Marine patrols.

2.2.2.4 Waterways

The plant is immediately adjacent to the Pacific Ocean. The principal uses of the coastal waters include pleasure boating, industrial cooling, military exercises, and sport and commercial fishing. The Coast Guard reports that commercial vessel traffic lanes lie at distances greater than 5 miles from the plant.

The Coast Guard estimates the majority of recreational boaters that use the ocean waters near the San Onofre site originates from Dana Point (10.5 miles, NW sector) and Oceanside Harbors (17 miles, SE sector). The Dana Point Harbor holds 2600 pleasure boats. The Oceanside Harbor includes nearly 800 pleasure boats. According to the Coast Guard and the two previously mentioned harbors, recreational boating activity is greatest on sunnier weekends. For 1975, the Coast Guard reported no serious accidents in the area.

The beaches south of the plant are used by the Marine Corps for maneuvers such as amphibious landings.(3) The waters adjacent to the site are reported to yield large quantities of fish and are attractive to sport and commercial fishermen.(3)

There are two intake structures (0.6 mile, SW and SSW sectors) each associated with Units 2 and 3 of the facility. Seawater from the Pacific Ocean is used for dilution intakes and discharges. The top of the intake structure is 12 feet below the water line. This 12-foot distance is sufficient to avoid interference with the operation of recreational boats. The Coast Guard reports that the draft of most recreational boats does not normally exceed 6 feet.

2.2.2.5 Aircraft Operations

2.2.2.5.1 Airports

Many air carrier, general aviation, and military airports are within 50 miles of the plant. There are no airports within 5 miles.

Figure 2.2-2 shows the location of airports near the site. Those with control towers, which serve as the source or destination for a large number of the planes flying airways in the vicinity are:

Airport	Distance (Statute Miles)
Long Beach	47
Orange County	28
Lindbergh	48
Montgomery	45
Palomar (Carlsbad)	23
Gillespie	51
Brown	66

Other general aviation airports along the southern California coast, which present a small contribution to airways in the vicinity are:

Airport	Distance (Statute Miles)
Meadowlark	37
Oceanside	15

Military airfields are:

Airport	Distance (Statute Miles)
Los Alamitos NAS	41
El Toro MCAS	24
Camp Pendleton MCALF	12.5
Miramar NAS	41.5
Santa Ana MCAS	29

2.2.2.5.2 Airport Operations

The current and projected operations for airports within 50 miles of the plant are shown in Table 2.2-2. Some of these airports are no longer in operation. None of the airports has sufficient operations to require statistics on aircraft accidents. A description of each airport with operations that could contribute to the airways in the vicinity of the plant follows:

2.2.2.5.2.1 Long Beach Airport

Long Beach Airport is located approximately 47 miles northwest of the site. It is basically a general aviation airport with a small number of flights associated with Douglas Aircraft testing and commercial service. The total number of operations in 1975 was 538,230. Of this number, 293,592 were itinerant operations.

2.2.2.5.2.2 Orange County Airport

Orange County Airport is approximately 29 statute miles from the plant. It is primarily a general aviation airport. Air California is based at the airport and there are jet flights. The majority of these flights are north-bound. There were 618,889 operations in calendar year 1975. Of these operations, 304,459 were itinerant operations. Although the Federal Aviation Administration(20) has forecast 690,000 operations by 1987, Orange County Airport has forecast 660,000 (± 10,000) by 1990.(21) The Airport reports that this number of operations represents a practical evaluation of present peak utilization of airport facilities and the potentially low probability of any major airfield improvements that might significantly extend this capacity.

2.2.2.5.2.3 Lindbergh Field

Lindbergh Field is approximately 49 statute miles southeast of the site. It is primarily an air carrier operation field and also has a number of general aviation operations. In the calendar year 1975, there were 195,016 operations at Lindbergh, of which 83,018 were general aviation and air taxi operations.

2.2.2.5.2.4 Montgomery Airport

Montgomery is located 46 statute miles southeast of the plant. It is primarily a general aviation field. In calendar year 1975, there were 341,339 operations, of which 131,547 were itinerant.

2.2.2.5.2.5 Palomar Airport

Palomar Airport is located approximately 22 miles southeast of the site. In calendar year 1975, there were 183,989 operations at the airport, of which 97,593 were itinerant operations.

2.2.2.5.2.6 Gillespie Airport

Gillespie Airport is located approximately 51 miles southeast of the site. In calendar year 1975, Gillespie had 243,601 operations, of which 116,018 were itinerant.

TABLE 2.2-2
CURRENT AND PROJECTED OPERATIONS FOR AIRPORTS WITHIN
A 50-MILE RADIUS FROM THE SAN ONOFRE SITE

Type, Name	Distance to Plant, Section		Operations[a] CY 1975	Projected Operations
Air Carrier				
Orange County	27	NW	618,889	660,000[b]
Long Beach	45	NW	538,230	800,000[c]
Ontario	45	N	153,958	298,000[c]
San Diego	50	SSE	195,016	320,000[c]
Los Angeles	63	NW	455,846	600,000[c]
Military				
Camp Pendleton MCB	15	ESE	67,100	NA
El Toro NCAS	20	NNW	140,000	NA
Los Alamitos NAS	40	NW	50,034	NA
March AFB	40	NNE	55,000	NA
Miramar NAS	45	SE	789,795	NA
Santa Ana MCAS	29	NW	103,033	NA
General Aviation				
Fallbrook	17	E	10,000	19,000[d]
Oceanside	17	SE	20,000	29,000[d]
Skylark	22	NE	30,000	55,000[d]
Palomar	25	SE	183,989	325,000[c]
Rancho California	25	ENE	5,000	10,000[d]
Perris Valley	30	NNE	6,000	9,000[d]
Corona	35	N	50,000	184,000[c]
Meadowlark	35	NW	58,000	65,000[d]
Fullerton	40	NW	223,248	400,000[c]
Hemet-Ryan	40	NE	45,000	60,000[d]
Riverside	40	N	124,176	218,000[c]
Chino	45	N	183,037	311,000[c]
Fla-Bob	45	N	36,000	42,000[d]
Ramona	45	ESE	36,000	51,000[d]
Montgomery	47	SSE	341,339	559,000[c]
Brackett	50	NNW	218,107	357,000[c]
Cable	50	N	75,000	224,000[c]
Gillespie	50	SE	243,601	423,000[c]
Tri-City	50	NNE	24,000	29,000[d]
Avalon	50	W	50,000	86,000[c]

(a) Personal Correspondence with Western Region FAA[22]
(b) 1990 Forecast by Orange County Airport[21]
(c) 1987 Forecast Federal Aviation Administration[20]
(d) 1982 Forecast by Western Region FAA[22]
NA = Not available

2.2.2.5.2.7 Brown Airport

Brown Airport is located approximately 66 statute miles southeast of the site. In calendar year 1975, Brown had 166,715 operations. Of these 49,884 were itinerant.

2.2.2.5.2.8 El Toro MCAS

El Toro is located approximately 24 miles northwest of the plant. In calendar year 1975, there were approximately 130,000 operations at El Toro. Of this number, approximately 40,000 were approaches which use a corridor that passes approximately 10 statute miles due west of the plant. From observations made at the radar scope at El Toro, these approaching aircraft tend to stay on a straight line approximately 10 miles away from the plant. The majority of the operations out of El Toro are high speed jet aircraft.

2.2.2.5.2.9 Camp Pendleton

Camp Pendleton Airport is located approximately 13 statute miles from the plant. In calendar year 1975, there were approximately 67,100 operations. These operations are primarily helicopter. However, there are some fixed-wing aircraft operating out of the field.

2.2.2.5.2.10 Miramar

Miramar Naval Air Station is located approximately 42 statute miles from the site in a southeast direction. In calendar year 1975, there were 789,795 operations.

2.2.2.5.2.11 Los Alamitos NAS

Los Alamitos Naval Air Station is located approximately 42 statute miles from the plant. In calendar year 1975, there were 50,034 operations. The majority of these operations were rotary wing military aircraft.

2.2.2.5.2.12 Meadowlark and Oceanside Airports

These general aviation airports are located 37 and 15 miles, respectively, from the site. Since they have no official control towers, they are assumed to have very little traffic. The FAA has provided an estimate of 24,000 movements per year for Meadowlark (Terminal Area Forecast, September 1974).

2.2.2.5.3 Air Traffic Descriptions

The following description of aircraft activity in the vicinity of the plant was determined by a survey conducted by the applicants at the El Toro Coast TRACON Facility.

There were three categories of air traffic observed.

A. General aviation

B. Commercial aviation and high speed private jets

C. Military operations

A description of each of these categories follows.

2.2.2.5.3.1 General Aviation

These aircraft generally fly parallel to the coast approximately along V-23. The observed distribution of aircraft is shown in Figure 2.2-3. The Airway V-23 centerline passes 1/2-mile seaward of the plant along bearing 301° north of Oceanside VORTAC. Restricted area R2533 requires that Visual Flight Rule (VFR) traffic along this airway be above 2000 feet MSL when passing the plant, unless authorized not to do so by the FAA Air Route Traffic Controller at El Toro, or the Commanding General Camp Pendleton. These airways are shown on Figure 2.2-4. Aircraft moving along V-23 are single-engine piston aircraft, twin-engine piston aircraft, and twin-engine turbo-prop aircraft. The estimated annual frequency of general aviation is 93,444.

2.2.2.5.3.2 Commercial and Other High Speed Jet Aircraft

These aircraft generally fly parallel to the coast approximately along V-25. Many are enroute to a landing at, or departing from, Lindbergh Field in San Diego. The remainder are making through flights at higher altitudes. The observed distribution of aircraft is shown in Figure 2.2-5. The Airway V-25-27 centerline passes 12 miles southwest of the plant along bearing 304° north of Mission Bay VORTAC. The location of the airway is shown on Figure 2.2-4. The estimated annual frequency of commercial air carriers and high-speed business jets is 71,656.

2.2.2.5.3.3 Military Aircraft

Military operations are either helicopter flights associated with Camp Pendleton or high speed jet flights associated with El Toro Marine Corps Air Station. The high speed military flights are concentrated 7.5 miles northwest of the plant in the El Toro landing corridor, and in a widely distributed pattern of traffic also associated with El Toro as shown in Figure 2.2-6. The estimated annual frequency of helicopter operations is 7,072, distributed as shown in Figure 2.2-7. The estimated annual frequency of military jet operations is 26,676.

2.2.2.6 Projections of Industrial Growth

There are no plans for expansion of existing facilities or new industrial development within the 5-mile radius of the plant. Existing pipelines and waterways are also not scheduled for expansion.[14][16][18]

The City of San Clemente reports no acreage zoned for industrial use in the southeastern section of the community within the 5-mile radius, nor are there plans to rezone for industrial use. The industrial land use in San Clemente, which is approximately 6 miles from the plant, is minimal and limited to light industry.

The Comprehensive Planning Organization of San Diego County, in conjunction with the California Department of Transportation, has forecast an increase of 45% by 1995 in truck traffic on Interstate 5 in the vicinity of the plant.

This forecast assumes a population increase of 60% by 1995 for San Diego County and a shift in truck activity to inland routes such as Interstate 15 and Highway 395. Hazardous cargo shipments are expected to decrease on Interstate 5 as a percent of total shipments because increased industrialization in San Diego will provide these products locally. Fuel shipments (gasoline, LPG, LNG, etc.) may decrease in absolute number because of the development of these processing facilities in San Diego and the increasing cost to ship fuels by truck. Explosive shipments by the U.S. Navy will remain constant to the U.S. Marine Corps Camp Pendleton and will decrease for other shipments. Industrial gas and chemical shipments will vary as a function of future industrial process requirements, availability from local sources, products manufactured and shipment costs. The largest increase in truck activity can be expected in food and other consumer products.

The Federal Aviation Administration "Aviation Forecast, Fiscal Years 1976-1987" forecasts a 45% increase in commercial aviation hours flown, and an 80% increase in general aviation hours flown. Military operations are forecast to remain constant. The resultant increases in air traffic in the vicinity of the plant are as follows:

	1976 Operations	1987 Forecast
General Aviation	93,444	168,198
Commercial	71,700	103,900
Military	33,700	33,700

2.2.3 EVALUATION OF POTENTIAL ACCIDENTS

This section historically addressed the determination of design basis events from the list of potential accidents and considers the postulated effects of these accidents on the plant in terms of design parameters or physical phenomena.

The accidents considered in this section include: explosions of hazardous materials, delayed ignition of flammable vapor clouds, release of toxic vapors, asphyxiation, fires, and accidents at sea.

2.2.3.1 Determination of Design Basis Events

Standard Review Plan 2.2.3 defines design basis events external to the station as those accidents for which a realistic estimate of the annual probability of exceeding 10CFR100 exposure guidelines is in excess of approximately 10^{-7} or for which a conservative estimate of this probability is in excess of approximately 10^{-6}.

Available statistical data were used to determine the probability of occurrence of potential accidents based upon their historical frequency of occurrence. In those cases where data relating to particular classes of accidents were not available, conservative assumptions were used to evaluate order-of-magnitude accident probabilities. A description of data sources, assumptions, and computation methods is presented in the following paragraphs.

2.2.3.1.1 Transportation Accidents on Interstate 5

Hazardous materials transported past the San Onofre plant site on Interstate 5 were tabulated in Table 2.2-1 but has been modified to reflect only potentially explosive chemicals. Historically, hazardous materials included military ordnance, flammable and explosive chemicals, toxic chemicals, and pressurized noncombustible gases. Only those with explosive potential remain relevant to the current design and licensing basis of the site.

2.2.3.1.1.1 Accident Rates for Motor Carriers of Hazardous Cargos

The probability of transportation accidents on Interstate 5 (I-5) involving hazardous materials was assumed to be the same as the accident rate for all trucks. The probability of an accident for all trucks is a function of the total number of accidents involving trucks and the annual number of trucks which travel past the plant on I-5.

The California Department of Transportation (CalTrans) provided truck[a] accident data for the 10.5 mile segment of the I-5, approximately five miles North and five miles South of the plant (Table 2.2-3). The data provided in Table 2.2-3 is for I-5 from milepost 65.2 to 72.37 in San Diego County and milepost 0.0 to 3.3 in Orange County. The data accounts for all traffic accidents involving trucks which had property damage exceeding $500.00.

Truck traffic rates for the period from 1982 through 1989 are based on data collected during the 1984, 1987, and 1990 offsite hazards surveys. Linear regression was used to estimate the traffic rate during the intermediate years.

For the period from 1990 through 2013, the truck traffic rate is based on data obtained from the California Highway Patrol. The California Highway Patrol collects data on the total number of trucks passing through the north and south bound weigh stations during their normal hours of operation. Data was extrapolated for the periods when one or both of the stations were closed.

TABLE 2.2-3
ANNUAL TRUCK TRAFFIC & TRUCK ACCIDENTS FOR A 10.5 MILE STRETCH OF I-5 ADJACENT TO SAN ONOFRE

Year	Actual Number of Accidents	Estimated Number of Trucks
1982	17	1.35×10^6(1)
1983	17	1.43×10^6(1)
1984	20	1.47×10^6(1)
1985	21	1.58×10^6(1)
1986	26	1.66×10^6(1)
1987	30	1.79×10^6(1)
1988	24	1.81×10^6(1)
1989	37	1.88×10^6(1)
1990-1992	77	2.1×10^6(3)
1993-1995	67	2.3×10^6(3)
1996-1998	110	2.3×10^6(3)
1999-2001	99	2.3×10^6(3)
2002-2004	105	2.9×10^6(3)
2005-2007	101	2.6×10^6(3)
2007-2010	49	2.5×10^6(3)
2011-2013	30	2.5×10^6(3)

(1) Truck traffic rates are based on data obtained during 1984, 1987 and 1990 offsite hazards analyses. Linear regression was used to estimate truck traffic during the interim years.
(2) (Deleted)
(3) Average annual truck traffic rate for given time period.

(a) Truck accident data excludes pickup trucks, panel trucks, school buses, emergency vehicles, fire trucks and highway construction equipment.

The information on truck accidents and truck transportation rates was used to calculate the truck accident probability. For the period of 2011 through 2013, the average truck accident probability in the vicinity of San Onofre was 3.82 x 10^{-7} accidents/truck-mile.

2.2.3.1.1.2 Explosions Due to Transportation Accidents on Interstate 5

A. Military Ordnance

Correspondence with the military identifies the maximum net explosive weight of any military shipment of explosives past San Onofre Nuclear Generating Station Units 2 and 3 on I-5 and the railroad. Assuming that the explosive shipments are composed of materials having a pound for pound equivalence with TNT, a shipment weight of 65,000 pounds(96) of TNT is required to exceed the peak positive normal reflected overpressure of 7 psi at the closest safety related structure (Fuel Handling Building) produced by the surface detonation of the TNT shipment. From the 2015 Offsite Hazards Analysis (OHA) update, military shipments did not exceed the maximum shipment weight; therefore, the hazard from shipment of military ordnance past the plant on I-5 is zero.

B. Explosive Chemicals

There are two classifications(30) of hazardous materials, detailed in Table 2.2-1, being shipped on I-5 past the San Onofre site, which can pose an explosion hazard: flammable liquids and flammable compressed gases.

1. Flammable liquids were evaluated in Reference 58 (pages 5-6 through 5-10) and Reference 82 (pages 29-33) to determine the impact on safety related structures resulting from a spill followed by an explosion. None of the chemicals evaluated are capable of causing a 7.0 psi peak reflective overpressure at the nearest safety related structure. There were no new flammable liquids identified in the 2015 survey, which need to be considered. Therefore, shipment of flammable liquids by tank truck on Interstate 5 do not contribute to the explosive hazards plant risk.

2. Five flammable gasses transported on Interstate 5 were evaluated, four were determined to have the capability of causing a 7.0 psi peak reflective overpressure; Liquefied Petroleum Gas (LPG), Liquefied Hydrogen, Compressed Hydrogen, and Acetylene. It was determined that Liquefied Natural Gas (LNG) is not capable of causing a 7.0 psi peak reflective over pressure. Table 2.2-4 contains the updated explosive hazard frequency of exceeding a 7.0 psi overpressure.

C. Flammable Vapor Clouds (Delayed Detonation)

The flammable cloud at the plant hazard analysis was based upon a review of flammable substances found in the survey to identify those, which may be capable of forming a cloud which could travel to the Control Room/Command Center HVAC air intake, ignite and cause damage due to the resulting fire or explosion. The materials evaluated to be capable of contributing to this risk are compressed gases and liquefied gases. The original 1979[58] analysis which was revised and updated in 1981[86] demonstrated that other materials do not have an evaporation rate large enough to create a flammable gas mixture at any significant distance (on the order of 500 feet) from the accident site.

There are five flammable gases transported on Interstate 5 which have the capability of forming a flammable vapor cloud hazard; Liquid Petroleum Gas (LPG), Liquefied Hydrogen, Compressed Hydrogen, Acetylene and Liquefied Natural Gas (LNG). Table 2.2-4 contains the updated flammable cloud hazard frequency of forming a flammable vapor cloud at the plant.

2.2.3.1.2 Transportation Accidents on the Railroad Track Adjoining the San Onofre Nuclear Generating Station

The update of offsite hazards performed every three years includes contacting the BNSF railroad for a list of all hazardous chemicals transported past San Onofre during the previous three years. Chemicals shipped by railroad can pose potential explosive, flammable cloud, toxic gas, and asphyxiation hazards. As previously noted, only potentially explosive chemicals are relevant to the current design and licensing basis of the site.

Based on the 2015 Offsite Hazards Update, there were no shipments of explosive, flammable, toxic, or asphyxiation materials by military transport. Therefore, hazard frequencies from shipments made specifically by the military on the railroad is zero.

The plant risk due to explosive hazards is directly proportional to the number of shipments past the plant. Shipments of LPG had increased significantly between the 1987 and 1990 OHA Updates. In 1987 there were 124 shipments and in 1990 there were 1499 shipments. Because of the uncertainty in the number of shipments and the increasing risk to the plant, SCE committed in 1991 to review the shipment rate every year as opposed to every three years. In 1991, the shipment rate increased to 2329 at which point SCE undertook an effort to revise the analysis to reduce the explosive hazards plant risk from the railroad by removing unnecessary conservatisms. The revised analysis allowed greater than 14,000 shipments of LPG before the shipment of LPG needed to be considered a design basis accident.[94] Because of the large margin between the actual number of shipments and the number of shipments required to exceed the allowable number of shipments, SCE is no longer required to update the shipment rate each year.

The explosive hazard analysis uses the 1992 analysis[94] for the baseline values to determine the updated explosive hazard frequency. For rail shipments, the accident probability is not updated since it was computed in 1992. The only factor, which needs to be updated is the current shipment frequency. The current explosive hazard frequency is therefore based on the baseline frequency multiplied by the ratio of the current shipment frequency to the baseline shipment frequency. The data is presented in Table 2.2-4.

Table 2.2-4
UPDATED FREQUENCY OF FLAMMABLE AND EXPLOSIVE HAZARDS

Substance	Baseline Flammable Cloud Hazard Frequency (per year)	2015 Flammable Cloud Hazard Frequency (per year)	Baseline Explosive Hazard Frequency (per year)	2015 Explosive Hazard Frequency (per year)
LPG-Hwy[3]	1.7 E-7[4]	2.6 E-7	2.8 E-8[4]	4.3 E-8
LPG-Rail[3]	1.3 E-8[4]	4.6 E-7	1.6 E-7[1]	3.0 E-7
Liquid Hydrogen-Hwy	9.0 E-9[4]	3.1 E-9	1.4 E-9[4]	4.8 E-10
Compressed Hydrogen-Hwy	8.8 E-9[4]	4.6 E-8	1.2 E-9[4]	6.2 E-9
Acetylene-Hwy	3.0 E-9[5]	2.5 E-8	2.0 E-10[5]	1.6 E-9
LNG-Hwy	1.6 E-8[5]	N/A	N/A	N/A
TOTAL		7.9 E-7		3.5 E-7

NOTES:

(1) Baseline values for LPG rail explosive hazards from NSG/PRA Report PRA-23-92-007.[94]

(2) (Deleted)

(3) Includes shipments of LPG, Butane, Propane, and Propylene.

(4) Revised baseline from 1996 OHA Update.[96]

(5) Baseline from Supplement 1 Analysis of Explosive Vapor Cloud for Rail and Highway Transportation Routes near SONGS.[86]

The plant risk due to flammable vapor clouds is also directly proportional to the number of shipments past the plant. However, the flammable vapor cloud plant risk attributed to the transportation of LPG on the railroad was sufficiently low in 1991 that the flammable risk did not need to be reevaluated with the explosive risk. In the 1992 analysis, the rail accident frequency was updated. The ratio of the 1981 to the 1992 accident frequencies is applied to reduce the LPG rail flammable vapor cloud baseline hazard frequency for an updated baseline value. The current flammable vapor cloud hazard frequency is then calculated by the same ratio method applied to the explosive hazard frequency. The data is presented in Table 2.2-4.

2.2.3.1.3 Accidents Involving Natural Gas Pipelines

A 12-inch natural gas pipeline is located approximately 450 feet from the nearest plant structure. A probabilistic analysis of the potential hazard to the plant due to postulated natural gas pipeline accidents has been performed. The results confirm that no undue risk to the plant and, subsequently, to the health and safety of the public exists. The probability of pipeline rupture leading to an unacceptable air intake concentration at the plant is exceedingly small.

The pipeline is described in Paragraph 2.2.2.3.2. The pipeline is 5 feet west of the east side of the Highway 101 right-of-way and parallel to Highway 101. The pipeline is owned by Southern California Gas Company. It is 12 inches in diameter and buried nominally 30 inches. The section of pipe nearest the plant was constructed in 1966. The contents of the pipeline are gaseous methane (91%), ethane (5%), and miscellaneous (4%).

An analysis has been performed to determine the likelihood of a pipeline accident that leads to an unacceptable concentration of 4.4% natural gas at the air intake. The assessment of hazards posed by the proximity of a natural gas pipeline to the San Onofre Nuclear Generating Station involves the toxicity and flammability of natural gas concentrations. Methane is not generally classified as a toxic substance.(69) So the flammability limit is controlling. A value of 4.4% was chosen as a lower limit.(70)(71)(72) The analysis considers the likelihood of pipeline rupture with accompanying release of natural gas and transport to the plant by wind.

The frequency of unacceptable consequences is calculated as follows:

$$F = F_r * P_v * P_d * P_s * P_i * P_c$$

where:

- F = Frequency of unacceptable consequences
- F_r = Frequency of pipe rupture
- P_v = Probability of low initial upward velocity
- P_d = Probability of wind direction
- P_s = Probability of a spill
- P_i = Probability of air intake open
- P_c = Probability of actual unacceptable consequences considering that a 4.4% natural gas concentration at an air intake will not always lead to an unacceptable plant effect

Conservative assumptions used in the analysis include:

A. All pipe ruptures are double-ended guillotine ruptures
B. The 30 inches of overburden does not create an upward velocity
C. Cloud formation occurs without turbulent mixing
D. The air intake is always open
E. Existence of a 4.4% concentration at the air intake is unacceptable

The equation can be conservatively simplified to:

$$F = F_r * P_d * P_s$$

The American Gas Association Report NG-18, No. 106, An Analysis of Reportable Incidents for Natural Gas Transmission and Gathering Lines, 1969 through 1975, contains data for 285,000 miles of pipe over a 6-year period. The frequency of reportable incidents is 10^{-3}/year-mile. Southern California Gas Company, owner of the pipeline near San Onofre, was contacted and confirmed that the AGA data was appropriate for the SCG system (i.e., conservative). Adjusting the frequency to account for ruptures results in a frequency of 3.3×10^{-4}/ year-mile as F_r. F_r is thus based on 33% of reportable incidents being pipe ruptures and 67% being small leaks that would not be expected to create a cloud. This approach conservatively assumes that all ruptures are double-ended.

To assess the possible air intake effects, it is necessary to perform a cloud formation analysis, including the effects of natural gas buoyancy and air flow. Cloud formation is dependent upon mass flowrate from the broken pipe.

For this analysis, all ruptures were assumed to be double-ended guillotine breaks without effects of impingement against opposite flow or overburden. The flow is shown in Figure 2.2-8. The initial upward velocity was considered to be essentially zero, with only buoyancy and diffusion accounting for cloud rise.

A cloud model was developed assuming axial conservation of species, conservation of total mass, conservation of x and y momentum, and conservation of energy. A contiguous plume with a Gaussian concentration distribution was used. A cross-section of the plant and terrain is illustrated in Figure 2.2-9, with cloud formation shown.

It is necessary to adjust the cloud movement to account for the downward displacement of the terrain past the bluff. The actual downward displacement is expected to be small due to flow separation at the bluff. Flow separation is indicated by diffusion data,[73] which shows steady separation to occur with half angles exceeding 24°. The bluff forms a 28° angle with the horizontal. To be conservative, however, it was assumed that the flow followed the terrain (also ignoring the obstructing buildings). Flow field was evaluated using an electrical analog method for potential flow. The plume was then deflected downward an amount corresponding to the displacement of streamline intersecting the 4.4% concentration line at the bluff. The resulting displacements are shown in Figure 2.2-10.

Each case was run for the high initial flowrate and the steady-state flow-rate. The high initial flowrate is artificially depicted as creating a steady cloud rather than the decreasing flowrate release expected to occur. The plumes are shown in Figures 2.2-11 through 2.2-18. The figures are overlaid on a plant and terrain depiction for simplicity. This orientation represents a break at the point along the pipeline that is nearest to the plant and would be more conservative in breaks farther away. The declination of the cloud due to the bluff is not depicted in the plume plot. It is necessary to subtract the declination from the elevation of the cloud where the cloud concentration is 4.4%.

Considerable margin exists for all cases with steady-state flow due to both buoyancy and the lack of sufficient travel of the 4.4% concentration to reach the intake points. For the high flow cases, considerable margin exists due to the height of the 4.4% concentration at the intakes. The closest case is the high flowrate with a 10 m/s wind that failed to intersect the intake. The minimum distance is approximately 45 feet.

The above analysis results in a negligibly small probability of intersection of the 4.4% concentration with the plant intake. The equation $F = F_r * P_d * P_s$ must be integrated to include all cases that lead to a calculated intersection of the unacceptable concentration and the air intake. Since no case results in such intersection, the summation of all unacceptable cases is not performed. Instead, a conservative margin demonstration is included. This supplemental analysis is based upon the dual assumptions that wind speeds greater than 10 m/s do not rapidly mix the cloud to an acceptably low concentration and that the buoyancy effects do not exist.

The margin demonstration analysis arbitrarily assumed that a wind speed greater than 10 m/s would create a contiguous plume with travel of 1000 feet and diameter of 100 feet. It was further assumed that the cloud would not be elevated above the plant - that is, every cloud was depicted as 100 feet wide with a 1.0 probability of being at the height of the intake.

Using the distance of 1000 feet plume travel, the critical pipe segment capable of rupture and cloud formation with sufficiently close proximity to the plant to reach the intake was determined to be 1400 feet. This critical pipe was broken into 200-foot segments. A break was assumed to occur at the midpoint of the segment; the probability of wind direction toward the plant was taken from Table 2.3.6.2-1 in Appendix 2C of the Environmental Report, Operating License Stage, San Onofre Nuclear Generating Station, Units 2 and 3. The probability of intersection was taken as the width of the cloud divided by the width of the section; and the probability of direction and speed was determined for each segment. The results are as follows:

Pipe Segment (200 ft/Segment)	Wind Direction	P (Wind) 10 m/s	P (Intersection)	P(d) * P(int)
1	N	0	.36	0
2	N	0	.36	0
3	NNE	.0001	.36	3.6×10^{-5}
4	NE	.0002	.36	7.2×10^{-5}
5	NE	.0002	.36	7.2×10^{-5}
6	ENE	0	.36	0
7	ENE	0	.36	0

where:

P (wind) = P(d) = probability of wind > 10 m/s = 1.8×10^{-4} in a given direction

P (intersection) = P(int) = $\frac{\text{width of plume}}{\text{width of sector}}$ at plant (over 600 ft of pipe)

F (pipe rupture) = 3.3×10^{-4} /year-mile

F (interaction) $= \frac{3.3 \times 10^{-4}}{\text{year mile}} * 1.8 \times 10^{-4} * \frac{600 \text{ ft}}{5280 \text{ ft}} = 6.75 \times 10^{-9}/\text{year}$

This analysis is based on a single intake. However, taking into account the existence of several air intakes at the plant would yield a probability of interaction significantly less than 10^{-7}/year. Therefore, the probability is low enough that the potential impact on the plant is insignificant.

2.2.3.1.4 Offsite Fires

The effects of a serious fire were estimated using fire data provided by the U.S. Forest Service[8] for coastal areas such as Camp Pendleton. It is estimated the worst case Santa Ana fire will consume 3000 to 4000 acre/hr with the fire front moving up to 200 ft/min and a 30 mi/hr offshore wind. This fire is considered more limiting than from other postulated offsite sources.

To predict the consequences of a fire, a line source model[74] provides a reasonable estimate of ground-level pollutant concentration downwind of the fire line. The fire is estimated to provide 10 ton/acre of fuel and emission rates of 200 lb. carbon monoxide/ton, 40 lb hydrocarbon/ton, and 50 lb particulant[75]/ton.

The maximum range of concentrations resulting from these conditions are found to be well below acceptable toxicity limits.[76] Therefore, offsite fires are not considered to present a credible hazard to the plant.

2.2.3.1.5 Accidents at Nearby Industrial and Military Facilities

As described in Subsection 2.2.2, there are no significant manufacturing plants, chemical plants, refineries, wells, oil or gas storage facilities, or mining operations within a 5-mile radius of the San Onofre site. Hazards associated with the Camp Pendleton Marine Corps base are discussed in Subsection 2.2.2.

2.2.3.1.6 Accidents at Sea

The closest shipping lane to the site is located more than 5 miles from shore. Therefore, postulated shipping accidents are not evaluated as possible design basis events.[77]

2.2.4 REFERENCES

1. Letter from G. A. Merrill, Colonel, U.S. Marine Corps, Assistant Chief of Staff, Facilities, U.S. Marine Corps Base, Camp Pendleton to Mr. David R. Poole, Southern California Edison Company, February 3, 1976.

2. Mr. Paul Campo, Head of Base Natural Resources Office, U.S. Marine Corp Base, Camp Pendleton, Notes of Meeting at Camp Pendleton with Mr. A. A. Robertson, Southern California Edison, August 28, 1975.

3. Southern California Edison Company, "Section 2.2, Human Activities in the Environs," Construction Permit Environmental Impact Report for San Onofre Nuclear Generating Station Units 2 and 3.

4. Southern California Edison Company, Preliminary Safety Analysis Report for San Onofre Nuclear Generating Station Units 2 and 3.

5. Letter from Col. J. R. Aichele, Assistant Chief of Staff, Facilities, U.S. Marine Corps., Camp Pendleton, California, to Mr. D. R. Poole, Southern California Edison Company, December 7, 1978.

6. Letter from G. A. Merrill, Colonel, U.S. Marine Corps, Assistant Chief of Staff, Facilities, Camp Pendleton, to Mr. David R. Poole, February 20, 1976.

7. Letter from G. A. Merrill, Colonel, U.S. Marine Corps, Assistant Chief of Staff, Facilities, Camp Pendleton, to Mr. L. D. Hamlin, Southern California Edison, April 19, 1976.

8. Clive Countryman, Project Leader for Fire Behavior Project, Riverside, California, Forest Fire Lab, Pacific Southwest Forest and Range Experiment Station, U.S. Forest Service, telephone communication of March 26, 1976 with Mr. David R. Poole, Southern California Edison.

9. Frank P. Lees, "Loss Prevention in the Process Industries," Butterworth and Company, First Edition, Reprinted 1986.

10. 13. DELETED

14. Letter from Mr. W. Y. Eskew, General Manager, San Diego Pipeline Company, Los Angeles, to Mr. David R. Poole, Southern California Edison Company, January 28, 1976.

15. Letter from Mr. W. T. Eskew, General Manager, San Diego Pipeline Company, Los Angeles, to Mr. Ralph G. Crouch, Southern California Edison, May 5, 1976.

16. Letter from Mr. H. D. Striff, Staff Supervisor, Mapping and Drafting, Southern California Gas Company, Los Angeles, to Mr. David R. Poole, Southern California Edison Company, January 22, 1976.

17. Letter from Mr. A. S. Olson, General Superintendent, South Basin Division, Southern California Gas Company, Los Angeles, to Mr. Ralph G. Crouch, Southern California Edison, May 12, 1976.

18. Letter from Mr. C. N. Stuart, Manager, Gas Engineering Department, San Diego Gas and Electric Company, San Diego, to Mr. David R. Poole, Southern California Edison Company, January 22, 1976.

19. Letter from Mr. C. N. Stuart, Manager, Gas Engineering Department, San Diego Gas and Electric Company, San Diego, to Mr. D. R. Poole, Southern California Edison Company, March 31, 1976.

20. Terminal Area Forecast 1976-1987, U.S. Department of Transportation, Federal Aviation Administration, January 1976.

21. Letter from Michael B. Maccarone, Airport Engineering, Orange County Airport, to Ralph G. Crouch, Southern California Edison, April 12, 1976.

22. Letter from Mr. Robert C. Huber, Assistant Public Affairs Office, Federal Aviation Administration, Lawndale, California, to Mr. David R. Poole, Southern California Edison Company, January 22, 1976.

23. 29. DELETED

30. Code of Federal Regulations, Title 49-Transportation, Parts 100-199.

31. 57. DELETED

58. Analysis of Explosive Vapor Cloud and Missile Hazards for Rail and Highway Transportation Routes Near the San Onofre Nuclear Generating Station Units 2 and 3; NUS Report 3367, July 1979.

59. 68. DELETED

69. Sax, Irving N., "Dangerous Properties of Industrial Chemicals," Chapter 1.

70. Sokolik, A. S., "Self-Ignition Flame and Detonation in Gases." Translated from Russian, Published by the Israel Program for Scientific Translations for the NSF and NASA, Moskva: 1960, Jerusalem 1963, pp 240-241.

71. Windholds, Martha, et al., ed. "Merk Index: An Encyclopedia of Chemicals and Drugs," Merk and Co., 1976.

72. British Gas Data Book. Volume, British Gas Corporation, 1974.

73. Fox, R. W., and Kline, S. J., Flow, Regime Data and Design Methods for Curved Subsonic Diffusers," TASME, Journal Basic Engrg., Volume 84, Series D, September 1962.

74. Turner, B. D., "Workbook of Atmospheric Dispersion Estimates," Environmental Protection Agency, Office of Air Programs, Publication No. AP-26, 1970 (revised).

75. Personal communication with Dr. Ellis Darley, U. C. Riverside, Riverside, California.

76. 78. DELETED

79. State of California Department of Transportation, District II, J. M. Markey letter to S. Fong, ERIN Engineering and Research, Inc., I-5 Truck Accidents near San Onofre, dated January 18, 1991.

80. 81. DELETED

82. Southern California Edison Company, "San Onofre Nuclear Generating Station 1984 Offsite Hazards Update," Revision 3, Erin Engineering and Research, Inc., November 1985.

83. 85. DELETED

86. "Analysis of Explosive Vapor Cloud Hazards for Rail and Highway Transportation Routes Near the San Onofre Nuclear Generating Station Units 2 and 3 Using a Best Estimate Analysis," NUS Report 3367, Supplement 1, April 17, 1981.

87. 93. DELETED

94. PRA Evaluation of LPG Railcar Transportation, NSG/PRA Report PRA-23-92-007, November 16, 1992.

95. DELETED

96. Letter from J. L. Rainsberry, SCE, to L. J. Callan, NRC, dated February 4, 1997, Hazardous Cargo Monitoring Report, San Onofre Nuclear Generating Station, Units 2 and 3.

97. DELETED

98. Letter from A.E. Scherer, SCE, to E.W. Merschoff, NRC, dated February 18, 2003, Hazardous Cargo Monitoring Report, San Onofre Nuclear Generating Station, Units 2 and 3.

99. DELETED

100. Letter from A.E. Scherer, SCE, to E.E. Collins, NRC, dated February 17, 2009, Hazardous Cargo Monitoring Report, San Onofre Nuclear Generating Station, Units 2 and 3.

101. DELETED

102. “San Onofre Nuclear Generating Station Units 2 and 3 2015 Offsite Hazards Update,” ERIN Engineering and Research, Inc., January 2016

2.2.5 BIBLIOGRAPHY

1. Letter from Captain R. Brooke, U.S. Navy, San Diego, to Mr. L. D. Hamlin, Southern California Edison, April 16, 1976.

2. Commander R. E. Hatcher, Jr., U.S. Navy, San Diego, Telephone notes of May 19 and 21, 1976 Communication with Mr. David R. Poole, Southern California Edison Company.

3. "Accident Statistics - Interstate 5," California Department of Transportation.

4. Personal communication with Mr. A. Golden, California Department of Transportation, Traffic Division.

5. "1969 Accidents of Large Motor Carriers of Property," Bureau of Motor Carrier Safety, Federal Highway Administration, U.S. Department of Transportation, December 1970.

6. "1970 Accidents of Large Motor Carriers of Property." U.S. Department of Transportation, Federal Highway Administration, Bureau of Motor Carrier Safety, March 1972.

7. Booz-Allen and Hamilton, Inc., An Appraisal of the Problem of the Handling, Transportation, and Disposal of Toxic and Other Hazardous Materials, prepared for Department of Transportation, Environmental Quality Council, Washington, D.C., Report No. PB-236599, January 1970.

8. Simmons, J. A. Edmann, R. C., and Naft, B. N., "The Risk of Catastrophic Spills of Toxic Chemicals," report prepared for the U.S. AEC, Division of Research, by the School of Engineering and Applied Science, UCLA. Report-No-UCLA-ENC.74-25, May 1974.

9. Personal communication with Mr. Roth of American Trucking Association October 8, 1976.

10. "Analysis of Explosive Vapor Cloud and Missile Hazards for Rail and Highway Transportation Routes Near the San Onofre Nuclear Generating Station Units 2 and 3 - NUS Report 3367, July 1979.

11. "Analysis of Explosive Vapor Cloud Hazards for Rail and Highway Transportation Routes Near the San Onofre Nuclear Generating Station Units 2 and 3 using a Best Estimate Analysis," NUS Report 3367, Supplement 1, April 17, 1981.

12. "Southern California Edison Company San Onofre Nuclear Generating Station Offsite Hazards Update 1984," Revision 1, Nucon Inc., September 1985.

13. "Southern California Edison Company San Onofre Nuclear Generating Station Offsite Hazards Update 1987," ERIN Engineering and Research, Inc., January 1988.

14. "Southern California Edison Company San Onofre Nuclear Generating Station 1990 Offsite Hazards Update," ERIN Engineering and Research, Inc., February 1991.

2.3 METEOROLOGY

This section presents the meteorological description of the site and its environs. Those meteorological factors which bear upon plant design, operation, and safety are presented and discussed.

The data and information contained in Sections 2.3.1, 2.3.2, 2.3.5 and referenced Appendixes were developed and verified during San Onofre's original design. The information was used to determine the plant's design basis. A general review has determined that this information, its basis, and its impact to the facility's design have not changed since the plant was licensed. As such, specific numerical values are not subject to review. Section 2.3.3 updates will occur with the normal change process to include more recent events where those events result in specific changes to the plant's physical description or surrounding areas, to its design basis, where necessary for plant programs such as emergency planning, or for other topics as committed to by SCE.

2.3.1 REGIONAL CLIMATOLOGY

2.3.1.1 General Climate

Due to its coastal location, the climate of the site can be characterized as marine and subject to daily land and sea breezes on which an annual monsoon oscillation is superimposed. During most of the year, daytime heating of the land surface makes it warm relative to the Pacific Ocean. This thermal difference produces an onshore wind (sea breeze) that normally begins shortly after sunrise and lasts until after sunset. At night, the land cools, reversing the thermal gradient, and an offshore wind (land breeze) develops. This diurnal reversal is most apparent during the spring and fall months.

During the summer, the Pacific anticyclone moves northward to a position off the coast from the site. This high pressure cell combines with the thermal low pressure trough over inland southern California to produce a strong onshore pressure gradient, stratus deck, fog, and cool summer days.

In winter months, the anticyclone drifts farther southward, allowing the jet stream and its associated migratory storm tract to reach southward to the site. Between storm passages, the land-sea breeze pattern returns. During this period, the Great Basin high pressure cell frequently builds sufficiently to produce a relatively strong offshore pressure gradient and resulting warm dry Santa Ana winds.

Winds at the site exhibit an onshore component somewhat more than half the time. The most frequent wind is the westerly to west-northwesterly sea breeze, which averages about 5 to 7 mi/h. Winds associated with frontal passages are generally out of the southwest and relatively stronger, frequently over 10 mi/h. The strongest winds are associated with the Santa Ana condition and blow out of the northeast, occasionally exceeding 30 to 50 mi/h.

The presence of the Pacific Ocean has a moderating influence over the temperatures in the site region. Climatological data for Los Angeles and San Diego indicate that daily temperature ranges are usually less than 15°F in the spring and summer and increase to about 20°F during the fall and winter. Temperatures below 40°F are rare. Prior to 1975, temperatures below freezing were recorded only once at both the Los Angeles and San Diego National Weather Service (NWS) stations. Correspondingly, temperatures above 85°F have occurred occasionally in every month of the year when air from the interior reached the coast. At San Diego, there have been only 15 days on which 100°F or higher was reached. The maximum recorded temperature was 111°F at San Diego. The record minimum was 31°F.

The average relative humidity ranges from about 60% during the day to about 75% at night. Occasionally, however, during Santa Ana conditions, the influx of the dry desert air can drop humidity in the area to less than 10%.

The normal annual precipitation for San Diego and Los Angeles is 9.45 inches and 11.59 inches, respectively. Laguna Beach, 17 miles north of the site, with a surrounding topography similar to San Onofre, has a normal annual precipitation of 11.75 inches. About 85% of the precipitation falls in the winter months of November through March during the passage of the migratory storm systems, with measurable rain falling on an average of 1 day in 4. Occasionally a wet month will occur, such as during one February when 11 inches fell in Los Angeles. A maximum of 6.19 inches of rain in 24 hours was recorded in Los Angeles. Measurable snow has never been recorded at a coastal location in southern California.

2.3.1.2 Regional Meteorological Conditions for Design and Operating Bases

2.3.1.2.1 Hurricanes

Tropical storms with hurricane force winds (72 mi/h or greater) have not been recorded to approach the southwestern United States. Although hurricanes do exist several hundred miles to the south off of the western coast of Mexico, their impact on the San Onofre area usually only takes the form of a summer thunderstorm.

2.3.1.2.2 Tornadoes

Between 1950 and 1975, a total of 177 tornadic storms were reported in California. Of these, 123 caused little or no damage and were virtually all waterspout or funnel cloud observations. Prior to 1950, the California State Climatologist compiled a list of known tornado occurrences in California. This list includes 17 events, covering the period 1892 through 1949. Listings of major California tornadoes and waterspouts since 1950 are provided in Appendix 2.3A.

Based upon the Construction Permit review by the NRC, it was agreed that the design basis tornado for San Onofre Units 2 and 3 will be as follows:

A. Maximum total wind speed of 260 mi/h

B. Peripheral tangential velocity of 220 mi/h

C. Forward translational rate of 40 mi/h

D. Resultant differential bursting pressure between the inside and outside of structures of 1.5 lb/in.^{2} positive pressure occurring in 4.5 seconds followed by a calm for 3 seconds and a repressurization.

A discussion of the conservatism of the above design basis tornado is provided in Appendix 2.3A.

2.3.1.2.3 Thunderstorms

The normal annual occurrence of thunderstorms in Los Angeles and San Diego is 3 days per year. The mean number of days per month is less than 1/2 day in all months.

2.3.1.2.4 Lightning

Estimates have been made of the frequency of occurrence of lightning ground strikes in the vicinity of the San Onofre Nuclear Generating Station utilizing a method developed by Pierce, et al (1) method utilizes an equation to estimate the lightning flashes going to the ground from the frequency of thunderstorm days. The calculated monthly flash density has been found to be less than 0.005 flashes per square kilometer.

2.3.1.2.5 Hail

Storm Data (2) indicates a total of 22 sightings of hail have been reported in California since 1959. About half of these occurred in the San Joaquin Valley, with the remainder scattered over the rest of California. It must be recognized, however, that hail, in itself, rarely causes sufficient damage to be reported. Therefore, the actual frequency of occurrence is probably greater. Few data are available on hailstone size. Although diameters of 1-1/2-inch have twice been reported in northern California, the largest diameter reported in the southern portion of the state was 1/2-inch.

2.3.1.2.6 Air Pollution Potential

The meteorological parameters that are considered to be basic in the evaluation of the air pollution potential of an area are the depth through which pollutants are vigorously mixed, and the average wind speed through this mixing layer. These parameters usually undergo seasonal variations and are the highest in midafternoon and lowest in early morning. They also tend to be lowest in valleys, especially where the ends are restricted, and highest on hilltops or other exposed locations.

Vigorous vertical mixing is most commonly accomplished by mechanical turbulence, or by convective action produced by transfer of heat from the earth's surface to the bottom layer of the atmosphere and by the subsequent overturning of the atmosphere as stable stratification is restored. The height through which this vertical mixing penetrates is called the depth of the mixing layer. Because the temperature change through this layer is near to, or greater than, the dry adiabatic rate, and because the layer is capped by a stable layer, this depth is usually treated as the vertical distance to the base of the stable layer.

The mixing layer in the region of the SONGS is due to the presence, some distance above the ground, of an inversion or layer of air through which the temperature increases upward instead of decreasing as is normal. This inversion is associated with the semi-permanent Pacific anticyclone. On the average, the inversion has its base at a height of about 1500 feet along the coast. It acts as a lid on moisture transport and convective activity.

There are two essentially different kinds of inversions present at locations along the California coast, such as at the plant site. The one type is the surface layer inversion produced by cooling of the air in contact with the ground, which has lost heat by radiation during the night. This type is referred to as a radiation inversion or ground inversion and is a common phenomenon over all land masses. In some areas of the United States it occurs almost every clear night. Along the California coast it occurs principally at night only in the colder half of the year.

The second type is the subsidence inversion due to the sinking motion of the air spiraling outward from the Pacific anticyclone. It is present over the eastern subtropical portions of the oceans and overlaps onto the western coasts of the continents. It occurs principally and most persistently in the warm months of the year (April through September), but occasionally takes place during the rest of the year.

In Table 2.3-1, the frequency of inversions at various heights at San Diego is summarized. These data are representative of the values at the plant site. The morning (0700 PST) observations show surface inversions more than one-half of the days during December (57%), January (54%), and February (54%). The evening soundings show fewer inversions, demonstrating that they are wiped out on many days, and they require several hours after the ground starts cooling to form again. The larger frequency of inversions between 500 and 1500 feet at 1900 hours rather than at 0700 hours suggests that in some cases the daytime heating lifts the inversion off the ground, but does not eliminate it. With respect to the rest of the year, surface inversions occur fairly often in March (25%), but in the succeeding months until October they are essentially absent, and the subtropical subsidence inversion is present most of the time. Surface inversions begin occurring again in September (14%) and October (24%) and are fairly frequent in November (49%).

In Table 2.3-1 it is seen that the base of the inversion at San Diego ranges in height mostly between 500 and 2500 feet, with maximum frequency in the morning in June and July between 1500 and 2000 feet, and in August between 1000 and 1500 feet. The most frequent height in the evening is consistently in the next lower interval.

Table 2.3-1
FREQUENCY OF INVERSIONS AT VARIOUS HEIGHTS AT
NAVAL AIR STATION, NORTH ISLAND, SAN DIEGO[3]

0700 PST Observations												
Height of Inversion Base (ft)	Frequency (%)											
	Jan	Feb	Mar	Apr	May	Jun	Jul	Aug	Sep	Oct	Nov	Dec
Surface(24)	54	54	25	2	3	1	3	3	14	24	49	57
25 – 500	2	2	6	3	2	2	5	3	11	6	8	0
501 – 1000	3	4	6	6	5	9	10	16	12	9	3	4
1001 - 1500	3	2	5	7	15	13	28	29	14	15	7	4
1501 - 2000	1	4	4	9	15	16	29	21	17	14	3	4
2001 - 2500	2	3	7	14	14	9	9	11	9	10	2	1
2501 - 3000	3	0	5	9	10	12	7	3	6	4	3	1
3001 - 3500	0	2	2	9	10	10	3	1	5	5	3	3
3501 - 5000	3	4	7	13	11	11	1	1	5	5	4	6
None	25	22	26	25	9	5	1	3	1	5	15	14
Missing	5	4	7	2	5	12	5	9	5	3	9	5
1900 PST Observations												
Height of Inversion Base (ft)	Frequency (%)											
	Jan	Feb	Mar	Apr	May	Jun	Jul	Aug	Sep	Oct	Nov	Dec
Surface(24)	22	18	14	2	2	1	5	2	17	16	24	28
25 – 500	3	1	4	2	3	1	9	9	11	8	8	3
501 – 1000	10	11	10	9	15	16	25	37	19	19	9	9
1001 - 1500	8	8	7	15	19	19	35	30	21	23	9	6
1501 - 2000	6	2	6	12	17	17	16	13	15	10	9	2
2001 - 2500	2	4	5	7	13	12	5	3	7	7	3	3
2501 - 3000	3	2	5	7	6	7	1	1	3	3	3	5
3001 - 3500	1	3	2	5	4	4	0	2	3	3	2	4
3501 - 5000	4	2	6	9	8	7	1	0	1	2	3	6
None	37	43	32	26	11	1	0	1	1	6	23	25
Missing	4	6	10	5	3	14	4	2	1	3	8	9

Table 2.3-2
AVERAGE HEIGHT AND TEMPERATURE OF INVERSION BASE AND TOP AND RANGE OF TEMPERATURE CHANGE IN INVERSION[4]

	Inversion Base Height (Meters)	Temp. at Inversion Base (°C)	Inversion Top Height (Meters)	Temp. at Inversion Top (°C)	Temp. Rise per 100 Meters in Inversion Layer (°C)
Long Beach					
June	640	12.8	1,237	19.0	1.04
July	370	16.3	1,015	23.3	1.08
August	398	15.9	1,062	23.2	1.10
September	435	15.5	996	22.9	1.32
Season	458	15.1	1,078	22.1	1.13
San Diego					
June	621	12.0	1,195	19.2	1.25
July	398	15.4	1,015	25.0	1.55
August	405	15.3	983	23.2	1.36
September	457	14.6	949	22.2	1.55
Season	471	14.3	1,038	22.4	1.38

Table 2.3-2 shows the characteristics of the subtropical inversion at San Diego and Long Beach for the summer months. There is very little difference between the two stations with respect to inversion characteristics. This shows the validity of regarding the San Diego data reasonably representative of the San Onofre plant site.

The lapse rate below the inversion is near the dry adiabatic, so that mixing goes on easily up to the inversion base. The inversion, in turn, is so sharp and strong that turbulent diffusion upward into it is practically absent.

The subsidence inversion is present almost every day in the warm months. Radiation surface inversions are present on about half the days in the cool months. The remainder of the days in the cool months are divided among stormy periods, when no low inversion is present, and warm periods that often have a subsidence inversion. Among the warm periods are the Santa Ana situations, when anticyclones build up over the Great Basin in such a fashion that air spreads outward from the continent and subsides along the coast. In these periods, subsidence inversions develop similar to those associated with the oceanic anticyclone, but in these cases the inversion frequently extends right down to the ground. These are cases of very strong and persistent surface inversions that prevent almost all vertical diffusion of pollutants. Fortunately, so far as the plant site is concerned, in these cases the wind is directed seaward where extensive horizontal dilution occurs.

2.3.1.2.7 Snow Accumulation

Significant snow accumulation has never been recorded at a coastal location in southern California.

2.3.1.2.8 Extreme Winds

The fastest mile of wind recorded at San Diego during the 31 years of record was 51 mi/h. The highest peak gust recorded at Los Angeles during 25 years of record was 62 mi/h. The probable maximum wind for surge and seiche flooding conditions is described in Section 2.4 as 75 mi/h.

The 100-year return period isotach map of the continental United States drawn by H. L. Crutcher (unpublished) 1975, from annual fastest mile wind speed data, shows a wind speed of less than 26.8 m/s (60 mi/h) at San Onofre. Additional 100-year return period estimates were made by plotting on Fisher-Tippet Type II Distribution Maximum Value Probability paper the fastest annual hourly wind speeds from 20 years of Los Angeles International Airport and North Island Naval Air Station, San Diego data. The 100-year return period wind for North Island Naval Air Station based on 1953-1972 data is approximately 21 m/s (47 mi/h). The fastest mile of wind from 31 years of record was 22.8 m/s (51 mi/h) from the SE. The 100-year return period fastest mile of wind for Los Angeles International Airport based on 1947-1966 data is approximately 25.5 m/s (57 mi/h). The peak gust from 25 years of record was 27.7 m/s (62 mi/h) from the W.

Los Angeles International Airport and the Naval Air Station, North Island are both located on relatively flat terrain and are well exposed to wind. San Onofre receives protection from the nearby hills and bluff and is, therefore, expected to have lower extreme winds. A 100-year return period maximum hourly wind speed of 28 m/s (63 mi/h) for San Onofre should be a conservative estimate.

The vertical distribution of velocity and appropriate gust factor is provided in Paragraph 3.3.1.1.

2.3.1.2.9 Dust and/or Sand Storms

Although soil types in the vicinity of San Onofre are conducive to dust production, the coverage of the soils by natural vegetation greatly reduces the potential of blowing dust or sand. The occurrence of blowing or drifting sand from the beach is also minimized because the sand becomes wet during strong onshore wind conditions.

The greatest potential for the occurrence of blowing dust exists during strong wind conditions from the northwest because of the existence of eolian sand in the San Onofre Creek area. However, the presence of natural vegetation in this area greatly reduces the potential for the production of blowing dust.

The dust storm potential at San Onofre is estimated utilizing data from the San Mateo Point, which is similar to San Onofre. Utilizing the climatology from San Mateo Point and wind rose data for San Onofre (see Subsection 2.3.3) it is estimated that the probable maximum frequency of blowing dust at San Onofre is about once every 2 years with a duration of 1 hour. The visibility restriction should not be less than 4 miles.

2.3.1.2.10 Freezing Rain

Instances of freezing rain have not been recorded at a coastal location in southern California.

2.3.2 LOCAL METEOROLOGY

2.3.2.1 Normal and Extreme Values of Meteorological Parameters

Monthly and annual summaries from long-term records of representative nearby stations are provided. Shorter term onsite summaries are also provided and these tables are described in the following subsections.

When evaluating the onsite data and comparing them with data from nearby stations, the complicating factors of the terrain can be very significant considerations. Strictly speaking, the meteorological measurements are only representative of the points at which they are taken. Changes in terrain cause changes in meteorological parameters. At San Onofre, the complicating terrain features include the coastal bluff, the nearby hills and valleys, and the Pacific Ocean.

The location of the meteorological tower was chosen so that it would provide the most representative measurements in the layer of air that governs the initial dispersion of the plant effluent. The representativeness of the data for other situations depends on how much the meteorological parameters are altered with distance and time.

Southern California coastal stations such as Los Angeles International Airport and San Diego airports are reasonably representative for providing much long- and short-term data applicable to the San Onofre site. Considerations of differences are sometimes important and are discussed when encountered.

2.3.2.1.1 Local Wind at the Plant Site

The large-scale characteristics of the air flow at the plant site show seasonal variations upon which are superimposed daily onshore and offshore wind effects. Warm season winds blow from sea to land with a reversal during the cold season. Such winds are a natural consequence of the large-scale weather factors determining climate. During the summer, the air flow shows considerable day-to-day regularity compared to the winter when frontal systems move into the region.

The daytime onshore wind and nighttime offshore wind result from greater heating and cooling of the air over land as contrasted with only very slight diurnal changes in air temperature over the sea. In summer, the large-scale meteorological features favor the daytime onshore breeze and oppose the nocturnal offshore breeze, while in winter the large-scale features have the opposite effect.

The Santa Ana wind, described in Section 2.3, is a feature that causes the autumn and winter flow patterns to deviate from the usual onshore and offshore circulations.

Small-scale characteristics of wind flow include drainage winds and winds resulting from the bluff effect. Drainage wind flow behaves in a very predictable, well-documented manner. This flow consists of a relatively dense fluid seeking equilibrium at a lower level in the same manner as water flowing down a canyon and spreading out over a flood plain. Because it is formed by cooling of the lowest layers by contact with the cold ground, the densest air tends to be at the surface. For this reason, the highest speed tends to be immediately above the surface friction layer and it tends to decrease with height. An examination of the data indicates that drainage breezes occur frequently in the late night and early morning hours.

The onshore wind circulation resulting from the bluff effect is subject to considerable variation because of the nature of the eddy structure produced by the flow of air over a bluff. A speedup of the air in the lower levels as it comes over the bluff is required to compensate for the restricted cross-section through which it must flow. Wind direction may be also changed. The tower is located well within the region of these effects and represents the conditions which would be encountered by a cloud release being lifted over the bluff.

The onsite wind data from January 25, 1973, through January 24, 1976, are summarized in joint frequency wind speed-wind direction tables for the 10m (33 ft) and 36.6/40m (120/131 ft) levels. Summaries were produced on an annual and monthly basis and are presented in Appendix 2.3H, Tables 2.3H-1 through 2.3H-26. Distribution by direction is tabulated in the 16 compass point sectors and 14 wind speed categories ranging from calm (0.25 m/s or less) to more than 10 m/s. Totals for all directions by speed class and for all speeds by direction are given, along with the average wind speed for each direction and for all directions combined. Shown on each page are two tables expressing the same data. The upper table presents the numbers of cases in each category and the lower table gives the percentages of those numbers from the total number of cases used in that table.

The overall view provided by the annual wind frequency summaries for both levels shows a roughly trimodal wind speed and direction distribution. Peak average wind speeds at the lower level occur in the NE, SSE-S, and NW directions and at the upper level in the NNE, SSE, and WNW directions. Wind direction frequencies of occurrence have similar direction peaks. Onshore wind frequencies of occurrence are spread more uniformly among the sectors and the two levels are in closer agreement than the offshore wind frequencies of occurrence. Calm wind frequency was less than 1% and the frequency of wind speed greater than 10 m/s was less than 1%. The overall average wind speed at both levels is about 3 m/s.

Wind direction persistence summaries list the number of occurrences within the categories of 16 compass-point directions and the number of continuous hours a direction persisted. Also tabulated are the sums of the number of occurrences listed in each direction and the total number of occurrences regardless of direction for each category of hours of persistence. Percentile levels and the maximum number of hours are included by direction category and for all directions. The tables were computed from the January 25, 1973, to January 25, 1976, data base for both levels for annual and monthly average periods. The summaries are presented in Appendix 2.3I, Tables 2.3I-1 through 2.3I-26.

An overall view is provided by the annual wind direction persistence tables for both levels. The 50 percentile level for both levels was calculated to be 0.7 hours for all directions combined. The lower level had more incidents of longer persistence overall than the upper level, although the maximum case occurred at the upper level when for 23 continuous hours the wind direction remained in the WNW sector. The roughly trimodal distribution observed in the joint frequency wind speed-direction summaries is evident in the wind direction persistence. The numbers of occurrence of a category of persistence generally tend to rise to a peak in the NNE or NE, drop off to a low level around E, then increase to a smaller peak around the SE and SSE, drop off a little to a low around the SW, increase to a peak around the W or WNW, and drop to a low around the NNW.

The diurnal variation of the wind at the plant site is dominated by the land - sea breeze oscillation. This oscillation, in which a sea breeze occurs in the daytime and a land breeze at night, results from the differential absorption and radiative characteristics of the land and sea. The diurnal variation of the wind is presented in Appendix 2.3J, Tables 2.3J-1 through 2.3J-26 for the 10-meter level and in Appendix 2.3K, Tables 2.3K-1 through 2.3K-26 for the 36.6-/40-meter levels. Data from these tables are summarized in wind roses for the annual and midseason months in Figures 2.3-1 through 2.3-5.

On an annual basis, the sea breeze begins about 0900 PST and persists through the afternoon and early evening. By 1900 PST, the land breeze begins and is well established by 2200 PST. The average speed of the sea breeze ranges from 3.1 to 4.5 m/s (7 to 10 mi/h). The land breeze is weaker and blows with average speeds of 2.2 to 3.6 m/s (5 to 8 mi/h).

Offshore winds do not occur very often in the afternoon, but when they do occur their average speeds range from 4.3 to 7.6 m/s (14 to 17 mi/h). These winds are associated with warm Santa Ana conditions which interrupt the usual land-sea breeze oscillation. Onshore winds which may occasionally occur in the late evening or early morning hours are usually very light, with average speeds of 0.9 to 1.3 m/s (2 to 3 mi/h).

During the winter the land-sea breeze oscillation is frequently interrupted by storms moving through the southern California region. Onshore winds of 8.9 to 11.2 m/s (20 to 25 mi/h) may occur during the morning hours under these situations. Offshore winds may be enhanced by offshore pressure gradient and winds of 4.5 to 6.7 m/s (10 to 15 mi/h) may occur with these conditions. These offshore winds generally blow from the northeast and north-northeast sectors as a result of the channeling effect of the San Onofre Canyon.

The summer months are dominated by the land-sea breeze oscillation. During the morning, the wind veers from south to southwest and by mid-afternoon the wind blows predominately from the west. The afternoon speeds average about 3.6 to 4.5 m/s (8 to 10 mi/h). The land breeze during the summer is weak and of relatively short duration, generally ceasing by 0800 PST. Average speeds are 1.3 to 2.7 m/s (3 to 6 mi/h).

The spring and autumn seasons are transitional periods when the land-sea breeze oscillation is occasionally interrupted by storms moving into southern California. Santa Ana conditions which occur during the autumn season may enhance the offshore winds with resulting average speeds of 3.6 to 4.9 m/s (8 to 11 mi/h).

2.3.2.1.2 Temperature

The small range in temperature from day to night and from winter to summer produces a very equable regime along the southern California coast. For example, long-term climatological data at San Diego and Los Angeles (see Table 2.3-3) show the average monthly temperature in January is 12.8°C (55°F), while the August value is 21.1-22.2°C (70-72°F). High temperatures along the coast, although infrequent, are associated with Santa Ana winds which occur in the autumn. Both Los Angeles and San Diego recorded their highest maximum temperatures in September, 1963: Los Angeles 43°C (110°F) and San Diego 44°C (111°F). Nighttime temperatures are generally cool, but minimum temperatures below 4.4°C (40°F) are rare and periods of over 10 years may pass with no temperatures below freezing along the coast.

The meteorological summaries for 1973 and 1974 for Los Angeles (Table 2.3-4) and for San Diego (Table 2.3-5) show that these years were rather typical of the normal year at these stations. Therefore, the San Onofre data taken during the 2-year period from 1974 through 1975 may be considered as representative of normal conditions at the site.

The temperature summary (Table 2.3-6) of onsite data presents monthly and annual means, mean maximums, mean minimums, absolute minimums, absolute maximums, and averages by hours of the day. The computations were made from data recorded at the 6.1 meter (20 foot) level during the period from January 25, 1974, through October 25, 1975, and raised to 10 meters through January 24, 1976.

Table 2.3-3
LONG TERM CLIMATOLOGICAL DATA FOR LOS ANGELES AND SAN DIEGO, CALIFORNIA
NORMALS, MEANS, AND EXTREMES (Sheet 1 of 4)

Los Angeles, California, International Airport[a][b]

Mth	Temperatures (F)							Normal Degree Days (Base 65 F)		Precipitation (in.)										
	Normal			Extremes						Water Equivalent							Snow, Ice Pellets			
	Daily Max	Daily Min	Mthly	Record Highest	Yr	Record Lowest	Yr	Heat-ing	Cool-ing	Normal	Max Mthly	Yr	Min Mthly	Yr	Max in 24 Hrs	Yr	Max Mthly	Yr	Max in 24 Hrs	Yr
(c)				16		16					39		39		39		39		39	
J	63.5	45.4	54.5	86	1971	30	1963	331	5	2.52	9.60	1969	0.00	1972	6.19	1956	(e)	1974	(e)	1974
F	64.1	47.0	55.6	92	1963	37	1965	270	7	2.32	11.07	1962	T	1964	4.16	1962	(e)	1951	(e)	1951
M	64.3	48.6	56.5	88	1964	39	1971	267	0	1.71	5.98	1938	0.00	1959	3.54	1968	0.00		0.00	
A	65.9	51.7	58.8	95	1966	43	1965	195	9	1.10	4.52	1965	0.00	1962	1.88	1960	0.00		0.00	
M	68.4	55.3	61.9	96	1967	45	1964	114	17	0.08	0.56	1956	0.00	1943	0.56	1956	0.00		0.00	
J	70.3	58.6	64.5	92	1973	50	1971	71	56	0.03	0.29	1964	0.00	1971	0.29	1964	0.00		0.00	
J	74.8	62.1	68.5	92	1960	55	1964	19	127	0.01	0.15	1969	0.00	1973	0.15	1969	0.00		0.00	
A	75.8	63.2	69.5	91	1967	59	1970	15	154	0.02	0.30	1961	0.00	1971	0.21	1961	0.00		0.00	
S	75.7	61.6	68.7	110	1963	55	1971	23	134	0.07	4.39	1939	0.00	1968	4.20	1939	0.00		0.00	
O	72.9	57.5	65.2	106	1961	43	1971	77	83	0.22	2.34	1936	0.00	1969	1.77	1972	0.00		0.00	
N	69.6	51.3	60.5	101	1966	38	1964	158	23	1.76	7.92	1946	0.00	1956	5.60	1967	0.00		0.00	
D	66.5	47.3	56.9	88	1959	32	1968	267	0	2.39	6.57	1936		1963	3.01	1951	(e)	1971	(e)	1971
					SEP		JAN					FEB		JUL		JAN		JAN		JAN
YR	69.2	54.1	61.7	110	1963	30	1963	1819	615	11.59	11.07	1962	0.00	1973	6.19	1956	(e)	1974	(e)	1974

Continues on sheet 2

a. Means and extremes above are from existing and comparable exposures. Annual extremes have exceeded at other sites in the locality as follows: Lowest temperature 25 in January 1913; maximum monthly precipitation 9.26 in December 1921; maximum precipitation in 24 hours 3.62 in December 1940; fastest mile of wind 53 from Southeast in February 1938. Normals - Based on record for the 1941-1970 period; Date of extreme - The most recent in cases of multiple occurrence; Prevailing Wind Direction - Record through 1963; Wind Direction - Numerals indicate tens of degrees clockwise from true north. 00 indicates calm; Fastest Mile Wind - Speed is fastest observed 1-minute value when the direction is in tens of degrees.

b. Source, Local Climatological Data, Environmental Data Service, NOAA.

c. Length of record, years, through the current year unless otherwise noted, based on January data.

d. 70° and above at Alaskan stations.

e. Trace.

f. Less than one half.

Table 2.3-3
LONG TERM CLIMATOLOGICAL DATA FOR LOS ANGELES AND SAN DIEGO, CALIFORNIA
NORMALS, MEANS, AND EXTREMES (Sheet 2 of 4)

Los Angeles California, International Airport [a][b]

Mth	Relative Humidity (%) Hour (Local Time) 04	10	16	22	Wind Mean Speed (mi/h)	Wind Prevailing Direction	Wind Peak Gust Speed (mi/h)	Wind Peak Gust Direction	Wind Peak Gust Yr	% of Possible Sunshine	Mean Sky Cover, Tenths, Sunrise to Sunset	Mean Number of Days: Sunrise to Sunset Clear	Partly Cloudy	Cloudy	Precipitation 0.01 Inch or More	Snow, Ice Pellets 1.0 Inch or More	Thunderstorms	Heavy Fog, Visibility 1/4 Mile or Less	Temperatures (°F) Maximum 90° and above (d)	Maximum 32° and below	Minumum 32° and below	Minumum 0° and below	Average Station Pressure (mbar) Elevation (104 feet ms1)
(c)	15	15	15	15	26	28	25	25			26	39	39	39	39	39	32	42	15	15	15	15	2
J	68	54	59	69	6.7	W	48	SW	1951		5.2	12	8	11	6	0	(f)	5	0	0	(f)	0	1014.7
F	72	57	61	70	7.3	W	57	N	1953		5.0	12	6	10	6	0	(f)	4	(f)	0	0	0	1014.7
M	78	61	65	74	8.0	W	62	W	1952		5.1	11	9	11	5	0	(f)	4	0	0	0	0	1012.2
A	79	59	63	75	8.4	WSW	59	N	1957		4.8	11	9	10	3	0	(f)	3	(f)	0	0	0	1012.2
M	81	65	65	79	8.2	WSW	45	N	1953		5.2	10	10	11	1	0	(f)	2	(f)	0	0	0	1010.9
J	85	70	68	82	7.9	WSW	32	W	1954		5.2	9	11	10	1	0	(f)	2	(f)	0	0	0	1008.5
J	86	68	68	83	7.6	WSW	29	W	1954		4.0	12	13	6	1	0	(f)	2	(f)	0	0	0	1009.9
A	85	68	69	83	7.5	WSW	33	SE	1955		3.9	13	12	6	(f)	0	(f)	3	(f)	0	0	0	1009.5
S	83	65	67	80	7.1	WSW	28	SW	1972		4.1	13	11	6	1	0	(f)	4	1	0	0	0	1009.2
O	78	58	64	77	6.8	W	46	W	1974		4.5	13	10	8	2	0	(f)	5	2	0	0	0	1011.4
N	75	59	64	74	6.6	W	55	N	1953		4.6	14	8	8	4	0	(f)	6	(f)	0	0	0	1013.6
D	70	55	61	69	6.6	W	49	S	1952		4.7	13	8	10	6	0	(f)	6	0	0	(f)	0	1015.4
									MAR														
YR	78	62	65	76	7.4	W	62	W	1952		4.7	143	115	107	35	0	3	45	5	0	(f)	0	1011.9

Table 2.3-3
LONG TERM CLIMATOLOGICAL DATA FOR LOS ANGELES AND SAN DIEGO, CALIFORNIA
NORMALS, MEANS, AND EXTREMES (Sheet 3 of 4)

San Diego, California, Lindbergh Field[(a)(b)]																					
Month	Temperatures (°F)							Normal Degree Days (Base 65°F)		Precipitation (in.)											Continues on Sheet 4
	Normal			Extremes						Water Equivalent							Snow, Ice Pellets				
	Daily Max	Daily Min	Mthly	Record Highest	Year	Record Lowest	Year	Heating	Cooling	Normal	Max Mthly	Year	Min Mthly	Year	Max in 24 Hrs	Year	Max Mthly	Year	Max in 24 Hrs	Year	
(c)				14		14					34		34		34		34		34		
J	64.6	45.8	55.2	86	1969	31	1963	314	10	1.88	6.26	1943	(e)	1948	2.65	1943	(e)	1949	(e)	1949	
F	65.6	47.8	56.7	85	1963	38	1965	237	0	1.48	5.31	1941	0.00	1967	1.71	1941	0.0		0.0		
M	66.0	50.1	58.1	85	1964	39	1971	219	5	1.55	5.89	1941	(e)	1972	2.40	1952	0.0		0.0		
A	67.6	53.8	60.7	91	1971	44	1965	144	15	0.81	3.58	1965	(e)	1966	1.40	1965	0.0		0.0		
M	69.4	57.2	63.3	91	1967	48	1967	79	26	0.15	0.95	1971	0.00	1952	0.42	1957	0.0		0.0		
J	71.1	59.9	65.5	90	1973	51	1967	52	67	0.05	0.38	1972	0.00	1946	0.28	1972	0.0		0.0		
J	75.3	63.9	69.6	92	1972	57	1964	6	149	0.01	0.13	1968	0.00	1964	0.10	1968	0.0		0.0		
A	77.3	65.4	71.4	90	1972	60	1968	0	201	0.07	0.87	1945	0.00	1970	0.83	1951	0.0		0.0		
S	76.5	63.2	69.9	111	1963	56	1966	16	163	0.13	1.90	1963	0.00	1964	0.90	1963	0.0		0.0		
O	73.8	58.4	66.1	107	1961	43	1971	43	77	0.34	2.90	1941	0.00	1967	1.20	1941	0.0		0.0		
N	70.1	51.5	60.8	97	1966	38	1964	140	14	1.25	5.82	1965	0.00	1956	2.44	1944	0.0		0.0		
D	66.1	47.2	56.7	88	1963	36	1974	257	0	1.73	7.60	1943	0.03	1953	3.07	1945	(e)	1967	(e)	1967	
					SEP		JAN					DEC		AUG		DEC		DEC		DEC	
YR	70.3	55.4	62.9	111	1963	31	1963	1507	727	9.45	7.60	1943	0.00	1970	3.07	1945	(e)	1967	(e)	1967	

Table 2.3-3
LONG TERM CLIMATOLOGICAL DATA FOR LOS ANGELES AND SAN DIEGO, CALIFORNIA
NORMALS, MEANS, AND EXTREMES (Sheet 4 of 4)

San Diego, California, Lindbergh Field [(a)(b)]

Month	Relative Humidity (%) In Hours (Local Time) 04	10	16	22	Wind Mean Speed (mi/h)	Wind Prevailing Direction	Wind Fastest Mile Speed (mi/h)	Wind Fastest Mile Direction	Wind Fastest Mile Yr	% of Possible Sunshine	Mean Sky Cover, Tenths, Sunrise to Sunset	Mean Number of Days Sunrise to Sunset Clear	Partly Cloudy	Cloudy	Precipitation 0.01 Inch or More	Snow, Ice Pellets 1.0 Inch or More	Thunderstorms	Heavy Fog, Visibility 1/4 Mile or Less	Temperatures (°F) Maximum 90° and above (d)	Maximum 32° and below	Minumum 32° and below	Minumum 0° and below	Average Station Pressue (mbar) Elevation (28 feet ms1)
(c)	14	14	14	14	34	15	31	31		34	34	34	34	34	34	34	34	34	14	14	14	14	2
J	69	54	55	68	5.6	NE	39	SW	1955	71	5.0	13	7	11	7	0	(f)	4	0	0	(f)	0	1017.7
F	72	56	57	71	6.3	WNW	35	S	1969	72	5.0	11	7	10	6	0	(f)	3	0	0	0	0	1017.6
M	74	59	59	72	7.2	WNW	46	SW	1945	71	5.1	11	10	10	7	0	(f)	2	0	0	0	0	1015.5
A	74	58	58	71	7.6	WNW	37	S	1958	65	5.2	10	10	10	5	0	(f)	1	(f)	0	0	0	1015.3
M	76	64	63	74	7.6	WNW	27	SW	1947	58	5.7	9	11	11	2	0	(f)	1	(f)	0	0	0	1013.9
J	80	69	67	78	7.5	SSW	26	S	1948	56	5.6	9	12	9	1	0	(f)	1	(f)	0	0	0	1011.5
J	81	69	66	79	7.1	WNW	23	NW	1968	68	4.5	13	13	5	(f)	0	(f)	1	(f)	0	0	0	1012.7
A	80	67	66	78	6.9	WNW	23	SW	1945	69	4.1	15	12	4	(f)	0	(f)	1	(f)	0	0	0	1012.2
S	78	65	65	77	6.7	NW	25	W	1955	68	4.0	16	9	5	1	0	(f)	3	1	0	0	0	1011.9
O	74	58	60	73	6.3	WNW	31	N	1961	67	4.3	15	9	7	2	0	(f)	4	1	0	0	0	1014.2
N	74	58	63	73	5.6	NE	51	SE	1944	73	4.2	15	8	7	5	0	(f)	4	(f)	0	0	0	1016.4
D	71	55	57	70	5.5	NE	34	S	1951	71	4.7	14	8	9	6	0	(f)	4	0	0	0	0	1018.2
									NOV														
YR	75	61	61	74	6.7	WNW	51	SE	1944	67	4.8	151	116	98	41	0	3	28	3	0	(f)	0	1014.8

Table 2.3-4
METEOROLOGICAL DATA FOR 1973 AND 1974 FOR LOS ANGELES, CALIFORNIA (Sheet 1 of 4)

Station: LOS ANGELES, CALIFORNIA, INTERNATIONAL AIRPORT, Standard time used: PACIFIC, Latitude; 33° 56' N, Longitude: 118° 24' W, Elevation (ground): 97 feet, Year: 1973

Mth	Temperatures (°F)							Degree Days (Base 65°F)		Precipitation (in.)						Rel Humidity(%)				Wind		
	Averages			Extremes						Water Equivalent			Snow, Ice Pellets			Hour				Resultant		
																04	10	16	22			
	Daily Max	Daily Min	Mthly	Highest	Date	Lowest	Date	Heating	Cooling	Total	Greatest in 24 Hrs	Date	Total	Greatest in 24 Hrs	Date	(Local Time)				Direction	Speed (mi/h)	
J	62.7	46.5	54.6	77	14	37	5	314	1	3.16	1.70	16	0.0	0.0		67	53	59	67	31	0.4	
F	65.6	51.4	58.5	78	20	45	17	177	0	4.87	1.82	6-7	0.0	0.0		81	68	67	79	17	1.2	
M	62.3	48.6	55.5	68	16(d)	43	21	87	0	2.42	0.75	8	0.0	0.0		80	63	68	73	25	4.7	
A(c)	67.8	52.3	60.1	80	4	48	21(d)	146	4	(e)	(e)	29(d)	0.0	0.0		74	55	61	76	25	4.8	Continues on Sheet 2
M	68.4	56.4	62.4	84	28	52	6(d)	89	14	0.01	0.01	30-31	0.0	0.0		87	71	70	84	24	6.0	
J	73.7	59.7	66.7	92	20	55	15	12	70	(e)	(e)	22(d)	0.0	0.0		87	68	68	85	24	6.1	
J	74.3	61.6	68.0	87	3	58	24(d)	0	99	0.00	0.00		0.0			89	70	68	87	24	5.7	
A	75.0	63.1	69.1	85	19	60	31(d)	0	134	0.02	0.02	13	0.0	0.0		88	70	70	84	25	5.7	
S	74.0	61.1	67.6	98	27	57	6	1	83	(e)	(e)	22(d)	0.0	0.0		84	68	68	82	24	4.4	
O	74.6	56.7	65.7	91	27	53	29(d)	24	52	0.08	0.04	23(d)	0.0	0.0		84	57	64	81	24	3.3	
N	67.1	51.9	59.5	77	28(d)	44	24	159	2	1.92	0.98	22	0.0	0.0		78	60	63	74	27	1.8	
D	67.8	48.8	58.3	85	9	42	3	207	8	0.45	0.30	1	0.0	0.0		72	52	57	71	34	0.2	
					SEP		JAN					FEB										
YR	69.4	54.8	62.1	98	27	37	5	1416	467	12.93	1.82	6-7	0.0	0.0		81	63	65	79	24	3.6	

a. To 8 compass points only.
b. 70° at Alaskan stations.
c. Data corrected after publication of the monthly issue.
d. Also on earlier dates, months, or years.
e. Trace, an amount too small to measure.
f. The National Weather Service considers the accuracy of solar radiation questionable; therefore, publication is suspended pending determination of corrected values.

Table 2.3-4
METEOROLOGICAL DATA FOR 1973 AND 1974 FOR LOS ANGELES, CALIFORNIA (Sheet 2 of 4)

Station: LOS ANGELES, CALIFORNIA, INTERNATIONAL AIRPORT, Standard time used: PACIFIC, Latitude; 33° 56' N, Longitude: 118° 24' W, Elevation (ground): 97 feet, Year: 1973

Month	Wind				Percentage of Possible Sunshine	Average Sky Cover Sunrise to Sunset	Mean Number of Days											Average Daily Solar Radiation-Langleys[f]
	Average Speed (mi/h)	Peak Gust					Sunrise to Sunset			Precipitation 0.01 Inch or More	Snow, Ice Pellets 1.0 Inch or More	Thunderstorms	Heavy Fog, Visibility 1/4 Mile or Less	Temperature (°F)				
														Maximum		Minimum		
		Speed (mi/h)	Direction[a]	Date			Clear	Partly Cloudy	Cloudy					90° and above (b)	32° and below	32° and below	0° and below	
J	7.4	46	N	19		4.8	11	11	9	5	0	0	1	0	0	0	0	
F	7.6	38	S	11		6.8	6	7	15	11	0	0	1	0	0	0	0	
M	9.6	40	W	20		4.8	14	8	9	6	0	0	0	0	0	0	0	
A	8.9	43	SE(c)	4		4.6	14	6	10	0	0	0	0	0	0	0	0	
M	7.6	25	W	5		6.4	7	10	14	1	0	0	1	0	0	0	0	
J	7.6	25	SW	23(d)		6.1	7	11	12	0	0	0	4	2	0	0	0	
J	7.6	23	SW	20(d)		5.1	8	16	7	0	0	0	3	0	0	0	0	
A	7.3	28	W	22		4.6	12	12	7	1	0	1	1	0	0	0	0	
S	7.0	23	W	5(d)		5.3	7	15	8	0	0	0	2	3	0	0	0	
O	6.3	25	W	10		3.8	15	12	4	2	0	0	6	1	0	0	0	
N	6.9	37	W	18		5.0	12	8	10	5	0	0	4	0	0	0	0	
D	6.0	36	NE	23		6.2	6	11	14	6	0	0	1	0	0	0	0	
				JAN														
YR	7.5	46	N	19		5.3	119	127	119	37	0	1	24	6	0	0	0	

Table 2.3-4
METEOROLOGICAL DATA FOR 1973 AND 1974 FOR LOS ANGELES, CALIFORNIA (Sheet 3 of 4)

Station: LOS ANGELES, CALIFORNIA, INTERNATIONAL AIRPORT, Standard time used: PACIFIC, Latitude; 33° 56' N, Longitude: 118° 24' W, Elevation (ground): 97 feet, Year: 1974

Mth	Temperatures (°F)							Degree Days (Base 65°F)		Precipitation (in.)						Rel Humidity(%)				Wind		
	Averages			Extremes						Water Equivalent			Snow, Ice Pellets			Hour				Resultant		Average Speed (mi/h)
																04	10	16	22			
	Daily Max	Daily Min	Mthly	Highest	Date	Lowest	Date	Heating	Cooling	Total	Greatest in 24 Hrs	Date	Total	Greatest in 24 Hrs	Date	(Local Time)				Direction	Speed (mi/h)	
JAN	61.1	47.5	54.3	79	14	39	2	323	0	5.68	1.93	3-4	(e)	(e)	6	83	70	71	79	16	0.7	6.8
FEB	66.8	48.1	57.5	80	24	43	7	208	3	0.13	0.13	28	0.0	0.0		67	48	56	63	28	1.4	6.4
MAR	62.1	51.0	56.6	68	14	43	4	256	0	2.49	1.05	1-2	0.0	0.0		91	76	78	86	25	3.4	7.1
APR	67.5	51.8	59.7	78	5	46	25	158	2	0.14	0.14	1-2	0.0	0.0		83	55	63	76	26	5.3	8.6
MAY	68.9	56.9	62.9	77	25	50	19	62	5	0.02	0.02	5	0.0	0.0		84	65	65	80	26	6.0	7.9
JUN	73.1	60.2	66.7	80	28	56	17	2	58	(e)	(e)	7	0.0	0.0		88	66	64	83	25	6.3	8.1
JUL	76.7	64.3	70.5	84	23	60	11	0	179	(e)	(e)	29	0.0	0.0		87	66	67	82	25	6.2	7.8
AUG	74.8	64.4	69.6	78	6	61	16	0	150	(e)	(e)	8	0.0	0.0		89	71	71	88	25	6.7	8.0
SEP	75.1	62.8	69.0	86	22	59	28	0	125	(e)	(e)	25	0.0	0.0		91	71	75	88	25	5.4	7.2
OCT	72.2	59.6	65.9	100	16	52	31	26	65	0.54	0.45	28	0.0	0.0		87	69	72	85	26	4.9	7.2
NOV	72.9	52.4	62.7	94	12	44	29	100	40	(e)	(e)	21-22	0.0	0.0		75	49	64	76	27	1.7	5.6
DEC	65.7	45.9	55.8	78	16	35	25	279	0	3.76	2.28	3-4	0.0	0.0		77	54	60	73	34	0.8	5.9
					OCT		DEC					DEC			JAN							
YEAR	69.7	55.4	62.6	100	16	35	25	1414	627	12.76	2.28	3-4	(e)	(e)	6	84	63	67	80	26	3.9	7.2

Continues on Sheet 4

Table 2.3-4
METEOROLOGICAL DATA FOR 1973 AND 1974 FOR LOS ANGELES, CALIFORNIA (Sheet 4 of 4)

Station: LOS ANGELES, CALIFORNIA, INTERNATIONAL AIRPORT, Standard time used: PACIFIC, Latitude; 33° 56' N, Longitude: 118° 24' W, Elevation (ground): 97 feet, Year: 1974

Month	Wind			% of Possible Sunshine	Average Sky Cover Sunrise to Sunset	Number of Days											Average Station Pressure (mbar) Elevation (104 feet ms1)
	Peak Gust					Sunrise to Sunset			Precip-itation 0.01 Inch or More	Snow, Ice Pellets 1.0 Inch or More	Thunder-storms	Heavy Fog, Visibility 1/4 Mile or Less	Temperatures (°F)				
													Maximum		Minimum		
	Speed (mi/h)	Direction (a)	Date			Clear	Partly Cloudy	Cloudy					90° and above(b)	32° and below	32° and below	0° and below	
J	40	W	1		6.5	7	9	15	11	0	1	7	0	0	0	0	1014.2
F	32	NW	19		3.6	15	7	6	1	0	0	1	0	0	0	0	1015 9
M	30	W	3		6.8	6	10	15	8	0	1	5	0	0	0	0	1013.2
A	46	W	9		2.5	22	5	3	2	0	0	2	0	0	0	0	1012.5
M	36	W	18		6.1	7	11	13	1	0	1	0	0	0	0	0	1010.5
J	30	W	25		4.3	15	4	11	0	0	0	0	0	0	0	0	1007.8
J	26	W	10		3.9	13	15	3	0	0	1	0	0	0	0	0	1010.2
A	24	W	13		4.7	11	15	5	0	0	0	0	0	0	0	0	1009.5
S	26	W	16		5.3	8	15	7	0	0	0	5	0	0	0	0	1008.5
O	46	W	28		5.9	7	13	11	3	0	0	4	2	0	0	0	1011.9
N	30	W	1		3.7	16	8	6	0	0	0	4	2	0	0	0	1013.2
D	41	N	22		4.2	16	7	8	6	0	1	4	0	0	0	0	1015.2
			OCT														
YR	45	W	28		4.8	143	119	103	32	0	5	32	4	0	0	0	1011.9

Table 2.3-5
METEOROLOGICAL DATA FOR 1973 AND 1974 FOR SAN DIEGO, CALIFORNIA (Sheet 1 of 4)

Station: San Diego, California, Lindbergh Field, Standard time used: PACIFIC, Latitude: 32° 44' N, Longitude: 117° 10' W,
Elevation (ground): 13 feet, Year: 1973

Month	Temperatures (°F)							Degree Days (Base 65°F)		Precipitation (in.)						Rel Humidity(%)				Wind	Continues on Sheet 2
	Averages			Extremes						Water Equivalent			Snow, Ice Pellets			Hour				Resultant	
																04	10	16	22		
	Daily Max	Daily Min	Mthly	Highest	Date	Lowest	Date	Heating	Cooling	Total	Greatest in 24 Hrs	Date	Total	Greatest in 24 Hrs	Date	(Local Time)				Direction	
JAN	63.9	47.2	55.6	76	13	38	5	286	0	1.68	0.48	16	0.0	0.0		63	51	53	63	29	
FEB(b)	67.3	52.5	59.9	75	20	47	1	131	0	1.63	0.54	11-12	0.0	0.0		73	60	57	71	24	
MAR	64.1	52.0	58.1	71	16	46	14	208	0	2.26	0.71	11	0.0	0.0		70	58	56	65	26	
APR	67.8	55.1	61.5	81	9	49	3(e)	107	10	0.05	0.03	29-30	0.0	0.0		64	53	52	62	28	
MAY	68.0	58.7	63.4	81	28(e)	55	5(e)	61	17	(f)	(f)	31	0.0	0.0		77	65	64	73	26	
JUN	73.4	62.5	68.0	90	20	59	9(e)	1	97	(f)	(f)	14	0.0	0.0		78	65	64	76	26	
JUL	74.3	63.8	69.1	80	3	62	26(e)	0	133	(f)	(f)	12	0.0	0.0		78	70	65	76	26	
AUG	75.5	65.4	70.5	83	20(e)	63	31(e)	0	176	(f)	(f)	20	0.0	0.0		76	67	66	75	27	
SEP	74.3	63.3	68.8	93	27	60	7	0	121	0.02	0.02	4	0.0	0.0		71	61	60	70	28	
OCT	74.7	58.9	66.8	90	28	54	30	6	70	0.01	0.01	8	0.0	0.0		67	55	57	69	30	
NOV	67.3	53.9	60.6	82	11	46	20	132	8	1.63	0.65	17-18	0.0	0.0		73	60	61	70	27	
DEC	67.0	49.3	58.2	81	9	44	3	205	1	0.19	0.13	22	0.0	0.0		68	52	59	67	29	
					SEP		JAN					MAR									
YEAR	69.8	56.9	63.4	93	27	38	5	1137	633	7.47	0.71	11	0.0	0.0		72	60	60	70	27	

a. To 8 compass points only.
b. Data corrected after publication of the monthly issue.
c. Climatological normals (1941-1970).
d. >70° at Alaskan stations.
e. Also on earlier dates, months, or years.
f. Trace, an amount too small to measure.

Table 2.3-5
METEOROLOGICAL DATA FOR 1973 AND 1974 FOR SAN DIEGO, CALIFORNIA (Sheet 2 of 4)

Station: San Diego, California Lindbergh Field, Standard time used: PACIFIC Latitude: 32° 44' N Longitude: 117° 10' W
Elevation (ground): 13 feet Year: 1973

Month	Wind					% of Possible Sunshine	Average Sky Cover Sunrise to Sunset	Number of Days												Average Daily Solar Radiation-Langleys
	Resultant	Average Speed (mi/h)	Peak Gust					Sunrise to Sunset			Precipitation 0.01 Inch or More	Snow, Ice Pellets 1.0 Inch or More	Thunderstorms	Heavy Fog, Visibility 1/4 Mile or Less	Temperatures (°F)					
															Maximum					
	Speed (mi/h)		Speed (mi/h)	Direction (a)	Date			Clear	Partly Cloudy	Cloudy					90° and above (d)	32° and below	32° and above (d)	0° and below	
J	2.1	6.8	30	S	18	78	5.1	12	7	12	8	0	0	2	0	0	0	0	
F	1.8	7.2	33	S	11	78	6.1	6	10	12	12	0	1	1	0	0	0	0	
M	4.3	9.8	25	NW	13	66	6.0	9	7	15	13	0	2	0	0	0	0	0	
A	4.2	8.4	26	N	4	63	5.0	13	8	9	3	0	0	0	0	0	0	0	
M	4.6	7.8	20	W	1	47	6.5	6	9	16	0	0	0	2	0	0	0	0	
J	4.4	8.2	19	NW	5	56	6.3	8	8	14	0	0	0	3	1	0	0	0	
J	4.4	8.0	18	W	2	54	5.7	8	14	9	0	0	0	1	0	0	0	0	
A	4.6	8.2	21	S	19	62	5.1	10	13	8	0	0	0	0	0	0	0	0	
S	4.3	8.0	19	NW	5	53	5.5	10	8	12	1	0	0	0	3	0	0	0	
O	4.3	7.0	18	NW	28(e)	73	3.7	18	6	7	1	0	0	7	1	0	0	0	
N	2.5	6.6	24	W	18	62	5.6	7	13	10	7	0	0	2	0	0	0	0	
D	1.4	4.5	19	NW	22	75	5.7	9	10	12	4	0	0	2	0	0	0	0	
					FEB														
YR	3.5	7.5	33	S	11	63	5.5	116	113	136	49	0	3	20	5	0	0	0	

Table 2.3-5
METEOROLOGICAL DATA FOR 1973 AND 1974 FOR SAN DIEGO, CALIFORNIA (Sheet 3 of 4)

Station: SAN DIEGO, CALIFORNIA, LINDBERGH FIELD, Standard time used: PACIFIC, Latitude: 32° 44' N Longitude: 117° 10' W, Elevation (ground): 13 feet, Year: 1974

Month	Temperatures (°F)							Degree Days (Base 65°F)		Precipitation (in.)						Rel Humidity(%)				Wind
	Averages			Extremes						Water Equivalent			Snow, Ice Pellets			Hour				Resultant
																04	10	16	22	
	Daily Max	Daily Min	Mthly	Highest	Date	Lowest	Date	Heating	Cooling	Total	Greatest in 24 Hrs	Date	Total	Greatest in 24 Hrs	Date	(Local Time)				Direction
JAN	63.9	49.8	56.9	73	14	44	31	243	0	2.96	1.28	7-8	0.0	0.0		71	57	60	72	27
FEB	67.9	48.4	58.2	80	25	44	14	184	0	0.04	0.04	19	0.0	0.0		58	43	45	61	31
MAR	64.8	53.4	59.1	72	1	46	5	176	0	1.70	1.15	7-8	0.0	0.0		76	65	63	74	28
APR	69.0	54.9	62.0	80	5	51	4	85	2	0.02	0.01	9	0.0	0.0		71	54	54	67	29
MAY	68.1	58.5	63.3	76	25	53	20	55	9	0.01	0.01	9	0.0	0.0		72	62	61	70	25
JUN	72.2	61.6	66.9	82	27	59	19	4	69	0.02	0.02	6-7	0.0	0.0		80	68	64	75	29
JUL	76.5	66.3	71.4	86	20	62	12	0	204	0.01	0.01	29	0.0	0.0		77	65	63	75	28
AUG	74.9	65.4	70.2	77	26	61	30	0	169	(f)	(f)	1	0.0	0.0		77	67	66	76	29
SEP	75.1	65.4	70.3	84	2	61	28	0	164	(f)	(f)	26	0.0	0.0		80	70	67	77	29
OCT	72.5	61.0	66.8	92	16	54	31	14	75	1.03	0.78	28-29	0.0	0.0		74	63	61	72	29
NOV	71.0	53.4	62.2	91	12	46	26	97	19	0.14	0.10	1	0.0	0.0		68	50	55	66	30
DEC	65.7	46.9	56.3	77	16	36	25	265	0	2.20	1.43	4	0.0	0.0		66	46	47	61	31
					OCT		DEC					DEC								
YEAR	70.1	57.1	63.6	92	16	36	25	1123	711	8.13	1.43	4	0.0	0.0		73	59	59	71	29

Continues on sheet 4

Table 2.3-5
METEOROLOGICAL DATA FOR 1973 AND 1974 FOR SAN DIEGO, CALIFORNIA (Sheet 4 of 4)

Station: SAN DIEGO, CALIFORNIA, LINDBERGH FIELD, Standard time used: PACIFIC Latitude: 32° 44' N Longitude: 117° 10' W, Elevation (ground): 13 feet, Year: 1974

Month	Wind					% of Possible Sunshine	Average Sky Cover Sunrise to Sunset	Number of Days											Average Station Pressure (mbar) Elevation (28 feet ms1)
	Speed (mi/h)	Average Speed (mi/h)	Fastest Mile					Sunrise to Sunset			Precipitation 0.01 Inch or More	Snow, Ice Pellets 1.0 Inch or More	Thunderstorms	Heavy Fog, Visibility 1/4 Mile or Less	Temperatures (°F)				
															Maximum		Minimum		
			Speed (mi/h)	Direction (a)	Date			Clear	Partly Cloudy	Cloudy					90° and above (d)	32° and below	32° and above (d)	0° and below	
J	1.3	6.6	32	SE	7	62	6.3	8	7	16	9	0	0	2	0	0	0	0	1017.3
F	3.4	5.9	23	NW	28	86	4.1	15	6	7	1	0	0	1	0	0	0	0	1018.6
M	3.2	7.2	33	SW	8	68	7.0	7	7	17	6	0	0	4	0	0	0	0	1016.3
A	4.7	7.7	26	NW	9	84	3.4	18	7	5	2	0	0	1	0	0	0	0	1015.6
M	4.6	7.5	21	W	19	49	7.2	5	8	18	1	0	0	0	0	0	0	0	1013.5
J	5.0	7.9	20	NW	19	62	4.7	13	9	8	1	0	0	0	0	0	0	0	1010.8
J	4.8	7.6	20	W	4	67	4.8	10	15	6	1	0	0	0	0	0	0	0	1012.9
A	5.2	7.7	17	W	26	58	5.3	10	15	6	0	0	0	0	0	0	0	0	1012.2
S	4.4	6.9	17	NW	21	60	5.2	11	11	8	0	0	0	2	0	0	0	0	1011.2
O	4.5	7.1	28	W	29	49	6.2	9	8	14	2	0	0	2	1	0	0	0	1014.9
N	2.1	5.1	19	W	1	73	4.1	16	7	7	3	0	0	1	1	0	0	0	1015.9
D	1.9	5.3	25	NW	22	87	3.9	16	9	6	3	0	0	5	0	0	0	0	1018.0
					MAR														
YR	3.6	6.9	33	SW	8	66	5.2	138	109	118	29	0	0	18	2	0	0	0	1014.8

Table 2.3-6

TEMPERATURE SUMMARY FOR SAN ONOFRE SITE : LEVEL: 6.1/10 METERS[(a)] (Sheet 1 of 2)

Period of Record 1/25/74 - 1/24/76

Hour	January		February		March		April		May		June		July	
	(°C)	(°F)	(°C)	(°F)	(°C)	(°F)	(°C)	(°F)	(°C)	(°F)	(°C)	(°F)	(°C)	(°F)
1	11.3	52.3	10.4	50.7	10.3	50.5	10.8	51.4	12.9	55.2	14.0	57.2	16.4	61.5
2	10.9	51.6	10.1	50.2	10.1	50.2	10.5	50.9	12.8	55.0	13.8	56.8	16.3	61.3
3	10.9	51.6	9.9	49.8	9.9	49.8	10.3	50.5	12.5	54.5	13.6	56.5	16.1	61.0
4	10.8	51.4	9.6	49.3	9.6	49.3	10.0	50.0	12.4	54.3	13.6	56.5	16.1	61.0
5	10.6	51.1	9.5	49.1	9.4	48.9	9.7	49.5	12.2	54.0	13.5	56.3	15.8	60.4
6	10.5	50.9	9.4	48.9	9.4	48.9	9.5	49.1	12.2	54.0	13.7	56.7	16.1	61.0
7	10.5	50.9	9.3	48.7	9.7	49.5	9.4	48.9	12.5	54.5	14.1	57.4	16.6	61.9
8	11.2	52.2	9.7	49.5	10.4	50.7	10.7	51.3	13.2	55.8	14.5	58.1	17.2	63.0
9	12.5	54.5	11.0	51.8	11.3	52.3	11.9	53.4	13.7	56.7	15.0	59.0	17.6	63.7
10	13.3	55.9	12.0	53.6	12.0	53.6	12.3	54.1	13.9	57.0	15.6	60.1	18.0	64.4
11	13.6	56.5	12.3	54.1	12.3	54.1	13.0	55.4	14.2	57.6	16.1	61.0	18.3	64.9
12	14.0	57.2	12.7	54.9	12.5	54.5	13.4	56.1	14.6	58.3	16.5	61.7	18.6	65.5
13	14.3	57.7	13.1	55.6	12.8	55.0	13.9	57.0	14.9	58.8	16.5	61.7	18.7	65.7
14	14.4	57.9	13.4	56.1	13.0	55.4	14.3	57.7	15.3	59.5	16.8	62.2	18.8	65.8
15	14.6	58.3	13.7	56.7	13.0	55.4	14.4	57.9	15.2	59.4	16.8	62.2	18.6	65.5
16	14.5	58.1	13.8	56.8	12.8	55.0	14.3	57.7	15.2	59.4	16.5	61.7	18.5	65.3
17	14.3	57.7	13.6	56.5	12.7	54.9	14.0	57.2	15.0	59.0	16.3	61.3	18.2	64.8
18	13.5	56.3	12.9	55.2	12.2	54.0	13.5	56.3	14.6	58.3	15.9	60.6	17.8	64.0
19	13.0	55.4	12.2	54.0	11.9	53.4	13.1	55.6	14.1	57.4	15.5	59.9	17.4	63.3
20	12.4	54.3	11.7	53.1	11.4	52.5	12.6	54.7	13.6	56.5	15.3	595	17.2	63.0
21	11.9	53.4	11.1	52.0	11.1	52.0	12.3	54.1	13.5	56.3	15.0	59.0	17.1	62.8
22	11.8	53.2	10.8	51.4	10.8	51.4	11.8	53.2	13.4	56.1	14.7	58.5	17.0	62.8
23	11.7	53.1	10.6	51.1	10.5	50.9	11.2	52.2	13.2	55.8	14.5	58.1	16.8	62.2
24	11.2	52.2	10.5	50.9	10.5	50.9	11.0	51.8	13.1	55.6	14.2	57.6	16.7	62.1
Mean	12.4	54.3	11.4	52.5	11.2	52.2	12.0	53.6	13.7	56.7	15.1	59.2	17.3	63.1
Mean Min	9.0	48.2	7.9	46.2	8.5	47.3	8.5	47.3	11.5	52.7	12.5	54.5	15.3	59.5
Mean Max	15.6	60.1	14.4	57.9	13.5	56.3	14.9	58.8	15.9	60.6	17.4	63.3	19.2	66.6
Absolute Min	0.6	33.1	3.5	38.3	3.8	38.8	4.0	39.2	5.7	42.3	9.5	49.1	10.4	50.7
Absolute Max	26.5	79.7	19.7	67.5	17.3	63.1	19.7	67.5	19.9	67.8	20.3	68.5	23.2	73.8

(a) Temperature measurement raised from 6.1 meters to 10 meters on October 25, 1975.

Table 2.3-6

TEMPERATURE SUMMARY FOR SAN ONOFRE SITE: LEVEL: 6.1/10 METERS[(a)] (Sheet 2 of 2)

Period of Record 1/25/74 - 1/24/76												
Hour	August		September		October		November		December		Annual Averages	
	(°C)	(°F)	(°C)	(°F)	(°C)	(°F)	(°C)	(°F)	(°C)	(°F)	(°C)	(°F)
1	15.3	59.5	16.1	61.0	14.5	58.1	12.9	55.2	11.2	52.2	13.0	55.4
2	15.3	59.5	16.0	60.8	14.7	58.5	13.0	55.4	11.1	52.0	12.9	55.2
3	15.0	59.0	15.8	60.4	14.5	58.1	12.3	54.1	11.1	52.0	12.7	54.9
4	14.9	58.8	15.7	60.3	14.3	57.7	12.4	54.3	10.7	51.3	12.5	54.5
5	14.5	58.1	15.5	59.9	14.4	57.9	12.1	53.8	10.7	51.3	12.3	54.1
6	14.7	58.5	15.6	60.1	14.4	57.9	12.0	53.6	10.8	51.4	12.4	54.3
7	15.2	59.4	16.0	60.8	14.7	58.5	12.1	53.8	10.5	50.9	12.6	54.7
8	15.6	60.1	16.3	61.3	15.9	60.6	13.1	55.6	11.1	52.0	13.3	55.9
9	16.1	61.0	17.0	62.6	16.3	61.3	14.2	57.6	12.4	54.3	14.1	57.4
10	16.6	61.9	17.6	63.7	16.6	61.9	14.6	58.3	13.3	55.9	14.6	58.3
11	17.0	62.6	18.0	64.4	17.1	62.8	15.0	59.0	13.8	56.8	15.0	59.0
12	17.6	63.7	18.5	65.3	17.4	63.3	15.3	59.5	14.1	57.4	15.4	59.7
13	17.8	64.0	13.6	65.5	18.0	64.4	15.6	60.1	14.3	57.7	15.7	60.3
14	18.1	64.6	18.7	65.7	17.9	64.2	16.0	60.8	14.5	58.1	15.9	60.6
15	18.2	64.8	18.7	65.7	18.0	64.2	16.1	61.0	14.6	58.3	16.0	60.8
16	17.8	64.0	18.5	65.3	17.8	64.0	15.9	60.6	14.5	58.1	15.8	60.4
17	17.5	63.5	18.1	64.6	17.3	63.1	13.7	60.3	13.9	57.0	15.6	60.1
18	17.0	62.6	17.8	64.0	16.9	62.4	15.1	59.2	13.1	55.6	15.0	59.0
19	16.5	61.7	17.6	63.7	16.5	61.7	14.6	58.3	12.7	54.9	14.6	58.3
20	16.4	61.5	17.4	63.3	16.1	61.0	14.0	57.2	12.4	54.3	14.2	57.6
21	16.1	61.0	16.9	62.4	15.8	60.4	13.6	56.5	12.0	53.6	13.9	57.0
22	15.8	60.4	16.8	62.2	15.3	59.5	13.6	56.5	11.9	53.4	13.7	56.7
23	15.7	60.3	16.5	61.7	15.0	59.0	13.4	56.1	11.6	52.9	13.4	56.1
24	15.4	59.7	16.4	61.5	14.9	58.8	13.2	55.8	11.6	52.9	13.2	55.8
Mean	16.2	61.2	17.1	62.8	16.0	60.8	14.0	57.2	12.4	54.3	14.1	57.4
Mean Min	13.8	56.8	14.8	58.6	13.2	55.8	10.8	51.4	9.4	48.9	11.3	52.3
Mean Max	18.6	65.5	19.5	67.1	18.7	65.7	16.9	62.4	15.3	59.5	16.7	62.1
Absolute Min	8.0	46.4	10.1	50.2	9.2	48.6	5.4	41.7	4.6	40.3	0.6	33.1
Absolute Max	25.2	77.4	34.3	93.7	30.3	86.5	27.5	81.5	23.7	74.7	34.3	93.7

The mean values at San Onofre are 2 to 3°C cooler than the mean values recorded at San Diego and Los Angeles. This variance is caused partially by differences in the instrument exposure. At San Diego and Los Angeles the temperature measurements are made in instrument shelters at a height of about 1 meter above the ground, while at San Onofre the temperatures are measured in a shielded aspirator mounted on a tower 6 meters above the surface. Another factor is the close proximity (60 meters, 197 feet) of the tower to the ocean, while both the observation sites at Los Angeles International Airport and San Diego Lindbergh Field are 1 to 4 kilometers (0.6 to 2.5 miles) from the immediate coast. This difference in distance from the sea coast is sufficient to cause slightly warmer temperatures to be experienced at the airport sites.

Noteworthy temperature statistics for the site include an annual mean temperature of 14.1°C (57.4°F) with a difference between the annual mean maximum at 16.7°C (62.1°F) and the annual mean minimum at 11.3°C (52.3°F) of only 5.4°C (9.8°F). The extremes were an absolute maximum of 34.3°C (93.7°F) on September 23, 1975, with an offshore Santa Ana wind, and an absolute minimum of 0.6°C (33.1°F) on January 25, 1975, with an offshore drainage breeze. The maximum temperature at the site may occasionally reach 38°C (100°F) or more in extreme Santa Ana conditions.

The difference between the monthly mean maximum and minimum temperatures varied from 6.6°C (11.9°F) in January to 3.9°C (7.1°F) in July. These very moderate mean temperatures reflect the strong influence of the adjacent Pacific Ocean. Extreme temperatures occur with offshore land breezes. Occasional Santa Ana winds bring the higher absolute maximum temperatures most evident during the fall and early winter.

2.3.2.1.3 Atmospheric Water Vapor (Relative Humidity)

No water vapor measurements were made at the San Onofre site during the period of record (1/25/74 - 1/24/76). However, because of the similarity of meteorological conditions and water temperatures along the southern California coast, the relative humidity climatology of Los Angeles and San Diego should be representative of the SONGS site.

Relative humidity is defined as the ratio of the actual amount of water vapor in the air to the maximum amount of water vapor the air can hold at the same temperature and pressure. It is inversely proportional to the temperature and shows an inverse relationship to the diurnal temperature cycle. Thus, with the same amount of water vapor in the air, the relative humidity increases as the temperature decreases, and vice versa.

The relative humidity data for Los Angeles and San Diego are given in Tables 2.3-3 to 2.3-5. The diurnal variation of relative humidity indicates high values in the late evening and early morning hours with minimums occurring in the late morning and early afternoon. The annual course of relative humidity shows the highest values in the summer months, coincident with the highest frequency of fog and stratus, and minimums during winter months. The early morning (0400 PST) average relative humidity in the summer are about 85% while during the winter they are near 70%. The late afternoon average values (1600 PST) in the summer are near 68% and in the winter near 58%. Extreme maximum relative humidity is 100% during fog and/or precipitation conditions. The extreme minimum relative humidity are associated with the hot Santa Ana winds when values may fall below 10%.

2.3.2.1.4 Precipitation

No precipitation measurements were made at the site during the period of record (1/25/74 to 1/24/76). However, precipitation measurements that were made from January 1968 to March 1970 are summarized in Table 2.3-7. For comparison, long-term (1943-1960) precipitation averages at Oceanside, California, approximately 24 kilometers (15 miles) southeast of the site, are also shown in Table 2.3-7. Long-term precipitation records for Los Angeles and San Diego are shown in Table 2.3-3. Maximum monthly and minimum monthly precipitation amounts and maximum 24-hour amounts are also shown in Table 2.3-3.

There is good agreement between the longer term normal data with the shorter term data from the plant site. The precipitation, averaging about 304.80 mm (12 in.) per year, occurs mostly in the winter; the total for the months of May through September averages 12.70 mm (0.5 in.) or less. The rainiest month is typically January, with an average of 63.50 mm (2.5 in.); the driest is July, with an average of 0.24 mm (0.01 in.). The total number of days per year with measurable precipitation averages only about 40.

As in many semi-arid regions, there is a marked variability in monthly and seasonal totals. Maximum monthly winter precipitation amounts may be as high as 279.40 mm (11 in.) and minimum monthly amounts near zero. Variations in the other seasons are also large, ranging from less than one-third of normal to nearly three times normal. The maximum 24-hour rainfall occurring at Los Angeles during the period of record (Table 2.3-3) is 157.23 mm (6.19 in.).

Measurable snow has never been recorded at a coastal location in southern California. Traces of snow have fallen only a few times, but the snow melted as it fell.

2.3.2.1.5 Fog and Smog

Fog and low clouds (stratus) are a characteristic feature of the southern California coastal climate. Although fog observations are not available for the San Onofre site, climatological data for Los Angeles International Airport and San Diego North Island Naval Air Station are representative of conditions at the site. Tables 2.3-8 and 2.3-9 give the percent frequency when the ceiling was less than 457 meters (1500-feet) and/or the visibility was less than 4.8 km (3 miles) and when the ceiling was less than 91 meters (300 feet) and/or the visibility was less than 1.6 kilometers (1 mile). From these tables, it may be concluded that the San Onofre site, during the summer months, has stratus and fog over 50%, of the time during the early morning hours. During the remaining portion of the year, the percent frequency drops to 30-35%. The fog and low clouds dissolve more often in the summer during the afternoon hours than in the winter when solar heating is at a minimum. The percentage frequency of fog and stratus in the afternoon hours ranges from 6-12% in the summer months and 12-18% for the remainder of the year. The lower ceilings and visibilities (<91 meters and 1.6 kilometers) occur most frequently in the winter months. During the early morning hours, these occur with a frequency of 10-15%

in the winter season and 5-9% during the other seasons. This higher wintertime frequency is related to the more frequent formation of surface inversions during the colder months of the year (see Section 2.3.1.2.6).

Table 2.3-7
MONTHLY PRECIPITATION AT THE SAN ONOFRE SITE
(JAN 1968-MAR 1970) AND OCEANSIDE, CALIFORNIA
(1943-1960)[a]

Month	San Onofre Site		Oceanside	
	(mm)	(in.)	(mm)	(in.)
January	49.78	(1.96)	51.31	(2.02)
February	43.18	(1.70)	42.16	(1.66)
March	29.72	(1.17)	32.00	(1.26)
April	44.45	(1.75)	21.34	(0.84)
May	4.06	(0.16)	6.60	(0.26)
June	0.76	(0.03)	1.27	(0.05)
July	0.76	(0.03)	0.76	(0.03)
August	0.25	(0.01)	3.56	(0.14)
September	4.57	(0.18)	1.78	(0.07)
October	2.29	(0.09)	8.38	(0.33)
November	7.91	(2.91)	26.16	(1.03)
December	69.85	(2.25)	36.07	(1.42)
Annual	310.64	(12.23)	230.63	(9.08)

[a] Source: Climatic Summary of the United States, Supplement for 1931 through 1952 and for 1951 through 1960, Environmental Data Services, National Oceanic and Atmospheric Administration.

Table 2.3-8
PERCENTAGE FREQUENCY OF LOW CEILINGS AND VISIBILITY AT LOS ANGELES, CALIFORNIA[5]

Los Angeles, California, International Airport Lat 33°56'N, Long. 118°24'W, Elev 126 ft															
Percent Frequency Ceiling Less Than 1500 Feet and/or Visibility Less Than 3 Miles															
Hours (LST)	Jan	Feb	Mar	Apr	May	Jun	July	Aug	Sept	Oct	Nov	Dec	Annual	POR (years)	No Obs
00-02	27.2	24.7	22.2	25.2	23.7	39.5	41.6	44.4	35.7	41.4	33.1	33.5	32.7	12	13137
03-05	27.2	25.4	29.1	31.4	28.1	47.7	49.6	49.7	47.0	48.0	34.2	29.1	37.2	12	13141
06-08	32.6	31.9	36.8	35.5	29.9	49.4	48.8	56.2	56.9	56.7	40.2	33.5	42.2	12	13142
09-11	31.7	29.1	23.4	21.2	15.8	26.8	23.2	29.9	33.8	38.5	34.4	31.1	28.2	12	13141
12-14	18.9	15.3	12.4	10.6	9.2	11.3	6.7	12.8	14.0	18.7	19.6	19.4	14.1	12	13137
15-17	15.1	14.2	8.2	13.3	12.6	12.7	11.1	14.5	14.6	18.2	16.0	19.0	14.1	12	13140
18-20	13.6	15.3	10.8	17.3	18.0	22.9	30.7	34.0	24.6	22.2	16.9	17.1	20.3	12	13134
21-23	20.4	19.4	13.5	20.6	22.0	31.6	37.5	39.9	28.0	29.1	24.3	26.7	26.1	12	13131
Percent Frequency Ceiling Less Than 300 Feet and/or Visibility Less Than 1 Mile															
Hours (LST)	Jan	Feb	Mar	Apr	May	Jun	July	Aug	Sept	Oct	Nov	Dec	Annual	POR (years)	No Obs
00-02	5.7	7.8	4.2	3.5	1.5	2.8	2.6	3.3	6.7	7.6	9.7	11.1	5.5	12	13137
03-05	7.3	9.0	8.6	7.0	3.3	4.9	4.8	5.4	11.9	13.1	11.6	11.1	8.2	12	13141
06-08	10.0	9.7	11.7	6.9	2.7	4.3	4.1	6.1	12.2	16.1	15.0	12.9	9.3	12	13142
09-11	7.2	5.5	3.1	0.5	0.6	0.7	0.1	0.9	1.8	4.8	7.5	8.4	3.4	12	13141
12-14	3.1	3.1	0.4	0.0	0.2	0.2	0.0	0.4	0.3	1.7	3.7	3.5	1.4	12	13137
15-17	2.4	2.5	0.9	0.6	0.0	0.0	0.1	0.3	0.6	1.3	3.9	5.3	1.5	12	13140
18-20	2.0	3.8	1.3	1.8	0.9	0.5	1.3	1.6	1.7	2.2	5.1	4.8	2.3	12	13134
21-23	3.3	5.3	2.1	1.7	2.0	1.6	2.2	2.3	2.3	4.0	7.8	7.6	3.5	12	13131

Table 2.3-9
PERCENTAGE FREQUENCY OF LOW CEILINGS AND VISIBILITY AT SAN DIEGO, CALIFORNIA[5]

San Diego, California, North Island NAS Lat 32°42'N, Long. 117°12'W, Elev 24 ft														
Percent Frequency Ceiling Less Than 1500 Feet and/or Visibility Less Than 3 Miles														
Hours (LST)	Jan	Feb	Mar	Apr	May	Jun	July	Aug	Sept	Oct	Nov	Dec	Annual	POR (years)	No Obs
00-02	16.8	17.5	18.3	22.0	25.3	49.6	53.8	43.3	39.5	34.9	22.9	21.7	30.5	12	13144
03-05	16.2	16.4	21.4	26.9	29.3	53.1	63.4	54.1	46.3	38.8	20.9	18.3	33.7	12	13145
06-08	16.7	16.8	19.3	24.6	24.8	46.3	54.5	48.8	41.5	37.8	18.5	15.0	30.4	12	13145
09-11	10.3	10.8	9.9	10.6	9.6	22.1	19.6	16.8	16.6	18.2	10.1	8.7	13.6	12	13146
12-14	9.0	6.8	6.2	6.9	6.5	9.4	9.1	7.4	9.8	13.7	6.9	5.0	8.1	12	13145
15-17	11.8	11.2	6.6	9.1	7.7	12.5	9.0	6.6	10.0	13.8	10.9	8.9	9.8	12	13143
18-20	12.8	13.2	7.9	12.8	14.7	25.7	17.4	13.1	16.9	18.9	14.6	14.9	15.2	12	13145
21-23	15.5	15.8	12.6	18.6	18.9	36.3	35.0	27.7	27.8	26.9	19.4	20.8	22.9	12	13140
Percent Frequency Ceiling Less Than 300 Feet and/or Visibility Less Than 1 Mile															
Hours (LST)	Jan	Feb	Mar	Apr	May	Jun	July	Aug	Sept	Oct	Nov	Dec	Annual	POR (years)	No Obs
00-02	6.8	7.5	5.1	4.4	0 4	2.2	2.1	0.7	6.9	6.6	9.9	9.8	5.2	12	13144
03-05	6.4	7.5	7.3	5.6	1.3	4.4	4.5	2.2	9.9	10.3	9.5	9.5	6.5	12	13145
06-08	5.6	6.9	5.7	3.4	0.5	2.4	2.9	1.4	7.8	10.3	8.1	5.6	5.1	12	13145
09-11	1.3	1.5	0.6	0.1	0.0	0.0	0.4	0.0	0.3	0.8	1.1	1.2	0.6	12	13146
12-14	0.3	0.5	0.0	0.2	0.0	0.0	0.0	0.0	0.3	1.2	0.5	0.4	0.3	12	13145
15-17	1.9	2.7	0.6	0.4	0.0	0.0	0.0	0.0	0.3	1.5	1.8	1.9	0.9	12	13143
18-20	2.2	2.5	0.6	1.5	0.0	0.0	0.0	0.1	0.7	1.4	3.8	5.6	1.5	12	13145
21-23	6.1	5.2	2.4	2.4	0.0	0.6	0.2	0.4	1.9	3.3	6.9	9.9	3.3	12	13140

Table 2.3-10
AVERAGE NUMBER OF DAYS WITH VISIBILITY LESS THAN 4.8 KILOMETERS (3 MILES) AND RELATIVE HUMIDITY LESS THAN 70% AT LOS ANGELES INTERNATIONAL AIRPORT (PERIOD 1950-1975)[6]

Jan	Feb	Mar	Apr	May	Jun	July	Aug	Sept	Oct	Nov	Dec
5	4	3	2	2	3	5	5	6	8	7	6

The term smog originated in Great Britain as a popular derivation of smoke-fog. However, in southern California the air pollution is referred to as photochemical smog. In photochemical smog, fog is not an essential constituent because, more often than not, low humidity conditions prevail and fog is absent. In southern California, where gas and oil, rather than coal, are the fuels employed, the photochemical smog is light-colored, consisting of solid and liquid aerosols in a fine state of subdivision together with numerous organic and inorganic gases. Its occurrence is accompanied by eye irritation, plant damage, haze, ozone formation, and a characteristic odor.

Smog along the immediate southern California coast occurs during periods in which offshore continental flow predominates. Days are mostly cloudless and warmer than usual. These situations are usually associated with weak Santa Ana conditions in which a high pressure area is over the Great Basin in such a fashion that air spreads outward from the continent and subsides along the coast. In these situations, the inversion is very low and frequently may extend to the ground. The frequency of occurrence of smog conditions along the coast reaches a maximum in the autumn with a minimum in the spring. This variation throughout the year is shown in Table 2.3-10, which gives the average number of days each month (period of record 1950-1975) in which the visibility was less than 4.8 kilometers (3 miles) and the relative humidity was less than 70% at the Los Angeles International Airport. A peak value of 8 days occurs in October with only 2 days in April and May.

The occurrence of smog at San Onofre has no effect on the plant operations and, since the plant does not employ fossil fuel or natural gas except during occasional testing of the emergency diesel, it has an insignificant impact on the photochemical smog.

2.3.2.1.6 Atmospheric Stability

Atmospheric stability was measured at the site over the period from January 25, 1973, to January 24, 1976, with sensors at the 6.1- and 36.5-meter (20- and 120-foot) levels on the tower. Two types of summary tables were computed. The Diurnal Stability and Inversion Frequencies table (Appendix 2.3L, Tables 2.3L-1 through 2.3L-13) lists stability categories and inversions by the hour of the day. Totals are also listed. The Stability and Inversion Persistence table (Appendix 2.3L, Tables 2.3L-14 through 2.3L-26) lists stability categories and inversions by the total number of hours of persistence. Totals are listed along with percentile levels and the maximum number of hours of persistence. These tables were produced for average monthly periods and for the entire data period.

The distribution of occurrences within these tables is influenced by the unequal sizes of the stability categories. Categories A (extremely unstable) and G (extremely stable) are open ends of the spectrum covering ΔT's of ≤0.58°C and >1.22°C, respectively, for the 30.4-meter (100-foot) interval of measurement. Categories B (moderately unstable) and C (slightly unstable) cover the narrow ranges of -0.58°C to -0.52°C to -0.46°C, respectively. Categories D (neutral), E (slightly stable), and F (moderately stable) cover the ranges of -0.46°C to -0.15°C to +0.46°C to 1.22°C, respectively.

The annual and monthly diurnal stability summaries (Appendix 2.3L, Tables 2.3L-1 through 2.3L-13) show stability category G was the most frequent category from 0100 PST until 0700 PST. Stability category D was most frequent at 0800 PST and 0900 PST. By 1000 PST category A is reached more than 50% of the time and remains dominant until 1800 PST. From 1900 PST to 2100 PST, category D is most common, then category G is regained for the rest of the night. Inversions occurred more than 50% of the time at 0100 PST and 2400 PST and more than 40% of the time from 2100 PST to 0600 PST. Inversion frequency was less than 10% from 1100 PST to 1600 PST.

The overall stability and inversion persistence summary (Appendix 2.3L, Table 2.3L-14) shows that persistencies are normally no longer than a few hours. The longest 50 percentile levels are for stability categories A and E and are less than 5 and 2 hours, respectively. Inversion persistence has a 50 percentile level of only 2 hours. All categories have 90 percentile levels of less than 11 hours.

The stability situation at San Onofre is influenced by important local factors. The trajectory of the air, first over the cold current some distance offshore and then over warmer and warmer water as it approaches shore, contributes to making ΔT more negative. A shallow, superadiabatic layer may be established as air in which the surface layer has assumed the temperature of the sea surface in the cold current and then absorbs heat as it moves over progressively warmer water.

The effect of scale compression is another important local factor. As onshore winds blow over the bluff, the general flow pattern would be such that the air nearest sea level would be lifted more and its speed accelerated more as it crosses the bluff than would air at greater heights. Under this common situation, if the lapse rate over the water is adiabatic, it will remain adiabatic as it raises over the bluff. However, an initially superadiabatic lapse rate will become even more unstable.

Further evidence of the prevalence of the tendency to instability is provided by some data from the Shoreline Diffusion Program (Smith and Niemann, 1969). Temperatures were measured at several levels on a 120-meter tower erected on a bluff at the coast near Leucadia, south of San Onofre. All measurements were made with onshore flow in the midafternoon to early evening period. The influences of sea surface temperatures and, possibly scale compression, were demonstrated by the tendency for instability to persist at least until near-sundown.

2.3.2.1.7 Mixing Heights

The mixing height (or depth) is defined as the height above the surface through which relatively vigorous vertical mixing occurs. The lapse rate (temperature change with height) in this layer is roughly dry adiabatic (-9.8°C/km). The depth of the mixing layer at the plant site is determined by the height of the base of the inversion that exists along the southern California coast (see Section 2.3.1.2.6). A climatology of mixing heights for the contiguous United States was made by Holzworth.(7) The morning and afternoon mixing heights were calculated approximately from routine meteorological measurements. The morning mixing height was calculated as the height above ground at which the dry adiabatic extension of the morning minimum surface temperature plus 5°C intersected the vertical temperature profile observed at 1200 Greenwich Meridian Time (GMT). The afternoon mixing height was calculated in the same way as the morning height except the maximum surface temperature observed from 1200 through 1600 PST was employed.

Vertically averaged wind speeds through the mixing layer for both morning and afternoon were computed as arithmetic averages of speeds observed at the surface and aloft within the mixing layer.

Mean seasonal and annual morning and afternoon mixing heights and wind speeds were presented for two southern California coastal stations, San Diego, and Santa Monica. The San Diego depths were obtained from the upper air soundings made at Montgomery Field and hourly surface reports for Lindbergh Field. Lindbergh Field is on the shore of San Diego Bay and Montgomery Field is on the coastal plain about 11 kilometers (7 miles) to the north-northeast. The Santa Monica depths were obtained from upper air soundings at Santa Monica Municipal Airport, Clover Field, and hourly surface weather observations at Los Angeles International Airport. Both locations are about 3 kilometers (2 miles) from the coast. The results obtained for these stations are climatologically representative of the plant site and are presented in Table 2.3-11.

The mixing heights at Santa Monica are in general lower than those found at San Diego. This reflects the known fact that the height of the subsidence inversion along the southern California coast slopes upward toward the south. Assuming a linear change of height with distance, the mixing heights over the plant site were obtained by interpolation of the values in Table 2.3-11 and are presented in Table 2.3-12.

Table 2.3-11
MEAN SEASONAL AND ANNUAL MORNING AND AFTERNOON
MIXING HEIGHTS AND WIND SPEEDS[7]
(Period of Record 1960-1964)

Station	Winter		Spring		Summer		Autumn		Annual	
	Mixing Height (m)	Wind Speed (m/s)	Mixing Height (m)	Wind Speed (m/s)	Mixing Height (m)	Wind Speed (m/s)	Mixing Height (m)	Wind Speed (m/s)	Mixing Height (m)	Wind Speed (m/s)
San Diego:										
Morning	468	2.0	807	2.6	531	2.0	558	2.0	591	2.2
Afternoon	989	4.2	1056	5.1	564	4.1	819	4.3	857	4.4
Santa Monica:										
Morning	376	2.8	651	2.7	552	1.9	487	2.3	516	2.4
Afternoon	863	4.4	946	5.9	603	5.1	785	4.8	799	5.1

Table 2.3-12
MEAN SEASONAL AND ANNUAL MORNING AND AFTERNOON
MIXING HEIGHTS AT SAN ONOFRE

	Winter (m)	Spring (m)	Summer (m)	Autumn (m)	Annual (m)
Morning	427	738	540	527	558
Afternoon	933	1007	581	804	831

The mixing heights at San Onofre reach a maximum in the spring and have a minimum during the winter. The winter minimum is caused by the relatively high frequency of surface inversions along the coast in this season. In the spring the surface inversions become less frequent and weaker and the persistent summertime subsidence inversion (see Section 2.3.1.2.6) has not yet formed along the coast. These conditions are favorable for the elimination of the inversions by insolational heating followed by the formation of a thick mixing layer. During the summer and autumn seasons the subsidence inversion is very strong and persistent. Although insolation may weaken its strength, it frequently persists continuously along the coast for many days. This condition restricts the height of the mixing layer to the base of the inversion. The summer and autumn mixing heights are in good agreement with the average inversion base heights given in Section 2.3.1.2.6.

The mixing heights are in general higher than the hills (450-500 meters) which lie to the east and southeast of the plant site. Only the morning mixing depths in the winter have an average height less than the hills. However, during this season the morning flow is generally offshore. Any pollutants released on the coast would, in general, be carried out to sea rather than trapped along the inland hills.

2.3.2.2 Potential Influence of the Plant and Its Facilities on Local Meteorology

The effect of the plant on the local meteorology in the mesoscale is insignificant. Modification of local terrain as a consequence of the construction of the plant and the additions of the plant and its facilities to the site will redistribute the natural terrain features and add roughness elements. The detectable micro-scale effect of the change will become undetectable to the average climate of the 20 square mile area around the plant.

The micro-scale effect of the plant and its facilities is both variable and complex. It is unlikely that this effect can be detected in the data from the meteorological tower on the bluff since the bluff effect will be larger than the building effects at the tower position when the wind is from the infrequent ESE direction. In all wind directions, the only notable effect will be the addition of mechanical turbulence to the air which enhances diffusion.

Operational cooling is accomplished entirely through the closed heat exchange with the Pacific Ocean. Modest increases in localized surface temperature of the water offshore will not add significantly to the air temperature or water vapor content of the local meteorology. What little heat is added will increase the instability of the air and enhance mixing and diffusion.

Figure 2.3-6 is a topographical map of the region within 5 miles of the plant. Figures 2.3-7 and 2.3-8 show the maximum elevation versus distance from the center of Units 2 and 3 within 22.5-degree compass point sectors. Elevations and distances are in feet and meters. The vertical exaggeration is a factor of five.

2.3.2.3 Local Meteorological Conditions for Design and Operating Bases

The meteorological conditions used as the design and operating bases are:

A. Temperature:

1.	Average annual	60°F
2.	Maximum monthly average (July)	72°F
3.	Minimum monthly average (Feb)	42°F
4.	Maximum	85°F[a]
5.	Minimum	36°F[a]

B. Precipitation:

1.	Average annual	12 in.
2.	Number of days With measurable	40
3.	Rate	3 in./h

[a] This temperature value is for San Clemente and is taken from Recommended Outdoor Design Temperatures, Southern California, Arizona, Nevada, published by the Southern California Chapter of American Society of Heating Refrigerating and Air Conditioning Engineers, Inc. (ASHRAE) Fourth Edition, October 1972.

2.3.3 ONSITE METEOROLOGICAL MEASUREMENT PROGRAM

The onsite meteorological program at the San Onofre Nuclear Generating Station began in the latter part of 1964. At this time a wind measuring system, consisting of a vector vane, was mounted at the top of a 19.5-meter (64-foot) mast about 150 meters (500 feet) northwest of the North Industrial Area (formerly the Unit 1 reactor site). Data was collected from the system through December 1969. The program resumed in December 1970 when a 36.6-meter (120-foot) tower was installed.

The meteorological tower is located on the Pacific Coast atop a bluff 29.6 meters (97.0 feet) above mean lower low water and approximately 60 meters (197 feet) inland from the mean high water line. The tower is situated approximately 38 meters (125 feet) from the edge of the bluff overlooking the beach and is approximately 423 meters (1390 feet) west-northwest from the Unit 2 containment structure. The tower location is marked on the site map.

The primary tower is an open face (latticed) Rohn model 45GSR, 42.55-centimeter (16-3/4-inch) equilateral triangle design with 3.175-centimeter (1-1/4-inch), solid steel rod for side rails and 1.11 centimeter (7/16 inch) solid rod cross braces in a zigzag pattern of 40-centimeter (15-3/4-inch) steps. The present tower is 43 meters (141 foot - 3 inches) high, is designed per ANSI/EIA-222-D-1986 for 100 MPH wind loads, and in accordance with UBC (1988) Zone 4 seismic criteria.

The legs of the equilateral triangle are oriented on bearings of 170°, 110°, and 230°. Instrument support booms are mounted on a two level instrument elevator at a bearing of 200°. Instrument distance from the tower is measured from the nearest point of the tower. Temperature sensors are 0.46 meters (18 inches) out and wind sensors are 1.22 meters (4 feet) out from the tower with the exception of a 36.6-meter level wind sensor which was located directly on top of the tower until the tower was extended. Guy wires on the extended tower are 0.794 and 0.635 centimeters (1/4 inches) in diameter and are located at 12.5 meters (44 feet), 24.7 meters (81 feet), and 39 meters (128 feet). There are three guy wire anchors, each located 21.3 meters (70 feet) from the base of the tower. The system installed on the tower measures wind speed, wind direction, and turbulence at the 40-meter level; temperature difference between the 10- and 40-meter levels; and wind speed and wind direction at 10- and 40-meter levels.

The system was again modified in October 1975, in April 1981, July 1987, December 1994, and in March 2008. A detailed description of these modifications is presented in Paragraph 2.3.3.1.1.

The data covers the 3-year period January 25, 1973, through January 25, 1976.

In addition to the 40-meter tower, which is considered the primary source of onsite meteorological information, a backup tower was installed in November 1982. This tower is also located atop the coastal bluff approximately 54.4 meters (178.3 feet) east of the primary 40-meter tower.

The backup tower is an open face (latticed) Tri-ex Model T-20, 30.5 feet in height. It is constructed with a 46.2-centimeter (18.2-inch) triangular design with 3.8-centimeter (1-1/2-inch) steel tubing for side rails and 1.1-centimeter (7/16-inch) solid rod cross braces in a zigzag pattern of 38-centimeter (15-inch) steps. The tower is unguyed and includes an instrument elevator for easy access to the sensors. The fully loaded tower structure is designed for a minimum horizontal wind pressure of 123.3 kg/m^2 (15 lb/ft^2) on flat surfaces.

The instrument sensors are mounted on a boom projecting from the instrument elevator. A detailed discussion of the back-up instrumentation is given in Paragraph 2.3.3.1.1.

A tracer test was performed in order to obtain a measurement of actual atmospheric dispersion at the site. An inert gas tracer was released from points approximating effluent release points and then collected downwind. The concentration of the collected tracer gas was used to compute the actual atmospheric dispersion at the site. These results are summarized in Subsection 2.3.4.

The 3-year onsite meteorological measurement program is discussed in Paragraphs 2.3.3.1 through 2.3.3.6.

2.3.3.1 Instrumentation

The San Onofre Units 2 and 3 meteorological measurement system is consistent with the recommendations of NRC Regulatory Guide 1.23.

As of November 10, 1975, the primary system records digital signals on magnetic tape. In 1988, the data logger and magnetic tape units were replaced with an industrial personal computer. The original analog signals are recorded on strip charts as a backup system. Prior to November 10, 1975, the recording was entirely analog. The instrumentation systems are described in more detail below.

2.3.3.1.1 Meteorological Measurement Systems

The system in operation during the period of January 25, 1973, to October 2, 1975, included the following:

Parameter	Level 6.1 (m)	10 (m)	36.6 (m)	6.1-36.5 (m)
Wind speed		x	x	
Wind direction		x	x	
Dry bulb temperature[a]	x			
Wet bulb temperature[b]	x			
Sigma			x	
Delta temperature				x

[a] The dry bulb sensor was installed January 25, 1974.
[b] The wet bulb sensor was installed January 25, 1974, and removed January 24, 1975.

Modifications to the instrument system occurred between October 2, 1975, and October 31, 1975. The tower was extended on October 3, 1975, by 6.1 meters. On October 10, 1975, the wind sensor previously at 36.6 meters was moved to 40 meters. A new wind sensor was installed at the 20-meter (66-foot) level on October 20, 1975. Installation and calibration of new primary and backup delta temperature systems were completed on October 30, 1975. The lower wind sensor level is 10 meters. Sigma measurement from 36.6 meters ends October 3, 1975, and begins at the 10-meter level October 29, 1975. The new instrument system which was completed on October 31, 1975, includes the following:

Parameter	Level 10 (m)	20 (m)	40 (m)	10-40 (m)	6.1-36.5 (m)
Wind speed	x	x	x		
Wind direction	x	x	x		
Temperature	x				
Sigma	x				
Delta temperature (primary)				x	
Delta temperature (secondary)				x	
Delta temperature (comparison)					x

Further modifications to the primary meteorological tower system were completed on April 20, 1981 with the addition of dew point and precipitation sensors and the elimination of the wind speed and wind direction sensors at 20 meters. The dew point sensor is located at the 10-meter level on the primary tower while the precipitation sensor is located near ground level adjacent to the instrument shelter. In July 1989, the primary tower was replaced with a ROHN 45GSR tower equipped with a two level TS2500 instrument elevator. All sensors were unchanged except for ΔT 6.1-36.5 meters which was removed from service. In March 2008, the 10m dew point sensor was replaced with a relative humidity sensor. The current configuration is as shown below:

Parameter	Level 3 (m)	10 (m)	40 (m)	10-40 (m)
Wind speed		x	x	
Wind direction		x	x	
Temperature		x		
Sigma		x		
Delta temperature (primary)				x
Delta temperature (secondary)				x
Relative Humidity		x		
Precipitation	x			

The backup meteorological tower, which became operational November 2, 1982, is comprised of sensors to record wind speed, wind direction, and sigma theta at the 10-meter level.

In 1994 the Meteorological Measurement System was upgraded by replacing all the sensing instruments on both the primary and backup meteorological towers and the removal of all the electronics and the electronics shelter at the reservoir and replacing them with two new dataloggers located in weatherproof enclosures. An alternate power supply was also added to supply both towers electronics by manually transferring from the primary power source on loss of power.

The sensors, related system equipment, model and serial numbers, and locations on the tower are listed in Tables 2.3-13, 2.3-14 and 2.3-15, respectively, for the system prior to the October 1975 modifications and after the modifications of October 1975 and April 1981. The specifications for the sensors and the analog and digital system accuracies are given in Table 2.3-16. The measurements are described in Paragraph 2.3.3.2.

Table 2.3-13
INSTRUMENTATION AND ASSOCIATED EQUIPMENT INSTALLED
IN THE SAN ONOFRE SYSTEM
UNTIL THE OCTOBER 1975 MODIFICATIONS

Sensors					
Sensor Type	Model Numbers[(a)]	Serial Numbers	Mounting Height (m)	Distance from tower (m)	Direction from tower
Wind	1074-2	114	36.6	On top	NA
Wind	1074-2	259	10	1.2	SW
Delta temperature	809-1	102/507B[(b)]	36.5	0.5	NNW
Delta temperature	809-1	101/507A[(b)]	6.1	0.5	NNW
Temperature[(c)]	809-1/832-1[(c)]	174/002[(c)]	6.1	0.5	NE
Wet bulb temperature[(d)]	809-1	147	6.1	0.5	SW
Backup temperature[(e)]	809/832-1[(e)]	147/002[(e)]	6.1	0.5	SW

Recording Equipment[(f)]		
Equipment Type	Model Number	Serial Number
EA recorder	602	153479
EA recorder	602	153480
EA recorder	602	317824
EA recorder	602	317823

Electronics	
Electronics Type	Model Number
Sigma	None
Delta temperature	170900
Temperature	13495
Transmuter	1034/1001[(g)]
Tachometer	12905
Nonlinear amplifier	13940
540° azimuth amplifier	12819

(a) Manufactured by Meteorology Research, Inc. (MRI), Altadena, CA

(b) Sensor serial numbers 102, 101 replaced May 13, 1975, by serial numbers 507A, 507B

(c) Sensor model 809-1 serial 147, installed January 25, 1974, replaced September 30, 1975, by model 832-1 serial 002

(d) Installed January 25, 1974, removed January 24, 1975

(e) Sensor model 809 serial 147, installed January 24, 1975, replaced by model 832-1 serial 002, January 18, 1975, until August 30, 1975

(f) Data up to October 19, 1975, was recorded entirely on this equipment

(g) Model 1034 was the specific transmuter originally installed for the San Onofre system in January 1973. Model 1001 is the general model number for the two identical transmuters in operation after the October 1975, modifications

Table 2.3-14
INSTRUMENTATION SYSTEM INSTALLED IN THE SAN ONOFRE SYSTEM
BETWEEN OCTOBER 1975 AND APRIL 20, 1981

Sensor Type	Model Numbers[a]	Serial Numbers	Mounting Height (m)	Distance from tower (m)	Direction from tower
Wind	1074-2	452	40	1.2	SW
Wind[b]	1074-2	539	20	1.2	SW
Wind	1074-2	259	10	1.2	SW
Temp	809-2	002	10	0.5	NNW
Delta T - primary	840-1	532B	40	0.5	SW
Delta T - primary	840-1	532A	10	0.5	SW
Delta T - secondary	840-1	539A	40	0.5	WNW
Delta T - secondary	809-1	539B	10	0.5	WNW
Delta T old	840-1	507B	36.5	0.5	WNW
Delta T old	840-2	507A	6.1	0.5	WNW

Recording Equipment[c]

Equipment Type	Model Number	Serial Number[d]
EA recorder	602	153479
EA recorder	602	153480
EA recorder	602	317824
EA recorder	602	317823
EA recorder	601C	195888
EA recorder	601C	197369
EA recorder	601C	194758-L
EA recorder	601C	517442
EA recorder	601C	194429
Data logger	1751A	10020
Tape recorder	1600/360	404 - 1474

Electronics

Electronics Type	Model Number
Tachometer	12905
Transmuter	1001
Sigma	None
Temperature	13495
Delta temperature	170900
Nonlinear amplifier	13940
540° azimuth amplifier	12819

(a) Manufactured by Meteorology Research, Inc. (MRI), Altadena, CA

(b) Discontinued April 20, 1981.

(c) EA recorder system was established October 20-24, 1975. The data logger, tape recorder digital system became fully operational November 10, 1975

(d) The serial numbers shown are those originally installed and may change during normal operation due to maintenance activities.

Table 2.3-15
INSTRUMENTATION SYSTEMS INSTALLED AT SAN ONOFRE
AFTER THE APRIL 20, 1981 MODIFICATIONS (Sheet 1 of 2)

Sensor Type	Model Numbers	Serial[a] Numbers	Mounting Height	Distance from tower	Direction from tower
Primary Tower					
Wind	1074-2	226	40	1.2	SW
Wind	1074-2	661	10	1.2	SW
Temp	809-1	1596602	10	0.5	NNW
Delta T - primary	840-1	B779	40	0.5	SW
Delta T - primary	840-1	A779	10	0.5	SW
Delta T - secondary	840-1	004-8	40	0.5	WNW
Delta T - secondary	840-1	004-7	10	0.5	WNW
Delta T old	809-1	004-2	36.5	0.5	WNW
Delta T old	809-2	004-1	6.1	0.5	WNW
Dew point	890-1	202	10	0.5	-
Precipitation	302	1987	3.0	-	E
Backup Tower					
Wind	1074	1137	10	1.2	SSW

Recording Equipment

Equipment Type	Model Number	Serial Number
Primary Tower		
EA Recorder	601C	195849-L
EA Recorder	601C	153479
EA Recorder	601C	153479
EA Recorder	601C	520493
EA Recorder	601C	522156
EA Recorder	601C	520774
EA Recorder	601C	522191
EA Recorder	601C	194758-L
EA Recorder	601C	522149
EA Recorder	601C	522154
Data Logger	1751A	10020
Tape Recorder	1600/360	404-1474
Backup Tower		
EA Recorder	1905-1	None
EA Recorder	1903-1	525771

[a] The serial numbers shown are those originally installed and may change during normal operation due to maintenance activities.

Table 2.3-15
INSTRUMENTATION SYSTEMS INSTALLED AT SAN ONOFRE AFTER
THE APRIL 20, 1981 MODIFICATIONS (Sheet 2 of 2)

Electronics	
Electronics Type	Model Number
Primary Tower	
Tachometer	12905-3
Transmuter	1001
Sigma	1431200
Temperature	1349500
Delta temperature	1709000
Nonlinear amplifier	-
540° azimuth amplifier	1430300
Precipitation	1594800
Backup Tower	
Tachometer	2043100
Transmuter	2001
Sigma	2093770
Nonlinear amplifier	-
540° azimuth amplifier	2094300

2.3.3.1.2 Data Logging and Recording

From January 25, 1973, until October 17, 1975, the equipment consisted of an analog strip chart system with Esterline-Angus model 602 series analog recorders. Voltages ranging from 0 to 5V-dc were accepted from sensors and appropriate circuitry and were used to drive the scribes on the recorders. This range of voltages was used to cover the range of the measured parameters. Effective chart width was 5.08 centimeters (2 inches) per parameter. Each chart had the capacity to record two parameters and was graduated with a 7.62 cm/h (3 in./h) time scale. From October 9, 1975, to October 24, 1975, new Esterline-Angus model 601C recorders were added to the existing recorders to handle the increase in parameters. The analog charts for the new recorder arrangement are of two types. One is as described above, the other has an effective chart width of 11.43 centimeters (4-1/2 inches) per parameter and one parameter per chart. The 11.43-centimeter chart widths apply to the 10- and 40-meter wind directions and all of the delta temperature measurements.

Table 2.3-15a
INSTRUMENTATION SYSTEMS INSTALLED AT SAN ONOFRE
AFTER THE 1988 MODIFICATIONS (Sheet 1 of 2)

Sensor Type	Model Numbers	Serial[a] Numbers	Mounting Height	Distance from Tower	Direction from Tower
Primary Tower					
Wind	1074-2	226	40	1.2	SW
Wind	1074-2	661	10	1.2	SW
Temp	809-1	1596602	10	0.5	NNW
Delta T - Primary	840-1	B779	40	0.5	SW
Delta T - Primary	840-1	A779	10	0.5	SW
Delta T - secondary	840-1	004-8	40	0.5	WNW
Delta T - secondary	840-1	004-7	10	0.5	WNW
Delta T old	809-1	004-2	36.5	0.5	WNW
Delta T old	809-1	004-1	6.1	0.5	WNW
Dew point	890-1	202	10	0.5	-
Precipitation	302	1987	3.0	-	E
Backup Tower					
Wind	1074	1137	10	1.2	SSW

Recording Equipment

Equipment Type	Model Number	Serial Number
Primary Tower		
EA Recorder	601C	195849-L
EA Recorder	601C	153479
EA Recorder	601C	153479
EA Recorder	601C	520493
EA Recorder	601C	522156
EA Recorder	601C	520774
EA Recorder	601C	522191
EA Recorder	601C	194758-L
EA Recorder	601C	522149
EA Recorder	601C	522154
Data Industrial PC	QPC 5000 Series	
Backup Tower		
EA Recorder	1905-1	None
EA Recorder	1903-1	525771

[a] The serial numbers shown are those originally installed and may change during normal operation due to maintenance activities.

Table 2.3-15a
INSTRUMENTATION SYSTEMS INSTALLED AT SAN ONOFRE AFTER THE 1988 MODIFICATIONS (Sheet 2 of 2)

Electronics	
Electronics Type	Model Number
Primary Tower	
Tachometer	12905-3
Transmuter	1001
Sigma	1431200
Temperature	1349500
Delta temperature	1709000
Nonlinear amplifier	-
540° azimuth amplifier	1430300
Precipitation	1594800
Backup Tower	
Tachometer	2043100
Transmuter	2001
Sigma	2093770
Nonlinear amplifier	-
540° azimuth amplifier	2094300

Table 2.3-15b
INSTRUMENTATION SYSTEMS INSTALLED AT SAN ONOFRE
AFTER THE 1994 MODIFICATIONS (Sheet 1 of 2)

Sensor Type	Model Numbers	Mounting Height	Distance from Tower	Direction from Tower
Primary Tower				
Wind	100075/ 100076	40	>1.2	SW
Wind	100075/ 100076	10	>1.2	SW
Temp	100093	10	>0.5	SW
Temp	100093	40	>0.5	SW
Delta T Primary Temp	100093	10	>0.5	SW
Delta T Primary Temp	100093	40	>0.5	SW
Delta T Secondary Temp	100093	10	>0.5	SW
Delta T Secondary Dew Point	101197	10	>0.5	SW
Backup Tower				
Wind	100075/ 100076	10	>1.2	SW
Precipitation	100097	~2	---	W

Recording Equipment

Equipment Type	Model Number
Primary Tower	
EA Recorder	601C
EA Recorder	601C
Westronic Recorder	DDR10
Backup Tower	
Westronic Recorder	DDR10

Table 2.3-15b
INSTRUMENTATION SYSTEMS INSTALLED AT SAN ONOFRE AFTER
THE 1994 MODIFICATIONS (Sheet 2 of 2)

Electronics	
Electronics Type	Model Number
Primary Tower	
Wind Speed Sensors	100075
Wind Direction Sensor	100076
Temperature Sensors	100093
Dew Point Sensors	101197
IMP 860 Processor	N/A
Backup Tower	
Tipping Bucket Rain Gauge	100097
Wind Speed Sensors	100075
Wind Direction Sensor	100076
IMP 860 Processor	N/A

Note: Instrumentation system changes at San Onofre after March of 2008 were limited to the dew point sensor. This sensor was replaced with a relative humidity sensor. The new sensor is described below in Table 2.3-15c.

Table 2.3-15c
MARCH OF 2008 MODIFICATIONS TO THE MAIN MET TOWER

Sensor /Type	Model #	Mounting Height	Distance From Tower	Direction From Tower
Relative Humidity (Capacitive)	102273	10	>0.5	SW

Table 2.3-16
METEOROLOGICAL SENSOR AND SYSTEM
SPECIFICATIONS AND ACCURACIES

Parameter	Specifications and Minimum System Accuracy
Wind speed	Minimum system accuracy = ±0.15 m/h or ± - 1% Response distance: 13.1 ft Operating temperature = -40°C to +60°C Starting speed = 0.5 m/h
Wind direction	Minimum system accuracy = +/- 2.0° Wind recovery = 3 ft Damping ratio = 0.4 at 10° Operating temperature = -40°C to +60°C Starting speed = 0.5 m/h
Temperature and wet bulb temperature	Minimum system accuracy = ±0.15°C Vendor Operating temperature = -30°C to +50°C Range = -30°C to +50°C Digital resolution = 0.16°C (Linearity)
Delta temperature	Minimum system accuracy = ±0.15°C Operating temperature = -30°C to +50°C Range = ±3°C Digital resolution = 0.16°C (Linearity)
Sigma	Minimum system accuracy ≈ ±2.0° Sampling time = 4 s Averaging time = 900 s Range = 0 to 45° Environment = - 40°C to + 60°C
Relative Humidity	Minimum system accuracy =< ±1% RH from 0 to 100% Operating temperature = -40°C to +60°C Range = 0 to 100%
Precipitation	Minimum system accuracy = ±3% (Rates 1 to 6 in/hr)

A digital system became the primary system on November 10, 1975. This system consists of a Kennedy model 1600/360 incremental magnetic tape recorder, a Spectra system data logger model 55-20 DLI (MRI model 1751 A), and MRI model 1001 transmuters containing signal conditioning circuit boards. The recorder was a nine-track 800 BPI unit that uses half-inch magnetic tape. In 1988, the data logger and magnetic tape units were replaced with an industrial personal computer. Analog charts are changed at intervals of 14 days.

2.3.3.2 Measurements

The nature of the various measurements is discussed in the following paragraphs.

2.3.3.2.1 Wind Direction

The sensor consists of a counterbalanced, lightweight vane attached to a shaft which is coupled to a precision low torque potentiometer. Wind direction via vane position is converted to a proportional DC voltage by a potentiometer.

The continuous analog output voltage from this unit is input to a fully programmable datalogger. With the digital system, the output voltage is sampled by a PC once every 10 seconds and the value averaged over 15 minutes is recorded on a hard disk.

2.3.3.2.2 Wind Speed

A disk with slots around its perimeter is driven by a cup assembly mounted on the wind speed shaft. A light and phototransistor is mounted in such a way that the perimeter of the wheel interrupts the passage of light to the phototransistor, thus producing pulses. With a potentiometer and linear amplifier, these pulses are converted into an output frequency proportional to wind speed. The operating range is 0-125 MPH. The output from the circuits is sampled at few second intervals, averaged over 15 minutes and then recorded on a hard disk. The output voltage is input to a data logger that drives the CDAS MET recorded data.

2.3.3.2.3 Temperature

The sensor is a shielded and power-aspirated linear thermistor network. The datalogger applies an excitation voltage to the thermistor network, makes a voltage measurement across a resistor in series with the thermistor and calculates the temperature. The datalogger transmits a digital signal with temperature information to the CDAS. In the digital system it is sampled every few seconds, averaged over 15 minutes, and then recorded on a hard disk.

2.3.3.2.4 Temperature Differential

Two temperature sensors, as described above, are located at different levels on the tower. The voltage output from each sensor is fed to the datalogger which combines the voltages and calculates the temperature. The datalogger transmits the differential temperature data to the CDAS.

2.3.3.2.5 Wet Bulb Temperature

The wet bulb sensor was the same as the temperature sensor described above, with the exception that a wetted wick was attached. The wick was kept wet by means of a siphon and reservoir system. The continuous output was a voltage which was recorded in the same manner as temperature. Relative humidity was obtained through the use of wet and dry bulb temperatures and a psychometric conversion.

Since the station will use once-through cooling, a humidity measurement is not specifically needed. For this reason, recovery of these data has been discontinued and was planned not to be a part of the normal systems of the extended tower.

2.3.3.2.6 Turbulence (Sigma)

Turbulence is determined through the use of a sigma calculation in the MET/PIC RTIME computer server. In this unit the fluctuating voltage output of the wind vane potentiometers is passed through a processor and averaged to obtain the standard deviation of the horizontal wind direction, commonly called sigma. The sigma meter works according to the principles presented by Jones and Pasquill in 1959.[8] In the 15-minute mode used at San Onofre, a continuously updated standard deviation of wind direction changes, in the frequency band between 3 minutes per cycle and the highest frequency to which the sensor can respond, is measured and averaged with a 15-minute time constant. This encompasses that portion of the turbulence spectrum that is responsible for initial diffusion of effluent clouds. The data is available in CDAS. The level of measurement was moved from 36.6 meters to 10 meters in October 1975, to meet the NRC guidelines for its use.

2.3.3.2.7 Dew Point (Measurement done with Relative Humidity Sensor)

Relative Humidity is measured with a capacitive Relative Humidity (RH) sensor; the sensor element is built out of a film capacitor on different substrates (glass, ceramic, etc.). The dielectric is a polymer that absorbs or releases water proportional to the relative environmental humidity, thereby changing the capacitance of the capacitor. The change in capacitance can be measured by an electronic circuit, allowing the relative air humidity to be determined. The sensor reports directly in dew point through a calculation based on measured relative humidity (RH) and the measured temperature of the heated capacitive element.

2.3.3.2.8 Precipitation

The precipitation sensor is a tipping bucket range gage with low inertia tipping bucket. One tip of the bucket is equivalent to 1/100 inch of rain. A deep funnel in the collector assures proper collection efficiencies. A frictionless magnetic reed switch gives a contact closure for each tip of the bucket. Precipitation data is available in the CDAS.

2.3.3.3 Calibration and Maintenance

All sensors and related equipment are calibrated according to written procedures. These procedures are designed to assure adherence to NRC specifications for accuracy. The first calibration is accomplished on the fully assembled system in the plant before delivery. A calibration check is made following installation. Additional calibrations are made on semiannual schedule. Minor checks and adjustments are made at other times.

All meters and other equipment used in calibrations are in turn calibrated at frequent intervals. All calibrated instruments used have evidence of accuracy in the historical record, which is traceable to the National Bureau of Standards.

2.3.3.3.1 (Deleted)

2.3.3.3.2 Maintenance

Inspection and maintenance of all equipment is accomplished in accordance with written procedures. Individual components are removed for servicing at intervals specified in the manual or more frequently if the need is detected. If the maintenance required cannot be accomplished at the site, the component concerned is returned to the manufacturer for refurbishing.

In case of major trouble in the system, an electronics technician or engineer is dispatched to the site on short notice to investigate and correct any malfunction.

2.3.3.3.3 Onsite Monitoring

The meteorological parameters at San Onofre are displayed in the Units 2/3 Control Room/Command Center on CDAS displays including recording capabilities. Control Room/Command Center personnel visually inspect CDAS display twice a day to ensure that the output appears accurate and reasonable. If a malfunction or failure is detected which cannot readily be corrected by the station personnel, appropriate SCE personnel are informed and instrument repair technicians are dispatched to identify and correct any malfunctions.

2.3.3.3.4 Data Monitoring

All meteorological CDAS digital data is screened manually and automatically checked for validity by the CDAS Software.

The primary purpose of this accuracy control procedure is to detect signs of malfunction or the need for maintenance as soon after the need arises as possible. When a need for servicing is detected, station personnel are advised immediately so they can plan and execute any corrective action.

The inspection criteria for data monitoring are given in the procedures. These criteria emphasize such factors as reasonableness and consistency among parameters as well as the presence of expected diurnal variations.

2.3.3.4 Data Analysis Procedures

The analysis procedures used on San Onofre data are designed to obtain the most accurate data and analysis possible. They are responsive to Regulatory Guide 1.23.

2.3.3.4.1 Data Accuracy Control

As described in Paragraph 2.3.3.3.4, all data are subjected to an accuracy check. The meteorological data is monitored via surveillances for validity, reasonableness and continuity including:

- Reasonableness of data:
  - The proper diurnal variations of temperature, humidity, and temperature difference
  - The absolute values of these and other variables
  - The relationships among such variables as wind speed, temperature, and temperature difference
- Continuity of data and of instrument operation
- Evidence of power interruptions or malfunctions.

The CDAS validates the MET signals and flags those which do not meet the established screening criteria. For usable data, a listing is obtained and the data are given a preliminary inspection for consistency and reasonableness and to locate any gaps. The accuracy control procedure is intended to detect electronic or sensor drift or malfunction, improper mechanical zero adjustment, or any other source of error in the data. All data gaps are filled, where possible, using data from other sources.

2.3.3.4.2 Data Reduction

Reduction of analog charts, prior to November 10, 1975, to obtain average values was accomplished on an Oscar S2 semi-automatic chart reader.

Averages of 15 minutes of data are representative of 1 hour of data and are hereafter referred to as hourly values. The reduced data were first punched on cards, and then converted to engineering units and transferred to magnetic tape. A preliminary data listing was made and reviewed.

Wind direction, temperature, wet bulb temperature, wind speed, and temperature difference are averaged over a 15-minute period centered on the hour. Because sigma is already averaged over a 15-minute period, the reading at 7.5 minutes past the hour is selected, yielding a 15-minute average centered on the hour. All data were entered on a master tape as hourly values.

Until November 10, 1975, all data came from analog charts. On November 10, 1975, the digital system became operational and became the primary source. Analog charts are reduced when necessary to fill gaps when digital data are missing or erroneous and uncorrectable. Digital data averages are for the same time periods as the analog.

As of summer of 2011 Meteorological data is no longer monitored via analog charts.

2.3.3.4.3 Analysis

The hourly data obtained as described are compiled into a series of summary tables as specified in the references named above and as illustrated in Subsection 2.3.2. Most of these tables are produced by month and year. They are used as input for evaluating local meteorological conditions and form the base line for potential influences of the plant and its facilities on the local meteorology.

2.3.3.5 <u>Data Recovery</u>

Data recovery percentage rates listed in Table 2.3-17 are computed from the total number of hours of valid data and the total number of possible hours between January 25, 1973, 0100 PST and January 24, 1976, 2400 PST for each parameter except temperature. The temperature sensor was installed and calibrated on January 26, 1974, with the first hour of valid data at 1100 PST; therefore, this date and time are used as the beginning. Because of the changes in instrument levels during October 1975, some parameters are for combined levels. The periods for each level do not overlap. The recovery rate list includes all the major parameters but not the auxiliary parameters installed for only brief periods.

Recovery rates are generally above the 90% target with the exceptions of the 36.6/40-meter wind direction and the ΔT. The wind direction parameter suffered a major loss of data because of a malfunction that caused erroneous scribe movements on the recorder. The entire interval from August 14, 1973, 2000 PST to January 25, 1974, 1000 PST was discarded in order to ensure a valid data base. The delta temperature data from January 25, 1974, 1000 PST through March 30, 1974, 1100 PST was unusable because of instrument malfunction.

Table 2.3-17
DATA RECOVERY

Parameter	Percent Data Recovered
10m wind speed	96.0
10m wind direction	96.0
36.6/40m wind speed	94.3
36.6/40m wind direction	80.2
6.1/10m temperature	97.2
36.6/10m sigma	91.0
6.1/36.5, 10/40m delta temperature	89.5

2.3.3.6 Wind and Stability at the Plant Site

The annual joint frequency wind speed-direction summaries stratified by Pasquill stability categories for both the lower and upper levels are shown in Appendix 2.3B, Tables 2.3B-1 through 2.3B-7 and Tables 2.3B-8 through 2.3B-14, respectively. The strong dependence of stability categories to onshore and offshore wind flow is indicated in Table 2.3-18. The unstable categories A, B, and C occur principally with onshore flow. The stable categories F and G are associated principally with offshore flow. The average wind speeds for the categories A through E for both onshore and offshore flow are nearly equal, i.e., 3 m/s. However, for the stable categories F and G there is an increasing tendency for the offshore flow to be stronger than onshore flow by 1 to 2 m/s.

Long-term (10 years) annual joint frequency wind speed-direction summaries stratified by Pasquill stability are presented in Appendix 2.3C, Tables 2.3C-1 through 2.3C-8 for San Diego (Lindbergh Field) and in Appendix 2.3D, Tables 2.3D-1 through 2.3D-8 for Los Angeles (Los Angeles International Airport). The stability categories were determined by the NWS STAR program and were obtained from the Environmental Data Service of the National Oceanic and Atmospheric Administration. A short-term (January 1973-December 1974) set of stability-wind summaries for each of these stations is given in Appendix 2.3E, Tables 2.3E-1 through 2.3E-16. The long-term tables from the STAR program are based on 24 observations per day, while the short-term STAR tables are based on 8 observations per day. The short-term tables are concurrent with the first 2 years of the San Onofre data. A comparison of the stability frequencies for San Diego and Los Angeles (see Table 2.3-19) shows rather good agreement between stations. At Los Angeles, the short-term distributions are quite similar to those for the long-term period. At San Diego, however, the D category shows a higher frequency for the short-term period while the G category shows a lower frequency for the short-term period. The average difference is about 3%. The short-term and long-term average wind speeds in each stability category also are in rather good agreement.

From this rather good agreement of the short-term data with the longer period of record of stability data and the previously noted agreement of long-term (30 years) climatological data normal with the averages of the individual years of 1973 and 1974, it may be concluded that the short-term data taken at San Onofre are representative of a long-term average.

A comparison of the frequency distribution of stability categories between the San Onofre tower measurements and those obtained by the STAR model for Los Angeles and San Diego is shown in Table 2.3-20. The unstable category (A + B + C) frequencies from the tower are about 10% higher and the stable category frequencies (F + G) about 10% lower than those obtained from the STAR model. The neutral (D + E) category frequencies, however, are in closer agreement.

These differences in the unstable category frequencies stem from two factors. The first is related to the fact that the STAR model tends to underestimate the frequency of unstable hours and overestimate the neutral and stable hours. The second factor is the passage of air over progressively warmer water as it moves toward the coast. During the summer months the water

surface temperature gradient, over which the air moves, reaches a maximum of about 40 per 180 kilometers (112 miles). Because frictional stresses over the water are a minimum, very little mechanical turbulence occurs. This permits the lapse rates in the lower levels to become super-adiabatic (≤9.8°C per kilometer) by the time the air reaches the coastline. The STAR model does not consider this type of phenomenon and consequently will underestimate the instability frequencies as well as the magnitude of the instability. Smith,[(9)] in a comparison of STAR model results with tower measurements at New Orleans, Louisiana, and Wilmington, Delaware, and vicinity showed the following results as given in Table 2.3-21.

Table 2.3-18
ANNUAL WIND CHARACTERISTICS AND PASQUILL STABILITY CATEGORIES
(Period of Record January 25, 1973-January 24, 1976)

Lower Level (10 meters)					
		Onshore Wind		Offshore Wind	
Stability Category	Percent Frequency	Frequency (%)	Average Speed (m/s)	Frequency (%)	Average Speed (m/s)
A	26.75	91.5	3.5	8.5	4.0
B	3.10	78.7	3.0	21.3	2.8
C	3.96	74.0	3.0	26.0	2.9
D	21.73	67.1	3.3	32.9	2.7
E	17.76	47.5	3.2	52.5	2.8
F	8.41	20.6	2.3	79.4	2.7
G	18.28	9.1	1.8	90.9	3.7
Upper Level (36.6m and 40m Combined)					
A	29.28	94.3	3.6	5.7	3.9
B	3.26	81.0	3.1	19.0	3.2
C	4.36	76.4	3.1	23.6	3.2
D	22.91	66.4	3.3	33.6	2.8
E	15.56	48.3	3.5	51.7	2.8
F	8.07	26.4	1.9	73.6	2.5
G	16.57	14.7	1.7	85.3	2.7

Table 2.3-19
ANNUAL LONG-TERM (10 YEARS) AND SHORT-TERM (2 YEARS)
DISTRIBUTION OF PASQUILL STABILITY CATEGORY (STAR)
AND AVERAGE WIND SPEED

Los Angeles, California				
	January 1955-December 1964		January 1973-December 1974	
Stability Category	Percent Frequency	Average Wind Speed (m/s)	Percent Frequency	Average Wind Speed (m/s)
A	0.34	0.8	0.07	2.0
B	6.51	2.7	6.42	2.8
C	14.43	4.2	13.66	4.3
D	21.63	4.8	22.48	4.4
E	22.00	3.4	23.82	3.3
F	11.04	3.5	9.93	3.4
G	24.05	1.6	23.61	1.8
San Diego, California				
A	0.26	2.2	0.17	1.4
B	9.06	2.9	6.32	3.1
C	16.43	4.0	13.36	4.2
D	16.80	4.2	23.03	4.3
E	23.02	2.9	26.25	3.2
F	8.21	3.2	9.25	3.1
G	26.21	1.5	21.63	1.5

Table 2.3-20
COMPARISON OF DISTRIBUTION OF STAR STABILITY CLASSIFICATIONS AT LOS ANGELES AND SAN DIEGO WITH SAN ONOFRE TOWER STABILITY MEASUREMENTS
(Percent Frequency of Occurrence)

	Los Angeles	San Diego	San Onofre	
(A + B + C) Unstable				
January 1955-December 1964	21.3	25.8	---	---
January 1973-December 1974	20.2	19.9	---	---
January 25, 1973-January 24, 1976	---	---	Lower[a] 33.8	Upper[a] 36.9
(D + E) Neutral				
January 1955-December 1964	43.6	39.8	---	---
January 1973-December 1974	46.3	49.3	---	---
January 25, 1973-January 24, 1976	---	---	Lower[a] 39.5	Upper[a] 38.5
(F + G) Stable				
January 1955-December 1964	35.1	34.4	---	---
January 1973-December 1974	33.5	30.9	---	---
January 25, 1973-January 24, 1976	---	---	Lower[a] 26.7	Upper[a] 24.6

[a] Based on stability joint frequency wind speed-wind direction summaries. Lower wind level 10m, upper wind level 36.6m and 40m combined.

Table 2.3-21
STABILITY CLASSIFICATIONS (Percent)

Location	Model/Tower	Measurements		
		Unstable	Neutral	Stable
New Orleans, Louisiana	STAR	25	36	39
	Tower	82	6	12
Wilmington, Delaware and Vicinity	STAR	16	51	33
	Tower (Delaware City, DE)	68	5	27
	Tower (Salem, NJ)	65	13	22

Monthly joint frequency wind direction-wind speed summaries stratified by stability category are presented in Appendix 2.3F, Tables 2.3F-1 through 2.3F-84 for the lower 10-meter level and in Appendix 2.3G, Tables 2.3G-1 through 2.3G-84 for the upper level. Table 2.3-22 summarizes the monthly frequency of occurrence of stability categories and their distribution by onshore and offshore wind direction. The unstable neutral categories reach their maximum frequency in the summer months, while the stable categories E, F, and G occur in the late autumn and winter seasons. As in the annual distributions, the unstable categories occur principally during onshore wind flow, while stable categories are predominant during offshore flow. In all cases, stability is determined by the original 6.1-36.5-meter delta temperature levels.

2.3.4 SHORT-TERM (ACCIDENT) DIFFUSION ESTIMATES

2.3.4.1 Atmospheric Dispersion

Cumulative frequency distributions of hourly centerline χ/Q parameters were calculated by means of the equation:

$$\chi/Q = \frac{1}{\bar{u}\,[\min\,(\pi\,\sigma_y\,\sigma_z + \frac{A}{2}\,3\pi\,\sigma_y\,\sigma_z)\,]} \quad (1)$$

where:

χ = concentration of contaminant, units /m 3
Q = source strength of contaminant, units/s
u = mean wind speed, m/s
σ_y = crosswind standard deviation of contaminant at downwind distance x, meters
σ_z = vertical standard deviation of contaminant at downwind distance x, meters
A = cross-sectional area of the containment building, 2121 m^3

Table 2.3-22
MONTHLY FREQUENCY DISTRIBUTION OF PASQUILL STABILITY CATEGORIES AND OFFSHORE AND ONSHORE FLOW (10m winds)

Stability Category	January Percent Frequency			February Percent Frequency			March Percent Frequency			April Percent Frequency		
	Category	Wind		Category	Wind		Category	Wind		Category	Wind	
		Onshore	Offshore		Onshore	Offshore		Onshore	Offshore		Onshore	Offshore
A	13.68	93.2	6.2	15.38	83.8	16.2	19.99	88.1	11.9	30.46	92.9	7.1
B	1.34	73.9	26.1	1.90	92.6	7.4	2.39	76.6	22.4	2.86	92.0	8.0
C	1.92	82.3	17.7	1.68	81.6	18.4	2.39	84.1	15.9	2.29	89.1	10.9
D	17.75	74.4	25.6	15.38	70.2	29.8	21.12	73.8	26.2	23.31	69.8	30.2
E	15.66	42.1	57.9	24.37	55.0	45.0	26.34	52.2	47.8	13.63	34.6	65.4
F	14.20	36.5	63.5	11.12	18.5	81.5	10.50	10.1	89.9	8.82	12.0	88.0
G	35.45	19.4	80.6	30.08	1.5	98.5	17.28	1.0	99.0	18.54	5.0	95.0

Stability Category	May Percent Frequency			June Percent Frequency			July Percent Frequency			August Percent Frequency		
	Category	Wind		Category	Wind		Category	Wind		Category	Wind	
		Onshore	Offshore		Onshore	Offshore		Onshore	Offshore		Onshore	Offshore
A	34.45	95.5	4.5	38.33	91.4	8.6	37.61	93.7	6.3	42.02	86.8	13.2
B	5.22	78.9	21.1	2.32	83.6	16.4	4.76	76.3	23.7	3.72	70.7	29.3
C	5.62	73.7	26.3	9.38	67.6	32.4	7.23	79.9	20.1	4.62	68.6	31.4
D	32.58	72.2	27.8	29.29	68.2	31.8	26.75	73.2	26.8	23.68	58.2	41.8
E	12.12	53.2	46.8	12.58	55.6	44.4	17.55	53.5	46.5	18.61	47.2	52.8
F	3.30	10.6	89.4	3.36	8.6	91.4	3.64	6.9	93.1	4.17	8.2	91.8
G	6.65	2.3	97.7	4.74	2.5	97.5	2.33	0.0	100.0	3.0	2.7	97.3

Stability Category	September Percent Frequency			October Percent Frequency			November Percent Frequency			December Percent Frequency		
	Category	Wind		Category	Wind		Category	Wind		Category	Wind	
		Onshore	Offshore		Onshore	Offshore		Onshore	Offshore		Onshore	Offshore
A	36.34	91.0	9.0	19.04	89.8	10.2	14.69	95.7	4.3	10.82	94.1	5.9
B	5.82	67.7	32.3	2.74	88.7	11.3	1.82	100.0	0.0	1.20	76.7	23.3
C	5.53	65.8	34.2	2.53	68.8	31.2	1.58	85.4	14.6	1.62	78.4	21.6
D	19.12	61.4	38.6	21.52	53.6	46.4	15.31	63.7	36.3	12.67	66.8	33.2
E	18.49	46.3	53.7	23.10	37.0	63.0	19.49	48.1	51.9	14.75	47.9	52.1
F	6.70	16.0	84.0	11.08	18.6	81.4	11.71	24.3	75.7	14.57	32.5	67.5
G	7.91	16.2	83.8	19.99	13.0	87.0	35.33	8.9	91.1	44.26	9.8	90.2

The minimum function ($\pi\sigma_y\sigma_z + \frac{A}{2}\ 3\pi\sigma_y\sigma_z$) is employed to limit the reduction of the dispersion parameter by a factor of three for additional dispersion produced by the turbulent wake of the containment.

Values for σ_y and σ_z corresponding to the first six stability categories were determined from Slade.(10) Those for the seventh, Category G, were determined by extrapolation in the manner suggested by Yanskey, Markee, and Richter.(11)

The temperature change with height (ΔT from 6.1 to 36.5 meters) was used in establishing the Pasquill stability category. Also, if the wind direction at the lower level (10-meter) was missing, the upper level (36.5 or 40-meter) direction was employed to establish the sector location of the χ/Q value.

The window model suggested by Woodard(12) was used to compute sector averaged cumulative frequency distributions of atmospheric dispersion factors for time periods of 8 hours to 26 days.

These frequencies were determined for each sector following computation of the average χ/Q for each window period by the equation:

$$\left(\frac{\chi}{Q}\right)_{dw} = \frac{1}{\beta N_W}\sqrt{\frac{2}{\pi}}\sum_{i=1}^{N_W}\frac{\delta_{d}, d_i}{\sigma_{zs_i} u_i x} \tag{2}$$

where:

$(\chi/Q)_{dw}$	=	mean atmospheric dispersion factor for the window period w in the sector downwind from wind sector d, s/m^3
d	=	sector from which wind blows the first hour of the window period
β	=	sector width for 22.5° sector = 0.3927 radians
σ_{zsi}	=	vertical standard deviation of contaminant at downwind distance x from wind direction sector d for stability index s_i, meters
s_i	=	stability index for the ith hour of the window period
u_i	=	average wind speed for the ith hour of the window period, m/s
x	=	downwind distance from containment
N_W	=	number of hours in window
$\delta_d\ d_i$	=	1 if $d = d_i$ 0 if $d \neq d_i$

Because a window begins each hour of the period, there are as many windows as hours. Hours of calm were included by using the wind direction recorded by the wind vane during the calm and a wind speed of 0.25 m/s.

The meteorological data summaries used as input to the diffusion model are discussed in Subsection 2.3.2 and presented in joint frequency form in Appendix 2.3H.

The cumulative frequency distribution of hourly χ/Q class intervals were computed for the exclusion distance of 576 meters for the onshore wind direction and sector (108°-S-299) and by 22-1/2° sector. The results are presented in Tables 2.3-23 and 2.3-24 respectively. The window model (equation (2)) was employed for 8- and 16-hour, and 3- and 26-day windows for the low population zone boundary at 3140 meters. The results are shown in Tables 2.3-25 through 2.3-28.

The dispersion environment on the shoreline at the plant site is highly complex from a meteorological standpoint. A diffusion study made in the Oceanside area,[13] about 35 kilometers (22 miles) southeast of the plant site, found that large eddy motions with periods of 5 minutes or more may exist in the offshore area. Tracer releases offshore showed increasing dispersion upon entering a transitional region near the coast. Moderate turbulence was found in this region, causing a rapid dispersion of the tracer cloud. The releases were made during the summertime, under sea breeze conditions. These conditions are similar to those encountered during periods of Pasquill A, B, C, and D categories at San Onofre, which occur predominately with onshore winds.

The short-term dispersion parameters obtained from equations (1) and (2) should be conservative at the exclusion and the low population zone boundaries with onshore flow. The σ_y and σ_z parameters employed in the model are much smaller than actually exist in the real atmosphere after it crosses the coastline. The impingement of the air on the 29.6 meters (97.0 feet) coastal bluff and the release of the gravitational instability that is developed in the lowest layer of air, as it moves over the warm coastal waters, causes the air flow to become very turbulent when it crosses the coastline and moves inland. The increasing frictional stresses overland cause a rapid increase in the mechanical turbulence. As the flow moves inland, the Santa Margarita y Las Flores Mountains are encountered. The presence of the mouth of the San Onofre Canyon north-northwest of the plant may cause the flow to split, with some of the air flowing over the mountains and some entering the canyon. The net result of the topography is to cause increasing mechanical turbulence and divergent flow as the air moves inland. Since the window model (equation (2)) utilizes uniform sector flow and σ_y, σ_z parameters are derived from relatively flat terrain, the χ/Q values obtained will be conservative. The aforementioned tracer study yielded short-term (0-2 hr) relative concentration χ/Q of 1.3×10^{-4} s/m^3 for releases from Unit 1.[14] This value is less than those computed using Regulatory Guide 1.145 (9.5×10^{-4} s/m^3). Therefore, the tracer tests support the conservatism of using the values obtained using Regulatory Guide 1.145 for accident analysis calculations.

Table 2.3-23
CUMULATIVE FREQUENCY DISTRIBUTION OF HOURLY χ/Q VALUES
ONSHORE WIND DIRECTIONS AT 576 METERS

SAN ONOFRE SITE **ONSHORE WIND DIRECTIONS (108-180-299 DEG)**
CUMULATIVE FREQUENCY DISTRIBUTION OF HOURLY χ/Q VALUES
DATA PERIOD FROM 1/25/73 TO 1/24/76
WINDS FROM 33.0 FOOT LEVEL
STABILITY FROM AEC DELTA T CRITERIA, 20-120 FEET
WAKE TURBULENCE FACTOR - 1060.5 METERS**2
THRESHOLD OF WIND INSTRUMENT - .75 MPH

UPPER CLASS INTERVAL	ACC.	ACC. PCT.	PASQUILL CLASS						
			A	B	C	D	E	F	G
1.00E+99	23390	100.00	0	0	0	0	0	0	15
2.00E-03	23375	99.94	0	0	0	0	11	15	124
1.00E-03	23225	99.29	0	0	0	0	7	35	129
7.00E-04	23054	98.56	0	0	0	22	44	48	83
5.00E-04	22857	97.72	0	0	2	58	247	133	69
3.00E-04	22348	95.55	0	0	3	196	353	104	6
2.00E-04	21686	92.71	0	4	27	1093	750	84	6
1.00E-04	19722	84.32	0	3	70	876	225	11	0
7.00E-05	18537	79.25	0	13	138	667	144	5	0
5.00E-05	17570	75.12	2	89	267	425	109	1	0
3.00E-05	16677	71.30	13	161	122	111	12	1	0
2.00E-05	16257	69.50	209	264	47	4	1	0	0
1.00E-05	15732	67.26	620	40	3	0	0	0	0
7.00E-06	15069	64.42	1539	4	0	0	0	0	0
5.00E-06	13526	57.83	2836	0	0	0	0	0	0
3.00E-06	10690	45.70	341	0	0	0	0	0	0
2.00E-06	10349	44.25	52	0	0	0	0	0	30
1.00E-06	10267	43.89	0	0	0	0	0	0	64
7.00E-07	10203	43.62	0	0	0	0	0	8	167
5.00E-07	10028	42.87	0	0	0	0	0	60	557
3.00E-07	9411	40.24	0	0	0	0	8	160	779
2.00E-07	8464	36.19	0	0	0	0	78	607	2040
l.00E-07	5739	24.54	0	0	0	0	153	377	174
7.00E-08	5035	21.53	0	0	0	0	268	238	0
5.00E-08	4529	19.36	829	178	269	1656	1511	86	0
		CALM	2	3	2	12	10	6	4

NUMBER OF INVALID OBSERVATIONS = 2881
5 PERCENT LEVEL: 2.72 E-04

Table 2.3-24
FREQUENCY DISTRIBUTION OF HOURLY χ/Q VALUES BY WIND DIRECTION AT 576 METERS

SOUTHERN CALIFORNIA EDISON - SAN ONOFRE SITE - 1/25/73 TO 1/24/76
WIND FROM THE 33.0 FOOT LEVEL.
FREQUENCY DISTRIBUTION OF 1-HOUR AVERAGE χ/Q VALUES
PERIOD OF RECORD SAMPLE POPULATION PER SECTOR = 23389 MINUS HOURS OF INTEREST PLUS ONE

UPPER CLASS INT OF χ/Q	NNE	-NE	ENE	-E-	ESE	-SE	SSE	-S-	SSW	-SW	WSW	-W-	WNW	-NW	NNW	-N-	ALL
0.	20784	20240	22690	22957	22811	22193	21714	21824	21919	22074	21832	21281	20814	21960	22622	22535	350250
1.0E-06	0	0	0	0	0	0	0	0	0	0	0	0	0	0	0	0	0
7.5E-06	29	17	4	8	14	63	198	386	529	543	767	1200	1524	380	27	9	5698
1.0E-05	9	11	3	1	2	7	22	49	76	73	122	84	53	20	10	7	551
2.0E-05	23	13	7	4	11	28	65	76	87	84	71	74	86	53	21	10	713
3.0E-05	14	19	6	6	24	36	51	67	53	48	41	66	71	56	19	3	580
4.0E-05	18	12	13	4	20	67	93	69	41	36	41	45	72	52	28	8	619
5.0E-05	13	24	9	24	19	69	107	83	59	44	47	62	63	75	41	25	764
6.0E-05	34	20	14	11	16	73	124	87	40	42	29	50	58	78	28	15	719
7.0E-05	25	35	21	9	22	93	89	86	64	43	44	38	48	65	30	20	732
8.0E-06	55	28	9	16	22	65	119	73	55	35	33	31	52	58	54	11	716
9.0E-05	56	45	9	11	29	67	91	58	41	27	19	35	45	69	45	21	668
1.0E-04	56	50	6	9	27	62	76	59	33	39	29	42	44	36	28	31	627
2.0E-04	705	621	116	92	144	304	390	262	209	148	144	199	240	271	219	292	4356
3.0E-04	667	995	129	54	71	87	111	86	78	65	80	90	92	91	94	147	2937
4.0E-04	418	555	84	35	32	45	39	49	34	29	32	32	42	50	37	90	1603
5.0E-04	201	284	59	26	17	29	24	24	18	17	21	15	33	25	19	55	867
6.0E-04	107	160	47	22	15	20	16	8	11	4	6	9	19	15	11	25	495
7.0E-04	55	74	31	22	18	18	11	5	11	7	6	10	8	9	19	22	326
8.0E-04	40	58	30	19	11	8	10	13	7	6	5	2	1	2	11	12	235
9.0E-04	20	38	26	11	15	15	11	5	4	8	3	4	4	3	6	12	185
1.0E-03	16	26	28	10	15	9	5	5	3	6	7	2	0	5	2	5	144
GREATER THAN 1.0E-03	44	64	48	38	34	31	23	15	17	9	10	18	20	16	18	34	439
TOTAL	23389	23389	23389	23389	23389	23389	23389	23389	23389	23389	23389	23389	23389	23389	23389	23389	374224

Table 2.3-25
CUMULATIVE FREQUENCY DISTRIBUTION OF χ/Q, TIME PERIOD 8 HOURS

DATA FROM 1/25/73 TO 1/24/76
WND LVL 10 m TEMP DIFF 6.1-36.5 m

CUMULATIVE FREQUENCY DISTRIBUTION OF χ/Q --- BY WIND SECTOR --- TIME PERIOD 8 HOURS --- STANDARD

CUMULATIVE PERCENT FREQUENCY																	
SECTOR DIRECTION	S	SSW	SW	WSW	W	WNW	NW	NNW	N	NNE	NE	ENE	E	ESE	SE	SSE	TOTAL
SECTOR DISTANCE (M)	3.140 E3	3.140 E3	3.140 E3	3.140 E3	3.140 E3	3.140 E3	3.140 E3	3.140 E3	3.140 E3	3.140 E3	3.140 E3	3.140 E3	3.140 E3	3.140 E3	3.140 E3	3.140 E3	
MAGNITUDE OF χ/Q																	
5.0E-05 TO 2.5E-05	.0	0.0	.0	0.0	0.0	0.0	0.0	0.0	.0	0.0	0.0	0.0	0.0	.0	0.0	0.0	0.0
2.5E-05 TO 1.0E-05	.0	.3	.9	.1	.1	.0	.1	.1	.1	.0	.0	.0	.0	.1	.1	.0	2.1
1.0E-05 TO 7.5E-06	.1	.9	2.0	.3	.1	.1	.2	.3	.3	.1	.1	.1	.1	.3	.1	.1	5.3
7.5E-06 TO 5.0E-06	.3	1.8	3.1	.5	.2	.3	.4	.7	.6	.5	.4	.4	.5	.8	.3	.2	11.0
5.0E-06 TO 2.5E-06	.7	3.1	4.9	.9	.5	.6	1.1	1.6	1.4	1.1	1.0	1.2	1.9	2.5	1.1	.6	24.2
2.5E-06 TO 1.0E-06	1.4	5.1	7.6	1.5	.9	1.1	2.4	3.4	3.1	2.8	2.4	2.9	4.4	5.4	2.3	1.2	47.9
1.0E-06 TO 7.5E-07	1.7	5.9	8.4	1.7	1.1	1.2	2.8	4.0	3.7	3.4	2.8	3.5	5.1	6.2	2.7	1.4	55.6
7.5E-07 TO 5.0E-07	1.9	6.7	9.5	2.0	1.2	1.5	3.2	4.7	4.3	4.0	3.4	4.1	6.0	7.2	3.2	1.6	64.6
5.0E-07 TO 2.5E-07	2.2	7.7	10.6	2.3	1.3	1.7	3.7	5.3	4.9	4.7	3.9	4.9	6.9	8.0	3.6	1.9	73.7
2.5E-07 TO 1.0E-07	2.5	8.3	11.1	2.4	1.4	1.8	4.0	5.6	5.3	5.0	4.3	5.2	7.4	8.5	3.9	2.0	78.8
1.0E-07 TO 7.5E-08	2.5	8.4	11.3	2.4	1.4	1.8	4.0	5.7	5.3	5.0	4.3	5.3	7.4	8.6	4.0	2.1	79.6
7.5E-08 TO 5.0E-08	2.5	8.5	11.3	2.5	1.4	1.9	4.0	5.8	5.4	5.1	4.4	5.4	7.5	8.7	4.0	2.1	80.5
5.0E-08 TO 2.5E.08	2.6	8.6	11.4	2.5	1.4	1.9	4.1	5.8	5.5	5.2	4.5	5.5	7.7	9.0	4.2	2.2	82.1
2.5E-08 TO 1.0E-08	2.9	9.4	12.0	2.6	1.5	2.0	4.9	6.3	6.0	5.7	5.0	6.0	8.3	10.0	5.2	2.6	89.8
1.0E-08 TO 1.0E-09	3.5	11.1	13.4	2.8	1.7	2.3	4.9	7.0	6.5	6.1	5.4	6.5	8.8	10.9	6.0	3.1	100.0
1.0E-09 TO 1.0E-10	3.5	11.1	13.4	2.8	1.7	2.3	4.4	7.0	6.5	6.1	5.4	6.5	8.8	10.9	6.0	3.1	100.0
1.0E-10 TO 1.0L-11	3.5	11.1	13.4	2.8	1.7	2.3	4.9	7.0	6.5	6.1	5.4	6.5	8.8	10.9	6.0	3.1	100.0
1.0E-11 TO 1.0E-12	3.5	11.1	13.4	2.8	1.7	2.3	4.9	7.0	6.5	6.1	5.4	6.5	8.8	10.9	6.0	3.1	100.0
1.0E-12 TO 0.	3.5	11.1	13.4	2.8	1.7	2.3	4.9	7.0	6.5	6.1	5.4	6.5	8.8	10.9	6.0	3.1	100.0
MAGNITUDE OF χ/Q																	
WORST CONDITION	2.885 E –5	2.063 E -5	3.273 E -5	2.366 E -5	1.956 E -5	1.818 E -5	1.647 E -5	2.060 E -5	2.965 E -5	2.277 E –5	1.474 E -5	1.524 E -5	2.201 E -5	3.310 E -5	2.450 E -5	1.453 E -5	3.310 E –5

5.0 PERCENTILE .772E-05
50.0 PERCENTILE .924E-06
NUMBER OF CASES INPUT 26280
NUMBER OF CASES CALC. 23317
PERCENT INCLUDED 88.73

Table 2.3-26
CUMULATIVE FREQUENCY DISTRIBUTION OF χ/Q, TIME PERIOD 16 HOURS

DATA FROM 1/25/73 TO 1/24/76
WND LVL 10 m TEMP DIFF 6.1-36.5 m

CUMULATIVE FREQUENCY DISTRIBUTION OF χ/Q --- BY WIND SECTOR --- TIME PERIOD 16 HOURS --- STANDARD

CUMULATIVE PERCENT FREQUENCY																	
SECTOR DIRECTION	S	SSW	SW	WSW	W	WNW	NW	NNW	N	NNE	NE	ENE	E	ESE	SE	SSE	TOTAL
SECTOR DISTANCE (M)	3.140 E3	3.140 E3	3.140 E3	3.140 E3	3.140 E3	3.140 E3	3.140 E3	3.140 E3	3.140 E3	3.140 E3	3.140 E3	3.140 E3	3.140 E3	3.140 E3	3.140 E3	3.140 E3	
MAGNITUDE OF χ/Q																	
2.5E-05 TO 1.0E-05	0.0	0.0	.0	0.0	0.0	.0	.0	.0	.0	.0	.0	.0	.0	.0	.0	.0	.2
1.0E-05 TO 7.5E-06	.0	.0	.0	.0	.0	.0	.0	.1	.1	.1	.1	.1	.1	.2	.1	.0	.9
7.5E-06 TO 5.0E-06	.1	.2	.4	.0	.1	.0	.1	.2	.4	.3	.3	.3	.6	.8	.3	.1	4.2
5.0E-06 TO 2.5E-06	.4	1.0	1.8	.3	.2	.2	.5	.7	.9	.8	.8	1.1	1.7	2.7	1.3	.6	14.8
2.5E-06 TO 1.0E-06	1.3	3.0	3.8	.8	.5	.6	1.4	2.1	2.4	2.2	2.0	2.6	3.8	5.4	3.0	1.4	36.4
1.0E-06 TO 7.5E-07	1.5	3.6	4.6	1.0	.7	.7	1.8	2.7	3.0	2.8	2.5	3.2	4.6	6.3	3.5	1.7	44.1
7.5E-07 TO 5.0E-07	1.9	4.4	5.6	1.3	.8	1.0	2.3	3.5	3.8	3.6	3.2	4.0	5.7	7.6	4.2	2.0	55.1
5.0E-07 TO 2.5E-07	2.4	5.9	7.3	1.8	1.0	1.3	3.0	4.8	4.9	4.8	4.3	5.1	7.0	9.1	5.1	2.4	70.1
2.5E-07 TO 1.0E-07	2.7	6.9	8.7	2.1	1.2	1.6	3.5	5.5	5.4	5.3	4.8	5.8	7.9	10.0	5.5	2.6	79.4
1.0E-07 TO 7.5E-08	2.7	7.0	8.9	2.1	1.2	1.6	3.6	5.6	5.5	5.4	4.8	5.9	8.0	10.1	5.6	2.7	80.8
7.5E-08 TO 5.0E-08	2.8	7.2	9.1	2.1	1.2	1.6	3.7	5.7	5.6	5.5	4.9	6.0	8.1	10.2	5.6	2.7	82.3
5.0E-08 TO 2.5E-08	2.9	7.4	9.3	2.2	1.3	1.7	3.9	5.8	5.7	5.6	5.0	6.0	8.2	10.3	5.7	2.8	83.7
2.5E-08 TO 1.0E-08	3.0	8.0	9.8	2.3	1.4	1.8	4.0	6.0	5.9	5.7	5.1	6.1	8.4	10.5	5.7	2.8	86.5
1.0E-08 TO 1.0E-09	3.5	11.1	13.4	2.8	1.7	2.3	4.9	7.0	6.5	6.1	5.4	6.5	8.8	10.9	6.0	3.1	100.0
1.0E-09 TO 1.0E-10	3.5	11.1	13.4	2.8	1.7	2.3	4.9	7.0	6.5	6.1	5.4	6.5	8.8	10.9	6.0	3.1	100.0
1.0E-10 TO 1.0E-11	3.5	11.1	13.4	2.8	1.7	2.3	4.9	7.0	6.5	6.1	5.4	6.5	8.8	10.9	6.0	3.1	100.0
1.0E-11 TO 1.0E-12	3.5	11.1	13.4	2.8	1.7	2.3	4.9	7.0	6.5	6.1	5.4	6.5	8.8	10.9	6.0	3.1	100.0
1.0E-12 TO 0.	3.5	11.1	13.4	2.8	1.7	2.3	4.9	7.0	6.5	6.1	5.4	6.5	8.8	10.9	6.0	3.1	100.0
MAGNITUDE OF χ/Q																	
WORST CONDITION	9.237 E –6	9.914 E -6	1.752 E -5	7.920 E -6	9.331 E -6	1.440 E -5	1.201 E -5	1.291 E -5	1.332 E -5	2.123 E -5	2.021 E -5	1.912 E -5	1.588 E -5	1.746 E -5	1.269 E -5	1.030 E -5	2.123 E-5

5.0 PERCENTILE	.474E-05
50.0 PERCENTILE	.603E-06
NUMBER OF CASES INPUT	26280
NUMBER OF CASES CALC.	23317
PERCENT INCLUDED	88.73

Table 2.3-27
CUMULATIVE FREQUENCY DISTRIBUTION OF χ/Q, TIME PERIOD 3 DAYS

DATA FROM 1/25/73 TO 1/24/76
WND LVL 10 m TEMP DIFF 6.1-36.5 m

CUMULATIVE FREQUENCY DISTRIBUTION OF χ/Q --- BY WIND SECTOR --- TIME PERIOD 3 DAYS --- STANDARD

CUMULATIVE PERCENT FREQUENCY

SECTOR DIRECTION	S	SSW	SW	WSW	W	WNW	NW	NNW	N	NNE	NE	ENE	E	ESE	SE	SSE	TOTAL
SECTOR DISTANCE (M)	3.140 E3	3.140 E3	3.140 E3	3.140 E3	3.140 E3	3.140 E3	3.140 E3	3.140 E3	3.140 E3	3.140 E3	3.140 E3	3.140 E3	3.140 E3	3.140 E3	3.140 E3	3.140 E3	
MAGNITUDE OF χ/Q																	
1.0E-05 TO 7.5E-06	.0	.0	.1	.0	.0	0.0	0.0	0.0	.0	.0	0.0	0.0	0.0	0.0	0.0	.0	.1
7.5E-06 TO 5.0E-06	.0	.2	.7	.1	.0	.0	.1	.0	.0	.0	.0	.0	.0	.0	.0	.0	1.3
5.0E-06 TO 2.5E-06	.4	1.8	3.1	.6	.3	.3	.6	.6	.4	.2	.2	.1	.2	.3	.3	.2	9.6
2.5E-06 TO 1.0E-06	1.2	4.3	6.0	1.4	.7	.9	1.8	1.8	1.2	.9	.8	.7	1.0	1.3	1.2	.9	26.1
1.0E-06 TO 7.5E-07	1.4	5.1	6.9	1.6	.8	1.1	2.2	2.4	1.7	1.3	1.0	1.1	1.4	1.8	1.6	1.1	32.4
7.5E-07 TO 5.0E-07	1.8	6.1	7.9	1.8	1.0	1.4	2.7	3.2	2.3	2.0	1.4	1.7	2.0	2.8	2.3	1.3	41.7
5.0E-07 TO 2.5E-07	2.4	7.9	10.2	2.2	1.2	1.7	3.5	4.6	3.6	3.2	2.5	2.8	3.7	5.0	3.5	1.9	60.0
2.5E-07 TO 1.0E-07	3.1	9.6	12.1	2.5	1.5	2.1	4.3	5.8	5.0	4.5	3.9	4.5	5.9	7.8	4.9	2.6	79.9
1.0E-07 TO 7.5E-08	3.2	9.9	12.4	2.6	1.5	2.1	4.4	6.1	5.3	4.8	4.1	4.8	8.4	6.4	5.1	2.7	83.8
7.5E-08 TO 5.0E-08	3.3	10.3	12.8	2.7	1.6	2.2	4.6	6.4	5.6	5.1	4.4	5.3	6.9	9.0	5.4	2.8	88.2
5.0E-08 TO 2.5E-08	3.3	10.6	13.1	2.8	1.6	2.2	4.7	6.6	5.9	5.4	4.6	5.6	7.4	9.7	5.6	2.9	92.0
2.5E-08 TO 1.0E-08	3.4	10.8	13.2	2.8	1.6	2.2	4.7	6.7	6.1	5.6	4.8	5.9	7.9	10.0	5.7	3.0	94.3
1.0E-08 TO 1.0E-09	3.5	11.0	13.3	2.8	1.6	2.3	4.9	7.0	6.5	6.0	5.3	6.4	8.7	10.7	6.0	3.1	99.2
1.0E-09 TO 1.0E-10	3.5	11.1	13.4	2.8	1.7	2.3	4.9	7.0	6.5	6.1	5.4	6.5	8.8	10.9	6.0	3.1	100.0
1.0E-10 TO 1.0E-11	3.5	11.1	13.4	2.8	1.7	2.3	4.9	7.0	6.5	6.1	5.4	6.5	8.8	10.9	6.0	3.1	100.0
1.0E-11 TO 1.0E-12	3.5	11.1	13.4	2.8	1.7	2.3	4.9	7.0	6.5	6.1	5.4	6.5	8.8	10.9	6.0	3.1	100.0
1.0E-12 TO 0.	3.5	11.1	13.4	2.8	1.7	2.3	4.9	7.0	6.5	6.1	5.4	6.5	8.8	10.9	6.0	3.1	100.0
MAGNITUDE OF χ/Q																	
WORST CONDITION	7.982 E -6	7.777 E -6	8.517 E -6	7.737 E -6	7.699 E -6	7.392 E -6	7.014 E -6	6.635 E -6	7.862 E -6	8.240 E -6	5.648 E -6	6.521 E -6	5.499 E -6	7.394 E -6	6.225 E -6	7.765 E -6	8.517 E –6

5.0 PERCENTILE	.367E-05
50.0 PERCENTILE	.365E-06
NUMBER OF CASES INPUT	26280
NUMBER OF CASES CALC.	23317
PERCENT INCLUDED	88.73

Table 2.3-28
CUMULATIVE FREQUENCY DISTRIBUTION OF χ/Q, TIME PERIOD 26 DAYS

DATA FROM 1/25/73 TO 1/24/76
WND LVL 10 m TEMP DIFF 6.1-36.5 m

CUMULATIVE FREQUENCY DISTRIBUTION OF χ/Q --- BY WIND SECTOR --- TIME PERIOD 26 DAYS --- STANDARD

CUMULATIVE PERCENT FREQUENCY																	
SECTOR DIRECTION	S	SSW	SW	WSW	W	WNW	NW	NNW	N	NNE	NE	ENE	E	ESE	SE	SSE	TOTAL
SECTOR DISTANCE (M)	3.140 E3	3.140 E3	3.140 E3	3.140 E3	3.140 E3	3.140 E3	3.140 E3	3.140 E3	3.140 E3	3.140 E3	3.140 E3	3.140 E3	3.140 E3	3.140 E3	3.140 E3	3.140 E3	
MAGNITUDE OF χ/Q																	
5.0E-06 TO 2.5E-06	.2	.7	1.5	.3	.2	.1	.3	.5	.3	.2	.1	.2	.2	.4	.2	.2	5.5
2.5E-06 TO 1.0E-06	.8	2.5	4.1	.9	.5	.5	1.2	1.4	1.1	.8	.8	.9	1.3	1.6	.9	.6	20.0
1.0E-06 TO 7.5E-07	.9	3.0	4.9	1.1	.5	.7	1.5	1.9	1.5	1.1	1.1	1.2	1.7	2.2	1.2	.8	25.1
7.5E-07 TO 5.0E-07	1.2	4.0	6.2	1.3	.7	1.0	2.1	2.7	2.2	1.8	1.5	1.7	2.4	3.0	1.7	1.1	34.6
5.0E-07 TO 2.5E-07	2.1	6.8	9.8	2.0	1.1	1.5	3.2	4.4	3.8	3.4	2.9	3.4	4.4	5.8	3.4	2.0	59.9
2.5E-07 TO 1.0E-07	3.1	9.9	12.6	2.6	1.5	2.1	4.5	6.5	5.8	5.5	4.8	5.7	7.5	9.5	5.3	2.8	89.8
1.0E-07 TO 7.5E-08	3.3	10.4	13.0	2.7	1.6	2.2	4.7	6.7	6.1	5.7	5.0	6.0	8.0	10.0	5.6	3.0	93.9
7.5E-08 TO 5.0E-08	3.4	10.8	13.2	2.8	1.6	2.2	4.9	6.9	6.3	6.0	5.3	6.3	8.5	10.5	5.8	3.1	97.7
5.0E-08 TO 2.5E-08	3.5	11.0	13.3	2.8	1.6	2.3	4.9	7.0	6.5	6.1	5.4	6.5	8.8	10.8	6.0	3.1	99.7
2.5E-08 TO 1.0E-08	3.5	11.1	13.4	2.8	1.7	2.3	4.9	7.0	6.5	6.1	5.4	6.5	8.8	10.9	6.0	3.1	100.0
1.0E-08 TO 1.0E-09	3.5	11.1	13.4	2.8	1.7	2.3	4.9	7.0	6.5	6.1	5.4	6.5	8.8	10.9	6.0	3.1	100.0
1.0E-09 TO 1.0E-10	3.5	11.1	13.4	2.8	1.7	2.3	4.9	7.0	6.5	6.1	5.4	6.5	8.8	10.9	6.0	3.1	100.0
1.0E-10 TO 1.0E-11	3.5	11.1	13.4	2.8	1.7	2.3	4.9	7.0	6.5	6.1	5.4	6.5	8.8	10.9	6.0	3.1	100.0
1.0E-11 TO 1.0E-12	3.5	11.1	13.4	2.8	1.7	2.3	4.9	7.0	6.5	6.1	5.4	6.5	8.8	10.9	6.0	3.1	100.0
1.0E-12 TO 0.	3.5	11.1	13.4	2.8	1.7	2.3	4.9	7.0	6.5	6.1	5.4	6.5	8.8	10.9	6.0	3.1	100.0
MAGNITUDE OF χ/Q																	
WORST CONDITION	4.560 E -6	4.655 E –6	4.700 E –6	4.621 E -6	4.711 E -6	4.445 E -6	4.686 E -6	4.668 E -6	4.792 E -6	4.655 E -6	4.779 E -6	4.632 E -6	4.761 E -6	4.748 E -6	4.590 E -6	4.716 E -6	4.792 E –6

5.0 PERCENTILE	.267E-05
50.0 PERCENTILE	.328E-06
NUMBER OF CASES INPUT	26280
NUMBER OF CASES CALC.	23317
PERCENT INCLUDED	88.73

The offshore flow reaches the station site after passing over the inland mountains or flowing from the mouth of the San Onofre Canyon. The mechanical turbulence is quite strong and is enhanced by the air spilling over the bluff and traveling through the plant yard. Even the E, F, and G categories must contain considerable mechanical turbulence because of the relatively high speeds which average 3 to 4 m/s. The model should provide conservative estimates near the plant and some distance out to sea. As the air moves over the water surface, the mechanical turbulence will decrease and the χ/Q values will become less conservative.

2.3.5 LONG-TERM (ROUTINE) DIFFUSION ESTIMATES

This section provides realistic estimates of annual average atmospheric dispersion parameter for annual average release limit calculations.

The sector-averaged equation for a ground-level release was used for calculating the long-term average dilution factors. This equation is

$$\left(\frac{\chi}{\mathrm{Q}}\right)_d = \sqrt{\frac{2}{\pi}}\frac{1}{\beta}\sum_{i=1}^{7}\sum_{x=1}^{14}\frac{f_{isd}}{\sigma_{zi}u_s x}\left(\frac{s}{m^3}\right) \qquad (3)$$

where:

$(\chi/\mathrm{Q})_d$	=	atmospheric dispersion parameter for wind from sector d, s/m^3
β	=	sector width for 22.5° sector = 0.3927 radians
f_{isd}	=	joint frequency of stability index i, wind speed class s, and wind direction section d
σ_{zi}	=	vertical standard deviation of containment at distance x for stability index i, meters
u_s	=	average wind speed for speed class s, m/s
x	=	downwind distance from containment, meters

Annual averages for χ/Q were computed from equation (3) for each sector at distance ranges from 0.1 mile to 50 miles. The results are presented in Table 2.3-29.

The χ/Q values obtained with this model over the inland sectors will be conservative. This results from the utilization of the coastal measurements for stability classification. Strong isolational heating over the interior southern California areas causes the air to become more unstable as it moves inland. Inversions that exist along the coast weaken or are totally absent over the inland areas. Mechanical turbulence induced by the rough inland terrain also increases the dispersion power of the air above that indicated by the model. Therefore, the overall result is to cause the model to show χ/Q values that are higher than those that would actually be found over the interior.

For the ocean sectors, the model will tend to predict values that are conservative for the reasons cited in Subsection 2.3.4.

Table 2.3-29
ANNUAL AVERAGES FOR χ/Q
DATA FROM 1/25/73 TO 1/24/76
WND LVL 10 m TEMP DIFF 6.1-36.5 m
AVERAGE χ/Q FACTORS

χ/Q DISPERSION FACTORS																
DOWN WIND DIST.	(FOR WIND DIRECTION FROM)															
(MI)	N	NNE	NE	ENE	E	ESE	SE	SSE	S	SSW	SW	WSW	W	WNW	NW	NNW
.1	5.9E-05	1.7E-04	2.1E-04	6.2E-05	3.8E-05	3.9E-05	5.5E-05	6.3E-05	5.1E-05	4.6E-05	3.6E-05	4.0E-05	4.7E-05	5.5E-05	4.7E-05	4.0E-05
.2	1.7E-05	4.8E-05	6.2E-05	1.8E-05	1.1E-05	1.1E-05	1.6E-05	1.8E-05	1.4E-05	1.3E-05	9.9E-06	1.8E-05	1.3E-05	1.5E-05	1.3E-05	1.1E-05
.3	8.2E-06	2.3E-05	3.0E-05	8.7E-06	5.4E-06	5.3E-06	7.5E-06	8.4E-06	6.7E-06	5.9E-06	4.6E-06	4.9E-06	5.8E-06	6.8E-06	6.3E-06	5.4E-06
.4	4.9E-06	1.4E-05	1.8E-05	5.2E-06	3.2E-06	3.2E-06	4.5E-06	5.0E-06	3.9E-06	3.4E-06	2.6E-06	2.8E-06	3.3E-06	3.9E-06	3.7E-06	3.2E-06
.5	3.2E-06	9.4E-06	1.2E-05	3.5E-06	2.1E-06	2.1E-06	3.0E-06	3.3E-06	2.6E-06	2.3E-06	1.7E-06	1.8E-06	2.2E-06	2.5E-06	2.4E-06	2.1E-06
.6	2.3E-06	6.8E-06	8.7E-06	2.5E-06	1.5E-06	1.5E-06	2.1E-06	2.4E-06	1.9E-06	1.6E-06	1.2E-06	1.3E-06	1.5E-06	1.8E-06	1.7E-06	1.5E-06
.7	1.8E-06	5.3E-06	6.8E-06	2.0E-06	1.2E-06	1.2E-06	1.7E-06	1.8E-06	1.4E-06	1.2E-06	9.3E.07	9.8E-07	1.2E-06	1.4E-06	1.3E-06	1.2E-06
.8	1.5E-06	4.3E-06	5.6E-06	1.6E-06	9.8E-07	9.7E-07	1.3E-06	1.5E06	1.2E-06	9.9E-07	7.4E-07	7.8E-07	9.3E-07	1.1E-06	1.1E-06	9.6E-07
.9	1.2E-06	3.6E-06	4.7E-06	1.3E-06	8.2E-07	8.1E-07	1.1E-06	1.2E-06	9.6E-07	8.2E-01	6.1E-07	6.5E-07	7.7E-07	9.1E-07	9.0E-07	8.0E-07
1.0	1.0E-06	3.1E-06	4.0E-06	1.2E-06	7.0E-07	6.9E-07	9.6E-07	1.0E-06	8.1E-07	6.9E-07	5.2E-07	5.4E-07	6.5E-07	7.7E-07	7.7E-07	6.8E-07
1.5	5.6E-07	1.7E-06	2.2E-06	6.3E-07	3.8E-07	3.8E-07	5.1E-07	5.5E-07	4.3E-07	3.6E-07	2.7E-07	2.8E-07	3.4E-07	4.0E-07	4.1E-07	3.6E-07
2.0	3.6E-07	1.1E-06	1.4E-06	4.1E-07	2.5E-07	2.4E-07	3.3E-07	3.5E-07	2.7E-01	2.3E-07	1.7E-07	1.8E-07	2.1E-07	2.6E-07	2.6E-07	2.3E-07
2.5	2.6E-07	7.9E-07	1.0E-06	3.0E-07	1.8E-07	1.7E-07	2.4E-07	2.5E-07	1.9E-07	1.6E-07	1.2E-07	1.3E-07	1.5E-07	1.8E-07	1.8E-07	1.7E-07
3.0	2.0E-07	6.0E-07	8.0E-07	2.3E-07	1.4E-01	1.3E-07	1.8E-07	1.9E-07	1.4E-07	1.2E-07	9.0E-08	9.4E-08	1.1E-07	1.4E-07	1.4E-07	1.3E-07
3.5	1.6E-07	4.8E-07	6.3E-07	1.8E-07	1.1E-07	1.0E-07	1.4E-07	1.5E-07	1.1E-07	9.6E-08	7.0E-08	7.4E-08	8.9E-08	1.1E-07	1.1E-07	9.9E-08
4.0	1.3E-07	3.9E-07	5.2E-07	1.5E-07	8.9E-08	8.6E-08	1.2E-07	1.2E-07	9.2E-08	7.8E-08	5.7E-08	6.0E-08	7.2E-08	8.7E-08	8.9E-08	8.1E-08
4.5	1.1E-07	3.3E-07	4.4E-07	1.2E-07	7.5E-08	7.2E-08	9.6E-08	1.0E-07	7.6E-08	6.5E-08	4.7E-08	5.0E-08	6.0E-08	7.2E-08	7.4E-08	6.7E-08
5.0	9.1E-08	2.8E-07	3.8E-07	1.1E-07	6.4E-08	6.1E-08	8.2E-08	8.5E.08	6.5E-08	5.5E-08	4.0E.08	4.2E-08	5.1E-08	6.1E-08	6.3E-08	5.7E-08
7.5	5.0E-08	1.6E-07	2.1E-07	6.0E-08	3.6E-08	3.4E-08	4.5E-08	4.6E-08	3.5E-08	3.0E-08	2.2E-08	2.3E-08	2.8E-08	3.3E-08	3.5E-08	3.1E-08
10	3.5E-08	1.1E-07	1.5E-07	4.2E-08	2.5E-08	2.4E-08	3.1E-08	3.1E-08	2.4E-08	2.0E-08	1.5E-08	1.5E-08	1.9E-08	2.3E-08	2.4E-08	2.1E-08
15	2.1E-08	6.7E-08	9.1E-08	2.6E-08	1.5E-08	1.4E-08	1.8E-08	1.8E-08	1.4E-08	1.2E-08	8.3E-09	8.8E-09	1.1E-08	1.3E-08	1.4E-08	1.3E-08
20	1.4E-08	4.7E-08	6.4E-08	1.8E-08	1.1E-08	9.9E-09	1.3E-08	1.2E-08	9.2E-09	7.8E-09	5.6E-09	5.9E-09	7.3E-09	9.0E-09	9.4E-09	8.6E-09
25	1.1E-08	3.6E-08	4.9E-08	1.4E-08	8.0E-09	7.5E-09	9.5E-09	9.2E-09	6.8E-09	5.8E-09	4.1E-09	4.4E-09	5.4E-09	6.7E-09	7.0E-09	6.4E-09
30	8.5E-09	2.9E-08	4.0E-08	1.1E-08	6.4E-09	5.9E-09	7.5E-09	7.2E-09	5.3E-09	4.6E-09	3.2E-09	3.4E-09	4.2E-09	5.3E-09	5.5E-09	5.1E-09
35	7.0E-09	2.4E-06	3.3E-08	9.2E-09	5.3E-09	4.9E-09	6.2E-09	5.9E-09	4.3E-09	3.7E-09	2.6E-09	2.8E-09	3.4E-09	4.3E-09	4.5E-09	4.1E-09
40	5.9E-09	2.0E-08	2.8E-08	7.8E-09	4.5E-09	4.1E-09	5.2E-09	4.9E.09	3.6E-09	3.1E-09	2.2E-09	2.3E-09	2.9E-09	3.6E-09	3.8E-09	3.5E-09
45	5.1E-09	1.7E-08	2.4E-08	6.8E-09	3.9E-09	3.8E-09	4.5E-09	4.2E-09	3.1E-09	2.7E-09	1.9E-09	2.0E-09	2.5E-09	3.1E-09	3.3E-09	3.0E-09
50	4.4E-09	1.5E-08	2.1E-08	6.0E-09	3.4E-09	3.1E-09	3.9E-09	3.7E-09	2.7E-09	2.3E-09	1.6E-09	1.7E-09	2.1E-09	2.7E-09	2.8E-09	2.6E-09

23331 CASES AVAILABLE OUT OF 26280 CASES POSSIBLE

EXIT ONE – GRND LEV REL; UNITS 2/3; CONT. REL.; SITE SPECIFIC TERR. RECIRC.
CORRECTED USING SITE-SPECIFIC FACTORS
SPECIFIC POINTS OF INTEREST

Release ID	Type of Location	Direction from Site	Distance (Miles)	Distance (Meters)	χ/Q (Sec/Cub. Meter) No Decay Undepleted	χ/Q (Sec/Cub.Meter) 2.260 Day Decay Undepleted	χ/Q (Sec/Cub.Meter) 8.000 Day Decay Depleted	D/Q (Per Sq. Meter)
S	Sector P,Q	WNW	0.37	600.	2.0E-06	2.0E-06	1.8E-06	8.8E-09
S	Sector P,Q	NW	0.37	600.	4.8E-06	4.8E-06	4.5E-06	2.8E-08
S	Sector R,A	NNW	0.37	600.	3.3E-06	3.3E-06	3.0E-06	2.2E-08
S	Sector R,A	N	0.37	600.	2.3E-06	2.3E-06	2.2E-06	1.9E-08
S	Sector B,C	NNE	0.37	600.	2.0E-06	2.0E-06	1.9E-06	2.0E-08
S	Sector B,C	NE	0.37	600.	2.1E-06	2.1E-06	1.9E-06	2.3E-08
S	Sector D,E	ENE	0.37	600.	1.9E-06	1.9E-06	1.8E-06	2.4E-08
S	Sector D,E	E	0.37	600.	3.1E-06	3.1E-06	2.9E-06	4.3E-08
S	Sector F,G	ESE	0.37	600.	3.2E-06	3.2E-06	2.9E-06	2.8E-08
S	Sector F,G	SE	0.37	600.	2.4E-06	2.4E-06	2.2E-06	1.3E-08
S	Sector H,J	SSE	0.37	600.	2.2E-06	2.2E-06	2.1E-06	9.5E-09
S	Sector H,J	S	0.37	600.	3.8E-06	3.8E-06	3.5E-06	1.4E-08
S	Sector K,L	SSW	0.37	600.	3.1E-05	3.1E-05	2.9E-05	1.1E-07
S	Sector K,L	SW	0.37	600.	3.8E-06	3.8E-06	3.5E-06	1.1E-08
S	Sector M,N	WSW	0.37	600.	2.2E-06	2.2E-06	2.1E-06	6.3E-09
S	Sector M,N	W	0.37	600.	2.5E-06	2.5E-06	2.4E-06	9.0E-09

VENT AND BUILDING PARAMETERS:

RELEASE HEIGHT (METERS)	54.00	REP. WIND HEIGHT (METERS)	10.0
DIAMETER (METERS)	0.0	BUILDING HEIGHT (METERS)	48.8
EXIT VELOCITY (METERS)	0.0	BLDG.MIN.CRS.SEC.AREA (SQ. METERS)	2121.0
HEAT EMISSION RATE (CAL/SEC)	0.0		

ALL GROUND RELEASES.

2.3.6 REFERENCES

1. Pierce, E. T. and Cianos, N., "A Ground-Lightning Environment for Engineering Usage," Stanford Research Institute, Project 1834, 1972.

2. National Weather Service - Environmental Data Service

   Local Climatological Data, Los Angeles, California, 1974 Annual Summary

   Local Climatological Data, San Diego, California, 1974 Annual Summary

   Climatology of the United States No. 81-California Storm Data, 1959-1975.

3. Holzworth and Blake, Meteorological Summaries of Importance to Air Pollution in Western San Diego County, California, Department of Public Health, Berkeley, California, 1957.

4. Neiburger, M., Johnson, D. S., and Chien, C. W., "Studies of the Structures of Atmosphere over the Eastern Pacific Ocean in Summer: I. The Inversion over the Eastern North Pacific Ocean," University of California Press, 1961.

5. United States Naval Weather Service, May 1969: World-Wide Airfield Summaries, Vol VIII, Part 1, United States of America (West Coast, Western Mountains and Great Basin).

6. Southern California Air Pollution Control District, Metropolitan Zone: Air Quality and Meteorology - 1975, Los Angeles, California.

7. Holzworth, G. C., "Mixing Heights, Wind Speeds, and Potential for Urban Air Pollution throughout the Contiguous United States," Office of Air Programs Publication No. AP-101, U.S. Environmental Protection Agency, 1972.

8. Jones, J. I. P. and Pasquill, F., "An Experimental System for Directly Recording Statistics of the Intensity of Atmospheric Turbulence," Quarterly Journal Royal Meteorology Society, 85, 365, pp 225-236, 1959.

9. Smith, M. E., Deficiencies in Data and Analyses for Environmental Impact Statements, Paper preprint presented at the 67th Annual Meeting of the Air Pollution Control Association, Denver, Colorado, June 9-13, 1974.

10. Slade, D. H. (editor), Meteorology and Atomic Energy, U.S. Atomic Energy Commission, Oak Ridge, Tennessee, 445 pp, 1968.

11. Yanskey, G. R., Markee, Jr., E. H., and Richter, A. P., Climatography of the National Reactor Testing Station, Environmental Science Services Administration, 1966.

12. Woodward, K., "Probability Treatment of Atmospheric Dispersion for Dose Calculations," Nuclear Technology, 12, pp 281-289, 1968.

13. Smith, T. B. and Niemann, B. L., "Shoreline Diffusion Program Oceanside, California," Meteorology Research, Inc., MRI Technical Report 69 FR-860, Vol 1 Contract DA 42-007-AMC-180(R), Altadena, California, 230 pp, 1969.

14. Septoff, M., Mitchell, A. E., and Teuscher, L. H., NUS-1927, Final Report of the Onshore Tracer Tests Conducted December 1976 Through March 1977 at the San Onofre Nuclear Generating Station, NUS Corporation, Rockville, Maryland, 1977.

2.3.7 BIBLIOGRAPHY

1. National Weather Service - Environmental Data Service - Local Climatological Data, Los Angeles, California, 1974.

2. National Weather Service - Environmental Data Service - Local Climatological Data, San Diego, California, 1974.

3. National Weather Service - Environmental Data Service Climatography of the United States No. 81 - California

4. Sellers, W. D., Physical Climatology, University of Chicago Press, Chicago, Illinois, p 272, 1965.

5. Data Sources

   A. United States Department of Commerce, Environmental Data Service, NOAA, 1964: Climatography of the United States, 86-4, Decennial Census of United States Climate - Climatic Summary of the United States, supplement for 1951 through 1960 - California, U.S. Government Printing Office, Washington, D.C.

   B. United States Department of Commerce, Environmental Data Service, NOAA: Storm Data, Monthly issues for the years 1960 through October 1975, U.S. Government Printing Office, Washington, D.C.

   C. United States Department of Commerce, Environmental Data Service, NOAA: Local Climatological Data - Annual Summary with Comparative Data - Los Angeles, California, International Airport, 1973 and 1974, U.S. Government Printing Office, Washington, D.C.

   D. United States Department of Commerce, Environmental Data Service, NOAA: Local Climatological Data - Annual Summary with Comparative Data - San Diego, California, 1973 and 1974, U.S. Government Printing Office, Washington, D.C.

   E. United States Department of Commerce Weather Bureau, 1970: Climatography of the United States, 60-4, Climates of the States - California, U.S. Government Printing Office, Washington, D.C., June 1970.

   F. United States Department of Commerce, Weather Bureau, 1954: Climatography of the United States, 11-4, Decennial Census of the United States Climate - Climatic Summary of the United States - Supplement for 1931 through 1952 - California, U.S. Government Printing Office, Washington, D.C.

G. United States Department of Commerce, Weather Bureau: Climatological Data, National Summary, Annuals for the years 1951 through 1959, U.S. Government Printing Office, Washington, D.C.

6. Holzworth, G. C. and Blake, D., Meteorological Summaries of Importance to Air Pollution in Western San Diego County, California Department of Public Health, 29 pp, 1957.

7. Neilburger, M., Beer, G. C. P., and Leopold, L. P., The California Stratus Investigation of 1944, U.S. Department of Commerce, Weather Bureau, Washington, D.C., 1945.

8. Pierce, E. T. and Cianos, N., A Ground-Lightning Environment for Engineering Usage, Stanford Research Institute, Project 1834, 1972.

2.4 HYDROLOGIC ENGINEERING

The data and information contained in Section 2.4 and referenced Appendices are historical information developed during San Onofre's original design to address Hydrologic Engineering. The information was used to determine the plant's design basis. Unless otherwise noted in the text, this information has not been updated to reflect data from later years.

2.4.1 HYDROLOGIC DESCRIPTION

2.4.1.1 Site and Facilities

The site is located on the southern California coast of the Pacific Ocean near the City of San Clemente, California in the SW1/4, NW1/4, Section 30, T. 9 S., R. 6 W., as shown in Figures 2.4-1 and 2.4-2 taken from the U.S. Geological Survey San Onofre Bluff Quadrangle. Bordering the site to the north is the existing San Onofre Nuclear Generating Station North Industrial Area (formerly Unit 1), to the south the San Onofre State Beach, and to the east the U.S. Marine Corps Base, Camp Pendleton. Access to the site is by way of Interstate Highway 5, approximately 300 feet to the east and the commercial railroad, approximately 200 feet to the east.

The power block finish grade elevation is +30.00 mean lower low water (mllw). A subsurface drainage system will carry normal storm drainage flows to the cooling-water intake structure. For consideration of flooding due to the thunderstorm probable maximum precipitation (PMP), all catch basins for the subsurface drainage system were assumed plugged; surface drainage facilities will transmit all thunderstorm drainage flows in the power block over the seawall to the ocean. Drainage areas contributing to the surface drainage flows in the power block area are shown on Figure 2.4-3.

A description of all exterior accesses, openings, or penetrations of safety-related structures subject to hydrologic considerations are tabulated in Table 3.4-1.

2.4.1.2 Hydrosphere

2.4.1.2.1 San Onofre Region

The San Onofre site is situated on a coastal plain at the base of the western foothills of the Santa Margarita Mountain Range. In this area the elevation rises sharply from sea level to a fairly level terrace formation 100-200 feet above sea level. At the terminus of the terrace formation, some 1500 feet inland, the foothills begin, rising with moderate slopes to an elevation of 3000 feet above sea level. The foothills belt extends approximately 28 miles inland and lies in a general northwest-southeast direction.

Natural plant cover in the coastal plain sector typically consists of coastal chaparral and grassland, while the foothill sector is composed mainly of chaparral and open woodland. The majority of the soil structure in the coastal plain is a combination of sandstone and shale.

Alluvial fans within this area are composed of sandy-clay and clayey-loam material. Soil structures within the foothill sector consist mainly of sandy loam over a layer of clayey subsoil.[1]

The mean annual temperature in the coastal plain region is 61˚F, with a mean minimum temperature of 42˚F in January. Annual rainfall amount falls between 10 to 16 inches, with 90% of this annual total occurring during the months of November through April. Soils generally remain thoroughly moistened during this period; however, they become dry by summer due mainly to the rapid plant growth period taking place during the months of April and May.

The foothills sector exhibits a climate similar to that of the coastal plains. The mean annual temperature is 60˚F with a January mean minimum of 38˚F. Annual rainfall ranges from 12 to 20 inches. Heavy rainfall usually occurs during the months of December through April. As in the coastal plains, the soils are usually thoroughly moistened at this time, drying by summer.[1]

2.4.1.2.2 Major Drainage Basins

There are no perennial streams in the general vicinity of the plant site. However, ephemeral streams and water courses do exist. The major streams are San Mateo Creek, located approximately 2 miles to the northwest, and San Onofre Creek located approximately 1 mile to the northwest.

2.4.1.2.2.1 San Mateo Creek

San Mateo Creek has a drainage area of 132 square miles in size. Records from the U.S. Geological Survey recording gage[2] at the mouth are available for water years October 1946 to September 1967, at which time management of and record keeping for the gage was discontinued. From an examination of the topography of the area, it was determined that the drainage divide separating San Mateo and San Onofre Creeks would preclude the plant site being influenced by San Mateo Creek.

2.4.1.2.2.2 San Onofre Creek

San Onofre Creek has a drainage area of 43 square miles. A U.S. Geological Survey recording gage is located at the mouth with available records covering a period from October 1946 to September 1967. The drainage basin is presented in Figure 2.4-5. The basin length is approximately 9.7 miles and is 4.7 miles in width.

San Onofre Creek and its watershed lies entirely on U.S. Marine Corps Base, Camp Pendleton. The origin of the basin is in the Santa Margarita Mountains to the northeast of the site. The maximum elevation in the basin is 3187 feet above mllw with the minimum at sea level. Ground slope within the tributary area varies from approximately 3% to 10%.

There are no existing or proposed water control structures within the San Onofre Creek Basin. Camp Pendleton currently uses surface runoff infiltration for purposes of recharging the base well system, otherwise there are no surface water users in the basin.

2.4.1.2.2.3 Foothill Drainage Basin

The foothill drainage basin identified in Figure 2.4-6 contributes to the hydrologic factors influencing the plant site. The basin totals 0.86 square mile in area. There are no gaging stations located within the basin and, consequently, stream flow records are not available.

The entire watershed lies within the boundaries of the Marine Corps Base, Camp Pendleton. Elevation in the basin varies between a maximum of 1200 feet and a minimum of 100 feet above msl. Ground slope varies from 8 to 22%. Ground cover is moderate within the basin consisting mainly of chaparral and grassland.

Water control structures consist of the 42-inch and 72-inch diameter concrete culverts under Interstate Highway 5, as shown in Figure 2.4-6. The culverts are maintained by the California State Department of Transportation. The capacity of these culverts is 180 and 520 ft^3/s, respectively. In addition to the two culverts identified above, a channel traverses the basin along the east side of Interstate Highway 5 diverting runoff to San Onofre Creek, as shown in Figure 2.4-6.

2.4.2 FLOODS

2.4.2.1 Flood History

There are four U.S. Geological Survey stream-gaging stations located within the general plant vicinity. Two are located on San Mateo Creek and two on San Onofre Creek. The period of record for these gages varies from 17 to 21 years. Peak recorded discharges are as presented in Table 2.4-1. An examination of stream flow data revealed that measurable flows occur only 4 to 5 months of the year, usually during the months of December through April.

Ocean storm surges and tsunami historical data are presented in Subsections 2.4.5 and 2.4.6, respectively. Ice jams and dam failures do not apply to the San Onofre site (2.4.7 and 2.4.4 respectively).

2.4.2.2 Flood Design Considerations

For purposes of determining and analyzing potential flood sources, consideration was given to the San Onofre Creek Basin, as shown in Figure 2.4-5, and the foothill drainage area east of the site, as defined in Figure 2.4-6. In both cases the probable maximum flood (PMF) was defined as the design basis event. Regulatory Guide 1.59, Design Basis Floods for Nuclear Power Plants, and references noted therein were employed as standards in the determination of the PMF.

Results of the PMF analysis concluded that the San Onofre Creek Basin exhibits no flooding potential to the site. The maximum flood stage, as a result of the PMF, was determined to be

24.1 feet at the mouth of the creek. Topographical features of the basin would contain this flow and thereby preclude flooding of the site by this source.

An analysis of the flooding potential of the foothill drainage area was also performed during San Onofre's original design. The results of this analysis produced evidence that the site could be subjected to flooding during the occurrence of the design basis PMF. In order to preclude flooding of the site by this source a diversion structure, as shown in Figure 2.4-4, was constructed to route the surface runoff from the foothill drainage area to the San Onofre Creek Basin. For purposes of design of the diversion structure, the PMF was used as the design basis event for determining the maximum water elevation. Following the decision to permanently cease power operations, an additional hydrologic analysis was performed that determined that the diversion structure was not required for site flood protection.(50)

As discussed in Paragraphs 2.4.5.2, 2.4.5.3, and 2.4.6.1, the occurrence of storm surge, storm wave action, and tsunami will not cause flooding of the site.

2.4.2.3 Effects of Local Intense Precipitation

The San Onofre region is susceptible to major storm activity during the months of October through April. U.S. Weather Bureau Hydrometeorological Report 36 was used to calculate the orographic and conveyance components of the frontal probable maximum precipitation (PMP).(5) Evaluation of the thunderstorm PMP was also determined for the San Onofre site based on the methods of the U.S. Weather Bureau.(6) The thunderstorm PMP event causes the highest flood level on the San Onofre site and was therefore used as the design basis event.

The distribution of precipitation in the 6-hour thunderstorm used to design the site drainage structures is presented in Table 2.4-2. Arrangement of the incremental values into the critical PMP storm is based on procedures used by the U.S. Army Corps of Engineers.(7)

The drainage area tributary to the Units 2 and 3 power block was divided into sub-basins as presented in Figure 2.4-3. Drainage characteristics and peak flows for the sub-basins are presented in Table 2.4-3.

The U.S. Soil Conservation Service soil-complex method(8) was used to construct the hydrograph resulting from the PMP. Runoff curves for the given soil types were selected on the basis of Antecedent Moisture Condition III. Due to the relatively short times of concentration and corresponding very short lag times of the sub-basins, the assumption was made that all precipitation excess within any period became runoff during that period. Precipitation intensities for durations less than 15 minutes were interpolated from the thunderstorm PMP data presented in Table 2.4-2. The resultant PMF hydrographs for the sub-basins are shown in Figures 2.4-7 through 2.4-11.

The subsurface drainage system is designed to accommodate the runoff from the onsite areas and offsite areas west of Interstate Highway 5, resulting from a precipitation intensity of 3 in./h.

Table 2.4-1
STREAM FLOW STATIONS IN VICINITY OF SAN ONOFRE SITE(2)(3)(4)

Station	USGS Station No.	Location	Period of Record	Drainage Area(mi^2)	Peak Flow		
					Date	Discharge (ft^3/s)	Gage Height (ft)
San Onofre Creek near San Onofre, California	11-0462	Lat 33˚23'23" Long. 117˚30'50"	Oct 1950 to Sept 1967	34.6	4/1/58	2,680	5.90
San Onofre Creek at San Onofre, California	11-0462.5	Lat 33˚23'00" Long. 117˚34'22"	Oct 1946 to Sept 1967	42.2	4/1/58	2,600	6.90
San Mateo Creek near San Clemente, California	11-0463	Lat 33˚28'15" Long. 117˚28'20"	Oct 1952 to Sept 1967	80.8	12/6/66	7,300	10.45
San Mateo Creek at San Onofre, California	11-0463.7	Lat 33˚23'46" Long. 117˚35'21"	Oct 1946 to Sept 1967	132	12/5/66	10,000	10.42

Table 2.4-2
6-HOUR, 1-SQUARE-MILE PROBABLE MAXIMUM THUNDERSTORM PRECIPITATION (PMP)

Time (hours)	PMP Total (inches)	PMP Incremental (inches)	PMP Critically Arranged (inches)
0.25	3.01	3.01	0.14
0.50	4.90	1.89	0.14
0.75	6.16	1.26	0.14
1.00	7.00	0.84	0.14
1.25	7.63	0.63	0.14
1.50	8.12	0.49	0.21
1.75	8.54	0.42	0.21
2.00	8.96	0.42	0.21
2.25	9.31	0.35	0.28
2.50	9.59	0.28	0.35
2.75	9.87	0.28	0.42
3.00	10.15	0.28	0.63
3.25	10.36	0.21	1.26
3.50	10.57	0.21	3.01
3.75	10.78	0.21	1.89
4.00	10.99	0.21	0.84
4.25	11.20	0.21	0.49
4.50	11.41	0.21	0.42
4.75	11.55	0.14	0.28
5.00	11.69	0.14	0.28
5.25	11.83	0.14	0.21
5.50	11.97	0.14	0.21
5.75	12.11	0.14	0.21
6.00	12.25	0.14	0.14

Table 2.4-3
SAN ONOFRE SITE SUB-BASIN DRAINAGE PARAMETERS

Sub-Basin[a]	Area (acres)	Time of Concentration (minutes)	Time Increment For Analysis (minutes)	Peak PMP Discharge (ft^3/s)
1	6.4	10/5	10/5	59
2	8.8	5	5	83[c]
3	8.8	5	5	83[c]
4	7.9	5	5	96
5	32.6	30	30	270[b]
6	1.0	15	15	12

(a) See Figure 2.4-3
(b) Ten ft^3/s of this contributes to surface drainage in the power block area.
(c) This value only includes discharge over the seawall.
(d) This value does not include the MUD tank area that will not contribute to surface drainage.

All catch basins for the subsurface drainage system, roof drains, and exposed floor drains were assumed plugged for the purpose of determining water surface elevations arising during the thunderstorm PMP event. Two 4-foot by 4-foot box culverts at Highway 101 were assumed to remain operational. The box culverts are sufficiently large and are in an area that would not supply materials capable of plugging them. Even if flow were restricted through them, the topography along Highway 101 is such that the resulting drainage flows would not impact the plant site.

The switchyard has an upper and lower bench as illustrated in Figure 2.4-13. With the normal catch basins plugged, the ponded water on the upper bench will drain to the south access road. A peak flow of 32 ft^3/s would be discharged from the upper bench as a result of the thunderstorm PMP event. This peak was calculated by routing the storm hydrograph through the upper bench by the storage routing procedure specified by Henderson.[9] The cross-section of the access road is sloped to prevent the upper bench drainage from entering the lower bench.

Drainage entering the lower bench includes not only drainage from the thunderstorm PMP event over this area, but also accounts for the possibility that water could enter the normal storm drain system at the upper bench and emerge from the normal catch basins in the lower bench. The resulting peak flow of 54 ft^3/s will overtop the berm and flow into the Unit 2 and 3 power blocks.

For the extreme thunderstorm PMP event, when the normal catch basins are assumed plugged, the upper site area will drain into the barranca to the west without impacting the Area 4 drainage (Figure 2.4-3). Area 5 will drain through the two 4-foot by 4-foot box culverts; one enters the subsurface storm drain line leading to the power block and one enters the line to the barranca. The capacity of each box culvert (135 ft^3/s) is less than the approximate 300 ft^3/s capacity of the 54-inch conduit to which each culvert drains.

A runoff flow of 10 ft^3/s from Area 5 is assumed to enter the Unit 3 power block area at the junction of Highway 101 and the Unit 2 and 3 power block access road (Figure 2.4-3). The balance of the runoff flow from Area 5 will be diverted from Highway 101 into the upper site area and away from the power block area at station coordinate S44+90 (approximate) (Figure 2.4-3). At the south entrance to the Unit 3 power block, the peak discharge to the power block area was determined by routing the hydrographs from the contributing areas, taking into account the time of concentration and lag times for Areas 1, 4, and 6, plus including 10 ft^3/s from Area 5 (Figure 2.4-3). The resulting peak flow, at the south entrance to the Unit 3 power block, is 154 ft^3/s. Construction of a diversion channel on the south side of the Service Building allows 80 ft^3/s to be diverted over the seawall outside of the power block resulting in 74 ft^3/s flowing into the Unit 3 power block.

Swales are provided in the asphalt areas around the power block to convey the drainage to the seawall where it will discharge to the ocean. During normal rainfall intensities, the subsurface drainage system will convey all drainage to the cooling water intake structure. A duration of 5 minutes was used in calculating the peak discharges in the power block areas. The maximum backwater elevations resulting from these peak flows are shown on Figure 2.4-13. Contributing roof drainage was derived by routing the PMP hydrograph for each roof through the parapet openings. Pertinent roof discharge points and the corresponding ponded water surface depths are presented in Figure 2.4-13.

Penetrations in the auxiliary building control area, at elevations 72 and 30 feet are protected against ponding resulting from roof drainage by openings in the seismic gap which allows the water to fall to elevation 7 in the turbine area. The areas contributing to the turbine buildings are roof drainage from the safety equipment building, the auxiliary building, and the turbine areas. The volume of floodwater entering elevation 7 of the turbine building during the PMP thunderstorm will not impact safety-related equipment.

Surface water will not enter the auxiliary building from the west because the bridge walkway over the intake structure has numerous parapet openings which would allow drainage to flow into the cooling water intake structure. Additionally, a berm on this bridge walkway prevents Control Room/Command Center complex flooding due to a possible surge in the circulating water system.

The maximum postulated flood level in the Units 2 and 3 power blocks has been established below elevation +31.0 feet mean lower low water (MLLW) level as shown on Figure 2.4-13. Those penetrations below elevation +31.0 are specified in Table 3.4-1. In the extreme event that the thunderstorm PMP occurs, no safety-related equipment will be impacted by flooding for the following reasons:

- Watertight barriers prevent water from reaching most safety-related areas.

- Negligible water will enter the exterior doors with sills below the floodwater elevation because they either open outwards, are locked/card coded, have weather stripping, and/or are protected by curbs.

- Drainage water in the structures which entered from other areas (e.g., from roofs, open areas) will not reach safety-related equipment.

The drainage features indicated previously and those presented below will prevent all but approximately 15 cfs of runoff from Units 2 and 3 from reaching the North Industrial Area (NIA):

- Grade elevations in the switchyard access and the railroad spur access are above the calculated flood elevations.

- A curb is located at the slope interface of the NIA and the Unit 2 power block areas, except at the stairway between the NIA and Unit 2. The small amount of runoff (approximately 15 cfs) from Unit 2 into the NIA is easily within the capacity of the NIA Yard Sump.

Storm drainage in the NIA will not flow to Units 2 and 3 because of the elevation differential; the NIA is at elevation 20 feet and Units 2 and 3 are at 30 feet. Although the NIA access road connects to the access road to the Unit 2 and 3 switchyard, the NIA access road will be graded to preclude drainage flows from entering the Unit 2 and 3 site.

2.4.3 PROBABLE MAXIMUM FLOOD ON STREAMS AND RIVERS

An analysis of the 0.86 square mile foothill drainage area and the 43 square miles San Onofre Creek Basin was conducted to determine the PMF and subsequent contribution to flooding at the San Onofre site. The recommendations of NRC Regulatory Guide 1.59 were used in conducting the PMF analysis.

2.4.3.1 Probable Maximum Precipitation

The San Onofre area is susceptible to frontal storms, usually occurring during the months of October through April, and local thunderstorms which are predominant during summer and early fall. A comparison of the PMP values associated with both types of storms was made to determine the critical event. HMR 36(5) was used to calculate the frontal storm PMP and the National Weather Service Report(6) was used in determining the thunderstorm PMP. By comparison, it was concluded that the thunderstorm PMP was the more critical and consequently was used as the design basis event. The 6-hour, 1-square mile thunderstorm PMP is presented in Table 2.4-2.

Table 2.4-4
6-HOUR PROBABLE MAXIMUM THUNDERSTORM PRECIPITATION
SAN ONOFRE CREEK BASIN (PMP)

Time (hours)	PMP Total (inches)	PMP Incremental (inches)	PMP Critically Arranged (inches)
0.25	1.96	1.96	0.16
0.50	3.19	1.23	0.16
0.75	4.00	0.81	0.17
1.00	4.55	0.55	0.17
1.25	4.94	0.39	0.18
1.50	5.32	0.38	0.19
1.75	5.71	0.39	0.20
2.00	6.09	0.38	0.21
2.25	6.35	0.26	0.25
2.50	6.60	0.25	0.26
2.75	6.86	0.26	0.38
3.00	7.11	0.25	0.39
3.25	7.32	0.21	0.81
3.50	7.51	0.19	1.96
3.75	7.71	0.20	1.23
4.00	7.91	0.20	0.55
4.25	8.10	0.19	0.39
4.50	8.28	0.18	0.38
4.75	8.47	0.19	0.26
5.00	8.65	0.18	0.25
5.25	8.82	0.17	0.20
5.50	8.98	0.16	0.19
5.75	9.15	0.17	0.19
6.00	9.31	0.16	0.18

Table 2.4-4 provides the 6-hour thunderstorm PMP for San Onofre Creek Basin. Because of the size of San Onofre Creek Basin, the 1-square mile PMP was adjusted and applied over the basin in accordance with the procedures outlined in Reference 6. As noted in Table 2.4-4, the PMP total for the San Onofre Creek Basin is 9.31 inches.

The thunderstorm PMP for the foothill drainage basin was derived in a manner similar to the method used for the San Onofre Creek Basin. The 1-square mile PMP total was calculated at 12.25 inches as presented in Table 2.4-2.

Occurrence of snow coincident with the PMP was not considered a probable event at the San Onofre Site.

2.4.3.2 Precipitation Losses

From results of PMP studies noted in the National Weather Service Report,[(6)] it was determined that the occurrence of antecedent precipitation preceding the design basis PMP is highly probable. For this reason, the assumption was made that a storm of significant magnitude occurred immediately prior to the PMP, resulting in complete saturation of the soil with minimum loss to infiltration.

After examining records of major storms in the general vicinity of San Onofre, the decision was made to use the major storms of January and February 1969 for analysis of infiltration capability. The Corps of Engineers Hydrologic Engineering Center HEC-1 computer program,[(10)] Unit Hydrograph and Loss Rate Optimization Subroutine, was used to determine infiltration rates for the above storms. Records available for San Onofre Creek were not precise enough to permit a valid reconstruction of the storm runoff hydrograph. For this reason an analysis was conducted of the Santa Margarita River Basin near Oceanside. The Santa Margarita River and San Onofre Creek Basins were judged similar in regard to soil type and average ground slopes, although the Santa Margarita River Basin is considerably larger in total drainage area. On the basis of results obtained from the analysis a uniform infiltration rate of 0.1 in./h was used. Initial abstraction was not considered since it was assumed that the soil was saturated at the beginning of the PMP.

2.4.3.3 Runoff and Stream Course Models

2.4.3.3.1 San Onofre Creek Basin

The San Onofre Creek Basin was subdivided as shown in Figure 2.4-5. Hydrologic parameters for each sub-basin were calculated and are tabulated in Table 2.4-5. The sub-basin lag times were calculated on the basis of Figure 2.4-15 derived by the Corps of Engineers and presented by Linsley.[(11)] As noted in the referenced publication, this basin lag curve was derived as a result of a study of various drainage basins in southern California conducted by the Corps. For purposes of conservatism, a 10% reduction of all calculated lag times was performed prior to their use in calculations.

Table 2.4-5
SAN ONOFRE CREEK BASIN SUB-BASIN DRAINAGE PARAMETERS

Sub-basin	Area (mi^2)	L[a] (mi)	L_a[b] (mi)		Slope[c] (ft/mi)	Lag Factor $L \bullet L_a / \sqrt{S}$	Lag Time[d] (h)	Adjusted Lag Time[e] (h)
A1	12.80	7.6	3.2		342	1.3	1.3	1.2
A2	12.10	7.6	5.5		380	2.1	1.6	1.4
A3	0.60	1.1	0.8		542	0.04	0.4	0.3
A4	9.10	6.3	2.8		308	1.0	1.2	1.1
A5	8.60	5.7	2.8		155	1.3	1.3	1.2

(a) Length of watercourse from sub-basin divide to sub-basin outlet.

(b) Distance from point on watercourse nearest centroid of sub-basin to outlet of sub-basin.

(c) Slope of sub-basin from divide to outlet.

(d) Time in hours from centroid of effective rainfall to peak of unit hydrograph.

(e) Adjusted lag time reflecting 10% reduction in calculated lag time.

Using the Corps HEC-1 computer program,[10] the PMF hydrograph for each sub-basin was derived. A Snyder peaking coefficient of 0.7 was used for unit hydrograph computations in the program for each sub-basin. This value was determined as a result of the analysis of the major storms of January and February 1969 referenced in Paragraph 2.4.3.2. As noted, the analysis was performed for the Santa Margarita River Basin where records permitted a valid reconstruction of the basin runoff hydrograph. After determining the PMF hydrograph for each individual sub-basin they were routed and combined to obtain a PMF hydrograph at the mouth of San Onofre Creek.

Flood routing was conducted using the Muskingum Method. The Muskingum storage coefficient K for each reach was taken as 50% of the basin's lag time. This value was arrived at by assuming low flow and high flow conditions in sub-basin A5, calculating the corresponding velocities and average flow velocity. The average velocity was combined with the reach length to yield the travel time through the reach. From this relationship, a proportionality constant was calculated (i.e., 0.5) and then used in calculating K for the remaining sub-basins. The routing coefficient X was assumed as 0.3. This value is recommended for use in mountainous regions.[11]

2.4.3.3.2 Foothill Drainage Basin

The analysis of the foothill drainage basin was conducted in a manner similar to that of San Onofre Creek Basin described above. The drainage area was subdivided as shown in Figure 2.4-6. Sub-basin hydrologic parameters are as defined in Table 2.4-6. Figure 2.4-15 was used for calculation of sub-basin lag times.

The HEC-1 computer program was used to develop the unit hydrograph and resultant PMF hydrograph for each sub-basin. As explained in Paragraph 2.4.3.3.1, a Snyder peaking coefficient value of 0.7 was used in the derivation of the unit hydrographs. The PMF hydrographs obtained from each sub-basin were routed to San Onofre Creek assuming the future structure as shown in Figure 2.4-4. Due to the relatively short distance between the outlets of sub-basins B1 and B2, approximately 0.75 mile, and narrow range of lag times for the sub-basins, it was decided to ignore lag and travel times and combine the individual sub-basin PMF hydrographs directly, yielding a conservative PMF hydrograph at the outlet of sub-basin B2.

2.4.3.4 Probable Maximum Flood Flow

2.4.3.4.1 San Onofre Creek Basin

The PMF hydrograph resulting from the PMP for San Onofre Creek Basin is presented in Figure 2.4-16. This hydrograph represents the PMF flow for the basin's tributary area above the mouth, station 8 on Figure 2.4-5. As shown in Figure 2.4-16, the PMF peak flow is 71,000 ft^3/s.

Table 2.4-6
FOOTHILL DRAINAGE BASIN
SUB-BASIN DRAINAGE PARAMETERS

Sub-basin	Area (mi^2)	L (mi)	L_a (mi)	Slope (ft/mi)	Lag Factor $L \bullet L_a / \sqrt{S}$	Lag Time (hr)	Adjusted Lag Time[a] (h)
B1	0.42	1.58	0.85	743	0.043	0.36	0.32
B2	0.14	0.92	0.26	1,108	0.007	0.18	0.16
B3	0.15	0.78	0.33	833	0.009	0.20	0.18
B4	0.08	0.56	0.17	1,000	0.003	0.13	0.12
B5	0.07	0.57	0.21	1,211	0.0035	0.14	0.13

[a] Adjusted lag time reflecting 10% reduction in calculated lag time.

2.4.3.4.2 Foothill Drainage Basin

The PMF hydrograph for the foothill basin was developed as discussed in Paragraph 2.4.3.3.2, assuming a diversion structure. PMF hydrographs for each of the sub-basins are presented in Figures 2.4-7 through 2.4-10. Figure 2.4-11 presents the PMF hydrograph for local inflow from sub-basin B2 to San Onofre Creek. The combined hydrograph for the entire area is presented in Figure 2.4-17. The PMF peak discharge was calculated to be 5225 ft^3/s for the basin.

An analysis of potential debris yield from the basin was performed in order to determine the amount of debris storage required behind the diversion structure. The debris runoff analysis was based on debris production curves derived by the Los Angeles County Flood Control District given in Reference 12. The curve selected for the basis of analysis was curve DPA-6, valid for the Puente Hills area in Los Angeles County. This curve is reproduced in Figure 2.4-18. From comparison, the Puente Hills was judged similar to the Foothill Basin on the basis of topograph, soil type, and ground cover. Since Curve DPA-6 was based on a less severe precipitation intensity than that of the PMP for the Foothill Basin an adjustment was made on the basis of the Universal Soil-Loss Equation.

$$A = R\ K\ L\ S\ C\ P$$

where:

A = annual soil loss (tons/acre-yr)

R = rainfall factor

K = soil erodibility factor

L = slope-length factor

S = slope-gradient factor

C = cropping

P = supporting conservation practice index

The factors K, L, S, C and P in the Universal Soil-Loss Equation are all functions of topography, soil type and ground cover. Since the Puente Hills area and the Foothill Basin were judged similar in these respects, the only variable factor is the rainfall factor, R. Reference 13 indicates that R is related to precipitation by the following equation

$$R = 35.1\ P^{1.96}$$

where:

P = 6-hour precipitation (inches)

The Los Angeles County curve was based on a 6-hour precipitation of 3.9 inches with a corresponding R of 505 whereas the PMP of 12.3 inches has an R of 4800. The resultant ratio of 10 was used to adjust the debris production curve as presented in Figure 2.4-18. Figures 2.4-7 through 2.4-11 show the calculated debris runoff and the resultant design hydrograph for each sub-basin. Figure 2.4-17 presents the composite PMF hydro-graph for the entire Foothill Basin. As noted, the design peak discharge was calculated to be 7335 ft^3/s. The debris production curve, DPA-6, was derived by Los Angeles County assuming a major watershed burn immediately prior to the debris producing storm. On this basis, the debris runoff calculated for the Foothill Basin is conservative in nature.

2.4.3.5 Water Level Determinations

Following the decision to permanently cease power operations, a new analysis was performed to determine the effect to site water levels during Probable Maximum Precipitation (PMP) event, assuming the condition that the Offsite PMF Berm and Channel was removed.[50] The calculation uses the FLO-2D model computer program which is a combined two-dimensional hydrologic and hydraulic model for assessment of flooding hazards. FLO-2D is designed to simulate river and overbank flows as well as unconfined flows over complex topography and variable roughness, split channel flows, mud/debris flows and urban flooding. FLO-2D moves flood volume on a grid for overland flow through stream segments for channel routing.

The analysis determined the maximum water (flood) levels onsite for the condition where the Offsite PMF Berm is removed, and compared those results to the baseline condition where Berm was present. Results of the analysis indicate that there is a small increase in the maximum onsite water levels for the condition where the PMF Berm is removed compared to condition with the berm present. The incremental increase in PMF depths at critical openings (defined as openings where water might infiltrate buildings with a flow path to equipment that is important-to-safety) due to postulated removal of the Offsite PMF Berm ranges from a minimum of 0.0 feet to a maximum of 0.1 feet. When this incremental increase is added to the maximum water (flood) levels, shown in Figure 2.4-13, the maximum water level for Units 2 and 3 would increase from 30.8 feet to 30.9 feet MLLW, which is less than the maximum elevation +31.0 feet MLLW stated in DSAR Section 3.4.1.1. Structures, systems, and components that are important-to-safety are not adversely impacted by the small increase in maximum water (flood) levels caused by the postulated removal of the Offsite PMF Berm.

Consequently, the offsite Probable Maximum Flood (PMF) Berm and Channel (referred to as the "diversion structure") is no longer required for external flood protection of the plant in the permanently defueled condition. Reference to the diversion structure in other DSAR sections and all other design basis documents, including drawings, are for historical information only.

2.4.3.5.1 San Onofre Creek Basin

The PMF peak discharge of 71,000 ft^3/s was used in determining the maximum flood stage in San Onofre Creek. A water surface profile was constructed using the Corps HEC-2 computer program.[14] Profile computations commencing at the mouth of San Onofre Creek were carried approximately 2.3 miles upstream. Locations of cross-sections used in the analysis are given in Figure 2.4-19.

For calculation purposes, a Manning's n value of 0.12 was used throughout the reach being analyzed. This value is representative of a natural channel or flood plain with heavy underbrush or growth of timber. San Onofre Creek and floodplain are scattered with light to medium brush and trees with the majority of the watercourse clean and clear, suggesting a Manning's n on the order of 0.07. The higher value of 0.12 was used for conservatism.

The analysis performed with HEC-2[14] concluded that flow through the bridge structure at the mouth was restricted to subcritical. Yarnell's energy equation was used for the calculation of the change in water surface elevation through the bridge. A shape coefficient of 1.25 for a square nose and tail pier was used. The results of the analysis ascertained that the flow is contained within the limits of the floodplain of San Onofre Creek not presenting any risk of flooding at the site. PMF flood stage values for San Onofre Creek are presented in Table 2.4-7.

2.4.3.5.2 Foothill Drainage Basin

As part of the Plant's original flood protection, runoff from the Foothill Drainage Basin was diverted to San Onofre Creek by a diversion structure as shown in Figure 2.4-6. The diversion structure consisted of an earth filled berm with excavated channel designed to convey the peak discharge associated with the PMF. Following the decision to permanently cease power operations, an additional hydrologic analysis was performed that determined the diversion structure was not required for site flood protection. [50]

Table 2.4-7
PMP WATER SURFACE PROFILE SAN ONOFRE CREEK

Cross-Section[a]	Discharge (ft^3/s)	Depth of Flow (ft)	Water Surface Elevation[b] (ft)	Average Velocity (ft/s)	Critical Depth (ft)	Manning's n
1	71,000	8.3	8.3	16.5	8.3	0.12
2	71,000	18.4	28.4	8.6	10.8	0.12
3	71,000	22.4	32.4	11.4	15.3	0.12
4	71,000	22.6	32.6	11.9	15.3	0.12
5	71,000	24.1	39.1	3.9	9.5	0.12
6	71,000	20.0	40.0	5.1	10.0	0.12
7	71,000	21.4	44.4	3.1	10.8	0.12
8	71,000	14.4	48.4	3.2	6.5	0.12
9	71,000	13.8	53.8	3.4	6.0	0.12
10	71,000	14.0	64.0	5.1	9.6	0.12
11	71,000	12.8	77.8	4.1	6.3	0.12
12	71,000	16.6	86.6	7.0	10.2	0.12
13	71,000	15.2	95.2	6.6	7.9	0.12
14	71,000	15.5	105.5	6.4	7.0	0.12

[a] Cross-sections as located in Figure 2.4-19
[b] Elevation based on datum of msl

2.4.3.6 Coincident Wind Wave Activity

Coincident wind wave activity for the San Onofre Creek and Foothill Drainage Basins was not considered critical.

2.4.4 POTENTIAL DAM FAILURES, SEISMICALLY INDUCED

There are no existing dams located within the vicinity of the plant site, whose seismically induced failure could result in adverse flooding at the site.

2.4.5 PROBABLE MAXIMUM SURGE AND SEICHE FLOODING

2.4.5.1 Probable Maximum Winds and Associated Meteorological Parameters

The probable maximum winds associated with maximum surge and seiche water levels at the San Onofre Nuclear Generating Station are caused by northeast Pacific tropical cyclones that reach the southern California coast. Although relatively strong winds may result from severe Santa Ana conditions or extratropical storms, these weather systems will not cause water levels along the southern California coast as high as those resulting from a tropical storm entering the coastal areas. The Santa Ana conditions cause winds that blow offshore and tend to cause low water levels rather than high levels. The winter and spring extratropical storms usually enter California from the west. The centers of these storms move into central or northern California. Cold fronts embedded in these storms move rapidly through southern California. Maximum winds speeds of 35 to 45 knots are associated with the frontal systems. The winds shift from southwest to west and then to northwest as the frontal system moves through the area. The rapid variation of the wind speed and directions are not conducive to producing high water levels along the coast. The tropical storm, on the other hand, moves more slowly with very high wind speeds embedded in the storm circulation. This provides the necessary time and fetch to generate maximum surge and seiche water levels as the storm moves across the coast.

Before meteorological satellite observations were available, it was generally believed that on the average about 10 tropical cyclones occurred each year during the tropical storm season, May to November. However, satellite data has shown that the average may be as high as 15 to 20 per year, making the northeast Pacific one of the most active regions of the world.(15)

Most of the northeast Pacific tropical storms form a few hundred miles off the west coast of Mexico between 10˚ and 20˚ north latitude over very warm waters. Massive moisture and cloudiness from the Intertropical Convergence Zone (located at around 10˚N latitude in the summer) are fed directly into the southern half of the cyclones. During the midsummer months, the storms move northwestward and westward, paralleling the coast of Mexico. During the early and late season months, several storms usually curve to the northeast and cross the Mexican mainland coast or Baja California and eventually die over land.

The forward speed of movement of the tropical cyclones usually ranges between 5 to 15 knots. The average observed duration is from 4 to 5 days, with late-season cyclones on the average being of slightly shorter duration. Several storms have been tracked for more than 10 days.[16]

While tropical storms in the northeast Pacific are rather frequent during the summer months, they are not as intense as their counterparts in the Atlantic and western Pacific. In these latter regions about 65% of the tropical storms reach hurricane or typhoon intensity, while in the northeast Pacific only about 33% reach hurricane force.[17]

The size of the average storm is smaller than that of its Atlantic and western Pacific counterparts. The radius of gale force winds is thought to be relatively small. Now and then, however, a cyclone of huge proportions is encountered. Due to the scarcity of observational data, the intensity of the cyclones is often difficult to determine or estimate. The more severe ones can be assumed to have maximum sustained winds in the 100- to 125-knot range, while most of the storms that reach hurricane force (>64 knots) barely do so. However, a majority of the storms do not attain even this force.

Only one of these tropical cyclones has entered southern California in the last 50 years, with high winds and extensive damage. This occurred on September 25, 1939, when a tropical storm moved inland near Los Angeles.[18] September 1939 was unusual in that five tropical cyclones crossed the coast from Baja California northward. In addition to the southern California case, two other storms passed less than 200 miles south of San Diego (see Figure 2.4-23).

The southern California tropical storm of September 25, 1939, was a violent storm in its early offshore history. On the morning of September 22, while west of the southern tip of Baja California, winds of 60 knots and barometer 971 millibars (28.67 inches) were reported near the center. Its offshore track from that point was parallel to the coast (see Figure 2.4-23). This track was made possible by a strong ridge over the western United States and another offshore separated by an elongated inverted trough extending along the coast both at the surface and aloft. This trough persisted from the 19th through the 23rd, resulting in extremely high coastal and coastal mountain temperatures in southern and central California.

By the 24th, the ridge over the west had weakened, allowing the storm to veer toward the north-northeast and then toward northeast as it approached the southern California coast. The wind speed at San Pedro reached 41 knots before the 996-millibars (29.47 inches) low center entered the coast in that vicinity about 0800 PST on the morning of the 25th. The severity of this storm along the coast is indicated by a loss of 45 lives at sea, and property damage of approximately $2 million, largely from wave action at the coast.[19]

Although only one tropical storm has caused severe damage in the last 50 years, it is possible for conditions to occur that may produce several storms over a shorter period of time. Conditions conducive to entry of tropical storms into the southern California coast are weak summer north-westerly winds and a sluggish California current which results in high water temperatures along the coast. In some periods in the early 1800's the southern California coast apparently was affected by these tropical storms several times a year. These conditions were probably accompanied by abnormally high temperatures in autumn.[20]

Utilizing the climatology of the northeast Pacific tropical cyclones and the structure of typical hurricanes,[21] the track and the surface wind structure of the hypothetical maximum probable storm for the San Onofre site were constructed and are shown in Figures 2.4-24, 2.4-25, and 2.4-26. The track of the storm is shown in Figure 2.4-24. The speed of the hurricane is about 10 knots. The wind field for the hurricane for positions 1, 2, and 3 is shown in Figure 2.4-25. Wind speeds in excess of 110 knots occur in these positions but diminish to 70-75 knots (Figure 2.4-26) as it moves to position 4 on the southern California coast. The center of the hurricane crosses the coast near San Onofre and moves inland and dissipates.

2.4.5.2 Surge and Seiche Water Levels

Water levels antecedent to probable maximum surge and seiche levels are first discussed. Accepted conservative high and low tide levels and sea level anomalies for the San Onofre area are considered in establishing the antecedent water levels.

2.4.5.2.1 Tides

The character of the San Onofre tides is semidiurnal; i.e., two high tides and two low tides of differing amplitudes occur each day, on the average. The average of only the lower of the two low water levels is taken as the local bathymetric chart datum: mean lower low water (mllw). Mean lower low water thereby acts as a reference point in sea level variation discussions. The tide reference station local to San Onofre is at San Diego Bay.[22]

The specific location of San Onofre along the open coast north of San Diego necessitates that an amplitude ratio of 0.92 be applied to the San Diego reference data. This restricts the diurnal tidal range of the reference data to accurately reflect the tidal conditions at San Onofre.

Historically, at San Diego, where accurate absolute tidal levels have been recorded since 1906, the highest tide observed was on December 20, 1968, and the lowest tide observed was on December 17, 1933.[23] The extreme tides of 1968 and 1933 adjusted for the San Onofre location are +7.18 feet mllw and -2.66 feet mllw, respectively.

To establish the accepted conservative high and low tide levels for San Onofre, the 10% exceedance monthly spring tide was calculated. Semi-monthly spring tidal elevations at San Diego were obtained for the years 1968, 1970, 1972, 1974, and 1976 from tables of predicted tides (U.S. Department of Commerce for cited years). These data are shown in Table 2.4-10. The cumulative of highest and lowest tides at San Diego is given in Tables 2.4-11 and 2.4-12, respectively; these have been constructed from the data presented in Table 2.4-10. In these, the 10 and 90% exceedance levels are identified to the nearest 0.1 foot, as being +7.6 feet and -1.9 feet mllw (the tide is above +7.6 feet and below -1.9 feet mllw, only 10% of the time). To these are applied the amplitude ratio correction (0.92) for San Onofre to convert San Diego tides to ones accepted as representative of San Onofre. This yields a spring high tide at San Onofre that has a 10% probability of exceedance of +7.0 feet mllw and a spring low tide that has only a 10% chance of being lower than -1.75 feet below mllw.

2.4.5.2.2 Sea Level Anomalies

Mean sea level variations (sea level anomalies) that are significant in a time frame of 2 weeks or larger and that occur off of coastal southern California are principally attributable to two factors: variations in atmospheric pressure and changes in the specific volume of sea water.(24) Both factors vary seasonally. Specific volume changes can be ascribed mainly to oceanic temperature variations. The sea can be expected to respond to the local atmospheric pressure changes at a rate of 1 cm or -1 cm change in water level for each millibar atmospheric pressure decrease or increase, respectively. The pressure and specific volume contributions summed together form isostatic sea level variations.

Table 2.4-10
SPRING TIDAL ELEVATIONS AT SAN DIEGO, CALIFORNIA (FEET, RELATIVE TO MLLW)

Month	1968			1970			1972			1974			1976		
	Day	High	Low	Day	High	Low	Day	High	Low	Day	High	Low	Day	High	Low
January	1	7.2	-1.6	8	7.7	-2.1	1	7.2	-1.6	8	7.7	-2.1	1	7.1	-1.5
	28	7.2	-1.8	21	6.4	-1.0	16	6.9	-1.3	22	6.3	-0.8	17	6.9	-1.3
							19	7.0	-1.5						
February	13	6.7	-1.3	5	7.5	-2.1	14	6.7	-1.3	6	7.3	-1.8	15	6.8	-1.2
	25	6.6	-1.5	19	6.1	-0.8	26	6.3	-1.1	20	6.0	-0.6	26	6.0	-0.8
March	13	6.3	-1.0	5	6.9	-1.6	13	6.2	-0.9	6	6.6	-1.3	14	6.2	-0.9
	25	5.8	-0.9	20	5.5	-0.3	25	5.4	-0.6	26	5.8	-0.3	26	5.2	-0.2
April	14	6.8	-1.4	6	6.5	-1.1	14	7.0	-1.6	7	6.4	-1.0	14	6.9	-1.5
	28	5.9	-0.5	23	6.2	-0.8	29	5.9	-0.5	23	6.4	-1.0	29	5.9	-0.5
May	12	7.3	-2.0	5	6.7	-1.3	13	7.3	-2.0	5	6.6	-1.2	13	7.2	-1.9
	27	6.2	-0.7	21	6.8	-1.4	27	6.2	-0.7	22	6.9	-1.6	29	6.2	-0.7
June	10	7.6	-2.1	2	6.8	-1.3	11	7.5	-2.0	3	6.6	-1.1	11	7.3	-1.8
	25	6.4	-0.8	19	7.3	-1.7	27	6.5	-0.9	20	7.4	-1.8	27	6.6	-0.9
July	9	7.7	-1.9	2	6.7	-1.1	10	7.5	-1.8	2	6.6	-0.8	10	7.3	-1.4
	25	6.7	-0.8	18	7.6	-1.8	25	6.8	-0.8	19	7.6	-1.7	26	6.8	-0.8
				31	6.6	-0.8									
August	7	7.5	-1.5	16	7.6	-1.5	7	7.2	-1.3	1	6.5	-0.5	7	7.0	-0.9
	22	6.7	-0.7	29	6.3	-0.4	23	6.7	-0.6	16	7.4	-1.3	24	6.8	-0.6
										30	6.1	0.1			
September	3	6.8	-1.1	13	7.1	-1.0	5	6.6	-0.7				5	6.4	-0.4
	24	6.5	-0.3	26	5.7	0.0	25	6.9	-0.5	14	6.8	-0.7	25	6.8	-0.5
October	3	6.1	-0.5	15	7.2	-1.0	2	5.7	-0.2	3	6.2	+0.2	8	6.1	+0.2
	23	7.2	-1.1	31	6.5	-0.4	23	7.4	-1.4	15	7.1	-0.9	24	7.4	-1.3
November	1	6.5	-0.4	13	7.3	-1.4	5	6.4	-0.4	1	6.7	-0.6	7	6.3	-0.3
	21	7.6	-1.8	29	6.9	-1.1	21	7.7	-1.9	13	7.2	-1.2	22	7.6	-1.8
										30	7.1	-1.3			
December	4	6.5	-0.7	12	7.2	-1.5	5	6.5	-0.7	12	7.0	-1.2	6	6.4	-0.6
	20	7.8	-2.1	29	7.2	-1.6	20	7.8	-2.1	29	7.4	-1.7	20	7.6	-1.9

Table 2.4-11
DISTRIBUTION OF SPRING HIGH TIDES AT SAN DIEGO
DURING FIVE YEARS

Elevation Above mllw (ft)	No. Occurrences	Percentage Probability of Occurrence	Cumulative Percentage Probability of Equaling or Exceeding Given Elevation
5.2	1	0.7	100.0
5.3	0	0	99.3
5.4	1	0.8	99.3
5.5	1	0.8	98.5
5.6	0	0	97.7
5.7	2	1.6	97.7
5.8	2	1.6	96.1
5.9	3	2.4	94.5
6.0	2	1.6	92.1
6.1	4	3.3	90.5
6.2	7	5.7	87.2
6.3	5	4.1	81.5
6.4	7	5.7	77.4
6.5	8	6.5	71.7
6.6	8	6.5	65.2
6.7	8	6.5	58.7
6.8	10	8.1	52.2
6.9	7	5.7	44.1
7.0	4	3.3	38.4
7.1	4	3.3	35.1
7.2	10	8.1	31.8
7.3	7	5.7	23.7
7.4	5	4.1	18.0
7.5	4	3.3	13.9
7.6	7	5.7	10.6
7.7	4	3.3	4.9
7.8	2	1.6	1.6
	123	100.0%	

Table 2.4-12
DISTRIBUTION OF SPRING LOW TIDES AT SAN DIEGO
DURING FIVE YEARS

Elevation Below mllw (ft)	No. Occurrences	Percentage Probability of Occurrence	Cumulative Percentage Probability of Equaling or Exceeding Given Elevation
+0.2	2	1.6	1.6
+0.1	0	0	1.6
0.0	1	0.8	2.4
-0.1	1	0.8	3.2
-0.2	2	1.6	4.8
-0.3	4	3.3	8.1
-0.4	5	4.0	12.1
-0.5	7	5.7	17.8
-0.6	6	4.9	22.7
-0.7	8	6.5	29.2
-0.8	10	8.1	37.3
-0.9	7	5.8	43.1
-1.0	6	4.9	48.0
-1.1	7	5.7	53.7
-1.2	4	3.3	57.0
-1.3	11	8.9	65.9
-1.4	5	4.0	69.9
-1.5	7	5.7	75.6
-1.6	6	4.9	80.5
-1.7	3	2.4	82.9
-1.8	8	6.5	89.4
-1.9	4	3.3	92.7
-2.0	3	2.4	95.1
-2.1	6	4.9	100.0
	123	100.0%	

Pattullo[25] has tabulated the monthly sea level anomaly found at the La Jolla pier of the Scripps Institution of Oceanography, 34 nautical miles southeast of San Onofre. Pattullo found monthly deviations from msl to vary anywhere between +8 cm to -9 cm. Therefore, a conservative estimate of the maximum isostatic sea level rise due to effects with monthly time scales would be +10 cm (0.33 foot), and the minimum stand of sea level due to such causes would be -0.33 foot. Referring to graphical presentations of La Jolla sea level data for a longer duration (Roden)[26] it is apparent that the +/- 0.33 foot figures for the isostatic anomaly, in fact, do represent appropriate extremes at perhaps even less than the 10% probability of exceedance level.

2.4.5.2.3 Maximum Surge Conditions

The maximum surge water level hypothetically possible and applicable to the site would result from the hypothetical maximum probable storm diagrammed in Paragraph 2.4.5.1. In developing the hypothetical maximum tropical storm, particular attention was given to the configuration of its radius of maximum winds, the storm's forward speed, and the storm's track. A storm center trajectory lying farther offshore than the 1939 event (Paragraph 2.4.5.1) was chosen. This would provide less frictional and thermal energy loss over land. Additionally, as with the 1939 storm this hypothetical storm would pass over an unseasonably warm seawater surface, which reduces the storm's dissipation rate as it moves northward. Just north of San Onofre the storm would curve sharply and slowly toward the coast; its center passing over the coast somewhat north of San Onofre so that its maximal south, south-southwest, and southwest winds would occur over San Onofre. For these wind directions, the tropical storm with the above mentioned combination of maximizing conditions would produce the highest sustained winds at San Onofre with virtually no risk of being exceeded.

The high wind speeds from the south and southwest were obtained by: (1) elongating the axis of the storm in a northeast-southwest direction so as to direct the maximum winds to be in the southeast quadrant, and (2) moving the storm at a slow forward speed of 10 knots. The 6-hour durations are: 60 knots from south, 55 knots from south-southwest, and 50 knots from southwest. The 1-hour maximum credible wind speed for this storm is 70 to 75 knots.

2.4.5.2.3.1 Barometric Pressure Contribution to Surge

The lowest pressure with virtually no chance of being lower at San Onofre, associated with the hypothetical tropical storm moving into the area would be 985 millibars (29.10 inches Hg). The hydrostatic change in water level at San Onofre associated with a 985-millibar tropical storm would be +1.00 feet and the barometric increase in water level would be +1.20 feet.

2.4.5.2.3.2 Wind Stress Tide and Coriolis Tide Contributions to Surge

Storm surges are transient in nature and exhibit a main peak that is manifest as a sharp rise in water level and occurs near the vicinity of maximum storm winds, just before the arrival of the tropical storm. A simplified steady-state surge model can be employed to treat the case of the main surge peak. The model which has been employed is due to Bretschneider[27][28] and his co-workers. Bodine[29] has refined this technique and reduced it to a digital computer code. The general methodology[23] assumes that convective momentum terms can be ignored, the response to onshore wind stress is instantaneous, and relies on the existence of parallel depth contours in the longshore direction, a condition rather well met at San Onofre. The computations are carried out along lines transverse and perpendicular to the assumed parallel bottom contours. The transverse bathymetry sections used for this purpose are shown in Figure 2.4-27. The fact that the storm center is necessarily over deep water most of the time where the phase velocity of long waves is great makes it indicative that large storm surges would not develop in the vicinity of San Onofre.

Besides the barometric surge of +1.20 feet already discussed, the model employed views a storm surge as composed of two parts: (1) the wind stress tide caused by winds directed normal to shore; and (2) the coriolis tide. The latter is a rise (or drawdown) of water caused by a current flowing parallel to shore, which may result from wind stress in that direction. However, the coriolis tide can persist even in the absence of local winds. Following passage of a storm, for instance, the longshore current it generates may inertially move along for days while slowly decaying through various frictional effects. Both surge components have been combined to give the heights above pre-existing elevations according to wind directions over a 6-hour duration: south, +0.78 foot; south-southwest, +0.40 foot; and southwest, +0.31 foot. Pre-existing water levels already discussed were added to the depths shown in Figure 2.4-27 prior to surge computations due to the nonlinear addition of the various effects.

2.4.5.2.3.3 Summation of Maximum Surge Contributions

The maximum likely storm surge height, therefore, has been determined to be +1.98 feet above the antecedent water level. This figure is the sum of the barometric surge of +1.20 feet and the maximum surge components derived from the model of +0.78 foot. Hence, it is concluded that large surges will not develop in the vicinity of San Onofre. This precludes the necessity for a detailed two-dimensional treatment of surge such as a surge hydrograph.

2.4.5.2.4 Seiche Water Levels

Some of the most detailed measurements and analyses of long-period waves (normal shelf seiching background levels) over the continental borderland have been conducted near Oceanside, California, about 17 miles southeast of San Onofre.[30][31] Seiche has been found to affect sea surface elevation by only 0.7 cm, which is considered negligible for water level calculations for southern California.

2.4.5.2.5 Still Water Level Extremes - Summary

Extreme high and low still water levels have been estimated at +9.3 and -2.6 feet mllw, respectively. These figures arise through the following causal factors, as discussed in Paragraphs 2.4.5.2 and 2.4.11.2.

Causal Factor	Elevation (ft, mllw) High Water	Elevation (ft, mllw) Low Water
Astronomical tides (Paragraph 2.4.5.2.1)	+7.0	-1.75
Isostatic anomaly (Paragraph 2.4.5.2.2)	+0.33	-0.33
Maximum surge (Paragraph 2.4.5.2.3)	+1.98	-0.55[a]
	+9.31	-2.63

2.4.5.3 Wave Action

Severe deep water storm waves determine the lowest and highest instantaneous water elevations in conjunction with long period phenomena; i.e, tide and storm surge. As severe waves are infrequent, it is usually necessary to determine their characteristics by hindcasting. A careful selection of past storms based on reported wave damage and strong winds is a prerequisite. Then, the deep water significant wave characteristics for each storm are hindcast from weather maps. A wave height distribution function[32] is used to determine the highest individual shallow water wave height, H_{max}, in the storm from the hindcasted significant wave height and period time histories.

Marine Advisors[33] and Intersea Research[34] examined a total of approximately 60 storms that occurred between 1900 and 1967 and that occurred near enough to San Onofre to be applied to this study. Twenty-five of the most severe storms were selected and hindcast (Table 2.4-13).

The deep water wave data were corrected for refraction and shoaling at the San Onofre site, and also for island sheltering.

As waves enter into shallow water they are transformed by the bottom topography. This transformation is apparent as a decrease in wave velocity and a change in wave height. These two changes are brought about by separate physical processes. One, shoaling, always applies when waves travel into shallow water. It is the effect of the shoaling bottom on the advance of the wave form. As a result of this restricting effect the wave velocity is reduced; at first the wave height decreases but upon traveling into shallower water it increases until the wave breaks. The other process, refraction, occurs when the wave crest advances toward shore over a shallow, irregular bottom or over a shallow and smooth bottom at an angle to the bottom contours. The portion of wave that is in deeper water has a greater velocity than the portions in shallow water. This causes a bending of the crest and as a result wave heights are increased in some shore areas and reduced in others. Corrections for island sheltering are made by proportionately decreasing

[a] Surge drawdown is discussed in Paragraph 2.4.11.2.

Table 2.4-13
HINDCASTED WAVES FOR PAST SEVERE STORMS

	Deep Water			Shallow Water
Storm Date	Direction (˚T)	H_{max} (ft)	T_s (s)	H_{max} (ft)
March 9-11, 1904	228	22.6	8.5	18.5
March 8-10, 1912	155	40.9	12.3	27.8
December 16-17, 1914	220	29.3	10.0	25.8
January 28-30, 1915	272	35.1	10.4	20.7
February 1-3, 1915	268	36.3	11.4	22.5
April 29 - May 1, 1915	278	34.2	10.5	19.8
January 26-28, 1916	260	50.0	12.9	33.5
June 28-30, 1922	165	40.0	11.7	29.2
February 1-2, 1926	266	32.3	13.8	20.7
April 6-8, 1926	262	23.5	12.8	15.7
March 14-15, 1930	265	23.3	9.5	14.9
December 6-7, 1937	270	26.5	16.0	16.7
September 15-25, 1939	165	60.0	16.1	43.8
January 20-23, 1943	255	44.2	12.7	30.5
March 13-14, 1952	268	33.3	12.8	21.0
January 6-8, 1953	268	38.0	18.0	25.1
April 2-4, 1958	285	49.2	20.7	30.0
February 14-17, 1959	265	37.0	14.3	24.4
February 8-10, 1960	290	51.6	18.8	29.9
March 13-15, 1961	273	32.8	16.8	21.0
March 4-7, 1962	280	31.6	15.5	18.6
December 11-15, 1962	270	32.7	20.5	21.9
January 20-22, 1964	267	21.2	8.9	13.4
November 15, 1965	280	34.0	14.2	20.1
November 18, 1965	289	29.0	14.8	15.7

wave height and shifting the resulting wave mean direction when the deep water wave data has a path that is interfered with either by coastal islands or by parts of the coast itself for waves approaching the mainland obliquely.[35] The storm waves given in Table 2.4-13 represent 64 years of record. The deep water wave data provided in this Table include correction for refraction, shoaling, and island sheltering. The shallow water H_{max} values at San Onofre have been treated statistically by the Weibull method of extremes[36] with the assumption that the 1-in-64-year wave equals the highest H_{max} of the period covered. An extrapolation gives the 100-year highest individual shallow water wave of 46 feet. The highest hindcast wave was produced by the tropical storm of September 24-25, 1939 (described in Paragraph 2.4.5.1). This is the only tropical storm in the past 75 years which followed such a trajectory as to produce severe waves in southern California waters. As shown in Table 2.4-13, the greatest shallow water wave height offshore at San Onofre during the 1939 storm was 43.8 feet.

A hypothetical tropical storm was considered based on the concurrence of individual worst parameters. This storm was designed around the 1939 hurricane which was able to reach latitude 34 N with strong winds. Certain modifications were made, however, so that higher extreme wind conditions would be postulated in the San Onofre area than experienced in the 1939 case. The track, size, and configuration of the storm were all designed with the idea of a realistic storm that could reach San Onofre. Specific storm parameter modifications are discussed in Paragraph 2.4.5.2.

Having an optimum final trajectory from the south, then credible conditions for worst storm wave generation includes an effective fetch of 400 miles with wind speed of 50 knots for 24 hours. This would generate a significant deep water wave height of 34 feet. The highest individual wave, corrected for sheltering, shoaling, etc., at the site is calculated at 54 feet (shallow water height). Its associated wave period would be 13 seconds. According to the extrapolation in Figure 2.4-28, it would be 200-year return interval wave.

Using techniques and graphs given in U.S. Army CERC,[23] calculations have been made of the extreme instantaneous water levels due to the hypothetical storm waves. The highest crest elevation was determined for a +9.3 feet mllw still water level, and the lowest wave trough elevation was derived for a -2.6 feet mllw still water level as discussed in Paragraph 2.4.5.2. Tsunami effects were not included because the simultaneous occurrence of the hypothetical worst storm and hypothetical worst tsunami is infinitesimal. Another objective of this calculation was to determine the lowest wave trough at the cooling system seawater intakes. The results of the calculation are presented in Figure 2.4-29. Figure 2.4-29 shows that the lowest wave trough remains above -10 feet mllw until farther than 9000 feet distance from the coast. In preparing Figure 2.4-29, the highest crest elevation is based on a 13-second breaking wave height that is limited by the still water depth. The lowest trough elevation is based on breaking waves of shorter period, yet whose height is depth-limited; these have a larger portion of their height lying below the still water level. As seen from the graph, the worst storm-generated wave of 54 feet would begin feeling the bottom at a distance offshore of approximately 11,000 feet and would be completely dissipated by the time it reaches the beach in front of the San Onofre seawall.

Intersea Research Corporation(37) calculated the seasonal frequency of occurrence of breaking wave significant height, period and direction at the San Onofre beach. The significant breaking wave height exceedance values from that report and the annual average values are presented in Table 2.4-14.

Table 2.4-14
BREAKING WAVE SIGNIFICANT HEIGHT (H_b)
(feet)

H_b>	1	2	3	4	5	6	8	10	12
Summer (J-S)	100.0	86.4	62.5	18.6	10.4	1.4			%
Transition (A,M,O,N)	100.0	67.2	47.2	16.4	10.2	3.9	0.5		%
Winter (D-M)	91.2	52.6	33.0	16.1	11.9	5.9	1.3	0.5	0.2%
Annual	97.2	68.7	47.6	17.0	10.8	3.7	0.6	0.2	0.1%

Inasmuch as the significant wave height is the average of the highest one-third of the waves present, then two-thirds of the waves would be lower, and on an annual basis, the 1% height exceedance for all waves would be about 6 feet.

Thus, the calculated highest run up at the seawall of +27 feet mllw due to storm waves occurring during an extreme high water level of 15.6 feet mllw (including tsunami) presented by Intersea Research Corporation(34) is far more severe than the 1% exceedance surf height.

Wave action will not generate water levels above the elevation at the top of the seawall (+30.00 feet mllw); therefore, no further design provisions for protection of safety-related structures from waves are necessary.

2.4.5.4 Resonance

The possibility of oscillations of waves at natural periodicity, defined as resonance, is most applicable to a closed body of water such as a lake or embayment. The San Onofre site contrasts these types of physical confinements by being located on a coastal marine terrace adjacent to a long straight stretch of coastal shelf.

Aside from the tsunami consideration (see Subsection 2.4.6), resonance of the entire continental borderland is responsible for the bulk of the evident seiche, which has been measured extensively (Paragraph 2.4.5.2.4) 17 miles south of San Onofre, at Oceanside. Seiche has been found to affect sea surface elevation by only 0.7 centimeter which is considered negligible for all practical purposes.

2.4.5.5 Protective Structures

The San Onofre Units 2 and 3 plant grade is elevation +30.0 feet mllw. This is well above the maximum seawater elevation predicted for the occurrence of a maximum tsunami coincident with storm surge. Special structures designed to protect the site against wave action include the seawall and screen well perimeter wall. The onshore intake structure is arranged so that all penetrations, except in the screen well and screen well perimeter wall, are sealed against leakage of rising or surging seawater.

The screen well is surrounded by perimeter walls with top elevation at +30.0 feet mllw. There are unsealed penetration openings on the east perimeter wall, with bottom elevation of +19.7 feet mllw. These penetrations are above the +15.6 feel mllw maximum seawater elevation predicted for the occurrence of a maximum tsunami coincident with the high tide and storm surge. Runup due to wind-driven waves is not a consideration for maximum seawater elevation at the screen well because the inlet for the circulating water system is located offshore.

The recirculation gate slot openings of the circulating water system are set at elevation +30.5 feet mllw.

The seawall is a poured in place reinforced concrete cantilevered retaining structure. The top of wall elevation matches the Units 2 and 3 plant grade at elevation +30.0 feet mllw. The seawall is designed to withstand, without loss of functional capability, the design basis earthquake (DBE) followed by the maximum predicted tsunami with coincident storm wave action.(38) Additional design criteria include:

A. Location - generally following the natural bluff line

B. A seismic design factor - Seismic Class II criteria with additional requirement to maintain functional under DBE followed by tsunami

C. Wind load: W = 15 lb/ft^2 (Uniform Building Code)

D. Vehicle surcharge on retained earth = 250 lb/ft^2 (assumed)

E. In-place density = 130 lb/ft^2, with coefficient of friction ϕ = 35 degrees (San Mateo sand)

The offshore intake terminal structures and diffuser ports are designed to withstand maximum uprush and withdrawal velocities of current associated with the postulated tsunami.

The offshore conduits are buried with a minimum cover of 4 feet. This prevents the conduits from being subjected to any forces created by wave actions or currents.

2.4.6 PROBABLE MAXIMUM TSUNAMI FLOODING

2.4.6.1 Probable Maximum Tsunami

The maximum possible tsunami wave heights that could occur at the San Onofre site would be generated by local offshore earthquake activity. Major tsunamis have been occurring in the Pacific Ocean at the rate of about one every 4 years. Over the period of adequate historical records, tsunamis of large energy, generated in all known seismically active regions around the Pacific, have been noticed at southern California, but have generally not produced damage.[39]

The effects of a distantly generated tsunami are minimized at southern California by the presence of a broad continental borderland, which apparently reflects much incident low frequency energy back out to sea. The regions of known high runup from remote tsunamis seem to be confined to those having steep offshore slopes (e.g., Japan, Hawaii, western South America).

Because of the moderating affect of southern California's offshore border-land on distant tsunami waves, local offshore fault zones are considered to be the most probable generators for large waves at San Onofre. The closest such zone to the Unit 2 and 3 site is the hypothesized offshore Zone of Deformation discussed in Paragraph 2.5.2.4.5. The closest portion of this zone is approximately 5 miles southwest of the Unit 2 and 3 site.

To study the affect at San Onofre caused by sea floor displacements on the offshore Zone of Deformation, detailed specific analyses were completed by Dr. Basil W. Wilson.[40]

Mathematical modelling of the hypothetical tsunami was conducted assuming an earthquake with a 7-foot vertical displacement component of the sea floor 5 miles offshore from San Onofre as the generating mechanism. This vertical displacement is much larger than would be expected to occur on the hypothesized offshore Zone of Deformation which, because of its northwest trend, should be characterized by predominately strike slip displacement. Dr. Wilson's study concluded that the wave induced by 7-foot sea floor displacement and occurring during simultaneous high tide and storm surge would have a maximum runup to elevation +15.6 feet mllw at the Unit 2 and 3 seawall. The event modelled by Dr. Wilson is certainly the maximum probable tsunami that could reach San Onofre.

Normal faulting was postulated for the hypothesized offshore Zone of Deformation because the conversion of large strike-slip movements on the sea floor to a tsunami wave near San Onofre would be inefficient. Further, there are no large topographic features oriented normal to the direction of strike-slip movement on the offshore Zone of Deformation. This is consistent with the lack of a tsunami associated with the 1906 San Francisco earthquake, which caused lateral motions of the floor of San Francisco Bay.

2.4.6.2 Historical Tsunami Record

Table 2.4-15 summarizes the available information concerning tsunami indications associated with offshore California earthquakes at various regional locations.

Table 2.4-15
EXAMINATION OF TIDE GAGE RECORDS ASSOCIATED WITH OFFSHORE CALIFORNIA EARTHQUAKES (Sheet 1 of 2)

Date Day/Mo/Yr	Earthquake Magnitude	Location	Tide Record Location	Tsunami Indication
14, 15 July 1918	6.5	Humboldt County	San Diego San Francisco	None None
19, 20 Nov 1918	VII[a]	Santa Monica Bay	San Diego San Francisco	None None
31 Jan 1 Feb 1922	7.6	Cape Mendocino	San Francisco	None
22, 23 June 1923	7.3	Cape Mendocino	San Francisco San Diego	Questionable None
29, 30 June 1925	6.3	Santa Barbara	San Diego Long Beach	None[b] Questionable
22, 23 Oct 1926	6.1	Monterey Bay	San Diego	Questionable
4, 5, Nov 1927	7.5	Point Arguello	La Jolla	Present Very small
			San Diego	Present Very small
			San Francisco	Present Very small
10, 11 Mar 1933	6.3	Long Beach	San Pedro	None[c]
		Newport Beach	San Diego	None
		Offshore	La Jolla	Questionable

(a) Modified Mercalli scale

(b) The time sequence of this record seems confused. There is a long period oscillation in the tide record (about 30 minutes) which seems to have preceded the earthquake by a few hours.

(c) Actual ground motion appears on this tide gage record. A 6-inch seiche of about 1-hour period was in oscillation at the time. The earthquake failed to produce a tsunami or materially disturb the existing seiche.

(d) Conspicuous lack of any long-period waves above background.

Table 2.4-15
EXAMINATION OF TIDE GAGE RECORDS ASSOCIATED WITH
OFFSHORE CALIFORNIA EARTHQUAKES (Sheet 2 of 2)

Date Day/Mo/Yr	Earthquake Magnitude	Location	Tide Record Location	Tsunami Indication
30 June - 1 July 1941	5.9	Carpenteria	San Diego La Jolla	None None
9, 10 Feb 1941	6.6	Cape Mendocino	San Diego	Slight increase in seiching 14 hours later
			La Jolla Santa Monica Port Hueneme	None None General increase in seiching 36 hours later
			San Francisco	Increase in what appears to be a harbor resonance 14 hours later.
25, 26 Dec 1951	5.9	San Clemente Islands	San Diego[d] La Jolla[d] Long Beach[d] Santa Monica[d] Port Hueneme[d]	None None None None None

2.4.6.3 Source Tsunami Wave Height

2.4.6.3.1 Distant Tsunami Generating Sources

The cumulative world incidence of severe tsunamis has averaged 10 per century for 2400 years; most of these are generated by earthquakes associated with the great oceanic trench systems and volcanic arcs. Three trench systems (the Atacama, Aleutian, and Japan Trenches) have accounted for 33% of all Pacific Ocean tsunamis in the past 200 years.

The closest active trench system which could cause tsunamis at San Onofre is the Aleutian Trench. Because of its broad shelf topography, the southern California coast is not sensitive to such distantly-generated waves. Remotely-generated tsunamis have amplitudes on the same order as the astronomical tides in southern California as given in Marine Advisors Report A-163.[39]

Besides the great trench systems, there are other large scale tectonic structures which might be considered capable of generating tsunamis. These include the large east-west trending fracture zones (Mendocino, Murray, and Clarion Fracture Zones) and the north-south trending East Pacific Rise, which enters the Gulf of California. These structures have earthquakes associated with them, and thus might generate tsunamis. However, the predominant displacement on these tectonic zones is strike-slip, which does not produce a large amount of tsunami wave energy. In contrast, the ocean floor displacements which occur in the ocean trench systems are predominantly vertical, and are relatively efficient in producing tsunami wave energy. Strike-slip structures in the East Pacific are therefore not regarded as significant sources for distantly generated tsunamis.

2.4.6.3.2 Tsunamis of Local Origin

The hypothesized offshore Zone of Deformation is the controlling generator for protective design at San Onofre as discussed in Paragraph 2.4.6.1. Estimates of the maximum tsunami wave height at this hypothesized Zone of Deformation is provided in Paragraph 2.4.6.4.

Other faults in the Pacific Ocean are at a greater distance from the San Onofre coast, and could not have a tsunami effect at the Unit 2 and 3 site greater than the Postulated event 5 miles southwest of the site discussed in the Wilson Report.[40]

2.4.6.4 Tsunami Height Offshore

The maximum hypothetical tsunami to approach San Onofre would be generated from an assumed earthquake with a 7.07-foot vertical displacement component of the sea floor 5 miles offshore from San Onofre. To simulate the wave generated from this assumed maximum situation, a Fourier series representation of a sawtooth wave form of maximum height was considered by Dr. Wilson.[40] The main objective of this analysis was to identify the principal wave components that can be considered to be present and to be representative of the approximate stroke of the initial sea disturbance set up by the earthquake. From Wilson's Table III[40] it can be seen that the maximum wave height generated from a maximum vertical (dip-slip) bottom offset of 7.07 feet would be 6.32 feet (with a period of 12.7 minutes).

2.4.6.5 Hydrography and Harbor or Breakwater Influences on Tsunami

The analysis used to translate design (controlling) tsunami waves from the 5-mile offshore generator location to the San Onofre site is presented by Wilson.[40] The fault location of the earthquake that would generate the controlling tsunami is approximately along the 60 meter (200 feet) depth contour between Dana Point and Oceanside as shown in Wilson's Figure 1. Wilson's Figure 13, a profile of the continental shelf off San Onofre, shows that the continental shelf off San Onofre cannot satisfactorily be approximated by a single uniform slope. Wave refraction diagrams were calculated numerically and computer plotted.

Wilson's Figure 14 gives part of the grid pattern of depths, in meters, used to define the topography of the area and Figure 15 shows the wave fronts and rays as computer plotted from calculations which determine the refraction of the waves. Furthermore, Wilson's Figure 16 gives the initial profile of the sea disturbance in conformity with the hydrodynamic properties of the continental shelf.

Bore formation and resonance effects would not become an influence in estimating the maximum tsunami run up from the controlling tsunami. No effect to safety-related facilities is expected from the occurrence of this tsunami.

2.4.6.6 Effects on Safety-Related Facilities

The controlling tsunami occurring during simultaneous high tide and storm surge produces a maximum runup to elevation +15.6 feet mllw at the Unit 2 and 3 seawall. When storm waves are superimposed, the predicted maximum runup is to elevation +27 mllw, as discussed in Paragraph 2.4.5.3.

Tsunami protection for the Unit 2 and 3 site is provided by a reinforced concrete seawall constructed to elevation +30.0 mllw. Design parameters for the seawall are presented in Paragraph 2.4.5.5.

No effect to safety-related facilities is expected from the occurrence of the controlling tsunami.

2.4.7 ICE EFFECTS

As described in Section 2.3 the mild climate and general lack of freezing temperatures in this region make ice formation highly unlikely and it is, therefore, not considered credible.

2.4.8 COOLING WATER CANALS AND RESERVOIRS

Cooling water for San Onofre Units 2 and 3 was supplied by the Pacific Ocean and was transported to each unit by one intake conduit. No reservoirs or cooling water canals were needed or used in the system.

2.4.9 CHANNEL DIVERSIONS

Upstream diversions associated with rivers, where low flow has an impact on dependable cooling water sources, is not a factor at the San Onofre site. Cooling water was exclusively supplied by the Pacific Ocean through conduits which were designed to supply the minimum of 4% total intake conduit flow required for emergency cooling during any conceivable accident.

2.4.10 FLOODING PROTECTION REQUIREMENTS

Runoff resulting from precipitation along Highway 101 and directly onsite will be diverted by the site drainage facilities to the ocean. In areas where water may pond against openings or structures special provisions have been made. These features are discussed in Section 3.4.

2.4.11 LOW WATER CONSIDERATIONS

2.4.11.1 Low Flow in Streams

Local rivers and streams are not involved in plant operations. Plant cooling water was supplied exclusively by the Pacific Ocean; therefore, low flow conditions in streams do not affect the plant.

2.4.11.2 Low Water Resulting from Surges, Seiches, or Tsunami

2.4.11.2.1 Surge and Seiche Low Water

Winds that blow offshore at San Onofre would cause the greatest lowering of water as a result of surge. Surge drawdown would be most pronounced during Santa Ana wind conditions. A maximum credible Santa Ana condition for San Onofre would produce northeast winds of 35 knots sustained for 12 hours. The greatest correspondent drawdown from the antecedent water level associated with maximum Santa Ana wind conditions is -0.55 foot.

As mentioned in Paragraph 2.4.5.2, seiche has been extensively measured near San Onofre and has been found to affect sea surface elevation by only 0.7 centimeter.

It is therefore concluded that neither surge- nor seiche-caused maximum drawdown conditions would affect the ability of safety-related features at San Onofre to function adequately.

2.4.11.2.2 Tsunami Low Water

The most severe low water that could hypothetically be assumed would involve the worst tsunami drawdown combined with the hypothetical extreme low still water level. The extreme low still water level at San Onofre is estimated to be -2.63 feet mllw. This is derived from a situation consisting of a severe Santa Ana wind condition, as discussed above, causing a 0.55-foot sea level depression, promptly following passage of a deep low-pressure center in a winter storm causing an isostatic anomaly of - 0.33 foot (from Paragraph 2.4.5.2.2) and occurring simultaneously with the lowest probable astronomical tide of -1.75 feet mllw (from Paragraph 2.4.5.2.1). The maximum high water level of +15.6 feet would also cause the worst tsunami drawdown, which would be -11.9 feet mllw at the coast. This incident could persist for only a few minutes and only under the improbable condition that all of the contributing influences occur and reach their limits simultaneously.

The worst low water case described above would not affect the ability of safety-related features to function at San Onofre. The circulating water system receives its cooling water from intakes located 3330 feet from the protective seawall and at maximum inlet depth of -20.75 feet mllw. Worst tsunami drawdown at the offshore intakes is -4.0 feet, as discussed in Dr. Wilson's report[40].

2.4.11.3 Historical Low Water

The lowest tide elevation determined for the site is -2.3 feet mllw. This is a historical low tide and was considered in determining the bottom of the circulating water pump suction bell. This was to ensure proper impeller submergence. For information on the calculated low water elevations associated with tsunamis, refer to Paragraph 2.4.11.2.

The above information is graphically shown in Figure 2.4-30 and was determined using tables from the Army Corp of Engineers Shore Protection Manual, and the U.S. Department of Commerce Tide Table (1976)[41].

2.4.11.4 Future Control

Plant cooling water is supplied exclusively by the Pacific Ocean. Anticipated future uses of the Pacific Ocean will not limit the cooling water flowrate. Therefore, there is no impact to safety-related facilities.

2.4.11.5 Plant-Requirements

As part of the Plant's original design, the Pacific Ocean provided minimum required safety-related cooling water flow, and the system was designed to ensure an adequate supply of cooling water during the most severe sequence of events that could reasonably be postulated. The Pacific Ocean is no longer used as a source for safety-related cooling water.

Seawater from the Pacific Ocean is used for dilution flows and discharge.

2.4.12 DISPERSION, DILUTION, AND TRAVEL TIMES OF ACCIDENTAL RELEASES OF LIQUID EFFLUENTS IN SURFACE WATERS

The only release point from the plant to the surface waters is the Unit 2 circulating water system (outfall diffusers) to the Pacific Ocean, which is not considered a source of potable water. The flowrate is provided by the Saltwater Dilution System discussed in Chapter 9. The locations and users of the surface waters are discussed in Paragraph 2.4.1.2.

Chapter 15 discusses the design features of the plant which mitigate the effects of a tank leak or failure. In addition, Chapters 15 and 11 discuss the administrative controls and automatic interlocks, together with the fail-safe design of the instrumentation and control devices, which provide assurance against any release of liquid waste to the environs in excess of 10CFR20 limits.

Failure or overflow from an unprotected tank could result in an uncontrolled, unmonitored release of radioactive liquid. The storm drain system would route the release to the circulating water system’s outfall and to the Pacific Ocean. Administrative controls would limit the total radioactive inventory in unprotected tanks in accordance with NUREG-0472 and NUREG-0133. Control of the radioactive inventory ensures that the concentrations of radioactive material will remain below the limits in 10 CFR 20, Appendix B, Table II, Column 2, in the event of an uncontrolled release. Doses resulting from an uncontrolled release will remain below the limits of 10 CFR 50, Appendix I, and 10 CFR 100.

Routine releases of radioactive liquids are performed in accordance with the requirements of the Effluent Control Program and the Offsite Dose Calculation Manual. All releases of radioactive liquids are routed to the Unit 2 circulating water system outfall for discharge to the unrestricted area. Section 11.2 describes the operation of the liquid radioactive waste systems.

The maximum liquid radwaste system discharge flowrate will be administratively limited to less than 95 gal/min. During a radioactive liquid radwaste release, the minimum required flowrate in the Unit 2 circulating water outfall is approximately 14,000 gal/min, or one saltwater dilution pump on each unit (Unit 3 saltwater dilution pumps discharge into Unit 2 outfall). Therefore, an accidental release of radioactive liquid radwaste effluent would result in approximately 290:1 dilution within the plant Unit 2 outfall. The initial dilution of the circulating water Unit 2 outfall being discharged through the Unit 2 outfall diffusers is about 10 times the total volume rate of flow. Therefore, any discharged radioactive liquid radwaste effluent would be diluted about 2,900:1 in the near field zone.

2.4.13 GROUNDWATER

2.4.13.1 <u>Description and Onsite Use</u>

San Onofre Units 2 and 3 are located at the southern boundary of the San Onofre Valley Groundwater Basin (Basin No. 9-3).[43] The Basin lies within the South Coastal Hydrologic subregion of California as defined by the California Region Framework Committee (1968).[43] The Basin extends inland from the coast about 21 kilometers (13 miles) and dissects the Santa Margarita Mountains which lie inland to the east (Figure 2.4-5). The Basin is bounded on the south by the northwest-trending San Onofre Mountains which form a barrier to drainage toward the coast. A southwest-trending ridge separates the San Onofre Valley Basin from the San Mateo Creek Basin which lies immediately north.

San Onofre Valley Groundwater Basin is drained by San Onofre Creek and its tributaries Jardine, San Onofre North Fork, and San Onofre Canyons to the northeast, and San Onofre Canyon South Fork to the east. The drainage area of the San Onofre Valley Basin covers about 112 square kilometers (43 square miles) of which about 85% consists of steep sided mountains, about 10% consists of unconsolidated alluvium in the valleys, and about 5% of elevated terrace deposits. The Santa Margarita Mountains range in elevation from 122 to 152 meters (400 to 500 feet) near the coast to 975 meters (3198 feet) at Margarita Peak near the eastern boundary of the San Onofre Creek drainage divide. The valley floor of the San Onofre Basin ranges in elevation from 3 meters (10 feet) near the ocean to a maximum of 244 meters (800 feet) at the head of Jardine Canyon.

Stream gradients in lower San Onofre Creek range below 1%. Gradients in the tributary canyons range from 1.5 to 2.5% in the lower reaches, increasing up to 7.5% in the upper reaches.

The important water-bearing formations in the San Onofre Valley Basin consist of sedimentary strata of Pliocene, Pleistocene, and Recent age.(44) Older formations are well indurated and are essentially nonwater-bearing.(45) These older rocks consist of the Miocene Monterey, the San Onofre Breccia, the older La Jolla Group and pre-Tertiary sedimentary rocks.

The oldest of the productive water-bearing strata is the Capistrano Formation. The Capistrano consists of poorly to semi-consolidated, thinly-bedded marine siltstone, fine-grained sandstone and shale with local limestone concretions, conglomerate, and breccia. The Capistrano Formation crops out immediately to the northwest of San Mateo Creek in southern Orange County.(45)

The water-bearing San Mateo Formation underlies the portion of the San Onofre Valley Basin west of the Cristianitos fault (see Figure 2.4-32). Beneath the San Onofre Generating Station, the San Mateo consists of about 274 meters (900 feet) of light brown to yellow, medium- to coarse-grained sandstone. The formation is massive to thickly bedded, poorly cemented and well consolidated.

Alluvium is the most important of the water-bearing strata of the San Onofre Valley Basin,(43)(45) and occurs as unconsolidated valley fill reaching a maximum depth of about 30 meters (100 feet) and an average depth of about 21 meters (70 feet).(44) Alluvium is composed of boulders, gravel, sand, and silt. Production wells in the San Onofre Basin are located exclusively in the alluvial area which is the primary source of groundwater.

The principal recharge areas are the stream channels and alluvium in the upper parts of valleys.(43) Percolation of precipitation is the principle source of recharge. Minor amounts of water recharge the basin from percolation of recycled sewage effluent.(46)

Figures 2.4-33 and 2.4-34 show locations of wells and groundwater contours for typical basin high and low groundwater conditions. Groundwater occurrence, east of the Cristianitos fault, is restricted almost entirely to the alluvium. This is due to the thick sequence of relatively impermeable formations underlying the alluvium in this location. Groundwater moves downstream through the alluvium and passes over the Cristianitos fault. West of the fault the alluvium is underlain by, and in hydraulic continuity with, the San Mateo Formation. The contours (Figures 2.4-33 and 2.4-34) indicate that groundwater flow through the alluvium has a shallower gradient and is less restricted than movement occurring within the San Mateo Formation. Contours indicate that groundwater movement is to the west and southwest toward the ocean. Geologists at Camp Pendleton have indicated that well data suggests that little groundwater movement occurs between the San Onofre Valley and San Mateo Valley groundwater basins. For this reason, groundwater conditions in the San Mateo Basin should have no effect on the groundwater conditions beneath or in the vicinity of the site.

Fresh water requirements of the San Onofre plant will be met totally by water obtained from local water agencies and therefore no water will be derived from aquifers beneath or in the vicinity of the site for plant-related use.

2.4.13.2 Sources

The San Onofre Valley groundwater basin lies completely within the boundary of the Camp Pendleton Marine Corps Base. Groundwater use within the basin is under the direction and control of the Marine Corps. Presently, all water derived from the San Onofre Basin is for military use. Military security dictates that detailed information concerning amounts of water withdrawn, water levels, and locations of production wells remains classified. However, general information is available, including a limited amount of well data. San Onofre Valley Basin groundwater supplies only a partial quantity of Camp Pendleton's total consumption and is limited directly by the amount of precipitation and recharge, which occurs. Marine Corps policy requires the maintenance of a seaward gradient of the groundwater table at all times to prevent intrusion of saline water into fresh water aquifers.(47) This policy prohibits the withdrawal of considerable amounts of groundwater stored in alluvium below or near sea level. Past groundwater withdrawals have fully utilized the basins potential up to the policy limits. Future groundwater usage from the San Onofre Basin is expected to remain the same as past usage with no projected changes.

Groundwater fluctuations within the San Onofre Basin are controlled primarily by recharge and groundwater pumpage by the Marine Corps. Indications are that the basin rapidly accepts recharge. Well data have shown the basin to be almost completely replenished within 1 year (1952) following a 6-year dry spell.(45)(44) Largest fluctuations of the groundwater table occur in the upper portion of San Onofre Creek and the area immediately west of the Cristianitos fault (see Figure 2.4-32).

The average groundwater elevation beneath the site is +5 mllw.(46) Fluctuations within the pumped regions of the San Onofre basin have had little impact on the level of groundwater at the San Onofre site. Monitoring of groundwater levels at the San Onofre site for a ten-year period between 1963 and 1974 has shown the water table to vary from +2.7 feet to +5.7 feet mllw in the vicinity of the containment spheres.

Tidal effects on the groundwater levels in piezometers at the site have been monitored. Wells located closer to the ocean are generally more responsive to tidal fluctuations. Amplitudes of the fluctuations in observation wells are proportional to amplitudes of tidal fluctuations. The ratio of observation well to tidal fluctuations range from 0.1 to 0.3 for wells located between the containment spheres and the shore. Wells located a few hundred meters east of the unit's centerline are less responsive. The time lag between tidal highs and lows and the corresponding change in observations wells is generally about an hour (Appendix 2.4A).

Groundwater contours are shown in Figures 2.4-33 and 2.4-34 for typical high and low groundwater conditions.(47) Groundwater gradients within the alluvium to the east of the Cristianitos fault range from about 0.83% to 1.00%. Gradients in the alluvial portions of the lower basin to the west of the Cristianitos fault range from about 0.11% to 0.50%. Gradients within the San Mateo Formation are slightly higher ranging from 0.17% to nearly 1.0% with groundwater elevations dropping to sea level at the coast. Groundwater gradients are steepest over the Christianitos fault ranging from 1.25% to 1.67%.

The San Mateo Formation underlies the site to a depth of approximately 274 meters (900 feet). Boring logs indicate that the San Mateo is quite homogenous from the surface to below 91 meters (300 feet).

Pump test data indicate an average horizontal permeability for the San Mateo Formation of 0.0076 m/min (0.025 ft/min). Data were evaluated on the basis of several approaches. These included: (1) equilibrium methods, i.e., methods based on the assumption that a steady-state drawdown condition had been reached, and (2) nonequilibrium methods: methods based on the mathematical relationship between the rate of water lowering to permeability prior to reaching a steady-state (Appendix 2.4A, page 3).

Detailed data and the pump test report are included in Appendix 2.4A. A minimum value for vertical permeability for the San Mateo Formation of 0.0015 m/min (0.005 ft/min) was determined on the basis of grain size (using Allen Hazen's formula and correction).[48]

Studies have shown that reversal of groundwater flow from the site toward pumping wells in San Onofre Valley Basin cannot reasonably occur. According to SCE San Onofre Unit 1, Final Engineering Report and Safety Analysis, page 8 (1965),[47] "The established minimum pumping level for San Onofre Creek wells is above the elevation of the water table at the site so that even under extreme pumping conditions in San Onofre Creek, a seaward gradient will exist. Hence, a flow of groundwater toward the ocean from both San Onofre Creek and the site will be assured."

The groundwater table beneath the site approaches sea level as movement toward the ocean occurs. The groundwater gradient across the site is therefore influenced by tidal fluctuations. Piezometer measurements at the site indicate the gradient ranges below 0.3%. Available groundwater elevation data at the nearest Marine Corps observation well (9/7 -24H1), which lies about 914 meters (3000 feet) northwest of the site (Figure 2.4-5), indicate that the groundwater table normally ranged between +10 feet and +12 feet mllw at that well from 1951 to 1972. The only time during this period when the measured level fell outside of this range was in 1964 when the elevation dropped to 7.8 feet mllw. This was probably caused by the continuous pumping of 15 dewatering wells at the site during construction of San Onofre Unit 1.

Recharge of the San Onofre Valley Basin occurs in the upstream parts of stream channels and alluvium in the upper region of the valley.[43] There are no potential groundwater recharge areas within the influence of the plant.

2.4.13.3 Accident Effects

As discussed in Paragraphs 2.4.13.1 and 2.4.13.2 there is a groundwater gradient toward the ocean of approximately 0.4 to 0.6%. The nearest water supply wells serve the Marine Corps and are located in San Onofre Creek over 1 mile inland from the plant site. Marine Corps policy is to maintain the groundwater table throughout Camp Pendleton sufficiently above mean sea level to eliminate the possibility of saline water intrusion from the ocean into the freshwater aquifers. The established minimum pumping level for the San Onofre Creek wells is above the elevation of the water table at the site. Thus, a seaward gradient will exist even under extreme pumping conditions in San Onofre Creek and the flow of groundwater toward the ocean from both San

Onofre Creek and the site is assured. Based upon this gradient, groundwater movement from the site toward any present or projected users will not occur. There is no present or projected usage of groundwater at the San Onofre site. In addition, Subsection 15.7.3.3 discusses the design features of the plant, which mitigate the effects of a tank leak or failure. Based upon the above, no analysis of an accidental release of liquid radioactive material is required.

2.4.13.4 Monitoring for Safeguard Requirements

Observation wells around the site were established and monitored during the construction phase of Units 2 and 3. Monitoring of these confirmed a seaward gradient.

2.4.13.5 Design Bases for Subsurface Hydrostatic Loading

The design bases for groundwater induced hydrostatic loading on subsurface portions of safety-related structures, systems and components are as follows:

A. Elevation +5.00 feet above MLLW is the design limit for hydrostatic loading.

B. The soil below elevation +5.00 feet is either compacted to 100% optimum density or is left in an undisturbed condition.

C. Hydrostatic lateral earth pressures are determined by the relative elevation of each structure with the maximum groundwater pressures added directly to the equivalent soil fluid pressures.

Dewatering during construction is carried out so that any portion under construction is completely dewatered. Water is not permitted to rise until the structure is completely stable against hydrostatic forces. When construction and backfill is complete, the dewatering system is removed. No permanent dewatering for San Onofre Units 2 and 3 is required. Dewatering is discussed in detail in Paragraph 2.5.4.6.

All safety-related structures are designed to withstand the appropriate design loads at the design groundwater condition.

An evaluation of the groundwater level at San Onofre Unit 1 was conducted as reported to the NRC in Reference 49. The results of this evaluation indicate that the median groundwater level would be 5.6 feet MLLW. The new value of 5.6 feet is in close agreement to the design value of 5.0 feet and is considered to impose equivalent structural loads. It is expected that additional data would provide additional small variations in the median groundwater value which would also not affect design.

2.4.14 TECHNICAL SPECIFICATIONS AND EMERGENCY OPERATION REQUIREMENTS

No technical specifications or emergency procedures are required in the event of probable maximum precipitation rainfall to minimize the impact on safety-related facilities.

2.4.15 REFERENCES

1. U.S.D.A., SCS, "Soil Survey, San Diego Area, California," December 1973.

2. "Compilation of Records of Surface Waters of the United States, October 1950 to September 1960, Part II, Pacific Slope Basins in California," U.S. Geological Survey, Water Supply Paper 1735.

3. "Surface Water Supply of the United States, 1961-65, Part II, Pacific Slope Basins from Tijuana River to Santa Maria River," U.S. Geological Survey, Water Supply Paper 1928.

4. "Water Resources Data for California, Part I, Surface Water Records, Vol I," U.S. Geological Survey, 1966-1967.

5. "Interim Report, Probable Maximum Precipitation in California," U.S. Weather Bureau, Hydrometeorological Report No. 36, Rev 1969.

6. Probable Maximum Thunderstorm Precipitation Estimates - Southwest States, Hydrometerological Branch, National Weather Service, August 1972, Revised March 30, 1973.

7. Standard Project Flood Determinations, EM1110-2-1411, Department of the Army, Office of the Chief of Engineers, Washington, D.C., March 26, 1952, revised 1965.

8. "A Method for Estimating Volume and Rate of Runoff in Small Watersheds", U.S. Department of Agriculture, Soil Conservation Service, SCS-TP-149, 1968.

9. Henderson, F. M., Open Channel Flow, McMillan, 1966.

10. "Flood Hydrograph Package, HEC-1 Generalized Computer Program," Corps of Engineers Hydrologic Engineering Center.

11. Linsley, R. K., Jr., Kohler, M. A., and Paulhus, J. L. H., Hydrology for Engineers, McGraw-Hill, 1958.

12. Hydrology Manual, Los Angeles County Flood Control District, 1971.

13. "Procedure for Computing Sheet and Rill Erosion on Project Areas," Technical Release No. 51, U.S. Department of Agriculture, Soil Conservation Service, 1972.

14. "Water Surface Profiles, HEC-2," Corps of Engineers Hydrologic Engineering Center.

15. Rosenthal, J., Point Mugu Forecasters Handbook, Technical Publication PMR-7P-72-1, Point Mugu, California, Pacific Missile Range, 1972.

16. de Violini, R., Climatic Handbook for Point Mugu and San Nicholas Island, Vol 1, Surface Data, Point Mugu, California, Pacific Missile Range, 1967.

17. Atkinson, G. D., Forecasters Guide to Tropical Meteorology, Air Weather Service Technical Report 240, Air Weather Service, USAF, 1971.

18. Weaver, R. L., Meteorology of Hydrologically Critical Storms in California, Hydrometeorological Report No. 37, U.S. Weather Bureau, Washington, D.C., 1962.

19. Hurd, W. E., North Pacific Ocean, September 1939, Monthly Weather Rev., Vol 67, pp 356-358, 1939.

20. Southern California Coastal Water Research Project, The Ecology of Southern California Bight: Implications for Water Quality Management, SCCWRP TR 104 Publication TR 104, 1973.

21. Riehl, H., Tropical Meteorology, Chapter 11, McGraw-Hill, New York, 1954.

22. U.S. Department of Commerce, "High and Low Water Predictions West Coast of North and South America Including the Hawaiian Islands. National Oceanic and Atmospheric Administration, National Ocean Survey," Tide Tables 1976, pp 64-67 and p 163, 1976, Also, Tide Tables for the years 1968, 1970, 1972, and 1974.

23. U.S. Army Corps of Engineers, Shore Protection Manual, Vol I., U.S. Army Coastal Engineering Research Center, Table 3-8 and pp 3-82 - 3-143, 1973.

24. Lisitzin, E. and Patullo, J., "The Principal Factors Influencing Seasonal Oscillation of Sea Level," Journal of Geophysical Research, Vol 66, No. 3, pp 845-852, 1961.

25. Pattullo, J. G., "Seasonal Variation in Sea Level in the Pacific Ocean During the International Geophysical Year, 1957-1958," Journal of Marine Research, Vol 18, No. 3, pp 168-184, 1960.

26. Roden, G. I., "On the Nonseasonal Variations in Sea Level Along the West Coast of North America," Journal of Geophysical Research, Vol 65, No. 9, pp 2809-2826, 1960.

27. Bretschneider, C. L., Storm Surges, University of Hawaii Press, 1967a.

28. Bretschneider, C. L., "How to Calculate Storm Surges Over the Continental Shelf," Ocean Industry Magazine, Vol 2, No. 6, pp 31-34; No. 7, pp 42-47; No. 8, pp 46-47, 1967.

29. Bodine, B. R., Storm Surge on the Open Coast: Fundamental and Simplified Prediction. TM-3S, U.S. Army Corps of Engineers, Coastal Engineering Research Center, Washington, D.C., 1971.

30. Munk, W. H., Snodgrass, F. E., and Tucker, M. J., Spectra of Low- Frequency Ocean Waves, University of California Press, Berkeley, 1959.

31. Snodgrass, F. E., Munk, W. H., and Miller, G. R.,"Long-period Waves Over California's Continental Borderland: Part I. Background Spectra," Journal of Marine Research, Vol 20, No. 1, pp 3-30, 1962.

32. Longuet-Niggins, "On the Statistical Distribution of the Heights of Sea Waves," Journal of Marine Research, Vol XI, No. 3, pp 245-266, 1952.

33. Marine Advisers, "Hindcasts for the Ten Most Severe Cases of Waves in Southern California 1900-1956," prepared for California Research Corporation, 1957.

34. Intersea Research Corporation, "Probable Maximum and Minimum Sea Elevations at San Onofre Excluding Tsunamis," prepared for Southern California Edison Company, 1976.

35. Pierson, W. J., Neumann, G., and James, R. W., Practical Methods for Observing and Forecasting Ocean Waves by Means of Wave Spectra and Statistics, H.O. Pub 603, U.S. Navy Hydrographic Office, Washington, D.C., 1955.

36. Chow, Ven Te., ed, Handbook of Applied Hydrology, McGraw-Hill, New York, 1964.

37. Intersea Research Corporation, "Water Transport Through a 5000-foot Long Section along SONGS Unit No. 1 Outfall Line," prepared for Southern California Edison Company, November 1972.

38. Seismic Category I Criteria and Implementation Program, San Onofre Generating Station, Units 2 and 3, Dockets 50-361 and 50-362, December 1975.

39. Marine Advisors, "Examination of Tsunami Potential at the San Onofre Nuclear Generating Station," Report A-163, 1965.

40. Wilson, B. W., Dr., "Estimate of Tsunami Effect at San Onofre Nuclear Generating Station, Units 2 and 3," December 1972.

41. U.S. Department of Commerce Tide Tables, 1976.

42. List, E. J. and Koh, R. C. Y., Interpretations of Results from Hydraulic Modeling of Thermal Outfall Diffusers for the San Onofre Nuclear Power Plant, Report No. KH-R-31, pp 52 and 53, November 1974.

43. Bader, J. S., "Groundwater Data as of 1967, South Coastal Subregion, California," U.S. Geological Survey Open File Report, 1969.

44. Worts, G. F., Jr., et al., "Tables of Basic Data for Wells on Camp Pendleton, California," U.S. Geological Survey Open File Report, 1953.

45. Babcock, B. A., "Geology and Hydrology of the San Mateo Creek Basin," Office of Groundwater Resources, Camp Pendleton Marine Corps Base, California, 1956.

46. California Department of Water Resources, "Reclamation of Water from Wastes - Coastal San Diego County," Bulletin No. 80-2, 1968.

47. Southern California Edison Company, "San Onofre Nuclear Generating Station, Unit 1, Final Engineering Report and Safety Analysis," Vol I, 1965.

48. Woodward-McNeill & Associates, "Offshore Liquefaction Evaluation for the Proposed Units 2&3, San Onofre Nuclear Generating Station, San Onofre, California," 1974.

49. Enclosure 2: "Summary of SONGS 1 Groundwater Data," to May 7, 1984 letter to D. M. Crutchfield (NRC) from M. O. Medford (SCE).

50. Areva, "San Onofre Nuclear Generating Station, Hydrologic Evaluation of Offsite Flood Berm," 2015.

2.5 GEOLOGY, SEISMOLOGY, AND GEOTECHNICAL ENGINEERING

The data and information contained in Section 2.5 and referenced appendices are historical information developed during San Onofre's original design to address Geology, Seismology, and Geotechnical Engineering. The information was used to determine the plant's design basis. Unless otherwise noted in the text, this information has not been updated to reflect data from later years.

2.5.1 BASIC GEOLOGIC AND SEISMIC INFORMATION

Geologic investigation of the San Onofre area began in 1960 with field studies of the Unit 1 site (an area now referred to as the North Industrial Area (NIA)), and continued during construction of Units 2 and 3. Prior to the application for the Unit 1 Construction Permit, a review was made of available geologic information pertaining to the San Onofre area. Most of the available geologic data at that time was obtained from Open File USGS Reports, prepared with the cooperation of the United States Marine Corps, at Camp Pendleton. Since construction of Unit 1, additional geologic mapping has been completed by the California Division of Mines and Geology in the San Clemente area and extending as far south as San Mateo Creek.

The preliminary geologic investigation for Units 2 and 3 was conducted in 1970 by Converse-Davis Associates, Consulting Engineers and Geologists. Their study included a thorough review of all investigations conducted for San Onofre Unit 1, a review of published and unpublished literature on the geology of the region, and a detailed geologic field study of the area surrounding the plant, with particular emphasis on faulting. During construction of Units 2 and 3, geotechnical monitoring and studies were conducted primarily by Fugro, Inc., Woodward-Clyde Consultants, Dr. Shawn Biehler, Mr. Jack C. West, Dr. Perry L. Ehlig, and Dr. Roy J. Shlemon. In addition, a number of specialty studies have been performed by other consultants and service companies.

2.5.1.1 Regional Geology

The site region encompasses areas of diverse geologic evolution and tectonics. Included within the site region, a 320-kilometer (200-mile) radius (Figure 2.5-1), is the entire southern California area, the broad continental shelf to the west, parts of northern Baja California, Mexico, and small areas of Arizona and Nevada. Many aspects of regional geology, which concern the site area (the area within a 5-mile radius of the site) are, however, more easily discussed on a somewhat smaller scale. In the following paragraphs, the size of the region considered varies depending on the relationship of the subject matter to the site area.

2.5.1.1.1 Regional Physiography and Geomorphology

The San Onofre Nuclear Generating Station is situated near the southwestern boundary of the Peninsular Ranges Geomorphic Province of California (Figure 2.5-1); an area characterized by northwest trending mountain ranges that extend southward into Mexico. The Peninsular Ranges

Province is bounded on the north by the Transverse Ranges Province, on the east by the Coachella and Imperial Valleys of the Salton Trough Province, and on the west by the Continental Borderland Province.

These geomorphic provinces are essentially the same as the natural provinces described by Jahns.[1] Parts of 10 natural provinces are located within 320 kilometers (200 miles) of the site (see Figure 2.5-1). The east-west trending Transverse Ranges Province drains south across the alluvium filled Los Angeles Basin. The Los Angeles and San Gabriel Rivers are the major drainage courses.

The physiography of the Peninsular Ranges and surrounding areas in California is shown on Figure 2.5-2. In the Peninsular Ranges Province, drainage is generally toward the southwest, nearly normal to the mountains. Runoff from the interior of the Peninsular Ranges drains to the ocean primarily via the Los Angeles, San Gabriel, and Santa Ana Rivers to the north of the site and the Santa Margarita and San Luis Rey Rivers to the south. Numerous smaller drainages dissect the alluvium filled basins and coastal plains. The drainages generally flow only during heavy and prolonged rains. There are several small lakes or reservoirs in the region; Lake Elsinore is one of the largest and closest lakes to San Onofre (see Figure 2.5-2).

Terraces of both marine and stream origin are abundant in this region of California. As many as 22 marine terrace platforms have been recognized along the coast. They are known to reach elevations of approximately 390 meters (1300 feet) above sea level in California and may reach 475 meters (1550 feet).[2] They represent periods of relative emergence of the coastal areas during Pleistocene time and are sufficiently complex to present problems in correlations and determination of origin. Nonmarine terraces were formed as inland streams adjusted to relative changes of sea level. As a result, nonmarine and marine terrace deposits interfinger at the coast.

A part of the offshore sea south of Los Angeles has been traditionally included in the Peninsular Ranges Province; however the more recently recognized Continental Borderland Province (the offshore area between Point Conception and Central Baja California), is physiographically distinct from the Peninsular Ranges.[3] The Borderland is characterized by basin and range topography. There are 19 major basins 40 to 150 kilometers (20 to 80 nautical miles) long, 10 to 40 kilometers (5 to 20 nautical miles) wide, and 350 to 2000 meters (200 to 1600 fathoms) deep.[4] Associated with these basins are several submarine canyons and gullies that vary considerably in size.

Topographic highs on the Borderland form the banks and islands offshore. The most prominent and continuous of the offshore banks is the Santa Rosa-Cortes Ridge, which trends southeastward from the Channel Islands to the Cortes-Tanner Bank Shoals (Figure 2.5-2).

The continental slope forms the seaward boundary of the Borderland. Here the sloping outer shelf drops off abruptly to abysmal depths. The continental slope is more than 185 kilometers (100 nautical miles) west of the California coast in the area of San Onofre.

2.5.1.1.2 Regional Stratigraphy

Geologic units which have been mapped in the southern California region range in age from Precambrian to Recent and in lithology from crystalline and metamorphic basement to alluvium. Figure 2.5-3 is a generalized geologic map of the region illustrating this diversity.

Of particular interest to the San Onofre site is the stratigraphy of the Peninsular Ranges Province and the adjacent Continental Borderland. Onshore, the geology is well known from the mapping of numerous investigators. In the Borderland, geologic relationships are known or inferred from exposures on the islands, from drill holes and bottom samples, and from geophysical exploration.

The following discussion presents an overview of the ages and lithology of geologic units within these two provinces with emphasis on units exposed in the vicinity of the site area.

2.5.1.1.2.1 Peninsular Ranges Province

The rocks exposed within the Peninsular Ranges Province are readily grouped into those which constitute the basement terrane and those which unconformably overlie the basement terrane. The relationship of these groups is shown on Figure 2.5-4. The basement terrane is about 60% Cretaceous intrusive rocks of the Peninsular Ranges Batholith and 40% pre-batholithic rocks of sedimentary and volcanic origin.

The pre-batholithic rocks are best preserved in the western part of the province, particularly in the Santa Ana and Santa Margarita Mountains, where they are referred to as the Bedford Canyon Formation and Santiago Peak Volcanics.(5) The Bedford Canyon Formation consists of unmetamorphosed to mildly metamorphosed sandstone and argillaceous shale with minor amounts of conglomerate and limestone. The formation appears to be very thick, but complex deformation prohibits determination of its true thickness. Isotopic data and sparse fossils indicate that it includes strata of Triassic and Jurassic age.(6)(7) The Santiago Peak Volcanics consist of a series of unmetamorphosed to slightly metamorphosed volcanic and volcaniclastic rocks which appear to include both marine and nonmarine facies. Upper Jurassic marine fossils have been found at one location within the formation.(8) The Santiago Peak Volcanics appear to overlie the Bedford Canyon Formation unconformably; however, the contact between the two formations is typically faulted.

Within the central and eastern part of the Peninsular Ranges Province, pre-batholithic rocks occur in large irregularly-shaped bodies surrounded by batholithic intrusions. They are moderately to severely metamorphosed and consist mainly of phyllite, schist, and gneiss derived from sandstone and shale.(9)(10) Marble and quartzite are abundant locally, particularly within the San Jacinto, Santa Rosa, and Coyote Mountains. Only a few, poorly preserved fossils have been found in pre-batholithic strata in the central and eastern parts of the province and they appear to be of Triassic and Jurassic age.(10)(11)

The Peninsular Ranges Batholith (also known as the Southern California Batholith) is composed of numerous individual intrusions. Rocks range in composition from gabbro to granite, with tonalite being most abundant. Gabbroic rocks are relatively abundant in the western part of the province and granodiorite is abundant in the east.

Zircon U-Pb ages indicate that most of the batholith ranges from 80 to 120 million years in age with intrusions older than about 105 million years restricted to the western half of the province, and intrusion younger than about 105 million years restricted to the eastern half.(12) The batholith is interpreted to have formed as a magmatic arc above an eastward dipping subduction zone.(11)(13)(14)

The rocks that unconformably overlie the basement terrain include marine and nonmarine strata of Late Cretaceous, Tertiary, and Quaternary age as well as local occurrences of volcanic rocks of Miocene age. Most marine strata occur near the present coast. The thickest and most complete stratigraphic section is exposed to the north and northwest of San Onofre in the western Santa Ana Mountains and the San Joaquin Hills. Relationships between this and other sections in the province are shown on Figure 2.5-5.

A sequence of upper Cretaceous and lower Tertiary sedimentary rocks are exposed overlying the Bedford Canyon Formation and the Santiago Peak Volcanics in the Santa Ana Mountains and in the foothills near San Onofre. Cretaceous rocks are represented by the Trabuco Formation, a reddish, bouldery, nonmarine conglomerate, and the Williams and Ladd Formations which comprise a thick marine section (>1200 meters; 4000 feet) of interbedded conglomerate, sandstone, siltstone, and shale.

Sedimentary rocks of Paleocene and Eocene age rest upon a widespread erosional surface of low relief that was developed at the close of the Cretaceous Period. The Silverado Formation of Paleocene age is primarily a marine sandstone and includes local interbeds of conglomerate, siltstone, and shale. The Eocene Santiago Formation consists of an extensive sequence of massively bedded sandstone with numerous lenses of siltstone and conglomerate. These units are conformable and have been mapped both separately and together as the La Jolla Group.

Sespe and Vaqueros rocks of Oligocene age are broadly distributed in the region to the north of the site. They comprise a complex sequence of volcanic rocks and marine and terrestrial sedimentary rocks.

The Topanga Formation, a sandstone similar to parts of the Oligocene Vaqueros Formation, forms the base of the Miocene under most of the Los Angeles Basin but does not extend as a distinct unit as far south as San Onofre. In the vicinity of the site area, the San Onofre Breccia represents the base of the Miocene.

Characteristically, the San Onofre Breccia consists of fragments, some greater than 2 meters (6 feet) across, and occasionally greater than 12 meters (40 feet), of glaucophane schist and related rocks derived from Catalina Schist terrain presently exposed in the region only on Catalina Island. This unit which reaches a maximum thickness of about 1400 meters (4600 feet) was apparently derived from a landmass located offshore from the present coast. The Breccia is mainly of nonmarine origin, but it is partly marine where it interfingers with the underlying marine Topanga Formation and overlying marine Monterey Formation in the San Joaquin Hills northwest of the site. In the vicinity of the site and to the east, the San Onofre Breccia unconformably overlies pre-Miocene rocks.(2)

The middle Miocene Monterey Formation unconformably overlies the San Onofre Breccia in the vicinity of the site. The Monterey consists of about 250 meters (800 feet) of interbedded sandstone, siltstone, mudstone, diatomite and siliceous shale deposited in a broad, deepening marine basin.(2)

The upper Miocene to lower Pliocene Capistrano Formation conformably overlies the Monterey Formation within the Capistrano Embayment. It consists of marine mudstone, siltstone, including diatomaceous siltstone, and fine-grained biotite-rich arkosic sandstone. More locally distributed within the embayment is the light brown to light gray, coarse-grained sandstone and conglomerate of the upper Miocene to lower Pliocene San Mateo Formation. This formation is apparently contained within the Capistrano Formation in the San Clemente area.(1) The two formations have a maximum combined thickness of about 900 meters (3000 feet).

Stratigraphic equivalents, both in age and in lithology, of the Monterey, Capistrano, and San Mateo Formations are found in the Los Angeles Basin. Pliocene deposition is represented within the Capistrano Embayment northwest of the site by the Niguel Formation and in the San Diego area by the San Diego formation.

Unconsolidated Pleistocene marine sands are exposed as the San Pedro Formation in the coastal Los Angeles area and as the Linda Vista Formation near San Diego. Inland, thick alluvial deposits accumulated in lowland areas during the Pleistocene.

Emergence and intermittent submergence of the coastal areas of southern California during later Pleistocene time led to development of extensive marine terraces, most of which are covered by a thin veneer of marine sediments that, in turn, are largely concealed by terrestrial deposits. These terrace surfaces and overlying sediments are well developed from San Diego to as far north as Point Conception.

Recent sediments are widespread. These include marine and lagoonal deposits in the coastal area; alluvial-fan and flood-plain sands and gravels in many of the valleys; and swamp and pond deposits in marshes of the mountain areas. Eolian deposits include dunes along the coastline and the western margins of the Imperial and Coachella Valleys.

Part of the Peninsular Ranges Province extends southward to encompass the northwestern corner of Baja California, Mexico. This part of the province can be divided into three provinces based on geology and physiography, see Appendix 2.5J, Figure 2.5J-4.

- A narrow coastal margin characterized by Tertiary marine and nonmarine sedimentary rocks and Tertiary-to-Holocene volcanic and volcanic-derived rocks.

- The gently seaward sloping foothills between the Pacific Coast and the central high Peninsular Ranges underlain by pre-batholithic eugeoclinal accumulations of volcanic and sedimentary rocks which were subsequently metamorphosed to varying degrees by intrusion of the batholith.

- The Peninsular Range of northeastern Baja California comprised of Middle Cretaceous plutonic rocks of the Peninsula Ranges batholith (Appendix 2.5J).

2.5.1.1.2.2 Continental Borderland

The lithology of the Continental Borderland is generalized in Figure 2.5-6. In the San Onofre Region, the sedimentary rocks directly offshore are Miocene in age and are overlain by a veneer of late Pleistocene or Holocene terrace deposits. Seaward of these are Pliocene strata, chiefly mudstones. Shallow parts of the continental shelf are overlain by clays, silts, and sands of Pliocene to late Pleistocene age. The basin are generally covered by thick muddy sediments that are as old as Pliocene age.(15)

The only accessible bedrock exposures within the Borderland are on Santa Catalina and San Clemente Islands. The northern two-thirds of Santa Catalina Island is composed of a variety of metamorphic rocks collectively referred to as the Catalina Schist and correlated with the Jurassic-Cretaceous Franciscan assemblage. A large hypabyssal intrusion is exposed in the southern third of the island. San Clemente Island consists of predominantly Miocene volcanic rocks.

The Continental Borderland is described in greater detail in Paragraph 2.5.3.5.

2.5.1.1.3 Regional Structure

The structural character of the southern California region can be described in relation to its principal faults. Figure 2.5-7 shows the faults in relation to the boundaries of the natural provinces of Jahns.(1) Figure 2.5-8 further illustrates the major fault trends with emphasis on those inferred in the Continental Borderland.

A series of northwest-trending fault zones extending from the Salton Trough westward into the Continental Borderland provide the structural framework for the site area. These are essentially right-lateral strike-slip zones with widely varying histories and degrees of activity. Of these zones, only the easternmost (San Andreas and San Jacinto) extend into or through the Transverse Ranges. Others to the west abut the east-west structural features of the southern boundary of that province.

Near the Mexican border, the southern part of the San Andreas, San Jacinto, and Whittier Elsinore zones become involved in the crustal spreading centers of the Gulf of California. Principal faults in northern Baja California appear to be structurally disassociated from faults to the north although some may be related to features of the Continental Borderland (Appendices 2.5J, 2.5K, and 2.5L).

The major regional northwest-trending zones which impact the structural setting of the site area are described in the following paragraphs. Later paragraphs in this subsection discuss the regional fabric of the Western Peninsular Range Province and lesser faults and structural relief in the vicinity of the site area.

2.5.1.1.3.1 San Andreas Fault Zone

The San Andreas fault zone consists of high-angle, right-lateral, strike-slip faults with northwesterly strikes. Faults in the system are commonly believed to have originated during the late Cenozoic.

The San Andreas fault refers to the most recent surface of rupture within the zone. The zone varies from a single, discrete fracture to a belt of fractures up to 10 kilometers (6 miles) wide.

The zone can be traced over 1000 kilometers from near Cape Mendocino; the north end is believed to interconnect with the Mendocino Transform fault.(16) The south end is near the Mexican Border(7) and is believed to interconnect with spreading centers in the Salton Trough.(18)

The trace of the San Andreas fault zone is readily visible along most of its length. Rocks within this zone are severely deformed and minor structures within the zone are locally chaotic. Because of intense deformation within the fault zone, the rocks are soft and easily eroded. The San Andreas is commonly marked by a broad, shallow trough within which is an array of recent fault landforms, such as fault scarps, fault slices, sag ponds, and shutter ridges.(17)

The San Andreas is believed to be the principal crustal discontinuity extending to depths of at least 6.5 to 13 kilometers (4 to 8 miles). It has an accumulated displacement of about 300 kilometers (180 miles) in southern California during the past 8 to 10 million year.(17)(19) There is abundant geomorphic evidence of Quaternary displacement along the zone and Sieh(20) has documented nine major earthquakes along it within a period of 1400 years at Pallett Creek, California. The most recent major earthquakes on the San Andreas were the 1857 event centered at Fort Tejon and the 1906 San Francisco earthquake.

The San Onofre Nuclear Generating Station is located 92 kilometers (57 miles) to the southwest of the San Andreas fault zone.

2.5.1.1.3.2 San Jacinto Fault Zone

The San Jacinto fault zone branches from the San Andreas in the Transverse Ranges and runs roughly parallel to it, through the eastern Peninsula Ranges Province, 70 kilometers (43 miles) to the southwest. It is a major right-lateral strike-slip fault zone characterized by long, straight, steep, breaks. The fault zone is some 270 kilometers (170 miles) long, extending from the Cajon Pass south to beyond the Salton Sea.

Some of the faults comprising the San Jacinto zone are the San Jacinto, the Casa Loma, the Hot Springs, the Buck Ridge, and the Coyote Creek faults. Small segments within the zone show thrust type movement, but in general movement has been right-lateral, strike-slip. A total displacement of about 25 kilometers (15 miles) is indicated by the offset of a steeply inclined mylonite zone within basement terrane cut by the fault.(21)

The San Jacinto fault zone has been active in post-Pleistocene times. The destructiveness of the 1918 San Jacinto earthquake and the amount of surface rupture in the 1968 Borrego Mountain earthquake attest to the activity of this fault.

The San Jacinto fault zone is approximately 70 kilometers (43 miles) northeast of the San Onofre Site.

2.5.1.1.3.3 Whittier-Elsinore Fault Zone

The Whittier-Elsinore fault zone extends from the Los Angeles Basin to the Mexican Border, a total length of 232 kilometers (145 miles), and passes about 37 kilometers (23 miles) to the east of the site. The main part of the zone, the Elsinore fault, 192 kilometers (120 miles) long, extends from the northern end of the Santa Ana Mountains to south of the Salton Sea. North of the Santa Ana Mountains the Whittier fault, 40 kilometers (25 miles) long, represents the continuation of the zone into the Los Angeles Basin.

Movement along the Whittier-Elsinore fault zone seems to have varied over its length. Motion along the central part appears to have been primarily vertical with the western side up relative to the eastern side where the fault dips steeply to the southwest.(22) Evidence of strike-slip displacement is found along the southern part of the Elsinore fault and on the Whittier fault. Major horizontal offsets seem to have occurred on the fault zone in pre-Pliocene time. The latest displacements have occurred since the end of the Pleistocene.(23)

2.5.1.1.3.4 Hypothesized Offshore Zone of Deformation

The U.S. Geological Survey has expressed the opinion that three structural zones which have been identified along the coast of southern California cannot be disassociated (Reference 24, Appendix C). The Newport-Inglewood Zone of Deformation (NIZD), the South Coast Offshore Zone of Deformation (SCOZD), and the Rose Canyon Fault Zone (RCFZ) are therefore discussed herein as components of a hypothetical continuous zone of capable faults (see Paragraphs 2.5.2.4 and 2.5.3.5) which roughly parallels more clearly defined northwest trending fault zones to the east.

The Applicant contends that the hypothesized Offshore Zone of Deformation comprises independent fault zones that should not be associated. Evidence for this position includes the results of reflection profiling offshore (References 25, 26, 27, 28, 29, Appendix 2.5I, and PSAR Appendix 2E) as well as other factors. A discussion of these factors is included in the following paragraphs, in paragraph 2.5.1.1.3.12, and in Appendix 2.5M.

Analysis of the Western Geophysical data indicates that the offshore area of the Continental Borderland, which contains part of all three fault zones, between Long Beach and San Diego, can be divided into three separate and distinct provinces, based on differing geologic characteristics. This division is supported by seismic velocity data, gravity and magnetic anomalies, seismic-reflection profiles other geologic information, and the instrumental records of earthquakes.[26]

Faults northwest of the San Joaquin Structural High, in general, strike northwest-southeast, cut acoustic basement (Horizon C), and extend upward into the section through Horizon B. Some, such as the Palos Verdes fault, cut the sea floor. Many of these faults are probably the seaward extension of the Palos Verdes fault system, and to a lesser extent, the Newport-Inglewood Zone of Deformation. The Newport-Inglewood Zone of Deformation in this area terminates at the Offshore San Joaquin Hills Structural High.[26] Many of the faults in this area are reverse faults.

In contrast, the area southeast of the San Joaquin Structural High is crossed by two fault trends on Horizon C; a series of faults striking from north-south to northeast-southwest are superimposed by faults with northwest-southeast strike. Also to the southeast a series of faults and the associated folds make up the South Coast Offshore Zone of Deformation (SCOZD). In this zone, the major feature is a northwest-southeast trending fault termed the South Coast Offshore fault.[26] This fault, which is most prominent on Horizon C, cuts Horizon B at places and not at others, whereas the Rose Canyon Fault to the southeast cuts Horizon B along its entire length. The system of faults normal to these does not cut Horizon B. Still further south, there are a number of igneous intrusions that protrude through Horizon B. Some have associated magnetic high anomalies. The Rose Canyon Fault Zone appears to turn inland near Oceanside and is separated from the South Coast Offshore fault by this series of intrusives and by a series of north-south faults which are probably extensions of the north-south fault system onshore.[30]

The fault style on the opposite sides of the San Joaquin Structural High have been produced by a different strain pattern and the two are not directly associated.

The South Coast Offshore fault crosses the San Joaquin Structural High; however, it dies out upward as well as to the northwest, as it approaches the Newport-Inglewood Zone of Deformation; and to the southeast, as it approaches the Rose Canyon Fault Zone.

For most of its length, the South Coast Offshore Fault has only one major trace, which is down-thrown seaward. Opposite the San Onofre plant site, it has another component, down-thrown to the Coast and separated from the principal trace by a high block with steeply dipping strata. Horizon B was not deposited over a part of the high structural block lying between the two traces of the fault.

Other faults in the SCOZD, which lie seaward from the South Coast Offshore fault, have less displacement and are not as long. The South Coast Offshore fault, approximately 40 miles in length, was active after the Offshore San Joaquin Hills structure was formed. The interrupted and limited lateral extent and the small vertical relief of this fault on Horizon B points out the decrease in displacement along it during late Miocene time.

In summary, seismic reflections from the acoustic basement reveal the presence of a central north-south structural high (San Joaquin Structural High) that has been stable since approximately middle Miocene and has its origin deep within the crust. The Southern California Subduction Zone, as described by Hill,[31] shifts seaward along this feature such that it is approximately 18 miles from and parallel to the coast opposite the San Onofre Plant site; thus, the subduction zone is not continuously aligned with a major break in the deep crust from the NIZD to the RCFZ.

This fault is disassociated from the Newport-Inglewood zone and from the Rose Canyon fault. Finally, it does not overlie the Southern California Subduction Zone.

2.5.1.1.3.4.1 Newport-Inglewood Zone of Deformation

The Newport-Inglewood Zone of Deformation forms the western boundary of the Los Angeles Basin and the Santa Ana Mountain block. It consists of a northwest-trending elongate complex of en-echelon folds and faults extending through a thick section of Miocene and younger rocks in the Los Angeles Basin. The zone is terminated to the northwest by the Malibu-Santa Monica fault zone of the Transverse Ranges; its apparent termination to the southeast is offshore between Newport Beach and Laguna Beach some 40 kilometers (25 miles) northwest of San Onofre.

A basement-rock discontinuity (the Southern California Subduction Zone) is inferred to underlie the Newport-Inglewood Zone of Deformation and to extend southward beneath the region offshore of southern California.

The Los Angeles basin lies at the northern end of the Peninsular Ranges Province and contrasts sharply with the southern Peninsular Ranges and the Transverse Ranges to the north. Tertiary and Quaternary sedimentary rocks which accumulated in the basin were continuously deformed by uplifts, down-warping, faulting, and folding. This deformation was most pronounced during Pliocene and Quaternary time and its effect can be seen along the Whittier fault and Newport-Inglewood Zone of Deformation as topographic rises across the lowland area of the basin.

The belt of en-echelon folds and faults, which constitute the Newport-Inglewood Zone of Deformation, dies out in the Los Angeles Basin and terminates at the San Joaquin Hills Structural High; see Paragraph 2.5.1.1.3.12.[26] Distributive faulting and the lack of folding in the Newport oil fields are also indicative of termination of this zone within the Los Angeles Basin.

Historic earthquakes associated with the Newport-Inglewood Zone of Deformation (the 1920 and 1933 events, for example), were generated by slip within basement rocks below the sedimentary fill of the Los Angeles Basin.

It is generally agreed that repetitions of right-slip displacements, on a fault within the underlying basement rocks, are responsible for the late Miocene-Holocene development of the

Newport-Inglewood Zone of Deformation. This inferred right-slip fault is presumed to follow a contact separating oceanic Catalina Schist facies from an eastern continental basement facies of granitic and associated metamorphic rocks. The contact, termed the California Subduction Zone, is of Mesozoic age. This contact is inferred to continue to the southeast, passing along the west side of Baja California, for more than 800 miles.[31] Reflection data from Western Geophysical[26] indicate that this contact, presumed coincident with the NIZD in the Los Angeles Basin, is offset to the south by the San Joaquin Hills Structural High and passes 24 to 29-kilometers (15 to 18 miles) southwest of San Onofre.

The distribution of San Onofre Breccia, or its equivalent, (for example, on the Coronado Islands) and the presence of eastern basement facies in the Shell core hole west of Point Loma, lend support to the offshore position of this contact; furthermore Western's interpretation of gravity and magnetic surveys also places this contact well offshore. There is no structural or seismic evidence of Quaternary tectonic displacement across this basement contact, except under the Los Angeles Basin, and the contact does not coincide with the SCOZD or the RCFZ. This further supports a lack of continuity along the hypothesized Offshore Zone of Deformation.

2.5.1.1.3.4.2 South Coast Offshore Zone of Deformation

The South Coast Offshore Zone of Deformation (SCOZD) was identified as a continuous trace, within a zone of en-echelon faults, in acoustic basement based on detailed seismic reflection surveys.[26] On acoustic basement, this fault zone is 67-kilometers (42 miles) long with its northern terminus approximately 8-kilometers (5 miles) south of Newport Beach, and its southern terminus southwest of Oceanside. The closest approach of the SCOZD to the San Onofre site is a point approximately 8 kilometers (5 miles) to the southwest.

The tectonic structure of the SCOZD, as evaluated through interpretation of offshore geophysical reflection profiles, indicates the apparent tectonic deformation of two deeply buried reflecting horizons and shows the SCOZD to consist predominantly of a zone of branching and discontinuous faults and folds trending north to northwest.[26] Local northwest- to west-trending folds in the shallower horizons are also associated with this zone. Individual faults are most continuous on the acoustic basement (Horizon C) and less continuous in the younger rocks, such as those represented by Horizon B. Acoustic basement is predominantly located on the lower to middle Miocene San Onofre Breccia through much of the region, but locally is on crystalline basement.[26][32] The earliest displacement of this horizon is considered to be post-middle Miocene.

Apparent vertical displacements of 1000 to 3000 feet down to the west are indicated on the faults that cut Horizon C; however displacement diminishes rapidly in both the northwest and southeast directions from the central part of the zone. Similarly, displacements diminish upward in the section where the fault zone is generally expressed as a series of short, discontinuous breaks in upper Miocene rocks (Horizon B).

Variations among the structural patterns through time suggest that two separate tectonic regimes have produced the recognized features. Structures along the SCOZD on Horizon C appear to be dominated by north- and northwest-oriented normal faulting. This suggests a period of east-west tension across the area.

Horizon B structures are consistent with a north-south compressional environment. The faults in Horizon B, which are younger and shorter faults, indicate continued deformation.

At the northern end of the zone, displacements die out on acoustic basement (believed to be Catalina Schist) near a north-south fault along the west side of the San Joaquin Hills Structural High. To the south, the SCOZD is terminated by a series of intrusions and north-south trending faults.[26]

Recent interpretation of high resolution reflection profiles near to and south of San Onofre[27][28][29] indicate that the SCOZD locally intersects the sea floor outside of the site area (Appendix 2.5I). The SCOZD is not extensively overlain by Pleistocene or Holocene sediments; no evidence has been found to demonstrate that these younger units are displaced.[33] Although there is an occurrence of sea floor irregularity, it is not known to be a tectonic feature.

Faulting and folding identified on the profiles[27][34] that lie eastward of the SCOZD, between the zone and the shore, are restricted to the Mio-Pliocene sediments. The folds are generally a few hundred feet long and are asymmetrical. The faults are intraformational, involving generally only portions of the vertical stratigraphic section. All of these structures are truncated by the Pleistocene unconformity, 40,000 to 80,000 years old, and are overlain by two ages of Pleistocene-Holocene sediments (Appendix 2.5I).

Faults east of the SCOZD are of two types; they are either very old faults deep within the section that cut the San Onofre Breccia and do not extend very far up through the older Monterey section, or they are types of faults that result from deformation associated with folding. These appear to be intraformational faults generated by the folding of the sediments. The seismic data does not show these faults extending deep into the section nor to the Pleistocene unconformity and their apparent zonal distribution is a function of their association with the broad folds east of the SCOZD (Appendix 2.5I). No historical seismicity is associated with this zone.

2.5.1.1.3.4.3 Rose Canyon Fault Zone

The Rose Canyon Fault Zone (RCFZ) is a structural feature in the San Diego region. Onshore the zone is coincident with a sublinear north-northwest trending topographic depression from La Jolla Cove, south through Rose Canyon, along the east side of Mission Bay to San Diego Bay, where it appears to die out as a widening zone of short, principally dip-slip faults (Appendix 2.5N).

Offshore from La Jolla Cove, seismic reflection surveying indicates a northwest continuation of the zone to the Oceanside area. Near its northern terminus, the offshore extension of the RCFZ trends shoreward at Oceanside and becomes two branches onshore. Detailed field mapping near the coast has shown that these branches join two previously mapped faults inland. The north-south trend of these faults and the igneous intrusions at the southeast end of the South

Coast Offshore Zone of Deformation indicate that the two zones are disassociated. The closest approach of the Rose Canyon fault to the site is a point approximately 21 kilometers (13 miles) to the southeast.

Faulting along the RCFZ in the area south of the Morena-Old Town is not well defined onshore. Evidence for faulting at the south end of the RCFZ consists primarily of faults identified by acoustic profiling in San Diego Bay and offshore of San Diego.(35)(36) Faults identified offshore are more prominent than the faults in the southern end of San Diego Bay. The offshore faults are also expressed as fault scarps where they come onshore at Coronado.(36) This evidence strongly suggests that southern extension of the RCFZ is associated with the faulting, and extends offshore of San Diego and not to the south through San Diego Bay. The summary discussion of the RCFZ is addressed in Appendix 2.5K.

The character of the faulting within the RCFZ changes in the southern part of San Diego and becomes a wide zone of faulting characterized primarily by a dip-slip component. Current data indicates that the faulting within this wide zone dies out to the south and does not connect to the Calabasas fault or the Vallecitos fault zone (Appendices 2.5J and 2.5K).

Estimates of sense and amount of displacement on the Rose Canyon fault vary considerably, but are predominantly vertical (west side up) on the northern portion, since at least early Pleistocene time. At least 137 meters (450 feet) of vertical separation on the lower Pleistocene Linda Vista Formation is recognized northeast of Mount Soledad toward Mission Bay, based on the steeply tilted early Pleistocene Linda Vista terrace. On the eastern side of Mission Bay, movement on the fault is apparently reversed with the west side down relative to the east side (Appendix 2.5N).

Offshore, detailed seismic reflection surveying along the northwest part of the fault indicates vertical displacement with the west side down, but the amount of displacement is not known.

The La Jolla terrace and other upper Pleistocene terraces are apparently slightly tilted. Kern(37) shows two upper Pleistocene terraces (120,000 ± 10,000 years old) which have elevation differences across the Rose Canyon fault at the coast near La Jolla. This suggests post-late Pleistocene and possibly Holocene deformation.

Discussion of a possible connection of the RCFZ to faults in northern Baja is presented in Appendices 2.5J, 2.5K, and 2.5L.

2.5.1.1.3.5 Palos Verdes Fault

The Palos Verdes fault is known onshore as a steeply dipping reverse fault separating the Palos Verdes Hills from the Los Angeles Basin. The fault extends northward into Santa Monica Bay, where it appears to bend toward the west and merge with the Transverse Ranges structure.(23) South of the Palos Verdes Peninsula, the offshore fault extension trends southeastward across the San Pedro shelf as a zone of subparallel fault break.(23) Further to the south, two unnamed secondary faults appear to branch southeast from, and trend subparallel to, the main traces of the Palos Verdes fault. All branches terminate just southeast of the Lasuen Seamount, approximately 33.4°N 118 °W (see Figure 2.5-7). The total length of the Palos Verdes fault system is estimated to be about 95 kilometers (60 miles). The southern terminus of the easternmost branch of this fault is approximately 21 kilometers (11 miles) to the west of the plant site. The tectonic history of the Palos Verdes fault is poorly documented in the literature and good estimates of age or amount of displacement are not available.[38] The Palos Verdes Fault trends roughly toward a zone of northwest trending structures offshore from San Diego which includes the Coronado Banks fault. Recent detailed seismic profiling shows several kilometers of unfaulted Miocene sediments between the two faults.

During the period 1932 to 1970, many small seismic events of magnitudes less than 4.0, and two to six events of magnitude 4.0 to 5.0 have occurred that could be associated with the Palos Verdes fault.[23] Direct association of these events is however, questionable because of the nearness of the Newport-Inglewood and San Pedro faults.[23] Additional information concerning the Palos Verdes fault is contained in Appendices 2.5O and 2.5P.

2.5.1.1.3.6 San Pedro Basin Fault

The San Pedro Basin fault, shown on Figure 2.5-7, is a little-studied feature which lies about 12 kilometers (8 miles) west of the Palos Verdes Peninsula. The fault trends northwest some 50 kilometers (31 miles) from north of Santa Catalina Island along the eastern edge of the San Pedro Basin.[32] Displacement across the fault in post-Miocene rocks is inferred to be up to 365 meters (1200 feet). The southern terminus of the fault is believed to be several kilometers northeast of Santa Catalina Island.

2.5.1.1.3.7 San Clemente Fault

The eastern face of San Clemente Island has long been recognized as a fault scarp because of its distinct linearity and evidence of uplift. In their study of submarine topography, Shepard and Emery state that this fault is part of a much longer feature.[3]

The San Clemente fault aligns with the general northwest grain of southern California. In the area of San Clemente Island, the fault scarp faces northeast, but further south, the vertical separation is reversed and the submarine scarp faces southwest.[40]

It is unclear how far south the San Clemente fault extends. It does align with the Agua Blanca fault of Northern Baja California, but presently there is insufficient data to connect the two faults with any certainty. Figure 2.5-8 shows this possible connection and other inferred major faults both onshore and in the Continental Borderland.

2.5.1.1.3.8 Northern Baja California Faults

In general, faults in northern Baja, California, exhibit considerably different trends and structural styles from those north of the border. The exception is the Laguna Salada fault which continues southeast along the trend of the Whittier-Elsinore zone into the Salton Trough Province.

Trending south from an area of discontinuous faulting between these zones is the Sierra Juarez fault zone which bounds the Peninsular Ranges Batholith to the east.

Three major zones cut the main structural block to the west. They are the Agua Blanca, the San Miguel and the Vallecitos fault zones which are shown on Figure 2.5-8. Two other prominent faults, the Calabasas and the Tres Hermanos, have been mapped in the area. These are described in the following paragraphs. Their relationship to faults in the north is discussed in Appendices 2.5J, 2.5K, 2.5L, and 2.5P. As these faults are contained in the Peninsular Ranges Province, they are also discussed in Paragraph 2.5.2.2.2.4.

2.5.1.1.3.8.4 Agua Blanca Fault Zone

The Agua Blanca fault zone extends about 129 kilometers (80 miles) across the western two-thirds of the Baja California peninsula as a relatively continuous trace.

The Santo Tomas fault branches off the western part of the Agua Blanca fault. These faults are distinctive for their west-northwest trend that is more westerly than the strike-slip faults to the north. The trace of the Agua Blanca fault is indicated by abundant geomorphic evidence.[41][42] Typical features are distinct scarps, offset streams, shutteridges, fault sags and saddles, and fault-controlled valleys. Quaternary fan gravels in the Valle de Agua Blanca are offset about 4.8 kilometers (2.9 miles) in a right-lateral sense; between 11.3 kilometers (7 miles) and 22.6 kilometers (14 miles) of similar separation may be indicated by discontinuous igneous contacts across the fault trace.[40]

The extension of the Agua Blanca fault west of Punta Banda is characterized by complex submarine topography.[43] Recent investigations show that the offshore-onshore fault relationship is not present as a continuous through-going feature. Legg and Kennedy, 1979,[115] recognized the offshore part of the Agua Blanca fault as a series of subparallel en-echelon segments trending toward either the San Clemente or the Coronado Banks fault zones.

2.5.1.1.3.8.5 San Miguel Fault Zone

The San Miguel fault zone consists of two segments. In 1956, a 20-kilometer (12.4-mile) length of the southern segment broke along a series of short en-echelon ruptures.[44] Measured fault displacements ranged from 0-78 centimeters (0 to 31 inches) horizontally and from 0-91 centimeters (0 to 36 inches) vertically; the sense of offset was uniformly right-lateral and down to the southwest. The southern segment is mapped as a principally dip-slip fault that dies out in the Sierra Juarez Mountains and does not connect with either the Agua Blanca fault or the dip-slip faults of the eastern escarpment.[10] There is no evidence that this fault offsets this escarpment or connects with faults in the Gulf of California (Appendix 2.5L)

2.5.1.1.3.8.6 Vallecitos Fault Zone

The Vallecitos fault zone is en-echelon to the northern segment of the San Miguel fault zone, but separate from it by a distance of 6 to 10 kilometers (4-6 miles). The Vallecitos fault has a nearly continuous trace that extends from the western edge of the Sierra Juarez 65 kilometers (40 miles) to the west end of the Valle de las Palmas, about 29 kilometers (18 miles) southeast of Tijuana. The main trace of the fault is marked by erosional topographic features and there is no evidence that the Vallecitos offsets anything younger than the crystalline basement rocks (Appendix 2.5L).

2.5.1.1.3.8.7 Calabasas Fault

The Calabasas fault is mapped about 5 kilometers (3 miles) east of the Vallecitos fault zone and trends parallel to it for about 30 kilometers (19 miles) in a northwest-southeast direction. In the Valle de Las Palmas area, recent movement is indicated by small sags and saddles, breaks in uplifted alluvial deposits, and relatively uneroded scarplets.(10) (Appendix 2.5L).

2.5.1.1.3.8.8 Tres Hermanos Fault

The Tres Hermanos fault zone is located midway between the San Miguel and Agua Blanca fault zones and essentially parallels the San Miguel fault zone. The trace, approximately 45 kilometers (28 miles) long, begins in the batholithic rocks of the Peninsular Ranges Province and dies out east of Ensenada. The fault is indicated by pronounced topographic expression and is apparent on high altitude photos. Recency of movement and sense of displacement are unknown (Appendix 2.5L).

2.5.1.1.3.8.9 Connection Between the Rose Canyon and the San Miguel or Vallecitos Fault Zones

Several authors have suggested that an en-echelon relationship may exist regionally between the Rose Canyon fault zone and the San Miguel and Vallecitos fault zones (Appendix 2.5K). A possible northwest extension of the presently mapped limits of either the Calabasas or Vallecitos faults has been inferred by these authors largely on the basis of the regional alignment of discontinuous topographic, structural, and geothermal features in the southern San Diego and southeast Tijuana area; however, geologic maps(10)(35) indicate a 55-kilometer (34-mile) distance between the south end of the Rose Canyon fault and the north end of the Vallecitos fault.

Gastil and others (1979)(45) suggest the possibility of a northwest-trending lineament that would continue from the northwesternmost mapped trace of either the Vallecitos or the Calabasas faults, through eastern Tijuana, and across the U.S.-Mexico Border just west of San Ysidro. The lack of faulting in the well-exposed Eocene and pre-batholithic bedrock, and the lack of fault features recognized on aerial photographs of the area by Gastil (personal communication, 1979), suggest that no significant faulting has occurred in this area.

Geophysical data gathered by Kennedy, 1975,(46) and Kennedy and others, 1977,(36) do not identify continuous faulting along the proposed connection of the Calabasas and Vallecitos faults and the RCFZ in the area south of San Diego Bay and north of the International Border (Appendix 2.5L).

2.5.1.1.3.9 Mission Viejo Fault

The Mission Viejo fault is a discontinuous series of breaks in the Aliso Hills of the Santa Ana Mountains. The Mission Viejo fault trends southerly from Plano Trabuco toward San Mateo Canyon. Its maximum length is approximately 16 kilometers (10 miles), with its southern terminus approaching within 8 kilometers (5 miles) of the site. At the surface, the fault forms the contact between Tertiary sediments on the west and upper Cretaceous marine rocks on the east. The youngest rocks known to be cut by the fault are Eocene in age.[47] Additional information concerning this fault is located in Appendix 2.5H.

2.5.1.1.3.10 Cristianitos Fault

The Cristianitos is a north-northwesterly trending fault which forms the eastern boundary of the late Miocene to early Pliocene Capistrano Embayment. It extends 32 kilometers (20 miles) inland from its exposure in the coastal bluffs approximately 0.8 kilometer (0.5 mile) south of Units 2 and 3. The fault apparently dies out into a series of folds immediately offshore. The age of last movement on the fault is limited by overlying undisturbed marine terrace deposits dated at 125,000 years.

Because of its proximity to the site, detailed studies of the Cristianitos have been performed. These studies and details of the fault are described in relation to site area structure in Paragraph 2.5.1.2.3.2. The fault is also discussed in relation to the Capistrano Embayment in Paragraph 2.5.1.1.3.13.

2.5.1.1.3.11 Santa Ana Mountain Block

In the broadest structural sense, the Peninsular Ranges Province is an uplifted and westward-tilted block of the continental crust that has been broken into sub-blocks by the San Jacinto and Whittier-Elsinore faults. The Santa Ana Mountains and the area to the west, which includes the site, constitute a block.

Basement terrane consisting of Triassic and Jurassic metasedimentary and metavolcanic rocks intruded by Cretaceous batholithic rocks, crops out over most of the block. Westward dipping sedimentary formations of Late Cretaceous and younger age unconformably overlie the basement in the western part of the Santa Ana Mountains. Bedding and foliation within the pre-batholithic rocks generally trend toward the northwest or north-northwest and have moderate to steep dips.

2.5.1.1.3.12 San Joaquin Hills Structural High

The San Joaquin Hills Structural High is a north-south trending acoustical basement high associated both onshore and offshore with a deep seated positive Bouguer-anomaly. This feature forms the western boundary of the Capistrano Embayment.

Offshore the San Joaquin Hills structure is approximately 3 to 8 miles wide. It is located west of Dana Point, and is clearly evident on seismic reflection lines.[27][28][29] Along this structure, the acoustic basement rises 6500 and 9400 feet above its position in the basins it separates on the northwest and southeast, respectively. Onlap of upper Miocene rocks suggests that it has been stable since middle Miocene. This feature appears to be the seaward extension of the San Joaquin Hills Anticline. The gravity and magnetic data show that the Southern California Subduction Zone, which lies below the Newport-Inglewood Zone, is displaced seaward along the west side of this structure to a position, approximately 24 to 29 kilometers (15 to 18 miles) southwest of the seacoast. In general, there is little sedimentation atop the structure but the sea bottom profile has not been affected by its presence.[26]

The Offshore San Joaquin Hills Structure clearly constitutes the southeastern limit of the Offshore Los Angeles Basin. Velocity curves from seismic reflection data indicate the presence of deeper and higher-velocity formations southeast of this structure than are present to the northwest. Onshore, progressively older rocks crop out southward from Dana Point to San Diego; ranging from Miocene near Dana Point through Eocene, and to Cretaceous near San Diego. Cretaceous rocks should possess higher velocities than Miocene rocks and this conforms with the difference observed in the velocity profiles.

Finally, the character of the reflection section is quite different on opposite sides of the Offshore San Joaquin Hills Structure. The section to the northwest is characterized by many reflections between the ocean floor and acoustic basement. To the southeast there is an absence of reflectors in the lower half of the section above the acoustic basement that corresponds to the higher velocity part of the strata. Such an absence of reflectors is conformable with the type of Cretaceous section present onshore; thus, the offshore San Joaquin Hills Structure separates the two distinct basin areas.[26]

Gravity and magnetic data provide further evidence for differentiation of the provinces. The area to the northwest of the structure is characterized by positive Bouguer-anomaly values and relatively low magnetic relief. This contrasts markedly with the area to the southeast which is characterized by negative Bouguer-anomaly values and an undulating magnetic surface, containing a series of high, closed, total-intensity anomalies. This is indicative of the difference in basement rock type in the two basin areas.

The gravity data (PSAR, Appendix 2E) also shows the positive anomaly to include the San Joaquin Hills, northeast of the site. This structural uplift, which was active during Miocene time extends to about 20 kilometers (12 miles) west of the San Onofre site. A large number of north to northwest-trending faults are exposed in the San Joaquin Hills. Many of these faults (especially the north trending ones) were active only during the middle Miocene. Some of the faults (e.g., the Shady Canyon Fault) are intruded by diabasic and andesitic dikes of middle Miocene age, and are unconformably overlain by unfaulted San Onofre and Monterey formations. The faults are dominantly normal-slip faults associated with east-west extension.

Some of the faults extend beneath the Capistrano Embayment as shown in maps and cross-sections prepared by West (Appendix 2.5H), but they are concealed beneath unfaulted strata of the Monterey and younger formations.

2.5.1.1.3.13 Capistrano Embayment

The Capistrano Embayment is a north-south trending structural trough about 35 kilometers (22 miles) long that is bounded by the Cristianitos fault on the east and the San Joaquin Hills on the west. The trough has a narrow wedge shape that opens southward from an apex in the Santa Ana Mountains about 8 kilometers (5 miles) north of El Toro. The trough is about 15 kilometers (9 miles) wide near the coast, where its structural relief dies out along a northwest-trending anticline located between the coast and the South Coast Offshore fault. The configuration and structure of the Capistrano Embayment are shown by structure contour maps and cross-sections prepared by Jack West (Appendices 2.5G and 2.5H).

The Capistrano Embayment is essentially a down-warped structure produced by westward extension in the upper crust along the west side of the Cristianitos fault. Normal displacement on the Cristianitos fault and the resulting development of the Capistrano Embayment occurred during the period between about 10 to 4 million years before present.(48)

2.5.1.1.4 Regional Geologic History

The geologic history of the San Onofre Region is expressed in the stratigraphic record (Paragraph 2.5.1.1.2) and structural features (Paragraph 2.5.1.1.3) of southern California. In particular, the evolution of the Peninsular Ranges and the Continental Borderland provide the historical framework for the site.

The oldest exposures in the Region are the early Mesozoic Bedford Canyon Formation and Santigo Peak Volcanics. These units were deposited on oceanic crust along the margin of the American Continental Plate. The magma which intruded these units and formed the Peninsular Ranges Batholith was generated during the late Mesozoic as the oceanic crust was subducted eastward beneath the American Plate.(12) During this time, the pre-batholithic rocks were compressed against the continent as the Peninsular Ranges were accreted onto the continental crust.(11)

Subduction is believed to have continued into the early Cenozoic but is not reflected in onshore geology. Instead, accretion of continental crust continued in the Borderland.

Late Cretaceous and early Tertiary sedimentary rocks were deposited in marine basins on the newly formed continental margin as the batholith and associated metamorphic rocks were uplifted and eroded. A period of relative stability at the close of the Cretaceous Period is suggested by the extensive low relief erosion surface which formed on Cretaceous rocks.

The middle Cenozoic Era is characterized within the Region by the development of fault controlled basins and structural uplifts within a broad zone of transform faulting between the

American and Pacific Crustal plates.[14] The change from subduction to transform faulting is thought to have occurred about 30 million years ago when the East Pacific Rise intersected the continental margin. Most of the northwest trending structural zones in southern California, including the proto San Andreas, the Whittier-Elsinore, the hypothesized Offshore Zone of Deformation and the San Clemente, probably became active during this onset of transform faulting.

The Los Angeles Basin was one of those which began to develop at this time. Early deposition in the basin, which included the site area, is represented by the late Oligocene Vaqueros and early Miocene Topanga Sandstones.

By middle Miocene time, a structural high had developed in the area which is now offshore from the site. Sediments shed from this relatively short-lived highland, formed the San Onofre Breccia.

The middle to late Miocene Monterey Formation, which overlies the Topanga Formation in the Palos Verdes area and the San Onofre Breccia near the site, was deposited in the broad deepening Los Angeles Basin. It is characterized by abundant laminated diatomaceous shale indicating sedimentation in stagnant bottom water.

Approximately 8 to 10 million years ago, the San Andreas fault system became the principal site of strain associated with the plate transform boundary. Changes in regional stresses accompanied this transfer of principal shear from the previously broad zone to its eastern edge. One of these changes was the development of the Cristianitos fault with accompanied down-warping of the Capistrano Embayment.

The initiation of movement on the Cristianitos fault is marked by the change in sedimentation from the Monterey Formation to the Capistrano Formation. The Capistrano Formation is limited to the Capistrano Embayment. Along the west side of the Cristianitos fault it consists of coarse-grained sandstone with conglomerate lenses that appear to have been deposited by turbidity currents coming off an escarpment along the Cristianitos fault. The sandstone undergoes a pronounced decrease in grain size toward the interior of the basin where it interfingers with micaceous siltstone and mudstone. A similar relationship exists along the west side of the Embayment indicating that the San Joaquin Hills were being uplifted and were shedding sediments eastward into the Embayment. Faunal assemblages within the interior of the Embayment indicate the presence of deep water during the entire period from 10 to 4 million years ago while the Capistrano Formation was being deposited. A pronounced seaward slop existed along the southern edge of the basin as shown by presence of numerous backfilled submarine channels present in coastal exposures of the Capistrano Formation and by the San Mateo Formation which has been shown by Ehlig[2] to be contemporary with the Capistrano. The youngest part of the Capistrano Formation is about 4 million years old and represents the final stages of subsidence along the west side of the Cristianitos fault.

During subsidence and continued deposition in the Embayment, several growth faults such as those northwest of the site developed. In general, deformation within the Capistrano Embayment consists mainly of uplift and gentle folding along fold axes trending northwest to west-northwest. This reflects a change from an earlier east-west extensional strain field, to a strain field marked by north-south shortening. The forming of the Capistrano Embayment may be associated with drag along the South Coast Offshore Fault Zone; however, little displacement occurred along the offshore fault during this time. The pinch out at the top of the Monterey Formation as a result of erosion or buttressing against the San Joaquin Hills Structural High extends southward off the coast with only about 3 kilometers (2 miles) of separation along the South Coast Offshore Fault Zone.

During the past 4 million years, most of the relative motion between the Pacific and the North American plates appears to have occurred along the present day San Andreas fault and its branches. This coincides approximately with the time of opening of the Gulf of California, as the spreading centers of the east Pacific rise moved eastward to approximately its present position. Crustal spreading has extended northward into the Salton Trough and ties directly with the San Andreas and San Jacinto faults.

The relative importance of the most prominent northwest trending structural zones during the Tertiary Period is demonstrated by a comparison of displacement.[33] Offset on the San Andreas has been as much as 700 kilometers (435 miles); the San Jacinto 24 kilometers (15 miles); the Whittier-Elsinore 13 kilometers (8 miles); and the Newport-Inglewood about 3 kilometers (2 miles). Total horizontal offset on the Newport-Inglewood is believed to be conservatively representative of the hypothesized Offshore Zone of Deformation (OZD) including that part offshore from San Onofre. Although the lateral offset history of the Rose Canyon fault is not well known, total displacements are believed to be less than those on the Newport-Inglewood (Appendix 2.5N).

As this change in the tectonic setting of the region was taking place, during the Pliocene Epoch, coastal southern California became less active and in the Miocene, the marine basins were filled. Regressive deposits such as the San Pedro Sand in the Los Angeles Basin and the Niguel Formation north of the site marked the end of widespread marine deposition in the region.

Periodic uplift continued along the coast into Pleistocene times, and were accompanied by eustatic changes in sea level during the glacial ages. Along the southern California coast, a series of wave-cut marine terraces occur up to several hundred feet above sea level. These terraces represent former long-term relative high stands of the Pacific Ocean. Inland streams responded to these changes in relative sea level, resulting in deeply incised stream channels (such as that of the Santa Margarita River) being formed when sea level was below its present elevation. The channels were then backfilled, causing complicated relationships between marine and nonmarine terraces and deposits.

Prior to the formation of the Terrace 1 (stage 5e) marine terrace at elevation 55; about 125,000 years ago[49][50] and perhaps earlier, the Cristianitos fault became inactive.

This terrace surface forms part of the coastal plain in the vicinity of the site. The terrace deposits and part of the underlying San Mateo Formation are well exposed in the recently formed sea cliffs. The importance of the Terrace 1 (stage 5e) and the sea-cliff exposures to demonstrating the stability of the site is discussed in Paragraph 2.5.1.2. Regional processes which may have affected the area; subsidence, uplift and landsliding, are discussed in the following paragraphs.

2.5.1.1.5 Historic Subsidence

Land subsidence in California has long been recognized as a serious and costly problem. As compared with the rest of the state, southern California has only a few areas of historic subsidence. The area in southern California affected by subsidence is minimal, as compared with the central part of the state, but the most extreme, and probably the most costly subsidence in California has been in the Wilmington area of Los Angeles approximately 80 kilometers (50 miles) northeast of San Onofre. There has been a close coincidence of the area of subsidence with the outline of the Wilmington Oil Field, and a close coincidence of the time and amount of subsidence with the time and amount of removal of oil and gas, thus decreasing the pressure and allowing resultant compaction of subsurface materials.(51)

In comparing San Onofre and Wilmington, the subsurface materials are similar; however, the type of structure which produces oil and gas is less developed near San Onofre and production will continue to be negligible compared to Wilmington. The potential for subsidence at San Onofre due to oil and gas extraction is, therefore, insignificant.

Tectonic movements, such as crustal warping, faulting and vibrations due to earthquakes, are also linked with land subsidence. The absence of significant earthquakes, tectonic movement, and vibrations preclude subsidence from this area.

A study has been made of settlement records of United States Coast and Geodetic Survey bench marks along the coastline between San Clemente and Oceanside to measure possible areal subsidence or uplift that might be related to tectonic adjustment or consolidation of geologically young sediments. Subsidence rates along this part of the coast have varied between less than 0.3 centimeter to .09 centimeter (00.01 to 00.03 inch) per year during the period 1933 to 1968.

This rate of subsidence, when compared for example to the historic rates of 0.6 to 0.9 centimeter (.24 and .35 inch) per year near Huntington Beach in Orange County, 40 kilometers (25 miles) distant, and 0.9 to 1.3 centimeters (00.35 to 00.51 inch) per year in the coastal area of the Oxnard Plain in Ventura County, 160 kilometers (100 miles) from the site, indicate that this part of the southern California coast is highly stable. Based on the study of recorded benchmark movement, it is believed that subsidence in the vicinity of the plant should be less than 2.5 centimeters (1 inch) during the life of the plant. Long-term geologic stability is discussed in the following paragraph.

2.5.1.1.6 Regional Rates of Coastal Uplift

The description and analysis of the coastal geomorphology and uplift discussion in Subsection 2.5.1 are located in References 49, 52 and 53.

Late Quaternary rates of deformation (regional uplift, longitudinal and seaward tilt) can be approximated for coastal areas by shoreline angle or elevations of dated terraces. The first (lowest) wave-cut platform and overlying marine terrace and continental deposits in the Camp Pendleton - San Onofre State Beach area (Terrace 1) is an excellent stratigraphic marker. It can be traced as an essentially continuous surface from San Diego to Dana Point and Laguna Beach along the coast in sea cliffs and adjacent arroyos and roadcuts. Terrace 1 regressive marine deposits are dated radiometrically and by faunal assemblage as approximately 125,000 years old (marine oxygen/isotope stage 5e).

Long-term average uplift rates, calculated for a postulated +6-meter stage 5e sea level, show that the Target Canyon area of Camp Pendleton, 12 kilometers (7 miles) south of the site, has undergone probably no more than about 6 centimeters/1000 years of uplift during the last 125,000 years. This rate increases to approximately 9 centimeters/1000 years northward at San Onofre. Dana Point is 36 centimeters/1000 years.

The San Diego-Point Loma area appears to have long-term average uplift rates in the order of 11-20 centimeters/1000 years. Northward, near San Onofre Units 2 and 3, the long-term uplift rate decreases to about 9 centimeters/ 1000 years, about one-half that at San Diego, a third of 26 centimeters/1000 years at Dana Point. Almost two orders of magnitude less than the controversial rate of 500-800 centimeters/1000 years reported for the Baldwin Hills. Large uplift rates of 620-640 centimeters/1000 years are reported in the Ventura/Pitas Point area.

In terms of local late Quaternary uplift, the 9 centimeters/1000 years rate at San Onofre Units 2 and 3 compares favorably with approximately 11-16 centimeters/1000 years for the San Diego area, 40-50 and conceivably 500-800 centimeters/1000 years for Rancho La Brea and the Baldwin Hills, respectively, and 620 centimeters/1000 years for the Ventura Coast. Compared with late Quaternary uplift rates elsewhere, the San Onofre Region is apparently one of the most tectonically stable coastal areas in southern California.

Seaward gradient of Terrace 1 of about 1^{o} that is seen at Target Canyon and Dana Point is comparable to the modern offshore platform. Thus there appears to be little, if any, seaward tilt in this stretch of the coast.

2.5.1.1.7 Landslide Potential

Southern California is marked by abundant landslides which appear to concentrate in areas mainly underlain by sedimentary bedrock.(54) They seem particularly abundant where streams have deeply eroded the terrain and under cut bedding planes.(55) In the Region of San Onofre, the Capistrano and Monterey Formations are particularly susceptible to landsliding because of their lithologies and laminated bedding; however, the San Onofre Breccia and Santiago Formations are less susceptible to sliding, and the San Mateo Formation (site foundation material) is considered stable, and not susceptible to landsliding. Physical properties and analysis of slope stability of the San Mateo Formation are presented in Paragraphs 2.5.4.2.1.3 and 2.5.5. A thorough discussion of landslides is presented in Paragraph 2.5.1.2.5.2.

2.5.1.2 Site Area Geology

The site area, as shown on Figure 2.5-9, is the area within an 8-kilometer (5-mile) radius of the plant site. Approximately half of the area is covered by the Pacific Ocean. Figure 2.5-9 shows the surface (bedrock) geology of the onshore site area. Geology of the offshore site area is presented on Figures 2.5-13, 2.5-14, and 2.5-15. The following discussions may reference geologic features outside the site area when they are significant to the site geology.

2.5.1.2.1 Site Physiography

The San Onofre Nuclear Generating Station site is located on the southern California coast within the Peninsular Ranges Province; an area characterized by northerly trending elongate mountain ranges and valleys. The site is located in the northwest part of the province, which extends southward into Mexico. Major drainage north of the site is provided by the Santa Ana River and south of the site by the Santa Margarita River. The site is located near the northwest corner of Camp Pendleton Marine Corps Reservation, approximately 3.2 kilometers (2 miles) southeast of the mouth of San Mateo Creek. The physiography of the site area (Figure 2.5-10) is typical of the region, with a rather narrow, gently seaward sloping, coastal plain.

The plain is terminated at the beach and forms a line of cliffs, which have been straightened over long distances by marine erosion. Landsliding along the coast south of the Cristianitos fault has contributed to coastal retreat of the bluffs.

Sea cliffs in the immediate vicinity of the site reach a height of about 18 to 38 meters (60 to 125 feet) above sea level, and are separated from the ocean by a narrow band of beach sand. In places, ephemeral streams are actively eroding gullies into the seaward parts of the coastal plain, and several deeply incised barrancas have been formed.

Local landforms of interest near the site are the San Onofre Mountains on the east, the more distant Santa Margarita Mountains to the northeast, and the San Joaquin Hills to the northwest. Streams draining from the Santa Margarita Mountains feed into San Onofre Jardine Canyon and San Mateo Canyon north of the site.

The trace of the Cristianitos fault, in the site area, is subtly expressed by topography, and the general trend is inferred from: (1) the prominent ridge projecting at about north 20^{o} west into the bend of San Mateo Creek; (2) the long, relatively straight alignment of a large tributary canyon into San Onofre Creek; and (3) a series of aligned, north-trending swales inland from the coastal exposure of the fault. With the exception of the coastal exposure, the traces of the fault are not readily observed in natural outcrops. Lithologic changes have provided most of the evidence for mapping of the fault.

The middle Miocene and early Pliocene formations which form the shallow bedrock between the coast and the hypothesized Offshore Zone of Deformation contain extensive, submarine channel and fan deposits similar to those seen in exposures along the coast from Dana Point to

Oceanside. Some features which appear to be folds, are probably the result of nonparallel bedding within the submarine channel and fan deposits.

2.5.1.2.1.1 Terraces

The flight of terraces at Camp Pendleton rivals in number and elevation the "classic" southern California sequence on the Palos Verdes Peninsula. Two alternative hypotheses may be invoked to account for the elevation and origin of the pre-Terrace 1 deposits: (1) sea floor spreading, expansion of ocean basins, and resultant lowering of sea level since late Tertiary time; and (2) general tectonic uplift of the California coast throughout the Quaternary. The lower marine terraces originated in response to Pleistocene glacio-eustatic fluctuations of the sea superimposed on either generally falling sea levels or on a rising land mass. The magnitude of possible hydro-isostatic movement is unknown, but undoubtedly very small compared with glacio-eustacy.[49][52]

The data and interpretations are based on the recent, detailed mapping of marine terrace deposits,[2] and the detailed logging of post-stage 5 deposits underlying the San Onofre Bluffs. The marine terraces on the San Onofre Mountains of Camp Pendleton were identified mainly by topographic expression. Onshore, there are at least nine distinct marine terrace deposits, eight of which are unburied and lie at successively higher elevations above the first terrace. The pre-stage 5 marine terrace deposits range in elevation from about 75 to 375 meters (250 feet to 1250 feet). The lower terrace deposits, designated 2 through 5, are best preserved; higher deposits occur mainly as gravel veneers 1 meter (3 feet) thick recognized by beach bars and well-rounded pebbles and cobbles.[49]

Terrace 1 deposits are about 125,000 years old, based on uranium-series and amino acid dating and on faunal assemblage. Terrace deposits topographically higher are interpreted to be progressively older.[49] There is a "break" in steps of elevation between terraces 1 and 2, and between 8 and 9, therefore it is possible that the approximate ages given for terrace 2 and older deposits may be too young by a factor of at least "one terrace interval" and there may be topographically higher and presumably older terraces not yet identified owing to either nondeposition or to subsequent erosion.

The marine terrace deposits topographically higher than the San Onofre Bluffs at Camp Pendleton seem to span most of middle Pleistocene time. Continuity of terraces, especially the lower ones indirectly dated as between about 250,000 to 500,000 years old, suggests no post-terrace fault displacement, at least within the resolution afforded by current mapping and elevation data. Terrace elevations appear to be related both to slow uplift as well as to falling seal levels in middle and late Pleistocene time upon which were superimposed several glacio-eustatic fluctuations.[49]

Young sediments and marine terraces are present offshore from San Onofre. The geophysical profiles identify two sedimentary units overlying the marine platform. The younger cover is dated by radiocarbon methods as in the order of 5,000 to more than 13,000 years before present. The absolute age of the older cover is unknown, however, from stratigraphic position, is older than about 20,000 years (stage 2). The geophysical profiles suggest that the offshore platforms were cut during isotope stages 3 and 5a, about 40,000 and 80,000 years before present, respectively (Appendix 2.5I).

2.5.1.2.1.2 Terrace 1 Deposits

The most extensive marine terrace in the San Onofre area is the first terrace above sea level. This terrace is exposed clearly in sea cliffs and coastal arroyos for over 12 kilometers (7 miles); from San Onofre Units 2 and 3 on the north to Las Flores Creek on the south. The planar contact with underlying Tertiary deposits is readily traceable almost 1.6 kilometers (1 mile) inland in canyons and roadcuts.

The Terrace 1 deposits in the Camp Pendleton-San Onofre State Beach area were laid down as a regressive sequence when the sea retreated from its stage 5 glacio-eustatic high stand. Near the shoreline angle, fine-grained beach sands are mixed with sediments derived from adjacent cliffs. Seaward, these sediments grade into coarse-grained marine sands, boulders, and cobbles.

Basal marine gravels on the Terrace 1 abrasion platform, range in thickness from approximately 0.6 to 2 meters (2 to 6 feet) and grade upward into coarse-grained sands and shell fragments. Fossils associated with these sands are common only locally; the best known site being sea cliff exposures at the boundary between Camp Pendleton and San Onofre State Beach, Location 26C-3, Figure 2.5-9.

The age of the marine deposits overlying the Terrace 1 abrasion platform has only recently been calculated by amino-acid assay to be about 125,000 years old. The underlying marine abrasion platform upon which the fossils rest is approximately 125,000 to 130,000 years old, associated with marine oxygen isotope substage 5e, an interglacial high stand of sea level.(49)

2.5.1.2.1.3 Continental Sediments

Continental deposits have been laid down primarily by a hierarchy of drainages as coalescing alluvial fan deposits (piedmont plain) that form the San Onofre Bluffs.

These continental sediments are all younger than about 125,000 years old (stage 5), for they generally overlie Terrace 1 marine deposits. Their stratigraphy, as exposed in sea cliffs, arroyos, and roadcuts of the San Onofre Bluffs, consist of channel gravels, overbank silts and clays, and buried paleosols.

2.5.1.2.1.4 Drainage Classes

The post-stage 5 continental sediments have been laid down mainly by three classes of drainages: (1) Class I or integrated drainages, of sufficient basin area to have graded to sea-controlled changes of base level; (2) Class II or modern arroyos, typically steep-walled and heading within the coastal bluffs; and (3) Class III or ephemeral streams debouching from old marine terraces and highland terrain onto the San Onofre Bluffs.(49)

The Santa Margarita River exemplifies a Class I or fully integrated drainage in the Camp Pendleton-San Onofre State Beach area. Other Class I drainages include San Mateo and Las Flores Creeks. The Santa Margarita has periodically cut and filled its lower course responding to climatically-controlled changes in hydraulic regimen and glacio-eustatic fluctuations of sea level. This is particularly evident by the late Wisconsinan buried channel grading to a low stand of the sea. The basal gravels, presumably fluvial, occur at about 10 meters (32 feet) below present sea level, and may be chronologically correlative to the late Wisconsinan channel underlying the Santa Margarita River and Las Flores Creek.

Class II drainages, such as Horno Canyon, are mainly steep-walled arroyos rapidly dissecting the San Onofre Bluffs, and giving rise to coastal badland topography. Topographically, Horno Creek has built up an alluvial fan on the San Onofre Bluffs with radiating distributaries laying down fine-grained sediments along the distal margins. All Horno Creek drainage is now funneled into one distributary causing rapid channel incision, and the dissection of the fan.

Most of the San Onofre Bluffs, from San Onofre Units 2 and 3 on the northwest to Las Flores Creek on the southeast, are a composite of coalescing alluvial fans laid down by Class III ephemeral streams. These fans apparently extended at least 1.6 kilometers (1 mile) beyond the present sea cliffs about 5,000 years ago and were graded to sea level in mid-Holocene time. Characteristically, poorly-sorted coarse-grained mudflow, debris flow, and fluvial deposits are laid down in proximal segments of the fan or are entrapped in gullies. Distal parts of the fan are fine-grained, usually clays and silts, which in some cases reach the present sea cliffs.

2.5.1.2.2 Site Stratigraphy

Geologic formations exposed within the site area range, oldest to youngest, from the Cretaceous Trabuco Formation to recent deposits of Holocene alluvium and beach sand. Figure 2.5-11 is a composite stratigraphic column for the San Onofre area. This figure shows the depositional sequence of the geologic formations exposed in the site area and gives the cumulative thickness, geologic age, and generalized lithology of each formation. The areal extent of the offshore exposures of each formation is seen on Figure 2.5-9. This figure also locates the area of the geologic cross-section (Figure 2.5-12) extending through the plant site landward across the site area. Plates III-V, Appendix 2.5Q show the surficial geology of the offshore site area.

Exposed within the immediate boundaries of the plant site are, from oldest to youngest, (1) San Mateo Formation of late Miocene to Pliocene age; (2) the overlying Pleistocene terrace deposits; and (3) recent beach sand. Units 2 and 3 are founded on the dense, slightly cemented sandstone of the San Mateo Formation; see Figure 2.5-9.

During late Pleistocene time, wave action along the coast cut an extensive, gently seaward sloping bench into the San Mateo Formation immediately north and south of the plant site.[49] Crudely stratified, late Pleistocene marine and nonmarine sediments varying from 9 to 15 meters (30 to 50 feet) in thickness were then deposited over the wave-cut bench. A typical geologic cross-sections through the site is shown in Figure 2.5-12.(2) Boring logs for the site are described in Appendix 2.5C.

The marine and nonmarine terrace sediments are essentially horizontal in the exposure between San Mateo Creek and the Cristianitos fault. Horizontal bedding is also present in the San Mateo Formation along the coast, between San Mateo Creek and the site; however, between the site and the Cristianitos fault, bedding steepens and the strike is variable.(2)
The following are lithologic descriptions of each geologic formation exposed within the site area. These descriptions are based on literature studies and observations of:

A. The rock units exposed during the excavation of San Onofre Units 1, 2, and 3

B. The naturally exposed rock units of the San Onofre Bluffs and San Onofre Mountains

C. Petrographic analysis of boring samples at the San Onofre Site

2.5.1.2.2.1 Pre-Tertiary Sedimentary Rocks

The oldest rocks exposed within 8 kilometers (5 miles) of the site are the Cretaceous Trabuco, Ladd, and Williams Formations. The youngest formation, the Williams, unconformably underlies the Tertiary La Jolla Group, and consists of fine- to medium-grained sandstone, conglomeratic sandstone, and interbedded concretionary siltstone.

In the site area, the great thickness of the Williams Formation, its variability in lithology, and its Maestrichian aged fossils suggest that this formation may be transitional to the Tertiary rocks.

2.5.1.2.2.2 La Jolla Group

Overlying the pre-Tertiary sedimentary rocks is the Paleocene to Eocene La Jolla Group consisting locally of the Silverado and Santiago Formations. This group is widely distributed on the east side of the Cristianitos fault and generally underlies elongated, gently sloping ridges. The Silverado Formation is probably nonmarine and consists of gray, coarse-grained arkosic sandstone interbedded with minor amounts of siltstone and claystone. The Santiago Formation overlies the Silverado Formation and consists of marine, white to gray, massive to poorly bedded, fine to medium grained, arkosic sand. Locally, the sandstone is interbedded with dark siltstone. The upper member of the Santiago Formation is generally a white to yellow, medium-grained sandstone with interbedded siltstone.

2.5.1.2.2.3 San Onofre Breccia

Between the coast and San Mateo Canyon, and east of the Cristianitos fault, surface exposures of the San Onofre Breccia are widely distributed. Offshore, shallow bedrock rests unconformably on the Breccia. The formation is hard, resistant to erosion and is usually well exposed along the flanks of the major drainage channels. The San Onofre Breccia is of late lower to early middle Miocene age as shown by its stratigraphic position; see Figure 2.5-11.

The Breccia consists of, in decreasing abundance, breccia, conglomerate, and sandstone. The conglomerate facies characteristically contain clasts of blue-green glaucophane schist, most of which range in size from granules a few millimeters across to small boulders, however, clasts 1 to 2 meters (3 to 6 feet) long are present in many places and the largest clast observed was 13 meters (43 feet) long.[2] Clasts within the Breccia are angular to subangular and are exclusively of metamorphic rock types characteristic of the Catalina Schist and other basement rocks. The light brown sandstone is coarse-grained, massive to thickly bedded and contains some vertebrate fossils. The coarseness of the San Onofre Breccia increases south to north along the San Onofre Mountains.

The lower part of the formation consists of relatively fine grained sediments representing distal fan deposits that are common near the base of the formation throughout the area. The middle and upper parts of the formation appear to represent rapid accumulation on a relatively steeply sloping alluvial fan.

Coarse, internally massive beds of probable mud-flow origin are fairly common. The most abundant lithology is breccia with clasts ranging from pebbles to small boulders in size and showing clast to clast support.

In several places there are thick massive units interpreted to be avalanche deposits. The individual units are typically monolithologic and consist of tightly packed angular fragments of highly variable size.

Tuff beds and tuffaceous sediments occur locally and are composed of fine grained ash and alternation products derived from ash.

2.5.1.2.2.4 Monterey Formation

The Monterey Formation crops out east of the Cristianitos fault south of San Mateo Creek. It is also exposed northeast of the City of San Clemente. This formation consists of light gray to brown, thin bedded shale and mudstone; locally, diatomaceous and siliceous shales are present. The upper 300 feet of the formation is a transitional section including siltstones and shales typical of both the Monterey Formation and the overlying Capistrano Formation. The basal part of the formation consists of rounded, reworked conglomerate and coarse grained sandstone derived from erosion of the San Onofre Breccia. South of the site, these basal sediments are as much as 50 meters (160 feet) thick in the area upslope from the lowest marine terrace.

The Monterey Formation unconformably overlies the San Onofre Breccia and contains abundant microfossils of middle Miocene age.[2] The San Onofre Breccia and Monterey Formation are separated by an angular unconformity and represent very different depositional environments. The San Onofre Breccia was deposited by an alluvial fan emanating from the southwest whereas the Monterey Formation was deposited by a sea encroaching from the southwest.

The base of the Monterey Formation overlaps the base of the San Onofre Breccia and rests unconformably upon underlying Eocene sandstone of the La Jolla Group, on the ridge between San Onofre and San Mateo Canyons. In part of this area the basal sandstone and conglomerate member is no more than 1 meter (3 feet) thick. Diatomaceous and calcareous shale lie directly above the unconformity.

The lithology of the Monterey Formation undergoes lateral facies changes along this segment of the coast. Close to the Cristianitos fault the exposed strata consists of dark brown to greenish gray thin bedded siltstone and clayey siltstone with thin tuff beds scattered throughout the section. Farther down the coast to the southeast these sediments grade laterally into interbedded clayey siltstone and fine grained arkosic sandstone rich in biotite. Still farther to the southeast, the exposed strata consists mainly of coarse grained arkosic sandstone which finally grades into an almost entirely massive coarse grained arkosic sandstone northwest of Las Pulgas Canyon. The lateral variation of sediments in this formation represent changes in depositional environments between fan derived and pelagic deposits.(2)

2.5.1.2.2.5 Capistrano Formation

The Capistrano Formation conformably overlies the Monterey Formation. Foraminifera examination indicates that the formation is of late Miocene and early Pliocene age.(56) This formation is well exposed west of the Cristianitos fault near San Mateo Canyon and east of the fault at San Onofre Bluffs. The Capistrano Formation has a maximum thickness of about 950 meters (3100 feet) in the vicinity of San Juan Capistrano and decreases in thickness both northward and southward. This thickness is approximately the same as the vertical separation along the Cristianitos fault (exhibit B, Appendix 2.5H).

Exposed strata consists of interbedded mudstone, siltstone, and biotiterich arkosic sandstone, diatomaceous siltstone also occurs locally.(2) The formation is moderately hard, thinly laminated, and is slightly resistant to erosion. The topography is characteristically low, rolling hills marked by numerous landslides on canyon slopes. The transition between the Capistrano Formation and underlying Monterey Formation exposed in Section 27, T8S, R7W,(57) contains thinly interbedded diatomaceous siltstone and clayey siltstone of the upper part of the Monterey Formation and interbedded mudstone, clayey siltstone and fine grained biotite-rich sandstone of the overlaying Capistrano Formation. This transition grades upward into a more thickly bedded sequence dominated by fine to medium grained biotite-rich sandstone. The Capistrano Formation appears to be time equivalent to and perhaps a lateral facies of the San Mateo Formation. This is discussed below in Paragraph 2.5.1.2.2.6.

2.5.1.2.2.6 San Mateo Formation

The San Mateo Formation appears to be entirely of marine origin. The formation has not yielded fossils or other material suitable for dating; however, stratigraphic relationships bracket its age between early late Miocene and late Pleistocene. This formation was previously considered to be younger than the Capistrano Formation; however, recent studies(2) indicate the lower part of the San Mateo Formation could have been deposited synchronous with the lower part of the Capistrano Formation, and the upper part of the formation is probably early Pilocene in age.

Exposures of the San Mateo Formation in the cliff along San Clemente State Beach are indicative of turbidite deposition in a submarine canyon within the Capistrano Formation and, therefore, it represents only a facies of the Capistrano Formation.[(2)]

Within the area covered by the geologic map, Figure 2.5-9, the San Mateo Formation is exposed only in a relatively small triangular area bounded on the east by the Cristianitos fault, on the southwest by the coast, and on the north by a line trending south 70 degrees west from where the Cristianitos fault crosses San Mateo Creek. The San Mateo Formation which underlies the site, is predominantly a massive, coarse-grained, light yellow-brown to light gray, arkosic sandstone with scattered lenses of pebble-cobble conglomerate (reworked from the underlying San Onofre Formation), and layers of fine silty sandstone and siltstone. The sandstone is poorly cemented but is dense and forms steep canyon walls and near-vertical cliffs along the coast. Discernible bedding is rare in most exposures although the upper part of the formation north of Basilone Road contains broad open cross-beds.

Locally the formation contains large fragments of siltstone, up to 3 meters (10 feet) in length, probably incorporated by turbidity currents or submarine slumping. There is also evidence that locally some siltstone interbeds exist.

The maximum thickness of the San Mateo Formation within its outcrop area is estimated to be less than 1000 feet. A drill hole at the site indicates the San Mateo Formation is at least 295 meters (900 feet) thick at the point along the coast. Based on drilling and mapping, the total thickness is inferred to be approximately 650 meters (2000 fee).[(58)]

2.5.1.2.2.7 Qt, Undifferentiated Terrace Deposits

Terrace sediments deposited along the San Mateo and San Onofre Creeks, and the terrace platforms inland from San Clemente have not been differentiated in Figure 2.5-9. The location and elevation of these deposits suggest their origin; however, there is insufficient evidence to label the sediments other than to show that they are terrace deposits unconformably overlying bedrock.

2.5.1.2.2.8 Qtm, Marine Terrace Deposits

Sediments laid down during the periods when sea level was at higher elevations occur in the wave-cut platform at an elevation of 10 meters (30 feet). The sediments are characterized by cobble and gravel beds locally interspersed with beach sands. Fossils are rare, found only at location 26C-3, south of the State Park-Marine Corps property line.[(2)] The age of the fossil assemblage is considered to be dated at 125,000 years before present.[(49)]

Marine gravels overlie wave-cut terrace platforms at several elevations. Precussion marked and chipped lag gravels and armoring boulders rest on the remnants of the old erosion surfaces.

Some terrace remnants can be traced laterally several thousand meters, beginning about 3 kilometers (2 miles) south of the plant site and extending to Las Pulgas Canyon and beyond.

The age of the first terrace platform above the coastal plane at elevation 325 feet is at least 251,000 years before present and the oldest terrace ranges to greater than 782,000 years before present and is at about elevation 1250 feet.[(49)]

A subsurface marine terrace located offshore in the site area has been dated at as young as 13,000 years (Appendix 2.5I). It is probably older.

2.5.1.2.2.9 Qtn, Nonmarine Terrace Deposits

The nonmarine sediments are defined in this area as representing continental deposits laid down on the wave-cut platform or on the veneer of marine deposits overlying a wave-cut platform. The nonmarine sediments seen in the bluffs north and south of the site are typical.

The first marine terrace platform is overlain at the shoreline angle with fine sands and debris accumulated from the adjacent cliff-face. This grades upward through a sequence of soil horizons interspersed with sand and gravel lenses. Near the source, the nonmarine section is relatively thick, thinning as the distance from the source increases. Near the plant site, the bluffs are about 425 meters (1400 feet) from the foothills and are 20 meters (70 feet) thick along the coast. At Target Canyon where the bluffs are about 1,370 meters (4500 feet) from the foothills, the nonmarine section is about 10 meters (30 feet) thick.[(49)]

2.5.1.2.2.10 Qtr, Fluvial Deposits

The stream profiles of San Mateo and San Onofre Creeks have responded to the fluctuations in sea level, developing temporary base levels, depositing flood plain sediments and with sea level lowering, readjusting the profile and downcutting. This resulted in river terraces being deposited along the channels as seen in Figure 2.5-9.

The sediments are representative of the source areas and periodic changes in stream gradient. The river terraces consist of rock derived from the topographic highlands to the east. Interfingering of river terrace sediments and nonmarine continental deposits occurred where the creek sediments were influenced by tidal action or sea level change. This is observed in the cut slopes of Units 2 and 3.[(50)]

2.5.1.2.2.11 Landslide Deposits

Many of the canyon slopes in the area under investigation are marked by landslides. These rounded hummocky features along the canyons are especially evident in areas underlain by the Capistrano and Monterey Formations and members of the La Jolla Group. Rocks influenced by the Cristianitos fault tend to be fractured, jointed, and otherwise weakened, allowing slump failures in the bedrock. Away from the area of the fault, the sliding usually occurs in soft formations where oversteepening of the canyons permits slumping. Some sliding is probably due to unsupported bedding planes.

Along the coast, a series of large landslides begins about a mile south of the site and extends down the coast 8 kilometers (5 miles). The slide nearest to the site exposes the Cristianitos fault. All of these slides are confined to the Monterey Formation and were probably the result of wave erosion undercutting along bedding planes.

Stability analyses of the San Mateo Formation, which underlies the site show the rock to be stable under severe loading and not susceptible to landsliding; see Paragraphs 2.5.5 and 2.5.1.2.5.2.

2.5.1.2.2.12 Alluvium, Slopewash, Fan, and Beach Deposits

Alluvium occurs chiefly as thick deposits of silt, sand, gravel, cobbles, and boulders in the channels of San Onofre and San Mateo Creeks. The fan deposits have a similar composition but merge into the main drainage courses from the mouths of tributary streams and have accumulated on the coastal plain landward of the San Onofre bluffs.

Slopewash debris represents thick accumulations of soil composed of silt, sand, and gravel on the surrounding hillsides. These deposits are generally porous and have low density.

Beach deposits consist of wave deposited sand and gravel along the coastal strand between the cliffs and ocean. These deposits merge laterally with the alluvium of San Mateo and San Onofre Creeks.(50)

The middle Miocene to early Pliocene formations which form the shallow bedrock between the coast and the hypothesized Offshore Zone of Deformation contain complex submarine channel and fan deposits as seen in exposures along the coast from Dana Point to Oceanside.(80)

Submarine channel and fan deposits dominantly consist of medium to coarse-grained sandstone and conglomeratic sandstone characterized by large scale low-angle cross-bedding and lenticular bedding and, near fan heads, by massive bedding.

Deposits of interfan and overbank origin consist of siltstone, mudstone, shale and fine-grained sandstone characterized by parallel bedding.

2.5.1.2.3 Structure

2.5.1.2.3.1 Stratigraphy and Folding

Within the onshore site area, bedrock geology has a pronounced change across the north-northwest trending Cristianitos fault. East of the fault and beyond the site area the region is part of a large structural block which extends from the Elsinore fault southwest to the coast and includes several mountain ranges. The area west of the fault is part of the Capistrano

Embayment, an uplifted structural trough which interconnects with the Los Angeles Basin; see Paragraph 2.5.1.1.3.13.

Two to four miles inland, the Eocene strata is overlain by the lower to middle Miocene San Onofre Breccia which has an average dip of about 35° to the southwest. Approximately 4600 feet of the Breccia is exposed in the site area. It forms the San Onofre Mountains that are subparallel to the coast.

Unconformably overlying the San Onofre Breccia and dipping southwest at low to moderate angles, is the middle to upper Miocene marine Monterey Formation. This is the youngest bedrock formation exposed in the site area east of the Cristianitos fault.

North of the site area and west of the Cristianitos fault is the uplifted Capistrano Embayment, a more or less flat bottomed trough, trending approximately north 10° west. The exposed bedrock within the interior of the trough is the upper middle to lower Pliocene marine Capistrano Formation. This formation, locally capped by subhorizontal siltstone and sandstone of the upper Pliocene marine Niguel Formation, has been gently folded in an irregular pattern.(2) Closer to San Onofre and near the north end of the site area, bedding dips at a low angle near the Cristianitos fault, and becomes horizontal to west dipping along the west side of San Mateo Creek. Bedding northeast of the San Clemente golf course dips 16° southeast to 5° northwest; see Figure 2.5-9.

The upper Miocene to lower Pliocene San Mateo Formation appears to be contained within the Capistrano Formation; see Paragraph 2.5.1.2.2.6. Near the coast, it crops out adjacent to the Cristianitos fault. Though near horizontal bedding is present in the San Mateo Formation, generally the bedding dips 8° to 10° to the southwest with steeper dips locally. Exposed bedding in San Mateo Canyon dips 28° to the south indicating a change in attitude near the Cristianitos fault.(47) This change in attitude may be due in part to tectonic movement.(2)

2.5.1.2.3.2 Faults

The Cristianitos fault is a major structural feature within 8 kilometers (5 miles) of the site. Several other small structural features are also present; see Figure 2.5-9 and Paragraph 2.5.3.2. The Cristianitos fault is exposed in the coastal bluffs approximately 0.8 kilometer (1/2 mile) south of Units 2 and 3. Because of its proximity to the site, extensive and detailed studies of the fault were conducted by various consultants to examine past activity. The offshore projection and limits have been thoroughly examined. The following is a brief discussion of the physical characteristics of the Cristianitos fault and a summary of the site geologic structure based on these investigations.

The Cristianitos fault trends approximately north 20° west for about 32 kilometers (20 miles) inland from its coastal exposure. The fault is a normal fault with displacement being down to the west. It has an average dip of 58° to the west. Within the site area, the fault is a structural boundary between middle Miocene and older rocks and upper Pliocene and possibly younger sediments. The fault is mapped where it brings dissimilar rocks together although faults and shears are present locally either side of the fault trace.[2] At the northern end of the fault where it crosses San Mateo Creek, the Monterey and Capistrano Formations are faulted against the La Jolla Group Formations. The fault is mapped as a single trace from San Mateo Creek to the coast where a zone of shears 45 to 49 meters (140 to 150 feet) wide is exposed. At the southeast end of the Cristianitos fault, where it is exposed in the coastal bluffs, the San Mateo Formation is down faulted against the Monterey Formation. Undisturbed terrace deposits of marine gravels and cobbles lie across the fault trace. A thick section of nonmarine sediments overlie the marine sediments.

The age of last movement of the Cristianitos fault has been established by dating the eroded marine platform which crosses the fault. The platform was eroded by a receding sea after the last fault movement. Marine gravels and cobbles were deposited across the fault trace and they are undisturbed. Fossils deposited in these sediments some 6 kilometers (4 miles) (location 26C-3, Figure 2.5-9) farther south have been dated by amino-acid assay at about 125,000 years.[49]

In order to assess the minimum age of last displacement, elsewhere, trenches were excavated at five locations where the fault is covered by either Pleistocene terrace deposits or late Quaternary soil and slope wash.[25][57][59][60][61]

The investigations have demonstrated the age of the fault to be greater than 125,000 years, based on the overlying terrace material which has not been offset where the contact with the underlying formation is exposed. In addition, there is no evidence of any fault movement in the past 500,000 years. Based on these investigations, it is concluded that the Cristianitos fault is not capable as defined by 10CFR100, Appendix A.

Offshore from the site, no clear seaward extensions of the Cristianitos fault or of any other continuous structural feature have been found in the several miles of geophysical profiling.[27][28][29] The most likely reasons for the fault dying out being accommodated by down-warping toward the east as seen in WCC sparker profile 849. Another explanation is that the down-warping reduced the driving force along the fault causing displacement to decrease in the offshore. Geophysical profiles several thousand feet offshore display continuous reflection-horizons across the projected trend of the Cristianitos fault, indicating the fault extends seaward no more than about 6,000 feet (Appendices 2.5I and 2.5Q).

These same profiles do reveal the presence of minor structural features in the shallow bedrock between the coast and the hypothesized Offshore Zone of Deformation and along the trend of the Cristianitos fault, however, these features consist mainly of small gentle folds arranged in two belts; see Paragraph 2.5.1.2.3.1 and Appendix 2.5Q.

Several intersecting faults have been mapped by Blanc and Cleveland[54] in the hills between the city of San Clemente and San Mateo Creek, about 4.8 kilometers (3 miles) northwest of the site; see Figure 2.5-9. The longest fault is a northwest striking fault. The northwest striking fault is 4.8 kilometers (3 miles) in length and shows evidence of left lateral movement displacing a 2-mile long northeast striking fault near San Clemente. To the south, near San Mateo Creek, the northwest striking fault is offset by the remaining two northeast striking faults. They have been mapped as having left-lateral, oblique-slip movement. These two northeast striking faults are 2 and 0.96 kilometers (1.3 and 0.6 miles) in length.

Two additional very short faults were mapped by Blanc and Cleveland[54] in the San Clemente area about 4 miles northwest of the site. One fault along the beach north of San Clemente State Beach is about 210 meters (700 feet) in length; a 150-meter (500-foot) long fault is located near the city of San Clemente.

All of the faults described by Blanc and Cleveland displace Miocene-Pliocene Capistrano and/or San Mateo Formations, however, each fault or its projection is covered by unbroken Pleistocene terrace deposits.[50] This series of intersecting faults is confined to Tertiary formations and does not correlate to any pre-Tertiary fault; therefore no relationship exists between this series of faults and the Cristianitos fault.[54]

The Mission Viejo fault crosses San Mateo Canyon approximately 8 kilometers (5 miles) northeast of the site and is discussed in Paragraph 2.5.1.1.3.9. The youngest rocks known to be cut by the fault are Eocene in age.[47]

Approximately 3.2 kilometers (2 miles) northeast of the site, a short 4.3-kilometer (2.7-mile) long fault has juxtaposed the Eocene La Jolla Formation against the Miocene Monterey Formation. Unbroken Pleistocene terrace deposits overlie this fault along San Onofre Creek.

A fault, designated Fault E, see Figure 2.5-9, begins near San Onofre Creek to the north and trends southward toward the coast near the U.S. Immigration and Naturalization Station on Interstate 5.[2] This fault juxtaposes different units of the Monterey Formation in some areas and juxtaposes the Monterey Formation against the San Onofre Formation in other areas. The fault has two traces in some areas and has apparent normal separation of approximately 100 meters (330 feet) with the north side down. This fault was first observed by Ehlig,1977,[2] and dated by Shlemon[49] who suggested "probable Late Pliocene" and "very likely at least 100,000 years before present," respectively as dates of occurrence for Fault E. However, a study by Fugro, 1978,[62] indicates that the fault is at least 300,000 years old and probably more than 400,000 years old. No in-place deposits remain in the marine terrace platform at Fault E; however, the absence of any perceptible disruption of the bedrock platform or abrupt change in erosional slope indicates no movement since beveling of the terrace platform. In addition, soil profiles are locally continuous across the fault.[62] This suggests a minimum age of the last movement of Fault E of at least 100,000 years and as much as 300,000 years.

Two short faults separating San Onofre Breccia from the Monterey Formation lie farther to the east, beyond Fault E, at elevations 1050 and 1150. The relationship of the formations at these faults is the same as seen at Fault E, with the younger Monterey down relative to the Breccia.

The Monterey Formation was down-dropped, and then preserved by the more resistant outcrop of the Breccia on the up-thrown block. Had faulting occurred during or after Pleistocene terrace development, the Monterey would have been completely stripped away along with the terrace sediments that may have been deposited during Pleistocene time. To the south of the site area, terrace deposits occur at elevations of 1050 and 1200 feet[2] (Figure 2.5-9) that are older than 700,000 years before present[49] providing a correlation to establish that movement along these faults has not occurred in at least the last 500,000 years.

Offsets of the stage 5e terrace platform are essentially absent with the only occurrence unrelated to landsliding occurring at Target Canyon, about 6-1/2 miles south of the site. The offsets are minor, on the order of a few centimeters (inches) and are found where the San Onofre Breccia is buried at shallow depth; thus they are likely related to compaction deformation. They are oriented tangential to the site area and are not considered of geologic or seismic significance.

Structural features offshore of San Onofre Nuclear Generating Station, depicted in the Marine Advisers report[40] (PSAR Appendix 2B) have been reinterpreted in light of more recent geophysical data.[26][27][28][29] These data indicate that there is no fault corresponding to Fault E as interpreted by Marine Advisers. The feature referred to as Fault 3 offshore is represented by three pairs of subparallel, discontinuous trending folds that are cut by several short faults which do not disrupt the surface (see Paragraph 2.5.1.2.3.3).

Figure 13 of Appendix 2.5I, shows the track lines of the majority of the seismic reflection data presently available in the offshore area of the site. This figure includes the reconnaissance network of early sparker data by Marine Advisers and General Oceanographics, and several 3.5K hz transects and a few high powered, deep penetration data lines of Western Geophysical. The most significant data however, are the closely spaced Woodward-Clyde sparker transects on the shelf just south of the site and the Nekton water gun and 3.5K hz survey lines that extend the study area data south of Oceanside. Definition of the hypothesized Offshore Zone of Deformation near the site and the area onshore of the Cristianitos fault are discussed in Appendix 2.5I and in Paragraphs 2.5.1.1.3.4, 2.5.1.1.3.10, and 2.5.3.6.[27][28]

2.5.1.2.3.3 Minor Faults

Though faults are present in onshore exposures of the San Onofre Breccia, only those which offset the contact between the Breccia and the Monterey Formation can be traced for any distance. Four faults were recognized in the northwestern part of the San Onofre Mountains.[2] The faults are not exposed but can be located by the offsets in the San Onofre, Monterey contact and projected across the Breccia to known faults. The faults are subparallel to the Cristianitos fault but three of the four have a reverse sense of movement and none appear to have been active during late Pleistocene or Holocene.[2] Although some fault-like features occur along possible projections of the Cristianitos fault offshore, unfaulted reflectors in intervening profiles make correlation highly doubtful and preclude the existence of a thoroughgoing fault. Recent interpretation of high resolution data (Appendix 2.5I) confirm an earlier interpretation which indicates that there is no seaward extension of the Cristianitos fault beyond 6000 feet offshore.

Faults outside the site area, such as the Shady Canyon or Pelican Hills fault, which trend southeasterly toward the area apparently die out before reaching the site area.

Geologic investigation and detailed mapping of previously reported capable faults in Horno and Target Canyons indicate that the Horno Canyon graben was created by mechanisms of landsliding, and that features in Target Canyon are not significant to the site design; see Paragraph 2.5.1.2.5.2.

The Stuart Mesa fault is overlain by terrace sediments deposited on the 120,000-year old wave-cut bench and the closest observed approach to the site is approximately 7 miles.(2)

Fault E offshore, as described by Marine Advisers has been re-interpreted and found to be three pairs of anticlines and synclines. A complete discussion of this deformation is in Paragraph 2.5.1.1.3, Regional Structure.

2.5.1.2.4 Site Area Geologic History

The Pre-Cenozoic geologic history is represented by thick accumulations of Triassic and Jurassic marine sedimentary rocks overlain by Upper Jurassic volcanic rocks. The mid-Cretaceous emplacement of the Peninsular Ranges Batholith is the significant tectonic event that completed the conversion of this terrane to continental crust.

Younger rocks of the site area are marine and nonmarine sediments of Late Cretaceous, Tertiary, and Quaternary age. These predominantly clastic rocks are deposited in several episodes with unconformities indicating changes in the depositional regime.

Sedimentary rocks of Paleocene and Eocene age (La Jolla Group) rest upon a widespread erosional surface of low relief that was developed at the close of the Cretaceous Period. Unconformably overlying this group are middle Miocene rocks.

The San Onofre Breccia is indicative of unusual conditions of sedimentation that were present in the southern California coastal environment during the middle Miocene.

A large offshore land mass, now below sea level, is believed to have been the source of glaucophane schist characteristic of the San Onofre Breccia. The Breccia was deposited as coalescing alluvial fans in a subsiding basin.

These deposits were uplifted, partially eroded and tilted to the southwest. A transgressive sea then covered the Breccia and deposited sediments of the middle Miocene Monterey Formation.(2)

The Monterey Formation is a marine sequence which varies in lithology, both laterally and stratigraphically. It comprises a basal coarse sandstone to conglomerate, overlain by siltstone and fine-grained arkosic sandstone. The sequence was deposited within a rapidly deepening basin. Lateral variation in the lithology of the upper part of the sequence represents interfingering between submarine fan and pelagic sediments. The basal member represents prograding of beach derived material. For additional description of this formation, see Paragraph 2.5.1.2.2.4 and Figure 2.5-5.

The Capistrano Embayment area lies between the San Joaquin Hills on the west and the Santa Ana Mountains to the north and east. The Embayment developed during late Miocene and early Pliocene. Crustal extension in an east-west direction caused the formation of the Embayment. Paleontological data indicates that the basin was also being deepened at this time, which suggests that the activity of the Cristianitos fault was associated with subsidence of the Embayment. The displacement along the fault and continued crustal down-warping of the area allowed for the deposition of some 600 meters (2,000 feet) of upper Miocene and Pliocene sedimentary rocks.

The upper Miocene - lower Pliocene Capistrano Formation conformably overlies the Monterey Formation within the Capistrano Embayment to the west of the Cristianitos fault. Subsurface coring and exposures suggest that the San Mateo Formation is time correlative with the Capistrano Formation and interfingers with it.(2) The San Mateo Formation is exposed in the coastal bluffs adjacent to the site and underlies the southern part of the ridge between San Mateo and San Onofre Creeks; see Figure 2.5-9.

The Pleistocene geologic history of the San Onofre area is characterized by slow regional uplift with occasional eustatic fluctuations of sea level. In the site area, a series of wave-cut marine terraces representing former high stands of the Pacific Ocean form a series of step-like benches extending from near the coast offshore up to several hundred meters (over 1,000 feet) above sea level.(49)(50) The height of these platforms increase inland toward the topographic highlands. Little is known about the maximum elevation of the sea during the Pleistocene, but the height of the sea during Sangomon time is believed to have reached about 10 meters (30 feet) above the present sea level.(63)(64)

The same geomorphic relationships of stream terraces to marine terraces exist at the mouth of the San Onofre Creek as at the mouth of San Juan Creek at Dana Point.(65) Stream terraces are graded to former high sea level altitudes and can be traced laterally to marine terraces. Because each terrace level represents a long-term sea level stand, the relationship of stream deposits to marine deposits is complex. Sea level probably fluctuated slightly during each of these intervals, and the volume of stream material entering the sea varied; therefore, a complex interfingering in marine and nonmarine sediments is present.

Analysis of well logs indicate that San Mateo Creek and Santa Margarita River were carved to a base level below present sea level and then backfilled as base level rose in response to sea level change. A cobble and gravel horizon about 50 meters (165 feet) below present sea level at the coastline represents a lowstand about 17,000 to 20,000 years ago.(49)

A. Early late Pleistocene time is primarily represented by a sequence of marine terraces 100 to 300 meters (325 to 1250 feet) in elevation. The terrace platforms are highly dissected but are best exhibited near Dana Point, about 16 kilometers (10 miles) north of the site, and from the U.S. Immigration Station about 3 kilometers (2 miles) south of the site area to beyond Las Pulgas Canyon, about 13 kilometers (8 miles) south of the site.

B. Early late Pleistocene through Holocene time (250,000 years before present to present) is represented by a sequence of interfingering marine and stream terrace deposits. This situation is observed where San Onofre Creek joins the sea.[50][53] An exposure near San Onofre shows evidence that sea level has successively risen and fallen (transgression-regression), and tributary streams have consequently aggraded and degraded in response to the changing base level. This fluctuation resulted in deposition of stage 4 gravels and development of younger stage 3 paleosol.[53]

C. The wave-cut platform presently developing has been progressively encroaching on the lowest terrace platform, Terrace 1, Reference 49, exposing the marine/nonmarine relationships. At the mouth of San Onofre Creek, the sea cliff now exhibits marine and nonmarine interlayers overlaying the channeled San Mateo Formation. The stream terrace deposits pinch out laterally (Figure 2 of Reference 50) as the channel deposits grade out onto the wave-cut platform. Beyond this gradational contact, the San Mateo Formation, as seen in the bluff, is no longer channeled but is uniformly beveled by the wave-cut platform. The wave-cut platform slopes gently toward the sea, and is mantled by a thin 0.3 to a 1.6-meter (1 to 5-foot) veneer of bouldery beach gravel. Overlying the gravel is a variable thickness of marine sediment and continental cover.[50] (Figures 2.5-53 through 2.5-55 are aerial photos which show many of these relationships.)

D. Receding seas, during the Pleistocene, cut at least two marine terraces in the area presently offshore. These are related to stage 3, 35,000 to 40,000 years ago and stage 5a, about 80,000 years ago. When the sea level rose, the terraces were then buried by at least two ages of sediments. The older is 11,000 to 13,000 years old and the younger sediments are 8,500 to 9,500 years old. The old sea floor and overlying young sediments lay across the folded bedrock without deformation (Appendix 2.5I).

E. Regional uplift rates between Target Canyon and Dana Point increase northward from about 6 centimeters to 26 centimeters/1000 years. This indicates up-to-the-northwest tilt of the coast across the Capistrano Embayment. Seaward tilt of about 1 $^{\circ}$ in Target Canyon is the same slope as the present offshore platform.

2.5.1.2.5 Site-Related Geologic Items

2.5.1.2.5.1 <u>Geologic Features Observed in the Excavations</u>

Five types of geologic features observed in the excavations for San Onofre Generating Station Units 2 and 3 were reported earlier:[58][66][67]

- Joint-like features strike approximately N60E (Feature C) dipping 5 $^{\circ}$ to 19 $^{\circ}$ N and N50W (Feature D) dipping 15 $^{\circ}$ to 20 $^{\circ}$ N; movement on Feature C cannot be demonstrated; Feature D demonstrates minor reverse movement.

- Slump structures, graded bedding and other structural features characteristic of the formation, and lithification of saturated and unconsolidated sediments which were rapidly deposited.

- Claystone lenses and fragments set within the San Mateo sandstone as inclusions.

- Color banding in the San Mateo Formation.

Of the five types of geologic features, Type A, B, C and D Features were of significant interest. The A and B Features appear as thin, white, resistant seams forming sinuous zones up to several centimeters wide. Amount and sense of shear movement on these features were up to 10 centimeters (4 inches) left-lateral for Type A, and a similar amount of right-lateral for Type B; no vertical movement could be measured. As grading continued, two other geologic features (Types C and D) were exposed in the deeper parts of the excavated area of Units 2 and 3.

Feature C consists of a sinuous zone of 0.4 to 0.8-centimeter (1/8 to 1/4-inch) thick, white resistant ribs that generally appear very similar to Type A and B Features. In contrast to Feature C, Feature D consists of individual hairline, planar fractures in the San Mateo Formation. No clear examples of displacement have been recognized on Feature C, but a questionable offset of a thin silty clay seam suggests about 6 centimeters (2-1/2 inches) of apparent right-lateral displacement. Apparent displacements along Feature D are consistently reverse, with amounts ranging from less than 0.8 to 7 centimeters (1/4 to 2-3/4 inches).

It is concluded that because of the relationship of these features to the overlying terrace/bedrock contact, (they do not displace this contact or the overlying deposits) these features have been demonstrated not to be capable in terms of NRC criteria and are not considered to be significant to the safety of the San Onofre site.[58][66][67]

The three other geologic features observed at the site during excavation are nontectonic depositional features. The graded bedding and slump type structures seen in the San Mateo Formation are indicative of rapid deposition. The claystone lenses and fragmentary blocks found as inclusions in the San Mateo Formation imply a high energy depositional environment that could rip up adjacent deposits and incorporate these fragments as lenses or blocks.

Banding is very common in the San Mateo Formation, however, it does not reflect any mineralization, increased or decreased resistance to brushing, change in grain size, or textural discontinuity. The banding appears to be the result of leaching or oxidation of the sand grains, probably by percolating groundwater.

Because of the limited areal extent and nontectonic origin of these features it is concluded that they are not significant to the safety of the plant site.

Geologic monitoring during excavation, a period extending from June 1974 through February 1976, was performed by Fugro, Inc. The results are presented in References 58, 66, and 67.

2.5.1.2.5.2 Landslides

Landslides are common throughout the area southwest of the Cristianitos fault, and east of the San Onofre Mountain ridge line.(2)(54) The work done by Blanc and Cleveland on natural slope stability in the San Clemente area(54) is the most comprehensive study of landslides in the site area to date. Based on their studies, the San Mateo Formation on which the plant site is situated is shown to be one of the most stable and is the least susceptible to landslides. This conclusion is based, in part, on field mapping which shows no landslides at or near the site in the San Mateo Formation.(2)(54)(57) The largest landslide close to the site is in the Monterey Formation some 1500 meters (5000 feet) southeast along the coast. This landslide exposes the Cristianitos fault. A detailed study of this landslide and the surrounding area was conducted by Ehlig in 1977.(2) This study includes cross-sections through the landslide. Detailed geologic investigations were performed on several area slides. A landslide 3 miles south of the plant site was mapped, hand-dug trenches were excavated to expose the slide plane, and samples were taken for paleontological examination. This slide was found to be in Monterey Formation.(2)

Investigation of the shears exposed in the southeasternmost landslide mass of the sea cliff slide complex, 3.9 miles southeast of the station, found that all observed evidence supported failure by landsliding and slumping.(2)

Detailed mapping of the Horno Canyon Landslide indicate that the graben was created by mechanisms landsliding. This area has undergone multiple episodes of sliding.(2)

The origin of the offset bedrock/marine terrace contacts seen in Target Canyon are believed to be nontectonic, however, if they are assumed to be of tectonic origin they would not be significant to the seismic design of the plant because of their length, distance from the site, and amount of displacement.(2) Additional landslide studies are discussed in Reference 2.

Investigation of the offset features the marine terrace deposits on Trail Five were also found to be the results of landsliding (Appendix 2.5I).

Landsliding is a significant feature along the bluffs for some 8 kilometers (5 miles) south of the plant. The slides vary in age from recent to over 125,000 years old and appear to have been the result of wave action undercutting seaward-dipping bedding planes of the Monterey Formation.

Detailed analysis of the San Mateo Sandstone, Paragraph 2.5.4.2, demonstrates landsliding is not significant to the site stability.

2.5.1.2.5.3 Subsidence

A study was made of settlement records of United States Coast and Geodetic Survey benchmarks along the coastline between San Clemente and Oceanside to assess possible areal subsidence or uplift; see Figure 2.5-16. Based on this study of recorded benchmark movement, it is believed that subsidence in the site vicinity should be less than 2.5 centimeters (1 inch) during the plant life. This amount of potential movement should not adversely affect the site. Subsidence rates along this part of the coast are discussed in Paragraph 2.5.1.1.7.

Subsidence due to groundwater withdrawal is not considered to be significant to the site since the groundwater table is maintained at a constant elevation by the United States Marine Corps. This is discussed in Subsection 2.4.13.

2.5.1.2.5.4 Erosion

A detailed study was conducted by Woodward-McNeill and Associates, consultants to the Applicants, to define the active erosional processes at San Onofre.[68] The effects of past erosion and recommendations for erosion control regarding short- and long-term stability of facilities were outlined. Existing slopes at the North IndustrailArea (NIA) demonstrate the long-term stability of the exposed material.

2.5.1.2.5.5 Fluid and Mineral Extraction

The only mineral extraction within 8 kilometers (5 miles) of the site is noncommercial sand and gravel quarrying maintained by the U.S. Marine Corps, and this activity will have no bearing on plant stability. One quarry is 2.4 kilometers (1-1/2 miles) distant from the site. Quarrying of San Mateo Sandstone has been done at locations in the vicinity of construction, but are remote enough to have no influence on the facility.

Less than 10,000 barrels of petroleum were extracted prior to 1960 from the San Clemente and San Juan Capistrano oil fields, which are no longer active. The extraction has caused no apparent undesirable disequilibrium in surrounding rock units or structures. Maps showing the areas of mineral and hydrocarbon extraction are not included since very limited areas are involved.

2.5.1.2.5.6 Liquefaction

Liquefaction is discussed in Paragraph 2.5.4.8.

2.5.1.2.5.7 Photolineament Analysis

A study of high altitude NASA U-2 color infrared aerial photography was conducted, of the area from San Onofre north to the vicinity of El Toro, this area is bounded by 33 º 16' to 33 º 38'N latitude and 117 º 23' to 117 º 44'W longitude. Lineaments disclosed by the photographic interpretation were then field checked.

The criteria used in selection of the lineaments for study in the field included length, and strength of expression. This study shows that the lineaments expressed in the photographs are caused by such features as faults, fracture zones, bedding, formation contacts, landslides, scarps, rock cleavage, foliations, fences, trails, firebreaks, changes in vegetation, resistant ridges, aligned valleys and ridges, and linear breaks in slope.

Of over 100 lineaments investigated in the field, only 10 were found to correspond with previously unmapped faults having probable traces greater than 1000 feet. Many of these faults are extensions of members of previously mapped fault zones. For these reasons, it has been concluded that no major active fault zones exist unrecognized within the study area.

2.5.1.2.5.8 Additional Geologic Items

Other geologic items such as cavernous or karst terranes, and collapse structures are not present at the site. Unrelieved residual stress in bedrock is not significant to the site as discussed in Subsection 2.5.4.

2.5.1.2.6 Dynamic Behavior of the Site During Prior Earthquakes

The response of the San Onofre site to seismic activity has been monitored since August 1966 by strong motion accelerographs owned and maintained by the applicants. The instruments have been set to trigger at an acceleration of 0.01g. Since their installation, the accelerographs have recorded 2 of 10 earthquakes: the 1968 Borrego earthquake and the 1971 San Fernando earthquake. The October 1979 Imperial Valley earthquake and aftershock, as were several others, was just sufficient to trigger the instruments, but not strong enough to provide a meaningful record. The accelerographs of the 1968 and 1971 events are presented on Figures 2.5-17 and 2.5-18, respectively. No damage to structures or earth slopes or unusually high structural response were noted at the site during these events.

2.5.1.2.7 Groundwater Conditions

Site groundwater conditions are described in Subsection 2.4.13.

2.5.2 VIBRATORY GROUND MOTION

2.5.2.1 Seismicity

2.5.2.1.1 Earthquake History

The seismic record in the southern California region extends back to the 18th century when tremors were noted in journals of Spanish explorers. Until the early part of the century, reports of earthquakes that were felt and caused damage were the only records. Few epicenters were reliably recorded instrumentally prior to 1932; however, from 1932 to the present, an essentially complete listing of instrumentally recorded epicenters is available and their locations are considerably more accurate since 1961 (see Paragraph 2.5.2.3.2).

Table 2.5-1 provides a listing of all noninstrumental earthquakes that had reported Modified Mercalli Scale intensities of IV or greater and that could have reasonably occurred within a 320-kilometer (200-mile) radius of the San Onofre site. These events were compiled from a number of earthquake catalogs which are referenced in the table. The approximate locations of these noninstrumented events are shown on Figure 2.5-19. Since more detailed data is not available, the locations assigned to these events are usually only to the nearest half degree, thereby biasing the locations toward nodes. Furthermore, the nature of felt reports tends to bias locations toward population centers.

Table 2.5-2 lists earthquake data from the California Institute of Technology catalog for the period between January 1932 through June 1980 (including refinement of some nearby epicentral locations) for all earthquakes within 320 kilometers (200 miles) of the site with a Richter magnitude of 5.0 and greater (M5+). Magnitudes of 3.0 to 4.9 are not included in this table because they would have no impact on the assessment of the design basis earthquake (DBE) at the site. (DBE is considered synonymous with SSE in this report.) Recorded events within the 320-kilometer (200-mile) radius, of magnitude 5.0 and greater, 4.0 to 4.9, and 3.0 to 3.9 for the same period are shown on Figures 2.5-20, 2.5-21 and 2.5-22, respectively.

Events lying outside the 320-kilometer (200-mile) radius were not included in the listing since they would have no impact on the assessment of the DBE. Structures such as the San Andreas or Whittier-Elsinore faults or the hypothesized Offshore Zone of Deformation are of more significance to the site than events lying outside the 320-kilometer (200-mile) radius.

Information such as seismic moment, source mechanism, source dimension, source rise-time, rupture velocity, total dislocation and fractional stress drop is not included on this table since it is not generally available for the earthquakes.

Table 2.5-3 provides a listing of noninstrumental earthquakes that may have occurred within an 80-kilometer (50-mile) radius of the site. Instrumented events greater than magnitude 3.0 within 80 kilometers (50 miles) for the period of January 1932 through June 1980, are listed in Table 2.5-4 and are shown on Figure 2.5-23.

2.5.2.1.2 Strong Motion Data

The number of strong motion instruments has been steadily increasing in the region since 1932. Table 2.5-5 lists the earthquakes within the 320-kilometer (200-mile) radius of the site for which peak ground accelerations were recorded. Discussion of these data and the effect of their use in estimates of peak ground acceleration and on design response spectra at the site is presented in Appendix 2.5T. The lower limit of acceleration is taken as 0.01g through 1971 and 0.05g thereafter. This change in trigger level was due to a change in the type of seismic trigger used.

2.5.2.1.3 Earthquake Induced Geologic Failure

Earthquakes that may have induced geologic failure within a 320-kilometer (200-mile) radius of the site are listed in Table 2.5-6. Geologic failure such as liquefaction, lurching, landsliding etc., are not specifically named for the majority of events described in available earthquake catalogs; however, where such failures may be inferred from the description, the associated event is included in the table. The maximum recorded level of strong motion listed for some events in the table does not necessarily apply to the area where geologic failure occurred. Only isolated cases exist where strong motion was recorded near a geologic failure.

2.5.2.2 Geologic Structures and Tectonic Activity

2.5.2.2.1 General

The present tectonic environment within a 320 kilometer (200-mile) radius of the San Onofre site is dominated by interaction between the Pacific and North American crustal plates. The Pacific Plate is moving northwestward at about 6 centimeters/year relative to North America.[16] The main plate boundary extends northward from the Gulf of California and Salton Trough where it is marked by a complex system of small spreading centers interconnected by right-slip transform faults. From the Salton Trough northwestward to Cape Mendocino, most of the interplate motion is taken up by right-slip on the San Andreas fault.[17] Smaller faults and a reduced order of seismicity are associated with structural adjustment away from the plate boundary.

Table 2.5-1
LISTING OF NONINSTRUMENTED EARTHQUAKES REPORTED
WITHIN 320 KILOMETERS (200 MILES) OF THE SITE[a] (Sheet 1 of 30)

No.	Source[b]	Date (GMT)			Time (GMT)	Approximate Location[c]		Maximum Intensity[d]	Comments[e]
		(day)	(mo)	(yr)	(hr-min)	(lat)	(long.)		
1	1	11	04	1769	--	(32	117)	?	Questionable
2	1, 2	28	07	1769	2100	34	118	X	--
3	1, 2	27	12	1775	0100	(33.5	116)	(VII)	--
4	2	--	--	1790	--	(36.5	118)	(XI)	Questionable, Mag=7, 8, Di
5	2	22	10	1800	2130	(33	117)	VIII	Mag=7; Dam
6	2	--	--	1800	--	34.5	119.5	VII	Dam
7	1, 2	25	03	1803	--	32.5	117	VIII	Dam
8	1, 2	25	03	1806	0800	34.5	19.5	VIII	Dam
9	1, 2	08	12	1812	1500	(33	117)	IX	Dam, Mag=7
10	1, 2	21	12	1812	1900	34	120	XI	Dam, Ts, Mag=7
11	1, 2	23	09	1827	--	34	118	VII	--
12	1, 2	23	06	1843	2330	(33	117)	IX	--
13	1, 2	26	10	1852	--	(34	119)	X	Mag=8 (?)
14	1, 2	09	11	1852	--	33	114	IX	Di, Liq, Lu

[a] See last page of table for notes.

Table 2.5-1
LISTING OF NONINSTRUMENTED EARTHQUAKES REPORTED
WITHIN 320 KILOMETERS (200 MILES) OF THE SITE[a] (Sheet 2 of 30)

No.	Source[b]	Date (GMT)			Time (GMT)	Approximate Location[c]		Maximum Intensity[d]	Comments[e]
		(day)	(mo)	(yr)	(hr-min)	(lat)	(long.)		
15	1, 2	27	11	1852	--	34.5	119	X	Di
16	2	--	12	1853	--	33	115	?	Geysers near Yuma (Liq)
17	1	31	05	1854	1310	34.5	120	VI	Ts
18	1, 2	25	06	1855	2200	34.5	120	V	--
19	1	07	04	1856	0730	34	118	V	--
20	1	03	05	1856	0810	34	18	V	--
21	1, 2	21	09	1856	0730	33	116.5	VIII	Di, Dam
22	1, 4	09	01	1857	1600	35	119	X+	Di, Dam, Se, Lu, Liq Mag=8+
23	1	17	01	1857	0100	(34	118)	V	--
24	1	20	01	1857	1130	(35	118)	VI	--
25	1	15	03	1857	0300	(34.5	120)	V	--
26	1	04	15	1857	0600	(34	118)	V	--

Table 2.5-1
LISTING OF NONINSTRUMENTED EARTHQUAKES REPORTED
WITHIN 320 KILOMETERS (200 MILES) OF THE SITE[(a)] (Sheet 3 of 30)

No.	Source[(b)]	Date (GMT)			Time (GMT)	Approximate Location[(c)]		Maximum Intensity[(d)]	Comments[(e)]
		(day)	(mo)	(yr)	(hr-min)	(lat)	(long.)		
27	1	23	05	1857	--	(35	119)	VI	--
28	1	14	06	1857	--	(32	115)	VI	--
29	1	29	08	1857	--	(35	118)	VI	--
30	1	02	09	1858	--	(34.5	120)	V	--
31	1	01	12	1859	2210	(34	117.5)	V	--
32	1	26	03	1860	--	(34	118)	VI	--
33	1	27	03	1860	--	(34	118)	VI	--
34	1,2	27	05	1862	--	33	117.5	VI	--
35	1	25	01	1863	2220	(32.5	117)	VI	--
36	1	15	04	1865	0840	(33	117)	VI	--
37	1,2	--	05	1868	--	33.5	115.5	X	Di, Mag=7
38	1	07	10	1869	--	(34	117.5)	V	--
39	1	04	01	1870	0700	(35.5	119)	V	--

Table 2.5-1
LISTING OF NONINSTRUMENTED EARTHQUAKES REPORTED WITHIN 320 KILOMETERS (200 MILES) OF THE SITE[(a)] (Sheet 4 of 30)

No.	Source[(b)]	Date (GMT)			Time (GMT)	Approximate Location[(c)]		Maximum Intensity[(d)]	Comments[(e)]
		(day)	(mo)	(yr)	(hr-min)	(lat)	(long.)		
40	1	--	--	1871	--	(35.5	119)	X	Mag=7
41	1	12	10	1873	0915	(32.5	119)	V	--
42	1	02	11	1875	--	(33	115)	VI	--
43	1, 2	11	06	1877	--	33	115	?	vol (?)
44	1, 2	Summer		1878	--	34	118.5	VIII	Dam
45	1	21	03	1880	1425	34	118	V	--
46	1	25	03	1880	1030	34	117	IV	--
47	1	12	04	1880	1240	(34	17.5)	V	--
48	1	19	12	1880	1140	(33	118)	V	--
49	1	22	12	1880	0700	(32.5	116.5)	V	--
50	1	28	12	1880	0700	(33.5	117)	V	--
51	1	14	05	1881	2109	(32.5	116.5)	V	--
52	1	30	06	1881	1600	(32.5	116.5)	V	--

Table 2.5-1
LISTING OF NONINSTRUMENTED EARTHQUAKES REPORTED WITHIN 320 KILOMETERS (200 MILES) OF THE SITE[a] (Sheet 5 of 30)

No.	Source[b]	Date (GMT)			Time (GMT)	Approximate Location[c]		Maximum Intensity[d]	Comments[e]
		(day)	(mo)	(yr)	(hr-min)	(lat)	(long.)		
53	1	02	10	1881	1700	(32.5	116.5)	V	--
54	1	03	02	1882	1040	(34	117)	IV	--
55	1	30	09	1882	1857	(32.5	16.5)	V	--
56	1	08	10	1882	1000	(32.5	117)	V	--
57	1, 2	05	09	1882	1230	34	119	VI	--
58	1	13	09	1883	2230	(34.5	120)	IV	--
59	1	07	04	1885	1030	(35.5	119)	IV	--
60	1	09	07	1885	0920	(34.5	120)	V	--
61	1	07	03	1888	1554	(34	118)	VI	--
62	1	09	04	1888	1550	(34	117.5)	IV	--
63	1	07	02	1889	0520	(34	117.5)	VI	--
64	1	17	05	1889	0515	(34	118)	V	--
65	1, 2	09	02	1890	1206	34	117	VIII	Dam

Table 2.5-1
LISTING OF NONINSTRUMENTED EARTHQUAKES REPORTED
WITHIN 320 KILOMETERS (200 MILES) OF THE SITE[a] (Sheet 6 of 30)

No.	Source[b]	Date (GMT)			Time (GMT)	Approximate Location[c]		Maximum Intensity[d]	Comments[e]
		(day)	(mo)	(yr)	(hr-min)	(lat)	(long.)		
66	1, 2	24	02	1892	0720	31.5	116.5	X	Dam, Mag=7.5
67	1	24	02	1892	1000	(32	115)	VII	Dam
68	1	28	05	1892	1115	(34	118)	VI	--
69	1, 2	04	04	1893	1940	34.5	118.5	IX	Dam, Di, Ls, Lu
70	1, 2	19	05	1893	2435	34	119	VII	--
71	1	01	06	1893	1200	(34.5	120)	VII	--
72	1, 2	30	07	1894	0512	35	118	VII	Dam
73	1, 2	23	10	1894	2303	33	117	VIII	Dam, Ls
74	1, 2	22	07	1899	2032	34.5	117.5	VIII	Di, Dam, Mag=6.5
75	1, 2	25	12	1899	1225	33.5	116.5	X+	Di, Dam, Mag=6.8, Lu
76	1	27	12	1901	1100	(34	117.5)	VI	--
77	1	08	07	1902	0945	(33.5	118)	V	--
78	1, 2	28	07	1902	0657	34.5	120.5	IX	Di, Dam

Table 2.5-1
LISTING OF NONINSTRUMENTED EARTHQUAKES REPORTED
WITHIN 320 KILOMETERS (200 MILES) OF THE SITE[a] (Sheet 7 of 30)

No.	Source[b]	Date (GMT)			Time (GMT)	Approximate Location[c]		Maximum Intensity[d]	Comments[e]
		(day)	(mo)	(yr)	(hr-min)	(lat)	(long.)		
79	1, 2	01	08	1902	0320	34.5	120.5	IX	Di, Dam, Ls, Lu
80	1	08	07	1902	0945	(33.5	118)	V	--
81	1, 2	2	12	1902	--	34.5	120.5	VII	Dam
82	1	08	01	1903	0030	(35.5	119)	VI	--
83	1, 2	24	01	1903	0530	31.5	115.5	VI	Dam
84	1, 2	25	12	1903	1745	34	118	VII	Dam--
85	1	01	05	1904	1830	(34	119)	IV	--
86	1	19	03	1905	0440	(35	119.5)	V	
87	1	16	07	1905	0741	(34	117.5)	VII	Dam
88	1	03	10	1905	0540	(34	18)	VII	Dam
89	1, 2	23	12	1905	2223	34.5	119	VII	Dam
90	2	03	02	1906	2025	32	115	VIII	--
91	2	19	04	1906	0030	33	115	VIII	Di, Dam, Ls

Table 2.5-1
LISTING OF NONINSTRUMENTED EARTHQUAKES REPORTED
WITHIN 320 KILOMETERS (200 MILES) OF THE SITE[a] (Sheet 8 of 30)

No.	Source[b]	Date (GMT)			Time (GMT)	Approximate Location[c]		Maximum Intensity[d]	Comments[e]
		(day)	(mo)	(yr)	(hr-min)	(lat)	(long.)		
92	1	21	05	1907	0652	(34	117.5)	VI	--
93	1, 2	20	09	1907	0154	34	117	VIII	Di, Dam, Ls
94	1	03	07	1908	1255	(34	118)	IV	--
95	1	04	09	1908	--	(35.5	119)	VI	--
96	1, 2	04	11	1908	0837	36	117	VIII	Mag=6.5
97	1	16	07	1909	1028	(34.5	120)	IV	--
98	1	10	04	1910	0757	(33.5	117.5)	V	--
99	1	12	05	1910	0620	(33.5	117.5)	V	--
100	1, 2	15	05	1910	1547	33.5	117.5	VIII	Di, Dam, Mag=6+,(**)
101	1	27	12	1910	1715	(33	115.5)	VI	--
102	1	29	03	1911	0425	(34	120.5)	VI	--
103	1	11	08	1911	1820	(33.5	117)	VI	Dam
104	1	21	08	1911	2141	(34	117)	IV	--

Table 2.5-1
LISTING OF NONINSTRUMENTED EARTHQUAKES REPORTED
WITHIN 320 KILOMETERS (200 MILES) OF THE SITE[a] (Sheet 9 of 30)

No.	Source[b]	Date (GMT)			Time (GMT)	Approximate Location[c]		Maximum Intensity[d]	Comments[e]
		(day)	(mo)	(yr)	(hr-min)	(lat)	(long.)		
105	1	18	10	1911	1910	(32.5	117)	IV	--
106	1	22	11	1911	0257	(34	117.5)	IV	
107	1	23	12	1911	0942	(34	118)	IV	--
108	1, 2	14	12	1912	--	34	119	VII	Dam--
109	1	13	04	1913	1045	(34	117.5)	V	--
110	1	19	07	1913	0010	32.5	115.5	IV	Lu
111	1	21	10	1913	0938	(34	118)	IV	--
112	1	16	06	1914	1052	(34.5	119)	IV	--
113	1	08	11	1914	1140	(34.5	118.5)	V	--
114	1	29	12	1914	1000	(33.5	117)	V	--
115	1, 2	12	01	1915	0359	34.5	120	VII	Dam, Ls, Lu
116	1	12	01	1915	1015	(33.5	117)	IV	--
117	1	16	02	1915	1330	(33	116.5)	V	--

Table 2.5-1
LISTING OF NONINSTRUMENTED EARTHQUAKES REPORTED
WITHIN 320 KILOMETERS (200 MILES) OF THE SITE[a] (Sheet 10 of 30)

No.	Source[b]	Date (GMT)			Time (GMT)	Approximate Location[c]		Maximum Intensity[d]	Comments[e]
		(day)	(mo)	(yr)	(hr-min)	(lat)	(long.)		
118	1	17	02	1915	1100	(33	115.5)	IV	--
119	1	01	03	1915	1715	(33	115)	IV	--
120	1	04	03	1915	1250	(33	16)	V	--
121	1	12	03	1915	1000	(33.5	116.5)	IV	--
122	1	04	03	1915	2000	(33	117)	IV	--
123	1	28	04	1915	0310	(33	115.5)	V	--
124	1	30	04	1915	1020	(33	116.5)	V	--
125	1	11	05	1915	1145	(33	116.5)	V	--
126	1	29	05	1915	0646	(35	118.5)	V+	--
127	1	18	06	1915	1505	(33.5	118.5)	V	--
128	1, 2	23	06	1915	0359	32.8	115.5	IX	Di, Dam Mag=7.5, Lu, Liq, Ls
129	1	03	07	1915	2345	(33	115.5)	VI	--
130	1	18	08	1915	2040	(33	115.5)	V	--

Table 2.5-1
LISTING OF NONINSTRUMENTED EARTHQUAKES REPORTED
WITHIN 320 KILOMETERS (200 MILES) OF THE SITE[a] (Sheet 11 of 30)

No.	Source[b]	Date (GMT)			Time (GMT)	Approximate Location[c]		Maximum Intensity[d]	Comments[e]
		(day)	(mo)	(yr)	(hr-min)	(lat)	(long.)		
131	1	06	09	1915	0220	(33	116.5)	IV	--
132	1	08	09	1915	2342	(32.5	117)	V	--
133	1	10	10	1915	0516	(34	117)	V	--
134	1	01	12	1915	1405	(34	117.5)	V	--
135	1	11	01	1916	0515	(33.5	116.5)	IV	--
136	1	25	02	1916	2330	(33.5	116.5)	IV	--
137	1	12	03	1916	0315	(33	115.5)	IV	--
138	1	02	05	1916	1432	(34	118)	IV	--
139	1	16	07	1916	1150	(35	117)	V	--
140	1	16	07	1916	1230	(35	117)	V	--
141	1	29	09	1916	0211	(33.5	116.5)	V	--
142	1	30	09	1916	0425	(33.5	116)	V	--
143	1	22	10	1916	0254	(34.9	118.9)	VI	--

Table 2.5-1
LISTING OF NONINSTRUMENTED EARTHQUAKES REPORTED
WITHIN 320 KILOMETERS (200 MILES) OF THE SITE[a] (Sheet 12 of 30)

No.	Source[b]	Date (GMT)			Time (GMT)	Approximate Location[c]		Maximum Intensity[d]	Comments[e]
		(day)	(mo)	(yr)	(hr-min)	(lat)	(long.)		
144	1	23	10	1916	0520	(33	115.5)	IV	--
145	1	01	11	1916	0555	(32.5	115.5)	V	--
146	1	26	11	1916	1705	(33.5	116.5)	V	--
147	1	07	12	1916	1855	(32.5	115.5)	V	--
148	1	07	12	1916	2045	(32.5	115.5)	V	--
149	1	13	02	1917	1305	(34	118)	VI	--
150	1	13	04	1917	0359	(34	120)	VI	--
151	1	21	04	1917	0659	(34	120)	V	--
152	1	19	05	1917	0635	(34	118)	V	--
153	1	20	05	1917	0945	(34	118)	V	--
154	1	27	05	1917	0930	(33	115.5)	V	--
155	1, 2	28	05	1917	0606	33	115.5	VIII	Dam
156	1	28	05	1917	1017	(33	116.5)	V	--

Table 2.5-1
LISTING OF NONINSTRUMENTED EARTHQUAKES REPORTED
WITHIN 320 KILOMETERS (200 MILES) OF THE SITE[a] (Sheet 13 of 30)

No.	Source[b]	Date (GMT)			Time (GMT)	Approximate Location[c]		Maximum Intensity[d]	Comments[e]
		(day)	(mo)	(yr)	(hr-min)	(lat)	(long.)		
157	1	30	05	1917	0210	(33	115.5)	VI	--
158	1	31	05	1917	0435	(33.5	116.5)	V	--
159	1	02	06	1917	0435	(33.5	116.5)	V	--
160	1	08	06	1917	0031	(32.5	116.5)	IV	--
161	1	11	06	1917	0354	(33	116.5)	V	--
162	1	18	06	1917	1600	(32.5	115.5)	V	--
163	1	18	06	1917	0955	(32.5	115.5)	IV	--
164	1	22	06	1917	0405	(33	116.5)	IV	--
165	1	25	06	1917	0800	(34	118)	IV	--
166	1	26	06	1917	2315	(34	118)	IV	--
167	1	29	06	1917	0550	(34	118)	IV	--
168	1	30	06	1917	0000	(34	118)	IV	--
169	1	30	06	1917	2338	(34	118)	IV	--

Table 2.5-1
LISTING OF NONINSTRUMENTED EARTHQUAKES REPORTED
WITHIN 320 KILOMETERS (200 MILES) OF THE SITE[a] (Sheet 14 of 30)

No.	Source[b]	Date (GMT)			Time (GMT)	Approximate Location[c]		Maximum Intensity[d]	Comments[e]
		(day)	(mo)	(yr)	(hr-min)	(lat)	(long.)		
170	1	15	07	1917	1905	(34.5	118.5)	IV	--
171	1	17	07	1917	2315	(34	118)	IV	--
172	1	26	07	1917	2031	(35	120.5)	V	--
173	1	02	08	1917	0420	(33.5	116.5)	IV	--
174	1	12	08	1917	1100	(33.5	116.5)	V	--
175	1	19	08	1917	0710	(33	116.5)	V	--
176	1	10	10	1917	2350	(33	115.5)	IV	--
177	1	08	12	1917	0945	(32.5	115.5)	V	--
178	1	20	12	1917	0825	(32.5	115.5)	V	--
179	1	05	03	1918	1106	(33.5	116.5)	IV	--
180	1	06	03	1918	1615	(33.5	116.5)	IV	--
181	1	06	03	1918	1820	(34	118.5)	VI	--
182	1	08	03	1918	1230	(34	118.5)	V	--

Table 2.5-1
LISTING OF NONINSTRUMENTED EARTHQUAKES REPORTED
WITHIN 320 KILOMETERS (200 MILES) OF THE SITE[(a)] (Sheet 15 of 30)

No.	Source[(b)]	Date (GMT)			Time (GMT)	Approximate Location[(c)]		Maximum Intensity[(d)]	Comments[(e)]
		(day)	(mo)	(yr)	(hr-min)	(lat)	(long.)		
183	1	21	03	1918	2325	(32.5	117)	V	--
184	1	30	03	1918	1605	(33.5	116.5)	VI	--
185	1, 2	22	04	1918	2315	(34	117.5)	VII	Dam
186	1	23	04	1918	0503	(32.5	115.5)	IV	--
187	1	23	04	1918	0700	(33.5	117)	IV	--
188	1	23	04	1918	1415	(33.5	117)	V	--
189	1	25	04	1918	0323	(33.5	117)	IV	--
190	1	26	40	1918	1730	(33.5	116.5)	IV	--
191	1	27	04	1918	1000	(33.5	116.5)	IV	--
192	1	28	04	1918	2330	(33	115.5)	IV	--
193	1	29	04	1918	0200	(33.5	117)	V	--
194	1, 2	01	05	1918	0432	32.5	115.5	VII	Dam
195	1	01	05	1918	0510	(32.5	115.5)	IV	--

Table 2.5-1
LISTING OF NONINSTRUMENTED EARTHQUAKES REPORTED
WITHIN 320 KILOMETERS (200 MILES) OF THE SITE[a] (Sheet 16 of 30)

No.	Source[b]	Date (GMT)			Time (GMT)	Approximate Location[c]		Maximum Intensity[d]	Comments[e]
		(day)	(mo)	(yr)	(hr-min)	(lat)	(long.)		
196	1	02	05	1918	1251	(32.5	115.5)	V	--
197	1	03	05	1918	0425	(32.5	116.5)	V	--
198	1	11	05	1918	2005	(33	115.5)	VI	--
199	1	16	05	1918	1745	(33.5	117)	IV	--
200	1	28	05	1918	1230	(33.5	117)	IV	--
201	1, 2	06	06	1918	2232	33.5	117	VI	Dam, Lu, Ls
202	1	12	06	1918	2047	(32.5	115.5)	IV	--
203	1	14	06	1918	1024	(33.5	117)	V	--
204	1	22	06	1918	0557	(32.5	117)	V	--
205	1	08	07	1918	0125	(33.5	117)	IV	--
206	1	24	08	1918	1629	(32.5	115.5)	IV	--
207	1	07	09	1918	0956	(32.5	115.5)	IV	--
208	1	14	10	1918	1205	(32.5	115.5)	V	--

Table 2.5-1
LISTING OF NONINSTRUMENTED EARTHQUAKES REPORTED
WITHIN 320 KILOMETERS (200 MILES) OF THE SITE[(a)] (Sheet 17 of 30)

No.	Source[(b)]	Date (GMT)			Time (GMT)	Approximate Location[(c)]		Maximum Intensity[(d)]	Comments[(e)]
		(day)	(mo)	(yr)	(hr-min)	(lat)	(long.)		
209	1	08	11	1918	1824	(32.5	115.5)	IV	--
210	1, 2	19	11	1918	2018	34	118.5	VII	Dam
211	1	14	12	1918	1000	(34	120)	IV	--
212	1	08	01	1919	0407	(33.5	117)	IV	--
213	1	25	01	1919	2229	(35	118)	V	--
214	1, 2	16	02	1919	1557	35	119	VII	Dam, Ls
215	1	19	02	1919	0345	(32.5	117)	IV	--
216	1	19	02	1919	0458	(33	115.5)	IV	--
217	1	19	02	1919	1130	(33	115.5)	IV	--
218	1	14	03	1919	0753	(32.5	115.5)	IV	--
219	1	15	03	1919	1030	(32.5	115.5)	IV	--
220	1	21	03	1919	1100	(34.5	115.5)	IV	--
221	1	27	03	1919	0750	(33.5	117)	IV	--

Table 2.5-1
LISTING OF NONINSTRUMENTED EARTHQUAKES REPORTED
WITHIN 320 KILOMETERS (200 MILES) OF THE SITE[a] (Sheet 18 of 30)

No.	Source[b]	Date (GMT)			Time (GMT)	Approximate Location[c]		Maximum Intensity[d]	Comments[e]
		(day)	(mo)	(yr)	(hr-min)	(lat)	(long.)		
222	1	24	06	1919	2112	(32.5	117)	IV	--
223	1	26	09	1919	1457	(34.5	120)	IV	--
224	1	30	09	1919	0409	(33	115)	V	--
225	1, 2	30	09	1919	0737	32.5	115	V	Lu, Ls
226	1	30	09	1919	0838	(32.5	115)	VII	--
227	1	30	09	1919	1000	(33	115)	IV	--
228	1, 2	01	10	1919	1307	32.5	115	IV	--
229	1	01	10	1919	1930	(33	115)	VI	--
230	1	01	10	1919	2146	(32.5	115.5)	V	--
231	1, 2	01	01	1920	0235	33	117	VII	Dam
232	1	09	02	1920	1130	(33	116.5)	IV	--
233	1	22	02	1920	1610	(34	118.5)	VI	Dam
234	1	04	03	1920	0325	(34	118.5)	IV	--

Table 2.5-1
LISTING OF NONINSTRUMENTED EARTHQUAKES REPORTED
WITHIN 320 KILOMETERS (200 MILES) OF THE SITE[a] (Sheet 19 of 30)

No.	Source[b]	Date (GMT)			Time (GMT)	Approximate Location[c]		Maximum Intensity[d]	Comments[e]
		(day)	(mo)	(yr)	(hr-min)	(lat)	(long.)		
235	1	09	03	1920	0603	(32	115.5)	IV	--
236	1	18	05	1920	0625	(32.5	115.5)	V	--
237	1	20	05	1920	1330	(32.5	117)	V	--
238	1	22	06	1920	2035	(34	118.5)	V	--
239	1	23	06	1920	1220	(34	118.5)	V	--
240	1	30	06	1920	0350	(34	118.5)	V	--
241	1	11	07	1920	0525	(34	118)	IV	--
242	1, 2	16	07	1920	2127	(34	118.5)	VII	Dam
243	1	26	07	1920	1215	(34	118)	V	--
244	1	28	07	1920	1540	(34	117.5)	IV	--
245	1	28	07	1920	1928	(34	118)	IV	--
246	1	29	07	1920	0300	(34	118)	IV	--
247	1	23	08	1920	2300	(34	118)	IV	--

Table 2.5-1
LISTING OF NONINSTRUMENTED EARTHQUAKES REPORTED
WITHIN 320 KILOMETERS (200 MILES) OF THE SITE[a] (Sheet 20 of 30)

No.	Source[b]	Date (GMT)			Time (GMT)	Approximate Location[c]		Maximum Intensity[d]	Comments[e]
		(day)	(mo)	(yr)	(hr-min)	(lat)	(long.)		
248	1	10	09	1920	1415	(34	117.5)	IV	--
249	1	12	10	1920	1748	(33	116.5)	VII	--
250	1	01	12	1920	0130	(35	119.5)	VI	--
251		05	12	1920	1158	(34.5	120)	V	--
252		18	12	1920	1726	(33.5	117)	V	--
253		20	12	1920	0529	(33	115.4)	V	--
254		20	12	1920	1447	(33	115.5)	VII	Mud geysers
255		21	12	1920	1452	(33	115.5)	VII	--
256		09	01	1921	0530	(34	118)	VI	--
257		20	01	1921	1946	(32.5	115.5)	IV	--
258		25	03	1921	0125	(33	115)	IV	--
259		27	03	1921	0210	(35	119.5)	IV	--
260		21	04	1921	1538	(34	118.5)	V	--

Table 2.5-1
LISTING OF NONINSTRUMENTED EARTHQUAKES REPORTED WITHIN 320 KILOMETERS (200 MILES) OF THE SITE[a] (Sheet 21 of 30)

No.	Source[b]	Date (GMT)			Time (GMT)	Approximate Location[c]		Maximum Intensity[d]	Comments[e]
		(day)	(mo)	(yr)	(hr-min)	(lat)	(long.)		
261		09	08	1921	2046	(32.5	115.5)	IV	--
262		10	08	1921	1906	(33	116.5)	V	--
263	1, 2	08	08	1921	1824	32.5	115.5	IV	--
264	1	26	09	1921	2252	(34	117.5)	IV	--
265	1	2	11	1921	2322	(34	118.5)	IV	--
266	1	17	11	1921	1956	(32.5	115.5)	V	--
267	1	17	11	1921	2323	(32.5	115.5)	IV	--
268	1	27	01	1922	0750	(32.5	115.5)	IV	--
269	1	05	02	1922	1915	(33	116.5)	V	--
270	1	06	02	1922	0235	(33	117)	IV	--
271	1	09	02	1922	0707	(33	116.5)	IV	--
272	1	26	02	1922	0200	(33	115.5)	IV	--
273	1	13	04	1922	0412	(33.7	118)	IV	--

Table 2.5-1
LISTING OF NONINSTRUMENTED EARTHQUAKES REPORTED
WITHIN 320 KILOMETERS (200 MILES) OF THE SITE[(a)] (Sheet 22 of 30)

No.	Source[(b)]	Date (GMT)			Time (GMT)	Approximate Location[(c)]		Maximum Intensity[(d)]	Comments[(e)]
		(day)	(mo)	(yr)	(hr-min)	(lat)	(long.)		
274	1	16	06	1922	2306	(33	115.5)	V	--
275	1	12	03	1923	0600	(34.5	120)	IV	--
276	1	23	04	1923	2313	(34	117.5)	V	--
277	1	30	06	1923	0022	(34	117.5)	V	--
278	1	20	07	1923	0700	(33.2	117)	V	--
279	1, 2	05	11	1923	2207	32.5	115.5	VII	Dam
280	1, 2	07	11	1923	2357	32.5	115.5	VII	Dam
281	1	28	11	1923	0350	(34.5	119)	IV	--
282	1	05	01	1924	2252	(32.5	115.5)	IV	--
283	1	18	07	1924	2120	(33	115.5)	IV	--
284	1	08	10	1924	0524	(33	116.5)	IV	--
285	1	24	10	1924	0739	(33	115.5)	VI	--
286	1	28	01	1925	1730	(34.5	119)	IV	--

Table 2.5-1
LISTING OF NONINSTRUMENTED EARTHQUAKES REPORTED
WITHIN 320 KILOMETERS (200 MILES) OF THE SITE[a] (Sheet 23 of 30)

No.	Source[b]	Date (GMT)			Time (GMT)	Approximate Location[c]		Maximum Intensity[d]	Comments[e]
		(day)	(mo)	(yr)	(hr-min)	(lat)	(long.)		
287	1	08	02	1925	0024	(32.5	115.5)	IV	--
288	1, 2	16	04	1925	0330	32.5	115.5	VII	Dam
289	1	01	05	1925	0925	(33.8	118)	IV	--
290	1, 2	29	06	1925	1700	(33	115.5)	IV	--
291	1	03	07	1925	1638	(34.5	120)	VII	--
292	1	29	07	1925	1400	(35	120)	V	--
293	1	30	07	1925	0950	(34.5	120)	IV	--
294	1	02	08	1925	1845	(34.2	119.5)	V	--
295	1	31	08	1925	0307	(33	115.5)	V	--
296	1	22	10	1925	0932	(34	118)	IV	--
297	1	13	11	1925	1100	(33.9	117.8)	IV	--
298	1	12	01	1926	1015	(34.5	119)	IV	--
299	1, 2	18	02	1926	1818	34	119.5	IX	Dam

Table 2.5-1
LISTING OF NONINSTRUMENTED EARTHQUAKES REPORTED
WITHIN 320 KILOMETERS (200 MILES) OF THE SITE[a] (Sheet 24 of 30)

No.	Source[b]	Date (GMT)			Time (GMT)	Approximate Location[c]		Maximum Intensity[d]	Comments[e]
		(day)	(mo)	(yr)	(hr-min)	(lat)	(long.)		
300	1, 2	03	04	1926	2008	34	116	IV	--
301	1, 2	19	04	1926	1517	32.5	115	IV	--
302	1	29	04	1926	1218	(34.5	119)	IV	--
303	1	06	05	1926	0230	(32.5	117)	IV	--
304	1	09	05	1926	0510	33.9	117.8	IV	--
305	1	14	05	1926	1800	(34.5	119)	IV	--
306	1	24	06	1926	1530	(34.5	120)	V	--
307	1	28	06	1926	0130	(34.3	119.5)	IV	--
308	1, 2	29	06	1926	2321	34.5	119.5	VIII	Dam, Ts, (?)
309	1, 2	30	06	1926	1331	(35.5	118.5)	VII	--
310	1	06	07	1926	1745	(34.5	120)	V	--
311	1	06	08	1926	1742	(34.5	120)	V	--
312	1	09	08	1926	0412	(34.5	120)	V	--

Table 2.5-1
LISTING OF NONINSTRUMENTED EARTHQUAKES REPORTED
WITHIN 320 KILOMETERS (200 MILES) OF THE SITE[a] (Sheet 25 of 30)

No.	Source[b]	Date (GMT)			Time (GMT)	Approximate Location[c]		Maximum Intensity[d]	Comments[e]
		(day)	(mo)	(yr)	(hr-min)	(lat)	(long.)		
313	1	28	09	1926	1749	(34.3	119.5)	V	--
314	1	02	11	1926	2325	(34.5	119)	IV	--
315	1	04	11	1926	2238	(33.9	117.8)	VI	--
316	1	07	11	1926	1948	(33.9	117.8)	VI	--
317	1	09	11	1926	1535	(33.9	117.8)	VI	--
318	1	10	11	1926	1523	(33.9	117.8)	VI	--
319	1	09	12	1926	0548	(32.5	115.5)	V	--
320	1	30	12	1926	0015	(33.8	118.5)	IV	--
321	1	02	01	1927	1600	(32.5	115.5)	V	--
322	1	06	01	1927	1637	(32.5	115.5)	IV	--
323	1	08	01	1927	0729	(33	115.5)	IV	--
324	1	13	01	1927	1038	(32.5	115.5)	V	--
325	1	16	01	1927	1905	(32.5	115.5)	VI	--

Table 2.5-1
LISTING OF NONINSTRUMENTED EARTHQUAKES REPORTED
WITHIN 320 KILOMETERS (200 MILES) OF THE SITE[(a)] (Sheet 26 of 30)

No.	Source[(b)]	Date (GMT)			Time (GMT)	Approximate Location[(c)]		Maximum Intensity[(d)]	Comments[(e)]
		(day)	(mo)	(yr)	(hr-min)	(lat)	(long.)		
326	1	18	01	1927	1130	(33	115.5)	VI	--
327	1	29	01	1927	2324	(34	118.5)	V	--
328	1	07	02	1927	0429	(34	118.5)	VI	--
329	1, 2	12	02	1927	0858	(33	115.5)	VI	--
330	1	16	04	1927	0448	(34.2	118)	IV	--
331	1	15	05	1927	1120	(34.3	119.5)	V	--
332	1	08	07	1927	0047	(35.5	119)	IV	--
333	1	16	07	1927	0155	(32.5	115.5)	V	--
334	1, 2	04	08	1927	0424	34	118.5	VI	--
335	1	14	08	1927	1448	(32.7	116)	VI	--
336	1	26	08	1927	1240	(34.5	120)	V	--
337	1	08	10	1927	1940	(33.9	118.2)	VI	--
338	1, 2	04	11	1927	1351	(34.5	121.5)	X	Dam, Ls, Liq, Ts, Mag=7.5

Table 2.5-1
LISTING OF NONINSTRUMENTED EARTHQUAKES REPORTED
WITHIN 320 KILOMETERS (200 MILES) OF THE SITE[a] (Sheet 27 of 30)

No.	Source[b]	Date (GMT)			Time (GMT)	Approximate Location[c]		Maximum Intensity[d]	Comments[e]
		(day)	(mo)	(yr)	(hr-min)	(lat)	(long.)		
339	1	06	11	1927	0006	(34.5	119)	IV	--
340	1	06	11	1927	2210	(34.5	119)	IV	--
341	1	07	11	1927	0328	(32.5	117)	IV	--
342	1	08	11	1927	1010	(34.5	119)	IV	--
343	1	09	11	1927	1055	(32.5	117)	IV	--
344	1	19	11	1927	0332	(35	120.5)	VII	--
345	1	05	12	1927	1145	(34.5	120.5)	IV	--
346	1	31	12	1927	1010	(34.5	120.51)	V	--
347	3	07	01	1928	2252	(34	118.5)	IV	--
348	3	01	03	1928	0500	(35.5	119)	IV	--
349	3	16	03	1928	0025	(35	120.5)	VII	--
350	3	03	04	1928	1240	(33.8	118.5)	IV	--
351	3	18	04	1928	2140	(34	120)	IV	--

Table 2.5-1
LISTING OF NONINSTRUMENTED EARTHQUAKES REPORTED
WITHIN 320 KILOMETERS (200 MILES) OF THE SITE[a] (Sheet 28 of 30)

No.	Source[b]	Date (GMT)			Time (GMT)	Approximate Location[c]		Maximum Intensity[d]	Comments[e]
		(day)	(mo)	(yr)	(hr-min)	(lat)	(long.)		
352	3	04	05	1928	1922	(34	118)	IV	--
353	3	09	06	1928	0822	(35	119.5)	V	--
354	3	06	07	1928	0440	(32.5	117)	IV	--
355	2, 3	05	09	1928	1442	34	116	V	--
356	3	23	09	1928	0830	(32.5	115.5)	V	--
357	3	02	10	1928	1901	(33	116)	IV	--
358	3	12	03	1929	0418	(32.5	115.5)	IV	--
359	3	13	03	1929	0428	(34.5	119)	IV	--
360	3	08	07	1929	1646	34	118	VIII	Dam, Mag=4.7
361	3	13	09	1929	1323	(33.5	118.5)	IV	--
362	3	24	09	1929	1727	(35	117)	IV	--
363	3	31	10	1929	1939	(33.5	118.5)	IV	--
364	3	02	12	1929	1124	(32	116.5)	V	--

Table 2.5-1
LISTING OF NONINSTRUMENTED EARTHQUAKES REPORTED
WITHIN 320 KILOMETERS (200 MILES) OF THE SITE[a] (Sheet 29 of 30)

No.	Source[b]	Date (GMT)			Time (GMT)	Approximate Location[c]		Maximum Intensity[d]	Comments[e]
		(day)	(mo)	(yr)	(hr-min)	(lat)	(long.)		
365	2, 3	15	01	1930	2242	34.2	116.9	VII	Dam
366	3	27	01	1930	2026	(34	118)	IV	--
367	3	07	02	1930	2323	(32.7	116)	V	--
368	2, 3	26	02	1930	0230	33	115.5	VIII	Dam, Liq
369	2, 3	01	03	1930	2344	33	115.5	VIII	Dam
370	3	26	06	1930	2209	(32.7	115.4)	V	--
371	2, 3	05	08	1930	1125	34.5	119.5	VII	Dam
372	2, 3	30	08	1930	2240	33.9	118.6	VIII	Dam, Lu
373	3	08	01	1931	1353	(35	117)	IV	--
374	3	28	01	1931	0850	34	118.1	IV	--
375	3	16	02	1931	1357	(34	117.5)	V	--
376	3	31	03	1931	2033	(33.9	117.8)	IV	--
377	3	23	04	1931	2334	35	118	IV	--

Table 2.5-1
LISTING OF NONINSTRUMENTED EARTHQUAKES REPORTED
WITHIN 320 KILOMETERS (200 MILES) OF THE SITE[a] (Sheet 30 of 30)

No.	Source[b]	Date (GMT)			Time (GMT)	Approximate Location[c]		Maximum Intensity[d]	Comments[e]
		(day)	(mo)	(yr)	(hr-min)	(lat)	(long.)		
378	3	24	04	1931	1828	33.5	118.3	V	--
379	3	29	04	1931	1241	(34.2	118.2)	IV	--
380	3	23	06	1931	1654	(34.1	117.7)	IV	--
381	3	17	07	1931	--	(35.5	119)	IV	--
382	3	30	09	1931	1546	(32	115)	IV	--
383	3	07	10	1931	0115	34	118.3	IV	--
384	3	03	11	1931	0605	33.7	118.3	V	--

(b) Earthquake catalog sources: 1. Townley and Allen, 1939; 2. Wood, Heck and Eppley, 1961; 3. Heck, Bodle, Newman and others, 1968; 4. Richter, 1958.

(c) Earthquakes listed are those which could reasonably have occurred within a 200-mile radius of the site. Locations without parentheses are those cited by the referenced catalog. Those with parentheses are approximated from catalog descriptions. All latitudes are north; all longitudes are west.

(d) Intensities listed refer to the Modified Mercalli (MM) Scale of 1931. In earlier catalogs, intensities are given in Rossi-Forel notation. These entries are converted to MM herein. Intensities in parentheses are assigned from descriptions in cases where no intensity is given in the catalog.

(e) Abbreviations used in this column are as follows: Di, Diastrophism; Ts, Tsunami; Se, Seiche; Ls, Landslide; Liq, Liquefaction; Lu, Lurching; Dam, Damage to works of man; Mag, Estimated Richter Magnitude.

Table 2.5-2
LISTING OF INSTRUMENTAL EPICENTERS WITHIN A 320-KILOMETER (200-MILE) RADIUS OF THE SITE, THROUGH JUNE 1980 (Sheet 1 of 9)

YEAR	MO	DA	HRMN	SEC	LATITUDE	LONGITUDE	DEPTH	MAG
1933	3	11	154	7.80	33 37.00	-117 58.00	0.00	6.30
1933	3	11	209	0.00	33 45.00	-118 5.00	0.00	5.00
1933	3	11	230	0.00	33 45.00	-118 5.00	0.00	5.10
1933	3	11	323	0.00	33 45.00	-118 5.00	0.00	5.00
1933	3	11	510	22.00	33 42.00	-118 4.00	0.00	5.10
1933	3	11	518	4.00	33 34.50	-117 59.00	0.00	5.20
1933	3	11	658	3.00	33 41.00	-118 3.00	0.00	5.50
1933	3	11	854	57.00	33 42.00	-118 4.00	0.00	5.10
1933	3	11	910	0.00	33 45.00	-118 5.00	0.00	5.10
1933	3	11	1425	0.00	33 51.00	-118 16.00	0.00	5.00
1933	3	13	1318	28.00	33 45.00	-118 5.00	0.00	5.30
1933	3	14	1901	50.00	33 37.00	-118 1.00	0.00	5.10
1933	10	2	910	17.60	33 47.00	-118 8.00	0.00	5.40
1934	5	14	1314	0.00	31 0.00	-114 30.00	0.00	5.50
1934	6	5	2148	0.00	35 48.00	-120 20.00	0.00	5.00
1934	6	8	430	0.00	35 48.00	-120 20.00	0.00	5.00
1934	6	8	447	0.00	35 48.00	-120 20.00	0.00	6.00
1934	11	25	818	0.00	32 5.00	-116 40.00	0.00	5.00
1934	12	24	1626	0.00	35 56.00	-120 29.00	0.00	5.00
1934	12	30	1352	0.00	32 15.00	-115 30.00	0.00	6.50
1934	12	31	1845	0.00	32 0.00	-114 45.00	0.00	7.10
1935	2	24	145	0.00	31 59.00	-115 12.00	0.00	6.00
1935	4	29	2008	0.00	31 45.00	-116 30.00	0.00	5.00
1935	9	8	1703	0.00	32 54.00	-115 13.00	0.00	5.00
1935	10	11	1406	0.00	32 54.00	-115 13.00	0.00	5.00
1935	10	24	1448	7.60	34 6.00	-116 48.00	0.00	5.10
1935	12	20	745	0.00	33 10.00	-115 30.00	0.00	5.00
1936	4	29	850	0.00	31 40.00	-115 5.00	0.00	5.00
1937	2	27	129	18.44	31 52.02	-116 34.26	10.00	5.00
1937	3	25	1649	1.83	33 24.51	-116 15.69	10.00	6.00
1938	5	31	834	55.41	33 41.93	-117 30.64	10.00	5.50
1938	6	6	242	0.00	32 54.00	-115 13.00	0.00	5.00

Table 2.5-2
LISTING OF INSTRUMENTAL EPICENTERS WITHIN A 320-KILOMETER (200-MILE) RADIUS OF THE SITE, THROUGH JUNE 1980 (Sheet 2 of 9)

YEAR	MO	DA	HRMN	SEC	LATITUDE	LONGITUDE	DEPTH	MAG
1939	5	1	2353	0.00	32 0.00	-117 30.00	0.00	5.00
1939	5	4	2044	46.75	35 58.00	-114 49.00	0.00	5.00
1939	6	24	1627	0.00	32 0.00	-117 30.00	0.00	5.00
1939	12	28	1215	38.00	35 48.00	-120 20.00	0.00	5.00
1940	5	18	503	58.50	34 5.00	-116 18.00	0.00	5.40
1940	5	18	551	20.25	34 4.00	-116 20.00	0.00	5.20
1940	5	18	721	32.70	34 4.00	-116 20.00	0.00	5.00
1940	5	19	436	40.90	32 44.00	-115 30.00	0.00	6.70
1940	5	19	455	0.00	32 46.00	-115 29.00	0.00	5.50
1940	5	19	551	34.00	32 46.00	-115 29.00	0.00	5.50
1940	5	19	633	20.00	32 46.00	-115 29.00	0.00	5.00
1940	5	19	635	40.00	32 46.00	-115 29.00	0.00	5.50
1940	6	4	1035	8.30	33 0.00	-116 26.00	0.00	5.10
1940	7	7	1843	0.00	31 40.00	-115 5.00	0.00	5.00
1940	12	7	2216	27.00	31 40.00	-115 5.00	0.00	6.00
1941	1	9	1028	42.00	31 42.00	-115 6.00	0.00	5.50
1941	2	5	1333	6.00	31 42.00	-115 6.00	0.00	5.00
1941	7	1	750	54.80	34 22.00	-119 35.00	0.00	5.90
1941	9	21	1953	7.20	34 52.00	-118 56.00	0.00	5.20
1941	11	14	841	36.30	33 47.00	-118 15.00	0.00	5.40
1942	3	3	103	24.00	34 0.00	-115 45.00	0.00	5.00
1942	5	23	1547	29.00	32 59.00	-115 59.00	0.00	5.00
1942	10	21	1622	13.00	32 58.00	-116 0.00	0.00	6.50
1942	10	21	1625	19.00	32 58.00	-116 0.00	0.00	5.00
1942	10	21	1626	54.00	32 58.00	-116 0.00	0.00	5.00

Table 2.5-2
LISTING OF INSTRUMENTAL EPICENTERS WITHIN A 320-KILOMETER (200-MILE) RADIUS OF THE SITE, THROUGH JUNE 1980 (Sheet 3 of 9)

YEAR	MO	DA	HRMN	SEC	LATITUDE	LONGITUDE	DEPTH	MAG
1942	10	22	150	38.00	33 14.00	-115 43.00	0.00	5.50
1942	10	22	1813	26.00	32 58.00	-116 0.00	0.00	5.00
1943	8	29	345	13.00	34 16.00	-116 58.00	0.00	5.50
1943	12	22	1550	28.00	34 20.00	-115 48.00	0.00	5.50
1944	6	12	1045	34.66	33 58.57	-116 43.24	10.00	5.10
1944	6	12	1116	35.97	33 59.67	-116 42.70	10.00	5.30
1945	3	20	2155	7.00	34 15.00	-116 10.00	0.00	5.00
1945	4	1	2434	42.00	34 0.00	-120 1.00	0.00	5.40
1945	5	12	733	0.00	31 36.00	-115 36.00	0.00	5.20
1945	8	15	1756	24.00	33 13.00	-116 8.00	0.00	5.70
1946	1	8	1854	18.00	33 0.00	-115 50.00	0.00	5.40
1946	3	15	1321	0.90	35 45.20	-117 59.18	0.00	5.20
1946	3	15	1349	35.90	35 43.51	-118 3.28	22.00	6.30
1946	3	15	1400	35.40	35 42.89	-118 4.44	0.00	5.30
1946	3	15	1918	53.60	35 42.86	-117 58.63	0.00	5.40
1946	3	15	2154	33.40	35 45.08	-118 1.74	0.00	5.20
1946	3	16	946	17.90	35 44.70	-118 2.33	0.00	5.10
1946	3	18	1550	42.65	35 44.80	-117 54.51	4.40	5.30
1946	7	18	1427	58.00	34 32.00	-115 59.00	0.00	5.60
1946	9	28	719	9.00	33 57.00	-116 51.00	0.00	5.00
1947	4	10	1558	6.00	34 59.00	-116 33.00	0.00	6.20
1947	4	10	1603	0.00	34 58.00	-116 33.00	0.00	5.10
1947	4	10	1718	22.00	34 57.00	-116 32.00	0.00	5.00
1947	4	11	747	0.00	34 58.00	-116 33.00	0.00	5.00
1947	7	24	2210	46.00	34 1.00	-116 30.00	0.00	5.50
1947	7	25	46	31.00	34 1.00	-116 30.00	0.00	5.00
1947	7	25	619	49.00	34 1.00	-116 30.00	0.00	5.20
1947	7	26	249	41.00	34 1.00	-116 30.00	0.00	5.10
1947	11	18	2159	3.00	33 16.00	-119 27.00	0.00	5.00
1948	2	24	815	10.00	32 30.00	-118 33.00	0.00	5.30
1948	12	4	2343	17.00	33 56.00	-116 23.00	0.00	6.50

Table 2.5-2
LISTING OF INSTRUMENTAL EPICENTERS WITHIN A 320-KILOMETER (200-MILE) RADIUS OF THE SITE, THROUGH JUNE 1980 (Sheet 4 of 9)

YEAR	MO	DA	HRMN	SEC	LATITUDE	LONGITUDE	DEPTH	MAG
1949	5	2	1125	47.00	34 1.00	-115 41.00	0.00	5.90
1949	9	16	2045	0.00	31 0.00	-115 0.00	0.00	5.10
1949	11	4	2042	38.00	32 12.00	-116 33.00	0.00	5.70
1949	11	5	435	24.00	32 12.00	-116 33.00	0.00	5.10
1950	7	28	1750	48.00	33 7.00	-115 34.00	0.00	5.40
1950	7	29	1436	32.00	33 7.00	-115 34.00	0.00	5.50
1951	1	24	717	2.60	32 59.00	-115 44.00	0.00	5.60
1951	9	2	1627	32.00	31 0.00	-117 0.00	0.00	5.20
1951	12	26	46	54.00	32 49.00	-118 21.00	0.00	5.90
1952	7	21	1152	14.00	35 0.00	-119 1.00	0.00	7.70
1952	7	21	1202	0.00	35 0.00	-119 2.00	0.00	5.60
1952	7	21	1205	31.00	35 0.00	-119 0.00	0.00	6.40
1952	7	21	1219	36.00	34 57.00	-118 52.00	0.00	5.30
1952	7	21	1513	58.00	35 11.00	-118 39.00	0.00	5.10
1952	7	21	1742	44.00	35 14.00	-118 32.00	0.00	5.10
1952	7	21	1941	22.00	35 8.00	-118 46.00	0.00	5.50
1952	7	23	38	32.00	35 22.00	-118 35.00	0.00	6.10
1952	7	23	319	23.00	35 22.00	-118 35.00	0.00	5.00
1952	7	23	753	19.00	35 0.00	-118 50.00	0.00	5.40
1952	7	23	1317	5.00	35 13.00	-118 49.00	0.00	5.70
1952	7	23	1813	51.00	35 0.00	-118 50.00	0.00	5.20
1952	7	25	1313	8.25	35 18.65	-118 29.95	2.80	5.00
1952	7	25	1909	44.62	35 19.04	-118 29.67	5.50	5.70
1952	7	25	1943	23.67	35 18.92	-118 30.95	11.20	5.70
1952	7	29	703	47.00	35 23.00	-118 51.00	0.00	6.10
1952	7	29	801	46.00	35 24.00	-118 49.00	0.00	5.10

Table 2.5-2
LISTING OF INSTRUMENTAL EPICENTERS WITHIN A 320-KILOMETER (200-MILE) RADIUS OF THE SITE, THROUGH JUNE 1980 (Sheet 5 of 9)

YEAR	MO	DA	HRMN	SEC	LATITUDE	LONGITUDE	DEPTH	MAG
1952	7	31	1209	9.00	35 20.00	-118 36.00	0.00	5.80
1952	8	1	1304	30.00	34 54.00	-118 57.00	0.00	5.10
1952	8	22	2241	24.00	35 20.00	-118 55.00	0.00	5.80
1952	8	23	1009	7.15	34 3.16	-118 11.89	13.10	5.00
1952	11	22	746	37.00	35 44.00	-121 12.00	0.00	6.00
1953	6	14	417	29.90	32 57.00	-115 43.00	0.00	5.50
1953	10	10	1849	6.00	31 48.00	-116 6.00	0.00	5.00
1954	1	12	2333	49.00	35 0.00	-119 1.00	0.00	5.90
1954	1	27	1419	48.00	35 9.00	-118 38.00	0.00	5.00
1954	2	1	423	57.00	32 18.00	-115 18.00	0.00	5.20
1954	2	1	432	2.00	32 18.00	-115 15.00	0.00	5.60
1954	2	1	1305	29.00	32 18.00	-115 18.00	0.00	5.10
1954	3	19	954	29.00	33 17.00	-116 11.00	0.00	6.20
1954	3	19	955	56.00	33 17.00	-116 11.00	0.00	5.00
1954	3	19	1021	17.00	33 17.00	-116 11.00	0.00	5.50
1954	3	23	414	50.00	33 17.00	-116 11.00	0.00	5.10
1954	5	23	2352	43.00	34 59.00	-118 59.00	0.00	5.10
1954	5	31	806	24.00	31 36.00	-115 12.00	0.00	5.20
1954	10	17	2257	18.00	31 30.00	-116 30.00	0.00	5.70
1954	10	24	944	8.00	31 30.00	-116 0.00	0.00	6.00
1954	10	24	1121	24.00	31 30.00	-116 0.00	0.00	5.40
1954	11	12	1226	47.00	31 30.00	-116 0.00	0.00	6.30
1954	11	12	1316	42.00	31 30.00	-116 0.00	0.00	5.00
1954	11	14	536	19.00	31 30.00	-116 0.00	0.00	5.40
1955	4	25	1043	8.00	32 20.00	-115 0.00	0.00	5.20
1955	11	2	1940	6.00	36 0.00	-120 55.00	0.00	5.20
1955	11	26	1736	0.00	31 36.00	-116 6.00	0.00	5.40
1955	12	17	607	29.00	33 0.00	-115 30.00	1.00	5.40

Table 2.5-2
LISTING OF INSTRUMENTAL EPICENTERS WITHIN A 320-KILOMETER (200-MILE) RADIUS OF THE SITE, THROUGH JUNE 1980 (Sheet 6 of 9)

YEAR	MO	DA	HRMN	SEC	LATITUDE	LONGITUDE	DEPTH	MAG
1956	2	9	1432	38.00	31 45.00	-115 55.00	0.00	6.80
1956	2	9	1434	0.00	31 42.00	-115 54.00	0.00	5.60
1956	2	9	1501	33.30	31 36.00	-115 42.00	0.00	5.30
1956	2	9	1524	26.00	31 45.00	-115 55.00	0.00	6.10
1956	2	9	1629	53.30	31 36.00	-115 42.00	0.00	5.80
1956	2	9	1659	53.00	31 45.00	-115 55.00	0.00	5.70
1956	2	9	1848	45.00	31 45.00	-115 55.00	0.00	5.70
1956	2	10	418	15.00	31 35.00	-115 40.00	0.00	5.00
1956	2	10	1509	29.00	31 45.00	-115 55.00	0.00	5.00
1956	2	10	1812	54.00	31 45.00	-115 55.00	0.00	5.50
1956	2	11	257	46.00	31 45.00	-115 55.00	0.00	5.10
1956	2	11	519	0.00	31 42.00	-115 54.00	0.00	5.00
1956	2	11	611	24.00	31 45.00	-115 55.00	0.00	5.00
1956	2	11	624	25.00	31 35.00	-115 40.00	0.00	5.40
1956	2	14	1445	32.00	31 30.00	-115 30.00	0.00	5.00
1956	2	14	1833	34.00	31 30.00	-115 30.00	0.00	6.30
1956	2	15	120	38.00	31 30.00	-115 30.00	0.00	6.40
1956	2	15	228	39.00	31 30.00	-115 30.00	0.00	5.30
1956	2	15	707	47.00	31 30.00	-115 30.00	0.00	5.20
1956	2	15	835	54.00	31 30.00	-115 30.00	0.00	5.00
1956	2	16	812	28.00	31 30.00	-115 30.00	0.00	5.00
1956	2	25	508	51.00	31 30.00	-115 30.00	0.00	5.10
1956	3	3	1823	13.00	31 35.00	-115 40.00	0.00	5.10
1956	3	9	32	40.00	31 45.00	-115 55.00	0.00	5.00
1956	3	10	1412	54.00	31 30.00	-115 30.00	0.00	5.00
1956	5	10	1148	54.00	31 50.00	-116 0.00	0.00	5.00
1956	8	25	1557	43.00	31 30.00	-115 30.00	0.00	5.00
1956	11	16	323	9.00	35 57.00	-120 28.00	0.00	5.00
1956	12	13	1315	37.00	31 0.00	-115 0.00	0.00	6.00

Table 2.5-2
LISTING OF INSTRUMENTAL EPICENTERS WITHIN A 320-KILOMETER (200-MILE) RADIUS OF THE SITE, THROUGH JUNE 1980 (Sheet 7 of 9)

YEAR	MO	DA	HRMN	SEC	LATITUDE	LONGITUDE	DEPTH	MAG
1957	4	25	2224	12.00	33 11.00	-115 51.00	0.00	5.10
1957	5	26	1559	33.64	33 13.88	-116 0.27	15.10	5.00
1958	12	1	321	18.00	32 15.00	-115 45.00	0.00	5.80
1958	12	1	350	0.00	32 15.00	-115 45.00	0.00	5.00
1958	12	1	602	0.00	32 15.00	-115 45.00	0.00	5.50
1961	1	28	812	46.18	35 46.69	-118 2.92	5.50	5.30
1961	11	15	538	55.49	34 56.47	-118 59.20	10.70	5.00
1962	1	27	2307	42.00	30 48.00	-114 36.00	0.00	5.30
1962	5	27	145	35.00	31 42.00	-115 36.00	0.00	5.10
1963	3	1	25	57.86	34 55.95	-118 58.55	13.90	5.00
1963	9	23	1441	52.58	33 42.61	-116 55.50	16.50	5.00
1963	10	20	1329	27.00	31 6.00	-155 36.00	0.00	5.00
1964	2	3	843	36.00	31 30.00	-114 12.00	0.00	5.00
1964	12	22	2054	33.16	31 48.65	-117 7.84	2.30	5.60
1965	9	25	1743	44.12	34 42.75	-116 30.16	10.60	5.20
1965	9	26	700	1.75	34 42.67	-116 1.61	8.30	5.00
1966	6	28	426	13.60	35 54.95	-120 32.00	18.60	5.60
1966	8	7	1736	26.70	31 48.00	-114 30.00	0.00	6.30
1967	9	21	1	54.60	31 25.55	-115 57.20	1.00	5.20
1968	4	9	228	59.06	33 11.40	-116 7.72	11.10	6.40
1968	4	9	303	53.54	33 6.81	-116 2.25	5.00	5.20
1968	7	5	45	17.22	34 7.06	-119 42.15	5.90	5.20

Table 2.5-2
LISTING OF INSTRUMENTAL EPICENTERS WITHIN A 320-KILOMETER (200-MILE) RADIUS OF THE SITE, THROUGH JUNE 1980 (Sheet 8 of 9)

YEAR	MO	DA	HRMN	SEC	LATITUDE	LONGITUDE	DEPTH	MAG
1969	3	20	817	41.90	31 18.00	-114 12.00	0.00	5.70
1969	3	21	307	31.90	31 18.00	-114 42.00	0.00	5.20
1969	3	21	353	42.40	31 12.00	-114 18.00	0.00	5.60
1969	3	21	412	26.80	31 12.00	-114 12.00	0.00	5.20
1969	3	21	421	54.20	31 18.00	-114 18.00	0.00	5.10
1969	3	21	426	24.00	31 12.00	-114 24.00	0.00	5.00
1969	3	21	444	28.80	31 0.00	-114 30.00	0.00	5.20
1969	3	21	447	4.40	31 12.00	-114 12.00	0.00	5.10
1969	3	21	456	20.30	31 12.00	-114 12.00	0.00	5.80
1969	3	21	539	56.40	31 24.00	-114 18.00	0.00	5.00
1969	3	21	550	43.80	31 18.00	-114 18.00	0.00	5.00
1969	3	21	559	19.10	31 24.00	-114 12.00	0.00	5.30
1969	3	21	634	22.20	31 6.00	-114 18.00	0.00	5.70
1969	3	21	721	11.60	31 18.00	-114 12.00	0.00	5.60
1969	3	21	754	11.50	31 0.00	-114 24.00	0.00	5.00
1969	3	21	838	52.70	31 6.00	-114 12.00	0.00	5.10
1969	3	21	856	15.80	31 12.00	-114 12.00	0.00	5.50
1969	3	21	1010	10.70	31 12.00	-114 18.00	0.00	5.50
1969	3	21	1219	54.00	31 12.00	-114 12.00	0.00	5.20
1969	3	21	1224	0.10	31 12.00	-114 16.00	0.00	5.30
1969	3	21	1557	42.00	31 12.00	-114 18.00	0.00	5.10
1969	3	21	1629	40.40	31 18.00	-114 18.00	0.00	5.00
1969	3	21	1800	20.60	31 6.00	-114 18.00	0.00	5.20
1969	3	22	1823	2.10	31 30.00	-114 12.00	0.00	5.20
1969	3	23	1132	22.40	31 24.00	-115 0.00	0.00	5.20
1969	3	24	902	32.10	31 18.00	-114 12.00	0.00	5.30
1969	3	28	1519	40.40	31 30.00	-114 18.00	0.00	5.30
1969	4	28	2320	42.87	33 20.60	-116 20.78	20.00	5.80
1969	10	24	829	12.11	33 17.46	-119 11.56	10.00	5.10
1970	9	12	1430	52.98	34 16.19	-117 32.40	8.00	5.40

Table 2.5-2
LISTING OF INSTRUMENTAL EPICENTERS WITHIN A 320-KILOMETER (200-MILE) RADIUS OF THE SITE, THROUGH JUNE 1980 (Sheet 9 of 9)

YEAR	MO	DA	HRMN	SEC	LATITUDE	LONGITUDE	DEPTH	MAG
1971	2	9	1400	41.83	34 24.67	-118 24.04	8.40	6.40
1971	2	9	1401	8.00	34 24.67	-118 24.04	8.00	5.80
1971	2	9	1402	44.00	34 24.67	-118 24.04	8.00	5.80
1971	2	9	1410	28.00	34 24.67	-118 24.04	8.00	5.30
1971	2	9	1443	46.66	34 18.48	-118 27.23	6.20	5.20
1971	9	30	2246	11.30	33 2.01	-115 49.24	8.00	5.10
1973	2	21	1445	57.30	34 3.89	-119 2.10	8.00	5.90
1973	8	6	2329	16.97	33 59.16	-119 28.52	16.90	5.00
1974	11	22	1625	37.95	30 31.66	-115 7.92	8.00	5.50
1975	6	1	138	49.23	34 30.94	-116 29.73	4.46	5.20
1975	7	17	1824	47.03	31 55.62	-115 46.62	17.30	5.00
1975	9	13	238	27.48	30 38.90	-116 17.37	8.00	5.20
1976	1	10	1258	15.79	32 5.02	-115 28.28	12.32	5.00
1976	12	7	1259	56.31	31 58.63	-114 46.73	8.00	5.00
1977	11	19	1323	39.20	35 23.92	-118 37.29	5.00	9.00
1978	5	5	2103	15.80	32 12.68	-115 18.21	6.00	5.20
1978	8	13	2254	53.42	34 20.82	-119 41.76	12.75	5.10
1979	1	1	2314	38.94	33 56.66	-118 40.88	11.28	5.00
1979	3	15	2107	16.53	34 19.64	-116 26.69	2.48	5.20
1979	8	6	1705	45.09	35 39.80	-120 36.56	5.00	5.90
1979	10	15	2316	53.44	32 36.82	-115 19.09	12.28	6.60
1979	10	15	2319	29.98	32 45.94	-115 26.45	9.25	5.20
1979	10	16	549	10.18	32 55.63	-115 32.38	10.42	5.10
1979	10	16	619	48.68	32 55.71	-115 32.36	9.20	5.10
1979	10	16	658	42.79	33 0.82	-115 33.31	9.14	5.50
1980	2	25	1047	38.53	33 30.06	-116 30.79	13.58	5.50
1980	6	9	328	19.37	32 11.12	-115 4.55	5.00	6.10

Table 2.5-3
LISTING OF NONINSTRUMENTED EARTHQUAKES REPORTED
WITHIN 80 KILOMETERS (50 MILES) OF THE SITE[(a)] (SHEET 1 of 12)

No.	Source[(b)]	Date (GMT)			Time (GMT)	Approximate Location[(c)]		Maximum Intensity[(d)]	Comments[(e)]
		(day)	(mo)	(yr)	(hr-min)	(lat)	(long.)		
1	1	11	04	1769	--	(32	117)	?	Questionable
2	1, 2	28	07	1769	2100	34	118	X	--
3	1, 2	27	12	1775	0100	(33.5	116)	(VII)	--
4	1, 2	22	10	1800	2130	(33	117)	VIII	Mag=7, Dam
5	1, 2	25	03	1803	--	32.5	117	VIII	Dam
6	1, 2	08	12	1812	1500	(33	117)	IX	Dam, Mag=7
7	1, 2	23	09	1827	--	34	118	VII	--
8	1, 2	23	06	1843	2330	(33	117)	IX	--
9	1	07	04	1856	0730	34	118	V	--
10	1	03	05	1856	0810	34	118	V	--
11	1, 2	21	09	1856	0730	33	116.5	VIII	Di, Dam
12	1, 2	09	01	1857	1600	34	119	X+	Di, Dam, Se, Lu, Liq, Mag=8+

(a) See last page of table for notes.

Table 2.5-3
LISTING OF NONINSTRUMENTED EARTHQUAKES REPORTED
WITHIN 80 KILOMETERS (50 MILES) OF THE SITES[a] (Sheet 2 of 12)

No.	Source[b]	Date (GMT)			Time (GMT)	Approximate Location[c]		Maximum Intensity[d]	Comments[e]
		(day)	(mo)	(yr)	(hr-min)	(lat)	(long.)		
13	1	04	15	1857	0600	(34	118)	V	
14	1	01	12	1859	2210	(34	117.5)	V	--
15	1	26	03	1860	--	(34	118)	VI	--
16	1	27	03	1860	--	(34	118)	VI	--
17	1, 2	27	05	1862	--	33	117.5	VI	--
18	1	25	01	1863	2220	(32.5	117)	VI	--
19	11	15	04	1865	0840	(33	117)	VI	--
20	1	07	10	1869	--	(34	117.5)	V	--
21	1	12	10	1873	0915	(32.5	119)	V	--
22	1, 2	Summer		1878	--	34	118.5	VIII	Dam
23	1	21	03	1880	1425	34	118	V	--
24	1	25	03	1880	1030	34	117	IV	--
25	1	12	14	1880	1240	(34	117.5)	V	--
26	1	19	12	1880	1140	(33	118)	V	--

Table 2.5-3
LISTING OF NONINSTRUMENTED EARTHQUAKES REPORTED
WITHIN 80 KILOMETERS (50 MILES) OF THE SITE[a] (Sheet 3 of 12)

No.	Source[b]	Date (GMT)			Time (GMT)	Approximate Location[c]		Maximum Intensity[d]	Comments[e]
		(day)	(mo)	(yr)	(hr-min)	(lat)	(long.)		
27	1	28	12	1880	0700	(33.5	117)	V	--
28	1	08	10	1882	1000	(32.5	117)	V	--
29	1	07	03	1888	1554	(34	118)	VI	--
30	1	09	04	1888	1550	(34	117.5)	IV	--
31	1	07	02	1889	0520	(34	117.5)	VI	--
32	1	17	05	1889	0515	(34	118)	V	--
33	1, 2	09	02	1890	1206	34	117	VIII	Dam
34	1	28	05	1892	1115	(34	118)	VI	--
35	1, 2	23	10	1894	2303	33	117	VIII	Dam, Ls
36	1, 2	25	12	1899	1225	33.5	116.5	X+	Di, Dam, Mag=6.8, Lu, Ls
37	1	27	12	1901	1100	(34	117.5)	VI	--
38	1	09	07	1902	0945	(33.5	118)	V	--
39	1	08	07	1902	0945	(33.5	118)	V	--
40	1, 2	25	12	1903	1745	34	118	VII	Dam

Table 2.5-3
LISTING OF NONINSTRUMENTED EARTHQUAKES REPORTED
WITHIN 80 KILOMETERS (50 MILES) OF THE SITE[a] (Sheet 4 of 12)

No.	Source[b]	Date (GMT)			Time (GMT)	Approximate Location[c]		Maximum Intensity[d]	Comments[e]
		(day)	(mo)	(yr)	(hr-min)	(lat)	(long.)		
41	1	16	07	1905	0741	(34	117.5)	VII	Dam
42	1	03	10	1905	0540	(34	118)	VII	Dam
43	1	21	05	1907	0652	(34	117.5)	VI	--
44	1, 2	20	09	1907	0154	34	117	VIII	Di, Dam, Ls
45	1	03	07	1908	1255	(34	118)	IV	--
46	1	10	04	1910	0757	(33.5	117.5)	V	--
47	1	12	05	1910	0620	(33.5	117.5)	V	--
48	1, 2	15	05	1910	1547	33.5	117.5	V	Di, Dam, Mag=6+, Ls
49	1	11	08	1911	1820	(33.5	117)	VI	Dam
50	1	21	08	1911	2141	(34	117)	IV	--
51	1	18	10	1911	1910	(32.5	117)	IV	--
52	1	22	11	1911	0257	(34	117.5)	IV	--
53	1	23	12	1911	0942	(34	118)	IV	--
54	1	13	04	1913	1045	(34	117.5)	V	--

Table 2.5-3
LISTING OF NONINSTRUMENTED EARTHQUAKES REPORTED
WITHIN 80 KILOMETERS (50 MILES) OF THE SITE[a] (Sheet 5 of 12)

No.	Source[b]	Date (GMT)			Time (GMT)	Approximate Location[c]		Maximum Intensity[d]	Comments[e]
		(day)	(mo)	(yr)	(hr-min)	(lat)	(long.)		
55	1	21	10	1913	0938	(34	118)	IV	--
56	1	29	12	1914	1000	(33.5	117)	V	--
57	1	12	01	1915	1015	(33.5	117)	IV	--
58	1	16	02	1915	1330	(33	116.5)	V	--
59	1	17	02	1915	1100	(33	115.5)	IV	--
60	1	04	03	1915	1250	(33	116)	V	--
61	1	12	03	1915	1000	(33.5	116.5)	IV	--
62	7	30	04	1915	1020	(33	116.5)	V	--
63	1	11	05	1915	1145	(33	116.5)	V	--
64	1	06	09	1915	0220	(33	116.5)	IV	--
65	1	08	09	1915	2342	(32.5	117)	V	--
66	1	10	10	1915	0516	(34	117)	V	--
67	1	01	12	1915	1405	(34	117.5)	V	--
68	1	11	01	1916	0515	(33.5	116.5)	IV	--

Table 2.5-3
LISTING OF NONINSTRUMENTED EARTHQUAKES REPORTED WITHIN 80 KILOMETERS (50 MILES) OF THE SITE[a] (Sheet 6 of 12)

No.	Source[b]	Date (GMT)			Time (GMT)	Approximate Location[c]		Maximum Intensity[d]	Comments[e]
		(day)	(mo)	(yr)	(hr-min)	(lat)	(long.)		
69	1	25	02	1916	2330	(33.5	116.5)	IV	--
70	1	02	05	1916	1432	(34	118)	V	--
71	1	26	11	1916	1705	(33.5	116.5)	V	--
72	1	13	02	1917	1305	(34	118)	VI	--
73	1	19	05	1917	0635	(34	118)	V	--
74	1	20	05	1917	0945	(34	118)	V	--
75	1	28	05	1917	1017	(33	116.5)	V	--
76	1	31	05	1917	0435	(33.5	116.5)	V	--
77	1	02	06	1917	0435	(33.5	116.5)	V	--
78	1	11	06	1917	0354	(33	116.5)	V	--
79	1	22	06	1917	0405	(33	117.5)	IV	--
80	1	25	06	1917	0800	(34	118)	IV	--
81	1	26	06	1917	2315	(34	118)	IV	--
82	1	29	06	1917	0550	(34	118)	IV	--

Table 2.5-3
LISTING OF NONINSTRUMENTED EARTHQUAKES REPORTED WITHIN 80 KILOMETERS (50 MILES) OF THE SITE[(a)] (Sheet 7 of 12)

No.	Source[(b)]	Date (GMT)			Time (GMT)	Approximate Location[(c)]		Maximum Intensity[(d)]	Comments[(e)]
		(day)	(mo)	(yr)	(hr-min)	(lat)	(long.)		
83	1	30	06	1917	0000	(34	118)	IV	--
84	1	30	06	1917	2338	(34	118)	IV	--
85	1	17	07	1917	2315	(34	118)	IV	--
86	1	02	08	1917	0420	(33.5	116.5)	IV	--
87	1	19	08	1917	0710	(33	116.5)	V	--
88	1	05	03	1918	1106	(33.5	116.5)	IV	--
89	1	06	03	1918	1615	(33.5	116.5)	IV	--
90	1	21	03	1918	2325	(32.5	117)	V	--
91	1	30	03	1918	1605	(33.5	117.5)	VI	--
92	1, 2	22	04	1918	2315	(34	117.5)	VII	Dam
93	1	23	04	1918	1415	(33.5	117)	V	--
94	1	23	04	1918	1415	(33.5	117)	V	--
95	1	25	05	1918	0323	(33.5	117)	IV	--
96	1	26	40	1918	1730	(33.5	116.5)	IV	--

Table 2.5-3
LISTING OF NONINSTRUMENTED EARTHQUAKES REPORTED
WITHIN 80 KILOMETERS (50 MILES) OF THE SITE[a] (Sheet 8 of 12)

No.	Source[b]	Date (GMT)			Time (GMT)	Approximate Location[c]		Maximum Intensity[d]	Comments[e]
		(day)	(mo)	(yr)	(hr-min)	(lat)	(long.)		
97	1	27	04	1918	1000	(33.5	116.5)	IV	--
98	1	29	04	1918	0200	(33.5	117)	V	--
99	1	16	05	1918	1745	(33.5	117)	IV	--
100	1	28	05	1918	1230	(33.5	117)	IV	--
101	1, 2	06	06	1918	2232	33.5	117	VI	Dam, Lu, Ls
102	1	14	06	1918	1024	(33.5	117)	V	--
103	1	22	06	1918	0557	(32.5	117)	V	--
104	1	08	07	1918	0125	(33.5	117)	IV	--
105	1	08	01	1919	0407	(33.5	117)	IV	--
106	1	19	02	1919	0345	(32.5	117)	IV	--
107	1	21	03	1919	1100	34	117.5	IV	--
108	1	27	03	1919	0750	(33.5	117)	IV	--
109	1	24	06	1919	2112	(32.5	117)	IV	--
110	1, 2	01	01	1920	0235	33	117	VII	Dam

Table 2.5-3
LISTING OF NONINSTRUMENTED EARTHQUAKES REPORTED WITHIN 80 KILOMETERS (50 MILES) OF THE SITE[(a)] (Sheet 9 of 12)

No.	Source[(b)]	Date (GMT)			Time (GMT)	Approximate Location[(c)]		Maximum Intensity[(d)]	Comments[(e)]
		(day)	(mo)	(yr)	(hr-min)	(lat)	(long.)		
111	1	09	02	1920	1130	(33	116.5)	IV	--
112	1	22	02	1920	1610	(34	118.5)	VI	DAM
113	1	04	03	1920	0325	(34	118.5)	IV	--
114	1	20	05	1920	1330	(32.5	117)	V	--
115	1	11	07	1920	0525	(34	118)	IV	--
116	1	26	07	1920	1215	(34	118)	V	--
117	1	26	07	1921	1215	(34	118)	V	--
118	1	28	07	1920	1540	(34	117.5)	IV	
119	1	28	07	1920	1928	(34	118)	IV	--
120	1	29	07	1920	0300	(34	118)	IV	--
121	1	23	08	1920	2310	(34	118)	IV	--
122	1	10	09	1920	1415	(34	117.5)	IV	--
123	1	12	10	1920	1748	(33	116.5)	VII	--
124	1	18	12	1920	1726	(33.5	117)	V	--

Table 2.5-3
LISTING OF NONINSTRUMENTED EARTHQUAKES REPORTED WITHIN 80 KILOMETERS (50 MILES) OF THE SITE[a] (Sheet 10 of 12)

No.	Source[b]	Date (GMT)			Time (GMT)	Approximate Location[c]		Maximum Intensity[d]	Comments[e]
		(day)	(mo)	(yr)	(hr-min)	(lat)	(long.)		
125	1	09	01	1921	0530	(34	118)	VI	--
126	1	10	08	1921	1906	(33	116.5)	V	--
127	1	26	09	1921	2252	(34	117.5)	IV	--
128	1	05	02	1922	1915	(33	116.5)	V	--
129	1	06	02	1922	0234	(33	117)	IV	--
130	1	09	02	1922	0707	(33	116.5)	IV	--
131	1	13	04	1922	0412	(33.7	118)	IV	--
132	1	23	04	1923	2313	(34	117.5)	V	--
133	1	30	06	1923	0022	(34	117.5)	V	--
134	1	20	07	1923	0700	(33.2	117)	V	--
135	1	01	05	1925	0925	(33.8	118)	IV	--
136	1	22	10	1925	0932	(34	118)	IV	--
137	1, 2	03	04	1926	2008	34	116	IV	--
138	1	06	05	1926	0230	(32.5	117)	IV	--

Table 2.5-3
LISTING OF NONINSTRUMENTED EARTHQUAKES REPORTED
WITHIN 80 KILOMETERS (50 MILES) OF THE SITE[(a)] (Sheet 11 of 12)

No.	Source[(b)]	Date (GMT)			Time (GMT)	Approximate Location[(c)]		Maximum Intensity[(d)]	Comments[(e)]
		(day)	(mo)	(yr)	(hr-min)	(lat)	(long.)		
139	1	09	05	1926	0510	33.9	117.8	IV	--
140	1	04	11	1926	2238	(33.9	117.8)	VI	--
141	1	07	11	1926	1948	(33.9	117.8)	VI	--
142	1	09	11	1926	1535	(33.9	117.8)	VI	--
143	1	10	11	1926	1523	(33.9	117.8)	VI	--
144	1	16	04	1927	0448	(34.1	118)	IV	--
145	1	08	10	1927	1940	(33.9	117.2)	VI	--
146	1	07	11	1927	0328	(32.5	117)	IV	--
147	1	09	11	1927	1055	(32.5	117)	IV	--
148	3	04	05	1928	1922	(34	118)	(IV)	--
149	3	06	07	1928	0440	(32.5	117)	(IV)	--
150	3	08	07	1929	1646	34	118	VIII	Dam, Mag=4.7
151	3	13	09	1929	1323	(33.5	118.5)	(IV)	--
152	3	02	12	1929	1124	(32	116.5)	(V)	--

Table 2.5-3
LISTING OF NONINSTRUMENTED EARTHQUAKES REPORTED
WITHIN 80 KILOMETERS (50 MILES) OF THE SITE[(a)] (Sheet 12 or 12)

No.	Source[(b)]	Date (GMT)			Time (GMT)	Approximate Location[(c)]		Maximum Intensity[(d)]	Comments[(e)]
		(day)	(mo)	(yr)	(hr-min)	(lat)	(long.)		
153	3	27	01	1930	2026	(34	118)	(IV)	--
154	3	28	01	1931	0850	34	118.1	IV	--
155	3	28	01	1931	0850	34	118.1	IV	--
156	3	31	03	1931	2033	(33.9	117.8)	IV	--
157	3	24	04	1931	1828	33.5	118.3	V	--
158	3	23	06	1931	1654	(34.1	117.7)	(IV)	--
159	3	07	10	1931	0115	34	118.3	(IV)	--
160	3	03	11	1931	1605	33.7	118.3	V	--

(b) Earthquake catalog sources: 1. Townley and Allen, 1939; 2. Wood, Heck and Eppley, 1961; 3. Heck, Bodle, Newman and others, 1968; 4. Richter, 1958.

(c) Earthquakes listed are those which could reasonably have occurred within an 80-km/50-mi radius of the site. Locations without parentheses are those cited by the referenced catalog. Those with parentheses are approximated from catalog descriptions. All latitudes are north; all longitudes are west.

(d) Intensities listed refer to the Modified Mercalli (MM) Scale of 1931. In earlier catalogs, intensities are given in Rossi-Forel notation. These entries are converted to ME, herein. Intensities in parentheses are assigned from descriptions in cases where no intensity is given in the catalog.

(e) Abbreviations used in this column are as follows: Di, Diastrophism, Ts, Tsunami; Se, Seiche; Ls, Landslide; Liq, Liquefaction; Lu, Lurching; Dam, Damage to works of man; Mag, Estimated Richter Magnitude.

Table 2.5-4
LISTING OF INSTRUMENTAL EPICENTERS WITHIN AN 80-KILOMETER (50-MILE) RADIUS OF THE SITE, THROUGH JUNE 1980 (Sheet 1 of 44)

YEAR	MO	DA	HRMN	SEC	LATITUDE	LONGITUDE	DEPTH	MAG
1932	1	10	1539	27.40	33 32.00	-116 56.00	0.00	3.00
1932	1	14	1935	51.70	33 55.00	-118 2.00	0.00	3.00
1932	1	20	2021	35.70	33 25.00	-118 20.00	0.00	3.50
1932	1	31	1429	15.70	33 53.00	-118 19.00	0.00	3.50
1932	2	1	104	50.00	32 47.00	-118 20.00	0.00	3.00
1932	2	5	1644	17.90	34 3.00	-117 2.00	0.00	3.00
1932	2	7	1008	47.50	33 56.00	-118 23.00	0.00	3.00
1932	3	21	1045	0.00	33 54.00	-118 17.00	0.00	3.00
1932	4	6	1457	45.10	33 14.00	-116 44.00	0.00	3.00
1932	4	23	1338	28.00	34 5.00	-117 30.00	0.00	3.00
1932	5	2	232	27.00	33 30.00	-118 20.00	0.00	3.00
1932	5	2	232	43.00	33 30.00	-118 20.00	0.00	3.00
1932	5	6	102	28.50	33 55.00	-117 10.00	0.00	3.00
1932	5	29	1227	41.50	33 52.00	-118 9.00	0.00	3.00
1932	7	30	1931	8.00	33 55.00	-118 10.00	0.00	3.00
1932	8	30	250	24.80	34 5.00	-117 5.00	0.00	3.50
1932	9	24	638	0.00	34 2.00	-116 55.00	0.00	3.00
1932	10	6	856	0.00	33 17.00	-116 48.00	0.00	3.50
1932	10	19	320	0.00	33 50.00	-117 40.00	0.00	3.00
1932	11	1	445	0.00	34 0.00	-11 15.00	0.00	4.00
1932	11	14	1709	0.00	34 0.00	-118 0.00	0.00	3.00
1932	11	16	947	0.00	33 35.00	-116 55.00	0.00	3.00
1932	11	16	1852	0.00	33 58.00	-118 3.00	0.00	3.50
1932	12	6	1807	0.00	33 55.00	-118 7.00	0.00	3.00
1932	12	9	1304	0.00	33 30.00	-116 55.00	0.00	3.50
1932	12	14	1913	0.00	33 38.00	-118 12.00	0.00	3.00
1932	12	14	1916	0.00	33 38.00	-118 12.00	0.00	3.00

Table 2.5-4
LISTING OF INSTRUMENTAL EPICENTERS WITHIN AN 80-KILOMETER (50-MILE) RADIUS OF THE SITE, THROUGH JUNE 1980 (Sheet 2 of 44)

YEAR	MO	DA	HRMN	SEC	LATITUDE	LONGITUDE	DEPTH	MAG
1933	1	25	1444	0.00	33 55.00	-116 45.00	0.00	4.00
1933	1	31	1956	0.00	33 40.00	-118 20.00	0.00	3.00
1933	1	31	2031	0.00	33 30.00	-116 45.00	0.00	3.50
1933	3	8	1058	0.00	33 30.00	-116 45.00	0.00	3.50
1933	3	11	154	7.80	33 37.00	-117 58.00	0.00	6.30
1933	3	11	204	0.00	33 45.00	-118 5.00	0.00	4.90
1933	3	11	205	0.00	33 45.00	-118 5.00	0.00	4.30
1933	3	11	209	0.00	33 45.00	-118 5.00	0.00	5.00
1933	3	11	210	0.00	33 45.00	-118 5.00	0.00	4.60
1933	3	11	211	0.00	33 45.00	-118 5.00	0.00	4.40
1933	3	11	216	0.00	33 45.00	-118 5.00	0.00	4.80
1933	3	11	217	0.00	33 36.00	-118 0.00	0.00	4.50
1933	3	11	222	0.00	33 45.00	-118 5.00	0.00	4.00
1933	3	11	227	0.00	33 45.00	-118 5.00	0.00	4.60
1933	3	11	230	0.00	33 45.00	-118 5.00	0.00	5.10
1933	3	11	231	0.00	33 36.00	-118 0.00	0.00	4.40
1933	3	11	244	0.00	33 45.00	-118 5.00	0.00	3.90
1933	3	11	252	0.00	33 45.00	-118 5.00	0.00	4.00
1933	3	11	257	0.00	33 45.00	-118 5.00	0.00	4.20
1933	3	11	258	0.00	33 45.00	-118 5.00	0.00	4.00
1933	3	11	259	0.00	33 45.00	-118 5.00	0.00	4.60
1933	3	11	305	0.00	33 45.00	-118 5.00	0.00	4.20
1933	3	11	309	0.00	33 45.00	-118 5.00	0.00	4.40
1933	3	11	311	0.00	33 45.00	-118 5.00	0.00	4.20
1933	3	11	323	0.00	33 45.00	-118 5.00	0.00	5.00
1933	3	11	328	0.00	33 45.00	-118 5.00	0.00	3.60
1933	3	11	332	0.00	33 45.00	-118 5.00	0.00	3.80
1933	3	11	333	0.00	33 45.00	-118 5.00	0.00	3.90
1933	3	11	336	0.00	33 45.00	-118 5.00	0.00	4.00
1933	3	11	339	0.00	33 45.00	-118 5.00	0.00	4.00

Table 2.5-4
LISTING OF INSTRUMENTAL EPICENTERS WITHIN AN 80-KILOMETER (50-MILE) RADIUS OF THE SITE, THROUGH JUNE 1980 (Sheet 3 of 44)

YEAR	MO	DA	HRMN	SEC	LATITUDE	LONGITUDE	DEPTH	MAG
1933	3	11	343	0.00	33 45.00	-118 5.00	0.00	3.60
1933	3	11	347	0.00	33 45.00	-118 5.00	0.00	4.10
1933	3	11	351	0.00	33 45.00	-118 5.00	0.00	3.80
1933	3	11	358	0.00	33 45.00	-114 5.00	0.00	3.60
1933	3	11	409	0.00	33 45.00	-118 5.00	0.00	3.70
1933	3	11	431	0.00	33 45.00	-118 5.00	0.00	3.70
1933	3	11	436	0.00	33 45.00	-118 5.00	0.00	4.60
1933	3	11	438	0.00	33 45.00	-118 5.00	0.00	3.90
1933	3	11	439	0.00	33 45.00	-118 5.00	0.00	4.90
1933	3	11	440	0.00	33 45.00	-118 5.00	0.00	4.70
1933	3	11	444	0.00	33 45.00	-118 5.00	0.00	3.60
1933	3	11	453	0.00	33 45.00	-118 5.00	0.00	3.70
1933	3	11	456	0.00	33 45.00	-118 5.00	0.00	3.60
1933	3	11	459	0.00	33 45.00	-118 5.00	0.00	3.70
1933	3	11	510	22.00	33 42.00	-118 4.00	0.00	5.10
1933	3	11	513	0.00	33 45.00	-118 5.00	0.00	4.70
1933	3	11	515	0.00	33 45.00	-118 5.00	0.00	4.00
1933	3	11	518	4.00	33 34.50	-117 59.00	0.00	5.20
1933	3	11	521	0.00	33 45.00	-118 5.00	0.00	4.40
1933	3	11	524	0.00	33 45.00	-118 5.00	0.00	4.20
1933	3	11	553	0.00	33 45.00	-118 5.00	0.00	4.00
1933	3	11	555	0.00	33 45.00	-118 5.00	0.00	4.00
1933	3	11	559	0.00	33 45.00	-118 5.00	0.00	3.90
1933	3	11	601	0.00	33 45.00	-118 5.00	0.00	3.60
1933	3	11	611	0.00	33 45.00	-118 5.00	0.00	4.40
1933	3	11	618	0.00	33 45.00	-118 5.00	0.00	4.20
1933	3	11	628	0.00	33 45.00	-118 5.00	0.00	3.60
1933	3	11	629	0.00	33 51.00	-118 16.00	0.00	4.40
1933	3	11	635	0.00	33 45.00	-118 5.00	0.00	4.20
1933	3	11	658	3.00	33 41.00	-118 3.00	0.00	5.50

Table 2.5-4
LISTING OF INSTRUMENTAL EPICENTERS WITHIN AN 80-KILOMETER (50-MILE) RADIUS OF THE SITE, THROUGH JUNE 1980 (Sheet 4 of 44)

YEAR	MO	DA	HRMN	SEC	LATITUDE	LONGITUDE	DEPTH	MAG
1933	3	11	702	0.00	33 45.00	-118 5.00	0.00	3.60
1933	3	11	727	0.00	33 45.00	-118 5.00	0.00	3.60
1933	3	11	751	0.00	33 45.00	-118 5.00	0.00	4.20
1933	3	11	759	0.00	33 45.00	-118 5.00	0.00	4.10
1933	3	11	808	0.00	33 45.00	-118 5.00	0.00	4.50
1933	3	11	810	0.00	33 45.00	-118 5.00	0.00	3.80
1933	3	11	822	0.00	33 45.00	-118 5.00	0.00	3.70
1933	3	11	832	0.00	33 45.00	-118 5.00	0.00	4.20
1933	3	11	837	0.00	33 45.00	-118 5.00	0.00	4.00
1933	3	11	852	0.00	33 45.00	-118 5.00	0.00	3.70
1933	3	11	854	57.00	33 42.00	-118 4.00	0.00	5.10
1933	3	11	910	0.00	33 45.00	-118 5.00	0.00	5.10
1933	3	11	911	0.00	33 45.00	-118 5.00	0.00	4.40
1933	3	11	922	0.00	33 45.00	-118 5.00	0.00	3.90
1933	3	11	926	0.00	33 45.00	-118 5.00	0.00	4.10
1933	3	11	936	0.00	33 45.00	-118 5.00	0.00	3.60
1933	3	11	945	0.00	33 45.00	-118 5.00	0.00	3.90
1933	3	11	1011	0.00	33 45.00	-118 5.00	0.00	3.60
1933	3	11	1015	0.00	33 45.00	-118 5.00	0.00	3.60
1933	3	11	1019	0.00	33 45.00	-118 5.00	0.00	3.70
1933	3	11	1025	0.00	33 45.00	-118 5.00	0.00	4.00
1933	3	11	1045	0.00	33 45.00	-118 5.00	0.00	4.00
1933	3	11	1100	0.00	33 45.00	-118 5.00	0.00	4.00
1933	3	11	1104	0.00	33 45.00	-118 8.00	0.00	4.60
1933	3	11	1129	0.00	33 45.00	-118 5.00	0.00	4.00
1933	3	11	1136	0.00	33 45.00	-118 5.00	0.00	4.00
1933	3	11	1141	0.00	33 45.00	-118 5.00	0.00	4.20

Table 2.5-4
LISTING OF INSTRUMENTAL EPICENTERS WITHIN AN 80-KILOMETER (50-MILE) RADIUS OF THE SITE, THROUGH JUNE 1980 (Sheet 5 of 44)

YEAR	MO	DA	HRMN	SEC	LATITUDE	LONGITUDE	DEPTH	MAG
1933	3	11	1147	0.00	33 45.00	-118 5.00	0.00	4.40
1933	3	11	1244	0.00	33 45.00	-118 5.00	0.00	3.90
1933	3	11	1250	0.00	33 41.00	-118 3.00	0.00	4.40
1933	3	11	1259	0.00	33 45.00	-118 5.00	0.00	3.70
1933	3	11	1303	0.00	33 45.00	-118 5.00	0.00	3.90
1933	3	11	1330	0.00	33 45.00	-118 5.00	0.00	3.60
1933	3	11	1350	0.00	33 44.00	-118 6.00	0.00	4.40
1933	3	11	1357	0.00	33 45.00	-115 5.00	0.00	4.00
1933	3	11	1403	0.00	33 45.00	-118 5.00	0.00	3.60
1933	3	11	1414	0.00	33 45.00	-118 5.00	0.00	3.70
1933	3	11	1425	0.00	33 51.00	-118 16.00	0.00	5.00
1933	3	11	1428	0.00	33 45.00	-116 5.00	0.00	3.90
1933	3	11	1447	0.00	33 44.00	-118 6.00	0.00	4.40
1933	3	11	1457	0.00	33 53.00	-118 19.00	0.00	4.90
1933	3	11	1509	0.00	33 44.00	-118 6.00	0.00	4.40
1933	3	11	1536	0.00	33 45.00	-118 5.00	0.00	3.90
1933	3	11	1547	0.00	33 45.00	-118 5.00	0.00	4.00
1933	3	11	1653	0.00	33 45.00	-118 5.00	0.00	4.80
1933	3	11	1757	0.00	33 45.00	-118 5.00	0.00	3.80
1933	3	11	1804	0.00	33 45.00	-118 5.00	0.00	3.70
1933	3	11	1843	0.00	33 45.00	-118 5.00	0.00	3.70
1933	3	11	1944	0.00	33 45.00	-118 5.00	0.00	4.00
1933	3	11	1956	0.00	33 45.00	-118 5.00	0.00	4.20
1933	3	11	2200	0.00	33 45.00	-118 5.00	0.00	4.40
1933	3	11	2231	0.00	33 45.00	-118 5.00	0.00	4.40
1933	3	11	2232	0.00	33 45.00	-118 5.00	0.00	4.10
1933	3	11	2240	0.00	33 45.00	-118 5.00	0.00	4.40
1933	3	11	2248	0.00	33 45.00	-118 5.00	0.00	3.80
1933	3	11	2305	0.00	33 45.00	-118 5.00	0.00	4.20

Table 2.5-4
LISTING OF INSTRUMENTAL EPICENTERS WITHIN AN 80-KILOMETER (50-MILE) RADIUS OF THE SITE, THROUGH JUNE 1980 (Sheet 6 of 44)

YEAR	MO	DA	HRMN	SEC	LATITUDE	LONGITUDE	DEPTH	MAG
1933	3	12	27	0.00	33 45.00	-118 5.00	0.00	4.40
1933	3	12	34	0.00	33 45.00	-118 5.00	0.00	4.00
1933	3	12	105	0.00	33 45.00	-118 5.00	0.00	3.80
1933	3	12	314	0.00	33 45.00	-118 5.00	0.00	3.70
1933	3	12	448	0.00	33 45.00	-118 5.00	0.00	4.00
1933	3	12	546	0.00	33 45.00	-118 5.00	0.00	4.40
1933	3	12	601	0.00	33 45.00	-119 5.00	0.00	4.20
1933	3	12	616	0.00	33 45.00	-118 5.00	0.00	4.60
1933	3	12	654	0.00	33 45.00	-118 5.00	0.00	3.80
1933	3	12	740	0.00	33 45.00	-118 5.00	0.00	4.20
1933	3	12	835	0.00	33 45.00	-118 5.00	0.00	4.20
1933	3	12	1035	0.00	33 45.00	-118 5.00	0.00	3.70
1933	3	12	1200	0.00	33 45.00	-118 5.00	0.00	3.80
1933	3	12	1502	0.00	33 45.00	-118 5.00	0.00	4.20
1933	3	12	1504	0.00	33 45.00	-118 5.00	0.00	3.70
1933	3	12	1651	0.00	33 45.00	-118 5.00	0.00	4.00
1933	3	12	1738	0.00	33 45.00	-118 5.00	0.00	4.50
1933	3	12	1825	0.00	33 45.00	-116 5.00	0.00	4.10
1933	3	12	2128	0.00	33 45.00	-118 5.00	0.00	4.10
1933	3	12	2228	0.00	33 45.00	-118 5.00	0.00	3.70
1933	3	12	2354	0.00	33 45.00	-118 5.00	0.00	4.50
1933	3	13	343	0.00	33 45.00	-118 5.00	0.00	4.10
1933	3	13	432	0.00	33 45.00	-118 5.00	0.00	4.70
1933	3	13	439	0.00	33 45.00	-118 5.00	0.00	3.70
1933	3	13	554	0.00	33 45.00	-118 5.00	0.00	3.60
1933	3	13	617	0.00	33 45.00	-118 5.00	0.00	4.00
1933	3	13	1318	28.00	33 45.00	-118 5.00	0.00	5.30
1933	3	13	1532	0.00	33 45.00	-118 5.00	0.00	4.10

Table 2.5-4
LISTING OF INSTRUMENTAL EPICENTERS WITHIN AN 80-KILOMETER (50-MILE) RADIUS OF THE SITE, THROUGH JUNE 1980 (Sheet 7 of 44)

YEAR	MO	DA	HRMN	SEC	LATITUDE	LONGITUDE	DEPTH	MAG
1933	3	13	1929	0.00	33 45.00	-118 5.00	0.00	4.20
1933	3	13	2131	0.00	33 45.00	-118 5.00	0.00	3.70
1933	3	14	36	0.00	33 45.00	-118 5.00	0.00	4.20
1933	3	14	1219	0.00	33 45.00	-118 5.00	0.00	4.50
1933	3	14	1453	0.00	33 45.00	-118 5.00	0.00	3.90
1933	3	14	1901	50.00	33 37.00	-118 1.00	0.00	5.10
1933	3	14	2003	0.00	33 45.00	-118 5.00	0.00	3.70
1933	3	14	2224	0.00	33 45.00	-118 5.00	0.00	3.80
1933	3	14	2242	0.00	33 45.00	-118 5.00	0.00	4.10
1933	3	15	208	0.00	33 45.00	-119 5.00	0.00	4.10
1933	3	15	432	0.00	33 45.00	-118 5.00	0.00	4.10
1933	3	15	434	0.00	33 45.00	-118 5.00	0.00	3.80
1933	3	15	540	0.00	33 45.00	-118 5.00	0.00	4.20
1933	3	15	924	0.00	33 45.00	-118 5.00	0.00	3.80
1933	3	15	1113	32.00	33 37.00	-118 1.00	0.00	4.90
1933	3	16	1456	0.00	33 45.00	-118 5.00	0.00	4.00
1933	3	16	1529	0.00	33 45.00	-118 5.00	0.00	4.20
1933	3	16	1530	0.00	33 45.00	-118 5.00	0.00	4.10
1933	3	17	1651	0.00	33 45.00	-118 5.00	0.00	4.10
1933	3	18	2052	0.00	33 45.00	-118 5.00	0.00	4.20
1933	3	19	553	0.00	33 45.00	-118 5.00	0.00	3.70
1933	3	19	2123	0.00	33 45.00	-118 5.00	0.00	4.20
1933	3	20	1358	0.00	33 45.00	-118 5.00	0.00	4.10
1933	3	21	326	0.00	33 45.00	-118 5.00	0.00	4.10
1933	3	23	840	0.00	33 45.00	-118 5.00	0.00	4.10
1933	3	23	1604	0.00	33 45.00	-118 5.00	0.00	3.90
1933	3	23	1831	0.00	33 45.00	-118 5.00	0.00	4.10
1933	3	24	513	0.00	33 45.00	-118 5.00	0.00	3.70
1933	3	24	1513	0.00	33 45.00	-118 5.00	0.00	3.60
1933	3	25	1346	0.00	33 45.00	-118 5.00	0.00	4.10

Table 2.5-4
LISTING OF INSTRUMENTAL EPICENTERS WITHIN AN 80-KILOMETER (50-MILE) RADIUS OF THE SITE, THROUGH JUNE 1980 (Sheet 8 of 44)

YEAR	MO	DA	HRMN	SEC	LATITUDE	LONGITUDE	DEPTH	MAG
1933	3	30	1225	0.00	33 45.00	-118 5.00	0.00	4.40
1933	3	31	1049	0.00	33 45.00	-118 5.00	0.00	4.10
1933	4	1	642	0.00	33 45.00	-118 5.00	0.00	4.20
1933	4	2	800	0.00	33 45.00	-118 5.00	0.00	4.00
1933	4	2	1536	0.00	33 45.00	-118 5.00	0.00	4.00
1933	4	5	2037	0.00	33 45.00	-118 5.00	0.00	3.80
1933	4	6	1145	0.00	33 45.00	-118 5.00	0.00	3.90
1933	4	6	1157	14.00	33 51.00	-118 13.00	0.00	3.70
1933	4	7	624	0.00	33 45.00	-118 5.00	0.00	3.70
1933	4	13	710	0.00	33 45.00	-118 5.00	0.00	3.20
1933	4	19	1417	0.00	33 50.00	-118 10.00	0.00	3.30
1933	4	29	1004	0.00	33 45.00	-118 5.00	0.00	3.60
1933	4	29	1500	0.00	33 50.00	-118 10.00	0.00	3.90
1933	5	9	2103	16.00	33 51.00	-115 2.00	0.00	3.90
1933	5	16	2058	55.00	33 45.00	-118 10.00	0.00	4.00
1933	6	3	2319	0.00	33 30.00	-118 0.00	0.00	3.00
1933	6	4	1002	0.00	33 48.00	-118 12.00	0.00	3.00
1933	6	5	1830	0.00	33 30.00	-118 12.00	0.00	3.50
1933	6	5	1950	0.00	33 45.00	-118 10.00	0.00	3.00
1933	6	6	232	57.00	33 46.00	-117 56.00	0.00	3.30
1933	6	7	721	58.00	33 38.00	-117 56.00	0.00	3.30
1933	6	11	628	54.00	33 47.00	-117 56.00	0.00	3.20
1933	6	20	1004	8.00	33 43.00	-118 4.00	0.00	3.00
1933	6	20	1614	13.00	33 46.00	-118 9.00	0.00	3.00
1933	6	30	2321	45.00	33 44.00	-118 7.00	0.00	3.40
1933	7	1	152	51.00	33 44.00	-118 7.00	0.00	3.00
1933	7	17	429	56.00	33 46.00	-118 11.00	0.00	3.00

Table 2.5-4
LISTING OF INSTRUMENTAL EPICENTERS WITHIN AN 80-KILOMETER (50-MILE) RADIUS OF THE SITE, THROUGH JUNE 1980 (Sheet 9 of 44)

YEAR	MO	DA	HRMN	SEC	LATITUDE	LONGITUDE	DEPTH	MAG
1933	7	23	2300	2.00	33 23.00	-116 59.00	0.00	3.20
1933	8	4	417	48.00	33 45.00	-118 11.00	0.00	4.00
1933	8	4	845	0.00	33 45.00	-118 11.00	0.00	3.60
1933	8	12	1647	37.00	33 51.00	-118 5.00	0.00	3.10
1933	8	29	416	34.00	33 52.00	-118 4.00	0.00	3.50
1933	9	9	359	21.00	33 37.00	-118 2.00	0.00	3.00
1933	9	9	1353	18.00	33 38.00	-117 20.00	0.00	3.00
1933	9	16	2211	54.00	33 16.00	-116 52.00	0.00	3.20
1933	9	25	39	2.00	33 40.00	-117 50.00	0.00	3.00
1933	9	27	607	5.00	33 49.00	-118 10.00	0.00	3.00
1933	10	2	910	17.60	33 47.00	-118 8.00	0.00	5.40
1933	10	2	923	0.00	33 50.00	-118 18.00	0.00	3.80
1933	10	2	931	54.00	33 46.00	-118 9.00	0.00	3.30
1933	10	2	937	22.00	33 52.00	-118 16.00	0.00	3.10
1933	10	2	1033	17.00	33 50.00	-118 18.00	0.00	3.40
1933	10	2	1326	1.00	33 37.00	-118 1.00	0.00	4.00
1933	10	2	1436	31.00	33 48.00	-118 3.00	0.00	3.30
1933	10	2	1541	40.00	33 49.00	-118 13.00	0.00	3.20
1933	10	2	1611	14.00	33 48.00	-118 14.00	0.00	3.30
1933	10	2	1730	4.00	33 52.00	-118 16.00	0.00	3.50
1933	10	2	2155	54.00	33 52.00	-118 13.00	0.00	3.10
1933	10	3	554	31.00	33 46.00	-118 11.00	0.00	3.00
1933	10	3	2222	51.00	33 55.00	-118 3.00	0.00	3.00
1933	10	5	1045	7.00	33 55.00	-117 21.00	0.00	3.70
1933	10	5	2020	22.00	33 30.00	-116 52.00	0.00	3.00
1933	10	5	2035	44.00	33 46.00	-118 16.00	0.00	3.50
1933	10	6	145	23.00	33 48.00	-118 13.00	0.00	3.00
1933	10	7	1914	31.00	33 48.00	-118 13.00	0.00	3.00
1933	10	9	1556	8.00	33 49.00	-118 10.00	0.00	3.60
1933	10	21	406	11.00	33 30.00	-116 56.00	0.00	3.30
1933	10	25	700	46.00	33 57.00	-118 8.00	0.00	4.30

Table 2.5-4
LISTING OF INSTRUMENTAL EPICENTERS WITHIN AN 80-KILOMETER (50-MILE) RADIUS OF THE SITE, THROUGH JUNE 1980 (Sheet 10 of 44)

YEAR	MO	DA	HRMN	SEC	LATITUDE	LONGITUDE	DEPTH	MAG
1933	11	13	2128	0.00	33 52.00	-118 12.00	0.00	4.00
1933	11	16	1014	0.00	33 47.00	-118 8.00	0.00	3.00
1933	11	18	1333	0.00	33 37.00	-118 2.00	0.00	3.00
1933	11	20	843	0.00	33 46.00	-118 7.00	0.00	3.50
1933	11	20	1032	0.00	33 47.00	-118 8.00	0.00	4.00
1933	11	20	1202	0.00	33 47.00	-118 8.00	0.00	3.00
1933	11	20	1327	0.00	33 47.00	-118 8.00	0.00	3.00
1933	11	20	1351	0.00	33 47.00	-118 8.00	0.00	3.00
1933	11	21	2248	0.00	33 47.00	-118 8.00	0.00	3.00
1933	12	6	1501	0.00	33 51.00	-116 57.00	0.00	3.50
1933	12	15	848	0.00	33 46.00	-118 8.00	0.00	3.00
1933	12	15	2316	0.00	33 37.00	-118 2.00	0.00	3.00
1933	12	28	18	0.00	33 47.00	-118 8.00	0.00	3.00
1933	12	30	1758	0.00	33 47.00	-118 8.00	0.00	3.50
1934	1	5	2308	0.00	33 58.00	-118 9.00	0.00	3.00
1934	1	13	2226	0.00	33 30.00	-116 55.00	0.00	3.50
1934	1	14	1252	0.00	33 34.00	-117 59.00	0.00	3.00
1934	1	20	2117	0.00	33 37.00	-118 7.00	0.00	4.50
1934	1	26	2309	0.00	33 35.00	-118 10.00	0.00	3.00
1934	2	4	220	0.00	33 47.00	-118 8.00	0.00	3.50
1934	2	11	2104	0.00	33 58.00	-117 35.00	0.00	3.00
1934	2	14	1742	0.00	33 46.00	-117 47.00	0.00	3.20
1934	2	16	2336	0.00	33 25.00	-117 10.00	0.00	3.00
1934	3	3	1505	0.00	33 37.00	-118 2.00	0.00	3.50
1934	3	3	2045	0.00	33 38.00	-118 12.00	0.00	3.00
1934	3	5	2203	0.00	33 0.00	-118 23.00	0.00	3.00

Table 2.5-4
LISTING OF INSTRUMENTAL EPICENTERS WITHIN AN 80-KILOMETER (50-MILE) RADIUS OF THE SITE, THROUGH JUNE 1980 (Sheet 11 of 44)

YEAR	MO	DA	HRMN	SEC	LATITUDE	LONGITUDE	DEPTH	MAG
1934	4	7	336	0.00	33 42.00	-118 7.00	0.00	3.00
1934	4	8	1014	0.00	33 30.00	-116 55.00	0.00	3.00
1934	4	8	1415	0.00	33 46.00	-117 47.00	0.00	3.00
1934	4	17	1833	0.00	33 34.00	-117 59.00	0.00	4.00
1934	4	20	738	0.00	33 47.00	-118 8.00	0.00	3.00
1934	5	10	248	0.00	33 47.00	-118 8.00	0.00	3.00
1934	5	20	943	0.00	34 4.00	-116 44.00	0.00	3.50
1934	5	23	2222	0.00	33 55.00	-118 20.00	0.00	3.00
1934	6	9	1250	0.00	33 47.00	-116 8.00	0.00	3.00
1934	6	22	224	0.00	33 34.00	-117 59.00	0.00	3.00
1934	6	28	15	0.00	33 47.00	-118 8.00	0.00	3.00
1934	7	22	718	0.00	33 37.00	-116 50.00	0.00	3.00
1934	8	27	1236	0.00	33 57.00	-117 39.00	0.00	3.00
1934	8	30	1250	0.00	34 4.00	-117 35.00	0.00	3.50
1934	9	13	1036	0.00	33 34.00	-117 59.00	0.00	3.50
1934	10	1	2015	0.00	33 42.00	-117 50.00	0.00	3.00
1934	10	2	1425	0.00	33 57.00	-117 33.00	0.00	3.00
1934	10	17	938	0.00	33 38.00	-118 24.00	0.00	4.00
1934	10	18	1007	0.00	33 46.00	-118 6.00	0.00	3.00
1934	10	23	1817	0.00	33 46.00	-118 6.00	0.00	3.00
1934	10	24	456	0.00	32 53.00	-118 15.00	0.00	3.00
1934	10	27	2146	0.00	33 47.00	-118 8.00	0.00	3.00
1934	10	28	547	0.00	33 23.00	-117 5.00	0.00	3.00
1934	10	30	451	0.00	33 30.00	-116 55.00	0.00	3.00
1934	11	5	238	0.00	33 47.00	-118 8.00	0.00	3.50
1934	11	13	2041	0.00	33 40.00	-117 15.00	0.00	3.00
1934	11	14	2130	0.00	33 11.00	-117 30.00	0.00	3.50
1934	11	16	2126	0.00	33 45.00	-118 0.00	0.00	4.00
1934	11	21	2249	0.00	33 42.00	-118 4.00	0.00	3.00
1934	11	26	23	0.00	33 50.00	-117 24.00	0.00	3.00

Table 2.5-4
LISTING OF INSTRUMENTAL EPICENTERS WITHIN AN 80-KILOMETER (50-MILE) RADIUS OF THE SITE, THROUGH JUNE 1980 (Sheet 12 of 44)

YEAR	MO	DA	HRMN	SEC	LATITUDE	LONGITUDE	DEPTH	MAG
1934	12	21	1224	0.00	33 42.00	-116 59.00	0.00	3.00
1934	12	27	1341	0.00	34 2.00	-117 19.00	0.00	3.00
1935	1	1	158	0.00	33 34.00	-117 59.00	0.00	3.50
1935	1	1	1322	0.00	33 56.00	-116 45.00	0.00	3.50
1935	1	22	928	0.00	33 53.00	-118 9.00	0.00	3.50
1935	1	23	306	0.00	34 1.00	-117 25.00	0.00	3.50
1935	2	14	2230	0.00	33 42.00	-118 4.00	0.00	3.50
1935	3	5	2152	0.00	33 52.00	-116 52.00	0.00	3.00
1935	3	7	2017	0.00	33 47.00	-118 8.00	0.00	3.50
1935	3	10	616	0.00	33 58.00	-116 45.00	0.00	3.00
1935	3	12	1351	0.00	33 45.00	-116 52.00	0.00	3.00
1935	3	15	225	0.00	33 40.00	-117 17.00	0.00	3.50
1935	4	19	839	0.00	34 2.00	-117 19.00	0.00	3.00
1935	4	23	226	0.00	33 57.00	-117 39.00	0.00	3.00
1935	5	14	714	0.00	33 53.0	-117 50.00	0.00	3.00
1935	5	15	1911	0.00	33 47.00	-118 8.00	0.00	3.00
1935	6	7	1633	0.00	33 16.00	-117 1.00	0.00	4.00
1935	6	15	826	0.00	33 34.00	-117 59.00	0.00	3.00
1935	6	19	1117	0.00	33 43.00	-117 31.00	0.00	4.00
1935	6	19	1121	0.00	33 43.00	-117 31.00	0.00	3.50
1935	6	19	1234	0.00	33 43.00	-117 31.00	0.00	3.00
1935	6	23	1816	0.00	33 43.00	-117 31.00	0.00	3.50
1935	6	23	2141	0.00	33 43.00	-117 31.00	0.00	3.00
1935	6	25	1708	0.00	33 43.00	-117 31.00	0.00	3.00
1935	7	15	629	0.00	33 32.00	-117 9.00	0.00	3.50
1935	7	15	1002	0.00	33 30.00	-116 55.00	0.00	3.00
1935	7	21	2208	0.00	33 37.00	-118 2.00	0.00	3.00

Table 2.5-4
LISTING OF INSTRUMENTAL EPICENTERS WITHIN AN 80-KILOMETER (50-MILE) RADIUS OF THE SITE, THROUGH JUNE 1980 (Sheet 13 of 44)

YEAR	MO	DA	HRMN	SEC	LATITUDE	LONGITUDE	DEPTH	MAG
1935	8	8	330	0.00	34 2.00	-117 48.00	0.00	3.00
1935	8	8	1547	0.00	33 52.00	-117 3.00	0.00	3.00
1935	8	23	836	0.00	33 52.00	-117 3.00	0.00	3.00
1935	9	2	344	0.00	33 30.00	-116 55.00	0.00	3.00
1935	9	3	647	0.00	34 2.00	-117 19.00	0.00	4.50
1935	9	15	2051	0.00	33 42.00	-118 4.00	0.00	3.00
1935	9	16	1228	0.00	33 45.00	-117 55.00	0.00	3.50
1935	9	17	513	0.00	33 55.00	-117 31.00	0.00	3.00
1935	10	24	1727	0.00	34 5.00	-117 25.00	0.00	3.00
1935	11	4	355	0.00	33 30.00	-116 55.00	0.00	4.50
1935	11	4	547	0.00	33 30.00	-116 55.00	0.00	3.00
1935	11	4	657	0.00	33 30.00	-116 55.00	0.00	3.00
1935	11	4	714	0.00	33 30.00	-116 55.00	0.00	3.00
1935	11	4	911	0.00	33 30.00	-116 55.00	0.00	3.00
1935	11	8	1002	0.00	33 30.00	-116 55.00	0.00	3.00
1935	11	10	21	0.00	33 30.00	-116 55.00	0.00	3.00
1935	11	11	1544	0.00	33 30.00	-116 55.00	0.00	3.00
1935	11	12	1145	0.00	33 30.00	-116 55.00	0.00	3.00
1935	11	12	1346	0.00	33 30.00	-116 55.00	0.00	3.00
1935	11	16	259	0.00	33 50.00	-117 40.00	0.00	3.00
1935	11	16	846	0.00	33 29.00	-118 18.00	0.00	3.00
1935	11	19	2205	0.00	33 30.00	-116 55.00	0.00	3.00
1935	11	20	1616	0.00	33 30.00	-116 55.00	0.00	3.00
1935	11	24	12	0.00	33 40.00	-117 50.00	0.00	3.00
1935	11	24	2352	0.00	33 30.00	-116 55.00	0.00	3.00
1935	11	26	1200	0.00	33 30.00	-116 55.00	0.00	3.00
1935	11	27	928	0.00	33 39.00	-117 4.00	0.00	3.50
1935	11	27	1413	0.00	33 39.00	-117 4.00	0.00	3.00
1935	12	1	1902	0.00	34 5.00	-117 30.00	0.00	3.00
1935	12	1	2353	0.00	34 4.00	-117 34.00	0.00	3.00

Table 2.5-4
LISTING OF INSTRUMENTAL EPICENTERS WITHIN AN 80-KILOMETER (50-MILE) RADIUS OF THE SITE, THROUGH JUNE 1980 (Sheet 14 of 44)

YEAR	MO	DA	HRMN	SEC	LATITUDE	LONGITUDE	DEPTH	MAG
1935	12	19	1708	0.00	33 46.00	-118 7.00	0.00	3.00
1935	12	25	1715	0.00	33 36.00	-118 1.00	0.00	4.50
1936	1	1	1557	0.00	33 37.00	-118 2.00	0.00	3.00
1936	2	1	501	0.00	33 30.00	-116 55.00	0.00	3.00
1936	2	3	2136	0.00	33 37.00	-117 27.00	0.00	3.00
1936	2	5	2109	0.00	33 30.00	-116 55.00	0.00	3.00
1936	2	10	946	0.00	33 30.00	-116 55.00	0.00	3.00
1936	3	1	1927	54.08	33 57.30	-118 14.56	10.00	3.50
1936	3	1	1942	0.00	33 59.00	-118 18.00	0.00	3.50
1936	3	11	2238	0.00	33 33.00	-118 21.00	0.00	3.00
1936	3	17	1227	0.00	33 30.00	-116 55.00	0.00	3.00
1936	3	19	1639	0.00	33 30.00	-116 55.00	0.00	3.50
1936	4	5	2334	0.00	33 50.00	-118 9.00	0.00	3.00
1936	4	9	1317	0.00	33 56.00	-116 45.00	0.00	3.00
1936	4	19	1617	0.00	33 46.00	-118 10.00	0.00	3.00
1936	4	28	236	0.00	32 53.00	-118 15.00	0.00	3.00
1936	5	12	1206	0.00	33 30.00	-116 55.00	0.00	3.00
1936	5	16	1337	0.00	34 3.00	-117 17.00	0.00	3.00
1936	5	23	34	0.00	33 56.00	-116 45.00	0.00	3.00
1936	6	1	221	0.00	33 37.00	-118 2.00	0.00	3.00
1936	6	11	1204	0.00	33 25.00	-118 10.00	0.00	3.00
1936	6	21	1419	22.57	33 29.97	-116 49.60	10.00	3.50
1936	7	14	1839	0.00	33 37.00	-118 2.00	0.00	3.00
1936	7	22	706	0.00	33 58.00	-117 34.00	0.00	3.00
1936	7	25	902	0.00	33 34.00	-117 59.00	0.00	3.00
1936	7	29	1422	52.79	33 27.25	-116 53.90	10.00	4.00
1936	8	1	807	0.00	33 50.00	-117 24.00	0.00	3.00

Table 2.5-4
LISTING OF INSTRUMENTAL EPICENTERS WITHIN AN 80-KILOMETER (50-MILE) RADIUS OF THE SITE, THROUGH JUNE 1980 (Sheet 15 of 44)

YEAR	MO	DA	HRMN	SEC	LATITUDE	LONGITUDE	DEPTH	MAG
1936	8	19	1318	0.00	33 30.00	-116 55.00	0.00	3.00
1936	8	22	521	0.00	33 46.00	-117 49.00	0.00	4.00
1936	9	5	1024	0.00	33 30.00	-116 55.00	0.00	3.50
1936	9	8	1354	0.00	33 34.00	-117 59.00	0.00	3.50
1936	9	8	1522	0.00	33 34.00	-117 59.00	0.00	3.00
1936	9	10	1045	49.26	32 57.98	-117 22.79	10.00	3.50
1936	9	10	1047	0.00	32 50.00	-117 30.00	0.00	3.00
1936	9	22	614	0.00	33 55.00	-116 55.00	0.00	3.00
1936	10	6	1613	0.00	33 43.00	-118 5.00	0.00	3.00
1936	10	24	257	2.26	33 55.55	-117 16.69	10.00	3.50
1936	12	2	433	0.00	33 30.00	-116 55.00	0.00	3.00
1936	12	5	2000	0.00	33 48.00	-117 38.00	0.00	3.00
1937	1	9	1041	0.00	33 55.00	-116 50.00	0.00	3.00
1937	1	15	1835	47.03	33 33.66	-118 3.48	10.00	4.00
1937	1	18	1034	0.00	33 57.00	-117 39.00	0.00	3.50
1937	2	6	914	0.00	33 55.00	-117 40.00	0.00	3.00
1937	2	12	900	0.00	33 34.00	-117 59.00	0.00	3.00
1937	2	26	1054	0.00	33 50.00	-116 58.00	0.00	3.00
1937	3	1	214	0.00	33 50.00	-117 50.00	0.00	3.00
1937	3	27	639	0.00	33 37.00	-118 2.00	0.00	3.00
1937	3	28	57	0.00	33 37.00	-118 2.00	0.00	3.00
1937	3	28	2330	0.00	33 42.00	-116 50.00	0.00	3.00
1937	3	29	148	0.00	34 4.00	-116 47.00	0.00	3.50
1937	3	29	157	0.00	34 4.00	-116 47.00	0.00	3.00
1937	3	29	435	0.00	34 4.00	-116 47.00	0.00	3.00
1937	4	5	400	0.00	33 30.00	-116 55.00	0.00	3.00
1937	4	5	1856	0.00	33 42.00	-116 59.00	0.00	3.00
1937	4	20	1524	33.69	33 56.71	-117 31.71	10.00	3.50
1937	5	26	1229	0.00	33 40.00	-117 40.00	0.00	3.00
1937	5	30	2003	0.00	32 53.00	-118 15.00	0.00	3.00
1937	6	10	501	0.00	32 53.00	-118 15.00	0.00	3.00

Table 2.5-4
LISTING OF INSTRUMENTAL EPICENTERS WITHIN AN 80-KILOMETER (50-MILE) RADIUS OF THE SITE, THROUGH JUNE 1980 (Sheet 16 of 44)

YEAR	MO	DA	HRMN	SEC	LATITUDE	LONGITUDE	DEPTH	MAG
1937	6	11	409	0.00	33 52.00	-116 45.00	0.00	3.00
1937	6	11	610	0.00	33 37.00	-118 2.00	0.00	3.00
1937	7	7	1112	0.00	33 34.00	-117 59.00	0.00	4.00
1937	8	10	2239	6.20	32 48.09	-116 48.01	10.00	3.50
1937	8	10	2240	0.00	33 1.00	-116 51.00	0.00	3.00
1937	8	14	2310	0.00	33 1.00	-116 51.00	0.00	3.00
1937	8	17	503	0.00	33 47.00	-118 8.00	0.00	3.50
1937	8	17	750	2.50	33 44.98	-118 8.76	10.00	3.50
1937	8	31	2352	29.90	33 49.84	-117 16.61	10.00	3.50
1937	9	6	1938	0.00	34 4.00	-118 16.00	0.00	3.00
1937	9	11	1526	0.00	34 2.00	-117 38.00	0.00	3.00
1937	9	22	2346	0.00	33 24.00	-117 9.00	0.00	3.00
1937	10	11	455	0.00	32 55.00	-116 55.00	0.00	3.00
1937	10	25	1028	0.00	33 0.00	-116 50.00	0.00	3.00
1937	11	5	517	0.00	33 37.00	-118 2.00	0.00	3.00
1937	11	22	2330	0.00	34 1.00	-117 16.00	0.00	3.00
1937	11	24	1944	0.00	33 34.00	-117 59.00	0.00	3.00
1937	11	24	2137	0.00	34 1.00	-117 16.00	0.00	3.00
1937	11	25	144	0.00	33 37.00	-118 2.00	0.00	3.00
1937	12	2	2334	0.00	33 55.00	-118 15.00	0.00	3.00
1937	12	11	1806	0.00	33 40.00	-117 13.00	0.00	3.00
1938	1	8	1842	0.00	33 46.00	-118 7.00	0.00	3.00
1938	1	9	1230	0.00	33 56.00	-116 45.00	0.00	3.00
1938	1	24	415	0.00	34 2.00	-117 41.00	0.00	3.00
1938	2	14	1425	12.40	33 57.35	-118 15.03	10.00	3.50
1938	2	22	140	0.00	33 22.00	-116 55.00	0.00	3.00

Table 2.5-4
LISTING OF INSTRUMENTAL EPICENTERS WITHIN AN 80-KILOMETER (50-MILE) RADIUS OF THE SITE, THROUGH JUNE 1980 (Sheet 17 of 44)

YEAR	MO	DA	HRMN	SEC	LATITUDE	LONGITUDE	DEPTH	MAG
1938	4	3	1844	46.24	33 49.24	-118 13.93	10.00	3.50
1938	4	5	207	0.00	33 23.00	-117 18.00	0.00	3.00
1938	4	16	223	0.00	33 56.00	-116 45.00	0.00	3.50
1938	4	20	158	0.00	33 46.00	-118 7.00	0.00	3.00
1938	4	20	359	0.00	33 46.00	-118 7.00	0.00	3.00
1938	4	24	743	0.00	33 50.00	-117 48.00	0.00	3.50
1938	4	26	1219	0.00	33 46.00	-118 7.00	0.00	3.00
1938	4	28	607	27.99	32 43.06	-118 10.34	10.00	4.50
1938	4	29	1929	0.00	33 50.00	-117 24.00	0.00	3.00
1938	5	21	944	0.00	33 37.00	-118 2.00	0.00	4.00
1938	5	31	834	55.41	33 41.93	-117 30.64	10.00	5.50
1938	5	31	844	0.00	33 41.00	-117 32.00	0.00	3.00
1938	5	31	857	0.00	33 41.00	-117 32.00	0.00	3.00
1938	5	31	1050	0.00	33 41.00	-117 32.00	0.00	3.00
1938	5	31	2248	0.00	33 41.00	-117 32.00	0.00	3.00
1938	6	1	920	0.00	33 41.00	-117 32.00	0.00	3.00
1938	6	2	1601	0.00	33 41.00	-117 32.00	0.00	3.00
1938	6	10	749	0.00	32 53.00	-118 15.00	0.00	3.00
1938	6	10	1229	0.00	33 30.00	-116 55.00	0.00	3.00
1938	6	11	529	0.00	33 41.00	-117 32.00	0.00	3.00
1938	6	15	226	27.17	33 42.70	-117 32.25	10.00	3.50
1938	6	16	559	16.95	33 27.38	-116 53.74	10.00	4.00
1938	6	16	2148	0.00	33 55.00	-118 23.00	0.00	3.00
1938	7	3	2322	0.00	34 32.00	-117 41.00	0.00	3.00
1938	7	5	1806	55.75	33 40.93	-117 33.20	10.00	4.50
1938	7	17	1822	0.00	33 41.00	-117 32.00	0.00	3.00
1938	7	24	644	0.00	33 50.00	-117 24.00	0.00	3.00
1938	7	25	121	0.00	33 42.00	-117 18.00	0.00	3.00
1938	7	25	1522	0.00	33 42.00	-118 4.00	0.00	3.00
1938	8	1	1547	0.00	33 46.00	-118 6.00	0.00	3.00
1938	8	2	712	49.91	33 17.86	-116 58.12	10.00	3.50

Table 2.5-4
LISTING OF INSTRUMENTAL EPICENTERS WITHIN AN 80-KILOMETER (50-MILE) RADIUS OF THE SITE, THROUGH JUNE 1980 (Sheet 18 of 44)

YEAR	MO	DA	HRMN	SEC	LATITUDE	LONGITUDE	DEPTH	MAG
1938	8	5	159	0.00	33 37.00	-118 2.00	0.00	3.50
1938	8	5	433	0.00	34 3.00	-118 22.00	0.00	3.50
1938	8	6	228	0.00	33 56.00	-116 45.00	0.00	4.00
1938	8	6	2200	55.96	33 43.00	-117 30.41	10.00	4.00
1938	8	29	1448	0.00	33 42.00	-118 4.00	0.00	3.00
1938	8	31	318	14.25	33 45.54	-118 15.20	10.00	4.50
1938	8	31	534	0.00	33 48.00	-118 14.00	0.00	3.50
1938	9	11	16	0.00	33 30.00	-116 55.00	0.00	3.00
1938	9	17	2208	0.00	33 50.00	-118 8.00	0.00	3.00
1938	9	23	1118	0.00	33 56.00	-116 45.00	0.00	3.00
1938	10	23	47	0.00	33 50.00	-117 24.00	0.00	3.50
1938	11	4	1824	0.00	33 59.00	-118 18.00	0.00	3.00
1938	11	24	48	0.00	33 46.00	-118 7.00	0.00	3.00
1938	11	26	2049	0.00	33 46.00	-117 58.00	0.00	3.00
1938	12	4	326	0.00	33 40.00	-117 13.00	0.00	3.00
1938	12	7	338	0.00	34 0.00	-118 25.00	0.00	4.00
1938	12	17	1320	0.00	33 55.00	-117 29.00	0.00	3.00
1939	1	2	49	0.00	33 34.00	-117 59.00	0.00	3.00
1939	1	5	2258	0.00	33 59.00	-118 18.00	0.00	3.00
1939	1	12	1600	0.00	33 0.00	-116 55.00	0.00	3.00
1939	1	21	915	0.00	33 47.00	-118 8.00	0.00	3.00
1939	1	31	410	0.00	33 20.00	-116 58.00	0.00	3.00
1939	2	4	2341	0.00	33 59.00	-118 18.00	0.00	3.00
1939	2	6	1015	0.00	33 47.00	-118 8.00	0.00	3.00
1939	2	11	834	0.00	33 59.00	-118 18.00	0.00	3.00
1939	2	18	1847	0.00	33 56.00	-116 45.00	0.00	3.00

Table 2.5-4
LISTING OF INSTRUMENTAL EPICENTERS WITHIN AN 80-KILOMETER (50-MILE) RADIUS OF THE SITE, THROUGH JUNE 1980 (Sheet 19 of 44)

YEAR	MO	DA	HRMN	SEC	LATITUDE	LONGITUDE	DEPTH	MAG
1939	3	15	1939	0.00	33 34.00	-117 59.00	0.00	3.00
1939	3	28	815	0.00	33 47.00	-117 23.00	0.00	3.00
1939	4	2	324	0.00	33 5.00	-117 50.00	0.00	3.50
1939	4	3	250	44.71	34 2.59	-117 13.71	10.00	4.00
1939	4	7	1230	0.00	33 50.00	-117 35.00	0.00	3.00
1939	4	19	1329	0.00	33 21.00	-117 53.00	0.00	3.00
1939	4	25	622	0.00	33 47.00	-118 8.00	0.00	3.00
1939	5	11	1707	0.00	32 54.00	-118 22.00	0.00	3.00
1939	5	14	1226	0.00	33 44.00	-118 20.00	0.00	3.00
1939	5	27	1449	0.00	33 52.00	-117 38.00	0.00	3.00
1939	5	30	409	0.00	33 50.00	-117 30.00	0.00	3.50
1939	6	9	157	0.00	32 48.00	-118 8.00	0.00	3.00
1939	6	25	149	0.00	32 45.00	-118 12.00	0.00	4.50
1939	7	10	1415	0.00	33 11.00	-118 2.00	0.00	3.50
1939	8	23	1422	53.00	33 35.00	-116 45.00	0.00	3.00
1939	9	18	858	9.00	33 59.00	-118 18.00	0.00	3.00
1939	9	28	1841	55.00	33 30.00	-116 55.00	0.00	3.50
1939	9	28	1915	58.00	33 59.00	-117 12.00	0.00	3.00
1939	10	10	1138	20.00	33 8.00	-117 58.00	0.00	3.00
1939	10	14	1755	15.00	33 47.00	-118 8.00	0.00	3.50
1939	11	4	2141	0.00	33 46.00	-118 7.00	0.00	4.00
1939	11	7	1852	8.40	34 0.00	-117 17.00	0.00	4.70
1939	11	11	511	12.00	33 50.00	-117 24.00	0.00	3.00
1939	11	21	1722	31.00	33 44.00	-117 1.00	0.00	3.00
1939	12	9	1846	39.00	33 40.00	-117 20.00	0.00	3.00
1939	12	24	1933	55.00	33 50.00	-117 24.00	0.00	3.00
1939	12	24	2346	29.00	33 50.00	-117 51.00	0.00	3.50
1939	12	27	1928	49.00	33 47.00	-118 12.00	0.00	4.70
1939	12	28	549	35.00	33 47.00	-118 8.00	0.00	3.00
1939	12	30	1920	14.00	33 47.00	-118 8.00	0.00	3.50

Table 2.5-4
LISTING OF INSTRUMENTAL EPICENTERS WITHIN AN 80-KILOMETER (50-MILE) RADIUS OF THE SITE, THROUGH JUNE 1980 (Sheet 20 of 44)

YEAR	MO	DA	HRMN	SEC	LATITUDE	LONGITUDE	DEPTH	MAG
1940	1	11	340	21.00	33 47.00	-118 8.00	0.00	3.50
1940	1	12	1600	43.00	33 40.00	-117 13.00	0.00	3.00
1940	1	13	749	7.00	33 47.00	-118 8.00	0.00	4.00
1940	1	18	516	58.00	33 46.00	-118 6.00	0.00	3.00
1940	1	28	2033	52.00	33 38.00	-118 12.00	0.00	3.00
1940	2	8	1656	17.00	33 42.00	-118 4.00	0.00	4.00
1940	2	9	1016	55.00	33 37.00	-117 25.00	0.00	3.00
1940	2	9	1111	44.00	33 0.00	-117 5.00	0.00	3.00
1940	2	9	1148	58.00	33 20.00	-117 5.00	0.00	3.00
1940	2	11	1547	33.00	33 58.00	-116 58.00	0.00	3.50
1940	2	11	1924	10.00	33 59.00	-118 18.00	0.00	4.00
1940	2	19	1206	55.70	34 1.00	-117 3.00	0.00	4.60
1940	2	19	1217	31.00	33 42.00	-117 26.00	0.00	3.00
1940	2	22	1038	2.00	33 45.00	-117 20.00	0.00	3.50
1940	2	25	2123	47.10	33 41.00	-117 32.00	0.00	3.40
1940	3	2	1028	15.00	33 42.00	-117 20.00	0.00	3.00
1940	3	3	1427	17.00	33 42.00	-117 20.00	0.00	3.50
1940	3	21	121	9.00	33 45.00	-117 15.00	0.00	3.50
1940	4	13	355	8.00	33 51.00	-117 25.00	0.00	3.00
1940	4	18	1843	43.90	34 2.00	-117 21.00	0.00	4.40
1940	4	24	1316	58.00	33 47.00	-118 23.00	0.00	3.50
1940	5	23	1331	5.00	33 50.00	-117 24.00	0.00	3.00
1940	6	5	827	27.00	33 50.00	-117 24.00	0.00	4.00
1940	6	6	227	16.00	33 57.00	-117 33.00	0.00	3.50
1940	6	8	30	1.00	33 59.00	-118 18.00	0.00	3.00
1940	6	24	530	12.00	33 33.00	-118 21.00	0.00	3.50
1940	7	20	401	13.00	33 42.00	-118 4.00	0.00	4.00

Table 2.5-4
LISTING OF INSTRUMENTAL EPICENTERS WITHIN AN 80-KILOMETER (50-MILE) RADIUS OF THE SITE, THROUGH JUNE 1980 (Sheet 21 of 44)

YEAR	MO	DA	HRMN	SEC	LATITUDE	LONGITUDE	DEPTH	MAG
1940	7	20	1807	49.00	33 42.00	-118 4.00	0.00	3.00
1940	7	22	322	2.00	33 46.00	-117 55.00	0.00	3.00
1940	7	22	624	14.00	33 59.00	-118 23.00	0.00	3.00
1940	8	7	2151	31.00	33 22.00	-116 55.00	0.00	3.00
1940	8	16	858	17.00	33 34.00	-117 59.00	0.00	3.00
1940	8	19	1824	42.00	34 2.00	-117 41.00	0.00	3.00
1940	8	31	639	1.00	33 47.00	-118 8.00	0.00	3.00
1940	9	2	630	21.00	33 34.00	-117 59.00	0.00	3.00
1940	9	12	2003	1.00	33 30.00	-116 55.00	0.00	3.00
1940	10	4	1054	21.00	33 54.00	-118 19.00	0.00	3.00
1940	10	9	1301	23.00	33 30.00	-116 55.00	0.00	3.00
1940	10	11	749	49.00	33 47.00	-118 25.00	0.00	3.50
1940	10	12	24	0.00	33 47.00	-118 25.00	0.00	4.00
1940	10	12	318	46.00	33 47.00	-118 25.00	0.00	3.50
1940	10	14	2051	11.00	33 47.00	-118 25.00	0.00	4.00
1940	11	1	725	3.00	33 47.00	-118 25.00	0.00	4.00
1940	11	1	1320	5.00	33 47.00	-118 25.00	0.00	3.00
1940	11	1	2000	46.00	33 38.00	-118 12.00	0.00	4.00
1940	11	2	258	26.00	33 47.00	-118 25.00	0.00	4.00
1940	11	5	604	35.00	33 57.00	-119 8.00	0.00	3.50
1940	11	6	2044	15.00	33 47.00	-118 25.00	0.00	3.00
1940	11	17	700	40.00	33 47.00	-118 25.00	0.00	3.00
1940	11	17	2005	51.00	33 55.00	-118 13.00	0.00	3.00
1940	12	4	2216	39.00	33 25.00	-116 45.00	0.00	3.00
1940	12	9	820	27.00	33 56.00	-116 45.00	0.00	3.00
1940	12	24	2144	35.00	33 37.00	-118 0.00	0.00	3.00

Table 2.5-4
LISTING OF INSTRUMENTAL EPICENTERS WITHIN AN 80-KILOMETER (50-MILE) RADIUS OF THE SITE, THROUGH JUNE 1980 (Sheet 22 of 44)

YEAR	MO	DA	HRMN	SEC	LATITUDE	LONGITUDE	DEPTH	MAG
1941	1	30	134	46.90	33 58.00	-118 3.00	0.00	4.10
1941	2	18	1951	4.00	34 1.00	-117 32.00	0.00	3.00
1941	2	22	1141	40.00	33 47.00	-118 25.00	0.00	3.50
1941	2	22	1819	1.00	33 47.00	-118 25.00	0.00	3.00
1941	3	21	313	57.00	33 41.00	-117 32.00	0.00	3.00
1941	3	22	822	40.00	33 31.00	-118 6.00	0.00	4.00
1941	4	11	120	24.00	33 57.00	-117 35.00	0.00	4.00
1941	4	19	146	20.00	33 48.00	-118 12.00	0.00	3.00
1941	4	24	1845	52.00	33 37.00	-118 2.00	0.00	3.00
1941	5	25	959	20.00	33 25.00	-116 57.00	0.00	3.00
1941	6	4	856	3.00	33 45.00	-117 50.00	0.00	3.50
1941	6	11	1326	55.00	33 47.00	-118 25.00	0.00	3.00
1941	6	14	1900	21.00	34 0.00	-117 24.00	0.00	3.00
1941	7	26	732	12.00	33 37.00	-118 2.00	0.00	3.00
1941	8	9	704	44.00	33 58.00	-117 27.00	0.00	3.00
1941	8	10	1207	39.00	34 1.00	-117 53.00	0.00	3.50
1941	8	17	1	24.00	33 24.00	-118 24.00	0.00	3.00
1941	8	28	1714	5.00	33 52.00	-117 29.00	0.00	3.00
1941	9	13	324	36.00	33 50.00	-117 20.00	0.00	3.50
1941	9	14	1350	53.00	33 53.00	-117 24.00	0.00	3.00
1941	10	13	2059	16.00	33 57.00	-116 48.00	0.00	3.00
1941	10	22	657	18.50	33 49.00	-118 13.00	0.00	4.90
1941	10	22	1032	21.75	33 52.00	-118 13.00	0.00	3.80
1941	11	14	841	36.30	33 47.00	-118 15.00	0.00	5.40
1941	11	14	941	36.00	33 47.00	-118 15.00	0.00	3.00
1941	11	27	1733	23.00	33 59.00	-118 12.00	0.00	3.00
1941	11	28	224	54.00	33 17.00	-117 5.00	0.00	3.00
1941	12	1	1400	3.00	33 18.00	-118 15.00	0.00	3.50
1941	12	6	1900	23.00	34 0.00	-117 22.00	0.00	3.00
1941	12	8	2001	24.00	33 50.00	-11 43.00	0.00	3.00
1941	12	9	1254	9.00	33 48.00	-117 31.00	0.00	3.00

Table 2.5-4
LISTING OF INSTRUMENTAL EPICENTERS WITHIN AN 80-KILOMETER (50-MILE) RADIUS OF THE SITE, THROUGH JUNE 1980 (Sheet 23 of 44)

YEAR	MO	DA	HRMN	SEC	LATITUDE	LONGITUDE	DEPTH	MAG
1941	12	23	119	3.00	33 34.00	-117 59.00	0.00	3.50
1942	1	9	628	7.00	33 53.00	-117 27.00	0.00	3.00
1942	1	13	928	18.00	33 41.00	-117 59.00	0.00	3.00
1942	1	24	2141	48.00	32 48.00	-117 50.00	0.00	4.00
1942	2	27	128	55.00	33 47.00	-118 25.00	0.00	3.00
1942	4	16	728	33.00	33 22.00	-118 9.00	0.00	4.00
1942	4	26	1510	23.00	33 57.00	-116 44.00	0.00	4.00
1942	4	29	1213	0.00	33 32.00	-117 18.00	0.00	3.00
1942	5	11	845	19.00	33 52.00	-117 3.00	0.00	3.00
1942	5	12	125	48.00	33 42.00	-118 0.00	0.00	3.00
1942	5	19	727	0.00	33 32.00	-116 43.00	0.00	3.00
1942	5	19	732	51.00	33 32.00	-116 43.00	0.00	3.00
1942	5	29	1703	9.00	33 45.00	-118 16.00	0.00	3.00
1942	6	22	1559	17.00	33 48.00	-118 4.00	0.00	3.00
1942	7	1	2040	8.00	33 14.00	-118 25.00	0.00	3.00
1942	7	15	1602	3.00	33 50.00	-117 21.00	0.00	3.50
1942	8	16	112	48.00	33 51.00	-117 24.00	0.00	3.50
1942	8	19	1557	10.00	33 47.00	-117 45.00	0.00	3.50
1942	9	25	907	10.00	33 57.00	-118 10.00	0.00	3.00
1942	10	19	2327	12.00	33 21.00	-117 23.00	0.00	3.00
1942	10	24	1906	26.00	34 0.00	-117 5.00	0.00	3.00
1942	11	25	1847	5.00	33 57.00	-118 8.00	0.00	3.50
1942	11	26	2116	34.00	33 57.00	-118 8.00	0.00	3.00

Table 2.5-4
LISTING OF INSTRUMENTAL EPICENTERS WITHIN AN 80-KILOMETER (50-MILE) RADIUS OF THE SITE, THROUGH JUNE 1980 (Sheet 24 of 44)

YEAR	MO	DA	HRMN	SEC	LATITUDE	LONGITUDE	DEPTH	MAG
1943	1	2	2349	17.00	33 52.00	-117 21.00	0.00	3.50
1943	1	30	1045	11.00	33 44.00	-117 0.00	0.00	3.00
1943	2	12	543	44.00	33 45.00	-117 58.00	0.00	3.00
1943	2	23	921	12.00	32 51.00	-117 29.00	0.00	4.00
1943	4	6	903	24.00	33 40.00	-116 51.00	0.00	3.00
1943	4	16	704	5.00	33 40.00	-117 0.00	0.00	3.00
1943	5	3	2322	47.00	33 59.00	-117 17.00	0.00	3.00
1943	5	8	1507	6.00	34 0.00	-118 12.00	0.00	3.00
1943	5	17	1921	20.00	33 40.00	-118 9.00	0.00	3.00
1943	5	18	2235	35.00	33 40.00	-118 5.00	0.00	3.00
1943	6	11	1328	13.00	33 50.00	-117 4.00	0.00	3.50
1943	7	4	2153	10.00	33 57.00	-117 37.00	0.00	3.00
1943	7	17	2133	22.00	33 48.00	-118 0.00	0.00	3.00
1943	7	27	2144	5.00	33 53.00	-116 52.00	0.00	3.00
1943	8	11	1601	2.00	33 48.00	-117 52.00	0.00	3.00
1943	10	20	314	10.00	33 51.00	-117 52.00	0.00	3.00
1943	10	24	29	21.00	33 56.00	-117 22.00	0.00	4.00
1943	10	29	1631	9.00	33 47.00	-117 52.00	0.00	3.50
1943	11	14	1221	7.00	33 46.00	-116 48.00	0.00	3.00
1943	11	22	39	53.00	34 5.00	-117 7.00	0.00	3.00
1944	1	4	1854	17.00	33 57.00	-116 49.00	0.00	3.00
1944	1	14	808	21.00	33 44.00	-118 9.00	0.00	3.30
1944	2	20	631	7.00	33 43.00	-118 2.00	0.00	3.00
1944	3	31	110	1.00	34 5.00	-117 27.00	0.00	3.30
1944	6	10	1111	50.49	34 0.85	-116 46.26	10.00	4.50
1944	6	10	1115	31.87	33 58.37	-116 46.12	10.00	4.00
1944	6	10	1126	12.09	34 0.74	-116 46.78	10.00	3.20
1944	6	12	1045	34.66	33 58.57	-116 43.24	10.00	5.10
1944	6	12	1051	0.03	33 47.04	-116 57.69	10.00	3.70
1944	6	12	1113	46.45	33 57.68	-116 44.63	10.00	3.50
1944	6	12	1116	35.97	33 59.67	-116 42.70	10.00	5.30
1944	6	12	1139	14.15	33 43.53	-117 2.60	10.00	3.60
1944	6	12	1148	49.84	33 51.01	-116 52.67	10.00	3.40
1944	6	12	1345	28.18	33 54.88	-116 47.91	10.00	3.80

Table 2.5-4
LISTING OF INSTRUMENTAL EPICENTERS WITHIN AN 80-KILOMETER (50-MILE) RADIUS OF THE SITE, THROUGH JUNE 1980 (Sheet 25 of 44)

YEAR	MO	DA	HRMN	SEC	LATITUDE	LONGITUDE	DEPTH	MAG
1944	6	12	1443	20.40	33 58.24	-116 43.21	10.00	3.30
1944	6	12	2023	1.38	33 48.50	-116 55.11	10.00	3.60
1944	6	12	2221	19.49	33 58.89	-116 42.13	10.00	4.20
1944	6	13	19	28.52	33 57.46	-116 44.81	10.00	3.70
1944	6	13	1320	49.09	33 58.82	-116 45.68	10.00	3.20
1944	6	13	1730	17.61	33 50.18	-116 55.05	10.00	3.70
1944	6	13	1837	5.96	33 59.83	-116 42.38	10.00	3.30
1944	6	14	4	35.58	33 59.16	-116 42.25	10.00	3.90
1944	6	14	120	44.40	33 59.14	-116 42.52	10.00	3.30
1944	6	14	331	49.83	33 57.57	-116 44.59	10.00	3.30
1944	6	15	2044	26.78	33 50.41	-116 56.02	10.00	3.80
1944	6	17	2341	8.14	33 44.12	-117 1.59	10.00	3.40
1944	6	19	3	33.00	33 52.00	-118 13.00	0.00	4.50
1944	6	19	306	7.00	33 52.00	-118 13.00	0.00	4.40
1944	6	20	1342	23.56	33 56.75	-116 47.67	10.00	3.20
1944	6	23	2128	42.65	33 59.77	-116 43.51	10.00	3.60
1944	6	25	50	20.00	33 44.00	-116 44.00	0.00	3.20
1944	6	27	1634	50.84	33 59.78	-116 47.14	10.00	3.40
1944	6	28	655	17.24	34 0.44	-116 47.26	10.00	3.50
1944	6	30	304	44.32	33 56.93	-116 42.18	10.00	3.30
1944	7	1	1053	59.08	33 57.74	-116 44.04	10.00	3.70
1944	7	22	202	55.00	33 29.00	-116 51.00	0.00	3.70
1944	7	25	820	54.00	33 53.00	-117 43.00	0.00	3.00
1944	7	26	2259	55.00	33 47.00	-118 15.00	0.00	3.80
1944	8	16	632	28.00	33 42.00	-118 6.00	0.00	3.50
1944	8	22	948	54.36	33 58.50	-116 42.24	10.00	3.00
1944	8	22	1822	30.91	33 29.83	-117 0.22	10.00	3.10
1944	8	28	1253	19.34	33 50.52	-117 2.11	10.00	3.10
1944	8	29	2246	47.00	33 57.97	-116 45.04	10.00	3.00
1944	9	20	1412	21.00	33 58.00	-116 45.00	0.00	3.60
1944	9	20	1639	33.00	33 50.00	-117 40.00	0.00	3.40

Table 2.5-4
LISTING OF INSTRUMENTAL EPICENTERS WITHIN AN 80-KILOMETER (50-MILE) RADIUS OF THE SITE, THROUGH JUNE 1980 (Sheet 26 of 44)

YEAR	MO	DA	HRMN	SEC	LATITUDE	LONGITUDE	DEPTH	MAG
1944	10	17	1907	49.00	33 53.00	-116 52.00	0.00	3.00
1944	10	23	2200	39.00	33 43.00	-118 10.00	0.00	3.60
1944	10	28	1830	16.00	33 56.00	-116 45.00	0.00	4.40
1944	11	1	1146	30.00	33 58.00	-116 45.00	0.00	3.10
1944	12	13	2351	56.00	33 50.00	-117 50.00	0.00	3.40
1945	1	19	510	45.00	33 56.00	-118 19.00	0.00	3.50
1945	2	3	736	23.00	32 53.00	-118 21.00	0.00	3.10
1945	2	6	2256	11.00	33 57.00	-118 21.00	0.00	3.50
1945	2	17	2009	36.00	33 41.00	-117 56.00	0.00	3.20
1945	2	23	1159	41.00	33 45.00	-116 49.00	0.00	3.40
1945	4	6	1546	45.00	34 0.00	-116 46.00	0.00	3.60
1945	5	2	2356	55.00	33 47.00	-118 8.00	0.00	3.00
1945	5	29	1404	55.00	33 40.00	-118 0.00	0.00	3.30
1945	5	30	929	8.00	33 58.00	-117 33.00	0.00	3.40
1945	6	17	903	18.00	34 5.00	-117 2.00	0.00	3.40
1945	8	25	2127	57.00	33 53.00	-116 53.00	0.00	3.40
1945	9	3	2308	13.00	34 3.00	-116 48.00	0.00	3.10
1945	9	7	1534	24.00	33 58.00	-116 48.00	0.00	4.30
1945	9	7	1545	29.00	33 59.00	-116 52.00	0.00	3.00
1945	9	22	905	40.00	33 33.00	-116 50.00	0.00	3.80
1945	10	5	809	51.00	33 26.00	-116 54.00	0.00	3.10
1945	10	7	1817	21.00	33 59.00	-116 52.00	0.00	3.10
1945	11	8	1119	27.00	33 57.00	-117 18.00	0.00	3.50
1945	11	8	1306	53.00	33 57.00	-117 18.00	0.00	3.30
1946	1	1	2356	32.00	32 43.00	-117 25.00	0.00	3.30
1945	1	11	2023	52.00	34 5.00	-116 48.00	0.00	3.10

Table 2.5-4
LISTING OF INSTRUMENTAL EPICENTERS WITHIN AN 80-KILOMETER (50-MILE) RADIUS OF THE SITE, THROUGH JUNE 1980 (Sheet 27 of 44)

YEAR	MO	DA	HRMN	SEC	LATITUDE	LONGITUDE	DEPTH	MAG
1946	3	31	1352	23.00	33 21.00	-116 59.00	0.00	3.20
1946	4	19	1555	13.00	33 53.00	-117 18.00	0.00	3.40
1946	5	9	13	59.00	33 53.00	-117 18.00	0.00	3.50
1946	5	12	1819	5.00	33 53.00	-117 18.00	0.00	3.50
1946	5	20	151	13.00	33 57.00	-118 9.00	0.00	3.00
1946	6	21	722	59.00	34 3.00	-116 55.00	0.00	3.20
1946	6	24	1710	12.00	33 42.00	-116 53.00	0.00	3.00
1946	6	27	316	35.00	33 53.00	-117 18.00	0.00	3.50
1946	7	2	628	35.00	34 4.00	-117 45.00	0.00	3.20
1946	7	2	728	35.00	34 4.00	-117 45.00	0.00	3.20
1946	8	10	1821	31.00	33 27.00	-118 6.00	0.00	3.10
1946	8	19	1208	2.00	34 0.00	-116 45.00	0.00	3.10
1946	8	23	1918	52.00	33 53.00	-117 48.00	0.00	3.10
1946	9	28	719	9.00	33 57.00	-116 51.00	0.00	5.00
1946	10	28	2202	38.00	33 25.00	-116 54.00	0.00	3.70
1946	10	28	2227	21.00	33 25.00	-116 54.00	0.00	3.00
1946	11	22	819	7.00	33 39.00	-118 6.00	0.00	3.00
1946	12	25	1937	59.00	33 59.00	-117 35.00	0.00	3.10
1946	12	29	718	46.00	33 23.00	-118 15.00	0.00	3.00
1947	1	9	220	35.00	33 40.00	-117 58.00	0.00	3.30
1947	1	9	1324	44.00	33 58.00	-117 14.00	0.00	3.00
1947	1	30	1103	35.00	34 0.00	-116 44.00	0.00	3.50
1947	2	22	2218	46.00	33 16.00	-118 20.00	0.00	3.00
1947	5	19	528	12.00	33 23.00	-117 2.00	0.00	3.60
1947	5	20	254	52.00	33 17.00	-116 56.00	0.00	3.10
1947	6	25	1230	39.00	33 59.00	-117 20.00	0.00	3.20
1947	8	10	739	23.00	33 53.00	-116 44.00	0.00	3.10
1947	8	28	759	38.00	33 37.00	-116 57.00	0.00	3.20
1947	11	8	302	8.00	33 51.00	-117 17.00	0.00	3.10
1947	11	23	1051	32.00	34 4.00	-116 45.00	0.00	3.10

Table 2.5-4
LISTING OF INSTRUMENTAL EPICENTERS WITHIN AN 80-KILOMETER (50-MILE) RADIUS OF THE SITE, THROUGH JUNE 1980 (Sheet 28 of 44)

YEAR	MO	DA	HRMN	SEC	LATITUDE	LONGITUDE	DEPTH	MAG
1948	2	18	1338	50.00	33 59.00	-117 33.00	0.00	3.30
1948	2	20	421	24.00	33 55.00	-118 13.00	0.00	3.60
1948	2	24	303	39.00	33 59.00	-117 32.00	0.00	3.40
1946	3	16	346	51.00	33 55.00	-117 19.00	0.00	3.10
1948	3	16	704	26.00	33 55.00	-117 19.00	0.00	3.00
1948	3	30	1625	36.00	34 5.00	-116 49.00	0.00	3.40
1948	4	5	1028	46.00	33 37.00	-117 24.00	0.00	3.00
1948	4	29	2144	59.00	33 59.00	-116 46.00	0.00	3.50
1948	5	24	1038	20.00	33 35.00	-118 1.00	0.00	3.60
1946	6	24	1806	6.00	33 28.00	-117 46.00	0.00	3.80
1948	6	25	2212	21.00	33 58.00	-117 39.00	0.00	3.00
1948	7	2	750	21.00	33 30.00	-117 8.00	0.00	3.00
1948	7	18	103	48.00	34 4.00	-117 49.00	0.00	3.60
1948	8	18	1421	40.00	33 58.00	-118 22.00	0.00	3.00
1948	8	28	1331	59.00	34 2.00	-117 31.00	0.00	3.20
1948	9	16	1922	58.00	33 45.00	-116 55.00	0.00	3.20
1948	10	6	2016	41.00	33 51.00	-117 20.00	0.00	3.10
1948	10	11	1829	34.00	33 59.00	-117 31.00	0.00	3.00
1949	1	22	2115	16.00	33 25.00	-116 57.00	0.00	3.20
1949	2	18	2159	52.00	34 3.00	-116 45.00	0.00	3.10
1949	4	15	233	36.00	33 30.00	-116 45.00	0.00	3.00
1949	5	13	1018	31.85	33 58.33	-118 10.63	3.30	3.70
1949	6	14	915	50.00	33 13.00	-117 44.00	0.00	3.00
1949	6	20	1835	29.00	32 55.00	-117 18.00	0.00	3.00
1949	6	25	213	18.00	32 52.00	-117 20.00	0.00	3.10
1949	7	3	950	21.77	34 5.11	-117 20.15	20.50	3.10
1949	7	18	1221	53.00	33 3.00	-116 49.00	0.00	3.00

Table 2.5-4
LISTING OF INSTRUMENTAL EPICENTERS WITHIN AN 80-KILOMETER (50-MILE) RADIUS OF THE SITE, THROUGH JUNE 1980 (Sheet 29 of 44)

YEAR	MO	DA	HRMN	SEC	LATITUDE	LONGITUDE	DEPTH	MAG
1949	7	26	1418	18.00	33 59.00	-116 48.00	0.00	3.10
1949	8	17	514	19.88	34 0.56	-117 12.35	16.00	3.40
1949	8	19	1057	50.59	33 57.39	-116 53.96	16.80	3.80
1949	8	27	2248	33.00	33 41.00	-118 11.00	0.00	3.00
1949	9	19	508	13.46	33 57.58	-118 11.16	0.30	3.10
1949	11	18	119	52.00	33 45.00	-118 15.00	0.00	3.70
1949	12	10	213	44.00	33 46.00	-117 43.00	0.00	3.10
1950	1	11	2141	35.05	33 56.37	-118 12.29	0.40	4.10
1950	5	29	303	5.00	34 2.00	-117 16.00	0.00	3.20
1950	6	24	143	34.00	33 25.00	-118 11.00	0.00	3.30
1950	6	25	758	13.00	33 22.00	-116 53.00	0.00	3.00
1950	7	7	438	35.00	33 57.00	-117 49.00	0.00	3.00
1950	7	27	619	30.00	33 59.00	-117 14.00	0.00	3.00
1950	8	25	517	24.00	34 2.00	-117 1.00	0.00	3.00
1950	9	5	1919	56.00	33 39.00	-116 45.00	0.00	4.80
1950	9	21	2245	12.00	34 0.00	-117 18.00	0.00	3.40
1950	10	14	1759	31.00	33 41.00	-116 47.00	0.00	3.10
1950	11	1	1655	13.00	34 0.00	-116 59.00	0.00	3.00
1950	11	6	2055	46.00	32 43.00	-117 50.00	0.00	4.40
1950	11	16	159	19.00	33 57.00	-118 24.00	0.00	3.10
1950	11	17	346	51.00	33 55.00	-118 19.00	0.00	3.80
1950	12	26	1205	49.00	33 57.00	-117 35.00	0.00	3.10
1951	1	27	2057	51.00	33 58.00	-117 6.00	0.00	3.00
1951	3	10	1552	24.70	34 1.00	-116 52.55	22.80	3.90
1951	8	15	723	0.00	33 30.00	-118 12.00	0.00	3.10
1951	8	19	1440	27.00	33 33.00	-117 17.00	0.00	3.30
1951	8	23	1408	11.00	33 57.00	-116 54.00	0.00	3.20
1951	9	2	610	13.00	34 0.00	-116 45.00	0.00	3.20
1951	9	7	333	18.00	33 57.00	-118 20.00	0.00	3.30
1951	9	28	508	12.00	33 58.00	-117 29.00	0.00	3.10
1951	12	4	703	50.00	32 54.00	-118 21.00	0.00	3.40
1951	12	14	1150	9.00	33 56.00	-118 18.00	0.00	3.30
1951	12	23	0	21.00	33 57.00	-117 2.00	0.00	3.00
1951	12	26	46	54.00	32 49.00	-118 21.00	0.00	5.90

Table 2.5-4
LISTING OF INSTRUMENTAL EPICENTERS WITHIN AN 80-KILOMETER (50-MILE) RADIUS OF THE SITE, THROUGH JUNE 1980 (Sheet 30 of 44)

YEAR	MO	DA	HRMN	SEC	LATITUDE	LONGITUDE	DEPTH	MAG
1952	1	27	1608	50.00	33 37.00	-117 5.00	0.00	3.20
1952	2	6	2314	2.00	33 23.00	-118 19.00	0.00	3.20
1952	2	7	447	10.00	32 52.00	-118 15.00	0.00	3.00
1952	2	7	1619	58.00	32 52.00	-118 15.00	0.00	3.10
1952	2	13	1513	37.00	32 52.00	-118 15.00	0.00	4.70
1952	2	14	731	4.00	32 55.00	-118 18.00	0.00	3.40
1952	2	17	1236	58.33	33 59.75	-117 16.19	16.00	4.50
1952	2	20	42	1.64	34 3.75	-117 13.26	16.10	3.40
1952	3	3	1614	16.00	33 29.00	-117 40.00	0.00	3.50
1952	5	24	2018	57.00	32 59.00	-117 44.00	0.00	3.40
1952	6	11	801	57.00	32 45.00	-117 20.00	0.00	3.00
1952	6	29	622	25.00	32 50.00	-118 16.00	0.00	3.20
1952	7	10	845	53.46	33 59.94	-118 13.02	5.60	3.70
1952	8	13	1821	33.00	32 56.00	-118 12.00	0.00	3.10
1952	9	28	400	10.00	34 4.00	-117 10.00	0.00	3.00
1952	11	4	1907	31.00	32 48.00	-116 54.00	0.00	3.20
1952	11	16	1348	23.81	34 0.64	-117 11.26	20.20	3.80
1952	12	8	901	20.00	33 31.00	-116 45.00	0.00	3.00
1953	1	16	342	34.00	34 3.00	-116 58.00	0.00	3.00
1953	2	11	1715	39.00	34 3.00	-117 34.00	0.00	3.00
1953	5	2	550	40.78	34 4.62	-117 37.07	10.50	3.90
1953	5	15	1920	50.00	33 58.00	-117 39.00	0.00	3.00
1953	6	14	1728	29.00	33 3.00	-117 18.00	0.00	3.50

Table 2.5-4
LISTING OF INSTRUMENTAL EPICENTERS WITHIN AN 80-KILOMETER (50-MILE) RADIUS OF THE SITE, THROUGH JUNE 1980 (Sheet 31 of 44)

YEAR	MO	DA	HRMN	SEC	LATITUDE	LONGITUDE	DEPTH	MAG
1953	7	12	133	52.00	33 44.00	-116 53.00	0.00	3.20
1953	7	20	920	13.69	33 55.22	-117 36.03	16.00	3.40
1953	8	30	226	26.00	34 0.00	-116 51.00	0.00	3.70
1953	12	4	1728	0.00	33 22.00	-118 14.00	0.00	3.60
1953	12	29	1039	35.00	34 1.00	-117 10.00	0.00	3.10
1954	1	6	348	44.00	33 57.00	-116 58.00	0.00	3.10
1954	1	21	217	7.00	34 2.00	-116 48.00	0.00	3.10
1954	1	23	509	14.00	33 50.00	-118 8.00	0.00	3.10
1954	3	8	104	54.00	33 42.00	-117 28.00	0.00	3.10
1954	3	31	1351	28.00	33 43.00	-117 33.00	0.00	3.10
1954	4	30	36	23.88	34 1.75	-116 47.21	11.10	4.20
1954	6	7	1721	2.00	33 42.00	-116 45.00	0.00	3.00
1954	7	14	749	40.00	33 20.00	-118 0.00	0.00	3.30
1954	8	30	2234	1.00	32 48.00	-117 52.00	0.00	3.10
1954	9	3	1614	17.00	33 53.00	-118 18.00	0.00	3.00
1954	9	24	1458	28.00	33 11.00	-117 56.00	0.00	3.00
1954	10	21	245	52.09	33 59.88	-117 9.65	14.90	3.40
1954	10	26	828	28.00	33 43.00	-117 28.00	0.00	3.30
1954	10	26	1622	26.00	33 44.00	-117 28.00	0.00	4.10
1954	11	7	839	31.00	33 52.00	-118 20.00	0.00	3.20
1954	12	7	542	58.00	33 47.00	-116 56.00	0.00	3.10
1955	1	2	336	20.00	32 46.00	-118 8.00	0.00	3.20
1955	1	23	1117	9.00	33 38.00	-116 48.00	0.00	3.30
1955	1	25	1223	0.00	33 46.00	-118 13.00	0.00	3.30
1955	2	21	1006	56.00	34 0.00	-118 20.00	0.00	3.10
1955	7	16	605	46.00	33 59.00	-116 46.00	0.00	3.20
1955	7	16	1139	47.32	34 2.74	-116 42.17	11.80	3.60
1955	7	27	135	2.00	33 52.00	-117 11.00	0.00	3.30
1955	8	3	1649	5.65	33 59.90	-116 58.37	13.50	3.70
1955	9	14	1019	54.00	33 45.00	-118 19.00	0.00	3.10

Table 2.5-4
LISTING OF INSTRUMENTAL EPICENTERS WITHIN AN 80-KILOMETER (50-MILE) RADIUS OF THE SITE, THROUGH JUNE 1980 (Sheet 32 of 44)

YEAR	MO	DA	HRMN	SEC	LATITUDE	LONGITUDE	DEPTH	MAG
1955	9	30	1500	10.00	33 44.00	-117 58.00	0.00	3.30
1955	11	9	2241	35.00	34 2.00	-116 50.00	0.00	3.30
1955	11	17	441	38.00	33 42.00	-116 52.00	0.00	3.20
1955	11	29	1208	53.00	33 41.00	-116 50.00	0.00	3.00
1955	12	24	1736	27.00	33 40.00	-118 0.00	0.00	3.00
1956	1	3	25	48.95	33 43.50	-117 29.91	13.70	4.70
1956	6	24	641	50.00	32 56.00	-117 39.00	0.00	3.30
1956	7	7	1241	54.00	32 59.00	-116 58.00	0.00	3.50
1956	7	8	548	55.00	33 53.00	-117 51.00	0.00	3.00
1956	7	11	221	6.00	33 28.00	-116 50.00	0.00	3.10
1956	8	6	531	9.00	33 32.00	-116 44.00	0.00	3.00
1956	10	2	2044	34.84	33 49.17	-117 2.59	16.20	3.80
1956	10	3	134	36.00	33 50.00	-117 0.00	0.00	3.30
1957	2	6	904	32.54	34 2.20	-117 19.07	5.30	3.60
1957	2	10	1954	47.00	33 43.00	-116 50.00	0.00	3.00
1957	3	18	955	28.00	33 46.00	-118 4.00	0.00	3.30
1957	3	30	920	53.00	34 4.00	-116 55.00	0.00	3.10
1957	4	14	1342	31.00	32 52.00	-118 9.00	0.00	3.50
1957	5	27	1704	41.00	33 52.00	-116 58.00	0.00	3.20
1957	7	8	2119	10.48	34 2.82	-117 48.52	2.70	3.10
1957	8	28	941	34.00	33 59.00	-117 17.00	0.00	3.00
1957	9	1	1302	13.00	34 5.00	-117 16.00	0.00	3.30
1957	10	30	2021	0.00	33 58.00	-117 54.00	0.00	3.10
1957	11	7	434	35.00	34 0.00	-117 0.00	0.00	3.50
1957	12	31	2	25.00	34 0.00	-118 10.00	0.00	3.20
1958	1	1	738	52.00	33 38.00	-118 2.00	0.00	3.00
1958	3	30	653	17.00	34 0.00	-116 44.00	0.00	3.00

Table 2.5-4
LISTING OF INSTRUMENTAL EPICENTERS WITHIN AN 80-KILOMETER (50-MILE) RADIUS OF THE SITE, THROUGH JUNE 1980 (Sheet 33 of 44)

YEAR	MO	DA	HRMN	SEC	LATITUDE	LONGITUDE	DEPTH	MAG
1958	3	31	1433	43.00	34 5.00	-117 11.00	0.00	3.40
1958	4	30	236	18.00	32 47.00	-118 6.00	0.00	3.60
1958	10	14	1642	39.00	33 39.00	-116 47.00	0.00	3.20
1958	10	15	1036	58.00	33 54.00	-118 8.00	0.00	3.20
1959	11	2	1608	26.00	33 43.00	-116 44.00	0.00	3.50
1958	11	13	909	3.00	32 44.00	-117 23.00	0.00	3.40
1958	11	23	2104	2.00	32 44.00	-117 23.00	0.00	3.40
1958	12	23	1116	17.00	34 5.00	-117 30.00	0.00	3.30
1959	2	7	2124	22.00	33 28.00	-118 20.00	0.00	3.00
1959	3	15	424	8.00	33 22.00	-116 48.00	0.00	3.30
1959	3	30	1417	32.00	33 22.00	-117 52.00	0.00	3.30
1959	5	6	2323	29.00	34 4.00	-117 22.00	0.00	3.30
1959	5	10	1542	57.00	33 2.00	-117 43.00	0.00	3.10
1959	5	21	1550	44.00	33 23.00	-116 48.00	0.00	3.60
1959	6	12	1103	12.98	33 29.30	-116 46.62	5.70	4.00
1959	6	27	1622	11.09	33 58.09	-116 52.94	13.80	4.00
1959	7	23	321	3.00	33 56.00	-117 15.00	0.00	3.50
1959	7	29	2014	0.00	34 0.00	-117 48.00	0.00	3.10
1959	7	29	2129	0.00	34 0.00	-117 48.00	0.00	3.30
1959	8	3	1526	0.00	34 0.00	-117 48.00	0.00	3.50
1959	10	6	1502	17.00	32 50.00	-118 21.00	0.00	3.20
1959	11	29	2342	14.00	34 0.00	-116 59.00	0.00	3.10
1959	11	29	2350	45.00	34 1.00	-116 56.00	0.00	3.10
1959	12	15	2123	17.00	33 59.00	-117 1.00	0.00	3.00

Table 2.5-4
LISTING OF INSTRUMENTAL EPICENTERS WITHIN AN 80-KILOMETER (50-MILE) RADIUS OF THE SITE, THROUGH JUNE 1980 (Sheet 34 of 44)

YEAR	MO	DA	HRMN	SEC	LATITUDE	LONGITUDE	DEPTH	MAG
1960	1	5	1807	43.00	34 2.00	-117 44.00	0.00	3.00
1960	1	10	514	8.00	34 3.00	-117 48.00	0.00	3.10
1960	2	24	1312	34.00	34 0.00	-117 34.00	0.00	3.80
1960	6	24	39	56.00	33 50.00	-117 3.00	0.00	3.00
1960	7	8	335	44.00	33 43.00	-117 52.00	0.00	3.30
1960	8	17	905	48.00	33 9.00	-117 58.00	0.00	3.10
1960	8	20	2327	42.00	33 41.00	-118 22.00	0.00	3.80
1960	10	30	416	17.00	33 0.00	-117 29.00	0.00	3.00
1960	11	6	1155	22.00	33 41.00	-118 2.00	0.00	3.30
1960	11	23	15	24.00	32 43.00	-118 15.00	0.00	3.00
1960	11	23	1744	28.00	32 43.00	-118 15.00	0.00	3.00
1960	11	25	2230	28.00	33 16.00	-117 31.00	0.00	3.40
1961	1	1	618	34.00	34 5.00	-116 49.00	0.00	3.00
1961	1	14	323	39.00	34 4.00	-118 13.00	0.00	3.00
1961	2	12	1032	28.00	33 0.00	-117 45.00	0.00	3.00
1961	2	21	920	18.00	34 0.00	-117 31.00	0.00	3.20
1961	6	15	459	12.00	34 0.00	-117 1.00	0.00	3.30
1961	8	26	2147	45.78	33 16.55	-116 48.29	0.20	3.30
1961	10	4	221	31.60	33 51.25	-117 45.12	4.30	4.10
1961	10	18	1111	54.00	33 31.00	-116 47.00	0.00	3.10
1961	10	20	1919	11.75	33 39.59	-117 58.62	5.10	3.80
1961	10	20	1920	18.00	33 40.00	-117 59.00	0.00	3.40
1961	10	20	1944	25.21	33 40.63	-117 58.18	7.10	3.20
1961	10	20	1949	50.50	33 39.24	-117 59.65	4.60	4.30
1961	10	20	1955	9.70	33 39.89	-117 57.95	5.80	3.50
1961	10	20	2007	14.46	33 39.57	-117 58.44	6.10	4.00
1961	10	20	2019	37.15	33 40.22	-117 58.93	6.80	3.20
1961	10	20	2142	40.74	33 39.91	-117 58.77	7.20	4.00
1961	10	20	2147	4.24	33 41.62	-117 57.99	10.30	3.00
1961	10	20	2235	34.21	33 40.29	-118 0.75	5.60	4.10
1961	10	21	438	52.00	33 40.39	-117 56.17	2.00	3.50
1961	10	21	847	58.60	33 39.27	-117 56.79	6.50	3.10
1961	11	7	612	54.74	33 38.12	-118 2.73	7.10	3.00

Table 2.5-4
LISTING OF INSTRUMENTAL EPICENTERS WITHIN AN 80-KILOMETER (50-MILE) RADIUS OF THE SITE, THROUGH JUNE 1980 (Sheet 35 of 44)

YEAR	MO	DA	HRMN	SEC	LATITUDE	LONGITUDE	DEPTH	MAG
1961	11	10	749	16.45	33 39.00	-117 59.31	1.00	3.00
1961	11	20	853	34.66	33 40.83	-117 59.57	4.40	4.00
1961	11	20	1133	20.36	33 54.17	-118 11.54	6.80	3.00
1962	1	15	432	2.10	33 45.28	-117 13.17	9.00	3.00
1962	2	2	2241	5.12	33 26.68	-116 55.36	17.30	3.40
1962	3	27	125	3.80	33 52.83	-117 39.21	6.80	3.10
1962	4	14	1542	14.19	33 49.87	-118 9.47	23.30	3.00
1962	4	27	912	32.06	33 44.26	-117 11.20	5.70	4.10
1962	5	5	1417	24.23	33 41.45	-116 42.93	10.70	3.60
1962	6	3	2057	10.70	33 22.68	-118 23.55	9.20	3.00
1962	7	10	627	1.76	33 31.78	-116 55.59	9.90	3.30
1962	8	31	326	43.06	33 56.65	-117 55.92	11.80	3.20
1962	9	1	1553	43.57	33 57.09	-118 21.85	5.90	3.00
1963	2	18	1658	53.15	33 55.43	-118 22.46	9.90	3.40
1963	3	11	607	0.95	33 45.21	-118 21.21	6.40	3.00
1963	3	30	1828	15.82	33 59.17	-116 46.25	1.10	3.20
1963	5	5	1351	48.55	33 54.01	-117 53.76	1.50	3.00
1963	5	7	1949	26.16	33 54.85	-118 23.43	3.40	3.30
1963	7	7	357	14.28	33 34.06	-117 14.59	11.20	3.00
1963	7	21	1835	47.27	33 37.77	-116 48.12	13.00	3.00
1963	7	26	733	51.52	34 2.27	-117 19.41	18.90	3.60
1963	8	6	1836	16.98	33 45.77	-117 44.25	9.60	3.00
1963	8	9	813	19.54	33 51.08	-118 10.83	7.40	3.20
1963	8	22	1213	11.16	33 43.02	-118 3.12	3.80	3.50
1963	9	6	44	18.20	33 52.57	-117 1.40	10.80	3.30
1963	9	14	351	16.24	33 32.56	-118 20.41	2.20	4.20
1963	9	14	415	39.95	33 34.90	-118 17.39	9.40	3.40
1963	9	22	34	42.08	33 58.47	-117 53.16	9.90	3.30
1963	9	23	1441	52.58	33 42.61	-116 55.50	16.50	5.00
1963	9	25	837	38.04	33 26.16	-118 12.85	13.50	3.80

Table 2.5-4
LISTING OF INSTRUMENTAL EPICENTERS WITHIN AN 80-KILOMETER (50-MILE) RADIUS OF THE SITE, THROUGH JUNE 1980 (Sheet 36 of 44)

YEAR	MO	DA	HRMN	SEC	LATITUDE	LONGITUDE	DEPTH	MAG
1963	10	8	2302	42.22	33 39.51	-117 10.94	7.20	3.70
1963	10	27	2036	6.10	33 32.05	-118 16.28	4.80	3.50
1963	11	2	2141	50.84	33 53.80	-117 47.79	4.50	3.00
1963	11	8	1625	29.97	33 58.70	-117 22.30	15.80	3.30
1963	12	14	248	13.56	32 45.28	-117 8.83	2.60	3.10
1963	12	27	1226	2.27	32 59.32	-116 42.43	11.80	3.10
1964	1	30	1150	19.38	34 0.68	-116 47.89	15.60	3.40
1964	2	20	2220	53.28	33 48.06	-118 7.96	9.40	3.20
1964	3	16	1638	42.91	34 3.94	-117 29.09	5.80	3.10
1964	3	21	27	3.44	33 56.17	-118 24.39	9.30	3.00
1964	5	22	506	41.81	34 3.32	-117 11.55	13.40	3.10
1964	6	6	1739	18.83	33 59.12	-116 42.64	15.10	3.20
1964	6	9	409	57.08	33 42.83	-116 44.45	4.20	3.00
1964	6	13	2258	26.71	33 47.90	-117 57.43	7.90	3.00
1964	6	21	1532	51.77	32 41.50	-117 9.66	2.70	3.70
1964	6	23	454	37.47	32 41.42	-117 7.45	7.60	3.60
1964	6	24	928	14.57	33 37.12	-118 17.35	3.30	3.00
1964	7	15	311	5.81	32 42.35	-117 6.81	5.80	3.50
1964	8	4	2045	44.56	33 29.48	-116 51.08	19.50	3.90
1964	12	6	1309	56.06	33 42.66	-116 49.05	15.40	3.10
1965	1	21	2109	50.50	34 2.88	-117 10.46	9.40	3.00
1965	10	17	945	18.99	33 58.55	-116 46.48	17.00	4.90
1965	10	17	1235	51.80	33 59.39	-116 45.53	17.60	3.00
1965	10	17	1536	52.84	33 59.71	-116 48.44	17.00	3.90
1965	10	19	2133	13.74	33 56.39	-116 52.46	27.80	3.70
1965	10	20	116	43.80	33 58.58	-116 45.75	16.00	3.50
1965	10	21	843	2.42	33 58.74	-116 45.49	17.40	3.60

Table 2.5-4
LISTING OF INSTRUMENTAL EPICENTERS WITHIN AN 80 KILOMETER (50-MILE) RADIUS OF THE SITE, THROUGH JUNE 1980 (Sheet 37 of 44)

YEAR	MO	DA	HRMN	SEC	LATITUDE	LONGITUDE	DEPTH	MAG
1965	10	21	1025	15.82	33 58.26	-116 47.55	10.90	3.10
1965	10	23	1939	54.73	33 59.32	-116 44.87	17.50	3.40
1965	10	30	2303	33.12	33 57.91	-116 46.99	17.70	3.00
1965	11	12	2355	9.81	33 58.78	-118 23.53	6.00	3.00
1965	11	17	2010	32.54	33 58.86	-116 52.53	25.20	3.30
1965	12	26	1425	0.89	33 19.57	-116 43.19	1.30	3.70
1966	1	14	153	35.69	33 48.11	-117 42.43	5.30	3.00
1966	3	10	0	43.98	32 53.06	-117 11.38	48.70	3.20
1966	5	15	912	52.49	34 3.09	-116 43.87	0.70	3.10
1966	5	31	1122	11.05	33 56.40	-117 19.43	11.30	3.00
1966	6	6	616	43.11	33 59.67	-117 20.03	18.80	3.00
1966	6	13	2105	36.87	33 44.84	-117 59.50	11.30	3.50
1966	6	23	1854	21.01	33 20.84	-117 48.72	1.30	3.40
1966	6	27	1415	30.68	33 44.44	-116 49.17	8.70	3.00
1966	8	3	2055	5.43	32 45.67	-118 7.14	7.70	3.00
1966	10	2	512	34.46	33 58.13	-118 19.62	1.90	3.50
1966	12	22	453	54.74	33 39.45	-118 20.55	12.40	3.50
1967	1	8	738	5.34	33 39.79	-118 24.80	17.70	4.00
1967	1	8	812	30.25	33 33.28	-118 20.56	14.00	3.60
1967	1	8	813	36.72	33 34.37	-118 19.04	15.70	3.30
1967	1	8	815	16.94	33 34.12	-118 23.46	7.30	3.30
1967	1	8	826	58.24	33 34.78	-118 21.72	9.20	3.80
1967	1	8	910	33.26	33 34.30	-118 18.91	8.60	3.00
1967	1	8	2047	44.44	33 34.74	-118 24.23	8.80	3.80
1967	1	24	8	30.96	33 14.09	-117 58.07	4.40	3.70
1967	1	24	1412	22.66	33 15.94	-117 57.54	2.10	3.20
1967	2	21	2045	48.68	33 49.45	-117 40.51	0.10	3.50
1967	6	15	458	5.52	33 59.79	-117 58.49	10.00	4.10
1967	6	17	2114	48.64	33 49.21	-117 45.14	3.30	3.10
1967	8	22	1730	44.53	33 52.82	-117 39.63	5.30	3.00
1967	12	1	909	27.59	33 5.04	-117 55.12	11.90	3.20

Table 2.5-4
LISTING OF INSTRUMENTAL EPICENTERS WITHIN AN 80-KILOMETER (50-MILE) RADIUS OF THE SITE, THROUGH JUNE 1980 (Sheet 38 of 44)

YEAR	MO	DA	HRMN	SEC	LATITUDE	LONGITUDE	DEPTH	MAG
1968	1	11	2317	0.51	33 19.84	-517 3.74	4.70	3.30
1968	1	19	1208	55.42	33 56.84	-115 16.09	8.10	3.00
1968	2	28	1458	47.53	34 0.44	-116 48.53	10.00	3.00
1968	4	29	2212	35.22	33 27.04	-116 54.81	5.00	3.30
1968	4	30	53	35.37	33 25.84	-116 55.98	5.00	3.40
1968	5	3	721	54.94	32 41.10	-117 5.67	11.30	3.50
1968	7	8	1518	3.26	33 59.51	-116 42.14	4.20	3.30
1968	7	14	826	45.81	33 49.92	-117 44.25	6.50	3.30
1968	9	12	26	42.47	32 40.57	-118 17.96	13.40	3.00
1968	9	13	39	30.33	32 44.82	-118 19.67	13.90	3.10
1968	10	4	1057	39.68	33 31.52	-117 21.71	6.60	3.50
1968	10	5	55	52.30	33 32.02	-117 20.65	8.10	3.20
1968	10	11	1419	19.12	33 26.40	-117 15.11	4.80	3.00
1968	10	28	1413	33.33	33 55.21	-117 13.06	15.40	3.00
1968	12	12	614	57.59	34 3.84	-116 59.78	10.00	3.00
1968	12	29	1330	15.65	33 40.27	-116 44.92	9.30	3.30
1969	1	13	1623	47.94	33 59.20	-116 52.73	14.60	3.50
1969	2	23	2011	24.21	33 44.12	-117 7.32	3.10	3.20
1969	4	4	605	24.06	33 31.40	-116 44.85	5.60	3.10
1969	4	13	1055	5.74	33 33.91	-118 18.55	7.30	3.50
1969	5	5	1537	15.51	33 55.26	-118 11.50	7.70	3.10
1969	5	20	416	44.91	33 35.19	-116 51.81	10.00	3.00
1969	7	16	2	27.65	33 39.45	-116 52.04	5.30	3.00
1969	8	29	1742	18.13	34 3.20	-117 17.54	8.50	3.00
1969	9	26	2057	5.76	32 45.70	-118 14.06	13.70	3.00
1969	9	27	225	55.12	32 42.60	-118 16.61	2.30	3.10

Table 2.5-4
LISTING OF INSTRUMENTAL EPICENTERS WITHIN AN 80-KILOMETER (50-MILE) RADIUS OF THE SITE, THROUGH JUNE 1980 (Sheet 39 of 44)

YEAR	MO	DA	HRMN	SEC	LATITUDE	LONGITUDE	DEPTH	MAG
1969	10	27	1316	2.32	33 32.71	-117 48.40	6.50	4.50
1969	11	15	1618	12.05	34 0.13	-116 44.67	10.00	3.10
1969	12	2	1049	14.54	33 58.75	-118 19.64	10.00	3.10
1970	1	3	1948	40.80	33 57.74	-116 50.63	10.00	3.20
1970	2	11	2226	36.75	33 41.72	-117 8.43	10.00	3.00
1970	3	1	49	6.90	33 11.26	-117 34.09	5.00	3.00
1970	5	12	1232	1.96	33 56.90	-117 45.44	5.00	3.30
1970	5	22	940	30.56	33 44.71	-118 6.93	8.00	3.00
1970	7	21	2030	34.45	32 56.78	-117 41.12	5.00	3.40
1970	7	26	1117	29.42	33 27.65	-117 44.56	5.00	3.10
1970	8	25	1426	51.21	32 55.41	-118 20.06	8.00	3.20
1970	9	14	1157	0.03	34 3.69	-118 20.95	8.00	3.00
1970	9	23	833	33.94	33 56.23	-118 17.84	8.00	3.70
1970	9	23	851	17.26	33 54.98	-118 15.06	5.00	3.30
1970	9	23	859	55.95	33 57.76	-118 19.15	8.00	3.00
1970	9	23	958	15.20	33 55.90	-118 15.93	8.00	3.00
1970	10	9	755	6.68	33 45.01	-118 23.42	8.00	3.50
1970	11	17	654	4.77	33 44.56	-117 29.48	8.00	3.20
1971	1	14	228	40.32	33 28.49	-116 43.21	8.00	3.40
1971	1	19	236	12.62	33 58.96	-116 44.51	8.00	3.70
1971	3	2	346	29.34	33 56.01	-117 51.47	12.50	3.70
1971	5	6	1945	58.92	33 14.92	-116 45.38	8.00	3.50
1971	5	26	1816	53.22	33 14.78	-116 45.99	8.00	3.20
1971	6	22	1041	19.01	33 44.86	-117 28.74	8.00	4.20
1971	7	9	404	50.18	33 50.19	-117 44.06	5.40	3.00
1971	7	25	1731	29.86	34 0.29	-117 14.05	8.00	3.10
1971	8	17	1146	9.35	33 25.34	-117 6.68	8.00	3.20

Table 2.5-4
LISTING OF INSTRUMENTAL EPICENTERS WITHIN AN 80-KILOMETER (50-MILE) RADIUS OF THE SITE, THROUGH JUNE 1980 (Sheet 40 of 44)

YEAR	MO	DA	HRMN	SEC	LATITUDE	LONGITUDE	DEPTH	MAG
1971	8	28	1535	59.90	33 14.61	-116 48.43	8.00	3.00
1971	9	24	22	9.29	33 13.74	-116 47.35	8.00	3.00
1971	9	28	353	19.80	33 57.46	-117 52.63	5.60	3.20
1971	9	29	2307	26.44	32 47.53	-118 17.84	8.00	3.00
1971	9	30	1810	46.62	32 46.17	-118 17.80	8.00	3.10
1971	10	1	1744	41.34	32 45.57	-118 18.83	8.00	3.10
1971	10	1	2310	11.14	32 43.58	-118 24.87	8.00	3.00
1971	10	4	1831	38.18	32 42.47	-118 18.52	8.00	3.00
1971	10	10	1526	35.89	33 44.58	-117 30.65	8.00	3.50
1971	10	21	2231	24.65	33 13.02	-118 21.71	8.00	3.00
1971	10	28	2352	30.81	33 15.58	-116 44.21	8.00	3.10
1971	11	26	1713	18.00	33 57.30	-118 19.82	8.00	3.00
1972	1	7	408	25.27	33 15.76	-116 50.28	11.70	3.40
1972	3	1	749	37.15	33 24.62	-117 0.44	8.00	3.00
1972	3	4	1529	20.93	33 13.39	-116 55.55	8.00	3.50
1972	3	17	1948	5.15	34 0.06	-117 9.90	8.00	3.00
1972	3	23	1601	0.43	32 57.90	-117 37.22	8.00	3.20
1972	4	25	226	31.51	32 53.21	-117 42.04	12.70	3.60
1972	4	27	2229	42.08	33 27.45	-116 51.22	1.80	3.10
1972	5	23	1019	44.38	34 3.71	-117 13.99	8.00	3.00
1972	6	12	357	18.16	33 42.88	-116 45.85	8.00	3.20
1972	6	19	1608	26.76	34 4.62	-117 26.80	5.50	3.00
1972	7	29	118	51.00	33 11.57	-116 47.58	8.00	3.20
1972	8	27	849	27.05	34 3.34	-118 23.10	8.00	3.20
1972	9	11	940	28.70	34 5.08	-117 14.10	8.00	3.80
1972	10	16	1234	14.20	33 49.14	-118 23.36	12.70	3.40
1972	10	20	1753	24.46	34 1.56	-117 36.83	3.00	3.00
1972	10	31	956	10.05	33 15.06	-116 51.40	8.00	3.20
1972	11	10	2102	52.44	34 1.70	-116 55.42	8.00	3.20
1972	11	16	2153	18.23	33 44.31	-117 31.40	8.00	3.10

Table 2.5-4
LISTING OF INSTRUMENTAL EPICENTERS WITHIN AN 80-KILOMETER (50-MILE) RADIUS OF THE SITE, THROUGH JUNE 1980 (Sheet 41 of 44)

YEAR	MO	DA	HRMN	SEC	LATITUDE	LONGITUDE	DEPTH	MAG
1972	11	18	1508	38.73	34 2.89	-116 46.36	8.00	3.40
1972	11	25	324	59.72	34 0.99	-117 36.15	8.00	3.00
1972	11	25	657	38.17	34 1.03	-117 35.76	8.00	3.40
1972	11	25	702	6.47	34 0.94	-117 36.43	8.00	3.50
1972	11	25	707	39.64	34 1.04	-117 36.28	8.00	3.20
1972	12	10	1022	10.10	33 59.99	-117 36.20	8.00	3.20
1972	12	13	504	19.92	34 1.43	-117 36.38	8.00	3.10
1972	12	13	512	55.79	34 1.15	-117 36.61	8.00	3.40
1973	1	2	245	48.57	33 37.41	-117 19.12	8.00	3.10
1973	1	8	738	27.06	34 1.57	-117 36.57	8.00	3.00
1973	1	12	356	34.97	33 0.34	-117 52.65	8.00	3.00
1973	2	3	2345	12.59	34 3.18	-116 44.44	8.00	3.00
1973	2	6	101	0.52	33 35.97	-118 21.28	8.00	3.50
1973	2	25	541	41.88	33 15.00	-116 47.41	8.00	3.40
1973	3	19	213	48.50	33 34.47	-118 22.15	8.00	3.50
1973	3	21	411	49.70	33 51.37	-118 20.70	8.00	3.50
1973	3	25	2153	51.78	33 23.68	-116 58.95	8.00	3.00
1973	3	30	1550	21.89	34 2.41	-117 16.35	8.00	3.20
1973	5	18	635	19.56	34 1.82	-117 8.14	8.00	3.30
1973	6	15	1942	30.08	34 1.68	-117 33.48	8.00	3.00
1973	6	19	1026	31.31	32 53.35	-117 38.64	8.00	3.90
1973	6	19	1050	11.22	32 52.54	-117 37.54	8.00	3.20
1973	6	25	1239	50.08	33 50.92	-116 49.29	8.00	3.20
1973	6	26	2337	56.52	34 1.22	-116 45.18	8.00	3.00
1973	7	1	32	10.09	34 1.18	-116 49.05	8.00	3.00
1973	8	5	1325	17.33	33 45.40	-117 29.72	8.00	3.30
1973	10	19	1837	19.80	33 36.17	-118 20.04	8.00	3.10
1973	10	23	457	57.07	33 49.08	-117 43.36	8.00	3.30
1973	10	28	2200	2.74	32 40.83	-118 4.64	8.00	4.50
1973	11	4	29	24.88	33 58.82	-116 48.70	8.00	3.00
1973	11	18	730	0.23	33 58.36	-118 21.55	8.00	3.20
1973	11	19	1857	56.38	33 57.66	-117 47.17	8.00	3.10
1973	11	19	2039	21.92	33 57.94	-117 46.61	8.00	3.00
1973	12	28	1530	26.56	33 34.73	-117 44.20	0.00	3.60

Table 2.5-4
LISTING OF INSTRUMENTAL EPICENTERS WITHIN AN 80-KILOMETER (50-MILE) RADIUS OF THE SITE, THROUGH JUNE 1980 (Sheet 42 of 44)

YEAR	MO	DA	HRMN	SEC	LATITUDE	LONGITUDE	DEPTH	MAG
1974	1	31	605	28.59	34 2.18	-117 1.93	11.40	3.80
1974	2	19	642	5.46	33 0.71	-117 48.23	11.50	3.00
1974	3	12	735	45.35	34 4.54	-118 13.50	8.00	3.10
1974	9	11	1216	37.86	32 40.50	-117 54.79	8.00	3.20
1974	9	21	1037	41.85	33 51.19	-117 6.60	13.40	3.90
1974	10	22	1213	39.11	33 59.09	-118 21.89	10.10	3.10
1974	10	29	1053	51.71	34 1.20	-116 47.44	20.10	3.00
1974	12	14	401	22.38	32 44.10	-117 24.39	8.00	3.10
1974	12	19	1236	16.94	34 4.38	-118 4.80	9.27	3.50
1974	12	19	1239	50.50	34 4.32	-118 5.00	8.00	3.20
1975	1	3	555	31.71	33 32.22	-117 39.14	3.95	3.80
1975	1	3	600	53.14	33 32.18	-117 39.25	3.78	3.40
1975	1	12	2122	14.84	32 45.39	-117 59.29	15.30	4.80
1975	1	13	1121	50.32	33 48.70	-118 2.23	8.00	3.80
1975	1	14	758	41.46	33 49.00	-118 4.13	11.60	3.40
1975	1	30	1403	17.97	33 59.82	-116 45.16	12.80	3.20
1975	3	3	1534	45.10	33 55.98	-118 17.36	11.60	3.40
1975	3	8	713	9.16	33 40.29	-116 43.71	12.80	3.00
1975	3	23	430	22.44	34 5.28	-117 19.13	14.50	3.20
1975	5	12	2141	25.82	33 47.92	-117 27.22	1.01	3.00
1975	8	1	1142	13.05	33 38.23	-116 45.18	11.20	3.30
1975	9	25	2013	19.81	32 43.06	-118 19.43	4.01	3.50
1975	9	26	2124	22.46	32 42.07	-118 19.63	3.76	3.60

Table 2.5-4
LISTING OF INSTRUMENTAL EPICENTERS WITHIN AN 80-KILOMETER (50-MILE) RADIUS OF THE SITE, THROUGH JUNE 1980 (Sheet 43 of 44)

YEAR	MO	DA	HRMN	SEC	LATITUDE	LONGITUDE	DEPTH	MAG
1975	11	18	1604	45.02	34 2.00	-117 35.20	5.02	3.00
1975	12	9	1101	43.33	34 1.86	-117 35.23	5.30	3.00
1976	1	1	1720	12.94	33 57.90	-117 53.19	6.17	4.20
1976	1	1	2007	1.99	33 57.85	-117 52.95	3.57	3.20
1976	1	15	312	6.53	33 53.46	-117 53.48	5.36	3.00
1976	2	29	1301	26.21	33 41.37	-118 1.16	8.00	3.00
1976	3	7	1034	15.34	33 1.84	-117 32.36	5.83	3.10
1976	3	12	149	16.99	32 49.75	-118 22.41	11.70	3.00
1976	3	30	2334	54.12	33 41.31	-116 49.54	14.00	3.00
1976	4	17	416	20.38	33 59.72	-116 43.36	13.50	3.00
1976	4	25	1751	8.37	33 44.41	-118 1.04	10.60	3.00
1976	5	23	1330	20.40	33 40.11	-116 47.81	16.70	3.30
1976	7	23	2053	55.94	33 51.92	-118 9.38	9.85	3.00
1976	8	22	809	59.67	34 2.69	-117 28.12	2.68	3.00
1976	9	5	2230	30.22	34 1.19	-117 14.18	15.50	3.00
1976	9	19	1111	42.03	33 27.11	-116 44.46	15.50	3.50
1976	10	18	1726	52.61	32 42.83	-117 54.61	15.10	4.20
1976	10	18	1727	53.10	32 45.56	-117 54.37	13.80	4.20
1977	1	18	1254	34.47	33 49.53	-116 54.76	12.96	3.00
1977	3	31	1330	29.21	33 24.20	-116 58.26	8.00	3.30
1977	7	2	122	37.68	33 37.68	-116 42.80	12.60	3.00
1977	7	13	812	48.55	33 59.93	-116 49.83	10.45	3.10
1977	7	16	501	6.91	33 40.40	-116 48.17	5.02	3.00
1977	9	27	1810	42.05	33 32.94	-118 14.41	5.53	3.10
1977	10	4	2322	16.70	33 49.73	-117 2.62	10.00	3.10
1977	10	6	816	3.40	34 1.08	-118 11.14	13.90	3.30
1977	10	10	1238	0.57	33 33.69	-118 4.52	5.01	3.00
1977	11	8	1052	27.15	33 53.36	-117 54.36	6.99	3.40
1977	11	24	153	24.03	33 42.17	-116 49.80	4.99	3.10
1977	12	26	1836	8.37	33 59.69	-116 50.91	5.69	3.30

Table 2.5-4
LISTING OF INSTRUMENTAL EPICENTERS WITHIN AN 80-KILOMETER (50-MILE) RADIUS OF THE SITE, THROUGH JUNE 1980 (Sheet 44 of 44)

YEAR	MO	DA	HRMN	SEC	LATITUDE	LONGITUDE	DEPTH	MAG
1978	1	11	1827	0.65	32 45.96	-118 23.40	1.07	3.10
1978	1	11	2335	9.67	32 46.24	-118 24.24	1.07	3.10
1978	1	12	1851	1.67	32 54.90	-118 17.21	1.06	3.10
1978	2	6	39	25.63	34 2.48	-116 46.55	14.38	3.10
1978	2	6	101	28.79	34 2.40	-116 46.72	12.12	3.30
1978	2	13	1804	6.25	34 1.13	-117 12.86	13.47	3.00
1978	3	8	1449	34.84	33 49.65	-117 53.03	10.91	3.00
1978	3	13	1638	15.63	33 56.22	-117 58.64	5.14	3.30
1978	4	18	2242	36.14	33 52.82	-117 32.48	11.68	3.10
1978	4	25	2206	32.10	33 59.31	-116 56.08	20.45	3.30
1978	4	29	332	11.98	33 50.61	-117 43.38	6.00	3.30
1978	6	1	1659	55.06	32 46.19	-117 3.95	4.70	3.00
1978	6	4	357	17.28	33 55.46	-117 50.13	13.10	3.70
1978	9	3	1810	46.44	33 57.08	-117 43.35	7.88	3.50
1978	10	29	809	59.42	33 54.89	-118 18.68	12.92	3.00
1978	11	19	1740	56.88	33 51.30	-118 11.11	13.04	3.00
1979	2	27	707	38.62	33 57.08	-118 19.41	5.00	3.00
1979	3	8	1040	51.56	33 20.07	-116 49.91	6.59	3.30
1979	3	8	2337	49.39	34 1.40	-117 2.25	5.04	3.00
1979	3	11	714	5.11	34 0.84	-116 43.94	5.00	3.40
1979	3	11	1054	31.92	33 41.74	-116 46.17	6.00	3.00
1979	3	29	217	11.61	33 38.72	-116 43.43	6.52	3.00
1979	4	21	600	38.30	33 46.90	-118 4.40	5.00	3.10
1979	6	20	530	35.53	34 0.24	-118 20.87	5.45	3.00
1979	7	10	520	27.55	32 56.22	-117 44.52	4.97	3.10
1979	8	22	201	36.33	33 42.06	-116 50.20	5.04	4.10
1979	10	4	1344	17.76	33 36.27	-117 14.43	5.01	3.40
1979	11	15	709	58.21	32 45.11	-118 10.22	11.13	3.20
1979	12	7	2354	36.06	33 59.16	-116 42.46	5.22	3.30
1979	12	18	1537	13.84	34 1.27	-117 7.40	7.63	3.30
1980	1	8	1910	11.52	34 2.06	-117 33.71	5.04	3.30
1980	1	18	909	30.91	33 55.63	-117 43.70	7.14	3.10
1980	6	22	1739	35.84	33 50.23	-116 51.91	13.54	3.10
1980	6	25	2232	19.29	34 0.89	-116 44.96	15.85	3.00

Table 2.5-5
STRONG MOTION RECORDINGS WITHIN 320 KILOMETERS (200 MILES)
OF SAN ONOFRE SITE[a][b] (Sheet 1 of 8)

Date (PST)					Maximum Recorded		
(day)	(mo)	(yr)	Earthquake Area	No. of Stations Recording Event	Acceleration (g)	Distance[c] (km)	Source[d]
10	03	1933	Long Beach	3	0.29	27	1, 2
02	10	1933	Signal Hill	8	0.13	24	1, 2
30	12	1934	Lower California	4	0.18	64	1, 2
08	09	1935	Imperial Valley	1	0.02	32	1
24	02	1936	Southern California	1	0.01	10	1
25	03	1937	Southern California	9	0.01	91	1
12	04	1938	Imperial Valley	1	0.04	13	1, 2
31	05	1938	Santa Ana Mts	5	0.01	88	1
05	06	1938	Imperial Valley	1	0.04	35	1, 2
06	12	1938	Southern California	1	0.01	8	1
21	03	1939	Imperial Valley	1	0.03	38	1
24	03	1939	Imperial Valley	1	0.05	38	1
27	12	1939	Southern California	5	0.01	5	1

[a] See last page of table for notes.

Table 2.5-5
STRONG MOTION RECORDINGS WITHIN 320 KILOMETERS (200 MILES)
OF SAN ONOFRE SITE[a][b] (Sheet 2 of 8)

Date (PST)					Maximum Recorded		
(day)	(mo)	(yr)	Earthquake Area	No. of Stations Recording Event	Acceleration (g)	Distance[c] (km)	Source[d]
18	05	1940	Imperial Valley	6	0.35	11	1, 2
10	10	1940	Santa Monica Bay	3	0.02	30	1
30	06	1941	Santa Barbara	6	0.17	16	1, 2
07	09	1941	Santa Barbara	1	0.03	16	1
14	09	1941	Santa Barbara	1	0.02	16	1
21	10	1941	Gardena	7	0.03	30	1
14	11	1941	Gardena	9	0.05	6	1, 2
21	10	1942	Borego Valley	8	0.06	48	1, 2
28	08	1943	Southern California	7	0.01	152	1
18	06	1944	Los Angeles Region	6	0.05	21	1
15	08	1945	Southern California	4	0.01	67	1
02	04	1947	Imperial County	1	0.01	8	1
10	04	1947	Imperial County	1	0.01	8	1

Table 2.5-5
STRONG MOTION RECORDINGS WITHIN 230 KILOMETERS (200 MILES)
OF SAN ONOFRE SITE[(a)(b)] (Sheet 3 of 8)

Date (PST)					Maximum Recorded		
(day)	(mo)	(yr)	Earthquake Area	No. of Stations Recording Event	Acceleration (g)	Distance[(c)] (km)	Source[(d)]
10	04	1947	Imperial County	12	0.10	189	1
24	07	1947	Imperial County	2	0.01	160	1
04	12	1948	Southern California	13	0.08	81	1
02	05	1949	Southern California	9	0.01	229	1
04	11	1949	Lower California	2	0.02	101	1
11	01	1950	Southern California	1	0.01	88	1
29	06	1950	Imperial Valley	2	0.02	27	1
23	01	1951	Imperial Valley	1	0.03	30	1, 2
25	12	1951	Southern California	8	0.03	125	1
17	02	1952	Colton	1	0.01	16	1
21	07	1952	Kern County	26	0.13	118	1, 2
Numerous Aftershocks Recorded							
16	10	1952	Kern County	1	0.02		1

Table 2.5-5
STRONG MOTION RECORDINGS WITHIN 320 KILOMETERS (200 MILES)
OF SAN ONOFRE SITE[a][b] (Sheet 4 of 8)

Date (PST)					Maximum Recorded		
(day)	(mo)	(yr)	Earthquake Area	No. of Stations Recording Event	Acceleration (g)	Distance[c] (km)	Source[d]
21	11	1952	S.W. California	9	0.06	77	1
22	05	1953	Southern California	1	0.02	32	1
13	06	1953	Imperial Valley	1	0.04	11	1, 2
15	12	1953	Southern California	1	0.06	1.6	1
15	01	1954	Wheeler Ridge	12	0.07	43	1, 2
27	01	1954	Wheeler Ridge	12	0.04	19	1
31	01	1954	Baja, California	1	0.02	64	1
19	03	1954	Southern California	12	0.02	80	1
12	11	1954	Southern California	6	0.02	150	1, 2
13	06	1955	Southern California	1	0.06	22	1, 2
16	12	1955	Southern California	1	0.08	22	1, 2
Largest of 3 with a ≥ 0.01 g that day.							
09	02	1956	Baja, California	12	0.05	118	1, 2

Table 2.5-5
STRONG MOTION RECORDINGS WITHIN 320 KILOMETERS (200 MILES)
OF SAN ONOFRE SITE[a][b] (Sheet 5 of 8)

Date (PST)					Maximum Recorded		
(day)	(mo)	(yr)	Earthquake Area	No. of Stations Recording Event	Acceleration (g)	Distance[c] (km)	Source[d]
Largest of 2 with a $\leq$ 0.01 g that day.							
08	08	1956	Santa Barbara	1	0.02	10	1
18	30	1957	Oxnard	4	0.17	6	1, 2
04	04	1961	Long Beach	1	0.03		1
20	10	1961	Huntington Beach	5	0.03	11	1
28	02	1963	Fort Tejon	4	0.06	8	1
30	08	1964	Los Angeles	3	0.05	24	1
22	12	1964	Baja, California	2	0.03	80	1
15	07	1965	Southern California	1	0.04		2
07	08	1966	Gulf of California	1	0.02		2
14	06	1967	Southern California	2	0.05		1
13	08	1967	Southern California	1	0.02		1
08	04	1968	Borego mountain	60	0.13	66	1, 2

Table 2.5-5
STRONG MOTION RECORDINGS WITHIN 320 KILOMETERS (200 MILES)
OF SAN ONOFRE SITE[(a)(b)] (Sheet 6 of 8)

Date (PST)					Maximum Recorded		
(day)	(mo)	(yr)	Earthquake Area	No. of Stations Recording Event	Acceleration (g)	Distance[(c)] (km)	Source[(d)]
29	06	1968	Santa Barbara	2	0.03		1
04	07	1968	Southern California	29	0.12		1
18	04	1969	Southern California	12	0.02		1
12	09	1970	Southern California	33	0.17	28	1, 2
09	02	1971	San Fernando	100+	1.25	8	5
Numerous aftershocks recorded.							
27	08	1972	Beverly Hills	32	0.15	1	4
21	02	1973	Point Mugu	127	0.13	18	4
30	11	1973	Los Angeles	3	0.09	1	4
11	02	1974	Los Angeles	12	0.18	6	4
11	03	1974	San Fernando	8	0.06	10	4
14	08	1974	San Fernando	6	0.12	10	4
12	10	1974	Hemet	4	0.09	9	4

Table 2.5-5
STRONG MOTION RECORDINGS WITHIN 320 KILOMETERS (200 MILES)
OF SAN ONOFRE SITE[a][b] (Sheet 7 of 8)

Date (PST)					Maximum Recorded		
(day)	(mo)	(yr)	Earthquake Area	No. of Stations Recording Event	Acceleration (g)	Distance[c] (km)	Source[d]
06	12	1974	Calexico	4	0.11	16	4
19	12	1974	San Gabriel	1	0.06	4.5	4
13	01	1975	Lakewood	3	0.06		4
23	01	1975	Brawley	6	0.11		4
08	02	1975	Los Angeles	1	0.25		4
31	10	1975	- Date uncertain - causitive earthquake unknown				
01	04	1975	Los Angeles	1	0.09		4
16	06	1975	- Date uncertain - causitive earthquake unknown				
12	05	1975	Maricopa	5	0.07		4
19	06	1975	Imperial Valley	6	0.10	9.6	4
20	06	1975	Imperial Valley	4	0.15	5.7	4

(b) Only events with recorded acceleration greater or equal to 0.01g (fraction of acceleration due to gravity) are included in table to 1971. From 1972 to present, 0.05g is the lower limit.

(c) Distance from epicenter to recording instrument included only when given in reference.

Table 2.5-5
STRONG MOTION RECORDINGS WITHIN 320 KILOMETERS (200 MILES)
OF SAN ONOFRE SITE[a][b] (Sheet 8 of 8)

[d] Reference sources cited are as follows:

1. U.S. Department of Commerce, Environmental Data Service, and Coast and Geodetic Survey, 1928-1970, United States Earthquakes.

2. California Institute of Technology, 1976, Excerpts from files, Earthquake Engineering Research Laboratory.

3. U.S. Geological Survey, 1975, Seismic Engineering Program Report, October-December 1974: Circular 713.

4. U.S. Geological Survey, 1975, Seismic Engineering Program Report, January-March 1975: Circular 717-A.

   U.S. Geological Survey, 1975, Seismic Engineering Program Report, April-June 1975: Circular 717-B.

   U.S. Geological Survey, 1975, Seismic Engineering Program Report, July-September 1975: Circular 717-C.

5. Cloud, W. K., and Hudson, D. E., 1975, Strong Motion Data from the San Fernando, California, Earthquake of February 9, 1971 in Oakeshott, G. B., ed., San Fernando, California, Earthquake of February 9, 1971: California Div. Mines and Geology, Bulletin 196, pp 273-303.

Table 2.5-6
GEOLOGIC FAILURES INDUCED BY EARTHQUAKES WITHIN A 320-KILOMETER RADIUS OF SAN ONOFRE SITE[(a)] (Sheet 1 of 9)

Date (GMT)					Maximum Strong Motion		
(day)	(mo)	(yr)	Locale of the Failure	Maximum Intensity	Acceleration (g)	Distance from Epicenter (km)	Description
09	11	1852	Fort Yuma	IX	-	-	Lurching suggested by cracks and fissures near the Colorado River. A "mud volcano" reported 64 km (40 miles) southwest of fort.
27	11	1852	Lockwood Valley	X	-	-	Fissures 30 miles long.
-	12	1853	Yuma	?	-	-	Mud geysers reported.
09	01	1857	Fort Tejon	X+	-	-	Flooding resulted from disturbance of Kern River, Los Angeles River, and Lake Tulare; new springs developed near San Fernando and Santa Barbara; lurching and possible liquefaction indicated by reported fissuring in San Gabriel Valley and near San Bernardino.
-	05	1868	North end of Salton Sea	X	-	-	Fissure opened, possibly on buried fault trace.

Table 2.5-6
GEOLOGIC FAILURES INDUCED BY EARTHQUAKES WITHIN A 320-KILOMETER RADIUS
OF SAN ONOFRE SITE[(a)] (Sheet 2 of 9)

Date (GMT)					Maximum Strong Motion		
(day)	(mo)	(yr)	Locale of the Failure	Maximum Intensity	Acceleration (g)	Distance from Epicenter (km)	Description
11	06	1877	Imperial County		-		Reported volcanic eruption has been discredited. (Wood, et al, 1901).
04	04	1893	Newhall	IX	-	-	Numerous rockfalls; reports of fissures.
23	04	1893	San Diego	VIII	-	-	Boulders dislodged from hillsides.
22	07	1899	Cajon Pass	VIII	-	-	Numerous landslides.
25	12	1899	San Jacinto	X+	-	-	Fresh cracking near old sinks along San Jacinto fault.
28	07	1902	Los Alamos	X	-	-	Fissures, cracks in ground; landslides.
19	04	1906	Brawley	VIII	-	-	Riverbanks caved in.
20	09	1907	San Bernardino	VIII	-	-	Rocks fell in quarries; landslides in mountains.
15	05	1910	Lake Elsinore	VIII	-	-	Rocks rolled down hillsides.
19	07	1913	El Centro	IV(?)	-	-	"Marked earth disturbance."

Table 2.5-6
GEOLOGIC FAILURES INDUCED BY EARTHQUAKES WITHIN A 320-KILOMETER RADIUS
OF SAN ONOFRE SITE[(a)] (Sheet 3 of 9)

Date (GMT)					Maximum Strong Motion		
(day)	(mo)	(yr)	Locale of the Failure	Maximum Intensity	Acceleration (g)	Distance from Epicenter (km)	Description
12	01	1915	Los Alamos	VII	-	-	Small landslides in epicentral area; cracks due to lurching in alluvial soils.
23	06	1915	El Centro	IX	-	-	Numerous small cracks in alluvium possibly due to lurching or liquefaction (area was under irrigation); river banks caved in.
21	11	1915	Volcano Lake	X	-	-	Levees, damp ground cracked.
23	10	1916	Tejon Pass	VI	-	-	Rock slides onto road.
21	04	1918	San Jacinto	X	-	-	Roads closed by slides; dust clouds rose from mountains, cracks formed along fault zone; dry ground in epicentral area cracked, harrowed; a number of sand and mud craterlets formed.
06	06	1918	Riverside County	VI	-	-	Boulders loosened on hillsides; cracks formed around large trees.

Table 2.5-6
GEOLOGIC FAILURES INDUCED BY EARTHQUAKES WITHIN A 320-KILOMETER RADIUS
OF SAN ONOFRE SITE[(a)] (Sheet 4 of 9)

Date (GMT)					Maximum Strong Motion		
(day)	(mo)	(yr)	Locale of the Failure	Maximum Intensity	Acceleration (g)	Distance from Epicenter (km)	Description
16	02	1919	Maricopa	VII	-	-	Landslide at Lebec.
30	09	1919	Imperial Valley	VII	-	-	Levees slumped; longitudinal cracks formed.
20	12	1920	Salton Sea	VII	-	-	Mud geysers active for several days after earthquake.
29	06	1925	Santa Barbara	IX	-	-	Ground cracked; spring flow increased.
04	11	1927	Pt. Arquello	X	-	-	Heavy earth and rock slides; spouting of water from cracks; sand craters.
26	02	1930	Imperial Valley	VIII	-	-	Mud craterlets formed east of Westmoreland.
30	08	1930	Santa Monica	VIII	-	-	Cracks appeared in bluffs at coast and at Chatsworth Dam.
26	07	1932	Kern River	VI	-	-	Rock slides.

Table 2.5-6
GEOLOGIC FAILURES INDUCED BY EARTHQUAKES WITHIN A 320-KILOMETER RADIUS
OF SAN ONOFRE SITE[(a)] (Sheet 5 of 9)

Date (GMT)					Maximum Strong Motion		
(day)	(mo)	(yr)	Locale of the Failure	Maximum Intensity	Acceleration (g)	Distance from Epicenter (km)	Description
11	03	1933	Long Beach	IX	0.26	27	Liquefaction widespread in water soaked alluvium; sand craters formed and water issued from numerous cracks; lurching caused minor slumps; buckling and cracking of mud and unstable ground. Rock and debris slides occurred particularly in road cuts, artificial embankments, and steep cliffs for several tens of miles from epicentral area.
03	12	1934	Calexico	X	0.18	64	Fissures opened in alkali flats and alluvial soils; hot water "geysers" formed with some fissures; water issued from dry canal bed.
24	10	1935	Beaumont	V	<0.01	125	Landslides on southwestern slopes of Mount San Gorgonio.
24	02	1936	Colton	V	0.03	10	Small rock slide.

Table 2.5-6
GEOLOGIC FAILURES INDUCED BY EARTHQUAKES WITHIN A 320-KILOMETER RADIUS
OF SAN ONOFRE SITE[a] (Sheet 6 of 9)

Date (GMT)					Maximum Strong Motion		
(day)	(mo)	(yr)	Locale of the Failure	Maximum Intensity	Acceleration (g)	Distance from Epicenter (km)	Description
19	05	1940	Imperial Valley	IX	0.35	11	Shattered earth banks, lurching and slumping reported; ground settled over large areas, geyser 100 ft high, and numerous mud and sand craters.
01	29	1941	Whittier	V(?)	-	-	Old slide moved 4.5 ft at Point Fermin.
01	07	1941	Santa Barbara Channel	VIII	0.17	16	Small slide across railroad.
21	10	1942	Borrego Valley	VII	0.06	48	Landslide at Jacumba.
10	04	1947	Barstow	VII	0.03	184	Numerous landslides in surrounding mountains, affecting railroad at Afton; cracks appeared in riverbank.
18	09	1947	San Nicolas Island	VI	-	-	Rockfall but no serious landslides.
04	12	1948	Desert Hot Springs	VII	0.08	91	Slumping of cliffs and riverbanks; some larger landslides.

Table 2.5-6
GEOLOGIC FAILURES INDUCED BY EARTHQUAKES WITHIN A 320-KILOMETER RADIUS
OF SAN ONOFRE SITE[(a)] (Sheet 7 of 9)

Date (GMT)					Maximum Strong Motion		
(day)	(mo)	(yr)	Locale of the Failure	Maximum Intensity	Acceleration (g)	Distance from Epicenter (km)	Description
04	11	1949	Ensenada	VI	0.02	100	Few small slides reported.
29	07	1950	Calipatria	VIII	0.02	27	Sand boil appeared; irrigation ditch banks sloughed.
23	01	1951	Calipatria	VII	0.03	30	Canal banks cracked; 100 ft of ground settled 1 in.
05	12	1951	Brawley	VII	-	-	Cracks formed in canal bank and gravel road; water spurted 10 ft from crack.
21	07	1952	Bakersfield	XI	0.18	125	Ground cracked and severely distorted over a large area; railroad tunnels collapsed.
13	06	1953	Brawley	VII	0.04	11	Landslide reported; canal bank cracked.
06	02	1956	Castaic	VI	-	-	Landslide reported.
09	02	1956	El Alamo, Baja	VI	0.05	118	Hot springs formed along new fault line.
25	04	1957	Calipatria	VII	-	-	Ground cracked; water flowed from "blowholes."

Table 2.5-6
GEOLOGIC FAILURES INDUCED BY EARTHQUAKES WITHIN A 320-KILOMETER RADIUS
OF SAN ONOFRE SITE[(a)] (Sheet 8 of 9)

Date (GMT)					Maximum Strong Motion		
(day)	(mo)	(yr)	Locale of the Failure	Maximum Intensity	Acceleration (g)	Distance from Epicenter (km)	Description
30	09	1959	Point Conception	VI	-	-	Boulders rolled onto highway.
28	10	1962	Big Bear	VI	-	-	Rockfall blocked highway.
07	08	1966	El Golfo, Mexico	VI	-	-	Earth cracks reported.
08	04	1968	Ocotillo Wells	VII	0.12	66	Minor ground ruptures.
28	04	1969	Borrego Springs	VII	0.02	67	Boulders fell from hillsides.
12	09	1970	Lyttle Creek	VII	0.17	27	Numerous ground cracks and landslides.
09	02	1971	San Fernando	XI	1.00	8	Widespread soil movements recorded in alluvial soils; several landslides and rockslides were triggered on steep slopes; massive slides occurred in relatively flat alluvial soils and fill areas. Numerous strong motion records 0.50g to 0.75g with 1 high frequency peak 1.00g from hillside site.

Table 2.5-6
GEOLOGIC FAILURES INDUCED BY EARTHQUAKES WITHIN A 320-KILOMETER RADIUS OF SAN ONOFRE SITE[(a)] (Sheet 9 of 9)

Date (GMT)					Maximum Strong Motion		
(day)	(mo)	(yr)	Locale of the Failure	Maximum Intensity	Acceleration (g)	Distance from Epicenter (km)	Description
31	03	1971	Granada Hills	VII	-	-	Rocks fell on road; dust clouds in hills may have been slides.
30	02	1973	Oxnard	VII	0.13	18	Boulders and several small rock slides blocked road; ground cracked at Point Mugu.
06	08	1973	Anacapa Island	VI	<0.05	27	Landslides on San Nicolas Island.

NOTE: References to Table 2.5-6. Reports of Geologic failures are abstracted from the following:

1769-1928 - Townley, S. D. and Allen, M. W., 1939, Descriptive Catalog of Earthquakes of the Pacific Coast of the United States, 1769-1928: Bulletin, Seismology Society of America, Vol 29, pp 1-297.

1769-1970 - Coffman, J. L., and Von Hake, C. A., 1973, Earthquake History of the United States: U.S. Department of Commerce, National Oceanic and Atmospheric Administration, Environmental Data Service, Boulder, Colorado.

1928-1970 - U.S. Department of Commerce, several editors, by year, United States Earthquakes.

1970-1975 - Seismological notes, bi-monthly, Bulletin, Seismology Society of America.

Right-slip transform faulting between the Pacific and North American crustal plates apparently began in the Continental Borderland off southern California about 30 million years ago.[14][16] The initial opening of the Gulf of California occurred as early as 10 million years ago, as did initial displacement on the San Andreas fault;[17][69] however, it was not until about 5 million years ago that the Gulf of California and San Andreas fault began to absorb most of the interplate motion.[16]

The northwest trending system associated with the San Andreas is evident on the regional map of faults with Quaternary displacement, Figure 2.5-24. This figure also shows the boundaries of the natural provinces and contains an inset map of the seismic-structural provinces defined by Richter.[70]

Differences in the tectonic styles of the provinces, discussed in detail in Paragraph 2.5.2.2.2, are explained on a broad scale by recent models, which explain the present day location of the Transverse and Peninsular Ranges in terms of translation and rotation of microplates from southern latitudes.

Other possible tectonic models for the southern California area consider the relative motion of the Pacific and North American plates, the role that the "big bend" and the Transverse Range play in dividing or concentrating shear motion on the various northwest oriented strike-slip faults and resultant rotation applied to southern California and Baja California by the variable spreading rates on the transform faults in the Gulf of California. The most compatible model of the known geologic and tectonic conditions combines the effects of the interference of the Pacific and North American plate motions due to the bend in the San Andreas fault at the Transverse Range, and the variable rates of crustal spreading in the Gulf of California. These models are consistent with the plate tectonic considerations[16] but differ somewhat from earlier models such as the one described by Hill.[71]

This model accommodates the existence of a compressive stress field in the Transverse Range, which would block the northward motion of the crust immediately to the west of the San Andreas system and would require right-lateral shear motion to be concentrated on faults to the east and west of the Transverse Range. This could be occurring on the San Clemente or Coronado Banks faults to the west and on the San Andreas, San Jacinto, and Elsinore faults to the east. In this manner, a lower stress field would exist south of the Transverse Range in the area of the hypothesized Offshore Zone of Deformation. This suggested lower stress field is consistent with the observed lower degree of activity and low total offset on the hypothesized Offshore Zone of Deformation as compared to other faults to the east and probably to the west.

2.5.2.2.2 Tectonic Provinces

Tectonic provinces coincide with the widely accepted natural provinces which have been delineated and described by numerous authors.[1][72][73] The region within 320 kilometers (200 miles) of the San Onofre site includes parts of 10 provinces. Each province demonstrates distinctive geologic and tectonic characteristics as well as differences in physiography by which they were originally defined.[1][74] These provinces are shown in relation to capable faults in Figure 2.5-24.

Richter[70] defined a set of provinces which differ somewhat from the natural province. The location of these "Seismic Provinces" are shown on the inset map, Figure 2.5-24. In the following paragraphs, the general features, structure, and seismic activity of each of the 10 natural provinces are discussed, and comparisons are made with the seismic provinces defined by Richter.[70]

2.5.2.2.2.1 Coast Ranges Province

The Coast Ranges Province extends southward to within 200 kilometers (125 miles) of the San Onofre site. The area is traversed longitudinally by two major northwest-trending fault zones, the San Andreas on the northeast and the Nacimiento to the southwest. Numerous smaller subparallel faults are also present. Granitic basement is exposed between the two major faults. Elsewhere, a thick Mesozoic and Cenozoic sedimentary section is found overlying the highly deformed rocks of the Franciscan Assemblage.

Strike-slip faulting, at least along the San Andreas zone, appears to be the dominant tectonic feature within the province. The Nacimiento and associated faults have exhibited vertical offsets during at least three episodes of deformation since mid-Tertiary time, but little evidence has been found for right-lateral movement since middle Miocene.[114] The San Andreas is a prominent linear feature within the province, while the Nacimiento is sinuous and discontinuous. The San Andreas continues to the south, but the Nacimiento is truncated by the Big Pine fault at the northern edge of the Transverse Range Province.

The Coast Ranges Province coincides with the province described by Richter as having moderate to major seismicity.[70] Most historic activity within the province has been centered on the San Andreas fault.

2.5.2.2.2.2 Transverse Ranges Province

The east-west structural trend of the Transverse Ranges is a major exception to the northwest grain of coastal California.

The province originates offshore northwest of Los Angeles and extends eastward to within 80 kilometers (50 miles) of the Colorado River,[1] and at the nearest point is about 88 kilometers (55 miles) northwest of the San Onofre site. The western part of the province is composed primarily of deformed Tertiary sedimentary rocks.

Pre-Cenozoic basement terrane is exposed over much of central and eastern parts of the province. Basement terrane west of the San Andreas fault is displaced from correlative terrane to the east of the Salton Trough.[17][75]

The province appears to have acquired its present-day location as a result of translation and rotation of major blocks ("micro-plates") from lower latitudes on the order of 20 million years before present. Many of the east-west structural trends may have been present during earlier deposition of the Miocene and older strata.

Changes in the San Andreas system within the Transverse Ranges Province since the Miocene are as follows: Movement continued on the combined San Gabriel-San Andreas system until late Pliocene. At that time, a bend developed in the San Andreas along the northern edge of the province. The San Gabriel strand was then abandoned in favor of the present strand along the northern boundary of the province to Cajon Pass. The San Jacinto fault became active at that time as a major spur of the San Andreas system.(17)

Most of the Quaternary faults in the Transverse Ranges on Figure 2.5-24 are reverse faults. Quaternary movement on the San Gabriel fault has been minor reverse dip-slip. Exceptions are the San Andreas, the San Jacinto, Santa Ynez and the Big Pine faults. The latter is an easterly trending left-lateral fault on the northern border of the province.

The Sierra Madre fault zone, which bounds the central part of the province on the south, has been the most recent site of seismicity. Historic seismicity and the occurrence of Quaternary faulting has been more frequent in the Transverse Ranges than in most adjacent provinces.

2.5.2.2.2.3 Salton Trough Province

The Salton Trough extends from San Gorgonio Pass to the Gulf of California and, at its closest approach, is about 110 kilometers (70 miles) east of the San Onofre site.

Sedimentary rocks within the Salton Trough Province are predominantly late Cenozoic in age and nonmarine in origin. These sedimentary rocks, with some volcanic rock, overlie a basement of pre-Cenozoic granitic and metamorphic rocks along the margins of the trough. Subsidence continues as a result of crustal spreading.

The northern part of the province follows the San Andreas fault zone south of the Transverse Ranges. To the south, the San Jacinto and the Elsinore fault zones cross into the province from the Peninsular Ranges. These zones, especially the San Andreas and the San Jacinto, are composed of a series of braided or en-echelon faults in contrast to linear major traces northwest of the province. Farther southeast, the zones become increasingly indistinct as they become part of the widening trough of the Gulf of California.(17)

The Salton Trough forms the eastern part of the Southern Seismic Zone seismic province.(70) The seismic province includes that part of the Peninsular Ranges natural province east of and including the Whittier-Elsinore fault zone, Figure 2.5-24. Historic seismicity within the Salton Trough Province is dominated by low magnitude, M4 or less, events in the Imperial Valley. Larger magnitude events have been plotted along the San Jacinto, and Imperial faults in the province.

2.5.2.2.2.4 Peninsular Ranges Province

The San Onofre site is located within the Peninsular Ranges Province as described in Paragraph 2.5.1.1.2.1. The Peninsular Ranges do not include the offshore area, which is discussed in Paragraph 2.5.1.1.2.2 as a separate province.

The western part of the Peninsular Ranges Province includes the Los Angeles Basin which has features in common with the Continental Borderland including Franciscan type basement in its western part. The Newport-Inglewood zone of en-echelon folds and faults trends northwest across the basin. This zone is seismically active within the Los Angeles Basin but activity dies out along its offshore extension south of Laguna Beach.

Investigations have indicated that the Newport-Inglewood Zone of Deformation dies out in the vicinity of Laguna Beach, California. Its extension seaward has not been shown to connect with the South Coast Offshore Zone of Deformation nor is its seaward extension seismically active (Appendix 2.5M).

To the east, both the Elsinore and San Jacinto fault zones cross the Peninsular Ranges Province. Both zones are seismically active in the province and are included in Richter's Southern Seismic Zone; see Paragraph 2.5.2.2.2.2.

That part of the Peninsular Ranges west of the Elsinore zone is referred to by Richter as the Coastal Stable Block on the basis of structure and seismicity.[70] This mostly nonseismic block appears to be bounded to the south, some 175 kilometers (110 miles), by a zone of epicenters associated with the Agua Blanca and San Miguel faults in Baja, California, both of which have been considered as capable faults on the basis of Quaternary displacement as well as seismicity.

Structurally, the western two-thirds of the northern part of Baja California consists of an uplifted and westwardly tilted fault block. The main structural block has been cut by two major fault zones: the Agua Blanca fault zone and the San Miguel fault zone.

Generally, the principal fault systems of the northwest peninsula region are considered to be primarily strike-slip but many show evidence of dip-slip displacement as well.

The Agua Blanca fault zone is characterized by a relatively continuous main trace while the San Miguel fault zone is characterized by en-echelon fault segments and associated shorter subparallel faults. Features along these two major fault zones suggest Quaternary activity (Appendix 2.5J). These zones are discussed further in Paragraph 2.5.1.1.3.8 and in Appendices 2.5J and 2.5L.

The historical seismicity of the northern Baja California area is dominated by the high level of activity on the San Miguel fault, although this level is about one-half as high as that on the plate boundary faults (Cerro Prieto, Imperial, and others) to the east. Based on seismological evidence, the San Miguel fault does not appear to be mechanically connected to the hypothesized Offshore Zone of Deformation to the north, Paragraph 2.5.2.3.4.1 (Appendices 2.5J and 2.5L).

Investigation of data suggesting an absence of southward extension of the Rose Canyon Fault Zone into Baja, a region of high seismicity, is presented in Appendix 2.5L.

2.5.2.2.2.5 Continental Borderland Province

The Continental Borderland has commonly been included in the Peninsular Ranges Province; however, several major differences have led to its designation as a separate province.[(74)(76)(77)] The Continental Borderland is underlain by Franciscan basement in contrast to granitic rocks beneath the Peninsular Ranges. The Borderland contains a basin and ridge topography similar to that of the Basin and Range Province and differs structurally from that of the Peninsular Ranges.

The province is bounded on the west by the continental slope, (or Patton Escarpment) approximately 320 kilometers (200 miles) offshore. Its eastern limit is generally placed near the present shoreline. Several relatively large faults have been inferred in the province on the basis of topography, geophysical data, and faults which are exposed on the channel islands.[(4)] The southern end of the Newport-Inglewood Zone of Deformation, the northern end of the Rose Canyon Fault Zone, and the South Coast Offshore Zone of Deformation are located within this province. These areas, termed the hypothesized Offshore Zone of Deformation, are discussed in greater detail in Paragraphs 2.5.1.1.3 and 2.5.1.2.3. For conservatism, these three zones have been considered as a single, capable zone composed of en-echelon segments. These zones are discussed in Paragraph 2.5.1.1.3.4, Appendix 2.5M, and Reference 33.

Seismicity in the province has been low and scattered except near the Los Angeles Basin. Richter[(70)] also considers the Continental Borderland a separate province and refers to its seismicity as moderate when compared to adjacent provinces.

2.5.2.2.2.6 Great Valley Province

The Great Valley Province is a northerly-trending, asymmetrical structural trough which extends southward to within 210 kilometers (130 miles) of the San Onofre Site. A major sedimentary basin, it has accumulated over 12,000 meters (40,000 feet) of sediment of Jurassic to Holocene age. The most prominent period of deformation occurred during mid-Pleistocene time and involved folding along the western margin. The most severe deformation, involving overturned folds and reverse faulting, occurred in the southernmost end of the province nearest the bend in the San Andreas.[(1)]

Richter considers the province almost aseismic with the scattered epicenters located around its perimeter more properly belonging to adjacent provinces.[(70)]

2.5.2.2.2.7 Sierra Nevada Province

The Sierra Nevada Province is about 190 kilometers (120 miles) from the site, and is bounded on the east by the Sierra Nevada fault and on the west by the Great Valley Province. The province is underlain by granitic rocks of the Sierra Nevada Batholith with sparse exposures of Paleozoic and Mesozoic metamorphic rocks and a fringe of Tertiary sedimentary rocks along the western side with local remnants of Cenozoic volcanic rocks capping ridges.

Several thousand meters (thousands of feet) of vertical offset on the Sierra Nevada fault has uplifted and tilted the range to the west, but otherwise it remains relatively undeformed by late Cenozoic tectonism. The Tehachapi Mountains in the southernmost end of the province, however, are involved in the strain system associated with the bend in the San Andreas fault. The range is located between the White Wolf and Garlock faults and is therefore considerably more deformed than the remainder of the province.(74) Richter considers the Tehachapi Mountains to be a separate structural province with high seismicity.(70)

The level of seismicity within the Tehachapi Mountains area has been historically the highest in the Sierra Nevada natural province. The Sierra Nevada fault is active and was the site of at least one great earthquake. Richter considers this fault to be more properly in the Basin and Range Province.(70) A lower level of seismicity has been associated with the western boundary faults.

2.5.2.2.2.8 Basin and Range Province

The Basin and Range Province is a large area encompassing parts of eastern California, the states of Nevada, Arizona, and most of Utah and Oregon. The San Onofre site is located about 200 kilometers (125 miles) south of the southern border of the province, which is coincident with the Garlock fault. The province is typified by north trending mountain ranges separated by broad alluvial valleys. Rock types are diverse and range in age from Precambrian to Quaternary.(1)

Although Mesozoic and early Cenozoic deformation has been recognized in the Basin and Range Province,(1) much of the present structure is thought to have developed within the last 17 million years as a result of east-west crustal extension.(78) This is expressed as a series of horsts and grabens with faults bounding each mountain range.(78) Right-lateral displacement occurs on several northwest trending faults. The two major faults in the southern Basin and Range, the Death Valley and Furnace Creek, are northwest-trending right-lateral faults.

Richter cites several large historic earthquakes that have occurred in Nevada in the eastern part of the province, some with surface faulting.(70) In California, historic seismicity in the Basin and Range Province is not as pronounced.

2.5.2.2.2.9 Mojave Desert Province

The Mojave Desert Province forms a wedge-shaped area in southeastern California bounded by the Garlock fault on the northwest and the San Andreas fault zone on the southwest. The nearest part of the province to the San Onofre site is about 105 kilometers (65 miles) to the north. Rock types are similar to those in the Basin and Range Province but range-front faults, and consequently the ranges themselves, are northwest-trending rather than north-south; see Figures 2.5-7 and 2.5-24.

The most recent deformation within the province has been described by Garfunkel as rotation of the block as a whole involving right-slip on the set of northwest-trending fault and conjugate left-slip on west-trending faults including the Garlock.(76)

Distinct geologic as well as seismic differences have been recognized between the western and eastern parts of the Mojave Dessert.(72) This has prompted a tentative division of the region into two separate provinces;(72) however, for the purpose of this report, the Mojave Desert is considered to be a single province.

Historic seismicity has been greatest in the center of the province. Richter considers the eastern part of the province to be almost nonseismic on the basis of instrumental records.(70)

2.5.2.2.2.10 Sonoran Desert Province

Only a small part of the Sonoran Desert Province approaches the site; at its closest approach, the province is about 290 kilometers (180 miles) from the site. This province is located in southern Arizona and northern Mexico.

The Sonoran Desert is often associated with the Basin and Range Province because of similar rock types, the fault controlled north-trending mountain ranges. Most faulting, however, appears to be older than the post-middle Miocene faults controlling the Basin and Range Province. Richter considers the province to be an extension of the eastern Mojave Desert.(70) Historic seismicity is low when compared to adjacent provinces.

2.5.2.2.3 Capable Faults

Major faults within a 320-kilometer (200-mile) radius of the site were discussed in the previous section in relation to the natural provinces where they occur. These faults and others that are considered capable of producing significant seismicity in the future are shown on Figure 2.5-24 and are listed on Table 2.5-7.

Faults and fault zones shown in Figure 2.5-2 in California are those reported to exhibit Quaternary displacement.(79) Faults in Mexico are generalized after those mapped by Gastil and others(80) which are reported in the literature to displace Quaternary features.

Table 2.5-7
LIST OF MAJOR FAULTS WITH EVIDENCE OF QUATERNARY MOVEMENT WITHIN 320 KILOMETERS (200 MILES) OF SAN ONOFRE SITE (Sheet 1 of 3)

Type of Fault	Name
A. Northwest Trending Faults (Coast Ranges, Transverse Ranges, Peninsular Ranges, Salton Trough)	1. San Andreas
	2. San Jacinto
	3. Elsinore
	4. Whittier
	5. Chino
	6. Santa Monica to Baja Zone of Deformation
	7. Superstition Hills
	8. Imperial
	9. Laguna Salada
	10. Hot Springs
	11. San Miguel
	12. Agua Blanca
	13. Sierra Juarez
	14. San Gabriel
	15. Nacimiento Zone
	16. San Juan
	17. Little Pine
	18. Palo Verde
B. Northeast Trending Faults (Sierra Nevada, Great Valley, Transverse Ranges, Basin and Range, Mojave Desert)	19. Garlock
	20. White Wolf
	21. Big Pine

Table 2.5-7
LIST OF MAJOR FAULTS WITH EVIDENCE OF QUATERNARY MOVEMENT WITHIN 320 KILOMETERS (200 MILES) OF SAN ONOFRE SITE (Sheet 2 of 3)

Type of Fault	Name
C. East Trending Faults (Transverse Ranges)	22. Malibu Coast
	23. Santa Monica
	24. Raymond
	25. San Fernando
	26. Sierra Madre
	27. Cucamonga
	28. Sawpit Canyon
	29. Northridge Hills
	30. Simi
	31. Santa Susana
	32. Oakridge
	33. Holser
	34. San Cayetano
	35. Red Mountain
	36. Arroyo
	37. Santa Ynez
	38. Pine Mountain
	39. Clear Water
	40. Pinto Mountain
	41. Blue Cut
	42. Unnamed-Santa Barbara Channel
	43. Santa Cruz Island
	44. Santa Rosa Island

Table 2.5-7
LIST OF MAJOR FAULTS WITH EVIDENCE OF QUATERNARY MOVEMENT WITHIN 320 KILOMETERS (200 MILES) OF SAN ONOFRE SITE (Sheet 3 of 3)

Type of Fault	Name
D. Basin and Range Faults	45. Furnace Creek
	46. Death Valley
	47. Panamint Valley
	48. Sierra Nevada
E. Mohave Desert Faults	49. Manix
	50. Ludlow
	51. Pisgah
	52. Calico
	53. Mesquite Lake
	54. Camprock
	55. Lenwood
	56. Helendale
F. Miscellaneous	57. Plieto
	58. La Nacion
	59. Kern Front

2.5.2.3 Correlation of Earthquake Activity With Geologic Structures or Tectonic-Provinces

2.5.2.3.1 General

Seismic activity in southern California is presumed to be associated with relative movement of two lithospheric plates as discussed in Paragraph 2.5.2.2.1. The San Andreas fault zone, which has historically produced the most and largest earthquakes in the region, is typical of large strike-slip faults on the perimeter of the Pacific and other oceanic crustal plates. The San Andreas and similar faults throughout the world have produced earthquakes of magnitudes up to M8.4 with shallow to intermediate hypocenters.(70)

The southern California region is seismically typical of other areas of slip along plate boundaries. Major seismicity is associated with the major strike-slip faults, and other large events are associated with well-established faults away from the plate boundary, which apparently respond to adjustments within the plates. Minor earthquakes appear to reflect a more random crustal adjustment. The level of seismic activity generally drops off with increasing distance from the plate boundary.

In southern California, earthquakes of M5.0 and greater are associated with previously recognized faults or fault zones. Many smaller events, M4.9 and below, occur more randomly and are not as readily associated with surface faults.(74) Figures 2.5-20, 2.5-21, and 2.5-22 show this pattern.

Assignment of an earthquake to a particular fault depends on several factors, including the accuracy with which the epicenter is located, the geometry of the fault, and its capability to produce the earthquake as shown by past associated seismicity or the geologic record. The capability of faults within a 320-kilometer (200-mile) radius of the San Onofre site is discussed in general terms in Paragraph 2.5.2.2.3. Other related factors are discussed in the following paragraphs.

In many cases where individual earthquakes cannot reasonably be assigned to a particular fault, seismicity over a period of time clearly shows a relationship to zones of faulting.(81) These fault-related seismic zones and their relation to structure are discussed below. The relationship of the more random pattern of smaller events to the seismic activity of the natural province in which they occurred is also discussed.

2.5.2.3.2 Accuracy of Epicenter Location

The principal source of seismological data in the southern California region is a network of seismograph stations operated by the California Institute of Technology (CIT). The system began routinely reporting epicenter locations in 1932. At that time seven stations in the vicinity of Los Angeles were producing data. Since then the network has been expanded, and that together with more advanced analytical techniques have produced increasingly more accurate epicentral locations.(81)

The present network consists of over 160 stations each occupied by a short period vertical seismometer.(82) In addition, some of the stations contain horizontal seismometers, long-period seismographs, or Wood-Anderson Torsion Seismographs. Location of the stations is shown on Figure 2.5-25. Coordinates for each station are listed in Table 2.5-8. Monitoring of each station is done either daily by trained personnel, by hard-wire telemetry, or by radio links. Each station is also equipped with a radio receiver programmed to receive U.S. Bureau of Standards time signals. Signals received throughout the network are currently read manually at the CIT Seismological Laboratory and entered directly into the computer for accurate epicentral calculation within a few minutes.

The station closest to the site, SNS, is approximately 10 kilometers northwest of the site near the city of San Clemente.

Beginning in 1961, computer methods have been used to routinely locate epicenters and calculate depth of focus. Prior to 1961, graphical methods assuming a focal depth of 16 kilometers (10 miles) were used. Also in 1961, a more accurate crustal velocity model was adopted following several years of development. Computer reduction and the crustal velocity data have been applied to several events recorded prior to 1961, producing more accurate hypocentral data and epicentral locations.(81)

Some of the instrumentally calculated epicenter locations listed in Table 2.5-1 are based, in part, on data obtained by teleseismic stations outside the Cal Tech system. This is particularly true for larger events and those located outside of the perimeter of CIT stations; however, the majority of epicenter determinations were obtained from the CIT southern California network.

Before instrumental data became available in 1932, epicenters were calculated by compilation of reported intensity data. These are considered reasonably accurate in southern California only within this century, when the area was more densely populated and when an interest in seismology was developing. The most accurate locations were produced by constructing isoseismal maps showing the areal distribution of reported felt intensities. Scales were used relating perception of an earthquake by individuals or damage caused by an earthquake to intensity. Epicenters are presumed to be located within the area of highest reported intensity.

The drawbacks to the isoseismal method are obvious. The effectiveness of the calculation depended on the density of population in the affected area and the objectivity of observers. Recent comparisons with instrumental data show that highest intensities are often experienced in other than the epicentral area, due to the response of the soil to seismic shaking.

Table 2.5-8
LIST OF SOUTHERN CALIFORNIA SEISMOGRAPHIC STATIONS (Sheet 1 of 6)

Station Identi-fication	Latitude		Longitude		Elevation (m)	Distance from Station to Site (km)
	(deg)	(min)	(deg)	(min)		
ABL	34	51.05	119	13.25	-	260
ADL	34	33.38	117	25.02	900	160
AMS	33	08.48	115	15.25	146	210
BAR	32	40.8	116	40.3	-	90
BCH	35	11.10	120	05.05	-	350
BC2	33	39.42	115	27.67	1,185	200
BLU	32	24.32	117	43.52	1,880	140
BMT	35	08.15	118	35.81	-	255
BON	32	41.67	115	16.11	14	220
BPK	34	07.48	114	12.58	504	330
BSC	32	43.49	115	02.64	-	240
BTL	34	15.43	117	00.29	2,520	130
CAM	34	15.27	119	02.00	-	200
CCM	33	25.75	115	27.88	-	190
CFT	34	02.11	117	06.66	671	100
CHM	34	33.18	114	34.32	940	320
CIS	33	24.4	118	24.2	-	100
CJP	34	10.92	118	59.19	-	190[a]
CKC	34	08.18	117	10.48	550	110
CLC	35	49.0	117	35.8	-	300
CLI	33	08.45	115	31.64	-	185
CLP	34	05.33	118	57.85	-	185[a]
COA	32	51.01	115	07.36	35	230
COK	32	50.95	115	43.61	15	170
COQ	33	51.63	117	30.58	-	75
COY	33	21.84	116	18.63	-	110
CO2	33	50.83	115	20.68	276	220
CPE	32	52.8	117	06.0	-	50

[a] Station not plotted on Figure 2.5-25

Table 2.5-8
LIST OF SOUTHERN CALIFORNIA SEISMOGRAPHIC STATIONS (Sheet 2 of 6)

Station Identi-fication	Latitude		Longitude		Elevation (m)	Distance from Station to Site (km)
	(deg)	(min)	(deg)	(min)		
CPM	34	09.24	116	11.80	937	165
CPT	38	18.2	117	20.4	61	10
CRG	35	14.53	119	43.40	-	330
CRR	32	53.18	115	58.10	82	145
CSP	34	17.9	117	21.4	-	130
CWC	32	26.35	118	04.7	-	380
DBB	33	44.0	117	05.83	672	75[a]
DB2	33	44.15	117	03.76	625	65
DC1	34	20.82	119	35.099	-	255[a]
DC2	34	19.54	110	35.769	-	255[a]
DC3	34	19.10	119	36.939	-	255[a]
DC4	34	16.10	119	42.179	-	260[a]
DC5	34	19.63	119	37.999	-	250
DC6	34	21.07	119	38.379	-	260[a]
DC7	34	20.40	119	36.959	-	255[a]
DVL	34	12.02	117	19.71	598	115
EAG	33	50.94	115	28.39	366	200
ECC	32	47.9	115	32.9	-	200[a]
ECF	34	27.48	119	05.44	-	220
EGG	34	07.95	119	08.82	-	200[a]
ELR	33	08.84	115	49.95	-	155
FMA	33	42.75	118	17.12	-	100
FNK	33	22.98	115	38.26	-	175
FTC	34	52.25	118	53.51	-	240
FTM	32	33.29	114	20.01	263	310
GAV	34	01.35	117	30.34	-	95
GLA	33	03.1	114	49.6	-	255
GRP	34	48.26	115	36.27	1,238	265

Table 2.5-8
LIST OF SOUTHERN CALIFORNIA SEISMOGRAPHIC STATIONS (Sheet 3 of 6)

Station Identi-fication	Latitude		Longitude		Elevation (m)	Distance from Station to Site (km)
	(deg)	(min)	(deg)	(min)		
GSC	35	18.1	116	48.3	-	250
HAI	36	08.2	117	56.85	-	350[(a)]
HAY	33	42.5	115	38.3	-	180
HDG	34	25.73	116	18.30	1,347	180
HOT	33	18.84	116	34.89	-	80
IKP	32	38.93	116	06.48	-	140
ING	32	59.30	115	18.61	2	205
INS	33	56.14	116	11.66	1,700	150
IRC	34	23.4	118	24.0	-	165
IRN	34	09.60	115	11.04	980	240
ISA	35	39.8	118	28.4	-	305
KEE	33	38.49	116	39.14	1,366	90
KYP	34	06.11	118	52.77	-	175
LCL	33	50.0	118	11.55	-	105
LED	34	28.06	115	56.19	853	205
LGA	32	45.58	114	29.57	68	290
LHU	34	40.30	118	24.70	-	195
LRR	34	31.50	118	01.70	-	160
LTC	33	29.34	115	04.20	458	235
LTM	33	54.90	114	55.10	744	260
LJC	32	51.9	117	15.15	-	45
MDA	33	54.78	116	59.97	845	190
MLL	34	05.48	116	56.18	1,513	110
MTE	32	28.07	118	08.74	1,305	165[(a)]
MWC	34	13.4	118	03.5	-	135
NWR	33	06.10	115	41.01	-	165
OBB	33	10.04	115	38.20	61	175
OCB	34	02.20	119	01.01	-	120[(a)]

Table 2.5-8
LIST OF SOUTHERN CALIFORNIA SEISMOGRAPHIC STATIONS (Sheet 4 of 6)

Station Identi-fication	Latitude		Longitude		Elevation (m)	Distance from Station to Site (km)
	(deg)	(min)	(deg)	(min)		
PAS	34	08.95	118	10.29	-	130
PEC	33	53.51	117	79.6	-	80
PEM	34	10.04	117	52.18	-	120
PCF	34	03.19	117	47.44	-	105
PIC	32	54.85	114	38.59	263	275
PKM	35	03.0	120	02.40	-	305
PLM	33	21.2	116	51.7	-	50
PLT	32	43.87	114	43.76	61	270
PNM	33	58.64	115	48.05	1,147	180
PSP	33	47.63	116	32.93	195	105
PTD	34	00.25	118	48.38	-	165
PYR	34	34.08	118	44.5	-	205
RAY	34	02.18	116	48.67	2,342	110
RDM	34	24.0	117	11.10	1,426	140
RMR	34	12.77	116	34.52	1,702	145
ROD	34	37.78	116	36.29	-	180
RUN	32	58.33	114	58.63	151	240
RVR	33	59.6	117	22.5	-	90
RVS	34	02.08	114	31.08	677	300
RYS	34	38.60	119	21.10	-	255
SAD	34	04.87	118	39.9	-	160
SBAI	34	00.80	119	26.23	113	220
SBB	34	41.3	117	49.5	-	175
SBC	34	26.5	119	42.8	-	260
SBCC	34	56.38	120	10.32	610	340
SBCD	34	22.12	119	20.63	213	230
SBCL	34	24.75	119	21.67	-	240[(a)]
SBLC	34	29.79	119	42.81	119	270

Table 2.5-8
LIST OF SOUTHERN CALIFORNIA SEISMOGRAPHIC STATIONS (Sheet 5 of 6)

Station Identi-fication	Latitude		Longitude		Elevation (m)	Distance from Station to Site (km)
	(deg)	(min)	(deg)	(min)		
SBLG	34	06.87	119	03.85	415	190
SBLP	34	33.57	120	24.02	134	330
SBSC	33	59.68	119	37.99	457	235
SBSM	34	02.24	120	2.01	72	300
SBSN	33	14.68	119	30.38	-	210
SCI	32	58.8	18	32.8	-	115
SCY	34	06.37	118	27.25	-	145
SDW	34	36.55	117	04.45	1,184	170
SGL	32	38.95	115	43.52	104	175
SHH	34	11.26	115	39.27	1,122	205
SIL	34	20.87	116	49.60	1,730	140
SIP	34	12.25	118	47.92	-	175
SLU	32	30.10	114	46.64	41	275
SME	33	49.36	117	21.32	494	70
SMO	33	32.15	116	27.7	-	105
SNS	33	25.9	117	32.9	190	30
SNR	32	51.71	115	26.21	29	200
SPM	34	28.32	115	24.16	915	245
SSK	34	12.97	117	41.32	1,765	120
SSV	34	12.46	117	29.98	1,609	115
SUF	32	24.58	119	12.15	-	230[3]
SUP	32	57.31	115	49.43	221	160
SWM	34	43.0	118	35.0	-	210
SYP	34	21.6	119	58.7	-	290
TCC	33	59.7	118	00.8	-	105
THR	34	33.19	117	43.10	1,025	344[a]
TIN	37	03.3	118	13.7	-	455
TMB	35	05.24	119	32.08	-	300
TPC	34	06.35	116	02.92	-	170

Table 2.5-8
LIST OF SOUTHERN CALIFORNIA SEISMOGRAPHIC STATIONS (Sheet 6 of 6)

Station Identi-fication	Latitude		Longitude		Elevation (m)	Distance from Station to Site (km)
	(deg)	(min)	(deg)	(min)		
TPO	34	52.70	118	13.80	-	210
TTM	34	20.12	114	49.65	1,098	285
TWL	34	16.7	118	35.67	-	170
VPD	33	48.9	117	45.7	-	75
VGR	33	50.25	116	48.53	1,500	95
VST	33	09.4	117	13.9	112	20
WHP	34	18.42	114	29.75	606	310[a]
WH2	34	18.87	114	24.55	1,245	315
WIS	33	16.56	115	35.58	-	175
WLK	33	03.08	114	29.44	44	190
WML	33	00.91	115	37.35	-	175
WWR	33	59.51	116	39.36	702	115
YEG	34	26.18	119	57.56	-	360
YMD	32	33.28	114	32.68	76	290

Prior to about 1900, the southern California region was sparsely populated. Only broad areas affected by larger events can be identified on the basis of felt reports from the few population centers that existed during that period. The earliest earthquake documented in the site region was in 1769.

2.5.2.3.3 Association of Noninstrumental Earthquakes with Faults

Only a very small percentage of earthquakes, which occurred prior to the advent of instrumented epicenter calculations, can be readily associated with faults. Most of these were associated with observed movement of a fault. Others occurred within populated regions where particular causative faults were indicated by well established areas of maximum felt intensity.

In the majority of cases, maximum felt intensity areas were probably biased toward population centers; therefore, no attempt is made herein to associate earthquakes with faults when documented only by felt reports.

2.5.2.3.4 Occurrence of Larger Earthquakes

The pattern of seismicity in the site region shows that most earthquakes of M5.0 and greater are associated with recognized zones of faulting which generally show evidence of movement during Quaternary time; see Figure 2.5-20. Earthquakes of M6.0 and greater that have occurred in the past 40 years have been assigned to specific faults. Events in the M5.0 to M5.9 range appear to be associated with more general zones of faulting.

The California Institute of Technology has located and listed all earthquakes between January 1932 and June 1980; see Table 2.5-2 and Figures 2.5-20, 2.5-21, and 2.5-22. The plots of instrumental epicenters within a 80-kilometer (50-mile) radius, Figure 2.5-23, show no earthquake epicenters recorded within 8 kilometers (5 miles) of the San Onofre site. In addition, there are no historically reported earthquakes that can reasonably be associated with faults that lie within 5 miles of the site; however, as discussed below, earthquakes have occurred within the site region that cannot be associated with geological structure. For a discussion of these earthquakes see Paragraph 2.5.2.3.5.

Studies show that the seismicity between January 1, 1975, and October 1, 1979, within 200 miles of the site is similar to the long-term pattern for 1932 to 1975, and no distinctive new patterns of activity are evident. Seismic activity suggests an apparent decrease westward between the San Andreas and San Jacinto faults and the hypothesized Offshore Zone of Deformation. There is a suggestion the offshore region is more active than the hypothesized Offshore Zone of Deformation for the post-1975 period (Appendix 2.5J).

2.5.2.3.4.1 Association of M6+ Earthquakes with Faults

The relationship between earthquakes and recognized, pre-existing faults is most apparent for M6 and greater events[74] as shown on Figure 2.5-20.

In southern California, most major faults are strike-slip faults with apparent near-vertical dips; however, only a few degrees of deflection are necessary to offset the fault plane several kilometers at typical hypocentral depths of 8 to 24 kilometers (5-15 miles); therefore, if an epicenter is located close to the surface expression of such a fault, it can reasonably be associated with it. This is the case for the M6.0 and greater historic earthquakes in the site region. Similar associations can be made for smaller events if the quality of epicentral location warrants.

Two notable cases have occurred in southern California in which M6+ epicenters were accurately located at considerable distances from surface rupture on major faults. These were a series of aftershocks following the 1952, M7.7, earthquake on the White Wolf fault and the 1971, M6.4, event on the San Fernando segment of the Sierra Madre fault zone. The White Wolf aftershock occurred 20 kilometers (12 miles) from the surface faulting. The epicenters were related to the fault when the fault plane was shown to dip towards the location of the focus.[74] The same was true of the San Fernando earthquake, where the epicenter was about 12 kilometers (7-1/2 miles) from the nearest surface faulting.[79] Both faults were previously recognized as reverse faults associated with mountain uplift.

The most prominent alignment of larger earthquakes in the region has occurred along the trace of the San Jacinto and Imperial faults south of the Transverse Ranges. Epicenters of M6.0 and M6.8 earthquakes were located within a few miles of the recognized trace of the San Jacinto fault adjacent to and north of the Salton Sea in 1918, 1923, 1937, 1954, and 1968. A similar shock in 1899 was attributed to the San Jacinto fault on the basis of reported surface faulting.[83]

An M6.5 earthquake occurred on the main trace of the San Andreas fault north of the Salton Sea in 1948.

South of the Salton Sea, the San Andreas-San Jacinto zone breaks into several segments including numerous mapped faults that show evidence of recent movement. In 1915, two M6.25 earthquakes took place near the trace of the Imperial fault, which ruptured at the surface during an M7.1 earthquake in 1940. The epicenter of the October 1979 El Centro M6.8 event occurred on the Imperial Fault where it extends into Mexico. Farther south along the trend of the San Andreas system, epicenter locations are not as well known. Six events of M6.0 to M7.1 occurred in that area between 1915 and late 1979.

Other than the events associated with the San Jacinto fault, only one earthquake of M6.0 or greater was recorded in either the northern Peninsular Ranges or the Continental Borderland Province. This was the 1933 M6.3 earthquake which was centered near the southern terminus of the Newport-Inglewood Zone of Deformation.

In 1925 and 1941, M6.0 and M6.3 events occurred along a complex zone of faulting in the west-central Transverse Ranges, which includes the Santa Ynez and Red Mountain Faults. In 1916, an M6 event was apparently located near the junction of the San Andreas and Garlock faults. A few kilometers to the north, an M7.7 earthquake was located on the White Wolf fault in 1952 and was followed by an M6.4 aftershock. Two M6.1 aftershocks were located several kilometers to the northeast on a projected extension of the fault plane as previously discussed.

In 1946, an M6.3 event was located a few kilometers west of the Sierra Nevada fault. The 1947 M6.2 Manix earthquake is the only M6+ event ever recorded in the Mojave Desert.

The two largest earthquakes reported in southern California, both thought to have been greater than M8, occurred before 1900. In 1857 major strike-slip displacement occurred on the San Andreas near Fort Tejon. In 1872, normal and right-slip movement was reported along the Sierra Nevada fault in the Owens Valley, slightly more than 320 kilometers (200 miles) from the site.

Northern Baja California is an area of high seismicity; at least 13 earthquakes of magnitudes greater than 6.0 have occurred since 1900 (Brune and others 1979). Previous epicenters in this region (Hileman and others 1973, Figure 2.5-20) appear to scatter across the peninsula, suggesting a broad zone of deformation. Recent investigations, including field studies (Reyes, et al., 1975; Johnson, et al., 1976) and the relocation of epicenters (Leeds, 1979; Brune and others 1979) in the region, indicate that the vast majority of earthquakes are associated with a few active faults (Appendix 2.5J).

The San Miguel Fault appears to be the seismically dominant fault in the northern Baja California region. In 1956, four large earthquakes (magnitude 6.1 to 6.8) occurred along the San Miguel fault near the town of San Miguel (Brune and others 1979). In addition, Leeds (1979) has relocated five earthquake epicenters with magnitudes greater than 5.0 on the San Miguel fault zone. Relocation errors as large as 90 kilometers have been noted in earlier catalog locations (Appendix 2.5J).

The historically high level of activity of the San Miguel fault, is about one-half as high as that on the plate boundary faults (Cerro Prieto, Imperial, and others) to the east. Based on seismological evidence, the San Miguel fault does not appear to be mechanically connected to the hypothesized Offshore Zone of Deformation to the north (Appendix 2.5J).

No large historic earthquakes are positively correlated with the Agua Blanca fault (Allen and others, 1960; Brune and others, 1979). Magnitude 6.0 and 6.3 earthquakes of 1954, previously located along this fault, have been relocated to the San Miguel fault (Leeds, 1979). Very low rates of micro-earthquake activity have been recorded on the Agua Blanca fault (Johnson and others, 1976) (Appendix 2.5J).

2.5.2.3.4.2 Association of M5.0 to M5.9 Epicenters with Zones of Faulting

Figure 2.5-20 also shows the location of instrumentally calculated epicenters within a 200-mile radius of the San Onofre site. Events in this magnitude range are associated with major zones of faulting. This is in contrast with many earthquakes of magnitude less than M5.0 which do not occur near recognized surface faults. These smaller events are discussed in Paragraph 2.5.2.3.5.

Fewer earthquakes of M5.0 to M5.9 were recorded in the Continental Borderlands Province than in adjacent provinces. Epicenters tend to lie along faults that have been postulated primarily from topographic expression and geophysical traverses. The M5.9 event of December 26, 1951, 105 kilometers (65 miles) west of San Diego is associated with the San Clemente fault.
In the Coast Ranges, the two epicenters within 320 kilometers (200 miles) of the site are only approximately associated with the San Andreas and Nacimiento fault zones. Farther to the north, most epicenters are aftershocks of the 1966, M5.6 Parkfield earthquake.

In the northern part of the Peninsula Ranges Province, earthquakes of M5.0 and greater are readily associated with faults. Thirteen events align with the Newport-Inglewood Zone, two with the Elsinore, and nine with the San Jacinto fault zone.

In the southern part of the province in Baja, California, several M5.0 and greater events have occurred in the vicinity of the Agua Blanca and San Miguel faults; see Paragraph 2.5.2.3.4.1.[74] The zone of seismicity apparently lies along the boundary of this block.

In the northern Salton Trough Province, the majority of epicenters are associated with faults of the San Andreas Zone. To the south, epicenters lie either within the San Jacinto fault zone or between the San Jacinto and San Andreas, apparently on the several subsurface fault traces delineated by geophysics. Further to the south, the pattern of epicenters follows the zone of faulting associated with spreading of the Gulf of California.

Of the epicenters of M5.0 or greater that were recorded in the Transverse Ranges Province, several are aftershocks to the 1971 San Fernando earthquake. Others lie close to the trace of the

San Andreas fault. At both the east and west ends of the province, scattered epicenters lie along general trends of faulting.

In the Mojave Desert, most of the M5.0 to M5.9 epicenters fall within zones of faulting, and several are aftershocks of the 1947, M6.2 Manix earthquake. In the Basin and Range Province and the Sierra Nevada Province, most epicenters were located near the Sierra Nevada fault and most of those are aftershocks of the 1946, M6.3 earthquake. Several epicenters lie along the White Wolf fault and are aftershocks of the 1952 M7.7 earthquake. Most of these aftershocks are located in the Great Valley Province. A few M5.0 to M5.9 epicenters were located along the alignment of a set of faults on the east side of the Great Valley.

2.5.2.3.5 Occurrence of Smaller Earthquakes

Earthquakes of magnitude smaller than M5.0 do not correlate well in most cases with specific faults or well defined zones of faulting. Only a few of these smaller events show approximate correlations with known structures. The density of these events varies among the provinces as discussed below.

2.5.2.3.5.1 Coast Ranges Province

Most of the epicenters instrumentally located in the Coast Range Province are greater than 320 kilometers (20 miles) from the site. A concentration of epicenters between the San Andreas and Nacimiento fault zones appears to be associated with larger earthquakes on the San Andreas fault near Parkfield.

2.5.2.3.5.2 Transverse Ranges Province

Most of the epicenters within the Transverse Ranges Province are located just east of the San Andreas fault zone. Many of these represent aftershocks of larger earthquakes. In the western part of the province, the general pattern is more scattered except for two areas of concentration. These areas are offshore of Santa Barbara and the epicentral area of the 1971 San Fernando earthquake.

2.5.2.3.5.3 Salton Trough Province

Seismicity within the Salton Trough Province is associated with the south end of the San Jacinto fault, the Imperial fault and other subsurface structures. Epicenters occur as aftershocks of events on the San Jacinto or other faults and as discrete events and swarms along the trough axis. The events are due to down-warping of the trough and slip along the plate boundary.

2.5.2.3.5.4 Sonoran Desert Province

No epicenters have been recorded in the part of the Sonoran Desert which lies within 320 kilometers (200 miles) of the site.

2.5.2.3.5.5 Continental Border Province

The area offshore from the San Onofre site is typified by a widely scattered pattern of epicenters. Minor concentrations of epicenters are found near the Los Angeles Basin and San Clemente Island.

2.5.2.3.5.6 Great Valley Province

Except for a few scattered epicenters, the instrumental seismicity of the province is concentrated at the southern end near the White Wolf fault. Most are part of the aftershock sequence of the 1952 Kern County earthquake. This concentration falls within the Tehachapi Mountains seismic province of Richter.(70)

2.5.2.3.5.7 Sierra Nevada Province

Many epicenters of the aftershock sequence of the 1952 Kern County earthquake extend into the Sierra Nevada Province. Other than the concentration along the White Wolf fault, and a few along the Sierra Nevada fault, epicenters of M4.9 and smaller events do not appear to follow any particular pattern within the province.

2.5.2.3.5.8 Basin and Range Province

Epicenters in the basin and Range Province are scattered and somewhat more concentrated to the west, near the Sierra Nevada fault. The density of Quaternary faults within the province follows a similar pattern.

2.5.2.3.5.9 Mojave Desert Province

Epicenters in the Mojave Desert are concentrated near the center, particularly in the vicinity of the Manix fault and along the northern boundary of the eastern Transverse Ranges. In the western Mojave, scattered epicenters have been recorded and only a few epicenters have been instrumentally located in the eastern part of the province.

2.5.2.3.5.10 Peninsular Ranges Province

Concentrations of small earthquakes within the Transverse Ranges have occurred along the San Jacinto and Elsinore fault zones, and to a lesser extent, the Newport-Inglewood Zone of Deformation. To the south, a scattered pattern of epicenters appears to be associated with the Agua Blanca, San Miguel, and Sierra Juarez faults. The part of the province adjacent to the San Onofre site has a relatively low density of historic epicenters; however, interest in the site and the nearby location of the Cristianitos fault has stimulated detailed study of earthquakes in this province. The results of this study are described below.

As stated in Paragraph 2.5.2.3.4, no earthquake epicenters have been recorded within 8 kilometers (5 miles) of the San Onofre site, and no historically reported earthquakes can reasonably be associated with faults that lie within 5 miles of the site; however, four groups of small earthquakes have occurred within the site region that cannot be associated with surficial geological structure:

A. The nearest reported earthquakes to the site are the small magnitude epicenters within the Capistrano Embayment reported by Morton, Edgington and Fife.[84] Only one epicenter appears to be associated directly with the surface trace of the Cristianitos fault. This event had a magnitude of 2.0 and occurred in 1937. Considering the magnitude of the event and the poor quality of timing and recording early years, the location is highly questionable.[59][85]

B. Four nearby earthquakes which occurred since 1960 were re-analyzed based upon the new crustal model.[59][85] These events consisted of three offshore earthquakes with magnitudes of 3.4 in 1960, 3.1 in 1967, and a 3.1 in 1970; the fourth, an M3.6 in 1973, was located onshore. The focal mechanisms of the four earthquakes are not consistent with either the later January 1975 earthquakes or the motion characteristic of any known geologic structure.[59][85]

C. On January 3, 1975 two small earthquakes (M3.8 and 3.3) occurred near San Juan Capistrano, California, approximately 20 kilometers (12 miles) north of the San Onofre site. These earthquakes were located, by the California Institute of Technology (CIT), several kilometers west of the Cristianitos fault. An extensive investigation was performed to assess their relationship to the Cristianitos fault, a fault that is not capable.

   The study concluded that these two events did not occur on the Cristianitos fault.[59][85] This conclusion was based primarily on the fact that the focal mechanisms for these two events are incompatible with the Cristianitos fault. The corresponding hypocenter location was also considered incompatible with the fault. The fault plane solutions for the two events are discussed in Reference 59.

   The events were located using one of the standard U.S. Geological Survey location programs, HYPO-71. Also taken into account were the limitations of the data and model in forming the above conclusion. The focal mechanism of the earthquakes is oblique with components of strike-slip and reverse motion whereas the movement observed from geologic mapping of the Cristianitos fault is normal.

   The vicinity of the Cristianitos fault is seismically very quiet compared to areas along active faults in southern California. This is clearly evident from comparisons made of this area to both the San Jacinto and Elsinore faults and to regional data.[49]

   The recurrence curve for the Cristianitos fault is based on the entire CIT catalogue of 45 years, as is the southern California curve. By using the CIT data, it was possible to compare all events both before and after larger earthquakes, without biasing the results.

The fault plane solutions for the two events are discussed in References 59 and 85.

D. An earthquake swarm with a magnitude of less than 2.5 occurred during late June - early July 1977 in Trabuco Canyon. The location very nearly coincides with the location of the two small earthquakes which occurred in January 1975.

Interest in the structural history of the Capistrano Embayment initiated a study of the seismic history in this region of the province.

In order to evaluate the correlation of seismicity with faulting in the Embayment, the entire California Institute of Technology catalog of recorded events in this area was analyzed. In all, 40 events were located and plotted.

Fault plane solutions were performed by Biehler[59] for several events within the Embayment. The direction of maximum compressive stress is a generally north-south orientation consistent with the regional stress field in Southern California; however, the randomness of the focal mechanisms supports the lack of any major through-going features.

Based on these data, there is no significant correlation between the seismicity and faulting in the Capistrano Embayment.

2.5.2.4 Maximum Earthquake Potential

The maximum earthquake potential at the site was analyzed by considering the maximum credible earthquake on all significant faults as discussed below.

Figure 2.5-26 and Table 2.5-9 identify faults significant to establishing the earthquake potential at the San Onofre site. Significance was assessed through consideration of the capability of the fault, its length and distance from the site, and whether any nearer fault would have more severe ground-motion characteristics. For the purposes of this discussion, a capable fault is considered to be one that has demonstrated activity during Quaternary time. Distant faults included on Table 2.5-9 are those for which the estimated predominant period of the maximum credible earthquake would be longer than for a nearby fault, so that all combinations of high and low acceleration, and short and long periods are considered.

The characteristics of the faults significant to the San Onofre site are presented in the following paragraphs and complete discussions of those faults are given in Paragraph 2.5.1.1.3. Only those faults capable of a site acceleration greater than 0.1g were considered here. Empirical relationships given in Figure 2.5-27 were used to assess the maximum bedrock acceleration level at the site for each fault. In this evaluation, with the exception of the San Andreas fault zone and the hypothesized Offshore Zone of Deformation, it was conservatively estimated that a fault can rupture up to half its recorded length.[77] In addition to this approach, data have been developed to compare the degree of activity of the various faults and specifically the geologically derived slip-rate on the plate boundary and related faults. Also utilized was an empirically derived slip rate vs. magnitude relationship and a ground-motion modeling approach (SSEP) developed by

TERA-DELTA. These approaches are presented in Reference 33 and on the San Onofre Nuclear Generating Station Unit 1 docket.

Table 2.5-9
COMPARISON OF SIGNIFICANT FAULT PARAMETERS
BASED ON EMPIRICAL RELATIONSHIPS

Fault or Zone of Deformation	Length		Nearest Approach to Site		Largest Associated Historical Magnitude	Maximum Theoretical Magnitude (Figure 2.5-27 or Intensity Part A)	Maximum Site Bedrock Acceleration [g] (Figure 2.5-27 Part B)	Estimated Predominant Period(s) (Figure 2.5-27 Part C)	Reference
	(km)	(mi)	(km)	(mi)					
San Andreas	965	600	92	57	8+	8+	0.2	0.5	Jennings, 1974[79]
San Jacinto	272	170	69	43	6.8	8	0.27	0.5	Jennings, 1974[79]
Whittier-Elsinore	233	145	37	23	5.1	7-3/4	0.32	0.4	Jennings, 1974[79]
Hypothesized Offshore Zone of Deformation[a]	240	150	8	5	[b]	X,7[d]	0.67[e]	0.4	Vedder, et al., 1974[32]
Palos Verdes	96	60	18	11	[c]	7	0.45	0.35	Vedder, et al., 1974[32]

[a] This feature is not considered capable over its full length (Paragraph 2.5.2.4.5). The Modified Mercalli intensity and the acceleration listed for this hypothesized feature are those discussed in Reference 59.

[b] The three fault zones that constitute this hypothesized zone of deformation have experienced different seismic histories (Paragraph 2.5.2.4.5). An M6.3 has occurred on the northern portion, the Newport-Inglewood fault. No historical seismicity has been associated with the central portion. The southern portion, the Rose Canyon fault, has not been associated with events greater than M4.0.

[c] No historic earthquakes are definitely associated with this structure.

[d] M_s =7 was developed as the maximum magnitude through subsequent work presented in Reference 86.

[e] This interpretation is conservative based on subsequent work that developed M_s=7 as the maximum magnitude on site specific analysis of empirical data showing a corresponding peak instrumental acceleration of 0.63g.

Based on magnitudes and corresponding bedrock accelerations for each capable fault, as indicated in Table 2.5-9, the maximum site bedrock acceleration level is 0.67g. The 2/3g site acceleration presented in Table 2.5-9 is consistent with the site design acceleration of 2/3g presented in the SER[(24)] and with the upper bound attenuation curves as shown in Figure 2.5-20B. This is conservative based on subsequent work that developed M_s = 7.0 as the maximum magnitude[(33)] and site specific analysis of empirical data showing a corresponding peak instrumental acceleration of 0.63g. The faults considered in evaluating the earthquake potential at the San Onofre site and which are listed in Table 2.5-9 are discussed below.

2.5.2.4.1 San Andreas Fault Zone

The San Andreas fault zone represents a plate boundary extending from well north of San Francisco to near the Mexican border, a total length of about 1000 kilometers (625 miles). Two great earthquakes have occurred on the fault in historic times. The 1906 San Francisco earthquake was estimated at M8+ and may have involved 415 kilometers (260 miles of surface rupture). In 1857 a M8+ was centered at Fort Tejon, and involved about 320 kilometers (20 miles) of surface rupture from Chalome to Cajon Pass. No historic break on the San Andreas has involved more than 415 kilometers (260 miles) (less than one-half of its length) and there is no geologic evidence that more than 415 kilometers (260 miles) rupture has ever occurred.

South of Cajon Pass on the segment of the San Andreas nearest the site, evidence of Quaternary displacement is much less pronounced than to the north. Present seismic and geologic evidence indicates that lateral stress along this segment is being absorbed by the adjacent San Jacinto fault. It has been suggested that the southern segment of the San Andreas is capable of no more than M7.5 earthquake.[(87)]

2.5.2.4.2 San Jacinto Fault Zone

As a continuous fault zone, the San Jacinto extends from west of Cajon Pass to south of the Salton Sea, and is discussed in Paragraph 2.5.1.1.3.2. Five earthquakes of M6.0 or greater have occurred on the fault since 1918. Possible rupture of 3.2 kilometers (2 miles) coincided with an earthquake in 1899.[(37)] Similar ground cracking may have occurred during the M6.4 Borrego earthquake in 1968.[(88)]

The San Jacinto fault appears to be the most active branch of the San Andreas system in southern California. The scatter of events M6.0 to M6.9 along the fault indicates that larger magnitude earthquakes may not be necessary to relieve the stress. The assignment of an M8 maximum event to the fault is therefore considered conservative.

2.5.2.4.3 Whittier-Elsinore Fault Zone

The Whittier-Elsinore fault zone is discussed in Paragraph 2.5.1.1.3.3. It extends from the Los Angeles Basin southeast to the vicinity of the United States-Mexico border. It parallels the San

Jacinto and San Andreas faults for virtually its entire length. The fault zone approaches within 35 kilometers (22 miles) of the site.

Although many small earthquakes have been associated with the Elsinore fault, no earthquakes greater than M5.1 have occurred on it in historic times.

Seismicity on the Whittier fault is even less pronounced. An M4.2 earthquake in January of 1976 was tentatively located in the immediate vicinity of the Whittier fault. This would represent the largest recorded event associated with that fault.

2.5.2.4.4 Palos Verdes Fault

The Palos Verdes fault is a steeply dipping reverse fault separating the Palos Verdes Hills from the Los Angeles Basin. To the north the fault extends into Santa Monica Bay and to the south it extends into the offshore where three branches have been tentatively identified.[(32)] Based on geophysical evidence, it appears that the southernmost of these may extend to within approximately 17 kilometers (11 miles) offshore of the San Onofre site. The fault is discussed in Paragraph 2.5.1.1.3.5. It was not considered in the earthquake analyses because of its greater distance from the site than the hypothesized Offshore Zone of Deformation with a comparable estimated magnitude.

Seismicity in the vicinity of the fault is scattered, with many smaller events, a few as high as M4.9, have been associated with the fault. No larger events have occurred near the trace of the Palos Verdes fault.

Based on the total length of the fault and its inferred offshore branches to the south, the fault could be capable of an M6.5 to M7 earthquake.

2.5.2.4.5 San Clemente Fault

A fault scarp along the east face of San Clemente Island is a part of a much longer feature. The alignment of small earthquake epicenters from near Santa Barbara Island to a point at least 64 kilometers (40 miles) southeast of San Clemente Island confirms the seismic activity of this feature and gives some indication of its length.

The largest known earthquake associated with the San Clemente fault, M5.9, occurred on December 26, 1951. Its epicenter was approximately 105 kilometers (65 miles) due west of Mission Bay, San Diego, California.

2.5.2.4.6 Hypothesized Offshore Zone of Deformation

The apparent alignment of structural features offshore along the southern California coast has resulted in the hypothesis of a continuous zone of deformation, extending from the Santa Monica Mountains, on the northern border of the Los Angeles Basin, to Baja California, a distance of 200 kilometers (125 miles) or more.[(24)] Extensive geophysical investigation indicates that the hypothesized OZD is in actuality composed of three structural features; from north to south: The Newport-Inglewood Zone of Deformation, South Coast Offshore Zone of Deformation, and Rose Canyon fault zone; however, in the interest of conservatism the hypothesized OZD has been evaluated as a continuous zone of deformation capable of generating significant shaking at the site[27][28][29] (Appendix 2.5I). This zone has been assumed to be a potential source of earthquake activity despite the geologic evidence that strongly suggests the different structural features exhibit differing degrees of activity and thus differing earthquake potential. The hypothesized OZD quantitative earthquake potential has been based on the conservative assumption that the maximum earthquake which could occur anywhere along the length of the zone could occur offshore of San Onofre (Appendix 2.5M).

The paragraphs below discuss each of these structural features and their relationships to each other. More detailed discussions are presented in Subsection 2.5.3, Paragraph 2.5.1.1.3.4, in Reference 33.

2.5.2.4.6.1 Newport-Inglewood Zone of Deformation

The Newport-Inglewood Zone of Deformation (NIZD) consists of a series of short, discontinuous, northwest-trending en-echelon, right-lateral faults, relatively shallow drag fold anticlines, and subsidiary normal and reverse faults. The NIZD extends from the Santa Monica Mountains to offshore of Newport Beach for a total length of 70 kilometers (45 miles).

Historical earthquake activity on the NIZD is dominated by the occurrence of magnitude 6.3 (M_s) Long Beach earthquake of March 11, 1933. The style of faulting of the 1933 earthquake was evaluated by waveform analysis of tele-seismic body wave records of the earthquake, as described in Reference 33. The best-fit focal mechanism is right-slip on a N40^{o} west-trending fault. This matches the geologic observations of orientation of the NIZD and also agrees with the aftershock pattern. The wave-form study indicates that the focal depth was 10 kilometers and the seismic moment is estimated to be 4.2 to 6.2 x 10^{25} dyne-cm. The calculated average displacement is 31 to 46 centimeters, and a low stress drop of approximately 10 bars is indicated. The seismicity of the zone is discussed in Paragraph 2.5.2.2.2.5.

2.5.2.4.6.2 South Coast Offshore Zone of Deformation

The tectonic structure of the South Coast Offshore Zone of Deformation (SCOZD) was evaluated through interpretation of offshore geophysical reflection profiles.[26][27][28][29] This interpretation indicates the apparent tectonic deformation of two deeply buried reflecting horizons, and shows the SCOZD to consist of a zone of branching and discontinuous faults trending south to southeast about 8 kilometers (5 miles) seaward of the San Onofre site. Local northwest- to west-trending folds in the shallower horizons are also associated with this zone and, together with the faults, appear to reflect a tectonic style similar to that of the NIZD.

These interpretations of the geophysical data show the individual faults to be most continuous within the acoustic basement, Horizon C, and less continuous in the younger rocks, such as those represented by Horizon B. This apparent decrease in fault length and continuity in the younger units is also similar to the NIZD. Major differences are the more gentle nature of the folds, and although there are sea floor irregularities of uncertain origin, there is a lack of any prominent fault scarps on the sea floor along the SCOZD, and there is a lack of physical evidence for estimating the amount of lateral displacement on the various fault segments of the SCOZD.

No historic seismic activity has been associated with the zone. A more detailed discussion of this zone is presented in Paragraph 2.5.1.1.3.4.2.

2.5.2.4.6.3 Rose Canyon Fault Zone

The Rose Canyon Fault Zone was originally mapped onshore to the north and southeast of San Diego. Recent detailed mapping south of San Diego has produced no evidence for a continuation of the main trace of the fault to the south.[89] This fault is discussed in Paragraph 2.5.1.1.3.4.3.

Several epicenters have occurred near the fault in the San Diego area, but none have exceeded M4.0.

2.5.2.4.6.4 Maximum Earthquake Potential for Hypothesized Offshore Zone of Deformation (OZD)

Geological data indicates that this zone is not continuous and not capable of significant seismicity. A conservative approach, however, to evaluating ground motion potential at the site was taken by considering the zone, as a whole, capable of generating significant earthquake shaking. The zone, at its closest approach, is approximately 8 kilometers (5 miles) from the site. Seismic parameters resulting from this approach are shown on Table 2.5-9.

Geologic, seismologic, and earthquake engineering analyses and reviews have been completed for the San Onofre site to estimate the magnitude of maximum earthquake that could be postulated for the hypothesized OZD[33] (Appendix 2.5M).

The specific approach used for the assessment of the maximum earthquake[33] considered all possible methods in evaluating maximum earthquake. Any one of these techniques does not consider the complexities for fault behavior and thus all were considered in comparison to one another for consistency of results. The use of this comparison has been called the degree-of-activity approach and has resulted in a fault ranking format for evaluation of maximum earthquake.

This fault ranking is applied to the hypothesized OZD relative to other faults in Southern California and in similar tectonic settings throughout the world. As a means of evaluating the earthquake potential of various faults the degree-of-activity approach considers both a qualitative comparison of features such as tectonic setting, style of faulting, degree of deformation, and geomorphic expression along a fault as well as a quantitative comparison of length of fault rupture, slip per event, maximum historical earthquake, total displacement, and geologic slip-rate on faults.

The basis for selection of degree-of-fault-activity methodology and the applicability of other methodologies to the hypothesized OZD is presented in Appendix 2.5R. Table 2.5R-2 summarizes the ranking criteria and fault zone characteristics used in the degree-of-activity analysis. In addition, this appendix places the role of the slip-rate maximum magnitude relationship in perspective with other fault parameter relationships used in the degree-of-fault-activity methodology. The specific application of the slip-rate maximum magnitude relationship as an element of the degree of fault activity methodology is fully developed in Appendix 2.5R.

Conclusions regarding the maximum earthquake magnitude of the hypothesized OZD can be summarized as follows: M_s = 6-1/2 is a reasonable maximum earthquake magnitude consistent with the geologic and seismologic features of the NIZD. Because the NIZD is considered to conservatively represent the earthquake potential of the hypothesized OZD, transferring M_s = 6-1/2 to the OZD provides a degree of conservatism for the maximum magnitude estimate for the hypothesized OZD opposite the site.

Based on incorporation of additional conservatism through evaluation of ranges in the slip-rate data and review of other elements for assessing the degree-of-fault-activity of the hypothesized OZD, the most conservative maximum magnitude is M_s = 7. A larger earthquake is inconsistent with the geologic and seismologic features of the hypothesized OZD and is therefore not credible.

2.5.2.5 Seismic-Wave Transmission Characteristics of the Site

Because the nonmarine terrace deposits were excavated at the plant area, the only soil/rock material participating in seismic-wave transmission at the site as the San Mateo Formation. The properties of San Mateo Sandstone are presented in Subsection 2.5.4. The properties important for seismic-wave transmission considerations are given in Table 2.5-10.

Table 2.5-10
SUMMARY OF MATERIAL SEISMIC WAVE TRANSMISSION PROPERTIES FOR SAN MATEO FORMATION SAND[(a)]

Item	Quantity
Seismic compressional velocity	
Above water table, ft/s	3,000 - 7,000
Below water table, ft/s	7,000 - 7,500
Seismic shear velocity	
Above water table, ft/s	1,000 - 2,000
Below water table, ft/s	1,900 - 2,750
Soil properties	
Natural water content	
Above water table, %	2
Below water table, %	11
Dry unit weight, lb/ft^3	123
Shear strength:	
Strength intercept, k/ft^2	0.8
Angle of shearing resistance, degrees	41
Relative density, %	100
Plasticity index	Nonplastic
Unified soil classification	SW
Shear modulus	Figure 2.5-31
Poisson's ratio	
High stress	0.25 - 0.33
Low stress	0.40 - 0.45
Hysteretic damping	Figure 2.5-31
Water table elevation, ft MLLW	+5
Water table variation	Minor (± 1.5)

(a) For more details of properties and the methods used to obtain them, see Paragraph 2.5.4.2.

Analysis of seismic-wave transmission characteristics of the site are based on estimating maximum amplitudes of motion from calculations of the shear-wave responses of the site to large earthquakes. The analyses, described in more detail in Appendix 2.5B, involved calculating the site response, by lumped-mass methods (Paragraph 2.5.4.7), to a number of recorded earthquake acceleration time histories. Those records were scaled so as to yield about 0.5g in the free field near the site surface and were used to aid judgement in shaping the response spectra. Later, the maximum ground acceleration was increased to 0.67g. Based on the observation from calculated strains (which are large) and the data from Figure 2.5-31, that the soil moduli were essentially the same for 0.50g and 0.67g earthquakes, response spectra accelerations at all periods were increased by a factor of 1.33 (i.e., 0.67/0.5). Those results are discussed in Paragraphs 2.5.2.6 and 2.5.2.7 and in Appendix 2.5B.

Essentially, the calculations consistently show that the site transmits short-period rather inefficiently, and long-period energy with some amplification. For this reason, the long-period end of the design spectrum was made more broad than would be normal for most sites. In addition, the analyses suggest that site accelerations for this flat site probably cannot exceed perhaps 0.5g to 0.6g because of the thickness of the deposit (900+ feet) and the fact that the sandstone responds to shaking as a soil.

Given the estimated maximum earthquake of $M_s = 7$, the known local soil conditions at the San Onofre site, and the regional tectonic setting, 56 earthquake records were selected to correspond closely to the conditions of the estimated maximum earthquake and analyzed to develop 84th-percentile response spectra for $M_s = 6\text{-}1/2$ and carefully extrapolated to $M_s = 7$. A comparison between the computed 84th-percentile spectrum and the design spectrum showed that the design spectrum exceeds the instrumental spectrum at all periods.[33]

Matters of site stability, including liquefaction potential and slope performance, are discussed in detail in Paragraphs 2.5.4.8 and 2.5.5. The work in those sections establishes that the site will not liquefy, and the slopes will not become unstable, even under very severe earthquake shaking.

2.5.2.6 Design Basis Earthquake (DBE)

The design basis earthquake (DBE), a term used synonymously with SSE in this report, was assessed during the construction permit phase of the project as documented in the Safety Evaluation Report.[24] The development of the response spectrum for the DBE is described in detail in Appendix 2.5B. In essence, that work, which involved calculating the response of the site to many earthquakes, showed that the site possibly could amplify long-period motions to some extent. For that reason the long-period part of the design response spectrum is more broad than for many sites.

The acceleration level of 0.67g is conservative when compared to the maximum earthquake potential as discussed in Paragraph 2.5.2.4. The DBE time history was fitted to the design response spectrum, scaled to a 0.67g reference acceleration, by the methods and with the results described in Paragraph 3.7.1.2. Because it is assumed that the acceleration results from a strong earthquake, the duration of DBE strong motion was taken as 80 seconds.

The methodology used to address the development of ground motion parameters for an earthquake magnitude 6-1/2 does not provide the means to extrapolate ground motion parameters to earthquakes with magnitudes greater than 6-1/2, however, by carefully extrapolating the San Onofre 84th-percentile instrumental response spectrum for an M_s = 6-1/2 earthquake, the 84th-percentile instrumental response spectra for M_s = 7 and 7-1/2 earthquakes were obtained.

An M_s = 6-1/2 is the most reasonable estimate of maximum magnitude for a postulated earthquake on the hypothesized OZD opposite the site;(33) however, an M_s = 7 is considered to be appropriate for purposes of assessing the conservatism of the present design basis. A response spectrum appropriate for design would of course be significantly below the 84th-percentile instrumental spectrum which in turn is enveloped by the DBE response spectrum as shown in Figure 2.5M-4; therefore, the DBE response spectrum is an extremely conservative representation of the appropriate design response spectrum for the site (Appendix 2.5M).

An earthquake greater than M_s = 7, considered to be inconsistent with the geologic and seismologic features along the hypothesized OZD. And although unrealistic as an estimate of maximum magnitude or as a basis for assessing conservatism of the present design, an M_s = 6-1/2 spectrum was extrapolated to include M_s = 7-1/2.

2.5.2.7 Operating Basis Earthquake (OBE)

The operating basis earthquake (OBE) is characterized by maximum ground shaking of 0.33g (1/2 of the DBE). As discussed in Paragraph 2.5.2.5, none of the tectonic features potentially capable of generating an earthquake that would have this level of ground shaking at the site have demonstrated this capability in historic times.

Based on procedures similar to those outlined by Haley and Hunt,(90) the average recurrence interval for 0.33g ground shaking at the San Onofre site would be in excess of 1000 years and, thus, the probability of occurrence in the 40-year design life of the plant would be less than 1 in 25. The studies also indicate that an M_s = 6 to 6-1/2 event would be the most likely earthquake to cause this acceleration level at the site. Correlations by Housner(91) and Lee and Chan(92) indicate the maximum duration for strong motion shaking for this magnitude range is less than 30 seconds. Conservatively, a 36-second duration has been assigned to the OBE.

2.5.3 SURFACE FAULTING

2.5.3.1 Geologic Conditions of the Site

The geologic conditions of an area extending a minimum of 8 kilometers (5 miles) from the site are discussed in Paragraph 2.5.1.2. The relationship of the foundations of the nuclear power plant to the geologic conditions at the site are discussed in Paragraphs 2.5.4.1 and 2.5.4.2.

2.5.3.2 Evidence of Fault Offset

The site stratigraphy is described in Paragraph 2.5.1.2.2. The plant will be founded on the San Mateo Formation (of probable late Miocene to Pliocene age) which is about 275 meters (900 feet) thick at the plant. Extensive exploration and excavation, revealed no geologic evidence of fault offset at the site. In addition, no evidence was found to suggest that unrecognized buried faults exist at depth beneath the site or that projections of other faults extend into the site; therefore, it is concluded that the likelihood of ground displacement within the plant site during its lifetime is negligible.

The Cristianitos fault is the nearest zone of faulting, 0.8 kilometer (1/2 mile), to the site and is the only major structural feature within 8 kilometers (5 miles). A detailed description of the fault is contained in Paragraph 2.5.1.2.3. To summarize, substantial evidence is presented that demonstrates there has been no movement within at least the last 125,000 years. In addition, no evidence was found to indicate movement in the last 500,000 years. This is based on three types of investigations: geologic mapping, trenching, and geomorphic studies. Exposures along the coastal bluffs south of the plant, and trenching performed at five locations along the fault indicate that it is overlain by unbroken Pleistocene terrace deposits or late Quaternary soil and slopewash that are estimated to be more than 125,000 years old. A geomorphic study of these terrace deposits indicates that no discernible faulting or warping has occurred in at least the last 125,000 years (see References 49, 52, 53, and Appendix 2.5I). The geologic structure of the basement in the area of the Capistrano Embayment and west of the Cristianitos fault has been studied by West[47] to establish type of movement and amount of displacement on the Cristianitos fault.

Displacement on the Cristianitos fault is greatest near the central part of the fault about 3 kilometers (2 miles) east of Arroyo Trabuco. Here vertical separation is between 1000 and 1200 meters (3,500 and 4,000 feet). Where the fault crosses Highway 74 (Ortega Highway) the vertical offset is only about 500 meters (1700 feet).[47] A few hundred feet east of the site, a boring estimated stratigraphic separation of the Monterey/San Onofre Breccia contact of about 550 feet (Appendix 2.5I).

Recent interpretation of high resolution seismic reflection profiles (see References 27, 28, 29, and Appendix 2.5I), by Moore, in the area of the Cristianitos fault offshore, indicates the fault dies out to the south and is not present beyond 6000 feet offshore.

Additional information on surface faulting within or near the site area is reported in Paragraph 2.5.1.2.3.2. This information includes interpretation of extensive offshore exploration which was performed in the site area and vicinity (see References 26, 27, 28, 29, 40 and Appendix 2.5I). The exploratory techniques include sparker, Aquapulse, gravity, and magnetics. No evidence for surface offset was found. For additional information on surface faulting outside the site area, see Paragraph 2.5.1.1.3.

2.5.3.3 Earthquakes Associated with Capable Faults

The plot of instrumental epicenters within an 80-kilometer (50-mile) radius, (Figure 2.5-23) show no earthquake epicenters recorded within 8 kilometers (5 miles) of the San Onofre site. In addition, there are no historically reported earthquakes that can reasonably be associated with faults that lie within 5 miles of the site; however, earthquakes have occurred within the site region that cannot be associated with geologic structures, see Paragraph 2.5.2.3.5.10.

The nearest reported earthquakes to the site are the small magnitude epicenters along the Cristianitos fault reported by Morton, Edgington and Fife.(84) Only the epicenter appears to be associated directly with the surface trace of the Cristianitos fault. This event had a magnitude of 2.0 and occurred in 1937. Considering the magnitude of the event and the poor quality of timing and recording in those early years, the location is highly questionable.(59)(85)

Four nearby earthquakes which occurred since 1960 were re-analyzed based upon the new crustal model.(59)(85) These events consisted of three offshore earthquakes with magnitudes of 3.4 in 1960, 3.1 in 1967, and a 3.1 in 1970; the fourth, an M3.6 in 1973, was located in the hills west of the Cristianitos fault. The focal mechanisms of the four earthquakes are not consistent with either the January 1975 earthquakes or the motion characteristic of any known geologic structure.(59)(85)

Earthquakes in California of the magnitudes below 4.5 often cannot be associated with geologic structures mapped at the surface. Such earthquakes are probably manifestations of minor re-adjustments in the crustal rocks resulting from residual compressional stresses which cannot be identified with regional tectonic strain patterns in southern California.

2.5.3.4 Investigation of Capable Faults

Paragraphs 2.5.3.2 and 2.5.1.2.3.2 discuss those structural features within 8 kilometers (5 miles) of the site that exhibit evidence of fault offset at the ground surface. There is no evidence of displacement at the ground surface in the past 125,000 years or of movement of a recurring nature in the past 500,000 years; therefore, these faults are not considered capable.

Offshore faults within the site area are discussed in Paragraph 2.5.1.2.3.2. No capable faults were identified within the site area offshore.

Capable faults outside the site area are discussed in Paragraph 2.5.1.1.3 as is the South Coast Offshore Zone of Deformation (SCOZD). The SCOZD is mentioned in this section because of its close proximity to the site (5 miles), its alignment with capable faults to the north and south, and because the U.S. Geological Survey reported that the "NIZD, the SCOZD and the RCFZ cannot be disassociated" (Reference 24, Appendix C). The applicant contends that these "segments" are structurally independent and should not be associated. Evidence supporting this contention is discussed in Paragraph 2.5.1.1.3.4 and in Appendix 2.5M; however for conservatism, this zone has been considered as a segment of the hypothesized Offshore Zone of

Deformation and therefore capable. Discussion of the relevance of this zone to the plant site is described in Paragraph 2.5.2.4.4.

2.5.3.5 Correlation of Epicenters with Capable Faults

As stated previously, (Paragraphs 2.5.1.2.3.2 and 2.5.3.2), no capable faults were found within the site area; however in the Regional area, both the Newport-Inglewood Zone of Deformation and the Rose Canyon Fault Zones contain capable faults. These regional features align with, but are considered by the applicant to be separate from, the South Coast Offshore Zone of Deformation[26] (Appendix 2.5M).

The hypothesis presented by the U.S. Geological Survey (Paragraph 2.5.3.4) which states that these zones cannot be disassociated, is inconclusive; however, in the interest of conservatism the applicant has considered the South Coast Offshore Zone of Deformation to be a continuous fault zone concomitant with the Newport-Inglewood Zone of Deformation and the Rose Canyon Fault Zone. Consideration of this zone as a continuous capable fault has provided for the establishment of a conservative DBE. The offshore area containing the SCOZD and the projections of both the NIZD and RCFZ is hereafter referred to as the hypothesized Offshore Zone of Deformation or the hypothesized OZD. The applicants have assumed the hypothesized OZD to be a potential source of earthquake activity despite the geologic evidence that strongly suggests the different structural entities exhibit differing degrees of activity and thus differing earthquake potential; see Paragraph 2.5.1.1.3.4.

Analysis of the Western Geophysical data indicates that the offshore area of the Continental Borderland, which contains part of all three fault zones, between Long Beach and San Diego can be divided into three separate and distinct provinces; the Northwest, Central and Southeast, based on differing geologic characteristics. This division is supported by seismic velocity data, gravity and magnetic anomalies, seismic-reflection profiles other geologic information, and the instrumental records of earthquakes.[26]

A detailed description of the offshore area is presented in Appendix 2.5M, Western's final report[26] and in Paragraph 2.5.1.1.3.4. Additional references that discuss the offshore area of the hypothesized OZD are 27, 28, 29 and Appendix 2.5I.

Faults in the northwest Province, in general, strike northwest-southeast, cut acoustic basement (Horizon C), and extend upward into the section through Horizon B. Some, such as the Palos Verdes fault, cut the sea floor, see Paragraph 2.5.1.1.3. Many of these faults are probably the seaward extension of the Palos Verdes fault system, and to a lesser extent, the Newport-Inglewood Zone of Deformation; see Paragraph 2.5.1.1.3.4.1. The Newport-Inglewood Zone of Deformation in the Northeast Province terminates at the Offshore San Joaquin Hills Structural High.[26] Many of the faults in this Province are reverse faults.

The fault style in the Southeast Province are predominately normal faults. The Southeast Province is crossed by two fault trends on Horizon C. A series of faults striking from north-south to northeast-southwest are superimposed by faults with northwest-southeast strike.

This series of faults and the associated folds make up the South Coast Offshore Zone of Deformation (SCOZD); see Paragraph 2.5.1.1.3.4.2. In this zone, the major feature is the northwest-southeast trending South Coast Offshore fault.[26] The South Coast Offshore fault crosses the Central Region and the northwest part of the Southeast Province about 5 miles offshore. To the north, it dies out as it approaches the Newport-Inglewood Zone of Deformation; and to the southeast, as it approaches the Rose Canyon Fault Zone. This fault, which is most prominent on Horizon C, cuts Horizon B at places and not at others.

Recent study of high resolution geophysical profiles indicate that the SCOZD intersects the sea floor locally; however the system is generally not overlain by Pleistocene and Holocene deposits and no evidence has been found to demonstrate that these young units are displaced (references 27, 28, 29, 33, and Appendix 2.5I).

The Rose Canyon Fault Zone in the Southeast Province appears to turn inland near Oceanside and is separated from the South Coast Offshore fault by a series of intrusive rocks and north-south faults, which are probably extensions of the north-south fault system onshore; see Paragraph 2.5.1.1.3.4.3. The Rose Canyon Fault Zone cuts Horizon B along its entire length.

Historic earthquakes associated with the Newport-Inglewood Zone of Deformation (the 1920 and 1933 events, for example) were generated by slip within basement rocks below the sedimentary fill of the Los Angeles Basin. It is generally agreed that repetitions of right-slip displacements, on a fault within the underlying basement rocks, are responsible for the late Miocene-Holocene development of the Newport-Inglewood Zone of Deformation. This inferred right-slip fault is presumed to follow a contact separating oceanic Catalina Schist facies from an eastern continental basement facies of granitic and associated metamorphic rocks. The contact, termed the California Subduction Zone is of Mesozoic age. This contact is further inferred to continue to the southeast, passing along the west side of Baja California, for more than 800 miles.[31] Reflection data from Western Geophysical[26] indicate that this contact presumed coincident with the NIZD in the Los Angeles Basin, is offset to the south by the San Joaquin structural high and passes 24 to 29 kilometers (15 to 18 miles) southwest of San Onofre; see Paragraph 2.5.1.1.3.4.

The distribution of San Onofre Breccia, or its equivalent, (for example, on the Coronado Islands) and the presence of eastern basement facies in the Shell core hole west of Point Loma, lend support to the offshore position of this contact. Furthermore Western's interpretation[26] of gravity and magnetic surveys also places this contact well offshore. There is no structural or seismic evidence of Quaternary tectonic displacement across this basement-rock contact, except under the Los Angeles Basin, and the contact does not coincide with the SCOZD or the RCFZ.

California Institute of Technology data listing all earthquakes between January 1932 and June 1980 were used for plotting instrumental epicenters within 320 kilometers (200 miles) of the site; see Paragraph 2.5.2.1.1. No earthquake epicenters were recorded within 8 kilometers (5 miles) of the site area and there are no historically reported earthquakes that can reasonably be associated with faults that lie within the site area. Several earthquakes have however, been reported within the site area and each of these reports has been investigated (see Paragraph 2.5.3.3). Though several earthquakes were reported, (early 1930s through January 1975) only one appeared to be directly associated with the surface trace of the Cristianitos fault. This event had a magnitude of 2.0 and occurred in 1937. Considering the magnitude of the event and the poor quality of timing and recording in those early years, the location is highly questionable;[59][85] in addition, the last movement on this fault is limited by overlying undisturbed marine terrace deposits dated at 125,000 years before present (Appendix 2.5I).

2.5.3.6 Description of Capable Faults

In accordance with the criteria set forth in 10CFR100, Appendix A, no capable faults exist within 8 kilometers (5 miles) of the plant site. As discussed in Paragraph 2.5.3.5, the hypothesized OZD has been considered capable in this report in order to assess a conservative DBE. This zone is composed of three fault zones. The Newport-Inglewood Zone of Deformation (NIZD) in the northwest contains capable faults as does the Rose Canyon Fault Zone (RCFZ) in the southeast; however, the South Coast Offshore Zone of Deformation (SCOZD) which lies between, but separate from them,[26] has no historic record of seismic activity (see Paragraph 2.5.3.3), and largely contains faults representative of a different stress regime than that of the other two zones. The hypothesized OZD is described in detail in Paragraph 2.5.1.1.3.4; however, a brief description of the three fault zones is included in Paragraph 2.5.3.5 and below.

The NIZD consists of a series of northwest trending en-echelon faults and folds that extend onshore, some 76 kilometers (48 miles) from Newport Bay to the Santa Monica Mountains. The displacement history of the faults within this zone is primarily defined from onshore oil fields to the northwest. The orientation of structural elements in this zone has been attributed to right-lateral shearing at depth. Displacements in lower Pliocene oil-bearing strata appear to be right-lateral, strike-slip movements. Vertical separation on basement rocks of Mesozoic age is 1200 meters (4000 feet). In Pliocene strata, lateral separation is 900 to 1400 meters (3000 to 5000 feet) and vertical separation is less than 300 meters. Vertical offset of the Plio-Pleistocene contact is only about 60 meters (200 feet).[93] This zone of deformation involves faults which cut more than 4500 meters (15,000 feet) of Tertiary sedimentary rocks. These rocks typically are displaced less at successively higher stratigraphic levels. Activity in this zone dates from at least middle Miocene through recent, and historic seismicity[70] confirms present activity. Additional description of this zone is presented in Paragraph 2.5.1.1.3.4.1.

The South Coast Offshore Zone of Deformation (SCOZD) was identified as a continuous trace within a zone of en-echelon faults in acoustic basement, based on detailed seismic reflection surveys.[26] This fault zone is 67 kilometers (42 miles) long with its northern terminus approximately 8 kilometers (5 miles) south of Newport Beach, and its southern terminus southwest of Oceanside. The closest approach of the Zone to the San Onofre site is approximately 8 kilometers (5 miles) to the southwest. The structure of the SCOZD indicates the tectonic deformation of two deeply buried reflecting horizons; and shows the SCOZD to consist predominantly of a zone of branching and discontinuous faults and folds trending north to northwest. Local northwest to west-trending folds in the shallower horizons are also associated with this zone. Individual faults are most continuous on the acoustic basement (Horizon C) and less continuous in the younger rocks, such as those represented by Horizon B. Apparent vertical displacements of 1000 to 3000 feet down to the west are indicated on the faults that cut Horizon C, however, displacement diminishes rapidly in both the northwest and southeast directions from the central part of the zone. Similarly, displacements diminish upward in sections where the fault zone is generally expressed as a series of short, discontinuous breaks in upper Miocene rocks (Horizon B). Expression of the fault on the ocean floor is questionable.

Structures along the SCOZD on Horizon C appear to be dominated by north- and northwest-oriented normal faulting. The younger and shorter faults in Horizon B indicate continued deformation. Maximum vertical separation within Miocene strata is 2675 meters (5500 feet). Pliocene strata have not been recognized overlying the fault, but a maximum vertical separation of 180 meters (600 feet) is seen in upper Miocene strata. The zone is locally overlain by as much as 300 meters (1000 feet) of undisturbed sediment.[25]

High resolution profiles near to and south of San Onofre[27][28][29] indicate that the SCOZD locally intersects the sea floor; however, the SCOZD is not intensively overlain by Pleistocene or Holocene sediments, and no evidence has been found to demonstrate that these young units are displaced (Appendix 2.5I); in addition, no historic seismicity has been associated with this zone.

At the northern terminus of the zone, displacements die out on acoustic basement (believed to be Catalina Schist) near a north-south fault along the west side of the San Joaquin Hills structural high. To the south, the SCOZD is terminated by a series of intrusions and north-south trending faults.[26] This zone is also described in Paragraph 2.5.1.1.3.4.2.

The Rose Canyon Fault Zone (RCFZ) has been studied offshore, north of Point La Jolla, and southwest of the San Diego Bay.[35][94] Faults mapped in these areas have been located on the basis of generally wide-spaced acoustic profiles and inferred correlation with bathymetric relief; see Appendix 2.5K. More detailed acoustic profile surveys[36][95] in these offshore areas have refined the location and current understanding of this part of the RCFZ. The specific information developed is summarized in Appendices 2.5K and 2.5N.

Offshore, detailed seismic reflection surveying along the northwest part of the fault indicates vertical displacement on Horizon B along the entire length of the fault. The west side is down, but the amount of displacement is not known.

Offshore from La Jolla Cove, seismic reflection surveying indicates a northwest continuation of the zone to the Oceanside area. Near its northern end, the offshore extension of the RCFZ trends shoreward at Oceanside and becomes two branches onshore. Detailed field mapping near the coast has shown that these branches joined two previously mapped faults inland. The north-south trend of these faults and the intrusions at the southeast end of the SCOZD indicate that the two zones are disassociated. The closest approach of the Rose Canyon fault to the site is a point approximately 40 kilometers (25 miles) to the southwest.

There is a series of topographic highs and lows in the San Diego area, and the southernmost of these alternating features is underlain by the San Diego Basin that is roughly defined by the down-to-the-west faults of the La Nacion system and the down-to-the-east faults offshore from

San Diego Bay. This structural low, or graben, implies that the southern part of the RCFZ is characterized by a widened zone of extensional style faults, and further indicates that the sense of displacement on this part of the RCFZ is dip-slip rather than strike-slip (Appendix 2.5K).

Faulting along the RCFZ in the area south of the Morena-Old Town is not well defined onshore. The bulk of evidence for faulting at the south end of the RCFZ consists of faults identified by acoustic profiling in San Diego Bay and offshore of San Diego.[35][36] Faults identified offshore are more prominent than the faults in the southern end of San Diego Bay. The offshore faults are also expressed as fault scarps where they come onshore at Coronado.[36] This evidence strongly suggests that a southern extension of the RCFZ is associated with the faulting, and extends offshore of San Diego and not to the south through San Diego Bay. A discussion of evidence for extension of the RCFZ to the south is found in Appendix 2.5K.

The character of the faulting within the RCFZ changes in the southern part of San Diego and becomes a wide zone of faulting characterized primarily by a dip-slip component. Current data indicates that the faulting within this wide zone dies out to the south and does not connect to the Calabasas fault or the Vallecitos fault zone (Appendix 2.5K).

Geologic data available from onshore investigations indicate that the RCFZ has been active since at least early Pleistocene. Kennedy[89] shows the late Pleistocene Bay Point Formation (approximately 120,000 years old), which occurs at the La Jolla terrace level, as undeformed overlying Eocene and Cretaceous rocks displaced by the fault; however, the La Jolla terrace and other upper Pleistocene terraces are apparently slightly tilted. Kern[37] shows two upper Pleistocene terraces (120,000 ± 10,000 years old) which have elevation differences across the Rose Canyon fault at the coast near La Jolla. This suggests post-late Pleistocene and possibly Holocene deformation.

2.5.3.7 Zone Requiring Detailed Faulting Investigation

There are no capable faults within 8 kilometers (5 miles) of the site; therefore, there is no zone requiring detailed analysis of seismic potential; however, detailed studies have been performed over many areas of each of the above mentioned fault zones that make up the hypothesized OZD that has been used to assess the DBE. Results of the studies and references to the various investigations performed are contained in several paragraphs including 2.5.1.1.2.2, 2.5.1.1.3.4, 2.5.1.2.3.2, 2.5.3.4, 2.5.3.5, and 2.5.3.6.

2.5.3.8 Results of Faulting Investigation

No capable faults were found within 8 kilometers (5 miles) of the site; therefore, no detailed faulting investigation was required; however, for the purpose of assessing a conservative DBE, the South Coast Offshore Zone of Deformation has been considered to join the offshore extension of the Newport-Inglewood Zone of Deformation to the northwest, and the Rose Canyon Fault Zone to the southeast thereby forming the continuous zone referred to as the hypothesized Offshore Zone of Deformation; an assumed capable feature. During the extensive offshore geophysical investigation, the region between Long Beach and Rose Canyon, about 130 kilometers (80 miles), was investigated seaward approximately 50 kilometers (30 miles). The results are discussed in Paragraphs 2.5.1.1.3.4, 2.5.3.4, 2.5.3.5, and 2.5.3.6. Geologic data which demonstrate that surface faults need not be considered is presented in Paragraph 2.5.3.2.

2.5.4 STABILITY OF SUBSURFACE MATERIALS AND FOUNDATIONS

2.5.4.1 Geologic Features

The following paragraph describes the geologic conditions of the soil and rock as they pertain to the stability and design of the power plant foundations.

A. Historic and potential uplift and subsidence are discussed in Paragraph 2.5.1.2.5.3.

B. The history of deposition, erosion, and sea level changes is given in Paragraphs 2.5.1.2.4. An analysis of A, B, C and D features[58][86] which were exposed during excavation for San Onofre Units 2 and 3, has contributed some additional data relative to the loading history of the foundation materials. A hypothetical sequence of events concluded from this analysis is that at some period after the deposition and at least partial consolidation of the San Mateo Formation, a north-south component of horizontal stress began to increase. At the same time, an east-west stress component decreased. These stress changes, probably caused by lateral extension of the San Mateo block, eventually resulted in the generation of the nearly vertical conjugate set of joint-like shears (A and B features). Down-dropping of the San Mateo block caused by dip-slip displacements along the Cristianitos fault could have caused such an extension. The presence of grain crushing associated with the A and B features indicates that at the time of their formation the thickness of sediment above the present plant grade was at least 90 meters (300 feet). The lateral extension permitting the reduction in the east-west component eventually stopped, when the shearing displacement reached the level currently observed. Erosion of the upper surface proceeded, lowering the surface by about 60 meters (200 feet), when the generally north-south compression continued, or was reactivated with some rotation towards a more northerly direction. The consequence was the development of the C and D features. It would appear that these features were generated when the upper level of the San Mateo block was in a position similar to its present elevation, but before deposition of the overlying terrace gravels.

C. Geologic discontinuities which were exposed within the San Mateo Formation during site excavation are discussed in Paragraph 2.5.1.2.5.1.

D. Erosion of several hundred meters of terrace material and San Mateo Formation in the geologic past may have resulted in some amount of unequal unloading of the subsurface rock. There is no indication, however, that the resulting unrelieved residual stresses would adversely affect the site. This is substantially supported by no noticeable changes in the material properties or by construction problems during excavation at the site.

E. Extensive studies have been performed to examine static and dynamic properties of rock units exposed at the site in order to evaluate their potential for becoming unstable or hazardous to the safety of the plant. The results of these studies are discussed in Paragraphs 2.5.4.8 and 2.5.5.2.

2.5.4.2 Properties of Subsurface Materials

The properties of the materials underlying the site were investigated by drilling, sampling and laboratory testing, and by geophysical techniques. Exploration techniques are presented in Paragraph 2.5.4.3 and geophysical surveys are summarized in Paragraph 2.5.4.4.

The descriptions of subsurface materials and their static and dynamic properties are presented in the following paragraphs. Specifically, the general soil conditions and static material properties are discussed in Paragraph 2.5.4.2.1 and the dynamic material properties are discussed in Paragraph 2.5.4.2.2. Details of material property testing and evaluation are presented in Appendix 2.5D.

2.5.4.2.1 General Soil Conditions and Static Properties

2.5.4.2.1.1 General

Static material properties were assessed by an evaluation of all the data obtained during field and laboratory phases of the investigation. Identification tests were made to confirm field classification and additional laboratory tests were completed to assess the strength and compressibility characteristics of foundation soils. Chemical and X-ray diffraction analyses were also performed on selected granular samples from the San Mateo Formation to identify potential cementing agents.

Based on the boring data presented in Appendix 2.5C and a careful inspection of surfaces exposed during excavation, simplified subsurface conditions along a typical east-west section through the plant area between stations 17+00 and 25+00 (Figure 2.5-32) are shown on Figure 2.5-33. Prior to the start of construction, the plant and switchyard areas were relatively flat at elevation +105 to elevation +120 feet, with near-vertical bluffs at the beach. During construction, the site is being excavated to the configuration shown on Figure 2.5-33. As is indicated on Figure 2.5-33, the soils underlying the site consist of two major geologic categories:

- Terrace deposits
- San Mateo Formation

As indicated on Figure 2.5-33, the plant area is underlain entirely by the San Mateo Formation below approximately elevation 50 feet. Major plant structures, including all Seismic Category I structures, will be founded in this material. The terrace deposits occur only in the area of switchyard slopes and will support switchyard structures.

Soil conditions and material properties for the two formations are described in the following paragraphs.

2.5.4.2.1.2 Terrace Deposits

The upper part of the terrace, elevations 24+ to 35 meters (+80 to +115 feet), consists of generally cohesive clayey sands to silty clays. In the lower part of the terrace, deposits at elevation +15 to ± 24 meters (+50 to +80 feet) are quite variable, and consist primarily of gravelly sand with occasional zones containing clay, silt and cobbles. Because of their variability, the properties of terrace deposits were specifically investigated in a drilling program described in Appendix 2.5C. The drilling program was designed to yield indicator properties of terrace deposits such as moisture content and dry density, unconfined compressive strength, grain-size distribution and triaxial strength of representative driven-tube samples. In addition, the properties of the terrace deposits were estimated by back-calculating the strength required for stability assuming that existing 1/2:1 slopes at the San Onofre Unit 1 site are at limit equilibrium. Those calculations yielded soil-strength values conservatively within the bounds of laboratory data (Appendix 2.5D). Based on all available data as summarized in Appendix 2.5D, the static strength properties of both the cohesive and granular parts of the terrace deposits are summarized in Table 2.5-11. Due to extreme variability, average grain-size distribution curves could not be drawn. Actual grain-size distribution curves for net individual samples are referenced in Appendix 2.5D.

Measured compressional and shear wave velocities for the terrace deposits ranged from 304 to 945 m/s (1000 to 3100 ft/s,) and 100 to 304 m/s (330 to 1000 ft/s), respectively.

2.5.4.2.1.3 San Mateo Formation

The plant and offshore areas are underlain to a depth of about 275 meters (900 feet) by very dense well graded sands of the San Mateo Formation. The range of grain-size distribution for the San Mateo sandstone is shown on Figure 2.5-34. Some variation in gradation was found at a few locations during excavation.[96] The range of grain-size distribution for the finer-grained zone constitutes less than 10% of the total San Mateo sandstone observed during excavation. The static properties of the San Mateo sandstone were calculated by extensive laboratory testing. The sand exhibits a high degree of effective cohesion due primarily to efficiency in grain packing. Static properties of the San Mateo sandstone are summarized in Table 2.5-12.

Table 2.5-11
TYPICAL STATIC SOIL PROPERTIES FOR TERRACE DEPOSITS

Soil Property	Cohesive Materials (El +80 to +115 ft)	Granular Materials (El +50 to +80 ft)
Natural water content, w (%)	10	4
Dry unit weight, γ_d (lb/ft^3)	118	115
Degree of saturation (%)	85	15
Unconfined compressive strength, q_u (k/ft^2)	6-10	Not applicable
Plasticity index	13	Nonplastic
Liquid limit	28	---
Shear strength:		
Strength intercept c (k/ft^2)	2.6	0.2
Angle of shearing resistance, ϕ (degrees)	17	38

Table 2.5-12
TYPICAL STATIC SOIL PROPERTIES OF SAN MATEO FORMATION

Property	Value
Natural water content, w(%)	2 (above water table) 11 (below water table)
Dry unit weight, γ_d lb/ft^3)	123
Shear strength:	
Strength intercept, c' (k/ft^2)	0.8
Angle of shearing resistance, ϕ' (degrees)	41
Relative density (%)	100
Plasticity index	Nonplastic

The measured compressional and shear wave velocities for the San Mateo sandstone ranged from 913 to 2286 m/s (3000 to 7500 ft/s), and 304 to 838 m/s (1000 to 2750 ft/s), respectively.

2.5.4.2.2 Dynamic Material Properties

A wide variety of procedures, including laboratory and field tests, are currently available to determine the shear modulus (G) and damping characteristics of foundation materials. In general, laboratory tests such as cyclic triaxial compression tests are employed for measuring moduli and damping factors under moderate to relatively high strains. Field measurements of wave velocities (compressional, shear, and Rayleigh waves) are commonly used to estimate soil moduli for low strain conditions. Dynamic material properties of the foundation soils were determined using field seismic surveys and laboratory cyclic triaxial tests. Data obtained during field testing for soil-structure interaction studies (Appendix 3.7C) were used to confirm the modulus and damping values obtained from field seismic and laboratory test results.

In addition to an evaluation of modulus and damping characteristics of the terrace deposits and San Mateo Formation, dynamic shear strength of the terrace deposits and San Mateo sand was determined by cyclic triaxial tests for slope stability and liquefaction evaluations.

2.5.4.2.2.1 Laboratory Dynamic Tests

Laboratory tests to determine the dynamic material properties included:

- Cyclic triaxial compression tests, stress-controlled, to estimate dynamic shear strength

- Cyclic triaxial compression tests, stress-controlled, to determine modulus and damping characteristics.

- Resonant column tests, to determine modulus

- Shock-scope tests, to determine the compressional wave velocities

Tests were conducted on reconstituted and intact pitcher tube samples. In addition, a number of hand-carved block samples were obtained to test undisturbed samples and to estimate sample disturbance effects. Details of the test apparatus, methods of testing, test results, and method of computation of modulus, damping, and cyclic strength parameters are given in Appendix 2.5D. Laboratory data were used to develop the high strain portion of the strain modulus and strain-damping relationships and the cyclic strength as discussed in Paragraph 2.5.4.2.2.4.

2.5.4.2.2.2 Field Seismic-Survey

Field seismic surveys including refraction, seismic velocity, micromotion surveys, down-hole, and cross-hole seismic measurements. The results of these surveys are discussed in Paragraph 2.5.4.4 and details of apparatus, method of testing, test results, and interpretation of data are given in References 32, 97, and Appendix 2.5A, Section 2.5A.3.

2.5.4.2.2.3 Soil-Structure Interaction Field Tests

A field testing program was initiated to confirm the laboratory derived modulus and damping parameters and to set the rules by which those parameters should be used in evaluating soil-structure interaction. The field tests included slab response, Rayleigh wave, and attenuation tests.

From the slab response tests, the stiffness was evaluated by analysis of response frequencies, and damping by analysis of the decay of response motions. The Rayleigh wave velocity measurements were carried out to verify: (1) near-surface shear wave velocity measurements obtained during field seismic studies and (2) the estimates of low-strain level shear modulus. The attenuation tests were used to determine the hysteretic damping of the soil and to verify the laboratory-determined relationship between damping and strain. The details of the tests and test results are presented in Appendix 3.7C.

2.5.4.2.2.4 Dynamic Stiffness and Damping

The cyclic triaxial test results for the terrace deposit soils are summarized in Table 2.5-13. Details of testing are presented in Appendix 2.5E. The stiffness and damping properties of the terrace soils obtained from the laboratory and field test results and correlations available in literature are presented in Figures 2.5-35 through 2.5-38. Strain-modulus and strain-damping curves for the San Mateo Formation are presented in Figures 2.5-39 and 2.5-40, respectively.

2.5.4.2.2.5 Dynamic Strength

Dynamic strength of terrace deposits was evaluated for use in slope-stability evaluations. The results of these tests are summarized in Figures 2.5-41, 2.5-42, and 2.5-43 for typical clayey and sandy terrace deposits and weaker soil lenses in terrace deposits, respectively. Laboratory tests were performed at field consolidated stress ratios (K_c) to 1.0 to 3.0. A majority of the tests were performed at K_c = 1.0 because analyses indicated most of the subsurface areas have low K_c (1.0 - 1.3) and a more meaningful data base was developed by running a larger number of tests under like stress conditions.

The dynamic strength of San Mateo Formation was evaluated for use in liquefaction analyses. The results of the laboratory cyclic strength tests on San Mateo Sand are summarized on Figures 2.5-44 and 2.5-45. A number of factors such as density and recompaction, confinement, anisotropy, degree of overconsolidation, and drainage affect the in-situ strength of the sand. As discussed in Appendix 2.5D, corrections and adjustments to the laboratory strength presented in Figures 2.5-44 and 2.5-45 were made to obtain the insitu dynamic strength values used in liquefaction analyses; these in-situ strengths are presented on Figures 2.5-46 and 2.5-47. As discussed in Paragraph 2.5.4.2.1.3, limited areas of finer-grained San Mateo Sand(61) and a summary of the test results is shown in Table 2.5-14. The test results fall within the range of strength data for the more predominant San Mateo Formation shown on Figures 2.5-46 and 2.5-47.

TABLE 2.5-13
SUMMARY OF CYCLIC TRIAXIAL TEST DATA TERRACE DEPOSIT SOILS

1	**2**	**3**	**4**	**5**	**6**	**7**	**8**	**9**	**10**	**11**	**12**	**13**	**14**	**15**
Test[a] No.	Sample No.[f]	K'_c	σ_{3c}'(lb/ft^2) Pre-test	σ_3'(lb/ft^2) Test	Unified Soil Classification	Dry Density lb/ft^2	D_{50} (mm)	% Passing #200	$\pm\sigma_d$ lb/ft^2	N Stress Cycles	ε(%) Axial Strain @ N Cycles [e]	E Calculated Modulus (k/ft^2)	γ Hysteretic Damping (%)	ε(%) Strain for Calculations of **13** and **14**
81	4A-ST3 Bottom	1.0	2300	1300	SM	111	0.5	27	1200	250	1.0	1200	24	1.0
82	1-ST1 Bottom	1.0	3400	2500	SM	111	[d]	[d]	2100	100	0.5	750	18	0.5
85[b]	4A-4 Bottom	1.0	2900	2800	SC	118	[d]	[d]	2300	25	10.0	[d]	[d]	[d]
97	4A-ST4 Middle	1.0	2900	2800	SC	109	0.14	43	2750	16	10.0	[d]	[d]	[d]
98	4A-ST6 Bottom	1.0	5400	5000	SP	102	0.5	3	4000	60	10.0	750	21	0.5
99	9-P2 Middle	1.0	1400	1000	SM	118	0.3	34	900	150	0.61	560	29	0.3
99A	9-P2 Middle	1.0	1400	1000	SM	118	0.3	34	900	150	0.73	[d]	[d]	[d]
99B	9-P2 Middle	1.0	1400	1000	SM	118	0.3	34	1460	31	10.0	[d]	[d]	[d]
100	9-P2 Top	1.0	1400	1000	SM	118	0.3	33	1650	31	10.0	76	25	0.4
101	10-P1 Bottom	1.0	1300	500	SM	118	0.3	45	500	150	0.2	1162	17	0.5
101A[c]	10-P1 Bottom	1.0	1300	500	SM	118	0.3	45	800	67	0.5	[d]	[d]	[d]
101B[c]	10-P1 Bottom	1.0	1300	500	SM	118	0.3	45	1150	150	6.4	[d]	[d]	[d]
102	10-P1 Middle	1.0	1300	1000	SM	110	0.2	38	1000	150	0.9	206	14	1.0
103	10-P2 Bottom	1.0	1300	1000	SM	121	0.1	47	1700	75	10.0	[d]	[d]	[d]
104	10-P2 Middle	1.0	1600	1000	SM	120	0.1	45	1850	13	10.0	192	23	3.4
105	10-P2 Top	1.0	1600	1000	SM	119	0.1	46	1750	11	10.0	120	19	1.6
106	7-ST2 Bottom	1.0	2600	1000	SC	122	0.25	35	980	150	0.12	300	26	1.0
106A[c]	7-ST2 Bottom	1.0	2600	1000	SC	122	0.25	35	1850	475	9.0	[d]	[d]	[d]
107	9-P4 Bottom	1.0	2000	1500	CL	118	[d]	[d]	1380	150	0.24	1250	16	0.4
107A[c]	9-P4 Bottom	1.0	2000	1500	CL	118	[d]	[d]	2500	150	0.74	[d]	[d]	[d]
107B[c]	9-P4 Bottom	1.0	2000	1500	CL	118	[d]	[d]	3380	152	10.0	[d]	[d]	[d]
108	9-P4 Top	1.0	2000	1500	CL	117	[d]	[d]	3200	229	10.0	600	19	1.0
109	9-P4 Middle	1.0	2000	1500	CL	122	[d]	[d]	4000	20	10.0	245	23	3.6
110	9-P5 Bottom	1.0	2500	2500	SC	122	0.1	45	2200	156	2.5	416	10	0.1
110A[c]	9-P5 Bottom	1.0	2500	2500	SC	122	0.1	45	4280	1	10.0	[d]	[d]	[d]

TABLE 2.5-13
SUMMARY OF CYCLIC TRIAXIAL TEST DATA TERRACE DEPOSIT SOILS

1	2	3	4	5	6	7	8	9	10	11	12	13	14	15
Test[a] No.	Sample No.[f]	K'_c	σ_{3c}'(lb/ft^2) Pre-test	σ_3'(lb/ft^2) Test	Unified Soil Classification	Dry Density lb/ft^2	D_{50} (mm)	% Passing #200	$\pm\sigma_d$ lb/ft^2	N Stress Cycles	ε(%) Axial Strain @ N Cycles [e]	E Calculated Modulus (k/ft^2)	γ Hysteretic Damping (%)	ε(%) Strain for Calculations of **13** and **14**
111	9-P5 Middle	1.0	2500	2500	SC	127	0.1	48	2500	150	0.4	120	32	0.4
112	9-P5 Top	1.0	2500	2500	SC	127	0.3	34	3380	2	10.0	[d]	[d]	[d]
113	9-P7 Bottom	2.0	3300	2000/1000	SW	116	0.1	47	1900	150	0.5	1100	22	0.35
113A[c]	9-P7 Bottom	2.0	3300	2000/1000	SW	116	0.1	47	2900	167	1.3	[d]	[d]	[d]
113B[c]	9-P7 Bottom	2.0	3300	2000/1000	SW	116	0.1	47	3000	1	10.0	[d]	[d]	[d]
114	9-P7 Middle	2.0	3300	2000/1000	CL	117	0.015	66	3000	150	2.0	[d]	[d]	[d]
114A[c]	9-P7 Middle	2.0	3300	2000/1000	CL	117	0.015	66	3600	50	10.0	[d]	[d]	[d]
115	10A-ST1 Bottom	2.0	1500	2000/1000	CL	119	0.02	62	2200	150	0.26	[d]	[d]	[d]
115A[c]	10A-ST1 Bottom	2.0	1500	3000/1500	CL	119	0.02	62	2850	150	0.31	[d]	[d]	[d]
115B[c]	10A-ST1 Bottom	2.0	1500	3000/1500	CL	119	0.02	62	3500	150	0.6	[d]	[d]	[d]
115C[c]	10A-ST1 Bottom	2.0	1500	3000/1500	CL	119	0.02	62	4500	150	1.0	[d]	[d]	[d]
116	9A-P5 Bottom	2.0	2000	3000/1500	SC	127	0.1	45	3850	1000	0.9	[d]	[d]	[d]
116A[c]	9A-P5 Bottom	2.0	2000	4000/2000	SC	127	0.1	45	4650	1000	1.5	[d]	[d]	[d]
117	9A-P6 Bottom	2.5	2000	1250/500	CL	127	0.008	76	4900	1000	7.5	[d]	[d]	[d]
117A[c]	9A-P6 Bottom	2.5	2600	1250/500	CL	127	0.008	76	5900	200	10.0	[d]	[d]	[d]
118	9A-P7 Bottom	2.5	3000	3250/500	CL	97	0.05	55	6850	1	10.0	[d]	[d]	[d]
119	9A-P4 Middle	3.0	1600	1500/600	SC	127	0.06	54	1800	1000	0.4	[d]	[d]	[d]
119A[c]	9A-P4 Middle	3.0	1600	1500/600	SC	127	0.06	54	2420	1000	1.75	[d]	[d]	[d]

[a] Test numbers not in sequence as other testing program in progress concurrently.
[b] Inadvertently saturated for 12 hours.
[c] Test numbers followed by A, B, or C are retests.
[d] Not analyzed, or not tested.
[e] These values are peak-to-peak (double amplitude). Ten percent axial strain is considered failure.
[f] All tests run on tube samplers. "ST" indicates Shelby Tube. "P" indicates Pitcher Tube.

Table 2.5-14
SUMMARY OF CYCLIC TRIAXIAL TEST RESULTS FINE-GRAINED SAN MATEO SAND

Test No.	Sample Type[a]	Sample Location	K_c[b]	σ_{3c}[b] (k/ft^2)	Dry Density (lb/ft^3)	$\pm\sigma_d$[b] (k/ft^2)	N[b]	ε (%)[b]	$\frac{\sigma_d^{(b)}}{2\sigma_{3c}}$
1	Block No. 1	Turbine Bldg No. 2 El -8.5 ft	1.0	4.0	111	3.8	19	10	0.483
2	Block No. 1	Turbine Bldg No. 2 El -8.5 ft	1.0	4.0	110	3.5	66	10	0.430
3	Block No. 2	Turbine Bldg No. 2 El -8.5 ft	1.0	4.0	106.5	4.0	9	10	0.505
4	Block No. 2	Turbine Bldg No. 2 El -8.5 ft	1.0	4.0	105	3.2	94	10	0.399
5	Block No. 2	Turbine Bldg No. 2 El -8.5 ft	1.0	4.0	107	3.7	144	10	0.465

(a) Sample diameter = 2.86 in. All samples saturated. Tests at frequency of 1 Hz.

(b) K_c = consolidation stress ratio $\left(\frac{\sigma_{1c}}{\sigma_{3c}}\right)$

σ_d = cyclic deviator stress

σ_{1c} = axial consolidation stress

N = number of stress cycles

σ_{3c} = confining stress

ε = axial strain at N cycles (peak to peak)

Note: Dynamic strength test data for the more predominant San Mateo sand are presented in Appendix 2.5A, pages 2.5A-57 and 2.5A-134.

2.5.4.3 Exploration

2.5.4.3.1 General

The site subsurface exploration included:

A. 55 onshore borings ranging in depth from 1.8 to 300 meters (6 to 987 feet)

B. 11 offshore borings ranging in depth from 0.9 to 6.7 meters (3 to 22 feet)

C. 3 onshore seismic investigations

D. 2 offshore seismic investigations

E. 19 backhoe trenches

F. 12 dewatering wells and one test well

G. 7 piezometers

The locations of all onshore borings, seismic lines, backhoe trenches, and dewatering wells along with safety-related facilities are shown on plot plan, Figure 2.5-32. Offshore seismic lines and locations of offshore borings are shown on Figures 2.5-48 through 2.5-50. The limits of required excavations are shown on Figure 2.5-51.

Borings were made by a variety of drilling techniques such as: rotary drilling, bucket auger, hollow-stem auger, jet probing, and vibracore. Both disturbed and intact samples were obtained during drilling by various techniques such as: Standard Penetration Test Method, Modified-California Sampler, Shelby Tubes, and Pitcher Barrel Sampler. In addition to sampling during drilling, a number of undisturbed, hand-carved block samples were obtained for comparison testing to evaluate sample disturbance effects of conventional sampling techniques. The number, type, depth, and purpose of borings and backhoe trenches and type of sampling are summarized in Table 2.5-15, Summary of Borings and Trenches (see Figure 2.5-32 for boring and trench locations.) The purpose and extent of geophysical surveys are described in Table 2.5-16, Summary of Geophysical Surveys.

Details concerning borings, trenches, drilling procedures, including Boring Logs, are included in Appendix 2.5C, Soil Borings. The geophysical investigation is summarized in Paragraph 2.5.4.4.

Table 2.5-15
SUMMARY OF BORINGS AND TRENCHES (Sheet 1 of 4)

No.	Boring Designation	Logged[(a)] by	Date	Diameter (in.)	Depth (ft)	El[(b)] (ft)	Method[(c)]	Purpose[(d)]	Sampling[(e)] Type
1	1	SCE	18 Sep 62	8	395	+22	R	SI	PT/SPT
2	2	SCE	24 Sep 62	8	155	+98	R	SI	PT/SPT
3	3	SCE	27 Sep 62	8	340	+97	R	SI	PT/SPT
4	4	SCE	2 Nov 62	8	140	+35	R	SI	PT/SPT
5	5	SCE	13 May 63	6	125	+88.2	R	SI	PT/SPT
6	6	SCE	8 May 63	6	126	+88.7	R	SI/P	PT/SPT
7	7	SCE	13 May 63	6	55	22 (est)	R	SI	PT/SPT
8	8	SCE	15 May 63	6	125	91.7	R	SI/P	PT/SPT

(a) WMA = Woodward-McNeill & Associates
D&M = Dames and Moore
SCE = Southern California Edison
FUGRO = FUGRO, Inc.
MAI = Marine Advisers, Inc., Solana Beach, Calif.
(b) Elevations are above MLLW
(c) A = Continuous Flight Auger
R = Rotary
B = Bucket
VC = Vibral Core
JP = Jet Probe
(d) SI = Soil Investigation
GI = Geologic Investigation
G = Geophysical
p = Piezometer
(e) MC = Modified California
ST = Shelby Tube
PT = Pitcher Tube
SPT = Standard Penetration Test

Table 2.5-15
SUMMARY OF BORINGS AND TRENCHES (Sheet 2 of 4)

No.	Boring Designation	Logged[a] by	Date	Diameter (in.)	Depth (ft)	El[b] (ft)	Method[c]	Purpose[d]	Sampling[e] Type
9	9	SCE	17 May 63	6	125	98.9	R	SI/P	PT/SPT
10	10	SCE	15 May 63	6	125	88.2	R	SI/P	PT/SPT
11	11	SCE	14 May 63	6	50	14.8	R	SI/P	PT/SPT
12	12	SCE	14 May 63	6	50	15.99	R	SI/P	PT/SPT
13	13	SCE	14 May 63	6	49	15.09	R	SI/P	PT/SPT
14	14	SCE	14 May 63	6	50	22.7	R	SI/P	PT/SPT
15	1	D&M	6 Mar 70	6	987	89	B/R	SI/G	PT/DM
16	2	D&M	10 Mar 70	6	252	88	B/R	SI/P	PT/DM
17	3	D&M	27 Feb 70	Not Known	55	97	B/R	SI	PT/DM
18	4	D&M	27 Feb 70	Not Known	58	90	B/R	SI	PT/DM
19	1	WMA		6	60	30	R	SI/G	PT
20	2	WMA	16 Aug 71	6	61	30	R	SI/G	PT
21	3	WMA	through	6	162	30	R	SI/G	MC/PT
22	4	WMA	24 Aug 71	6	63	30	R	SI/G	MC/PT
23	5	WMA		6	61	30	R	SI/G	MC
24	6	WMA		6	65	30	R	SI/G	None
25	7	WMA		6	30	30	R	SI/G	None
26	1	WMA		5	109	89	R	SI	MC/PT
27	2	WMA		5	301	89	R	SI	MC/PT
28	3	WMA	23 Aug 72	5	57	91	R	SI	MC/PT
29	4	WMA	through	5	302	91	R	SI	MC/PT
30	5	WMA	14 Sep 72	5	43	84	R	SI	MC/PT
31	6	WMA		5	62	107	R	SI	MC/PT
32	7	WMA		5	240	115	R	SI	MC/PT
33	1	WMA	19 Mar 74	6	57-1/2	102	A	SI	MC/ST
34	2	WMA	21 Mar 74	6	60-1/2	112	A	SI	MC/ST

Table 2.5-15
SUMMARY OF BORINGS AND TRENCHES (Sheet 3 of 4)

No.	Boring Designation	Logged[(a)] by	Date	Diameter (in.)	Depth (ft)	El[(b)] (ft)	Method[(c)]	Purpose[(d)]	Sampling[(e)] Type
35	3	WMA	22 Mar 74	6	70	112	A	SI	MC/ST
36	4	WMA	25 Mar 74	6	51-1/2	112	A	SI	MC
37	4A	WMA	27 Mar 74	6	80	112	A	SI	MC/ST
38	5	WMA	26 Mar 74	6	66-1/2	103	A	SI	MC
39	6	WMA	29 Mar 74	6	56	107	A	SI	MC/ST
40	7	WMA	29 Mar 74	6	66	116	A	SI	MC/ST
41	8	WMA	25 Mar 74	6	56-1/2	104	A	SI	MC
42	9	WMA	29 Mar 74	6	59	104	R	SI	PT
43	9A	WMA	29 Mar 74	6	51-1/2	98	R	SI	PT
44	10	WMA	28 Mar 74	6	38	94	R	SI	PT
45	10A	WMA	2 Apr 74	6	35	94	R	SI	MC/ST
46	1	WMA	16 Apr 74	6	61	3	R	SI	PT
47	2	WMA	4 Apr 74	6	41	3	R	SI	PT
48	3	WMA	5 Apr 74	6	40	3	R	SI	PT
49	1	FUGRO	5 Jul 74	Not Given	26	34	B	GI	None
50	2	FUGRO	5 Jul 74	Not Given	6	34	B	GI	None
51	3	FUGRO	5 Jul 74	Not Given	24-1/2	34	B	GI	None
52	4	FUGRO	5 Jul 74	Not Given	14	34	B	GI	None
53	5	FUGRO	5 Jul 74	Not Given	Not Given	34	B	GI	None
54	6	FUGRO	5 Jul 74	Not Given	12	34	B	GI	None
55	7	FUGRO	5 Jul 74	Not Given	15	34	B	GI	None
56	3	WMA		4	3	-35	VC	SI	VC
57	4	WMA		4	5	-55	VC	SI	VC
58	8	WMA	26 Mar 74	4	5.5	-38	VC	SI	VC
59	14	WMA	and	4	4.0	-35	VC	SI	VC
60	15	WMA	27 Mar 74	4	4.0	-48	VC	SI	VC

Table 2.5-15
SUMMARY OF BORINGS AND TRENCHES (Sheet 4 of 4)

No.	Boring Designation	Logged[a] by	Date	Diameter (in.)	Depth (ft)	El[b] (ft)	Method[c]	Purpose[d]	Sampling[e] Type
61	19	WMA		4	7.0	38	VC	SI	VC
62	24	WMA		4	5.0	-55	VC	SI	VC
63	1	MAI	Mar 70	Not Given	10	-28	JP	GI	None
64	2	MAI	Mar 70	Not Given	22	-20	JP	GI	None
65	3	MAI	Mar 70	Not Given	21	-18	JP	GI	None
66	4	MAI	Mar 70	Not Given	21	-27	JP	GI	None
67	1	FUGRO	10 Jun 74	19	9.5	34	BH	GI	None
68	2	FUGRO	11 Jun 74	36	15	34	BH	GI	None
69	3	FUGRO	10 Jun 74	135	6	34	BH	GI	None
70	4	FUGRO	4 Jun 74	7	4	34	BH	GI	None
71	5	FUGRO	6 Jun 74	14	12	34	BH	GI	None
72	6	FUGRO	5 Jun 74	12	30	34	BH	GI	None
73	7	FUGRO	11 Jun 74	25	7	34	BH	GI	None
74	8	FUGRO	11 Jun 74	15	5	34	BH	GI	None
75	9	FUGRO	11 Jun 74	15	5	34	BH	GI	None
76	10	FUGRO	11 Jun 74	65	8	34	BH	GI	None
77	11	FUGRO	11 Jun 74	35	3	34	BH	GI	None
78	12	FUGRO	11 Jun 74	8	3	34	BH	GI	None
79	13	FUGRO	5 Jun 74	30	19	34	BH	GI	None
80	14	FUGRO	11 Jun 74	19	5	34	BH	GI	None
81	15	FUGRO	1 Nov 74	30	8	34	BH	GI	None
82	16	FUGRO	1 Nov 74	15	3	34	BH	GI	None
83	17	FUGRO	1 Nov 74	36	3	34	BH	GI	None
84	18	FUGRO	1 Nov 74	46	4	34	BH	GI	None
85	19	FUGRO	1 Nov 74	50	4	34	BH	GI	None

Table 2.5-16
SUMMARY OF GEOPHYSICAL STUDIES

Report Title and Date	Location	Purpose	Measurements
Seismic and Foundation Studies, Proposed Units 2 and 3, San Onofre Nuclear Generating Station, San Onofre, California, April 15, 1970, Dames & Moore	PSAR Appendix 2B	Determine seismic velocities to evaluate the response of materials to earthquake loadings	Seismic Refraction and velocities Micromotion
		Obtain bore hole geophysical data for geologic interpretation	Bore hole geophysical data
Elastic and Damping Properties, Laydown Area, San Onofre Nuclear Generating Station, October 14, 1971, Woodward-McNeill & Associates	Appendix 2.3 PSAR, Amend 11 Appendix 2E	Determine compressional and shear wave velocities to evaluate soil response to earthquake loading velocities	Cross-hole and down-hole measurements of shear and compressional wave
Offshore Liquefaction Evaluation for the Proposed Units 2 and 3, San Onofre Nuclear Generating Station, San Onofre, California, December 19, 1974, Woodward-McNeill & Associates	UFSAR Appendix 2.5A.3	Offshore sub-bottom profiling to estimate thickness of sediments above San Mateo Sand in the area of offshore conduits	Reflection seismic record using boomer survey
Development of Soil-Structure Interaction Parameters, Proposed Units 2 and 3, San Onofre Generating Station, San Onofre, California, January 31, 1974, Woodward-McNeill & Associates	UFSAR Appendix 3.7C	Determine soil-structure interaction parameters	Rayleigh wave velocity
Continuous Seismic Profiling Investigation of the Continental Shelf off San Onofre, California, April 24, 1970, A. J. MacKay, Marine Advisors, Inc., Solana Beach, California, A subsidiary of the Bendix Corporation	PSAR Appendix 2B	Investigate the offshore faults and geologic structure of the Continental Shelf and upper slope off San Onofre	Continuous seismic profiling by sparker, high-resolution boomer and 7-KH_z high-resolution profiler

Details of groundwater conditions including the results of water well and piezometer measurements are discussed in Paragraphs 2.4.13 and 2.5.4.6.

2.5.4.3.2 Generalized Soil Profile

A generalized soil and geologic profile through the center of the two containment buildings, Units 2 and 3, is presented as Section A-A on Figure 2.5-52. The section location, number, and identification of the borings are given on plot plan, Figure 2.5-32. The generalized profile indicates that the contact between the terrace deposits and San Mateo Formation varies between about elevation +40 and elevation +50 in the plant area. The finished grade in the plant will be elevation +29 and all safety-related structures are founded below elevation +29 in San Mateo Formation. A simplified east-west section is shown on Figure 2.5-33. Because all Class I structures are founded below elevation +29 in the generally uniform San Mateo sand, as shown on Figure 2.5-33, the borings and structures were not shown on the east-west section, Figure 2.5-33.

2.5.4.3.3 Photographs of Excavations

Figure 2.5-53 shows the site on February 11, 1974, 1 month prior to the start of excavation. Figure 2.5-54 shows the site on October 15, 1974, after all of the site (except the Unit No. 3 containment and turbine area) has been cut to finished subgrade elevation. Figure 2.5-55, taken on July 8, 1975, shows the Unit 3 containment structure excavation.

2.5.4.4 <u>Geophysical Surveys</u>

2.5.4.4.1 General

A number of geophysical surveys were made to determine the subsurface conditions in the plant area and offshore areas adjacent to the plant. Table 2.5-16 lists the investigations and summarizes the main purpose and the measurements made during each investigation. The table also indicates the location where details of each investigation can be found. Locations of all onshore seismic lines are shown on Figure 2.5-32. Offshore seismic lines for study No. 4 in Table 2.5-16 are indicated on Figure 2.5-48. Slip track lines for study No. 5 are shown in Subsection 2.5.3.

2.5.4.4.2 Seismic Velocity Measurements

Seismic velocity measurements were made during the first three investigations indicated on Table 2.5-16. The results of the first two investigations, including compressional and shear wave velocities are presented in Figures 2.5-56 through 2.5-58. The Rayleigh wave velocity tests made in exposed San Mateo Formation between elevation +30 feet and elevation +15 feet during the third investigation indicated velocities in the range of 850 to 1200 ft/s, with a velocity of 930 ft/s as a representative average for the upper 15 feet of soils. Because, for all practical purposes, the Rayleigh wave velocity is equal to the shear wave velocity, the shear wave velocity in the near-surface soils (upper 15 feet) was assumed to be of the order of 900 to 1000 ft/s.

Based on the geophysical velocity measurements presented in Figures 2.5-56 through 2.5-58, the range of shear and compressional wave velocities are summarized as follows:

	Velocity (ft/s^2)	
Material	Shear Wave	Compressional Wave
Terrace	330-1000	1000-3100
San Mateo Formation:		
(upper 50 ft)	1000-2200	3000-7000
(below 50 ft)	1900-2750	7000-7500

The values of shear and compressional wave velocities in the upper 50 feet of San Mateo Formation measured in two different investigations (Figures 2.5-56, 2.5-57, and 2.5-58) vary considerably. The smaller near-surface values shown on Figures 2.5-57 and 2.5-58 are due to the reduced overburden since the measurements were made after the removal of the overlying terrace deposits to about elevation 30 feet. The measurements in San Mateo Formation shown in Figure 2.5-56 were made with at least 45 feet of overlying terrace deposits.

From the seismic tests the low-strain range Poisson's ratio was found to lie between 0.4 and 0.45.

2.5.4.4.3 Offshore Seismic Profiling

The results of shallow seismic profiling indicated that generally 3 to 5 feet of sand, cobbles, and other surface sediment overlie the San Mateo Formation in the area of the offshore conduits. This mantle could be as thick as 10 feet locally.

The results of the seismic profiling investigation of the continental shelf are summarized in Subsection 2.5.3.

2.5.4.5 Excavation and Backfill

2.5.4.5.1 Excavation Plan and Sections

The as-constructed excavation plan for all Seismic Category I structures is shown on Figure 2.5-59. Typical as-constructed cross-sections through the following structures are shown on Figure 2.5-60:

Section	Direction	Building
A	E-W	Containment Unit 2
		Fuel Handling Building 2
		Safety Equipment Building
		Turbine Building Area
B	E-W	Auxiliary Building
		Intake Structure
C	N-S	Containment Unit 2
D	N-S	Turbine Building Area
		Intake Structure

All buildings are founded below finished plant grade at elevation +30 feet in San Mateo sand.

2.5.4.5.2 Dewatering and Excavation Methods

In general, dewatering to a maximum depth (elevation -35 feet) was accomplished by a multi-level well point system. The methods used, field monitoring and details of dewatering are discussed in Paragraph 2.5.4.6, Groundwater Conditions. The only foundation material below the original groundwater level is dense San Mateo sand; therefore, dewatering operations should not have any adverse effects (e.g., long-term consolidation settlements) on the foundation soils.

The foundation excavations were made with conventional earth-moving equipment in San Mateo sand. Since no expansive or water sensitive materials such as plastic clays or collapsible sands or silts are present in the foundation area, no special foundation protection or treatment measures were considered necessary. All foundation excavations at the base of slab were protected against disturbance and where over-excavation was done, the excavation was backfilled with concrete or San Mateo backfill to the specifications indicated in Paragraph 2.5.4.5.3.

No measurements of foundation rebound or heave were considered necessary because the foundation heave is expected to be small and occurs simultaneously with the excavation unload. No long-term heave or rebound is expected due to high permeability of the foundation materials.

2.5.4.5.3 Backfill

All soil backfill use in Seismic Category I areas of the site consists of San Mateo Sand which was excavated for construction of the plant facilities. Properties of this material are discussed in Paragraph 2.5.4.2.

No test fills were constructed at the site, as experience with the construction of existing Unit 1 provided sufficient data for evaluation of compaction characteristics.

All backfill on the site is compacted to a density of at least 95% and 100% of the maximum determined in accordance with ASTM Test Method D1557-70 for fill above and below elevation +5 feet, respectively. The backfill was placed and compacted while at a moisture content within about 2% of optimum moisture content determined from ASTM D1557-70. Grain-size bands for the material are presented on Figure 2.5-34.

2.5.4.6 Groundwater Conditions

Groundwater conditions are described in the following paragraphs.

2.5.4.6.1 Groundwater Conditions Relative to Plant Facilities

A detailed description of groundwater conditions is given in Subsection 2.4.13. Studies have shown that the groundwater table beneath the site is quite stable. Monitoring of piezometers near the site has shown that the average elevation of the groundwater table at the site is 1.5 meters (+5 feet) MLLW datum. Design of structures at the site is based on this value. Because any changes of the groundwater level beneath the site will be minor as discussed in Paragraph 2.4.13.2, they will have no impact upon the stability of plant facilities.

2.5.4.6.2 Control of Groundwater Levels

Because groundwater conditions at the site are stable, there is no need for control of groundwater levels. The groundwater table lies approximately 7.6 meters (25 feet) below the surface elevation at the site. Groundwater seepage at the surface is not expected to occur and, therefore, systems for collection and control of seepage are unnecessary.

2.5.4.6.3 Dewatering During Construction

Plans showing the excavation levels lying below the existing water table at elevation +5 feet are shown on Figure 2.5-59. Sections and details are shown on Figure 2.5-60.

The dewatering system plan, sections, and details are shown on Figure 2.5-61.

The initial design of the San Onofre Nuclear Generating Station Units 2 and 3 dewatering system was based on permeability studies provided by the following sources:

A. The San Onofre Nuclear Generating Station Unit 1 pump test.

B. The San Onofre Nuclear Generating Station Unit 1 dewatering system.

C. United States Geological Survey well data for the surrounding area.

D. Analysis of grain size at the project site.

In addition, economical and practical considerations dictated that the system should consist basically of a limited number of widely spaced, relatively deep wells. Such a design permitted the use of large capacity deep well turbine pumps having better operational efficiencies than smaller, submersible type pumps.

The plant cooling water lines are located in an area contiguous to the plant west property line. This area is shown on Figure 2.5-59, as that enclosed by the temporary seawall. Due to the proximity of the open water to the deep (-30-foot ± elevation) excavation for the intake lines, supplementary local wellpoint dewatering was required for this area as shown on Figure 2.5-61. The estimated permeability of 0.016 ft/min based on the foregoing permeability studies served as the basis for the initial design which consisted of 12 deep wells and one test well with a total combined pumping rate of 9000 gal/min. Subsequently, before actual dewatering commenced, a pump test was conducted at the test well. The results of this test are detailed in a report by R. Y. Bush, dated June 7, 1974, and titled "Report on Pumping Test, San Onofre Nuclear Generating Station, Units 2 and 3". The revised permeability of 0.025 ft/min required a corresponding increase in the pumping capacity of the dewatering system.

The final dewatering system consisted of 12 deep wells each containing an electric motor-driven turbine pump rated at 1500 gal/min at 80 feet (TDH). The test well, containing an electric motor-driven turbine pump rated at 1500 gal/min at 100 feet TDH, was incorporated into the permanent dewatering system. Two stand-by pumps rated at 1500 gal/min at 80 feet TDH were provided as part of the permanent design. The pumping rate from the deep well system, excluding the well point system, was estimated at 15,000 gal/min. The actual design rate of 19,500 gal/min provided approximately 30% additional capacity to allow for occasional pump failures. The maximum estimated water draw-down elevation was between -40.0 to -50.0 feet and was not expected to extend beyond the ring of dewatering wells more than about 1000 feet. The configuration of the water table after a steady state is reached will be an inverted saucer with deep points at the wells and following a parabolic path outward.

The deep wells ranged in depth from 195 ± to 204 feet ± and were drilled to a minimum 30 inch diameter. The test well depth was 300 feet ± and was also drilled to a minimum 30 inch diameter. The well steel casing was 14-inch diameter with a minimum wall thickness of 5/16 inch. The bottom 100 feet of the deep well casing and the bottom 200 feet of the test well casing was provided with louver-type slotted openings 1/8 inch wide and of sufficient number so that an area of at least 10 $in.^2$/ft of pipe was provided. The remaining top portions of the casings were of the solid type.

In addition to the deep wells, a supplementary well point system was required in the intake area. The system as originally designed consisted of two stages of well points at respective elevations of +2 feet and -14 feet. Two pumps, one operating and one standby, both connected to the well point header manifold, were included. As dewatering progressed, it became necessary to expand the well point system. A third stage of well points was installed at elevation -23 feet along with a 200 hp electric pump and two backup diesel pumps of 100 hp and 160 hp. In addition, a fourth stage of well point system at elevation -26.75 feet was later added along with an electric motor-driven pump rated at 5000 gal/min at 120 feet TDH. A backup diesel powered unit rate at 5000 gal/min at 100 feet TDH was also included. The maximum rate of pumping during dewatering at the lower stage was estimated to be approximately 2000 gal/min.

Dewatering operations commenced in August 1974 and continued on an intermittent basis through February 1978. Individual wells were decommissioned as construction needs dictated starting in June 1976. The last stage of the well point system at elevation -26.75 feet was removed in May 1975.

For details of the demobilization program refer to Paragraph 2.5.4.14.1.

2.5.4.6.4 Groundwater Conditions Experienced During Construction

Typical amounts of water discharged with the entire system in operation is approximately 15,500 gal/min. Actual flow measured was 12,915 gal/min with pumps 1, 10, and 11 off and 12,792 gal/min with pumps 8, 10, and 11 off. Actual draw-down curves are available in the form of field reports (see Appendix 2.4A).

Seven observation holes of 8-inch minimum diameter were provided at the locations indicated on Figure 2.5-61. The piezometers located at these observation holes consisted of 2-inch PVC pipe with performations consisting of holes or slots. The piezometer data are available in the form of field reports (see Appendix 2.4A).

2.5.4.6.5 Permeability Tests

The San Mateo Formation underlies the site to a depth of approximately 275 meters (900 feet). Permeability of this formation has been determined by field pump testing and laboratory mechanical analysis. Results of these tests are discussed in Paragraph 2.4.13.2.

2.5.4.6.6 History of Groundwater Fluctuation

The history of groundwater fluctuations is discussed in Paragraph 2.4.13.2. Observation wells nearest to the site have shown only minor fluctuations in response to maximum fluctuations occurring in the central basin area. Observed fluctuations in groundwater levels at the site are related directly to tidal fluctuations. Future groundwater fluctuations are projected to correspond closely to past fluctuations which at the site have been less than 0.46 meters (1.5 feet). Because of the semi-impermeable nature of the San Mateo Formation, flooding on the San Onofre Creek area is expected to have little effect on groundwater levels at the site.

2.5.4.6.7 Periodic Monitoring of Local Wells and Piezometers

The Marine Corps owns, operates, and monitors all wells in the San Onofre Valley Basin. Their monitoring program consists of one continuous strip-chart water level recorder at a representative well in addition to supplemental data on water levels in observation wells around the basin determined by field measurement on a biweekly basis. The aim of this program is to insure that a flow of fresh groundwater toward the coast is maintained, thus preventing the possibility of saline water intrusion.

2.5.4.6.8 Direction of Groundwater Flow, Gradients, and Velocities

Direction of groundwater flow, including groundwater contour maps, which indicate gradients and velocities is discussed in Paragraph 2.4.13.2.

2.5.4.7 Response of Soil and Rock to Dynamic Loading

2.5.4.7.1 Introduction

The terrace deposits have been removed from the plant area, so that the only soil/rock responding to dynamic loading in the plant area is the San Mateo sand. The properties of the San Mateo sand have been presented in Paragraph 2.5.4.2. The fundamental dynamic relationships between stiffness, damping and strain for the San Mateo sand, used in analyses for its response to dynamic loading, have been presented in Paragraph 2.5.4.2.2, and are presented for reference in Figure 2.5-62. Response analyses were made to develop the shape of the response spectrum for the design basis earthquake (DBE) (Paragraph 2.5.2.6), to study the stability of switchyard slopes (Subsection 2.5.5), to study the liquefaction potential at the site (Paragraph 2.5.4.8), to evaluate stresses on buried pipelines and conduits (Paragraph 3.7.1.4), and to evaluate the sliding potential of shallowly buried structures (Paragraph 3.7.1.4).

2.5.4.7.2 Analyses

To develop the shape of response spectrum for the DBE, the dynamic response of the soil/rock at the site was studied by using lumped-mass models of the site and strain-dependent values of shear modulus and hysteretic damping. An abstract of the program is presented in Paragraph 2.5.4.7.3.1. The San Mateo sand at the site was modeled as being 300- and 1000-foot thick, with a few calculations done for a 2500-foot thick model, in order to cover the possible ranges in the site-stiffness characteristics. Details of the various analyses and their results are presented in Appendix 2.5B.

Dynamic stability analyses of switchyard slopes, liquefaction evaluation, and evaluation of sliding potential of shallowly buried structures were made by static and dynamic finite-element procedures. The computer program LOCKS was used for static finite-element analyses, and the computer program QUAD4 was used for the dynamic finite-element analyses. Abstracts of these programs are presented in Paragraphs 2.5.4.7.3.2 and 2.5.4.7.3.3. Details of the slope-stability analyses are presented in Subsection 2.5.5, the liquefaction analyses in Paragraph 2.5.4.8, and sliding-potential analyses in Paragraph 3.7.1.4.

The response of buried pipelines and conduits were evaluated by examining their critical instantaneous profiles which were calculated by traveling wave dynamic finite-element procedures. These analyses are presented in Paragraph 3.7.2.1.1.4. An abstract of the traveling-wave finite-element program used is presented in Paragraph 2.5.4.7.3.4. Other response analyses for soil-structure interaction studies are also described in Paragraph 3.7.2.1.

2.5.4.7.3 Program Abstracts

2.5.4.7.3.1 Response of Homogeneous, Horizontal Soil Deposits

To compute the response of homogeneous, horizontal oil deposits to earthquake motion at their bases, a lumped-mass computer program developed at the University of California, Berkeley, was used.[34][98][99][100] The horizontal soil deposit shown in Figure 2.5-63 was analyzed using the lumped-mass idealization shown in Figure 2.5-64. The program is based on the solution of a set of simultaneous equations of motion describing motion of each layer modeled by a mass, stiffness (spring constant) and damping value. The nonlinearities of stiffness and damping, both of which depend on the strain level (Figure 2.5-62) are accounted for by the use of equivalent linear soil properties in an iterative procedure to obtain values for stiffness and damping compatible with the effective strain in each layer. The following assumptions are implied in the analysis:

A. The soil system extends infinitely in the horizontal direction.

B. Each layer in the system is completely modeled by a mass, a spring constant which is based on the shear modulus of the layer and a damping value.

C. The response of the system is calculated for a multi-degree system subjected to an acceleration-time history at the base.

D. The strain-dependence of modulus and damping is accounted for by an equivalent linear procedure based on an average effective strain level computed for each layer.

The program accepts input motion as horizontal acceleration-time history at the base of the profile, and provides response values, in terms of acceleration-time histories and/or maximum values of accelerations, shear stresses, and strains at any desired location in the profile.

2.5.4.7.3.2 Static Finite-Element Program

The static finite-element program, LOCKS, used for the preceding, analyses was developed at the University of California, Berkeley.(101) The program accepts quadrilateral, triangular, and joint elements and follows the standard finite-element approach with the following provisions for geotechnical purposes:

A. A simplified procedure has been used to represent stress-dependent soil stress-strain behavior. The nonlinear stress-strain relationship is approximated by a series of straight lines. This procedure is convenient for use in incremental finite-element stress analysis.(102)

B. The program can simulate an excavation or buildup sequence.

C. Analyses can be made using either a plane-strain or plane-stress relationship.

D. The program is capable of obtaining existing stresses, by a gravity-turn-on procedure.(102)

The output of the program consists of stresses, strains, and displacements for each construction sequence (excavation or buildup). In addition, the program computes principal stresses for each element and the values of modulus for each element used in each iteration of calculations.

2.5.4.7.3.3 Dynamic Finite-Element Program

The finite-element program QUAD4 for dynamic geotechnical analysis of structures was developed at the University of California, Berkeley.(100) The program uses triangular and quadrilateral elements, and uses strain-dependent dynamic properties of modulus and damping. The computations begin with assumed values of modulus and damping, and then iterations are carried out until the values of each parameter used are strain-compatible. The response calculations are done by the step-by-step direct integration method.

The maximum values of horizontal and vertical accelerations, and the time at which they occur for each nodal point are printed at the end of each iteration cycle. The maximum stresses and the maximum shear strain in each element are also printed. The values of modulus and damping in each element computed using the iterated strain values in the element are compared to the previously used values and printed at the end of each iteration cycle so that the strain-compatibility of the values of modulus and damping used in the last iteration could be examined. Acceleration-time histories of selected nodal points can be obtained.

2.5.4.7.3.4 Traveling-Wave Finite-Element Program

This program is a two-dimensional, dynamic, finite-element analysis procedure in which the base motion is considered as a shear wave traveling at a velocity depending on the properties of the bedrock. The program was developed at the University of California, Berkeley.[86]

The input to the program consists of data defining the triangular elements, the material properties (only constant elastic properties are considered), the earthquake time history, and the velocity, and direction of its propagation with respect to the structure.

The program performs the following operations in the order listed:

A. Read-in the structural data including geometry and material properties

B. Calculate the tributary masses for each nodal point and assemble structural mass matrix

C. Calculate finite-element stiffness matrices and combine them to establish an overall stiffness matrix

D. Find the static displacements for nodal points above the base due to a unit horizontal displacement placed separately at each base nodal point.

E. Compute normal frequencies and mode shapes

F. Read-in input data for the response, including ground accelerations and damping ratios

G. Integrate the ground acceleration to get velocity and displacement

H. Calculate the dynamic nodal-point displacements, and quasi-static nodal-point displacements, and their sums

I. Find the internal stresses in each finite element due to the total nodal point displacement

J. Keep a record of the peak major and minor principal stresses in each finite element and the corresponding times at which these peak stresses occurred

K. Print out dynamic response data.

1. The output from the program consists of the following:

    a. Reprint of the first set of input data, i.e., structural and material properties, options, etc.

    b. Static nodal-point displacements due to a unit horizontal displacement separately placed at each base nodal point

    c. Frequencies

    d. Mode shapes

    e. Participation coefficients

    f. Reprint of second set of input data, i.e., ground acceleration, initial stresses, damping ratios, etc.

    g. Ground velocity and displacement

    h. Nodal point displacements

    i. Element stresses

    j. Peak values of major and minor principal stresses of each individual element and the time at which those stresses occurred.

2.5.4.8 <u>Liquefaction Potential Evaluation</u>

2.5.4.8.1 General

Soil conditions at the site are described in Paragraphs 2.5.4.1 and 2.5.4.2. Of particular relevance to this subject are the facts that: (1) the upper terrace deposits were removed from the plant area, thus, all safety-related structures are founded on San Mateo sand; (2) in the onshore area, the water table is at elevation +5 feet and the top of San Mateo sand is at elevation +50 feet, thus, only San Mateo sand lies below the water table; and (3) in the offshore region, San Mateo sand is the principal soil. Thus, the liquefaction potential of only San Mateo sand was examined. A generalized section, showing soil conditions in the switchyard slope area, plant area, and offshore conduit area is presented in Figure 2.5-33.

2.5.4.8.2 Field Investigation

A number of field investigations have been made to explore the onshore subsurface soil conditions. Details of these explorations are presented in Paragraphs 2.5.4.3 and 2.5.4.4, and Appendix 2.5A, Section 2.5A.2.

In the area of offshore conduits, subsurface soil conditions were determined by geophysical survey and vibracore drilling. Details of these explorations are presented in Woodward-McNeill & Associates report of December 19, 1974 (Appendix 2.5A, Section 2.5A.3).

2.5.4.8.3 Soil Properties

2.5.4.8.3.1 Laboratory Testing and Field Measurements

A. Laboratory Testing

Static and dynamic properties of the San Mateo sand have been studied in detail and are described in Paragraph 2.5.4.2. For the evaluation of liquefaction potential, dynamic strength tests were accomplished on carved block samples, intact pitcher tube samples and remolded samples. A total of 112 cyclic triaxial tests were made at several different densities, confining pressures and anisotropic consolidation ratios to evaluate the in-situ strength of San Mateo sand. Results of these tests are presented in Appendix 2.5A, pages 2.5A-57 and 2.5A-134. Dynamic strength was defined as the cyclic shear stress required to induce initial liquefaction or the stress required to cause ±5% strain in a given number of stress applications, whichever was the smaller.

B. Field Measurements

Standard penetration tests were performed in borings yielding very high values of blow count N (i.e., N = 100) as shown on Figures 2.5A-39 and 2.5A-40. Also 125 field density tests were made in native San Mateo sand using the Sand Cone Method (ASTM D1556-70). The results of these tests are summarized on Figure 2.5-65. The dry density of the native San Mateo sand was interpreted to be 123 lb/ft^3 from Figure 2.5-65. This density was used for the analysis of the offshore area. A lower value of 120 lb/ft^3 was used in the plant area to account for the small areas of the plant to receive fill below the water table. The minimum density required for the compaction of such fill was set at 120 lb/ft^3.

2.5.4.8.3.2 Evaluation of In-situ Dynamic Strength of San Mateo Sand

A number of factors such as density and recompaction, confinement, anisotropy, degree of overconsolidation and drainage were studied to evaluate the in-situ dynamic strength of San Mateo sand, used in the analyses described in Appendix 2.5A. A schematic explanation of the various steps involved in determining the field dynamic strength of San Mateo sand from laboratory tests is presented in Table 2.5-17. The in-situ dynamic strength curves used in those analyses are presented in Figures 2.5-46 and 2.5-47. Subsequent to the analyses described in Appendix 2.5A there have been recent changes in the static-of-the-art of evaluating in-situ dynamic strength from dynamic strength tests.[103][104][105][106][107][108] These changes in the state-of-the-art and their implementation in obtaining the in-situ dynamic strength of San Mateo Sand are described below.

Table 2.5-17
EVALUATION OF FIELD DYNAMIC STRENGTH OF SAN MATEO SAND (Sheet 1 of 3)

1.	A total of 112 cyclic triaxial tests were conducted on samples of San Mateo sand. These included 8 tests on carved block samples, 40 tests on intact Pitcher tube samples and 64 tests on recompacted samples. Tests were done at different dry densities, confining pressures, and anisotropic consolidation ratios to incorporate these factors in evaluating in-situ dynamic strength (Appendix 2.5A, pages 2.5A-62 and 2.5A-141). The results are plotted as $\sigma_d/2\sigma_{3c}$ vs. N as shown for σ_{3c} = 4000 lb/ft^2 and γ_{d1} through γ_{d3} for remolded samples and γ_{d2} for intact samples.	
2.	Results of a large number of field density tests on the native soils were plotted as a histogram of a number of tests yielding different densities. Based on this plot, an average dry density of 123 lb/ft^3 was adopted for the in-situ San Mateo sand. For the compacted, backfilled San Mateo sand and native soils in the plant area, a conservative value of dry density of 120 lb/ft^3 was corresponding to the minimum density specification for compaction of backfill (Appendix 2.5A, page 2.5A-138).	

Table 2.5-17
EVALUATION OF FIELD DYNAMIC STRENGTH OF SAN MATEO SAND (Sheet 2 of 3)

3.	Because it was not possible (without degradation of material) to reproduce small lab samples to densities as high as indicated in Step-2, the lab test results for remolded samples at lower densities from Step-1 were used to extrapolate strengths of in-situ densities by cross-plotting data from Step-1 as the normalized strength ($\sigma_d/2\sigma_c$) vs. dry density (γ_d) for various members of cycles required to induce ±5% strain. From these plots, the normalized strengths at various cycles for San Mateo sand in the plant area were obtained for a dry density of 120 lb/ft^3 and in the offshore area for a dry density of 123 lb/ft^3 (Appendix 2.5A, page 2.5A-63).	
4.	To evaluate the effect of remolding on dynamic strength, the test results on carved block samples were compared with those for sister remolded samples compacted at the same dry density as that of the carved sample. The results were compared for K_c = 1. From this comparison, it was found that the carved block sample had a strength about 15% larger than the recompacted sample. This factor was used to obtain in-situ strength from recompacted samples tested at various densities, confining pressures, and K_c values (Appendix 2.5A, pages 2.5A-64 and 2.5A-65).	

Table 2.5-17
EVALUATION OF FIELD DYNAMIC STRENGTH OF SAN MATEO SAND (Sheet 3 of 3)

5.	Using the results of Steps-3 and 4 and state-of-the-art interpretation discussed in Paragraph 2.5.4.8.3.2, field dynamic strengths of San Mateo sand in the plant and offshore areas were obtained by first obtaining the laboratory strength at field density from Step-3, then increasing it by 15% to account for remolding from Step-4, and multiplying by appropriate C_r values listed in Table 2.5-19. For the plant area the field strength was conservatively based on the strength of in-situ material at a dry density of 120 lb/ft^3 and K_c = 1. Similar interpretations were made to obtain strengths at other K_c values. For the offshore area, the in-situ strength was based on a dry density of 123 lb/ft^3 and K_c = 1 (Figures 2.5-74 and 2.5-75).	
6.	Many of the tests in Step-1 were done at confining pressures higher than 4000 lb/ft^2. Based on interpretation procedures outlined in Steps-3, -4 and -5 field dynamic strengths at other confining pressures for the plant area were obtained. These strengths were normalized at σ_{3c} = 4000 lb/ft^2 as indicated and used in the development of field strength parameters. Strengths at lower confining pressures, appropriate for the offshore area are shown on Figure 2.5-75 (Appendix 2.5A, page 2.5A-69).	

Table 2.5-18
LIST OF DEFINITION OF TERMS USED IN
FIGURES 2.5-66
THROUGH 2.5-73 AND TABLE 2.5-17

C_r	-	Correction factor to obtain in-situ dynamic strength from cyclic triaxial test results
F.S.	-	Factor of safety
K_c	-	Ratio of principal stress used to consolidate the sample in cyclic triaxial tests
K_o	-	Coefficient of earth pressure at rest
OCR	-	Overconsolidation ratio
τ_{max}	-	Maximum cyclic shear stress
σ_3,σ_{3c}	-	Confining stress used to consolidate the sample for cyclic triaxial tests
σ_{fc}	-	Normal stress on the potential failure plane of a sample
σ_d	-	Dynamic deviator stress applied to the sample
γ_d	-	Dry density of the soil sample

Table 2.5-19
SUMMARY OF C_r FACTORS

Area	X(ft)[a]	Elevation (ft)[a]	Approximate OCR	Updated C_r Values[b]
Plant area	600	0	3.75	0.75
	600	-20	3.25	0.72
	600	-40	2.25	0.65
Offshore conduit	2000	-10	5 to 8	0.83 to 1.0
	2000	-20	5 to 8	0.83 to 1.0
	2000	-40	5 to 8	0.83 to 1.0

(a) For location see Figure 2.5-33.

(b) C_r based on overconsolidation ratio (OCR).

Table 2.5-20
SUMMARY OF PARAMETERS USED IN THE ANALYSIS

No.	Report[a]	Value of C_r Used	Basis for Choice of C_r	Number of Uniform Equivalent Stress Cycles @ 65% Maximum Stress	Minimum Factor of Safety[b]	
					Local	Areal
1	Site Liquefaction Study	0.8	$D_r \sim 100\%$	variable w/elevation ~30 to 80	1.3	1.5
2	Offshore Liquefaction	0.9	$K_o = 0.8$	30	1.2[c]	1.5

[a] See Appendix 2.5A.

[b] Factor of Safety defined as: stress to cause ±5% strain/induced stress.

[c] Very near surface.

A. Field Dynamic Strength (C_r Parameter)

For the studies reported in Appendix 2.5A, the parameter C_r (parameters used herein are defined in Table 2.5-18) used to obtain in-situ dynamic strength from cyclic triaxial tests was based on relative density and coefficient of earth pressure at rest, K_o. Recent studies[103][104] indicate that C_r is relatively insensitive to relative density, and is principally sensitive to K_o in the form of the overconsolidation ratio (OCR). The relationship between K_o or OCR and C_r developed in these studies[107] is presented in Figure 2.5-68. Utilizing the available information about the overburden which existed at the site in its geologic history[101] and the known amount of overburden removal in the switchyard and plant areas, along with the measured values of K_o in the offshore area, presented in Appendix 2.5A, new values for C_r were obtained. Table 2.5-20 presents the C_r values used in the previous analyses. New value of C_r, along with the estimated values of OCR, are presented in Table 2.5-19. Applying these modified C_r factors to the laboratory strength curves, developed in Appendix 2.5A, Sections 2.5A.2 and 2.5A.3, new field strength curves were developed for the plant and the offshore areas and are presented in Figures 2.5-74 and 2.5-75, respectively. The effect of confinement above σ_{3c} = 4000 lb/ft^2 on the curves on Figure 2.5-74 is presented on page 2.5A-69 of Appendix 2.5A.

B. Number of Uniform Equivalent Stress Cycles

In the previous calculations for the plant area, the number of equivalent uniform cycles of loading at 65% of the maximum stress during the DBE was conservatively selected to be between 30 and 80 (Table 2.5-19). Recent studies[108] have shown that the number of equivalent uniform cycles at 65% of the maximum stress are about 10 to 30 cycles for actual high-magnitude earthquakes, as shown in Figure 2.5-69. On this basis, a conservative analysis of liquefaction at the site would incorporate dynamic strengths from the field strength curves corresponding to 30 uniform equivalent stress cycles. Therefore, the use of 30 uniform equivalent stress cycles was adopted for the modified analyses described below.

C. Limiting Shear-Strain Potential

Based on the results of large-scale laboratory tests[103] a limiting shear-strain potential has been established as a function of relative density, as shown in Figure 2.5-71. For the San Mateo sand which has an average relative density of 100% (Paragraph 2.5.4.2), the shear-strain potential is quite small (much smaller than 5%), as indicated on Figure 2.5-71. Such a small value of limiting shear strain indicates that large strains which are associated with complete liquefaction are not possible for the San Mateo sand, due to effects of dilatency. This is further substantiated by the standard penetration resistance measured at the site compared to the values presented in the literature as relative to limiting strain for sands,[105][107] as shown on Figure 2.5-72. Because of the very low shear-strain potential for the soils at the site, factors of safety higher than 1.0 for the development of ±5% strain from cyclic triaxial testing are considered ample.

D. Effects of Drainage on Stability

Recent work[106] indicates that material such as gravels and coarse sands with high permeability do not liquefy, due to the drainage-caused reduction of pore pressures. For the San Mateo Formation sand, the permeability ranges between 0.005 and 0.025 ft/min (Appendix 2.5A, Section 2.5A.2). For these permeabilities, and based on the results of parametric studies,[106] the potential for liquefaction near the water table (or other free-draining boundaries at the site) is lower than would be calculated from the analyses which assume no drainage. Further, the results of tests incorporating small amounts of drainage (presented in the offshore liquefaction report, Appendix 2.5A, Section 2.5A.2), indicate about a 15% increase in strength due to the effects of drainage.

2.5.4.8.4 Analysis

2.5.4.8.4.1 General Approach

Basically the evaluation of liquefaction potential is accomplished by a comparison of the stresses induced by the DBE to the in-situ dynamic shear strength of the soil. The induced stresses are obtained by analyzing two-dimensional plane-strain models using dynamic finite-element procedures. The in-situ dynamic strength of the San Mateo sand was evaluated by dynamic triaxial tests as discussed in Paragraph 2.5.4.8.3 and summarized on Figures 2.5-74 and 2.5-75.

2.5.4.8.4.2 Induced Stresses

The dynamic shear stresses induced by the DBE were obtained by two-dimensional finite-element procedures. Both horizontal and vertical acceleration components were used in the analyses. These analyses are described in detail in Appendix 2.5A, Sections 2.5A.2 and 2.5A.3.

2.5.4.8.4.3 Results and Conclusions

The induced shear stresses obtained as described in Paragraph 2.5.4.8.4.2 were compared with the in-situ strength obtained as described in Paragraph 2.5.4.8.3 to obtain factors of safety against liquefaction (ratio of stress necessary to cause ±5% strain to earthquake induced stress). The stresses necessary to cause ±5% strain were determined from Figures 2.5-74 and 2.5-75 for plant and offshore areas, respectively, for 30 cycles of loading and for the in-situ stress conditions (k_c and σ_{3c}) as defined in Appendix 2.5A, Sections 2.5A.2 and 2.5A.3. The earthquake-induced stresses as described in Appendix 2.5A, Sections 2.5A.2 and 2.5A.3, for plant and offshore areas were used directly without modifications. As a result, a composite cross-section of the site was developed showing factor-of-safety contours for the San Mateo sand below water in plant and offshore areas of the site as presented on Figure 2.5-73. It is noted that the potentially beneficial effect of drainage described in Paragraph 2.5.4.8.3.2 was not incorporated into the determination of factor-of-safety presented in Figure 2.5-73. As indicated on Figure 2.5-73, the minimum factor-of-safety in the plant area is 1.5 to 2 and in the offshore area is 1.2 to 1.5. Based on the discussions of limiting shear strain potential and effects of drainage on stability presented in Paragraph 2.5.4.8.3.2, it is concluded that these calculated factors-of-safety against liquefaction of San Mateo sand at the site, for the DBE loading, are ample. Therefore, there should be no adverse effects due to liquefaction at the site.

2.5.4.9 Earthquake Design Basis

2.5.4.9.1 Derivation of the DBE and the OBE

The synthetic acceleration-time history for the DBE was developed so that its response spectrum appropriately matched the design response spectrum (Paragraphs 2.5.2.6 and 3.7.1.2). The general shape of the design response spectrum was developed from an analysis of the response of the site to earthquakes scaled so that the maximum acceleration at or near the site surface was 0.5 to 0.67g. This shape was verified by analyzing the response of the site to a number of earthquakes credible to the site. This time-history has a maximum acceleration of 0.67g and a duration of 80 seconds. The development of the response spectrum for the DBE and its verification are discussed in Paragraph 2.5.2.6 and described in detail in Appendix 2.5B.

The OBE (Paragraph 2.5.2.7) is characterized by a maximum acceleration of 0.33g (one-half of the maximum acceleration for the DBE) and a duration of 36 seconds.

2.5.4.9.2 Selection of Earthquakes for Liquefaction and Switchyard Slope Stability Analyses

The evaluations of the potential for liquefaction of the San Mateo sand at the site and the stability of switchyard slopes are presented in Paragraph 2.5.4.8 and Subsection 2.5.5, respectively. These evaluations depend on the level of the maximum acceleration, number of cycles of loading and the spectral characteristics of the earthquake motion. The liquefaction and slope stability analyses presented in Paragraph 2.5.4.8 and Subsection 2.5.5 were done for the DBE which is an extremely severe event as described above. As described in Paragraph 2.5.4.8 and Subsection 2.5.5, an equivalent number of uniform cycles of loading for the DBE was developed from the upper bound of the available data for large-magnitude earthquakes.

2.5.4.10 Static Stability

All Seismic Category I structures were analyzed for static loading conditions. Foundation bearing capacity, soil heave, total and differential settlement were evaluated under the excavation unload and design loads due to the plant structures. Lateral earth pressures on structures from backfills were considered. Design soil parameters used in the foundation stability analyses and the results of the analyses are discussed in the following sections. Soil and foundation conditions observed during construction were compared with those assumed in the analyses and the impact of different conditions on the design was evaluated.

2.5.4.10.1 General

All Seismic Category I structures are shown on the plot plan, Figure 2.5-32, and relationships of the plant structures to the subsurface conditions are presented in Figure 2.5-13. All Seismic Category I structures are founded in the San Mateo sand below finished plant grade, elevation +30. Since the San Mateo sand supports all major plant structures, its properties and selected design parameters used in the analyses are summarized in Paragraph 2.5.4.10.2. The size, embedment below elevation +30, unloading due to excavation below elevation +30 and, gross structure loading are summarized in Table 2.5-21. Bearing capacity, settlement and heave and lateral earth pressures are discussed in Paragraphs 2.5.4.10.3 through 2.5.4.10.5. Differences in observed and assumed soil conditions are discussed in Paragraph 2.5.4.10.6.

2.5.4.10.2 Soil Parameters

The preconstruction site grade in the plant area was between elevation +95 and elevation +110. The finished plant grade at elevation +30 was attained by excavating more than 65 feet of terrace deposits and San Mateo sand.

Figure 2.5-52 indicates that all Seismic Category I structures are founded below elevation +30 in the San Mateo sand. The foundation soils have thus been unloaded to the extent of at least 8 k/ft^2 and are reloaded in relation to the overburden pressures from the finished plant grade, elevation +30. Details of the pertinent properties of the San Mateo sand are given in Paragraphs 2.5.4.2 and Appendix 2.5D. Soil parameters used in the subsequent analyses are summarized in Table 2.5-22.

The shear strength properties used in the bearing capacity analyses are: strength intercept, $c = 800$ lb/ft and angle of internal friction $\phi = 41^{o}$.

The shear strength was evaluated by means of extensive triaxial compression and direct-shear testing as described in Appendix 2.5D. Strength values were also confirmed by back-calculating the shear strength required for stability assuming that the existing one-half to one (horizontal to vertical) slopes at San Onofre Unit 1 are in limiting equilibrium.

Table 2.5-21
STRUCTURE DIMENSIONS AND LOADING

Structure	Foundation Dimensions[a] (ft)	Foundation Embedment[b] (ft)	Excavation Unload[c] (k/ft^2)	Gross Load (k/ft^2)
Containment	92 radius	43.5	-5.65	4.63
Auxiliary building	221 x 280	30	-3.9	4.89
Fuel handling building	80 x 134	19.5	-2.58	6.17
Safety equipment	74 x 174	10-50	-3.25	3.54
Electrical and piping gallery building	67 x 86	35.5	-4.61	3.5
Intake structure	113 x 240	30-60	-5.85	3.23

(a) Dimensions are generally outside plant dimensions. See Figure 2.5-51 for building configuration.

(b) Embedment below finished plant grade elevation +30.

(c) Unload below plant grade at elevation +30. For varying excavation depth, average unload was estimated.

Table 2.5-22
SUMMARY OF MATERIAL SEISMIC WAVE TRANSMISSION PROPERTIES FOR SAN MATEO FORMATION SAND[(a)]

Item	Quantity
Seismic compressional velocity	
Above water table, ft/s	3,000 - 7,000
Below water table, ft/s	7,000 - 7,500
Seismic shear velocity	
Above water table, ft/s	1,000 - 2,000
Below water table, ft/s	1,900 - 2,750
Soil properties	
Natural water content	
Above water table, %	2
Below water table, %	11
Dry unit weight, lb/ft^3	123
Shear strength:	
Strength intercept, k/ft^2	0.8
Angle of shearing resistance, degrees	41
Relative density, %	100
Plasticity index	Nonplastic
Unified soil classification	SW
Shear modulus	Figure 2.5-31
Poisson's ratio	
High stress	0.25 - 0.33
Low stress	0.40 - 0.45
Hysteretic damping	Figure 2.5-31
Water table elevation, ft MLLW	+5
Water table variation	Minor

(a) For more details of properties and methods used to obtain them, see Paragraph 2.5.4.2.

2.5.4.10.3 Bearing Capacity

Ultimate bearing capacity was computed by using the following properties for San Mateo sand:

Cohesion	= 800 lb/ft^2
Angle of internal friction	= 41 ^{o}
Total unit weight	= 130 lb/ft^3
Buoyant unit weight	= 68 lb/ft^3

Calculated ultimate bearing capacity for the structures listed in Table 2.5-21 is greater than 400 k/ft^2 and the factor of safety against shear failure for the most heavily loaded building is in excess of 100.

Other buildings have correspondingly higher factors of safety. Therefore, it is concluded that all Seismic Category I structures have very high factors of safety against shear failure under static loading conditions.

2.5.4.10.4 Settlement and Heave

The heave of foundation soils due to excavation depends upon the magnitude of unload, areal extent of the excavation and the compressibility of the foundation soils. The settlements of structures depend upon size, shape, depth of embedment, configuration and intensity of the applied loading and soil compressibility.

To evaluate the elastic settlement and heave under various loading and unloading conditions, a formula of the following form was used:

$$S = \frac{P\,T\,(1-\nu^2)\,I\rho}{E}$$

where:

S = settlement or heave

P = bearing pressure or unload

B = foundation width

ν = Poisson's ratio

E = modulus of elasticity of the soil

$I\rho$ = influence factor depending upon foundation shape and rigidity.

Effects of adjacent structures were included in the calculation for settlement and heave.

A number of methods were used to estimate the compressibility of over-consolidated, dense San Mateo sand.

These methods included:

A. Back-calculations of a modulus based on measured settlements of the containment building, Unit 1.

B. Standard penetration test (SPT) blow counts (N-value) obtained during sampling (ASTM D1586).

C. Seismic modulus based on shear wave velocity measurements corrected for strain levels.

It has been shown[109] that, for small strains experienced under large nuclear plant structures, elastic modulus of dense sands determined by laboratory odometer or triaxial tests is not appropriate. Consequently, laboratory data were not used to estimate the sand compressibility.

Measured settlement at the center of the reactor containment for Unit 1 under a load of 3.4 k/ft^2 and equivalent radius of 70 feet was 0.38 inches. For a circular area of 140 feet diameter loaded to 3.4 k/ft^2 and a Poisson's ratio of 0.35, the elastic modulus is calculated by equation[1] to be about 13,000 k/ft^2.

The minimum SPT N-value in the San Mateo sand is about 100 blows/ft with the average value exceeding 200. Estimated settlement for containment Unit 2, using Mayerhoff's[110] equation is:

$$S = \frac{P\,(B)^{1/2}}{N}$$

where:

S = settlement, in.

P = soil bearing pressure, k/ft^2

B = foundation width, ft

N = SPT blow count, blows/ft

for

S = 0.63 in.

P = 4.63 k/ft^2

B = 184 ft

N = 100 (minimum)

Using equation(1) for a circular area, this settlement yields a minimum elastic modulus of about 14,000 k/ft^2.

The seismic moduli determined from shear wave velocity measurements(110) and corrected for strain levels have been used for estimated in-situ compressibility of sand deposits. Average shear wave velocity in the top 100 to 150 feet (zone of influence of structure loads) is about 1900 ft/s yielding a seismic shear modulus of G = 14,700 k/ft^2 and seismic elastic modulus E = 40,000 k/ft^2. For reloading conditions which are applicable to San Onofre sands due to the removal of more than 8 k/ft^2 of loads (Paragraph 2.5.4.10.2), a static modulus equal to about 40 to 50% of the seismic modulus is suggested.(110) This yields a minimum static modulus of E = 16,000 k/ft^2. This modulus is also compatible with the average estimated strain below the containment.

From the above analyses, the minimum static modulus was estimated to be on the order of 13,000 k/ft^2 for the size of structures under consideration. This was used for subsequent settlement calculations.

Settlement and heave calculations were made using equation(1) for the loading and unloading on structures shown in Table 2.5-21, an elastic modulus of 13,000 k/ft^2 and a Poisson's ratio of 0.35. The results of these calculations indicate that the maximum heave due to the excavation unload and settlement due to the gross structure loads are on the order of 1 inch, and occur at the center of the auxiliary building. The maximum computed settlements under other structures range between 1/2 to 1 inch. The maximum differential settlements are less than 1/2 inch. Due to the high permeability of the San Mateo sand, all settlements are expected to occur simultaneously with the application of loads and the post-construction settlements will be negligible. The computed settlements are based on a conservatively estimated minimum elastic modulus of 13,000 k/ft^2. The actual soil modulus is expected to be significantly higher and consequently the settlements to be lesser than the computed values. Results of stability analyses will be confirmed with as-built data as it becomes available.

2.5.4.10.5 Lateral Earth Pressures

For static conditions the at-rest pressure is considered applicable for the evaluation of static lateral earth pressure against rigid walls from the in-situ or backfill San Mateo sand. An at-rest earth pressure coefficient K_o equal to 0.34 was used in the design. This yields an equivalent fluid pressure from a fluid with a unit weight of 45 lb/ft^3 above the water table and 85 lb/ft^3 below the water table. Ultimate passive resistance due to static lateral loads was estimated by using a passive pressure coefficient, K_p, of 4.8 yielding an equivalent fluid weight of 625 lb/ft^3 above the water table and 390 lb/ft^3 below the water table (including hydrostatic pressure).

2.5.4.10.6 Design Verification and Variations from the Assumed Conditions

2.5.4.10.6.1 Density Verification

Strength data for the San Mateo sand used in bearing capacity analyses in Paragraph 2.5.4.10.4 were obtained by testing intact and recompacted samples. The dry intensity of these samples ranged between 118 and 122 lb/ft^3. During construction, in-situ density measurements were made at all structure locations at the exposed foundation grade level to verify the density of the natural San Mateo sand. The results of these tests are presented in Figure 2.5-65. These tests indicate that the in-place density at all locations was in the range of laboratory-test densities.

2.5.4.10.6.2 Fine-Grained San Mateo Sand

After excavations were made to the foundation grade, it was found that the San Mateo sand encountered in about 10% of the plant areas had a gradation finer than the sand obtained from borings and found in the majority of the plant areas. Samples of this material were obtained to determine its static and dynamic properties, and the results are given in Appendix 2.5D. These studies indicated that the strength of the finer-grained San Mateo sand is as high or higher than the strength of the coarse-grained material. Consequently, the different gradation material encountered during the excavation does not have any adverse impact on the strength properties used in the design analyses.

2.5.4.11 Design Criterion

The size, embedment, relative configuration, and loading of all Seismic Category I facilities were determined from safety and operational considerations. The geotechnical design criteria used for evaluation of various structures were:

A. The structure foundation is safe against a bearing capacity failure in the supporting soil.

B. The heave and settlements under the excavation unload and structure loading are small and within reasonable limits for the safe operation of the structure and equipment.

C. The preceding two criteria are satisfied under static as well as seismic or other severe loading conditions.

$$q_u = cN_c\zeta_c + qN_q\zeta_q + 1/2\gamma BN_\gamma\zeta_\gamma$$

The ultimate static bearing capacity was evaluated by the formula:[101]

where:

q_u = ultimate bearing capacity

c = cohesion

γ = unit weight

q = overburden

N_c, N_q, N_γ = bearing capacity factors

B = foundation width

$\zeta_c, \zeta_q, \zeta_\gamma$, = shape factors

Using conservatively estimated strength parameters for San Mateo sand, cohesion c = 800 lb/ft^2 and angle of shearing resistance, $\phi = 41\,^{o}$ C the computed ultimate bearing capacities for various structures have factors of safety in excess of 100 against static loading (Paragraph 2.5.4.10).

The maximum stresses in the soil below the basemat of any structure during seismic or other severe loading are less than 10 times the maximum static stresses (Subsection 3.7.2). This represents an adequate factor of safety against bearing capacity failure of greater than 10.

The settlement and heave analyses presented in Paragraph 2.5.4.10 indicate maximum settlements of less than 1 inch and maximum differential settlements of less than 1/2 inch. Post construction settlements are negligible, less than 1/10 inch. The total and differential settlements are very small, and there are virtually no post construction settlements; therefore, the structures are considered safe against detrimental settlement or heave.

The San Mateo sand is very dense and no instability due to liquefaction during the DBE loading conditions is expected (Paragraph 2.5.4.8).

In summary, the structures are safe against bearing failure or detrimental settlements under all conditions.

2.5.4.12 Techniques to Improve Subsurface Conditions

The undisturbed San Mateo sand, upon which all safety-related structures are founded, is a material which has 100% relative density and which exhibits extremely efficient grain packing. The strength of this material in its natural state is very high, consequently, no techniques were implemented to improve its properties.

2.5.4.13 Subsurface Instrumentation

Groundwater level measurements are continuing as a part of the dewatering operations at the site as discussed in Paragraph 2.5.4.6. Settlement measurement devices will be installed on selected foundations upon completion of construction.

2.5.4.14 Construction Notes

No construction problems that would adversely effect the safety of the plant facilities have been encountered. A few modifications in the planned procedures were adopted due to changed conditions observed during construction, and these are discussed in the following sections.

2.5.4.14.1 Dewatering System

The specified dewatering system was designed to lower the water table to approximately elevation -35 feet. However, after installation and operation, it was found that additional well points were required. These were installed along the center and perimeter of the intake structure excavation, as discussed in Paragraph 2.5.4.6.

During decommissioning of the 12 construction dewatering wells and one test well at the San Onofre 2 and 3 site (well locations shown on Figure 2.5-61), evidence of subsurface anomalies associated with these wells was detected. The decommissioning procedure was then modified to include an evaluation of the possibility of anomalies associated with these wells and an assessment of the effects of the detected anomalies on adjacent Seismic Category I structures. The results of the field and laboratory investigative work and the analyses performed during the well investigation/demobilization effort are summarized in Reference 111. In brief, the field work included: (1) drilling a total of 634 borings, some to the maximum depth of the wells (about 200 feet); (2) removal of the well casing and filter gravel from the well-bore and subsequent filling of the well-bore with concrete at three of the wells; (3) exploration drilling and cross-hole seismic surveys at four of the wells; (4) down-hole inspection of 12 well casings by a bore hole television camera; and, (5) pressure grouting with cement grout around four wells close to Seismic Category I structures where cavities were detected. This work led to the demobilization of all wells and to the detection of cavities at wells 6, 7, and 8 and either small or possible small cavities at wells 3, 5, and 10. Locations and configuration of these wells are shown in Figure 2.5-61. The significant characteristics of these cavities are that they were sand-filled, limited in areal extent, rather lobate in shape, and are predominately located in the draw-down zone developed during construction dewatering. These observed characteristics are consistent with the mechanism of cavity formation postulated in Section 2 and Appendix A of Reference 111.

The results of extensive exploration drilling and grouting programs indicate that all cavity areas are filled with sand or grout and contain no open voids. Analyses were performed to evaluate the maximum effects of the detected cavities on the performance of Seismic Category I structures, considering static as well as DBE-induced loading conditions. The results of these analyses indicate that maximum effects of any detected cavity on the adjacent Seismic Category I structures are very small and are well within the variation in design parameters used in initial design.

In conclusion, the findings of the investigations show no detrimental effect from the detected cavities to Seismic Category I structures. All onsite wells have been demobilized by backfilling with sand, gravel, and/or grout.

2.5.4.14.2 Support of Structures on Backfill

At certain locations, the structure subgrade materials did not consist of undisturbed San Mateo sand; i.e., along the beach. At other locations, structure subgrades were over-excavated and concrete or San Mateo sand backfill, compacted in accordance with the specifications (95% relative compaction above elevation +5 feet and 100% relative compaction below elevation +5 feet, was used to bring the area to grade. Prior to the implementation of this procedure, analyses were performed to determine the effects of these changes on design. To date, the only structures which have any backfill beneath them are the seawall and the turbine area of Unit 3. The locations of these fills are shown on Figure 2.5-76. In each of these areas, field verification was made to ensure that all unsuitable soils and debris were removed prior to placement of compacted backfill and that the backfill was placed on undisturbed San Mateo sand.

2.5.4.14.3 Concrete Backfill

Concrete with a minimum 28-day compressive strength of 2000 lb/in.^{2} was used in lieu of compacted San Mateo sand or backfill in some locations on the site which were too confined for access with compaction equipment.

Additional applications of concrete or Portland cement grout as backfill material are discussed in Paragraph 2.5.4.14.1 and Reference 111. These materials were used to backfill the well-bores and numerous exploration borings and to stabilize regions of formational material disturbed by operation of the wells as identified by the investigation/demobilization program for the construction dewatering well system described in Reference 111. The minimum unconfined compressive strength for bulk concrete placements was 2000 lb/in.^{2} at 28 days while Portland cement gravity or pressure grout was required to have a minimum unconfined compressive strength of 200 lb/in.^{2}. The 200 lb/in.^{2} specified minimum unconfined compressive strength for

Portland cement gravity or pressure grout yields an in-situ material with compatible strength characteristics to the native undisturbed formational material.

2.5.4.14.4 Backfill Outside the Seawall

Backfill placed outside the seawall was compacted to a density of at least 100% of the maximum determined by ASTM D1557-70, below elevation -1.5 feet. Above this elevation, San Mateo sand backfill was placed and compacted in accordance with the specifications (see Figure 2.5-77) in a zone extending 10 feet out from the seawall. Beyond this point, the backfill was placed with no compaction requirements. A schematic cross-section showing zones of fill in this area is given on Figure 2.5-77.

2.5.4.14.5 Units No. 2 and 3 Fuel Handling Buildings Soldier Beam Cutoff

As a construction aid, temporary retaining walls running north-south along the east side of the Units 2 and 3 fuel handling buildings were installed. The walls consisted of wide-flanged soldier beams placed in 24-inch diameter augered holes at 4-foot center-to-center spacing. Holes extended to approximately elevation -1 foot, and were backfilled with approximately 8 feet of concrete (up to elevation +7 feet, then backfilled with San Mateo sand and jetted). Subsequently the soldier beams were cut off at elevation +15 feet, and the backfill was placed in accordance with the specifications between elevation +15 and +17 feet. The effective change in specifications is that there are soldier beams in 24-inch diameter holes at 4-foot center-to-center spacing, encased in concrete below elevation +7 feet, and backfilled with uncompacted sand between elevation +7 and +15 feet. No safety-related structure is bearing on these areas, and the maximum groundwater level (elevation +5 feet) is below the zone of the uncompacted fill.

2.5.4.14.6 Siltstone

Pockets of very stiff siltstone and claystone were encountered on the site at the locations shown on Figure 2.5-78. To evaluate the index and strength properties of this material, drive-tube and carved-block samples of the material were taken from the site for laboratory testing. Classification and strength tests (triaxial) were performed in representative samples for comparison with the data from San Mateo sand tests. Strength tests indicate that for the confining pressures being investigated, the siltstone has a higher Young's Modulus under lower confining pressure and a low Young's Modulus under higher confining pressure than the San Mateo sand. These data were used for analysis of potential differential settlement of the Unit 2 crane extension footings (shown on Figure 2.5-78), assuming that one end of the footing would bear on the siltstone and the other on the San Mateo sand. The calculations indicated a maximum differential settlement of about 1/4 inch. Subsequent observations of all excavations for structures indicated that only very small isolated areas of the site have siltstone, therefore, their effects on settlement are negligible.

2.5.4.14.7 Trench Along Base of Switchyard Slopes

An electrical trench, 10 feet deep, was excavated parallel to and approximately 5 feet from the base of the temporary construction slope. San Mateo sand backfill was placed in the trench; however, no density tests were made at the time of backfilling. Subsequently, two field density tests were made in the backfill at depths of 3 and 5 feet below the surface. These tests indicated that the backfill was at a relative compaction of 80 to 90%. Analyses were made of the effects of this backfill on switchyard slope stability. These studies indicated that overall switchyard slope stability would not be compromised by leaving the existing trench backfill in place. Only minor surficial sloughing (which would not affect Quality Class I and II facilities) during a DBE is indicated by the analyses.

2.5.4.14.8 Finer-Grained San Mateo Sand

After excavation to the finished subgrade elevations, careful examination of the exposed San Mateo sand indicated that some areas had a material of a slightly finer gradation than had been encountered during preliminary studies. Therefore new studies were undertaken to determine the extent and properties of this material. A geologist and a soil engineer examined all excavations and logged areas where the finer-grained material exists. These areas are delineated on Figure 2.5-79.

To estimate the properties of this material, bulk and block samples were taken from the site for laboratory testing. Grain-size distribution tests, compaction tests, triaxial compression tests, and dynamic triaxial tests were performed. All test results indicated that the strength of the finer-grained material is as high or higher than for the more coarse-grained material. Background information, test results, and details of these studies are presented in Appendix 2.5D.

2.5.4.14.9 Gravel Backfill

Because of functional requirements and groundwater considerations, gravel backfill was used below the Unit 2 and 3 fuel storage tank sumps. The small quantity of backfill was placed in space measuring 2 feet by 8 feet in plan and 4 feet deep. This backfill extended approximately 6 inches below the groundwater table which is at elevation +5 feet. The gradation of this backfill varied between 3/4 inch to No. 4 which was verified for grain size distribution and was found to be a suitable bedding material.

2.5.5 SLOPE STABILITY

All native near-vertical bluffs and cut slopes to the north and south of the Unit 2 and 3 site are at great enough distances from Unit 2 and 3 structures so as not to affect safety of these structures. Switchyard slopes northeast of Units 2 and 3 are the only permanent slopes in the vicinity of plant structures. Therefore, these were the only slopes studied in detail for evaluation of plant safety. These 2:1 cut slopes are about 90 feet high and have two benches. The characteristics and design of these slopes are discussed in summary in this section. The antecedent background subsurface information and details of previous studies are given in Appendix 2.5E.

2.5.5.1 Slope Characteristics

The switchyard slopes are located to the northeast of Unit 2 and 3 reactors, and rise from elevation +30 feet at the plant level to about elevation +120 feet, Figure 2.5-80. The slopes are a little over a thousand feet in length, extending alongside the various plant structures, which are located in a flat area at the base of the slopes. The plan width of slopes is about 280 feet, including the two benches, which constitutes an overall slope inclination slightly flatter than 3 (horizontal) to 1 (vertical). All the slope surface is composed of cut materials with the exception of approximately 5 feet of fill along the base of slopes from about elevation +30 to +35 feet.

2.5.5.1.1 Cross-Sections and Profiles

A typical section across the switchyard slope area showing the pre- and post-construction conditions is given in Figure 2.5-81. Before construction began, the ground surface sloped gently toward the southwest and had an average elevation of approximately +110 feet. The gentle slope terminated near the beach at near-vertical bluffs.

After construction, the area adjacent to the beach is planned to be generally at elevation +30 feet, the finished grade around the plant. The switchyard slopes are to rise at an inclination of 2:1 from elevation +30 to +120 feet away from the beach, being interrupted by two benches at elevation +55 and +78 feet.

As indicated in Figure 2.5-81, the upper portions of the switchyard slope consist of terrace deposits. These materials, which extend beneath the surface to approximately elevation +50 feet, consist of very dense and very stiff soils. The upper portions of the terrace deposit (above approximately elevation +80 feet) are generally clayey sands to silty clays. These materials are underlain by predominantly gravelly sand materials, with occasional lenses of clay, silt, and cobbles. The soils which constitute the base of the terrace deposit (approximately elevation +50 to +60 feet) are quite variable. In some areas, coarse gravel and cobbles are present, while in others silty sand, sandy silt, or silty clay exists. These materials are underlain by the San Mateo Formation, which extends to approximately elevation -850 feet. This formation consists of a dense to very dense, well graded sand with apparent cohesion due to efficient particle arrangement.

The soil profile shown in Figure 2.5-81 is an idealized representation of boring and other field identification data. Materials exposed in temporary construction slopes in the switchyard area were logged as a field check, and a simplified representation is given in Figure 2.5-82, providing a general confirmation of the idealized profile.

Stability analyses, as described in Paragraph 2.5.5.2, have been performed on not only the most likely stratification of terrace deposit soils (as evidenced by boring logs and slope-face logging during construction), but also on two additional terrace-deposit profiles (the first assuming the terrace deposit to consist of only clay materials, and the second of only sand).

2.5.5.1.2 Groundwater

The normal groundwater elevation at the site is approximately +5 feet, as measured during the period 1963 to 1975. No significant rise or drop in this level is anticipated, as discussed in Appendix 2.5E, and Subsection 2.4.13.

The base of switchyard slopes is at approximately elevation +30 feet, or about 25 feet above the maximum groundwater level as shown on Figure 2.5-81. Temporary dewatering for construction of facilities has lowered the groundwater surface to approximately elevation -36 feet at the lowest point (intake structure). The temporary groundwater surface beneath the switchyard slope area was probably at an elevation substantially higher than -36 feet as a result of this dewatering, although no measurements were made. However, stability analyses indicate that groundwater level reduction has no appreciable adverse effect on slope stability (Appendix 2.5E).

2.5.5.1.3 Field Investigation

Subsurface soil exploration consisted of making borings and obtaining tube and hand-carved block samples. The drilling and sampling were done in several phases. All boring locations in the plant and switchyard slope area are shown in Figure 2.5-80.

Two sets of borings (7 borings in 1972, and 13 borings in 1974) were made specifically for the slope stability studies. These borings are listed in Table 2.5-23. The seven borings in 1972 were all drilled by rotary wash methods with the use of drilling mud. All seven were 5-inch diameter, and ranged in depth from 43 feet to 301 feet below the ground surface. Sampling in these borings was done with a Pitcher Barrel Sampler and a Modified California Sampler. The Pitcher method yields high-quality tube samples needed for laboratory strength testing. The Modified California Sampler yields tube samples of somewhat lower quality, however this method provides blow-count data that is a measure of in-situ soil strength.

Of the 13 borings made in 1974, 4 were drilled by rotary-wash methods, and 9 by use of a hollow-stem truck-mounted flight auger. Sampling was done by Pitcher Sampler, Modified California Sampler and Shelby Tubes. The number and type of samples are listed in Table 2.5-23. Holes were backfilled with native material upon completion of the project.

Hand-carved samples were dug from the face of the switchyard slope during site excavation.

2.5.5.1.4 Soil Properties

The major soil types are of interest in these slope-stability studies: San Mateo Formation sand, and terrace deposit soils. The properties of San Mateo sand were studied in detail for the plant structures foundation design and are described in Paragraph 2.5.4.2. In addition to the laboratory tests on drive-tube, carved-block, and bulk soil samples, strength parameters of existing slopes were back-calculated from static finite-element analysis.

Table 2.5-23
SUMMARY OF BORING AND SAMPLING OPERATIONS FOR SLOPE STABILITY STUDIES
(Location of all borings shown on Figure 2.5-80) (Sheet 1 of 2)

Boring Designation	Boring Description						Sampling Description		
	Logged By[a]	Date	Diameter (in.)	Depth (ft)	Method[b]	Purpose[c]	Number	Type[d]	Purpose[e]
1	WMA	3/19/74	6	57-1/2	A	I	8	MC	LT
							2	ST	LT
							2	SK	VO
2	WMA	3/21/74	6	60-1/2	A	I	10	MC	LT
							2	ST	LT
							3	SK	VO
3	WMA	3/22/74	6	70	A	I	10	MC	LT
							1	ST	LT
							5	SK	VO
4	WMA	3/25/74	6	51-1/2	A	I	9	MC	LT
4A	WMA	3/27/74	6	80	A	I	5	MC	LT
							7	ST	LT
5	WMA	3/26/74	6	66-1/2	A	I	11	MC	LT
6	WMA	3/29/74	6	56	A	I	7	MC	LT
							4	ST	LT
7	WMA	3/29/74	6	66	A	I	7	MC	LT
							6	ST	LT

(a) WMA = Woodward-McNeill and Associates

(b) A = Continuous flight auger
R = Rotary
SK = Sack sample

(c) I = Investigative

(d) MC = Modified California
ST = Shelby Tube
PT = Pitcher Tube

(e) LT = Laboratory Testing
VO = Visual observation

Table 2.5-23
SUMMARY OF BORING AND SAMPLING OPERATIONS FOR SLOPE STABILITY STUDIES
(Location of all borings shown on Figure 2.5-80) (Sheet 2 of 2)

Boring Designation	Boring Description						Sampling Description		
	Logged[a] By	Date	Diameter (in.)	Depth (ft)	Method[b]	Purpose[c]	Number	Type[d]	Purpose[e]
8	WMA	3/25/74	6	56-1/2	A	I	9	MC	LT
9	WMA	3/29/74	6	59	R	I	11	PT	LT
							4	SK	VO
9A	WMA	3/29/74	6	51-1/2	R	I	12	PT	LT
							4	SK	VO
10	WMA	3/28/74	6	38	R	I	4	PT	LT
							1	SK	VO
10A	WMA	4/2/74	6	35	R	I	5	MC	LT
							2	ST	LT
WM B-1	WMA	8/23/74	5	109	R	I	5	MC	LT
WM B-2	WMA	8/23/74	5	301	R	I	7	PT	LT
WM B-3	WMA	8/23/74	5	57	R	I	3	PT	LT
WM B-4	WMA	8/23/74	5	302	R	I	3	PT	LT
WM B-5	WMA	8/23/74	5	43	R	I	5	PT	LT
							2	MC	LT
WM B-6	WMA	8/23/74	5	62	R	I	8 1	PT MC	LT LT
WM B-7	WMA	9/14/74	5	240	R	I	8	PT	LT

2.5.5.1.4.1 Static Soil Properties

The San Mateo sand is a homogeneous dense deposit of sand that derives its high strength and some apparent cohesion from an efficient grain-packing arrangement. The overlying terrace deposit is composed of a variable sandy portion overlain by a clayey portion.

Because of the variability of terrace deposit materials, their properties were somewhat difficult to characterize. For this reason, the 1972 drilling and sampling program was designed to yield indicator properties such as moisture and density, unconfined compressive strength, grain-size distribution, and triaxial strength of representative driven-tube samples of the terrace deposit soils.

These data, boring log data, and observation of existing slopes and bluffs on the site indicate the terrace deposits consist of interbedded dense to very dense sandy soils and stiff clays, with occasional lenses of gravel and silt in a clay matrix (conglomerate). A generalized profile of the existing soil profile is given on Figure 2.5-81. The clayey soils appear to predominate in the upper portions of the terrace deposit (elevation +80 to +120 feet), while the sandy soils generally constitute the material directly above the San Mateo Formation sand (elevation +45 to +80 feet).

Finite-element calculations were made to estimate the required strength of the soils, assuming that the existing 1/2 to 1 slopes at San Onofre Unit 1 are just at limit equilibrium (which is probably quite conservative). Those calculations yielded soil-strength values conservatively within the bounds of the laboratory data. More recent in-situ bearing-capacity tests, conducted in the San Mateo sands at the plant elevation and taken to complete failure, indicate that the laboratory and calculated strength values for San Mateo sand used for all analyses could be conservative with respect to cohesion by a factor of 2 to 2-1/2. Based on the finite-element analyses and laboratory tests the static strength properties of San Mateo sand and the sandy and clayey portions of the terrace deposit materials were conservatively estimated and are summarized in Table 2.5-24.

2.5.5.1.4.2 Dynamic Soil Strength

For slope stability analyses, dynamic testing of terrace deposits was performed on Pitcher, Shelby-tube, and carved-block samples by stress-controlled cyclic triaxial techniques. For conservatism, the strength values from the more disturbed drive-tube samples were used for analysis. A total of 28 specimens were tested.

Table 2.5-24
STATIC STRENGTH PARAMETERS

Material Property	Materials		
	Terrace Deposit Clays	Terrace Deposit Sands	San Mateo Formation Sand
Bulk unit wt, γ_t (lb/ft^3)	130	120	130
Angle of shearing resistance, ϕ (degrees)	17	38	41.5
Cohesion, c, lb/ft^2	2,600	200	750

In general, the results of the dynamic testing program indicate the terrace soils have strengths as high as, or higher than, the static strength used during initial stability studies. There do appear to be occasional thin lenses of weaker materials in the lower part of the terrace deposit which: (1) appear to be horizontally stratified; (2) are not continuous through the slopes; and (3) are generally less than 3 feet thick. Our analyses have considered the possibility that weak lenses exist throughout the sandy lower portion of the terrace deposit. A summary of the interpreted strengths for this material, as well as others presented in terrace deposits is presented in Figure 2.5-83 for ease of reference. These curves were drawn considering the lower bound of strength data to be defined at ±5% strain or 10% total strain, whichever occurred first.

2.5.5.2 Design Criteria and Analyses

The primary criterion for the switchyard slope design is that slopes be stable through the design basis earthquake.

The basis for selection of the methods of analysis was that they be the most reliable, up-to-date procedures available. Therefore, static and dynamic finite-element analyses were used to estimate in-situ and earthquake-induced stresses in the slope-foundation system. Details of the computer programs are given in Appendix 2.5A. The output stresses from the computer programs were compared with appropriate soil strengths in order to evaluate stability. The Bishop Modified Method of Slices was used for comparison of results. Analyses were made assuming: (1) the most likely soil conditions which exist (based on boring log data, examination of graded slopes, etc.); and (2) weak lenses are present throughout the lower portion of the terrace deposit.

Based on the results of these analyses it is concluded that, during DBE loading: (1) the overall factor-of-safety of the switchyard slopes is in excess of unity; (2) surficial sloughing to a maximum depth of 5 feet may occur on the uppermost switchyard slope; and (3) overstressed zones may develop in localized portions of the terrace deposit. These zones are shown schematically on Figure 2.5-84. Interpreted factors of safety of each finite element in the slope are presented on Figure 2.5-84. It is expected that the overstressed zones will not cause instability because they are localized between understressed stable zones (Appendix 2.5F).

Further dynamic analyses were done recently to incorporate changes in the state-of-the-art of the evaluation of dynamic strength tests.[103][104][105][106][107] The factor of safety results of the previous evaluations were modified by a correction factor C_r (stress-correction factor for cyclic triaxial tests). A composite cross-section of the site showing factor-of--safety contours for the switchyard slope and other areas is presented on Figure 2.5-73. Only one small area near the surface of the upper slope shows a factor of safety of unity or less. This would likely manifest itself as minor surface sloughing which would be accommodated by the upper bench just below this area. No safety-related structures or equipment are located on this area. Furthermore, it is likely that the zone of surficial sloughing would not be continuous along the length of the slope because only the worst soil conditions found were used in the analysis. All other areas show a factor of safety of 1.1 or substantially higher.

Based on the above considerations, it is concluded that the factors of safety against slope and liquefaction instability (see Paragraph 2.5.4.8) presented on Figure 2.5-85 for the DBE condition are ample and that the response of the site to DBE excitation in terms of stability would not lead to any adverse consequences to structures or equipment.

2.5.5.3 Logs of Borings

The location of borings made at the plant site are shown in Figure 2.5-80. The 20 borings that were done specifically for slope stability studies are listed in Table 2.5-23. The logs of seven borings made in 1972 are summarized in Figure 2.5-86. The 13 borings made in 1974 are presented in separate logs on Figures 2.5-87 through 2.5-99.

2.5.5.4 Compacted Fill

Virtually all of the switchyard slopes are of excavated material. The only compacted fill materials present will be the trench and structure backfill, and backfill along the base of the slope. All backfill below elevation +45 feet will consist of San Mateo sand (excavated from the site) compacted to at least 95% of its maximum density determined in accordance with ASTM Test No. D1557-70. All backfill above elevation +45 feet will consist of either (1) San Mateo sand, (2) select terrace deposit soil, or (3) imported granular soil; compacted to at least 95% of its maximum density in accordance with ASTM Test No. D1557-70. Details of construction procedures are discussed in Paragraph 2.5.4.14.

2.5.6 EMBANKMENTS AND DAMS

There are no earth fill embankments or dams located in the general vicinity of the San Onofre site. A flood protection structure is located as shown in Figure 2.4-4.

Following the decision to permanently cease power operations, an additional hydrologic analysis was performed that determined that the diversion structure was not required for site flood protection as discussed in Section 2.4.3.5.

2.5.7 REFERENCES

1. Jahns, R. H., "Investigations and problems of Southern California," California Division of Mines, Bulletin 170, Ch. I, pp 5-29, 1954.

2. Ehlig, P. L., "Geotechnical Studies Northern San Diego County, October 1977," Consultants Report to Southern California Edison Company and San Diego Gas and Electric Company, 1977.

3. Shepard, F. P., and Emery, K.O., "Submarine Topography of the California Coast," Geological Society of America, Special Paper 31, 1941.

4. Moore, D. G., "Reflection Profiling Studies of the California Continental Borderland: Structure and Quaternary Turbidite Basins," Geological Society of America, Special Paper 107, 111 pp, 1972.

5. Larsen, E. S., Jr., "Batholith and Associated Rocks of the Corona, Elsinore and San Luis Rey Quadrangles, Southern California," Geological Society of America, Memoir 29, 182 pp, 1948.

6. Imlay, R. W., "Middle and Upper Jurassic Fossils from Southern California," Journal Paleontology, Vol 38, pp 505-509, 1964.

7. Criscione, J. J., Davis, T. E. and Ehlig, P. L., "The Age of Sedimentation/Diagenesis for the Bedford Canyon Formation and the Santa Monica Formation, in Southern California". A Rb/Sr evaluation, Howell, D. G. and McDougall, K. A., eds., Mesozoic Paleogeography of the Western United States: Pacific Section, Soc. Economic Paleontologists and Mineralogists, Pacific Coast Paleogeography Symposium 2, pp 385-396, 1978.

8. Fife, D. L., Minch, J. A. and Crampton, P. J., "Late Jurassic Age of the Santiago Peak Volcanics, "Geological Society of America Bulletin, Vol 78, pp 299-304, 1967.

9. Schwarcz, H. P., "Pre-Cretaceous Sedimentation and Metamorphism in the Winchester Area, Northern Peninsular Ranges, California," Geological Society of America, Special Paper 100, 63 pp, 1969.

10. Gastil, R. G., Phillips, R. P. and Allison, E. C., "Reconnaissance Geology of the State of Baja California," Geological Society of America, Memoir 140, 170 pp, 1975.

11. Gastil, R. G., Morgan, G. J. and Krummenacher, D., "Mesozoic History of Peninsular California and Related Areas East of the Gulf of California," in Howell, D. G., and McDougall, K. A., eds., Mesozoic Paleogeography of the Western United States: Pacific Section, Soc. Economic Paleontologists and Mineralogists, Pacific Coast Paleogeography Symposium 2, pp 107-115, 1978.

12. Silver, L. T., Taylor, H. P. and Chappell, B., "Some Petrological and Geochronological Observations of the Peninsular Ranges Batholith Near the International Border of the U.S.A. and Mexico," in Abbott, P. L. and Todd, V. R., eds., Mesozoic Crystalline Rocks Peninsular Ranges Batholith and Pegmatities Point Sal Ophiolite: Department of Geological Sciences San Diego State University, pp 83-110, 1979.

13. Hamilton, W., "Mesozoic California and the Underflow of the Pacific Mantle," Geological Society of America Bulletin, Vol 80, pp 2409-2430, 1969.

14. Blake, M. C., Campbell, R. H., Dibblee, T. W., Howell, D. G., Nilsen, T. H., Normark, W. R., Vedder, J. C. and Silver, E. A., "Neogene Basin Formation in Relation to Plate-Tectonic Evolution of San Andreas Fault System, California," American Association Petroleum Geologists Bulletin, Vol 62, pp 344-372, 1978.

15. Emery, K. O., The Sea off Southern California, John Wiley and Sons, New York, 366 pp, 1960.

16. Atwater, T., "Implications of Plate Tectonics for the Cenozoic Tectonic Evolution of Western North America," Geological Society of America Bulletin, Vol 81, pp 3513-3536, 1970.

17. Crowell, J. C., "The San Andreas Fault in Southern California," California Division of Mines, Special Report 118, pp 7-27, 1975.

18. Elders, W. A., Rex, R. W., Meidav, T., Robinson, P. T. and Biehler, S., 1972, "Crustal Spreading in Southern California," Science, Vol 178, pp 15-24, 1972.

19. Ehlig, P. L., Ehlert, K. W. and Crowe, B. M., "Offset of the Upper Miocene Caliente and Mint Canyon Formations along the San Gabriel and San Andreas Faults," in Crowell, J. C., ed., "San Andreas Fault in Southern California," California Division Mines and Geology Special Report 118, pp 83-92, 1975.

20. Sieh, K. E., "Prehistoric Large Earthquakes Produced by Slip on the San Andreas Fault at Pallett Creek, California," Journal Geophysical Research, Vol 83, pp 3907-3939.

21. Sharp, R. V., "San Jacinto Fault Zone in the Peninsular Ranges of Southern California," Geological Society of America Bulletin, Vol 78, pp 706-730, 1967.

22. Engle, R., "Geology of the Lake Elsinore Quadrangle California," California Division of Mines, Bulletin 146, 154 pp, 1959.

23. Fugro, Inc., "Recurrence Interval of the 0.22g Operating Basis Earthquake at San Onofre Nuclear Generating Station Unit 1," Unpublished Consultants Report to Southern California Edison Company, 1975.

24. "Safety Evaluation of the SONGS Units No. 2 & 3," U.S. Atomic Energy Commission, 1972.

25. "San Onofre Nuclear Generating Station, Units 2 & 3, Preliminary Safety Analysis Report," Southern California Edison Company, 1970.

26. Western Geophysical Company, "Final Report: San Onofre Offshore Investigations," for Southern California Edison Company and San Diego Gas and Electric Company, March 1, 1972.

27. Woodward-Clyde Consultants, Unpublished Seismic Reflection Profiles, developed for the California Coastal Commission, LNG Terminal Sites, 1978.

28. Fugro, Inc., Unpublished Seismic Reflection Profiles, 1977.

29. Nekton Inc., "Interpretive Results High Resolution Geophysical Survey In Selected Areas Between Dana Point and Oceanside, Offshore California," for Southern California Edison Company, 1980.

30. Fugro, Inc., "Report of Geologic and Fault Reconnaissance, Vicinity of Oceanside, California," for Southern California Edison Company, 1972.

31. Hill, M. L., "Newport Inglewood Zone and Mesozoic Subduction, California," Geological Society of America Bulletin, Vol 82, pp 2957-2962, 1971.

32. Vedder, J. G., et al, "Preliminary Report on the Geology of the Continental Borderland of Southern California," United States Geological Survey, Miscellaneous Field Studies. Map MF 624, 1974.

33. Woodward-Clyde Consultants, "Report of the Evaluation of Maximum Earthquake and Site Ground Motion Parameters Associated with the Offshore Zone of Deformation San Onofre Nuclear Generating Station," Consultants Report to Southern California Edison Company, June 1979.

34. Idriss, I. M. and Seed, H. B., "Response of Horizontal Soil Layers During Earthquakes," Research Report, Soil Mechanics and Bituminous Materials Laboratory, University of California, Berkeley, August 1967.

35. Moore, G. W. and Kennedy, M. P., "Quaternary Faults at San Diego Bay, California," Journal of Research of the U.S. Geological Survey, Vol 3, No. 5, pp 589-595, 1975.

36. Kennedy, M. P., et al., "Studies of Surface Faulting and Liquefaction as Potential Earthquake Hazards in Urban San Diego, California," California Division of Mines and Geology Final Technical Report, 1977.

37. Kern, J. P., "Origin and History of Two Upper Pleistocene Marine Terraces at San Diego, California," Geological Society of America, Cordilleran Section, 69th Annual Meeting, Abstract No. 1, pp 66, 1973.

38. Wagner, H. C. and Junger, A., "Geology of the San Pedro Basin and Shelf, Offshore Southern California," Geological Society of America Abstracts, Vol 7, No. 3, pp 383-4, 1975.

39. Greene, H. G., "Quaternary Tectonics, Offshore Los Angeles-San Diego Area," U.S. Geological Survey, National Earthquake Hazards Reduction Program, Summaries of Technical Reports, Vol 9 pp 11-12, 1980.

40. Marine Advisers, Inc., "Continuous Seismic Profiling Investigation of the Continental Shelf off San Onofre, California," Consultants Report for Southern California Edison Company and San Diego Gas and Electric Company, April 24, 1970.

41. Allen, C. R., Silver, L. T. and Stehli, F. G., "Agua Blanca Fault--a Major Transverse Structure of Northern Baja California, Mexico," Geological Society of America Bulletin, Vol 71, pp 457-482, 1960.

42. Hamilton, Warren, "Recognition of Space Photographs of Structural Elements of Baja California," U.S. Geological Survey Professional Paper 718, 26 pp, 1971.

43. Krause, D. C., "Tectonics, Bathymetry, and Geomagnetism of the Southern Continental Borderland West of Baja California, Mexico," Geological Society of America Bulletin, Vol 76, pp 617-650, 1965.

44. Shor, G. and Roberts, E. E., "San Miguel, Baja California Norte, Earthquakes of February, 1956--A Field Report," Seismological Society of America Bulletin, Vol 48, pp 101-116, 1958.

45. Gastil, R. G., Kies, R. and Melius, D. J., "Active and Potentially Active Faults: San Diego County and Northernmost Baja California," Abbott, P. L., and Elliott, W. J., eds., Earthquakes and Other Perils, San Diego Region: San Diego Association of Geologists, for Geological Society of America, Field Trip Guidebook, pp 47-60, 1979.

46. Kennedy, M. P., "Geology of the Western San Diego Metropolitan Area, California, Del Mar, La Jolla, and Point Loma Quadrangles," California Division of Mines and Geology, Geology of the San Diego Metropolitan Area, California, Section A, pp 9-39, 1975.

47. West, Jack C., "Generalized Sub-surface and Geophysical Study, Capistrano Area, Orange County, California," Consultant's Report for Southern California Edison Company, 1975.

48. Ehlig, P. L., "Miocene Stratigraphy and Depositional Environments of the San Onofre Area and Their Tectonic Significance," in Miocene Lithofacies and Depositional Environments, Coastal California and Northwestern Baja California, SEPM Guidebook, pp 43-51, 1979.

49. Shlemon, R. J., "Late Quaternary Evolution of the Camp Pendleton San Onofre State Beach Coastal Area Northwestern San Diego County, California," Consultants Report to Southern California Edison, 1978.

50. Fugro, Inc., "Summary of Geomorphic and Age Data for the First Emergent Terrace (Qt1) at the San Onofre Nuclear Generating Station," Unpublished Consultant's Report to Southern California Edison Company, 1975.

51. "Land Subsidence in California," California Division of Mines, Mineral Information Service, Vol 8, No. 7, 1955.

52. Shlemon, R. J., "Late Quaternary Rates of Deformation, Laguna Beach San Onofre State Beach, Orange and San Diego Counties, California," Consultants Report to Southern California Edison Company and San Diego Gas and Electric Company, 1978.

53. Shlemon, R. J., "Late Cenozoic Stratigraphy, Capistrano Embayment Coastal Area, Orange County, California," a Consultant's Report for Southern California Edison Company and San Diego Gas and Electric Company, 17 pp, 1979.

54. Blanc, R. P. and Cleveland, G. B., "Natural Slope Stability as Related to Geology, San Clemente Area, Orange and San Diego Counties," California Division of Mines and Geology, Special Report 98, 1968.

55. Cleveland, G. B., "Landsliding in Marine Terrace Terrain, California," California Division of Mines and Geology, Special Report 119, 1975.

56. White, W. R., "Pliocene and Miocene Foraminifera from the Capistrano Formation, Orange County, California," Journal of Paleontology, Vol 30, pp 237-260, 1956.

57. Converse, Davis and Associates, "Geologic Report on the Probability of Ground Displacement of Faults in the Vicinity of the San Onofre Nuclear Power Plant Site, Units 2 & 3, San Diego County, California," Consultant's Report for Southern California Edison Company and San Diego Gas and Electric Company, April 30, 1970.

58. Fugro, Inc., "Analysis of Geologic Features at the San Onofre Nuclear Generating Station," Consultant's Report for Southern California Edison Company, 1974.

59. "Recent Geotechnical Studies, Southern Orange County, California, San Onofre," Southern California Edison Company, 1976.

60. Fugro, Inc., "Geologic Investigation of the Mission Viejo (F. Beach Leighton) Bulldozer Excavation," Unpublished Consultant's Report to Southern California Edison Company, 1974.

61. Fugro, Inc., "Geologic Investigation of the Bulldozer Excavation at the Proposed Viejo Substation Site," Unpublished Consultant's Report to Southern California Edison Company, 1975.

62. Fugro, Inc., "Geologic Investigation of Fault 'E', Southeast of The San Onofre Nuclear Generating Station, San Onofre, California," 1978.

63. Ku, T. L., Kimmel, M. A., Easton, W. H. and O'Neill, T. J., "Eustatic Sea Level 120,000 Years Ago on Oahu, Hawaii," Science, Vol 183, No. 4128, pp 959-962, 1974.

64. Steinen, R. P., Harrison, E. S. and Matthews, R. K., "Eustatic Low Stand of Sea Level Between 125,000 and 105,000 b.p.: Evidence from the Sub-Surface of Barbados, West Indies," Geological Society of America Bulletin, Vol 84, pp 63-70, 1973.

65. Fugro, Inc., "Geomorphic Analysis of Terraces in San Juan and Bell Canyons, Orange County, California," Unpublished Consultant's Report to Southern California Edison Company, 1975b.

66. Fugro, Inc., "Analysis of C and D Type Features at SONGS," Unpublished Consultant's Report to Southern California Edison Company, 1974.

67. Fugro, Inc., "Final Report on Grading (Analysis of Geologic Features) at the San Onofre Nuclear Generating Station," Consultant's Report to Southern California Edison Company, 1976.

68. Woodward-Clyde & Associates, "Erosion Study for the Proposed Units 2 & 3, San Onofre Nuclear Generating Station, San Onofre, California," Unpublished Consultant's Report to Southern California Edison Company, 1975.

69. Ingle, J. C., "Paleobathymetric History of Neogene Marine Sediments, Northern Gulf of California," in Gastil, G. and Lillegraven, J., The Geology of Peninsular California: Pacific Sections AAPG, SEPM and SEG, pp 121-138, 1974.

70. Richter, C. F., Elementary Seismology, W. H. Freeman and Company, San Francisco, California, 768 pp, 1958.

71. Hill, M. L., "A Test of New Global Tectonics: Comparisons of Northeast Pacific and California Structures, American Association of Petroleum Geologists Bulletin, Vol 55, pp 3-9, 1971.

72. Sharp, R. P., Geology Field Guide to Southern California, Wm. C. Brown Publishers, Dubuque, Iowa, 181 pp, 1972.

73. Jenkins, 0. P., "Geomorphic Provinces of California," California Division of Mines and Geology, Bulletin 118, pp 83-88, 1943.

74. Allen, C. R., et al, "Relationship Between, Seismicity and Geologic Structure in the Southern California Region," Bulletin of the Seismological Society of America, Vol 55, No. 4, pp 753-797, 1965.

75. Ehlig, P. L., "Basement Rocks of the San Gabriel Mountains, South of the San Andreas Fault, Southern California," in Crowell, J. C., ed., San Andreas Fault in Southern California, California Division Mines and Geology Special Report 118, pp 177-186, 1975.

76. Garfunkel, Z., "Model for the Late Cenozoic Tectonic History of the Mojave Desert, California and for Its Relation to Adjacent Regions," Geological Society of America Bulletin, Vol 85, pp 1931-1944, 1974.

77. Albee, A. L. and Smith, J. L., "Earthquake Characteristics and Fault Activity in Southern California," in Engineering Geology in Southern California, R. Lung, and R. Proctor, eds., Association of Engineering Geologists, Los Angeles Section, Special Publication, 1966.

78. Stewart, J. H., "Basin and Range Structure - A System of Horsts and Grabens Produced by Deep Seated Extension," Geological Society of America Bulletin, Vol 82, pp 1019-1044, 1971.

79. Jennings, C. W., "State of California Preliminary Fault and Geologic Map, Scale 1:750,000," California Division of Mines and Geology, Preliminary Report 13, 1974.

80. Gastil, R. G., Phillips, R. P. and Edwin, C. A., "Reconnaissance Geologic Map of the State of Baja California, Plate 1A, Scale 1:250,000," Geological Society of America, Memoir 140, 1971.

81. Hileman, J. A., Allen, C. R. and Nordquist, J. M., "Seismicity of the Southern California Region: January 1, 1932 to December 31, 1972," Division of Geological and Planetary Sciences, Contribution No. 2385, California Institute of Technology, 1973.

82. Allen, C. R., "The Southern California Seismographic Network," Engineering and Science, Vol. XXXVIII, No. 1, California Institute of Technology, 1974.

83. Townley, S. D. and Allen, M. W., "Descriptive Catalog of Earthquakes of the Pacific Coast of the United States, 1769 to 1928," Geological Society of America, Bulletin 29, No. 1, 1939.

84. Morton, P. K., Edgington, W. J., and Fife, D. L., "Geology and Engineering Geologic Aspects of the San Juan Capistrano Quadrangle, Orange County, California," California Division of Mines and Geology, Special Report 112, 66 pp, 1974.

85. Biehler, S., "Seismological Investigation of the San Juan Capistrano Area, Orange County, California," Consultant's Report for Southern California Edison Company, 1975.

86. Dibaz, M. and Penzien, J., "Dynamic Response of Earth Dams to Traveling Seismic Waves," Soil Mechanics and Bituminous Laboratory, Research Report No, TE-67-8, University of California, Berkeley, 1967.

87. Greensfelder, R. W., "Maximum Credible Rock Acceleration from Earthquakes in California," California Division of Mines and Geology, Map Sheet 23, 1974.

88. Coffman, J. L. and von Hake, C. A., "Earthquake History of the United States,"U.S. Department of Commerce, Publication 41-1, 1973.

89. Kennedy, M. P., Stratigraphy of the San Diego Embayment, California, Unpublished PhD Dissertation, University of California, Riverside, 1973.

90. Haley, S. C. and Hunt, G. S., Determination of Design Earthquake Characteristics, American Society of Civil Engineers, National Meeting, January 21-25, Los Angeles, 21 pp, 1974.

91. Housner, G. W., "Strong Ground Motion," in Earthquake Engineering, R. L. Wiegel, ed., Prentice-Hall, New Jersey, 517 pp, 1970.

92. Lee, K. L. and Chan, K, "Number of Equivalent Significant Cycles in Strong Motion Earthquakes," Microzonation Conference Proceedings, October 30-November 3, 1972, Seattle, Washington, pp 609-627, 1972.

93. Yerkes, R. F., et al, "Geology of the Los Angeles Basin, California; An Introduction," U.S. Geological Survey, Professional Paper 420A, 1965.

94. Moore, G. W., "Offshore Extension of the Rose Canyon Fault, San Diego, California," U.S. Geological Survey Professional Paper 800-C, pp 113-116, 1972.

95. Kennedy, M. P., "Recency and Character of Faulting Offshore From Metropolitan San Diego, California--U.S. Geological Survey Contract No. 14-08-001-17699," U.S. Geological Survey, National Earthquake Hazard Reduction Program, Summaries of Technical Reports, Vol 8, pp 27-28, December 1979.

96. Woodward-McNeill and Associates, "Analyses of Properties of Finer-Grained San Mateo Sand, SONGS Units 2 and 3, San Onofre, California," Consultant's Report to Southern

California Edison Company and San Diego Gas and Electric Company, December 31, 1974.

97. Woodward-McNeill and Associates, "Material Property Studies, San Onofre Nuclear Generating Station," Consultant's Report to Southern California Edison Company.

98. Idriss, I. M. and Seed, H. B., "Seismic Response of Horizontal Soil Layers," Journal of the Soil Mechanics and Foundations Division, ASCE, Vol 94, No. SM4, pp 1003-1031, July 1968.

99. Idriss, I. M. and Seed, H. B., "Seismic Response of Soil Deposits," Journal of the Soil Mechanics and Foundations Division, ASCE, Vol 96, No. SM2, pp 2, pp 631-638, March 1970.

100. Idriss, I. M., Lysmer, J., Hwang, R., and Seed, H. B., "QUAD4, A Computer Program for Evaluating the Seismic Response of Soil Structures by Variable Damping Finite-Element Procedures," Earthquake Engineering Research Center, Report No. EERC 73-16, University of California, Berkeley, 1973.

101. Vesic, A. S., "Bearing Capacity of Shallow Foundations," Foundation Engineering Handbook, Hans, F. Winterkorn and Hsai-Yang Fany, eds., Van Nostrand Reinhold Co., New York, pp 121-147, 1975.

102. Duncan, J. M. and Cheng, C. Y., "Nonlinear Analysis of Stress and Strain in Soils," Journal of the Soil Mechanics and Foundations Division, ASCE, Vol 96, No. SM5, pp 1629-1654, September 1970.

103. De Alba, P., Chan, C. K., and Seed, H. B., "Determination of Soil Liquefaction Characteristics by Large-Scale Laboratory Tests," Earthquake Engineering Research Center, Report No. EERC 75-14, University of California, Berkeley, May 1975.

104. Mulilis, J. P., Chan, C. K., and Seed, H. B., "The Effects of Method of Sample Preparation on the Cyclic Stress-Strain Behavior of Sands," Earthquake Engineering Research Center, Report No. EERC 75-18, University of California, Berkeley, July 1975.

105. Seed, H. B., Mori, K., and Chan, C. K., "Influence of Seismic History on the Liquefaction Characteristics of Sands," Earthquake Engineering Research Center, Report No. EERC 75-25, University of California, Berkeley, August 1975.

106. Seed, H. B., Martin, P. P., and Lysmer, J., "The Generation and Dissipation of Pore Water Pressure During Liquefaction," Earthquake Engineering Research Center, Report No. EERC 76-26, University of California, Berkeley, August 1975.

107. Seed, H. B., Arrango, I., and Chan, C. K., "Evaluation of Soil Liquefaction Potential During Earthquakes," Earthquake Engineering Research Center, Report No. EERC 75-28, University of California, Berkeley, October 1975.

108. Seed, H. B., Idriss, I. M., Makdisi, F., and Banerjee, M., "Representation of Irregular Stress Time Histories by Equivalent Uniform Stress Series in Liquefaction Analyses," Earthquake Engineering Research Center, Report No. EERC 75-29, University of California, Berkeley, October 1975.

109. Swiger, W. G., "Evaluation of Soil Moduli," in Proceedings of the Conference on Analysis and Design in Geotechnical Engineering, University of Texas, Austin, Texas, pp 74-92, June 9-12, 1974.

110. Mayerhoff, G. G., "Bearing Capacity and Settlement of Pile Foundations," Journal of the Geotechnical Engineering Division, ASCE, Vol 102, No. GT3, Proc. Paper 11962, 219 pp, March 1976.

111. "Summary Report of the Investigation/Demobilization of Construction Dewatering Wells, San Onofre Nuclear Generating Station, Units 2 & 3," Woodward-Clyde Consultants, Consultant's Report, prepared for Southern California Edison Company, July 1979.

112. Deleted

113. Deleted

114. Barrows, A. G., "A Review of the Geology and Earthquake History of the Newport-Inglewood Structural Zone, Southern California," California Division of Mines and Geology, Special Report 114, 1974.

115. Legg, M. R., and M. P. Kennedy, 1979, Faulting Offshore San Diego and Northern Baja California, in Abbott, P. L., and W. J. Elliott, editors, Earthquakes and Other Perils, San Diego Region: San Diego Association of Geologists Special Publication for 1979 National Geographical Society of America Meeting Field Trip, p. 29-46.

2.5.8 BIBLIOGRAPHY

1. Eardley, A. J., "Tectonic Divisions of North America, American Association of Petroleum Geologists, Bulletin, Vol 35, 1951.

2. Fife, D. L., "Geology of the South Half of the El Toro Quadrangle, Orange County, California," California Division of Mines and Geology Special Report 110, 1974.

3. "Geotechnical Studies, Northern San Diego County," Southern California Edison Company, October 1977.

4. Hill, M. L. and Troxel, B. W., "Tectonics of Death Valley Region, California," Geological Society of America Bulletin, Vol 77, pp 435-438, 1966.

5. "Information Concerning Site Characteristics: Vidal Nuclear Generating Station, Units 1 and 2," Southern California Edison Company, 1974.

6. Isacks, B., Oliver, J., and Sykes, L. R., "Seismology and the New Global Tectonics," Journal of Geophysics Research, Vol 73, pp 585-5899, 1968.

7. Jumikis, A. R., "Soil Mechanics", Fourth Edition, D. Van Nostrand Company, Inc., Princeton, New Jersey, 791 pp, 1968.

8. Kanamori, H. and Anderson, D. L., "Theoretical Basis of Some Empirical Relations in Seismology," Bulletin of the Seismological Society of America, Vol 65, pp 1073-1095, 1975.

9. King, P. B., "The Tectonics of North America - A Discussion to Accompany the Tectonic Map of North America, Scale 1:5,000,000," U.S. Geological Survey, Professional Paper 628, 1969.

10. McCulloh, T. H., "Gravity Variations and the Geology of the Los Angeles Basin of California," U.S. Geological Survey Research, Professional Paper 400-B, 150 pp, B-325, 1960.

11. Morton, P. K., editor, "Geologic Guidebook to the Northern Peninsular Ranges, Orange and Riverside Counties, California," National Association Geology Teachers, 1972.

12. Murphy, L. M., "Report on the Site Seismicity for the SONGS Units 2 and 3," Seismological Investigations Group of the Earth Sciences Laboratories, NOAA, U.S. Atomic Energy Commission, Safety Evaluation of the SONGS Units No. 2 and 3, 1972.

13. "Report of Geologic and Fault Reconnaissance, Vicinity of Oceanside, California," Fugro, Inc., for Southern California Edison Company and San Diego Gas and Electric Company, April 6, 1972.

14. Schnabel, P. B., Lysmer, J., and Seed, H. B., "SHAKE, A Computer Program for Earthquake Response Analysis of Horizontally Layered Sites," Research Report, EERC 72-12, Earthquake Engineering Research Center, University of California, Berkeley, 1972.

15. Schoelhammer, J. E., et al, "Geologic map of the Northern part of the Santa Ana Mountains, Orange and Riverside Counties, California," U.S. Geological Survey Oil and Gas Inventory, map 154, 1953.

16. Seed, H. B. and Idriss, I. M., "Soil Moduli and Damping Factors for Dynamic Response Analysis," Earthquake Engineering Research Center Report No. EERC 70-10, University of California, Berkeley, 1970.

17. "Seismic and Foundation Studies for Proposed Units 2 & 3, San Onofre Nuclear Generating Station," Dames and Moore, Inc., for Southern California Edison Company and San Diego Gas and Electric Company, April 15, 1970.

18. Slemmons, D. B., "State-of-the-Art for Assessing Earthquake Hazards in the United States, Report 6: Faults and Earthquake Magnitude," U.S. Army Corps of Engineers, Miscellaneous Paper S-73-l, 129 pp, 1977.

19. Smith, R. B. and Sbar, M. L., "Contemporary Tectonics and Seismicity of the Western United States with Emphasis on the Intermountain Seismic Belt," Geological Society of America, Bulletin 85, pp 1205-1218.

20. Stuart, C. J., "The San Onofre Breccia in the Camp Pendleton Area, California: in, Studies on Geology of Camp Pendleton, and Western San Diego County, California," San Diego Association of Geologists, pp 15-32, 1976.

21. U.S. Army Corps of Engineers, "Hydraulic Design of Flood Control Channels," EM 1110-2-1601, 1970.

22. U.S. Department of the Interior, Bureau of Reclamation, "Design of Small Dams," 1974.

23. Vedder, J. G. and Brown, R. D., Jr., "Structural and Stratigraphic Relations Along the Nacimiento Fault in the Southern Santa Lucia Range and San Rafael Mountains, California," Proceedings, Conference on Geologic Problems of San Andreas Fault System, Stanford University Publication, Geologic Sciences II, 1968.

24. Vedder, J. G., et al., "Geology of the Los Angeles Basin, California; An Introduction," U.S. Geological Survey, Professional Paper 420A, 1965.

25. Wagner, H. C. and Junger, A., "Geology of the San Pedro Basin and Shell Offshore, Southern California," Geological Society of America Abstracts, Vol 7, No. 3, pp 383-384, 1975.

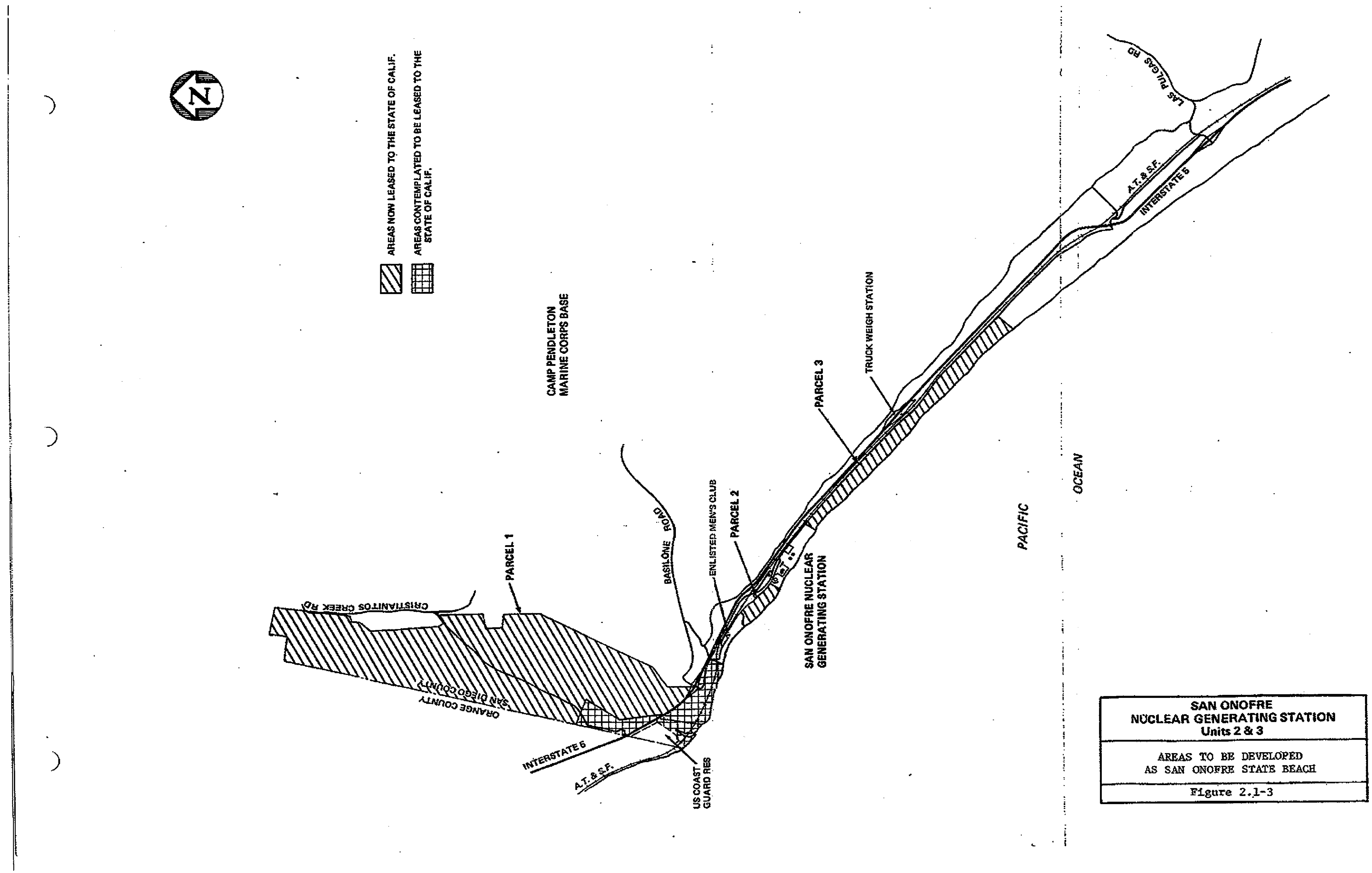

SAN ONOFRE NUCLEAR GENERATING STATION Units 2 & 3

AREAS TO BE DEVELOPED AS SAN ONOFRE STATE BEACH

Figure 2.1-3

Site File Copy

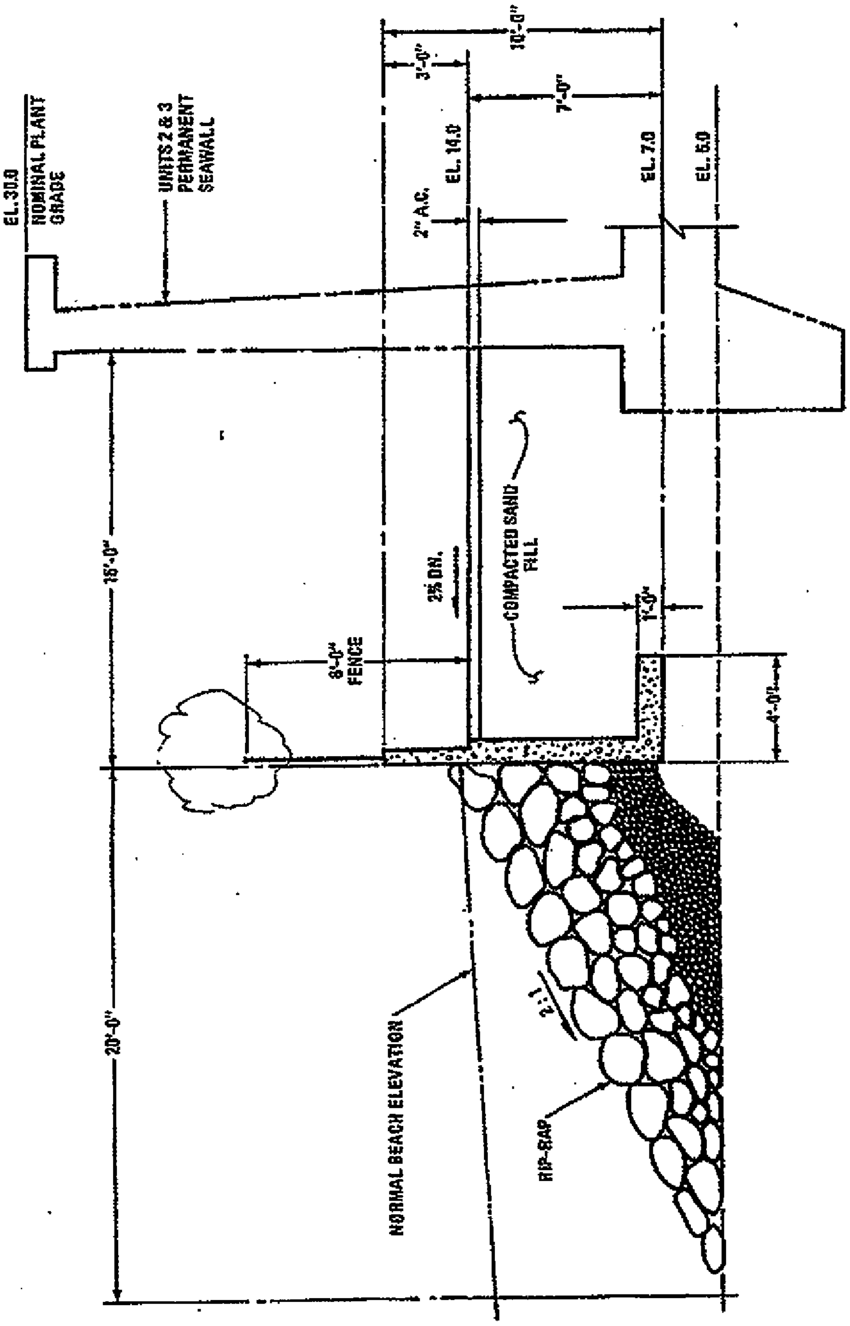

SAN ONOFRE NUCLEAR GENERATING STATION
Units 2 & 3
Updated Final Safety Analysis Report

BEACH PASSAGEWAY

Figure 2.1-4

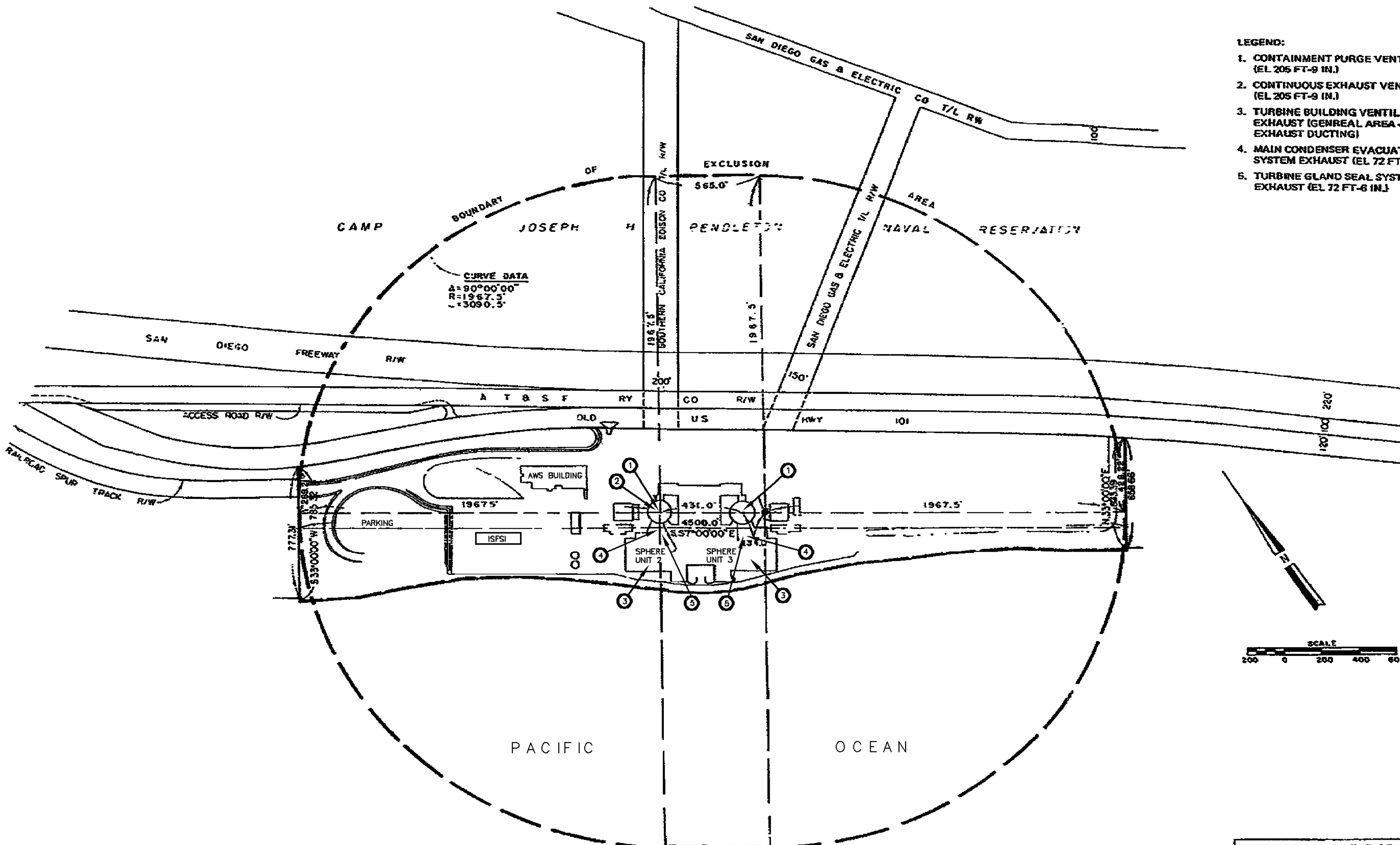

LEGEND:

1. CONTAINMENT PURGE VENT STACK (EL 205 FT-9 IN.)
2. CONTINUOUS EXHAUST VENT STACK (EL 205 FT-9 IN.)
3. TURBINE BUILDING VENTILATION EXHAUST (GENREAL AREA – NO EXHAUST DUCTING)
4. MAIN CONDENSER EVACUATION SYSTEM EXHAUST (EL 72 FT-6 IN.)
5. TURBINE GLAND SEAL SYSTEM EXHAUST (EL 72 FT-6 IN.)

SAN ONOFRE NUCLEAR GENERATING STATION, UNITS 2 & 3
Updated Final Safety Analysis Report

Effluent Release Points

Figure: 2.1-5

REV. 5

ACAD2009

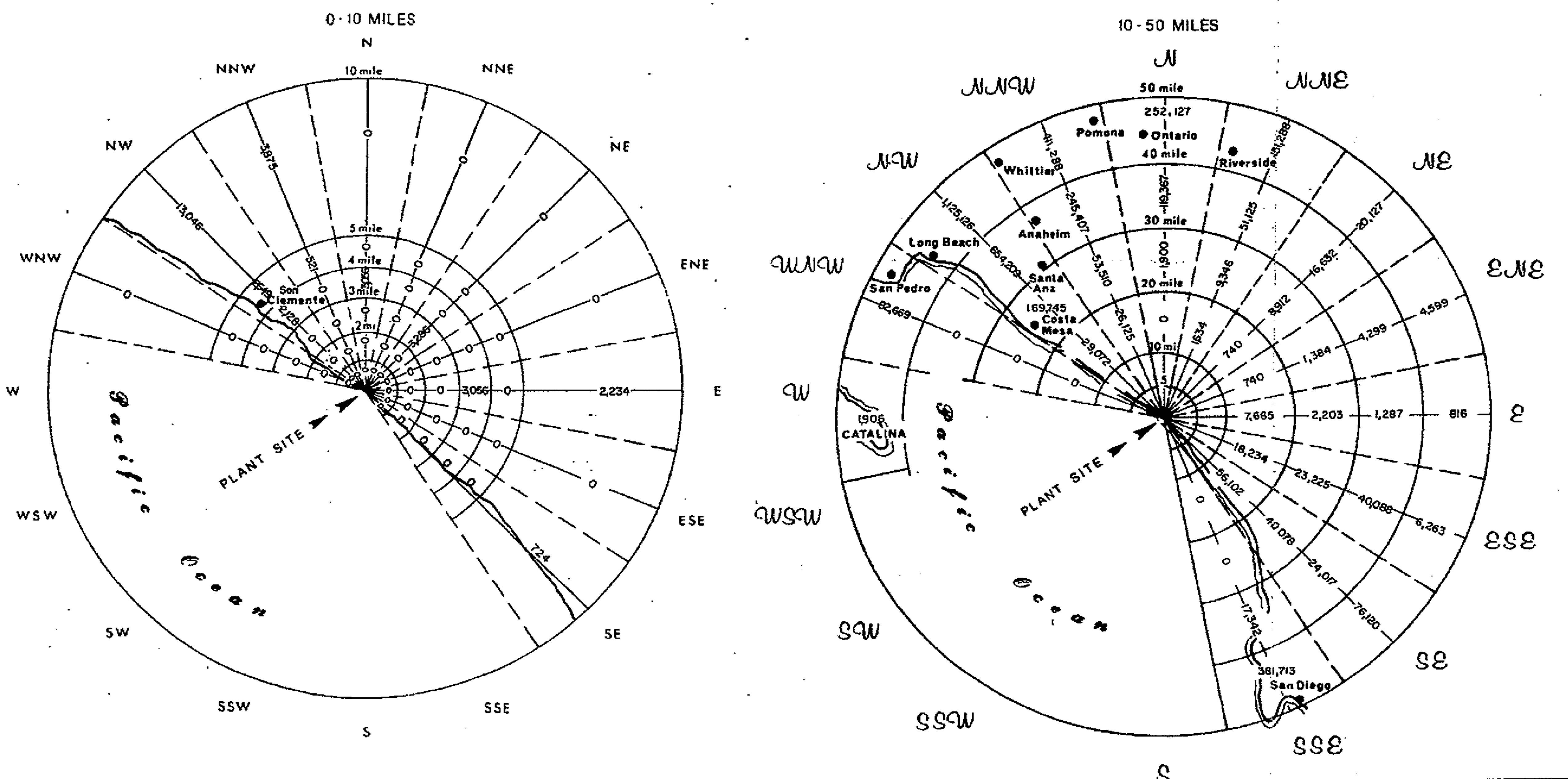

Radius in Miles	1	2	3	4	5	10	20	30	40	50
Accumulative Total	0	0	3,286	11,526	14,696	34,575	174,887	485,190	1,658,963	4,173,005

SAN ONOFRE
NUCLEAR GENERATING STATION
Units 2 & 3

1970 CENSUS POPULATION
DISTRIBUTION SECTOR MAP

Figure 2.1-6

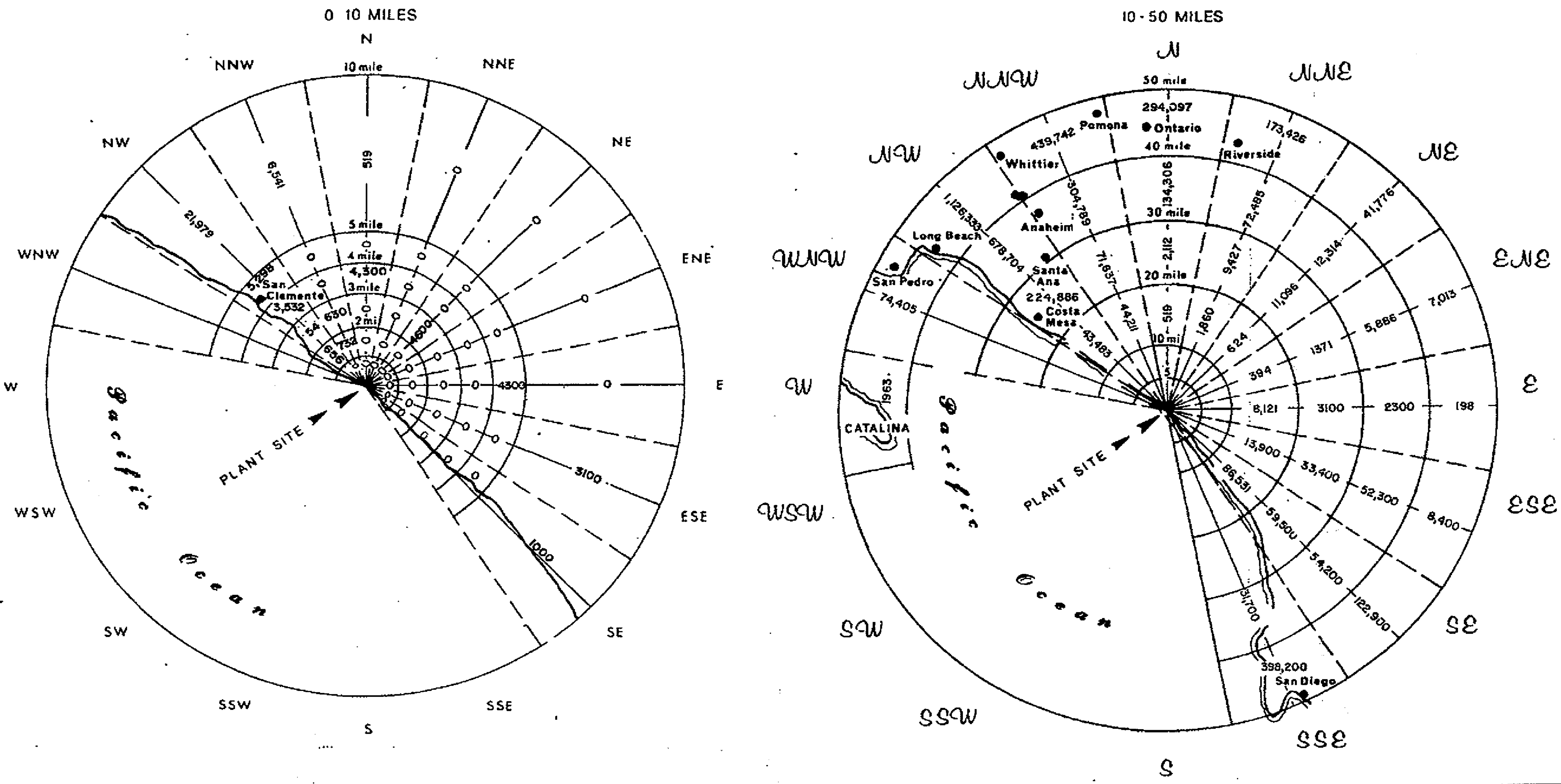

Radius in Miles	1	2	3	4	5	10	20	30	40	50
Accumulative Total	0	1,388	6,672	14,504	24,102	57,241	256,884	673,413	2,022,397	4,710,850

SAN ONOFRE
NUCLEAR GENERATING STATION
Units 2 & 3

1976 POPULATION
DISTRIBUTION SECTOR MAP

Figure 2.1-7

0 – 10 MILES

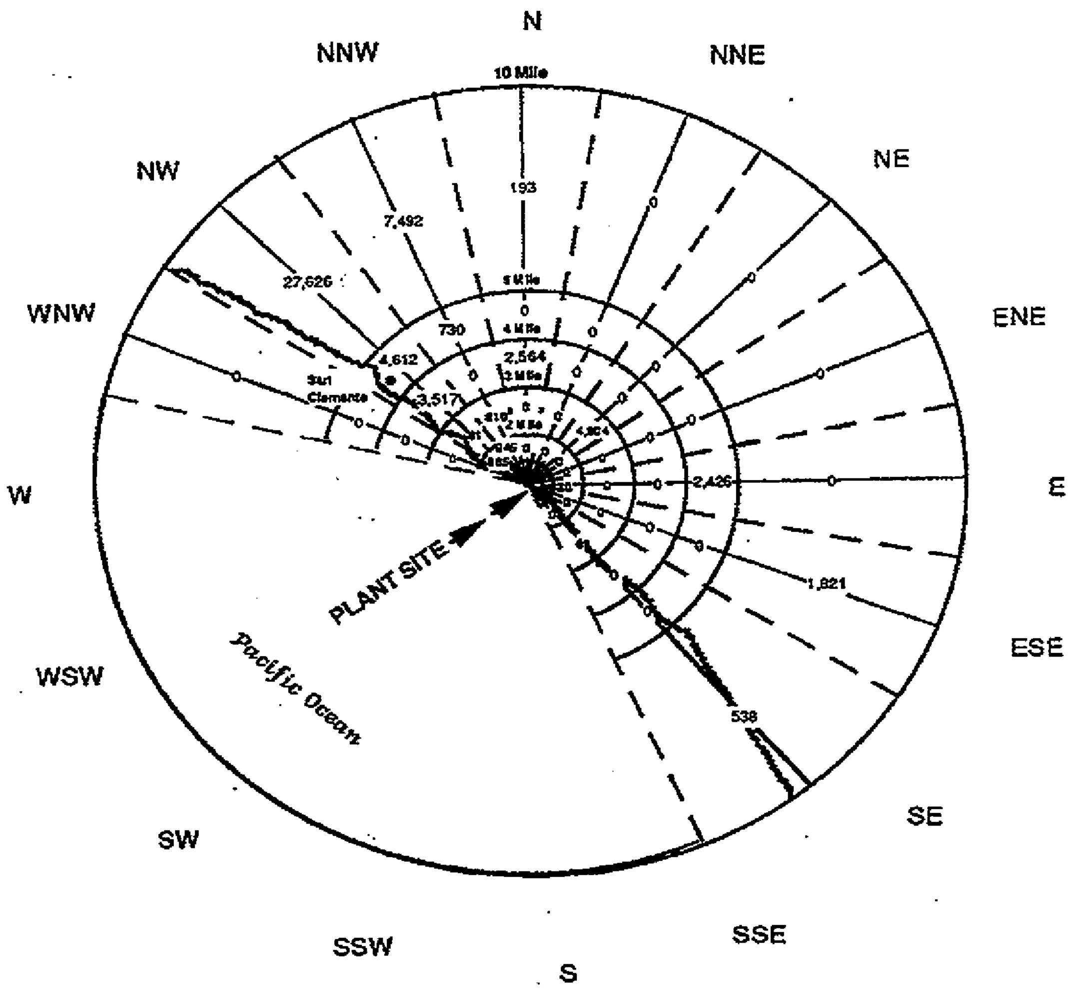

10 – 50 MILES

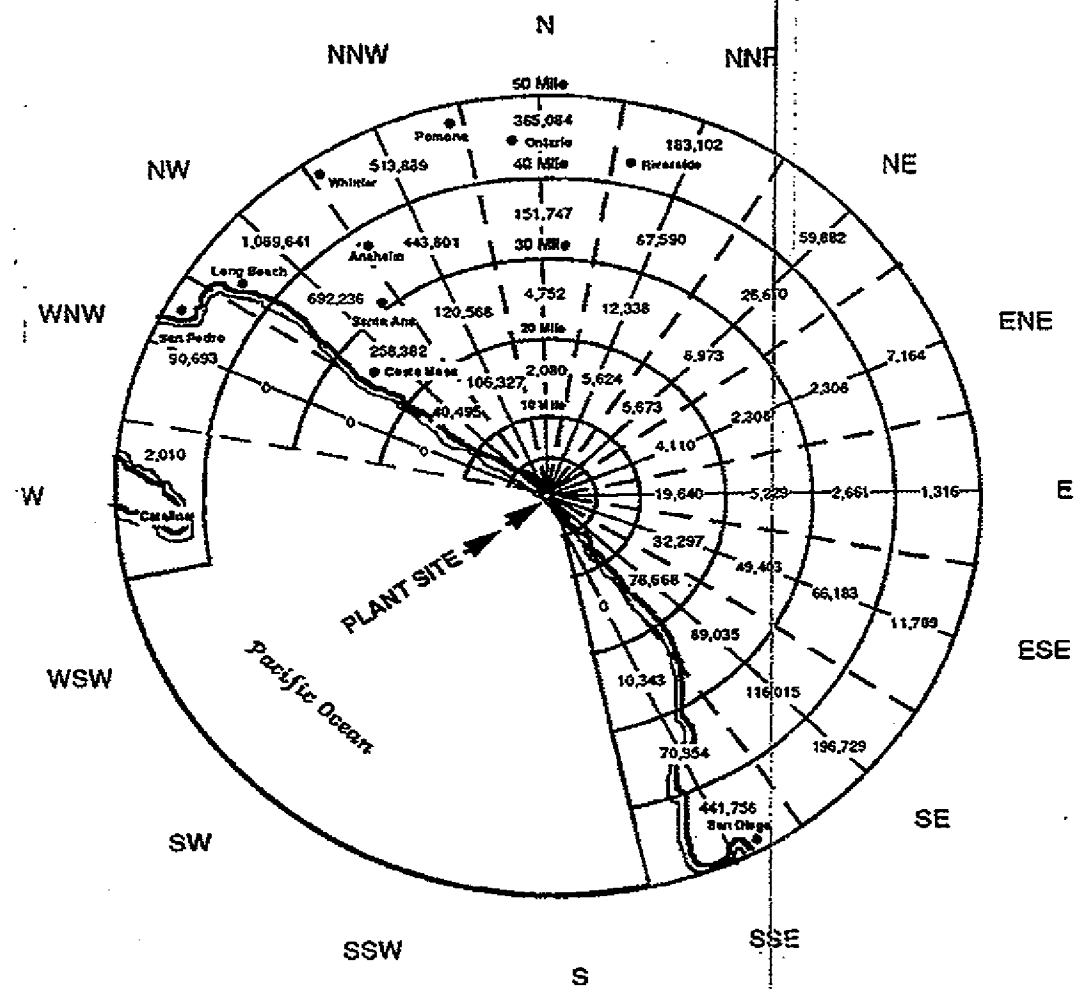

Radius in Miles	1	2	3	4	5	10	20	30	40	50
Accumulative Total	0	1,810	7,505	13,586	21,354	59,024	353,938	913,267	2,552,830	5,515,885

SAN ONOFRE NUCLEAR GENERATING STATION,
UNITS 2 & 3
Updated Final Safety Analysis Report

1980 Population Distribution Sector Map

Figure: 2.1-8

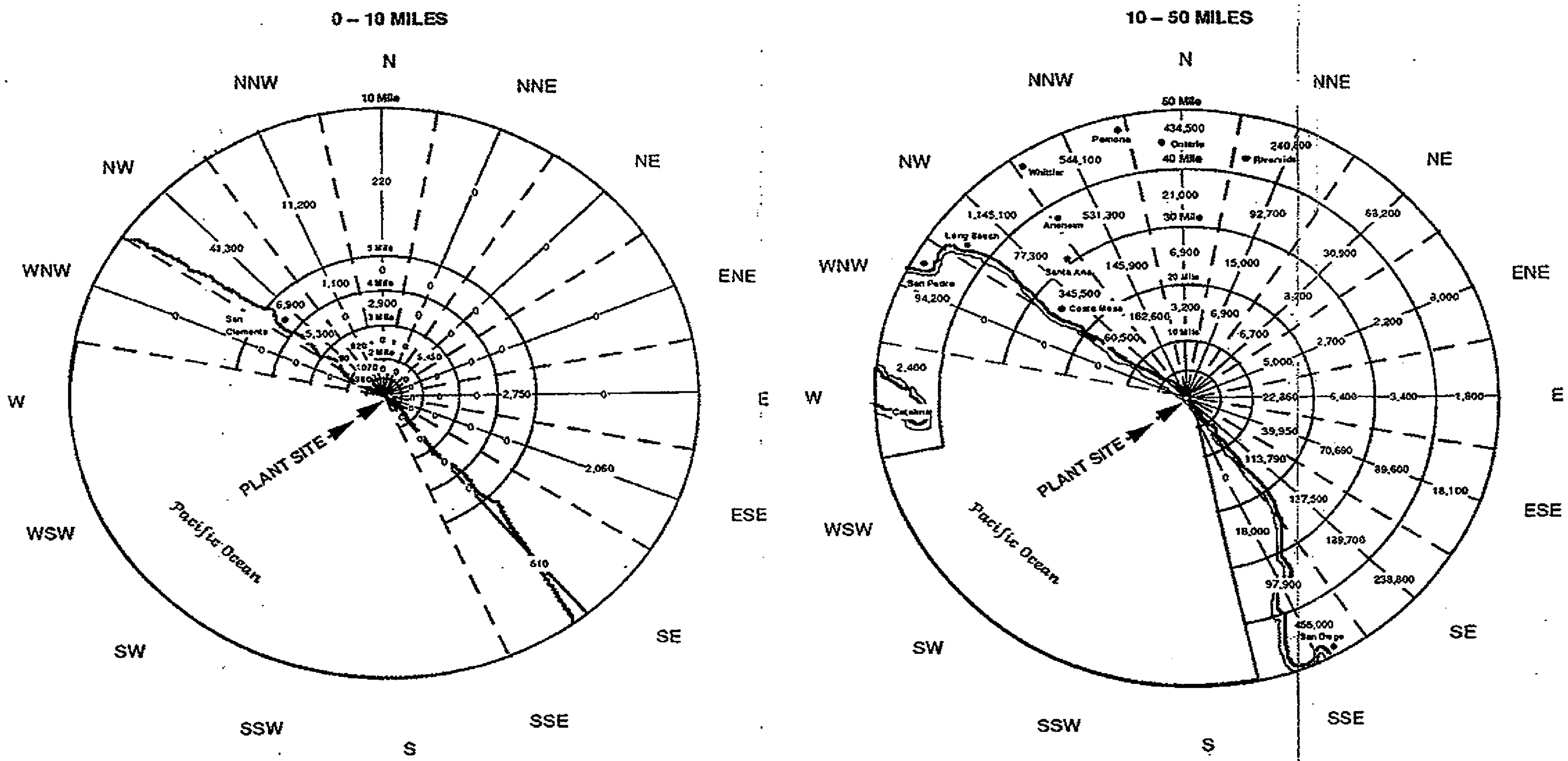

Radius in Miles	1	2	3	4	5	10	20	30	40	50
Accumulative Total	0	2,050	8,510	16,710	27,460	82,850	504,350	1,261,140	3,282,840	6,533,840

SAN ONOFRE NUCLEAR GENERATING STATION
UNITS 2 & 3
Updated Final Safety Analysis Report

Projected 1990 Population Distribution Sector Map

Figure: 2.1-9

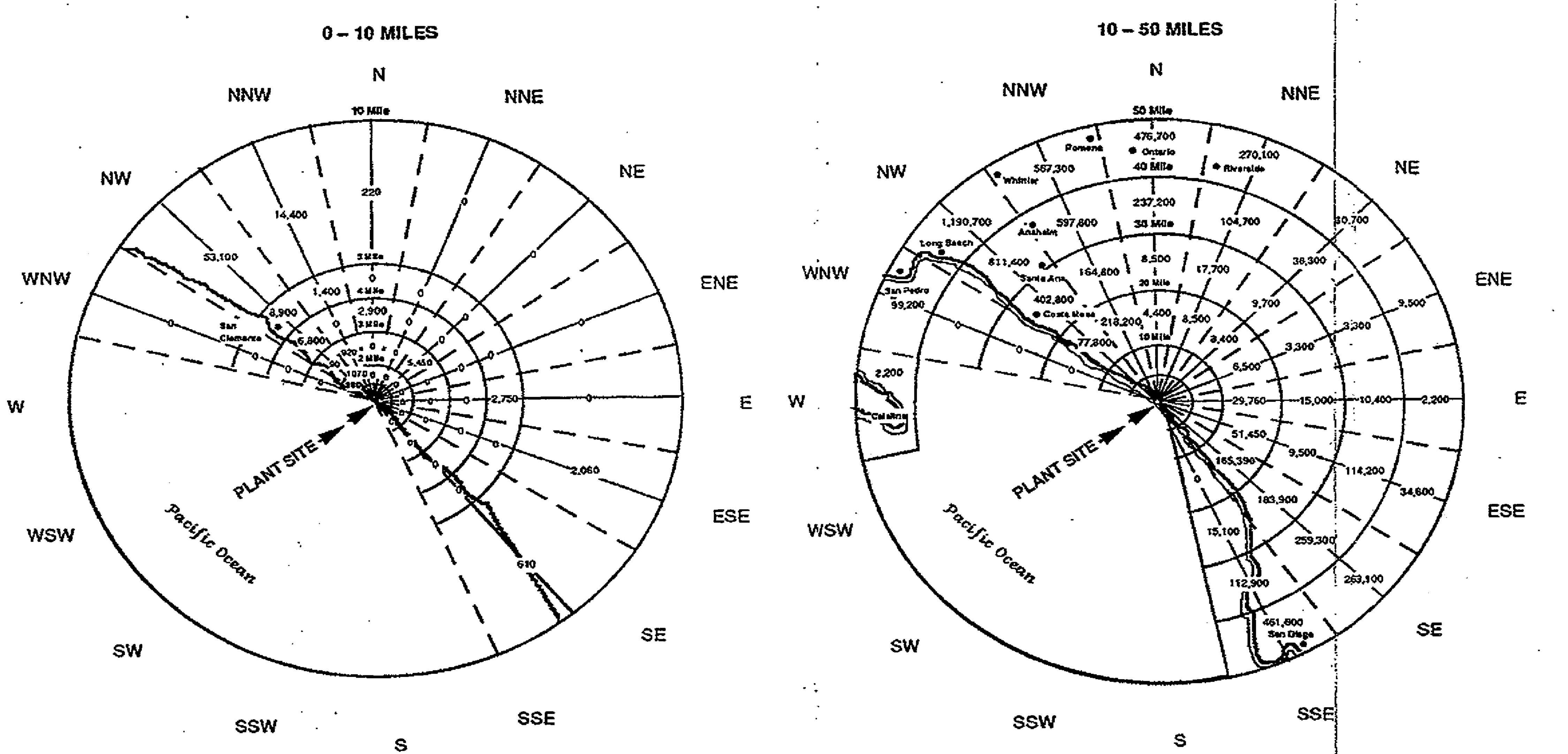

Radius in Miles	1	2	3	4	5	10	20	30	40	50
Accumulative Total	0	2,050	8,510	18,210	31,260	101,650	672,050	1,502,350	3,789,850	7,247,750

SAN ONOFRE NUCLEAR GENERATING STATION, UNITS 2 & 3 Updated Final Safety Analysis Report
Projected 2000 Population Distribution Sector Map
Figure: 2.1-10

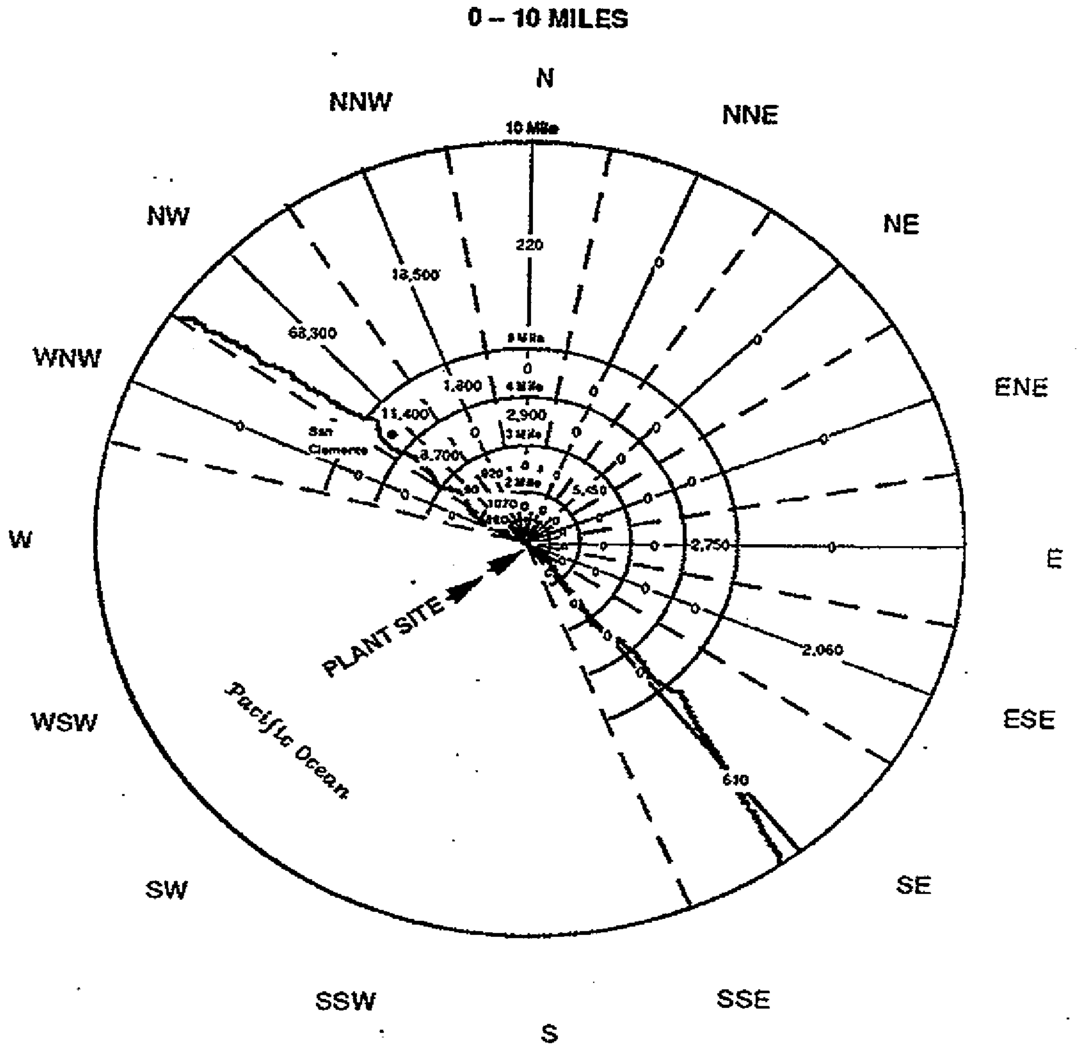

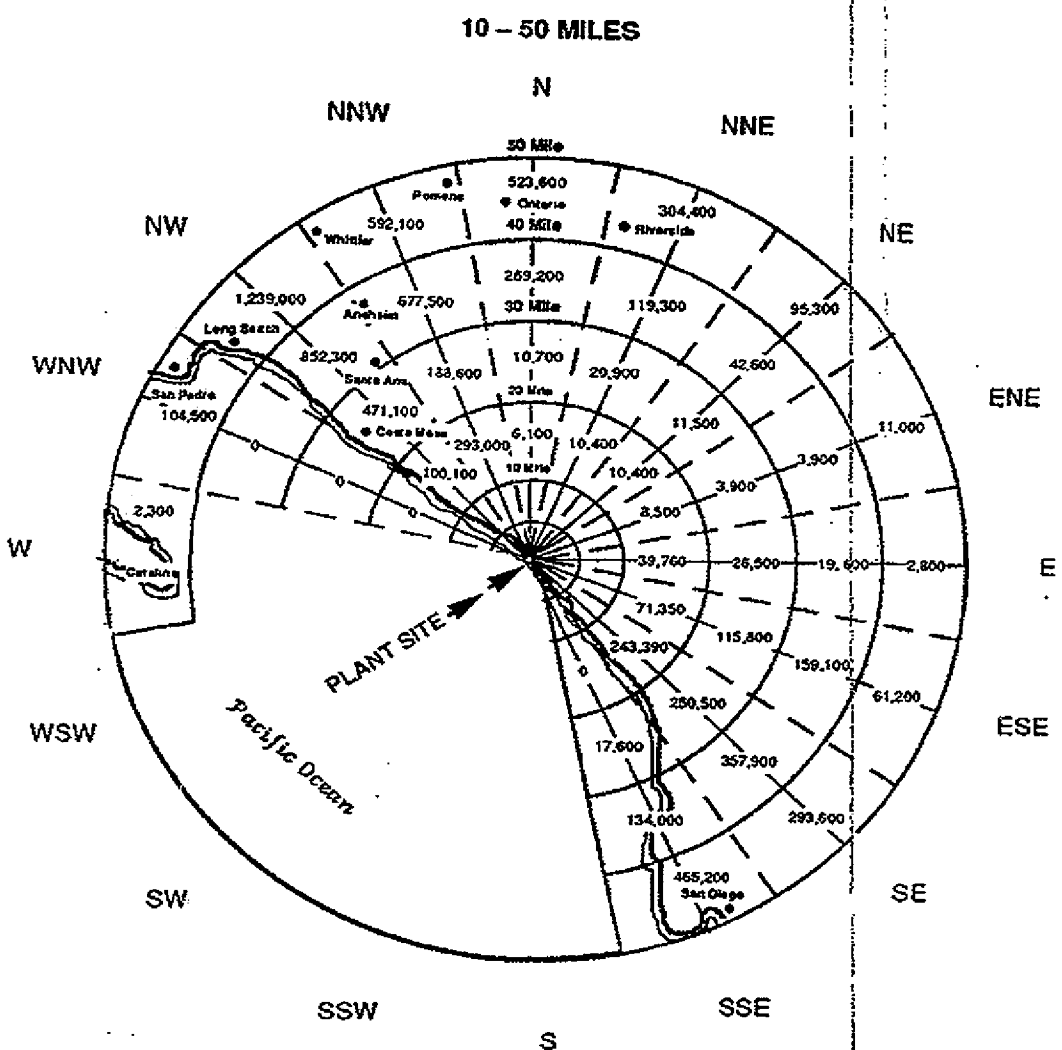

Radius in Miles	1	2	3	4	5	10	20	30	40	50
Accumulative Total	0	2,050	8,510	20,110	36,060	125,750	908,750	2,025,850	4,661,250	8,356,250

SAN ONOFRE NUCLEAR GENERATING STATION
UNITS 2 & 3
Updated Final Safety Analysis Report

Projected 2010 Population Distribution Sector Map

Figure: 2.1-11

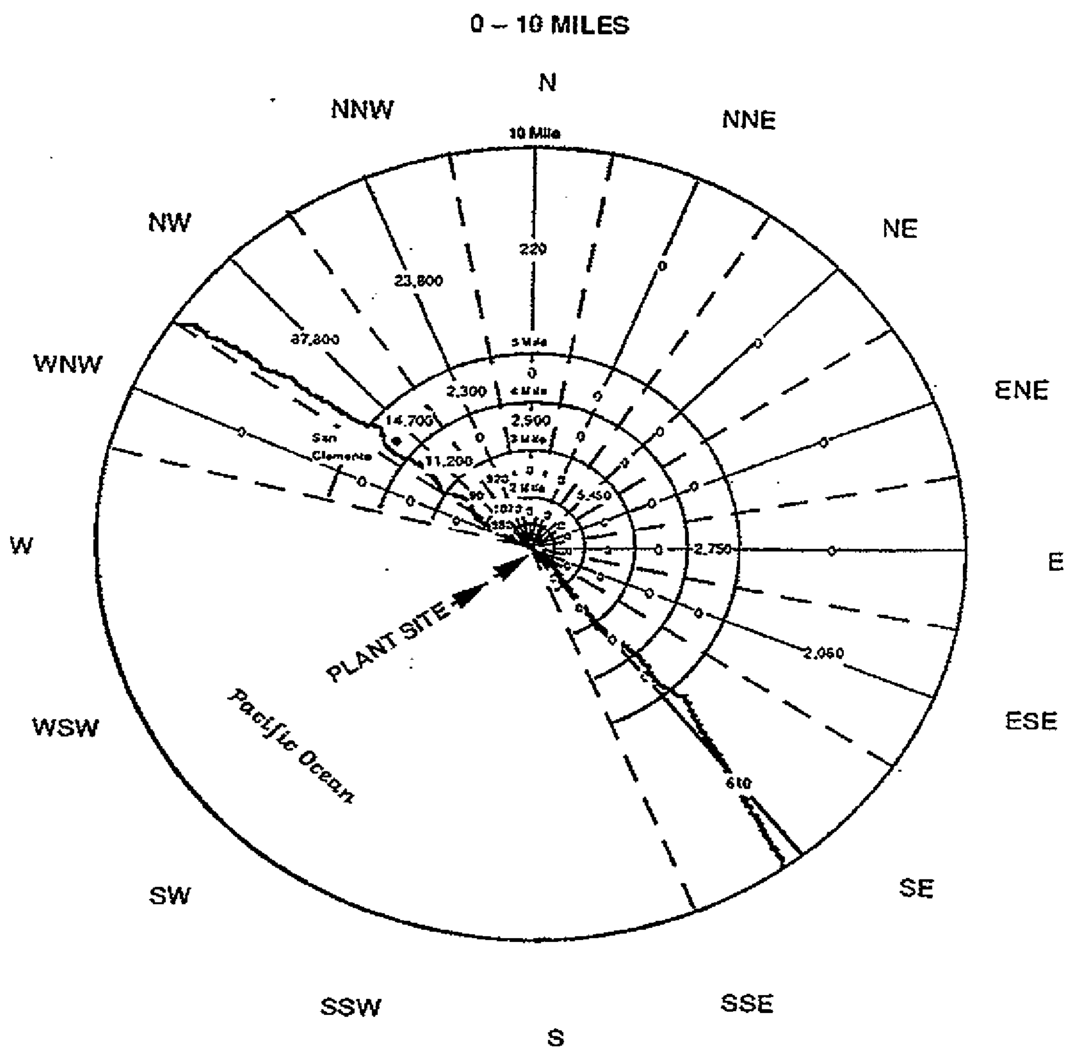

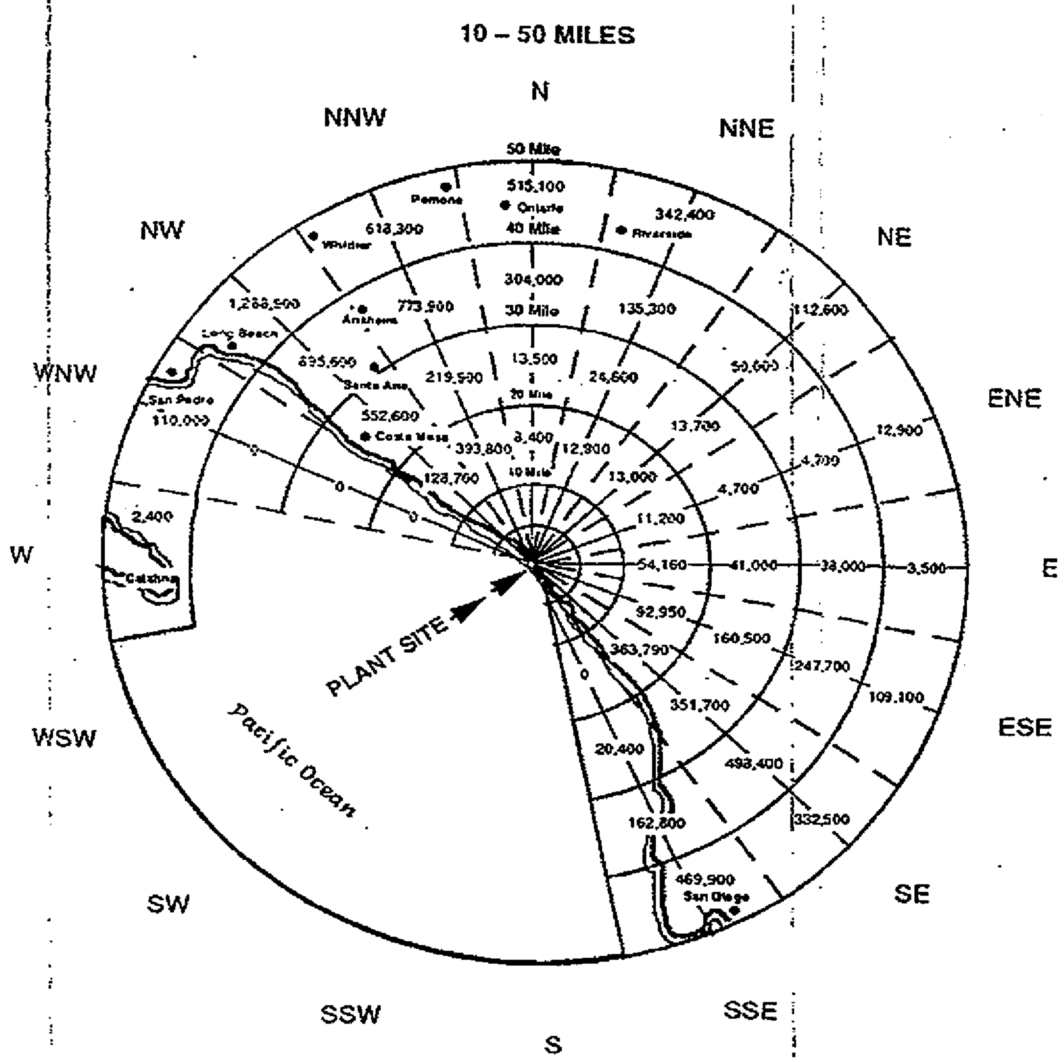

Radius in Miles	1	2	3	4	5	10	20	30	40	50
Accumulative Total	0	2,050	8,510	22,610	42,360	156,850	1,235,750	2,638,350	5,748,750	9,666,350

SAN ONOFRE NUCLEAR GENERATING STATION
UNITS 2 & 3
Updated Final Safety Analysis Report

Projected 2020 Population Distribution Sector Map

Figure: 2.1-12

SAN ONOFRE NUCLEAR GENERATING STATION
Units 2 & 3
Updated Final Safety Analysis Report

LOW POPULATION ZONE

Figure 2.1-13

REV. 5

ACAD2009

REV 5

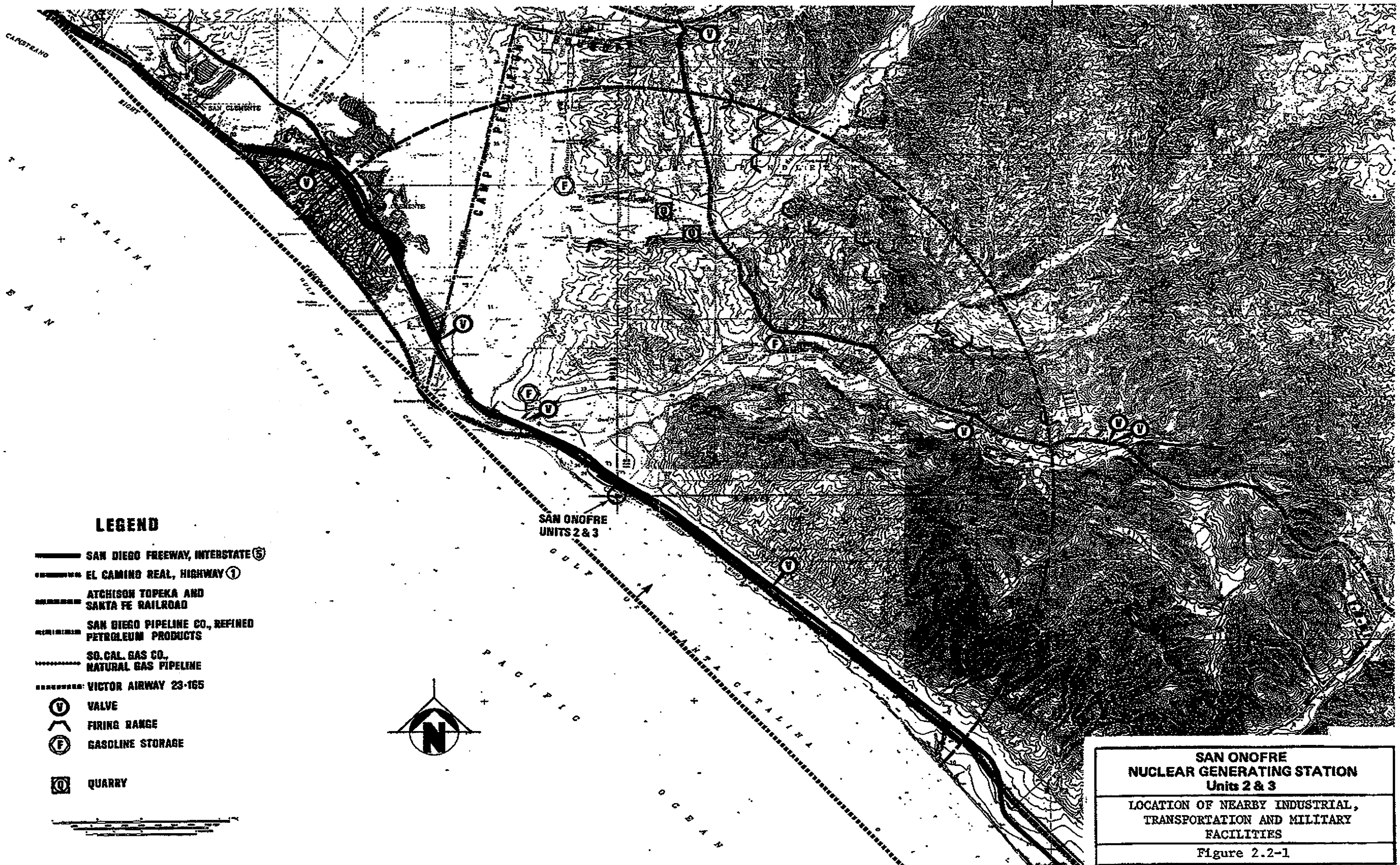

SAN ONOFRE
NUCLEAR GENERATING STATION
Units 2 & 3

LOCATION OF NEARBY INDUSTRIAL, TRANSPORTATION AND MILITARY FACILITIES

Figure 2.2-1

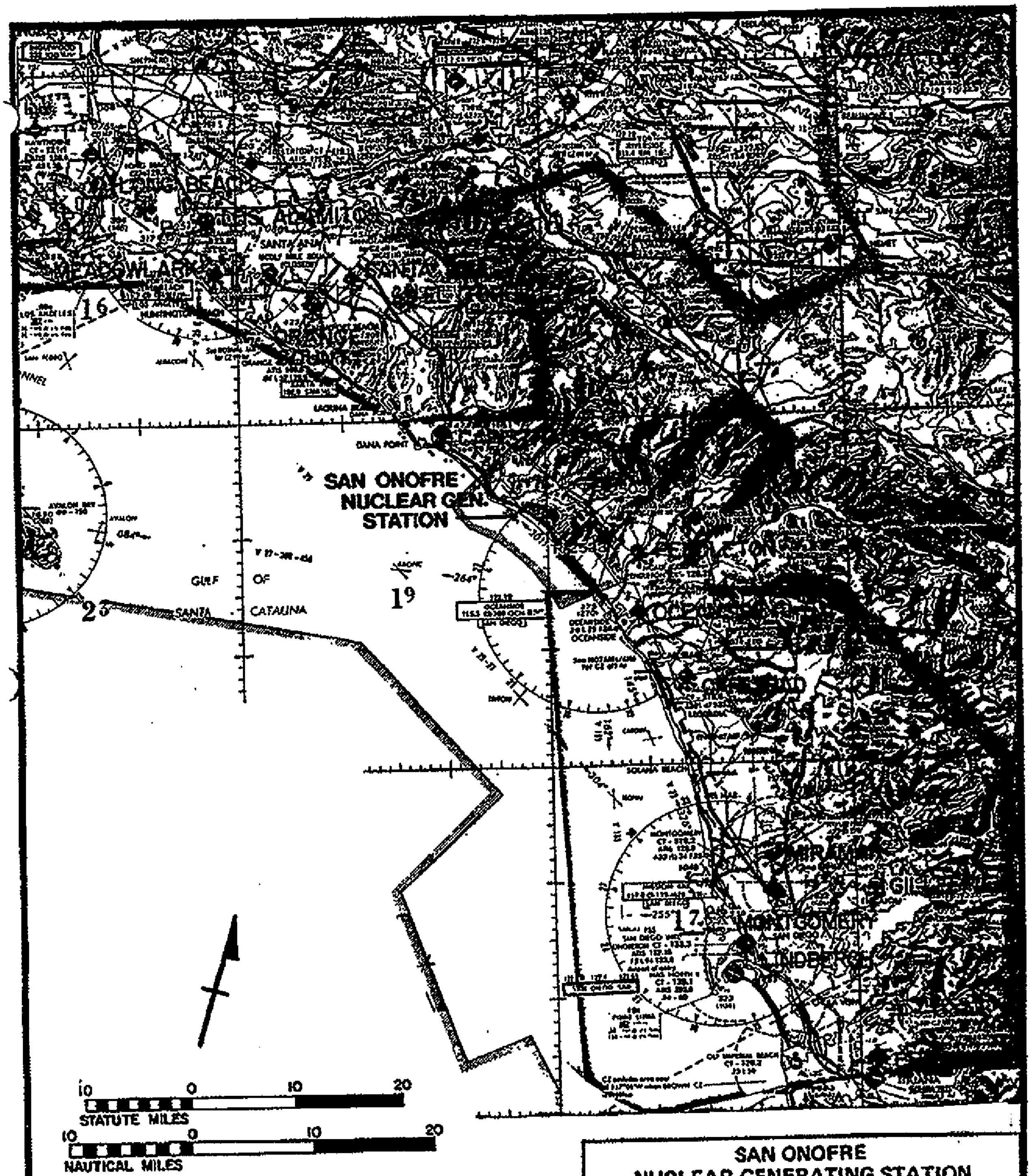

SAN ONOFRE NUCLEAR GENERATING STATION Units 2 & 3

COASTAL AIRFIELDS

Figure 2.2-2

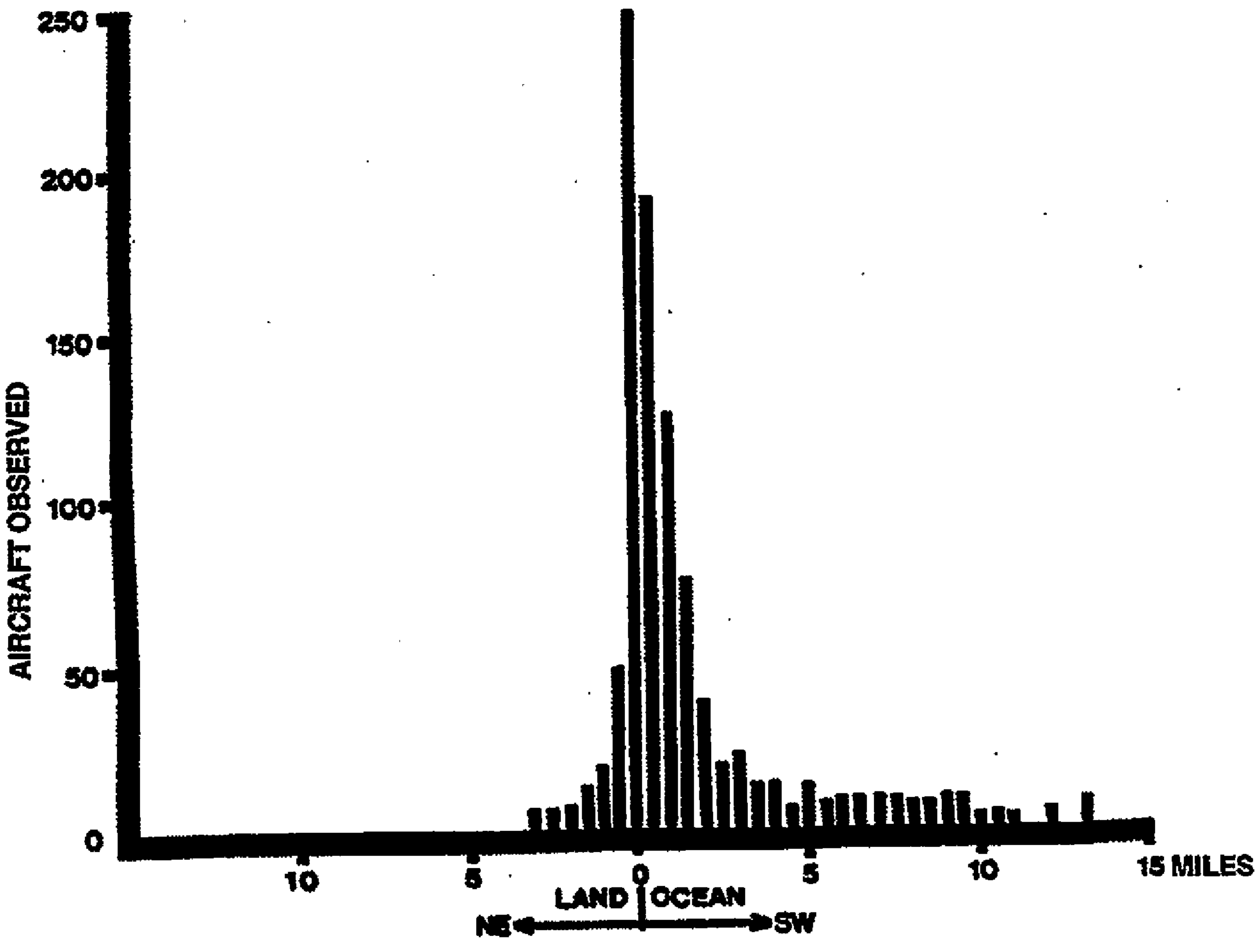

SAN ONOFRE NUCLEAR GENERATING STATION
Units 2 & 3
Updated Final Safety Analysis Report

GENERAL AVIATION

Figure 2.2-3

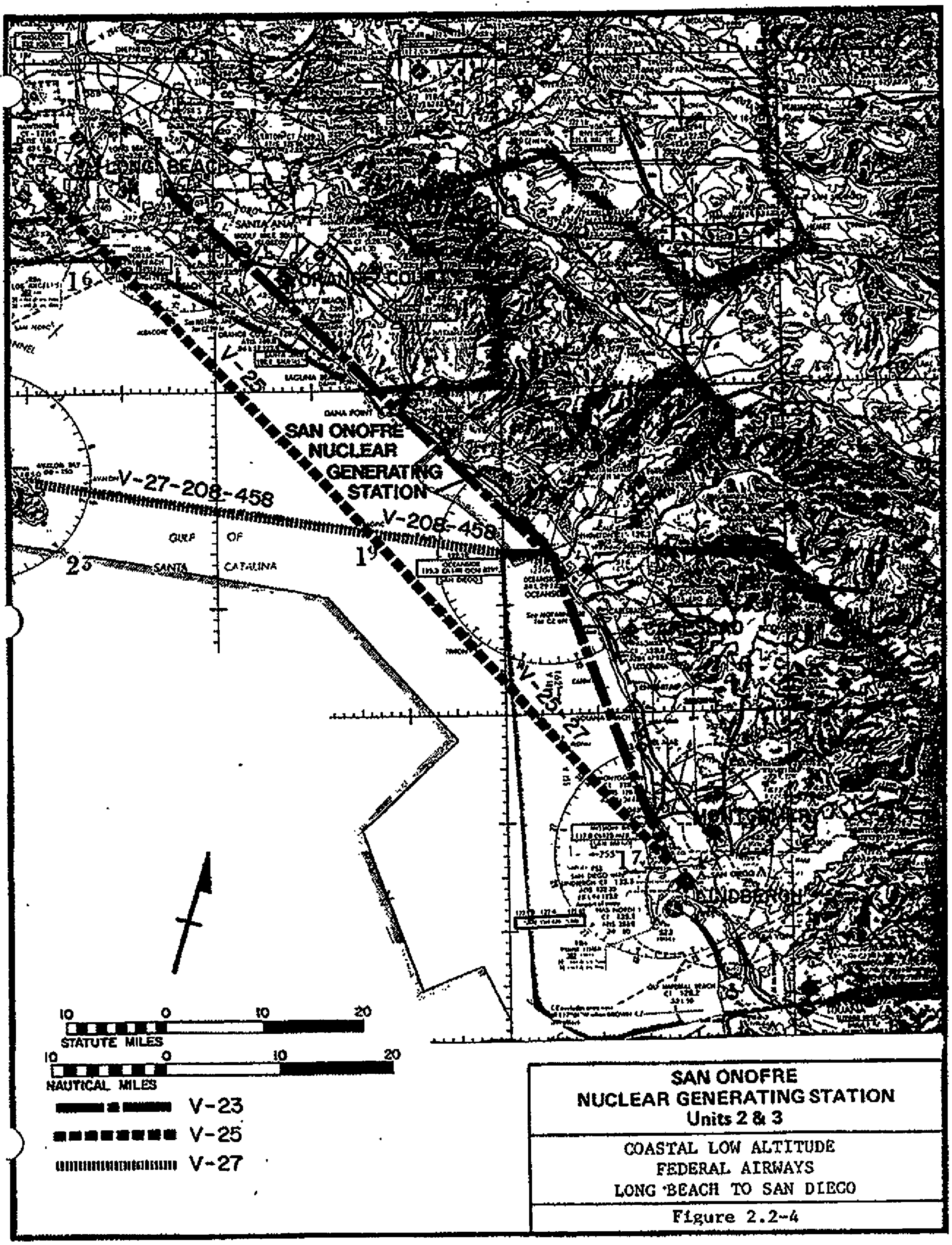

SAN ONOFRE
NUCLEAR GENERATING STATION
Units 2 & 3

COASTAL LOW ALTITUDE
FEDERAL AIRWAYS
LONG BEACH TO SAN DIEGO

Figure 2.2-4

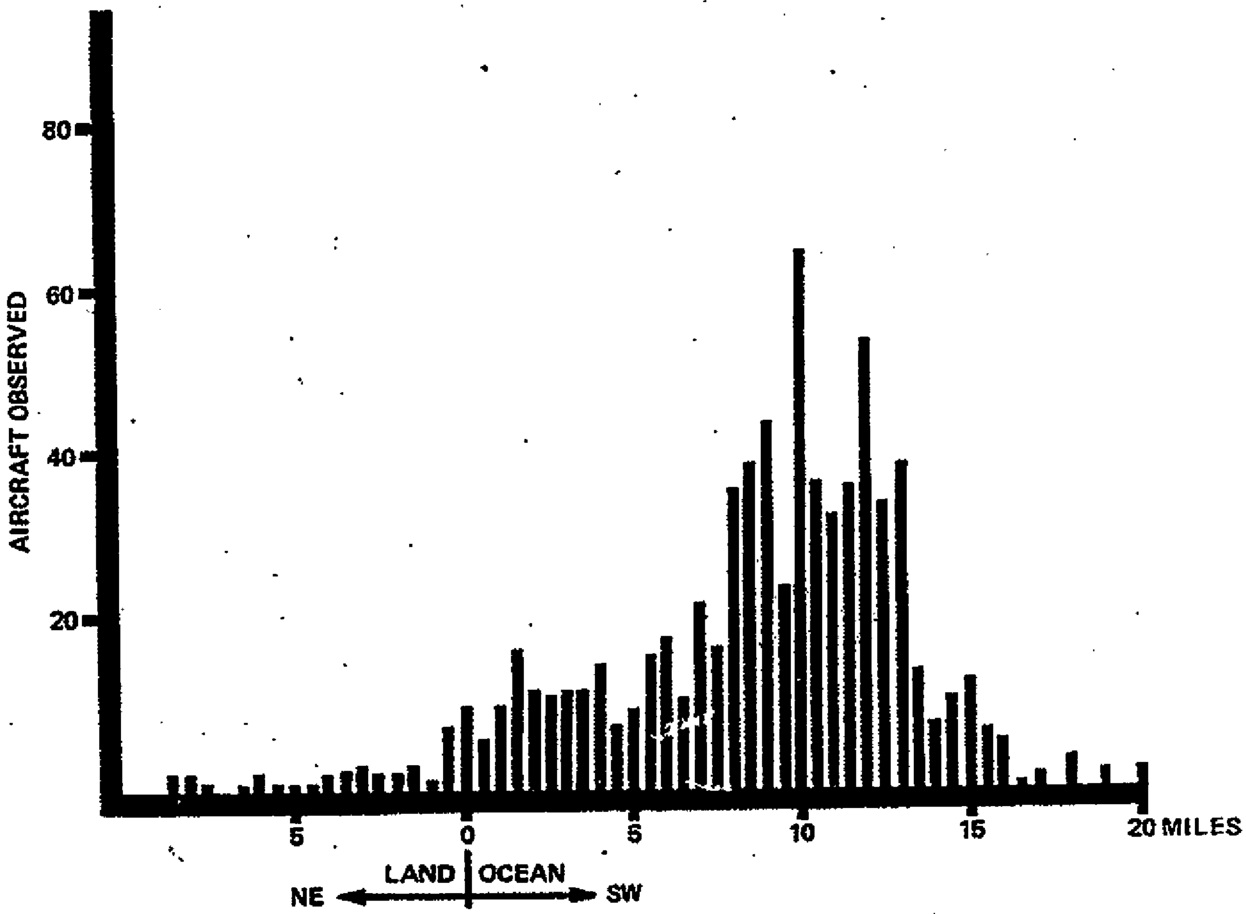

SAN ONOFRE
NUCLEAR GENERATING STATION
Units 2 & 3

COMMERCIAL AND OTHER
GENERAL JET AIRCRAFT

Figure 2.2-5

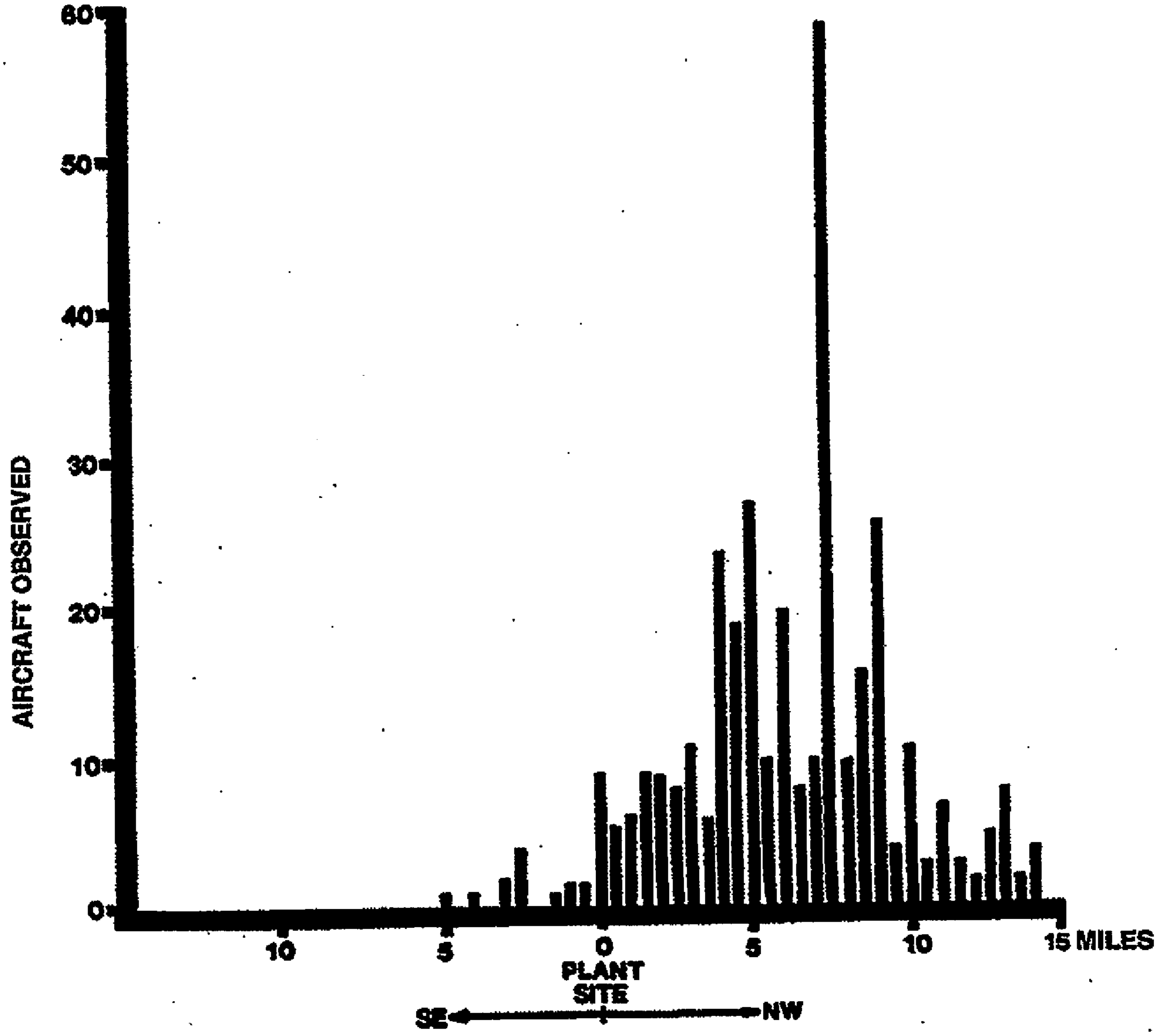

SAN ONOFRE NUCLEAR GENERATING STATION
Units 2 & 3
Updated Final Safety Analysis Report

MILITARY FIXED WING AVIATION

Figure 2.2-6

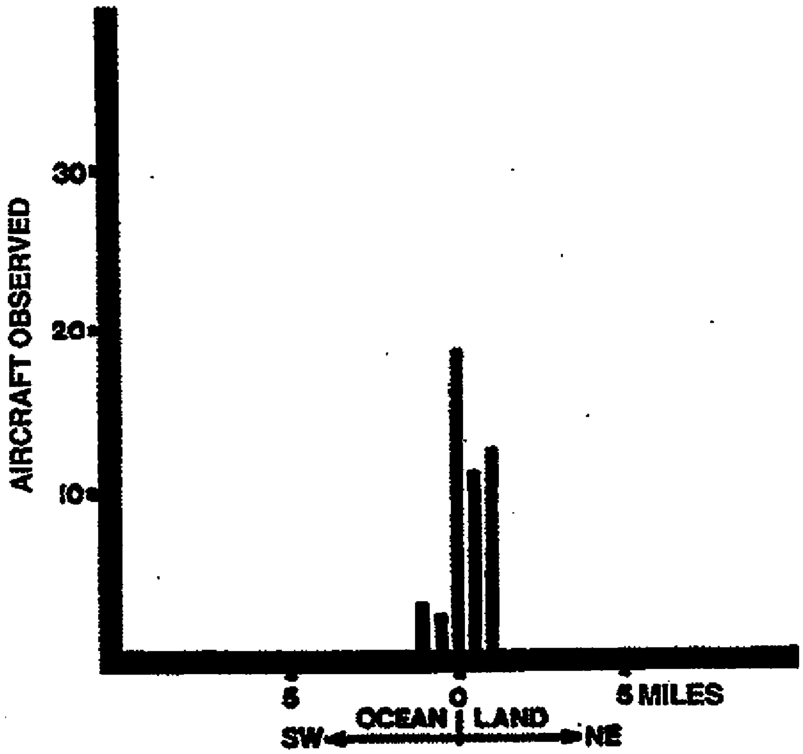

SAN ONOFRE NUCLEAR GENERATING STATION
Units 2 & 3
Updated Final Safety Analysis Report

MILITARY HELICOPTER AVIATION

Figure 2.2-7

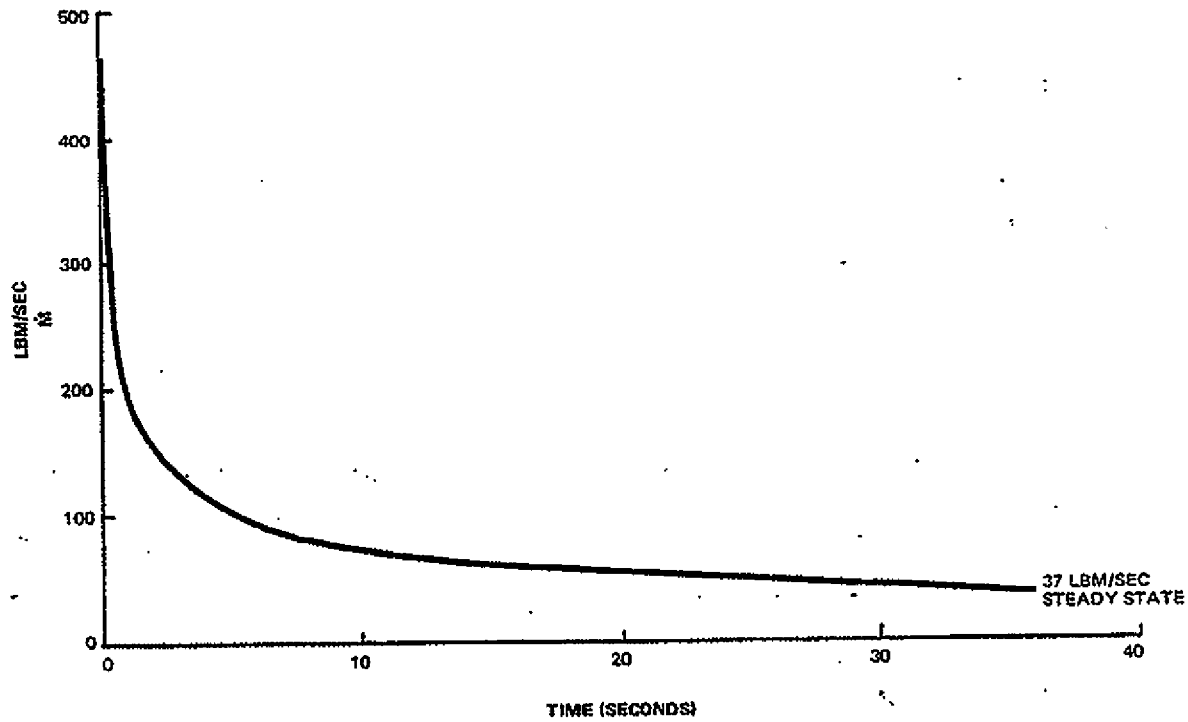

SAN ONOFRE
NUCLEAR GENERATING STATION
Units 2 & 3

TRANSIENT FLOWRATE AS A FUNCTION OF TIME FOLLOWING A RUPTURE (FROM EACH SIDE OF BREAK)

Figure 2.2-8

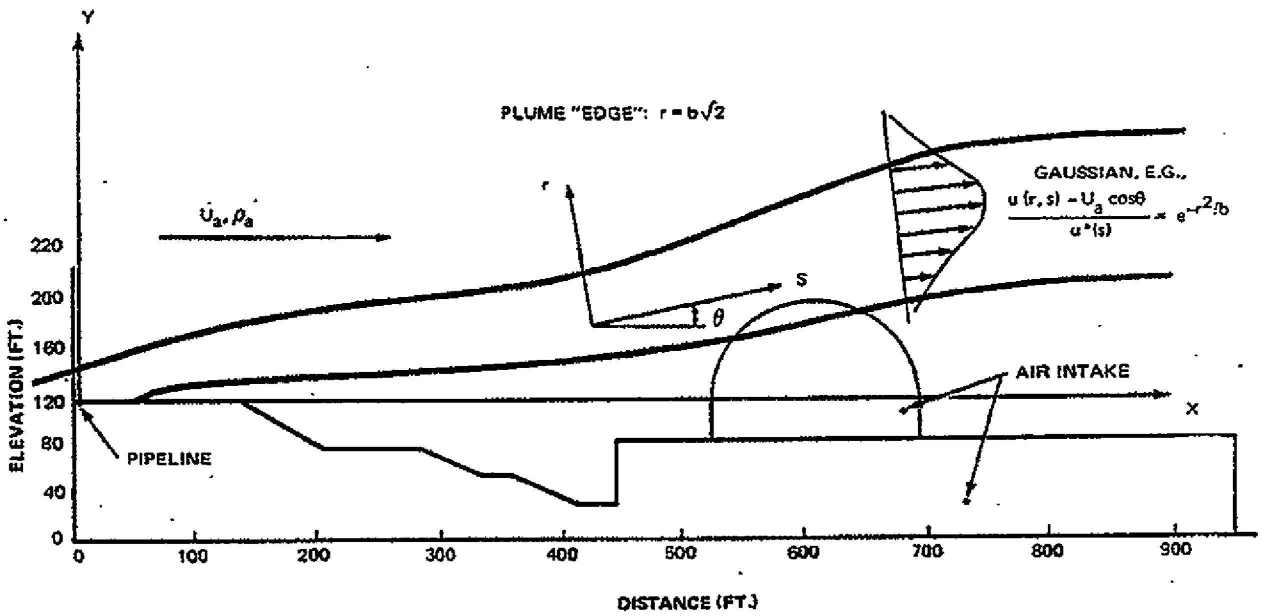

SAN ONOFRE
NUCLEAR GENERATING STATION
Units 2 & 3

SCHEMATIC OF PHYSICAL SITUATION AND PLUME COORDINATES

Figure 2.2-9

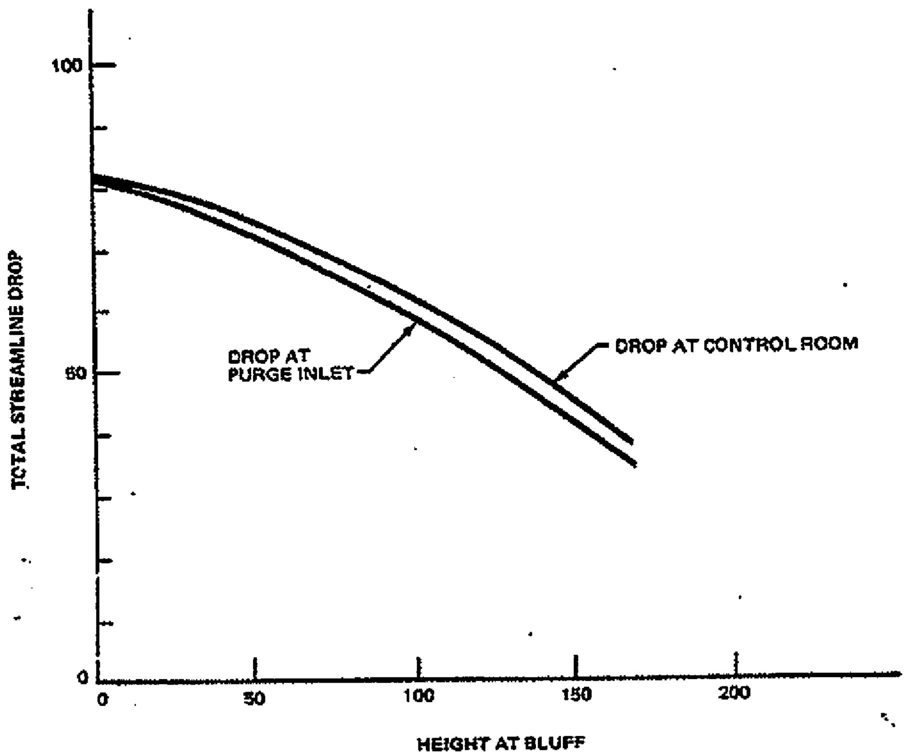

SAN ONOFRE
NUCLEAR GENERATING STATION
Units 2 & 3

DISPLACEMENTS

Figure 2.2-10

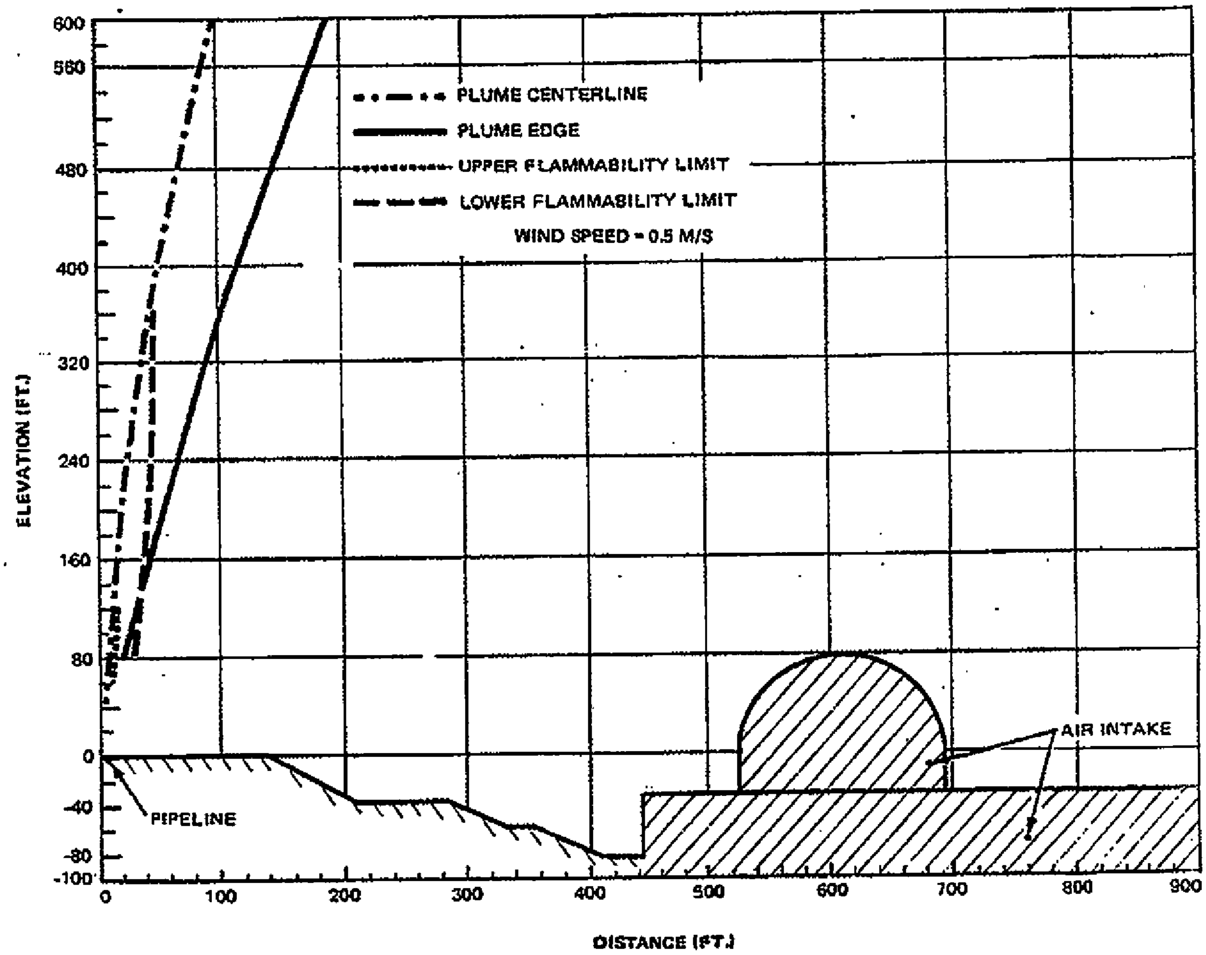

SAN ONOFRE NUCLEAR GENERATING STATION Units 2 & 3
PLUME TRAJECTORY WIND SPEED = 0.5 M/S STEADY-STATE BREAK FLOW
Figure 2.2-11

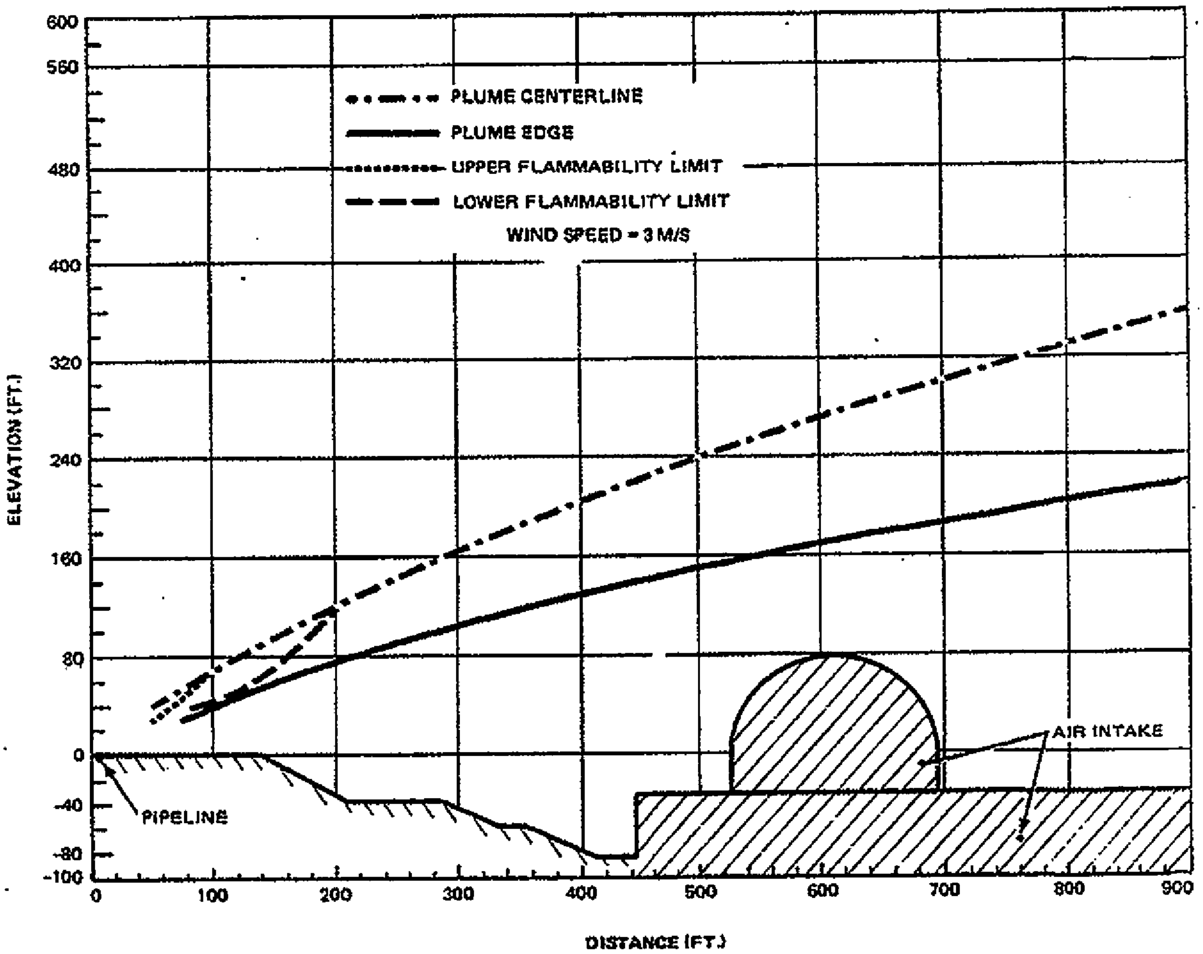

SAN ONOFRE NUCLEAR GENERATING STATION Units 2 & 3
PLUME TRAJECTORY WIND SPEED = 3 M/S STEADY-STATE BREAK FLOW
Figure 2.2-12

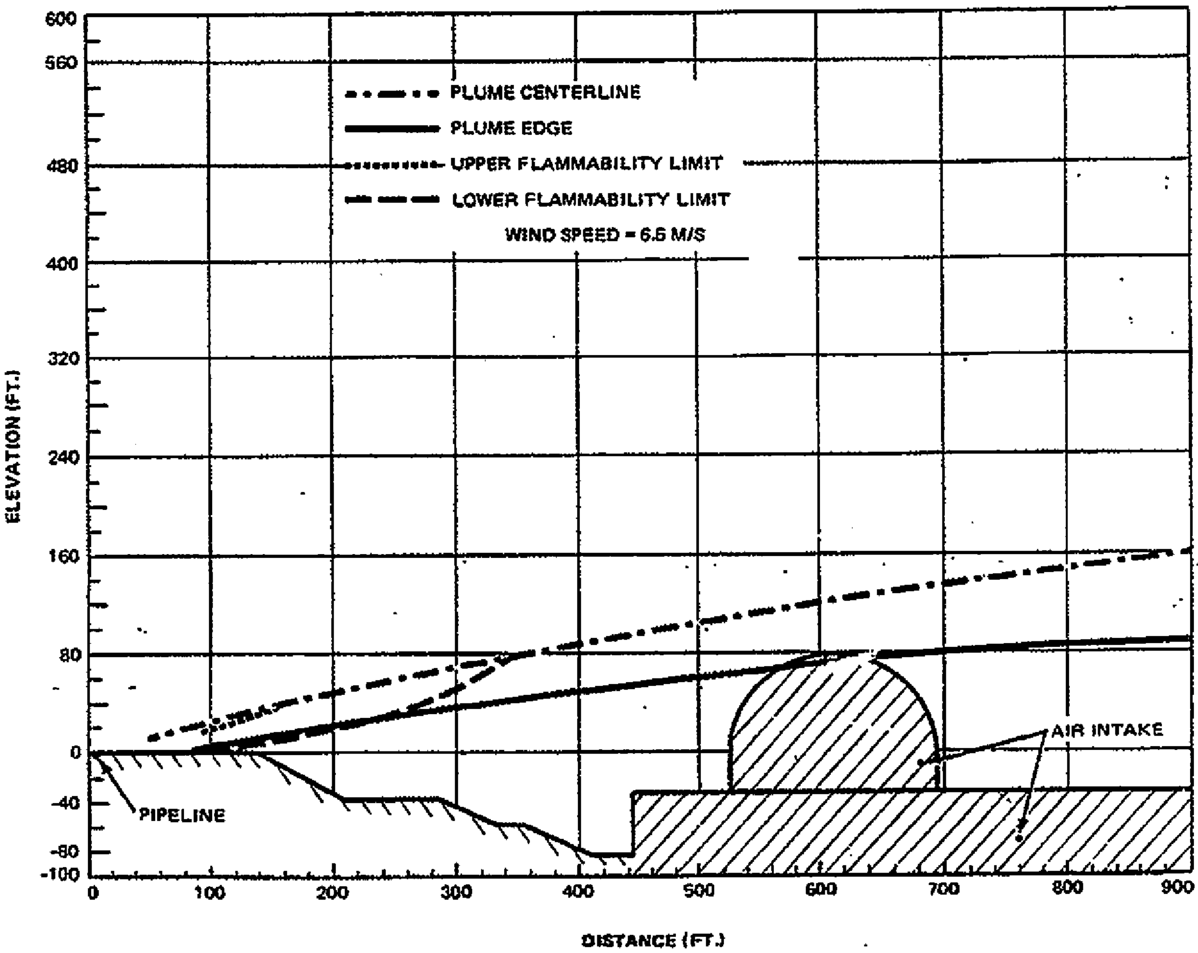

SAN ONOFRE NUCLEAR GENERATING STATION Units 2 & 3
PLUME TRAJECTORY WIND SPEED = 6.5 M/S STEADY-STATE BREAK FLOW
Figure 2.2-13

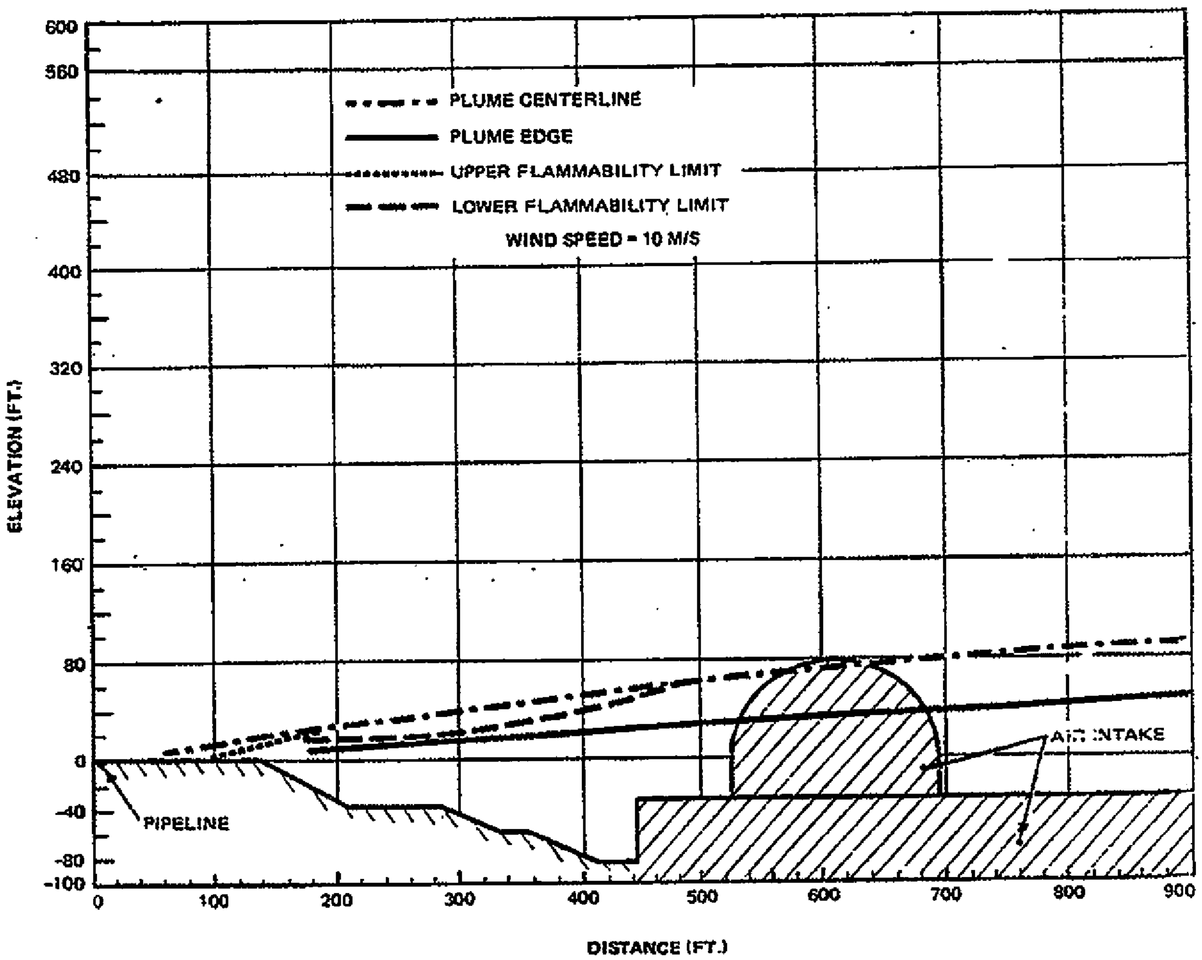

SAN ONOFRE NUCLEAR GENERATING STATION Units 2 & 3
PLUME TRAJECTORY WIND SPEED = 10 M/S STEADY-STATE BREAK FLOW
Figure 2.2-14

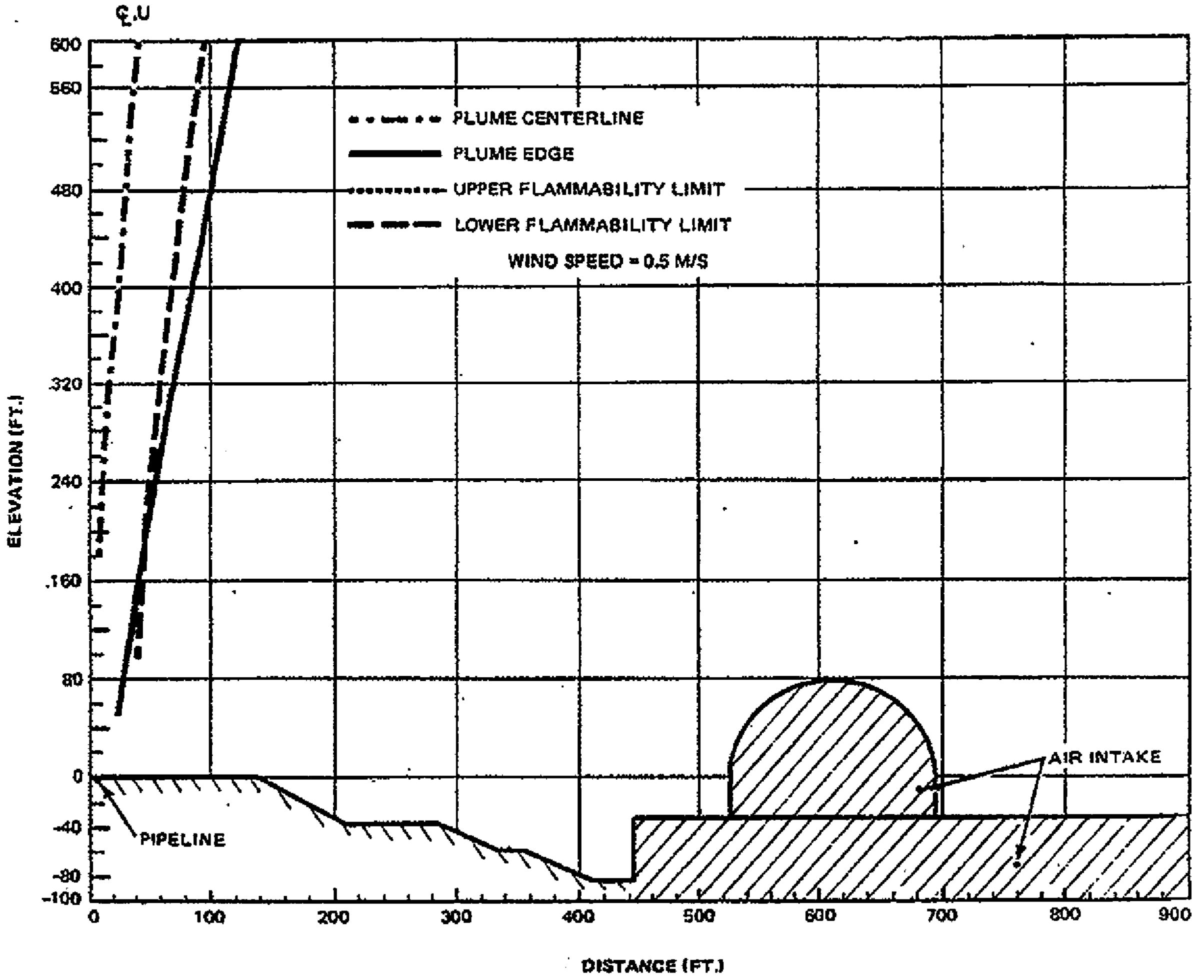

SAN ONOFRE NUCLEAR GENERATING STATION Units 2 & 3
PLUME TRAJECTORY WIND SPEED = 0.5 M/S INITIAL BREAK FLOW
Figure 2.2-15

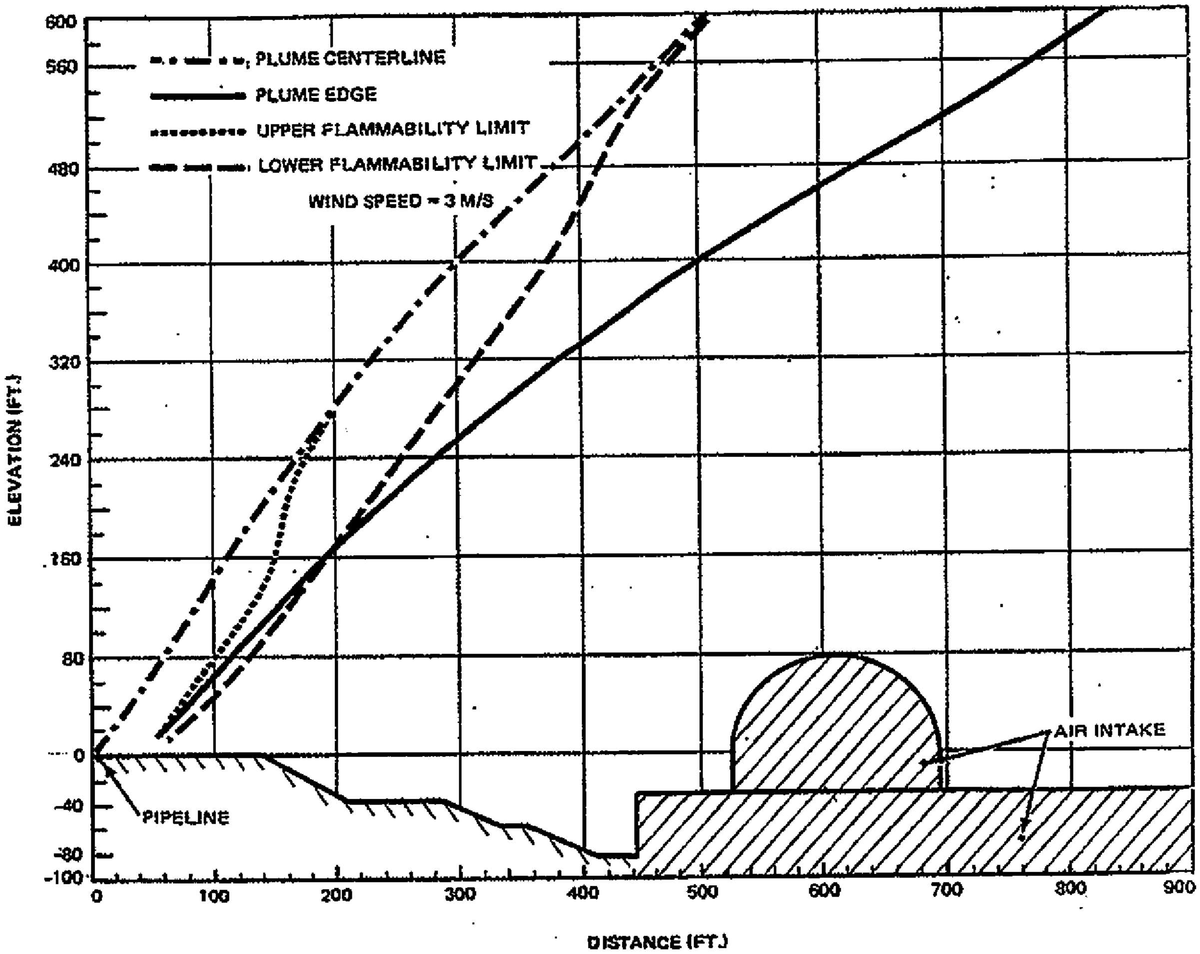

SAN ONOFRE
NUCLEAR GENERATING STATION
Units 2 & 3

PLUME TRAJECTORY
WIND SPEED = 3 M/S
INITIAL BREAK FLOW

Figure 2.2-16

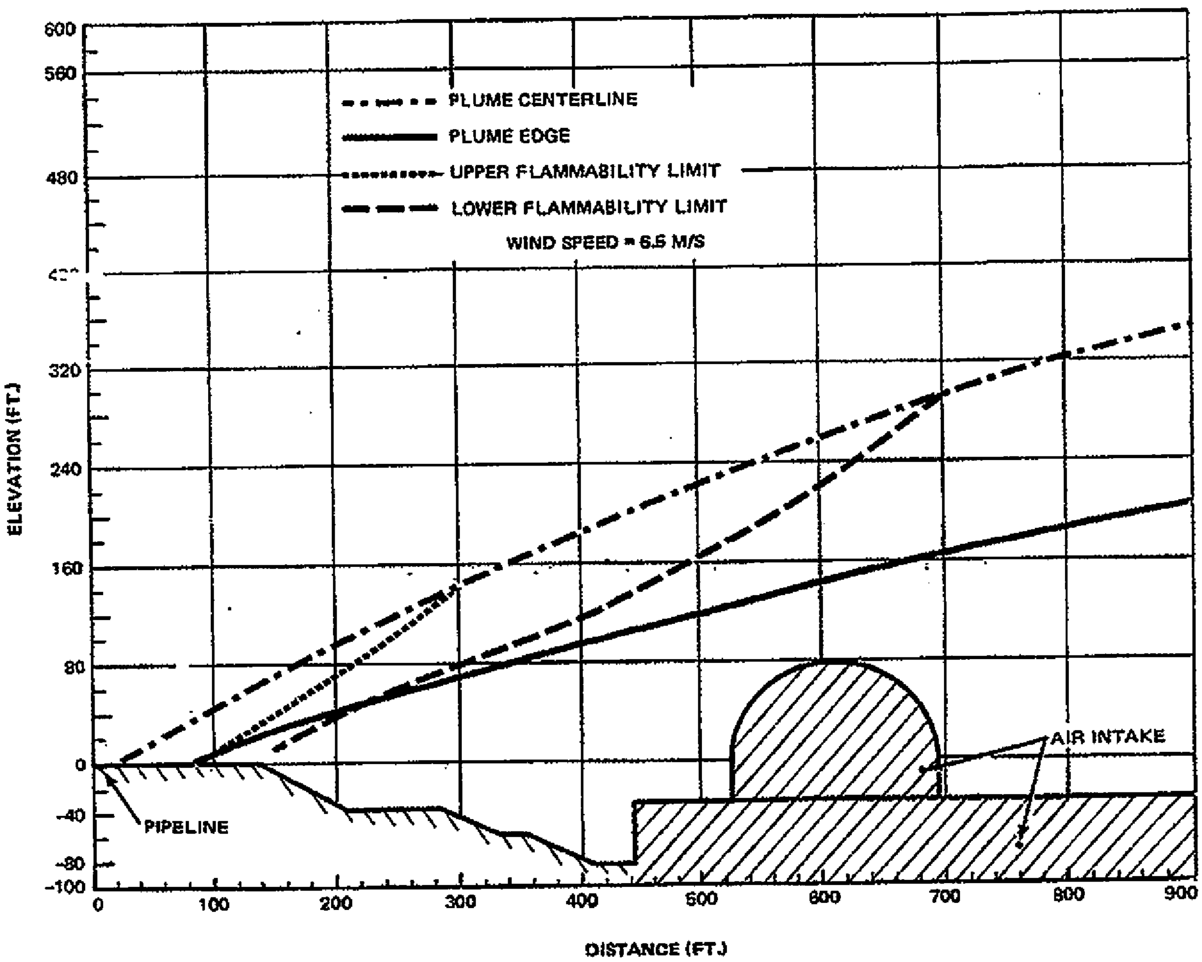

SAN ONOFRE NUCLEAR GENERATING STATION Units 2 & 3
PLUME TRAJECTORY WIND SPEED - 6.5 M/S INITIAL BREAK FLOW
Figure 2.2-17

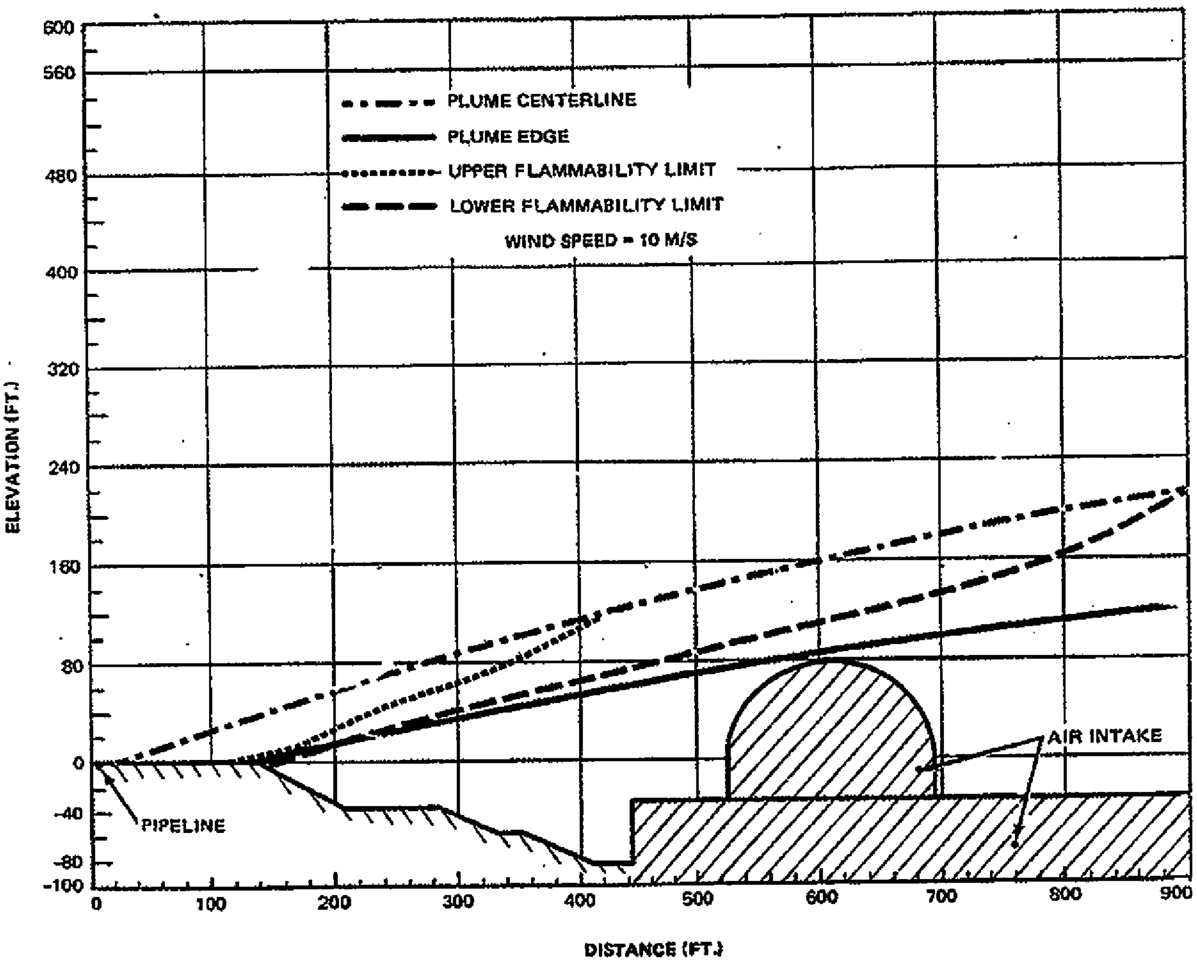

SAN ONOFRE
NUCLEAR GENERATING STATION
Units 2 & 3

PLUME TRAJECTORY
WIND SPEED = 10 M/S
INITIAL BREAK FLOW

Figure 2.2-18

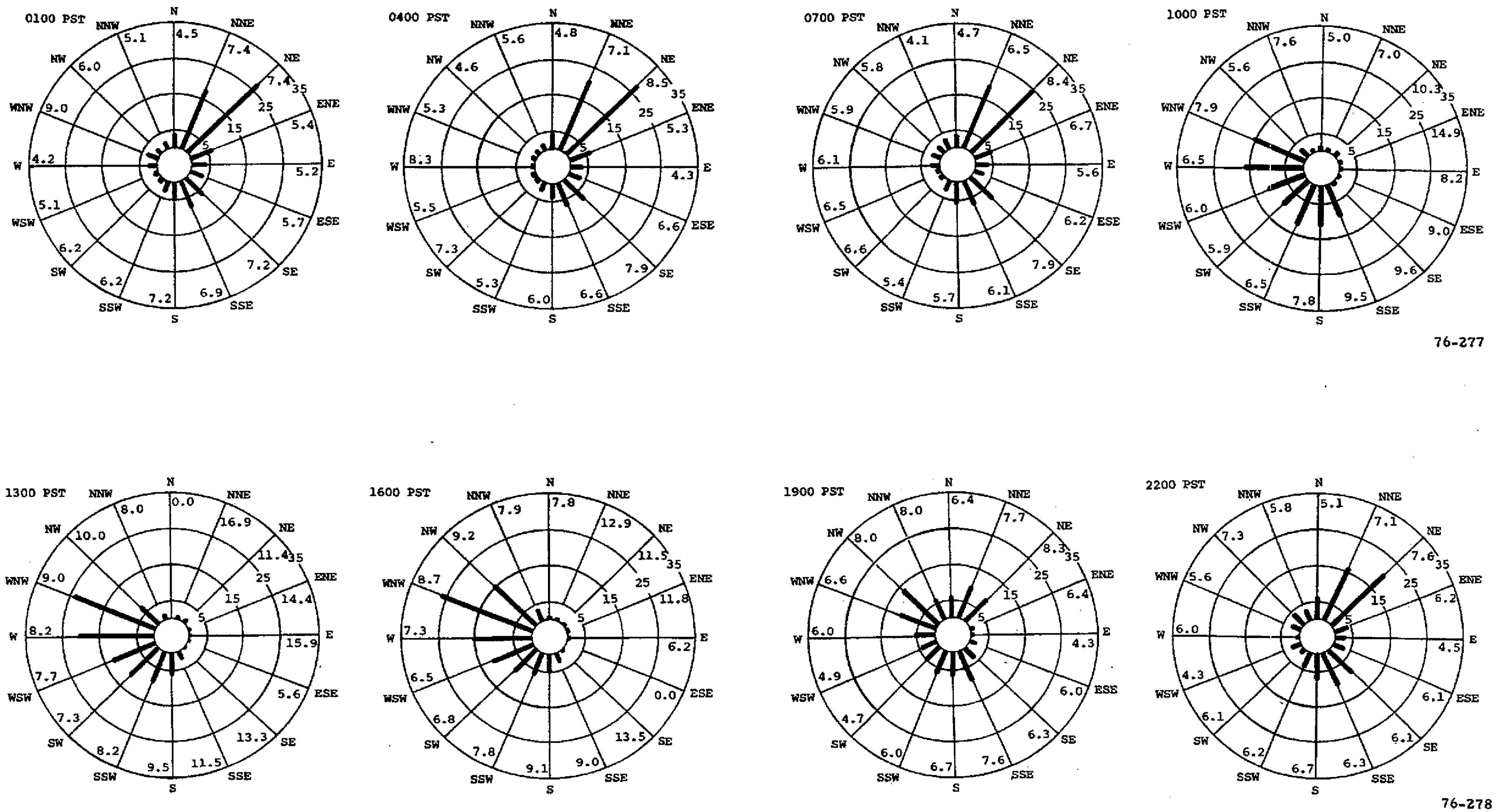

SOLID LINE REPRESENTS PERCENTAGE FREQUENCY OF OCCURRENCE BY SECTOR
AVERAGE WIND SPEED BY SECTOR IS MI/H.

SAN ONOFRE
NUCLEAR GENERATING STATION
Units 2 & 3

SAN ONOFRE ANNUAL AVERAGE
3-HOURLY WIND ROSES, 10m LEVEL
(DATA PERIOD 1/25/73 THROUGH 1/24/76)

Figure 2.3-1

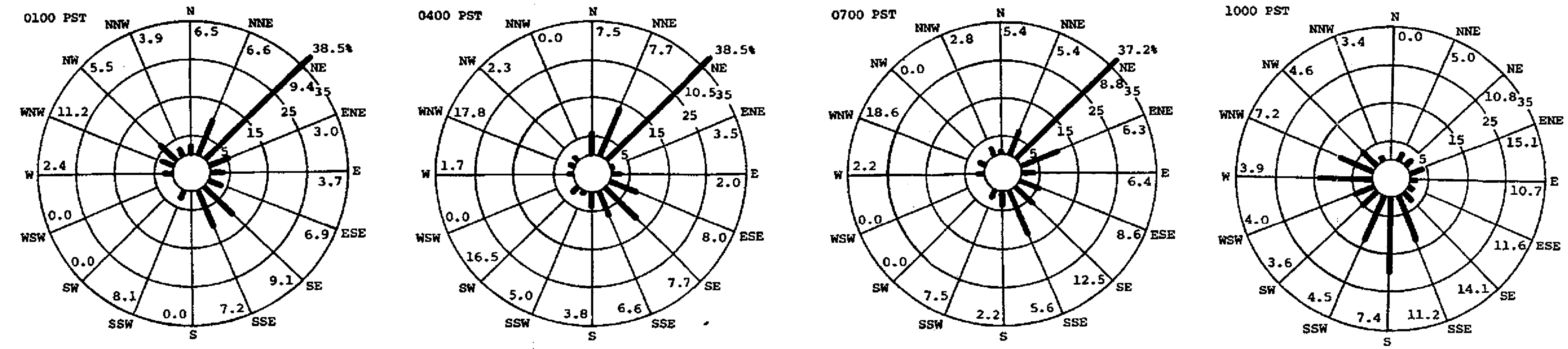

76-279

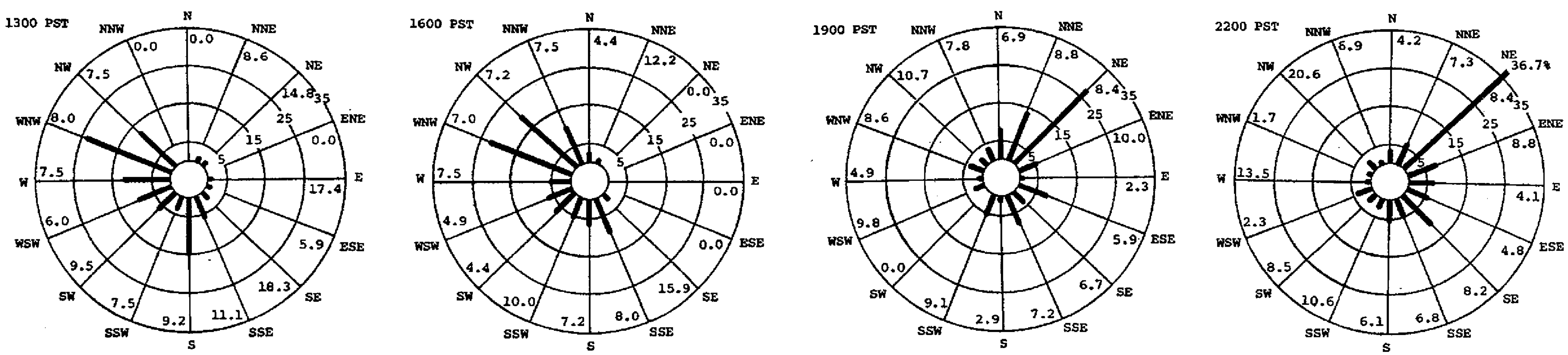

76-280

SOLID LINE REPRESENTS PERCENTAGE FREQUENCY OF OCCURRENCE BY SECTOR
AVERAGE WIND SPEED BY SECTOR IS MI/H.

SAN ONOFRE NUCLEAR GENERATING STATION Units 2 & 3

SAN ONOFRE JANUARY AVERAGE
3-HOURLY WIND ROSES, 10m LEVEL
(DATA PERIOD 1/25/73 THROUGH 1/24/76)

Figure 2.3-2

10079-11D-365
27JL6

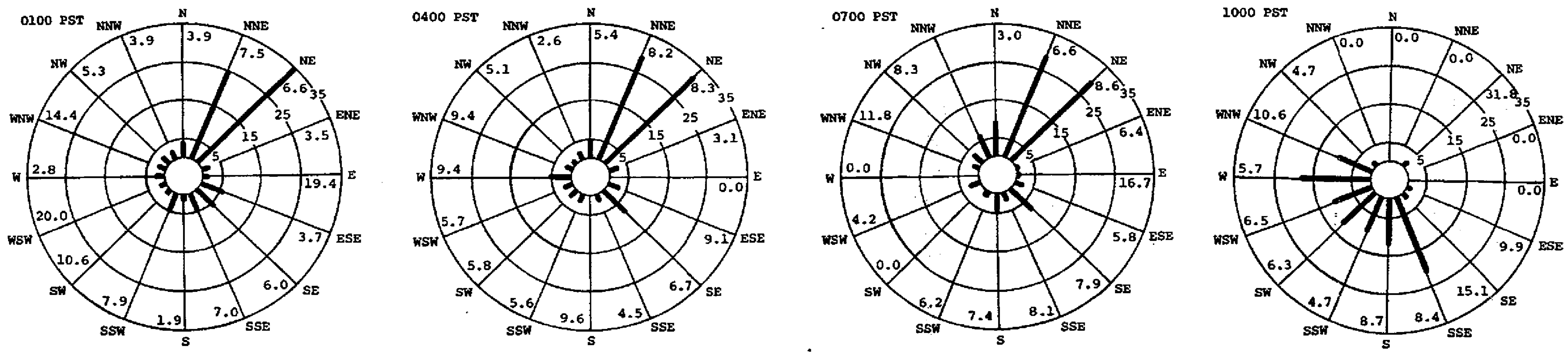

76-281

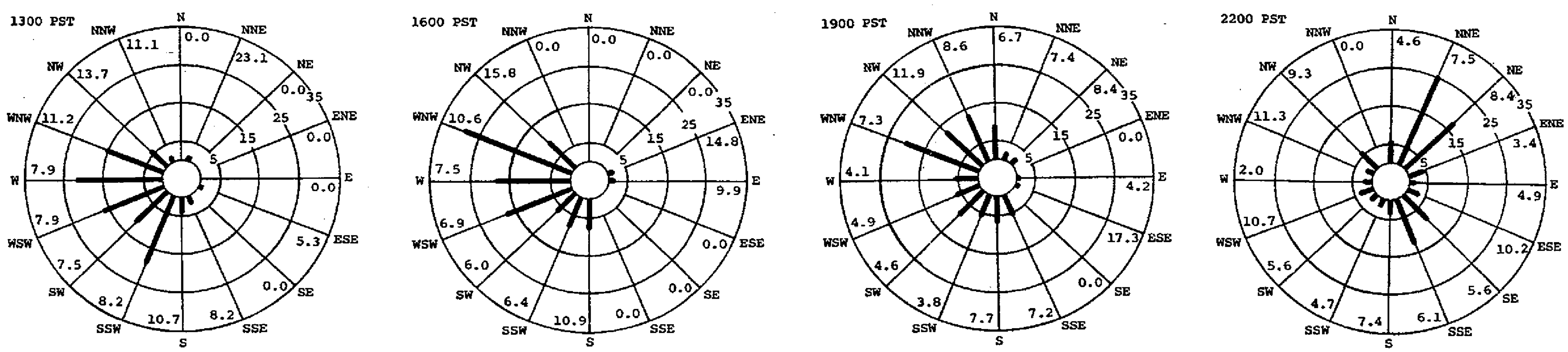

76-282

SOLID LINE REPRESENTS PERCENTAGE FREQUENCY OF OCCURRENCE BY SECTOR
AVERAGE WIND SPEED BY SECTOR IS MI/H.

10079-11D-366
27JL6

SAN ONOFRE NUCLEAR GENERATING STATION Units 2 & 3
SAN ONOFRE APRIL AVERAGE 3-HOURLY WIND ROSES, 10m LEVEL (DATA PERIOD 1/25/73 THROUGH 1/24/76)
Figure 2.3-3

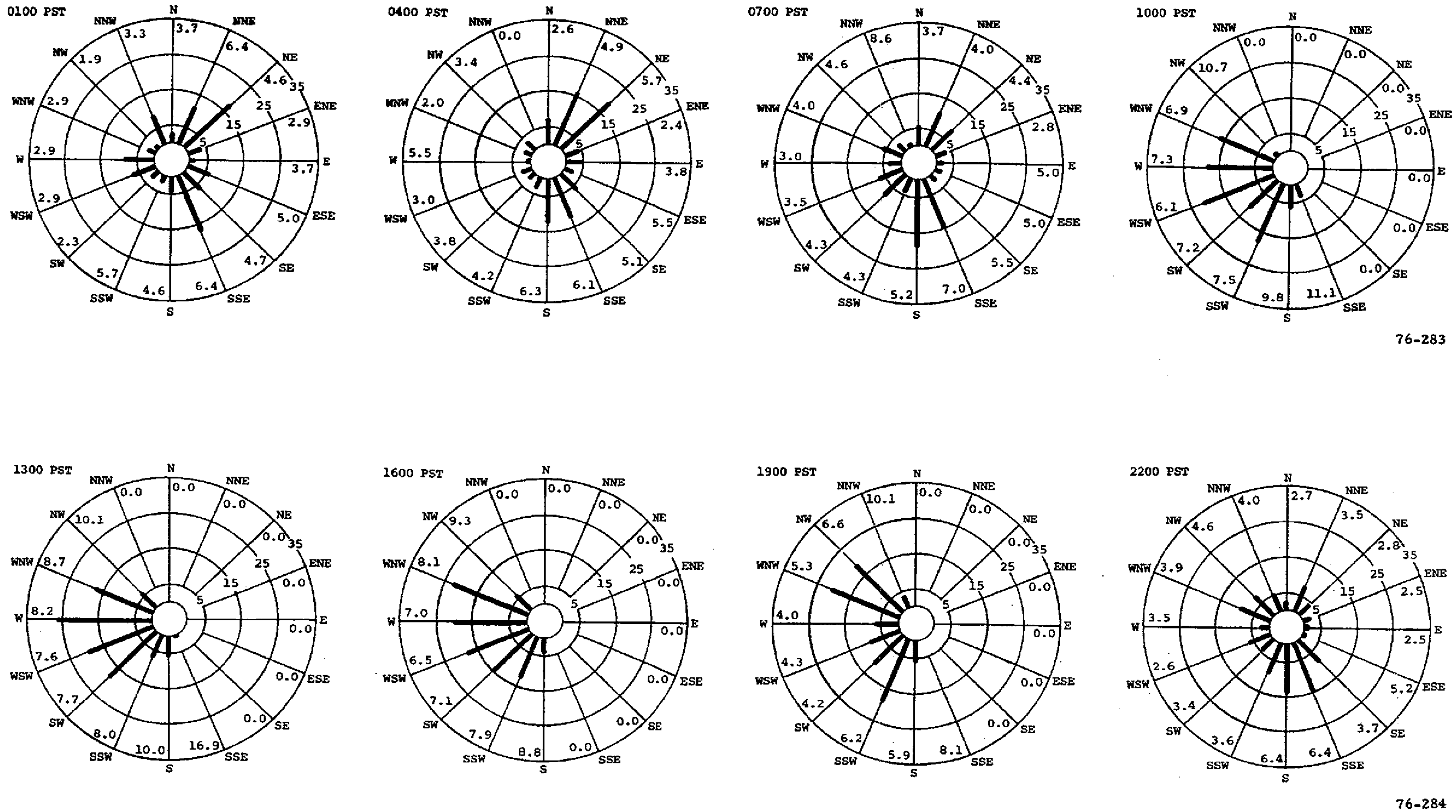

SOLID LINE REPRESENTS PERCENTAGE FREQUENCY OF OCCURRENCE BY SECTOR
AVERAGE WIND SPEED BY SECTOR IS MI/H.

10079-110-367
27JL6

SAN ONOFRE NUCLEAR GENERATING STATION Units 2 & 3

SAN ONOFRE JULY AVERAGE
3-HOURLY WIND ROSES, 10m LEVEL
(DATA PERIOD 1/25/73 THROUGH 1/24/76)

Figure 2.3-4

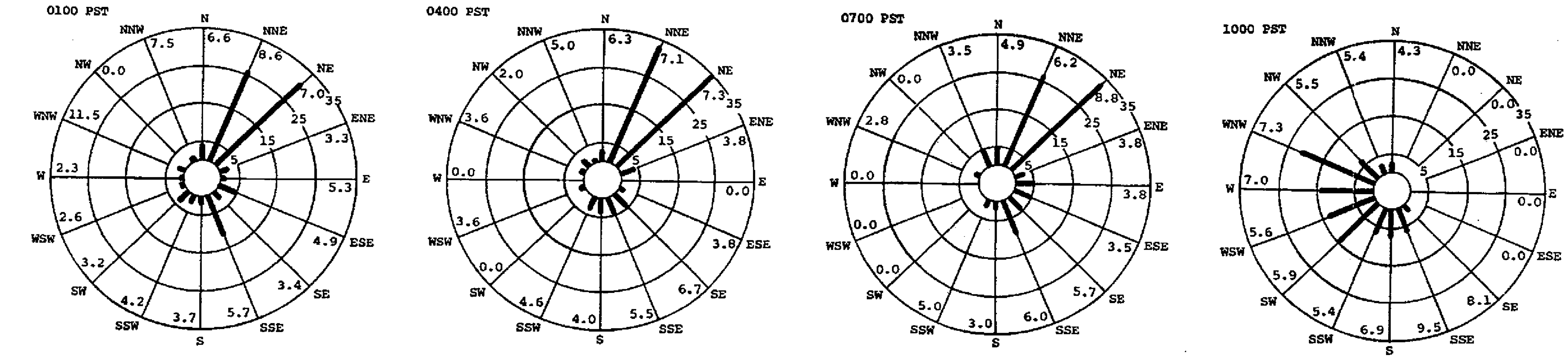

76-285

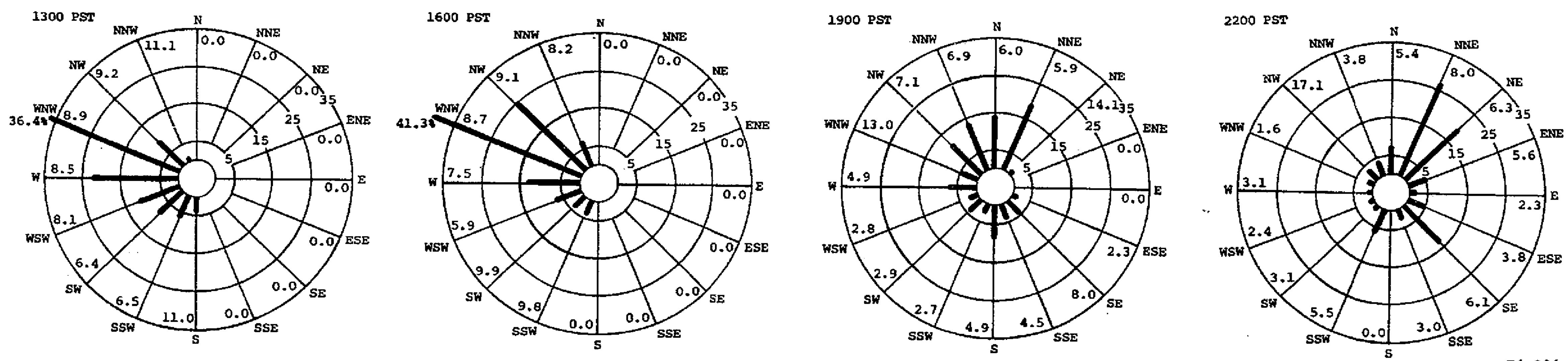

76-286

SOLID LINE REPRESENTS PERCENTAGE FREQUENCY OF OCCURRENCE BY SECTOR
AVERAGE WIND SPEED BY SECTOR IS MI/H.

SAN ONOFRE NUCLEAR GENERATING STATION Units 2 & 3
SAN ONOFRE OCTOBER AVERAGE 3-HOURLY WIND ROSES, 10m LEVEL (DATA PERIOD 1/25/73 THROUGH 1/24/76)
Figure 2.3-5

10079-11D-368
27JL6

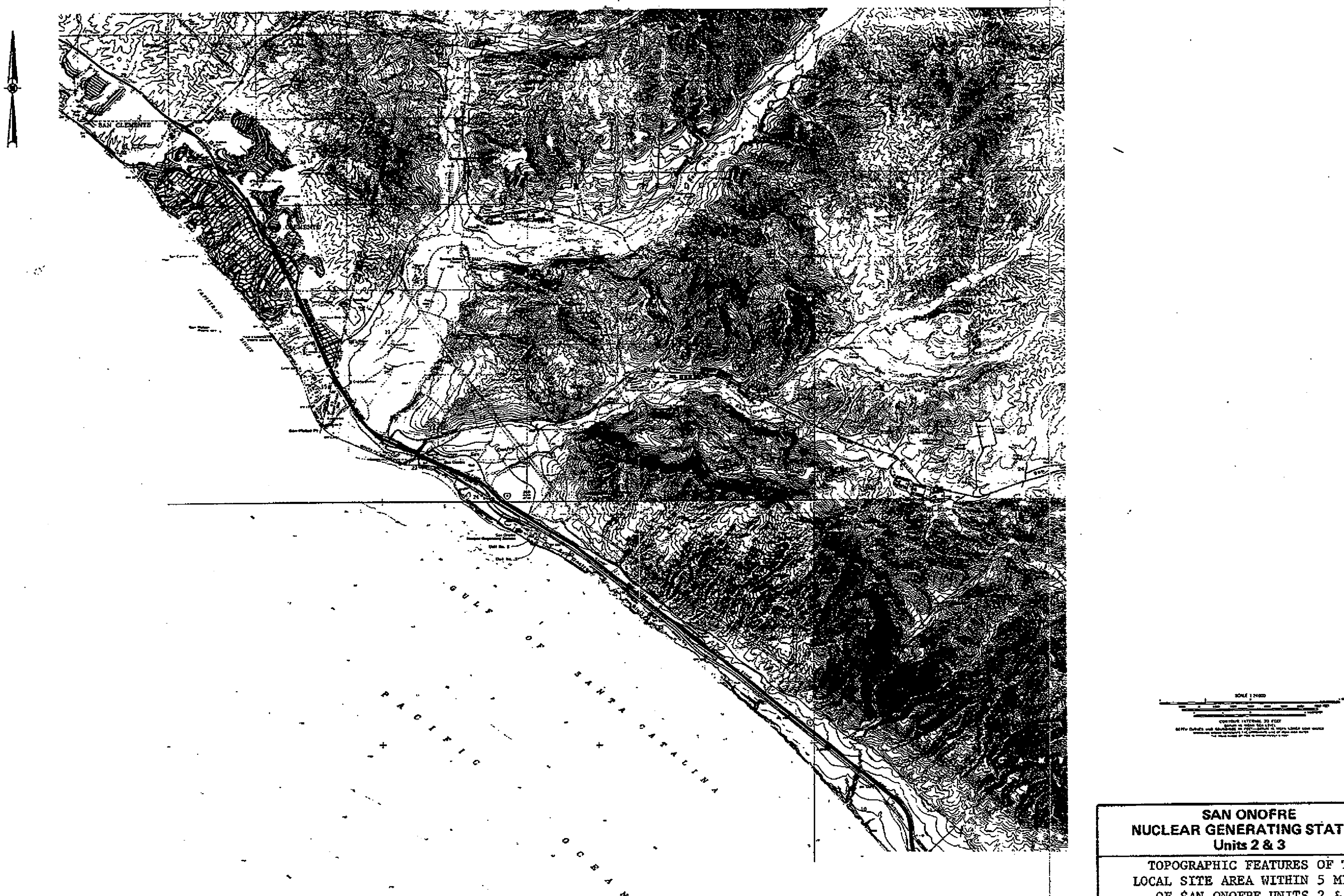

SAN ONOFRE
NUCLEAR GENERATING STATION
Units 2 & 3

TOPOGRAPHIC FEATURES OF THE LOCAL SITE AREA WITHIN 5 MILES OF SAN ONOFRE UNITS 2 & 3

Figure 2.3-6

10079-11D-458
273L6

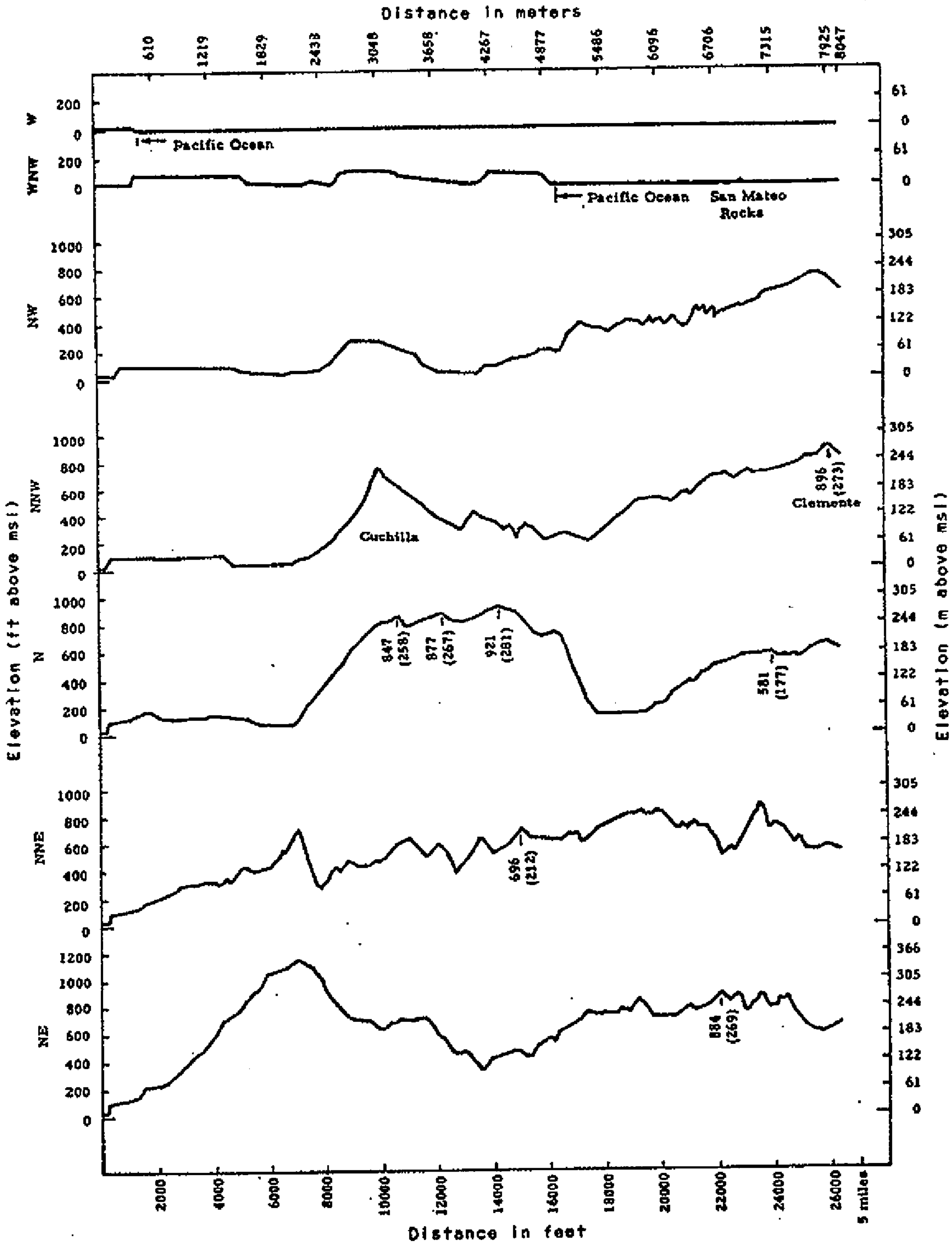

SAN ONOFRE NUCLEAR GENERATING STATION Units 2 & 3

ELEVATION vs. DISTANCE (NE, NNE, N, NNW, NW, WNW, W)

Figure 2.3-7

10079-11D-749
235E6

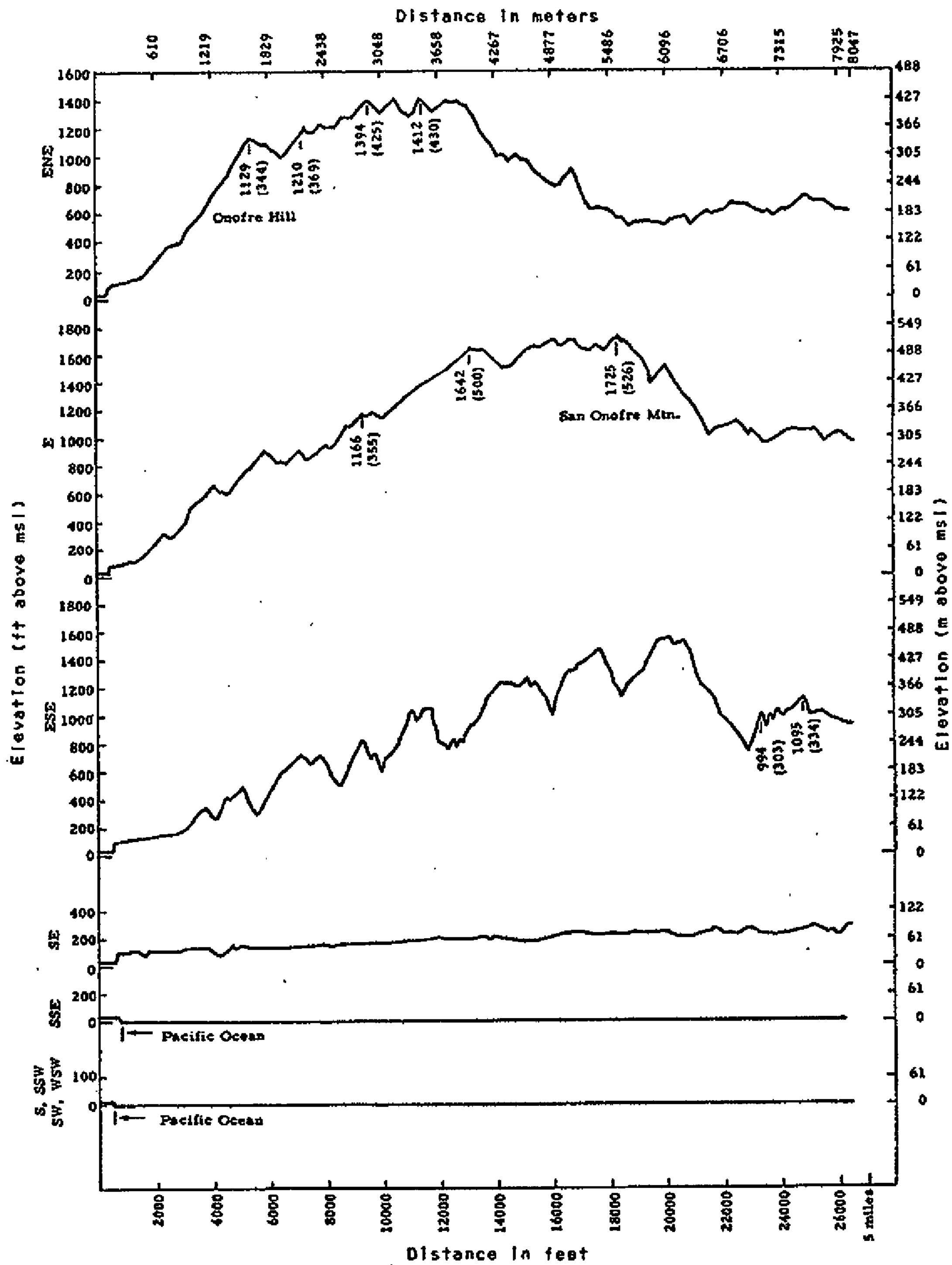

10079-11D-750
235E6

SAN ONOFRE
NUCLEAR GENERATING STATION
Units 2 & 3

ELEVATION vs. DISTANCE
(S, SSW, SW, WSW, SSE, SE,
ESE, E, ENE)

Figure 2.3-8

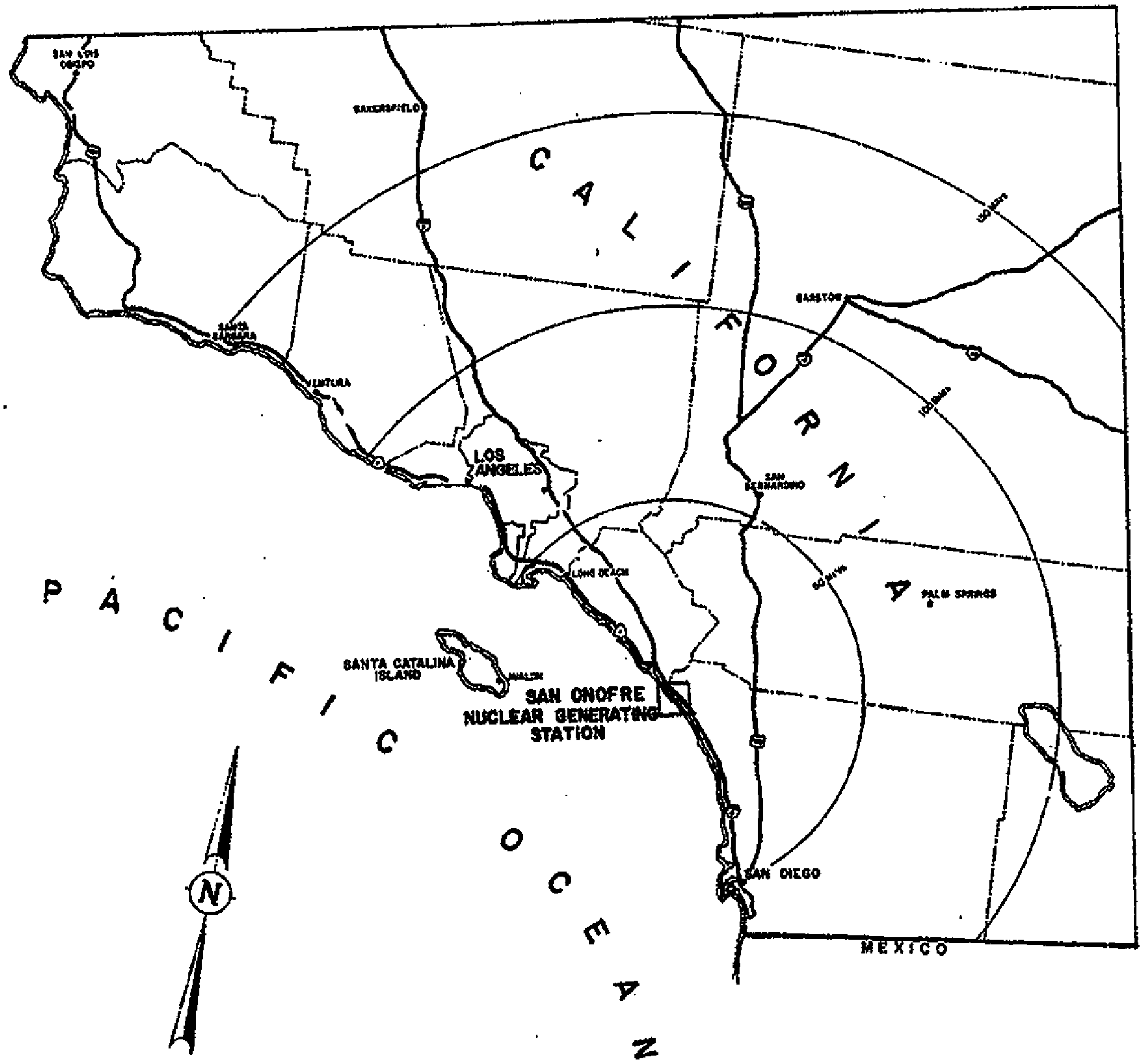

SAN ONOFRE NUCLEAR GENERATING STATION Units 2 & 3
SITE LOCATION
Figure 2.4-1

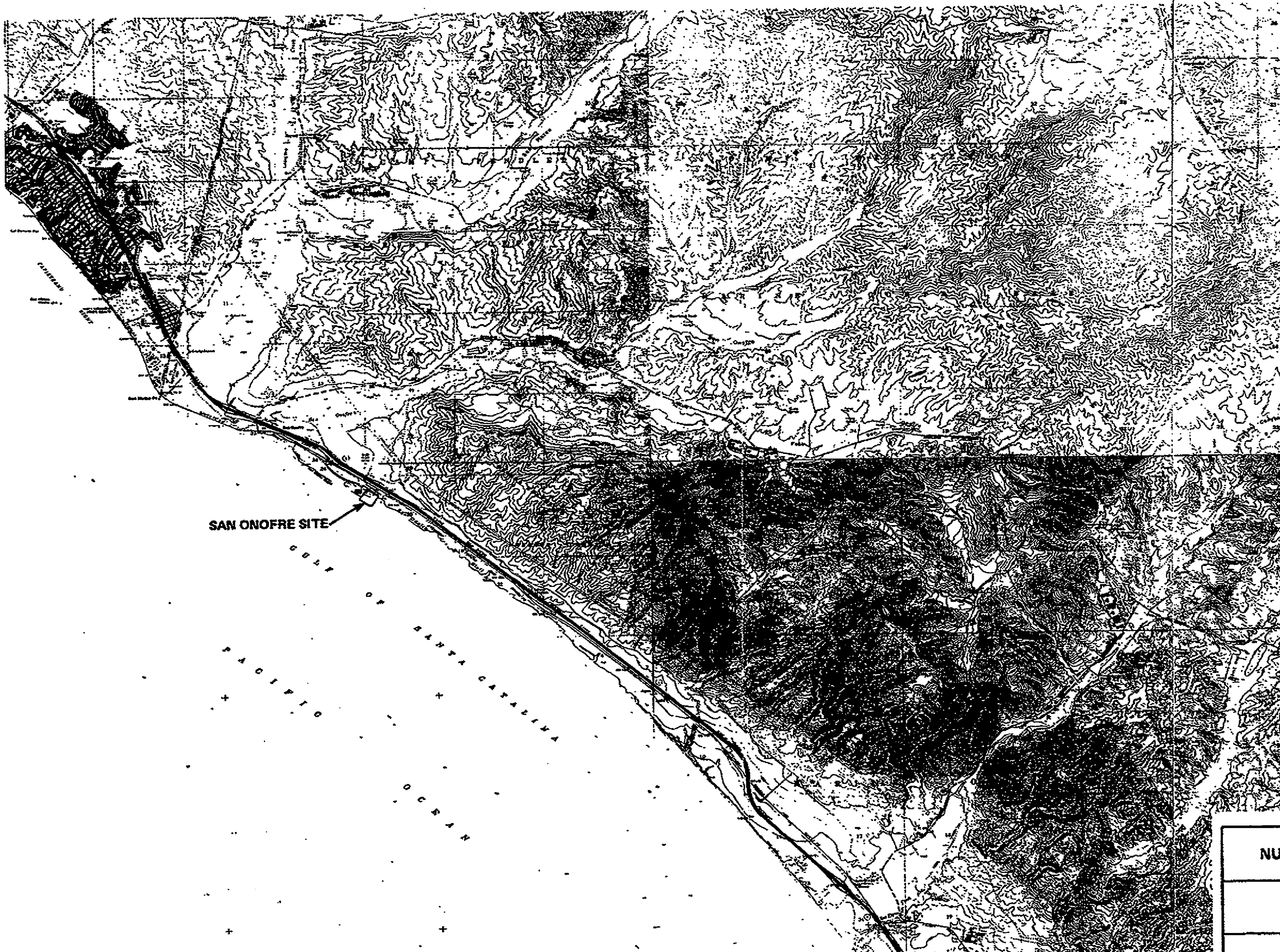

SAN ONOFRE
NUCLEAR GENERATING STATION
Units 2 & 3

SITE VICINITY MAP

Figure 2.4-2

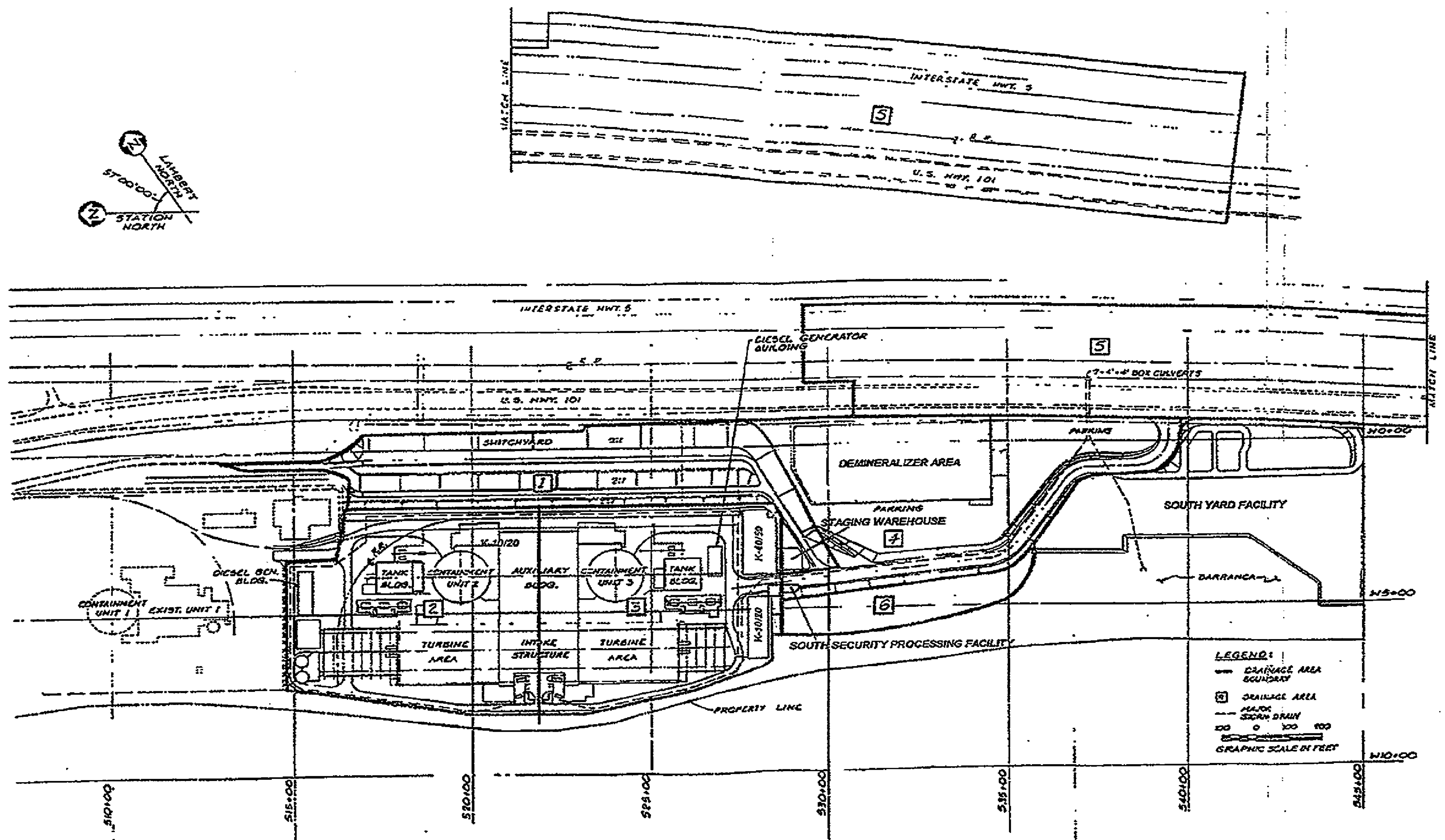

SAN ONOFRE NUCLEAR GENERATING STATION
Units 2 & 3
Updated Final Safety Analysis Report

SITE SUB-BASIN DRAINAGE AREAS

Figure 2.4-3

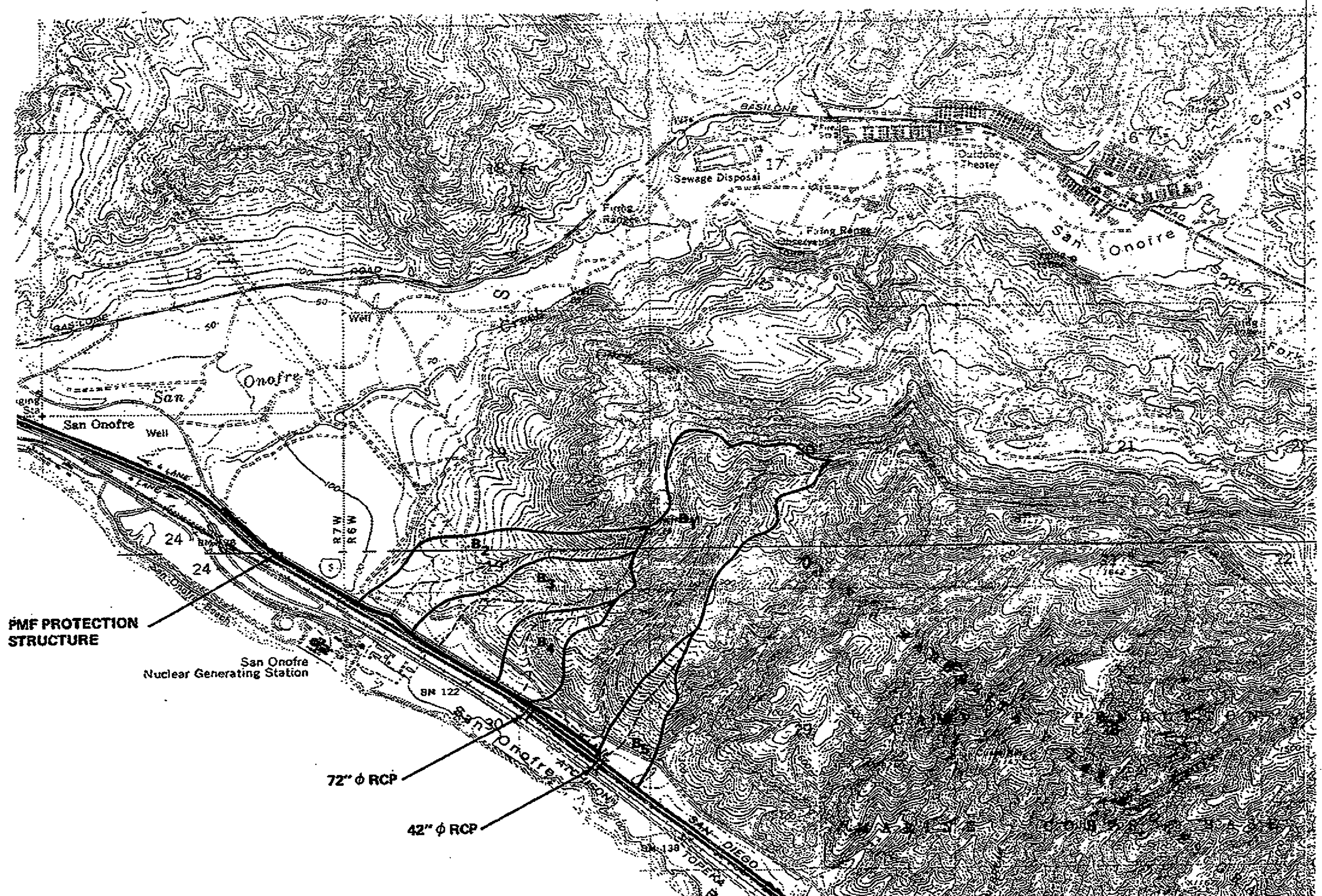

SAN ONOFRE NUCLEAR GENERATING STATION Units 2 & 3

PMF PROTECTION STRUCTURE ALIGNMENT

Figure 2.4-4

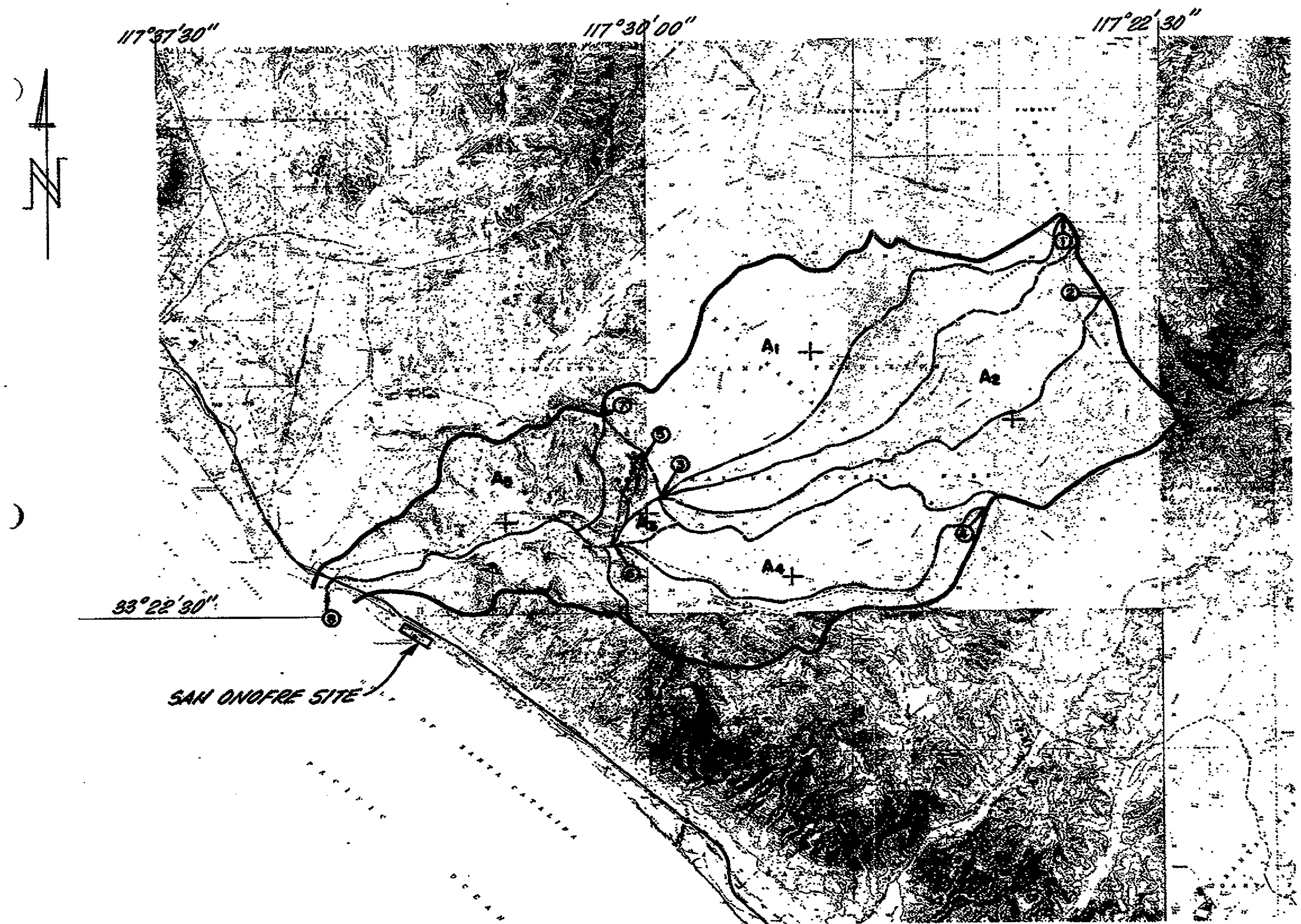

SCALE 1"=8000'

LEGEND

- SAN ONOFRE BASIN DIVIDE
- SUB-BASIN DIVIDE
- MAIN DRAINAGE COURSE
- \+ CENTROID OF SUB-BASIN
- ② STATIONING FOR ROUTING REACH
- A_1 SUB-BASIN IDENTIFICATION.

SAN ONOFRE NUCLEAR GENERATING STATION Units 2 & 3
SAN ONOFRE CREEK DRAINAGE BASIN
Figure 2.4-5

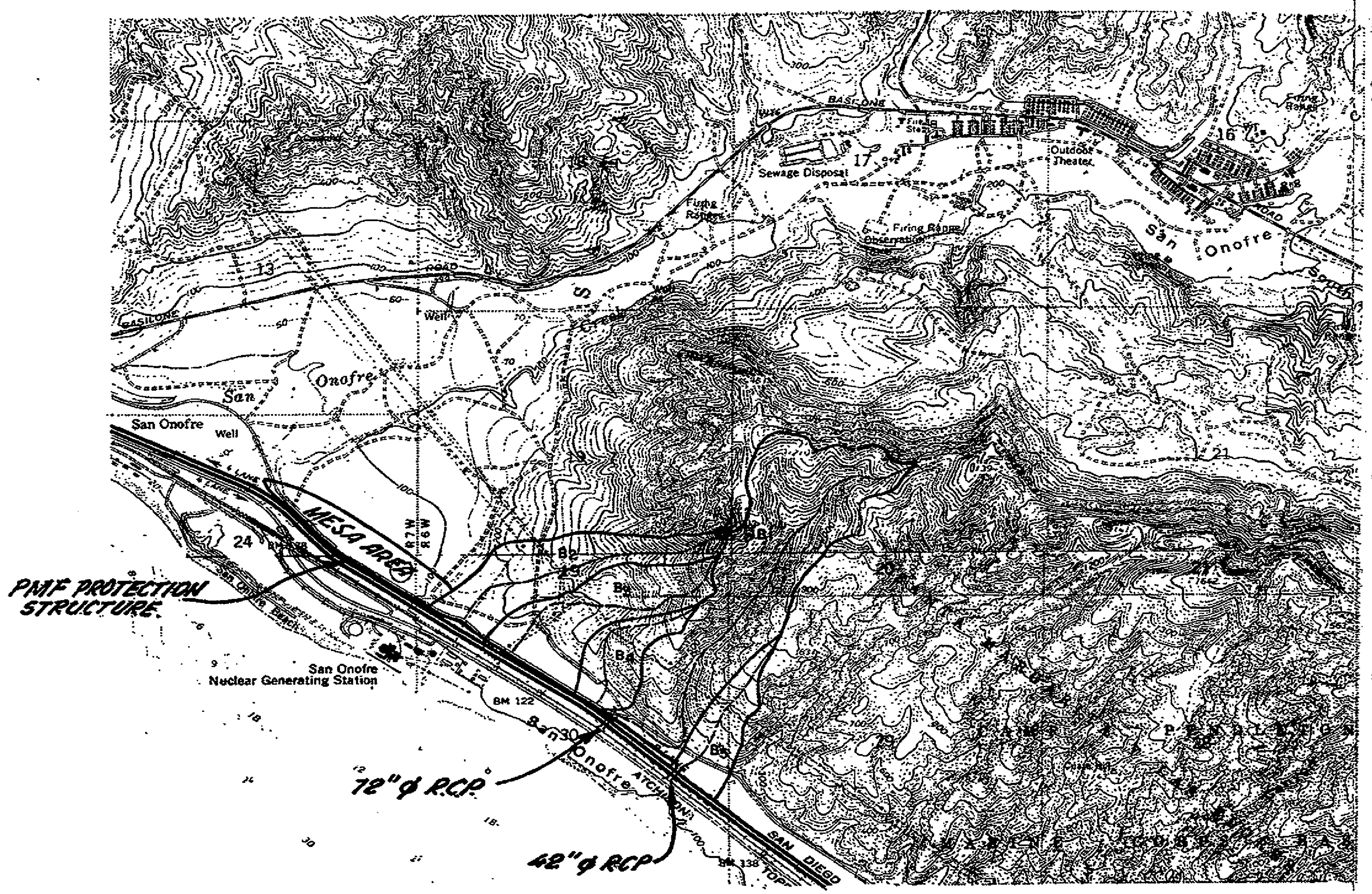

SAN ONOFRE
NUCLEAR GENERATING STATION
Units 2 & 3

FOOTHILL DRAINAGE BASIN

Figure 2.4-6

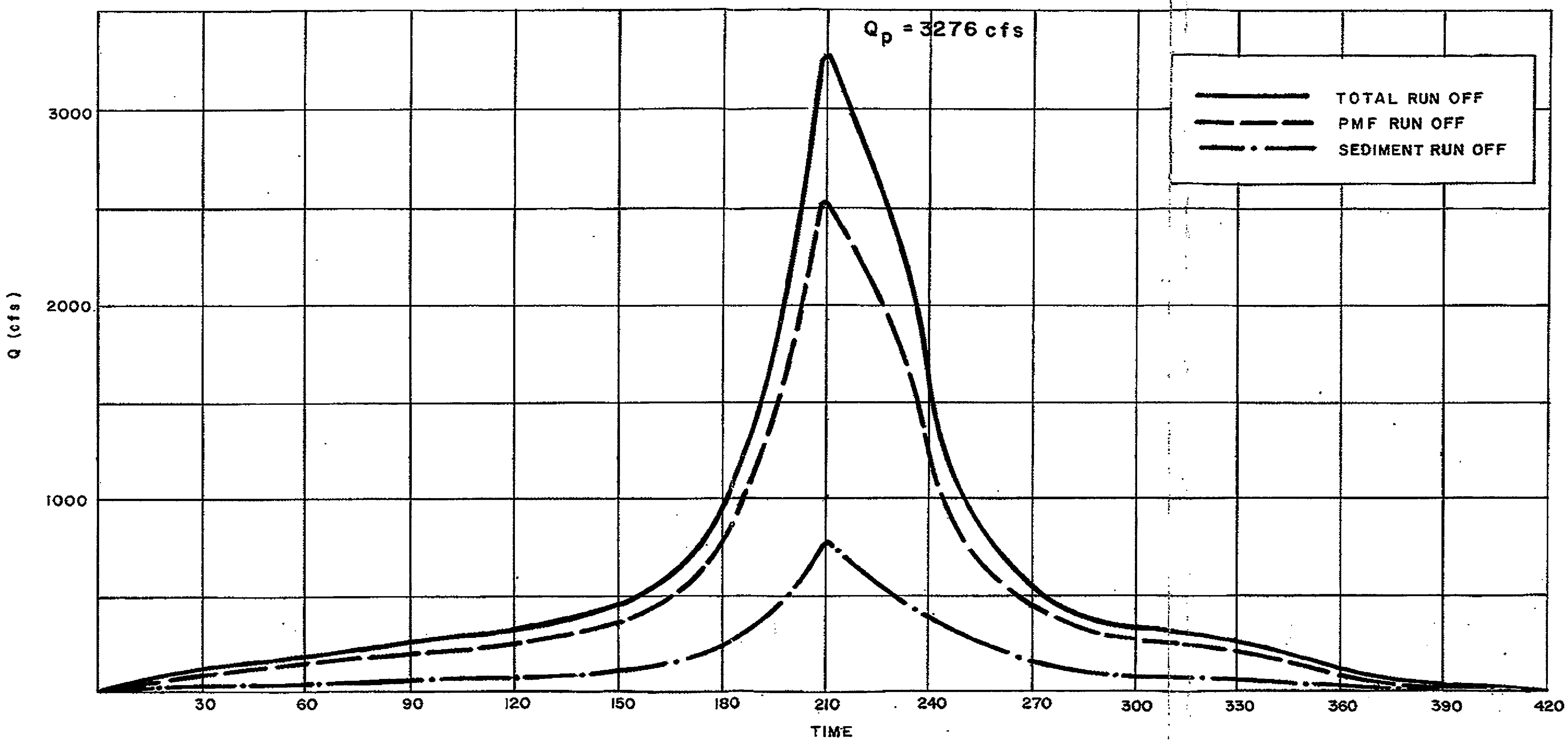

SAN ONOFRE
NUCLEAR GENERATING STATION
Units 2 & 3

PMF HYDROGRAPH
FOOTHILL DRAINAGE BASIN
SUB-BASIN B-1

Figure 2.4-7

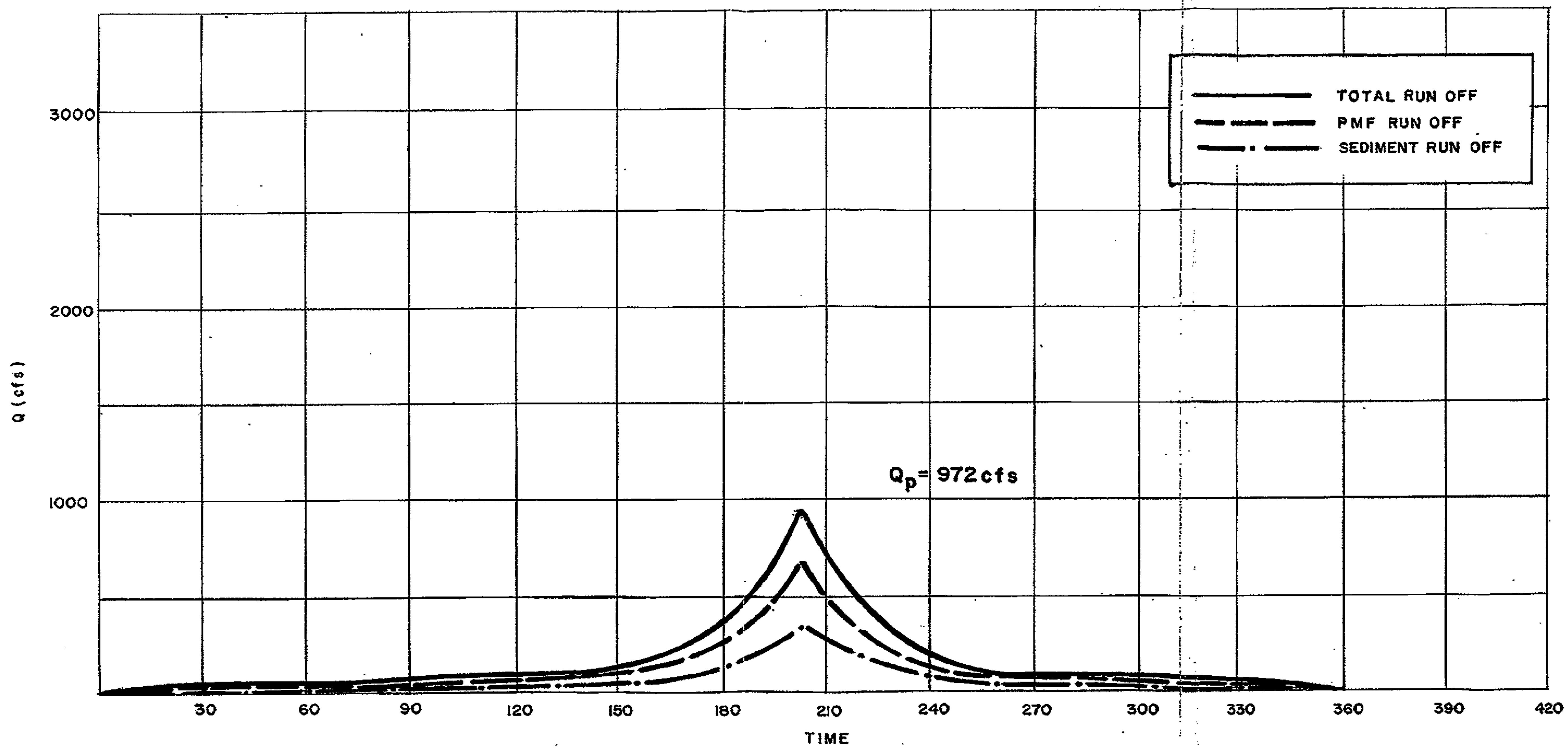

SAN ONOFRE
NUCLEAR GENERATING STATION
Units 2 & 3

PMF HYDROGRAPH
FOOTHILL DRAINAGE BASIN
SUB-BASIN B-4

Figure 2.4-8

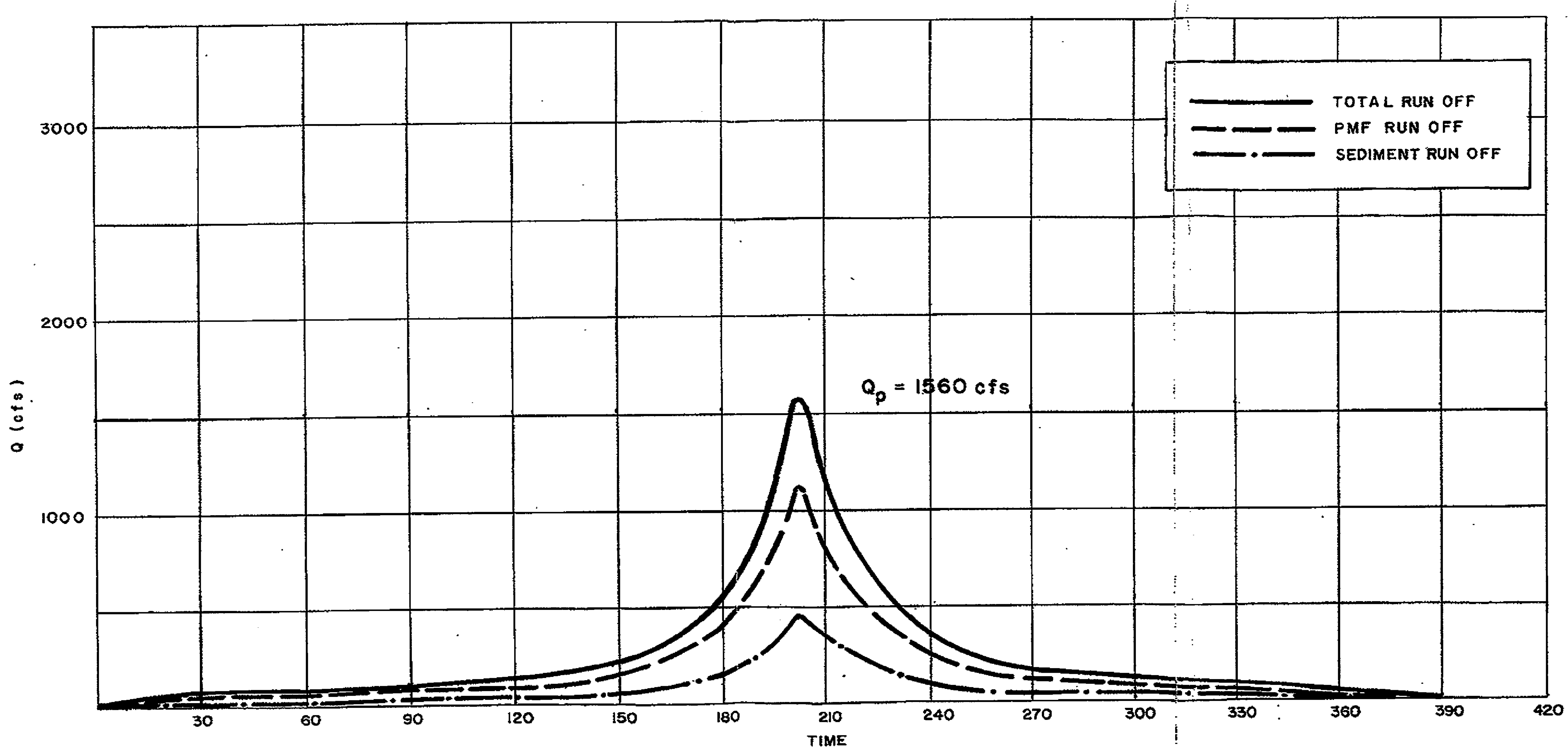

SAN ONOFRE
NUCLEAR GENERATING STATION
Units 2 & 3

PMF HYDROGRAPH
FOOTHILL DRAINAGE BASIN
SUB-BASIN B-3

Figure 2.4-9

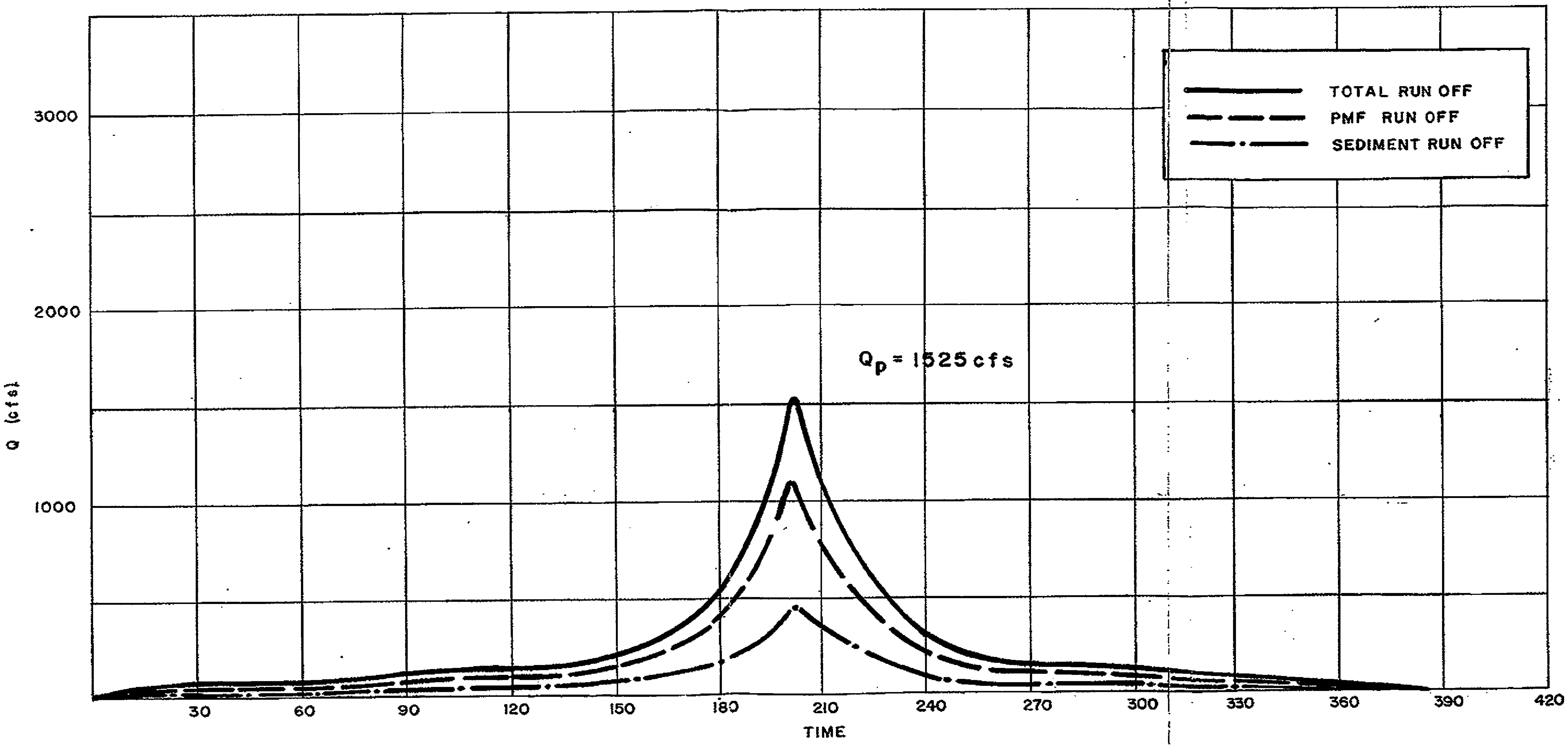

SAN ONOFRE
NUCLEAR GENERATING STATION
Units 2 & 3

PMF HYDROGRAPH
FOOTHILL DRAINAGE BASIN
SUB-BASIN B-2

Figure 2.4-10

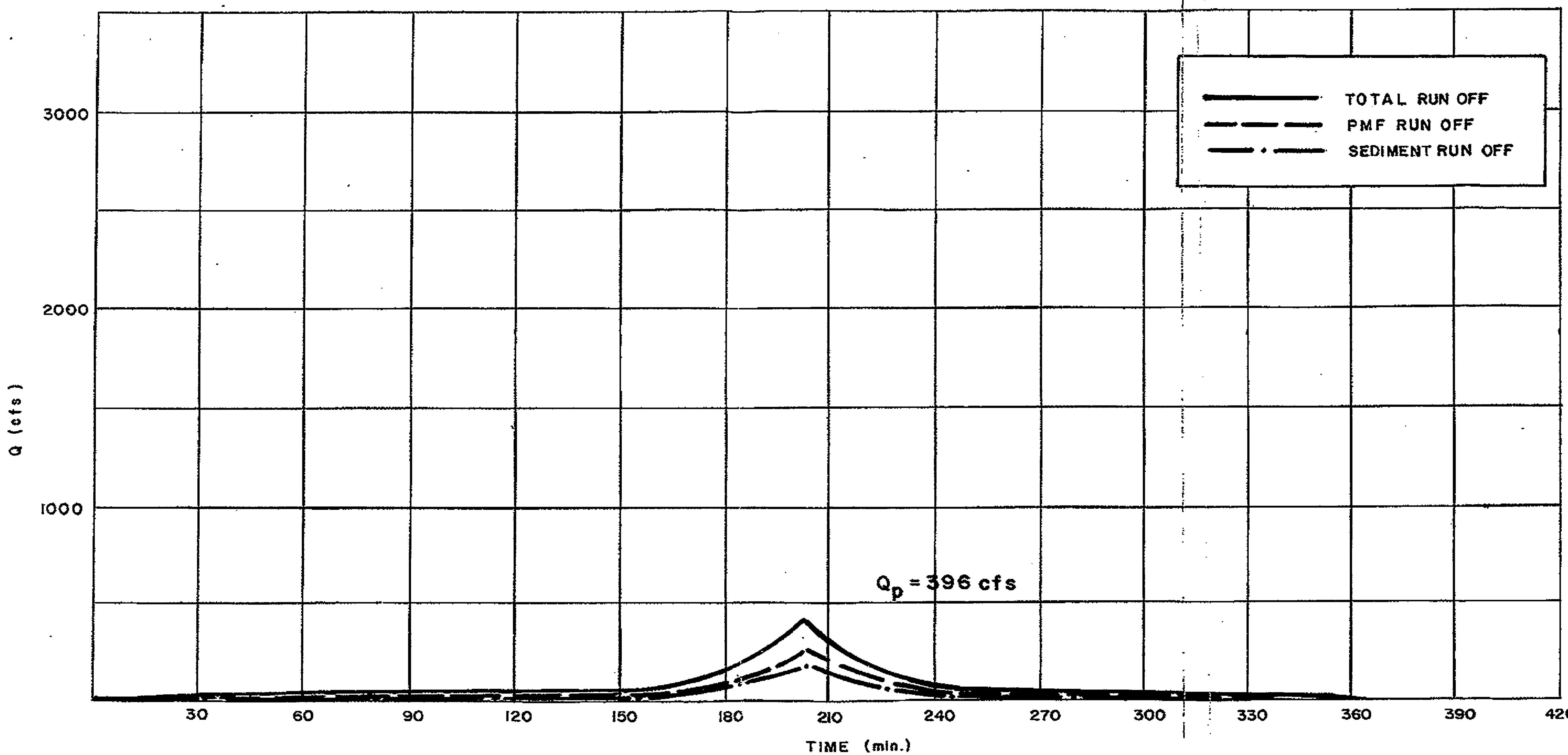

SAN ONOFRE
NUCLEAR GENERATING STATION
Units 2 & 3

PMF HYDROGRAPH
FOOTHILL DRAINAGE SYSTEM
SUB-BASIN MESA

Figure 2.4-11

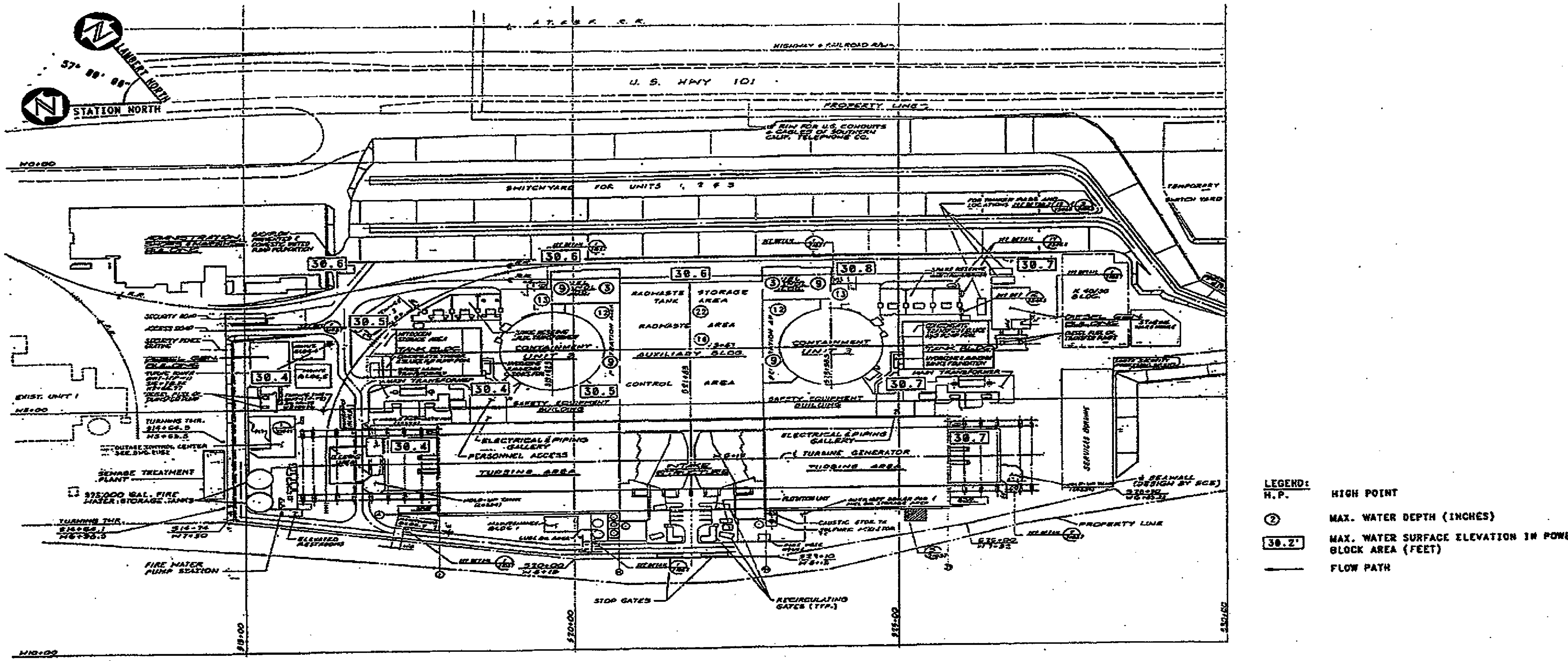

NOTE: FOR FACILITIES NOT SHOWN SEE PLOT PLAN FIGURES 1.2-1 AND 2.1-1

SAN ONOFRE NUCLEAR GENERATING STATION
Units 2 & 3
Updated Final Safety Analysis Report

FLOOD ELEVATIONS AND WATER DEPTHS

Figure 2.4-13

SOURCE: REFERENCE 8

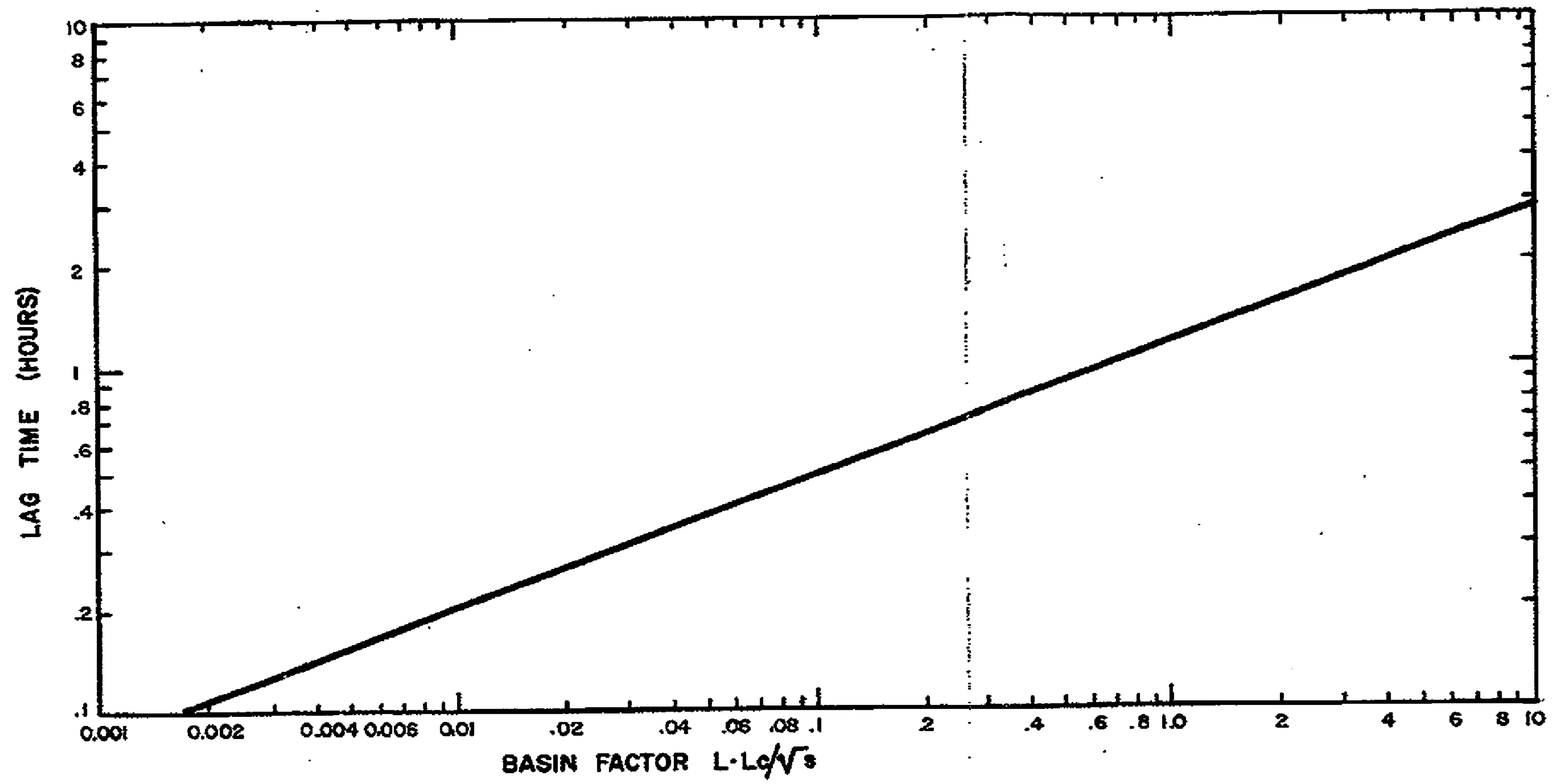

SAN ONOFRE
NUCLEAR GENERATING STATION
Units 2 & 3

BASIN LAG CURVE

Figure 2.4-15

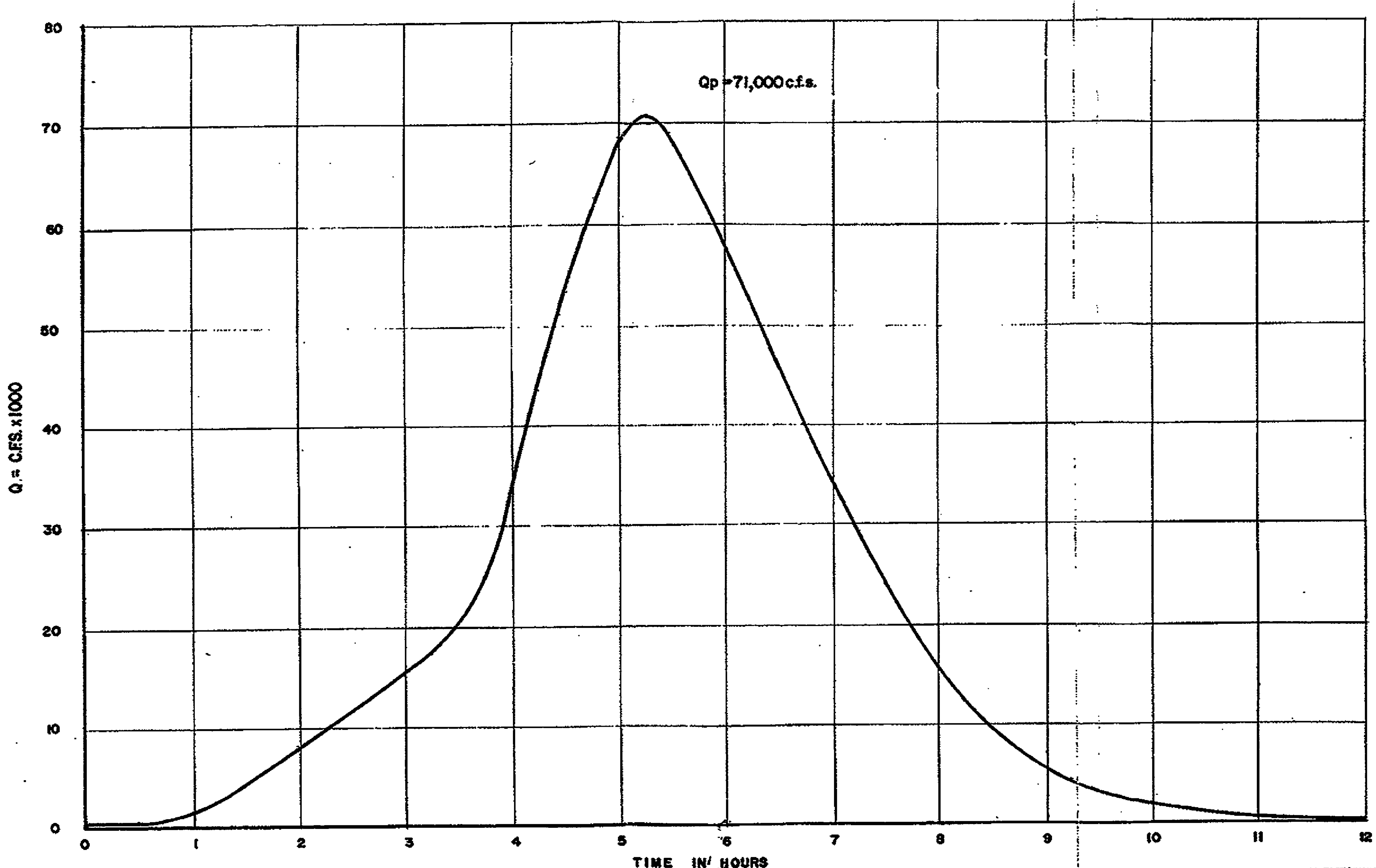

SAN ONOFRE
NUCLEAR GENERATING STATION
Units 2 & 3

PMF HYDROGRAPH
SAN ONOFRE CREEK
AT MOUTH

Figure 2.4-16

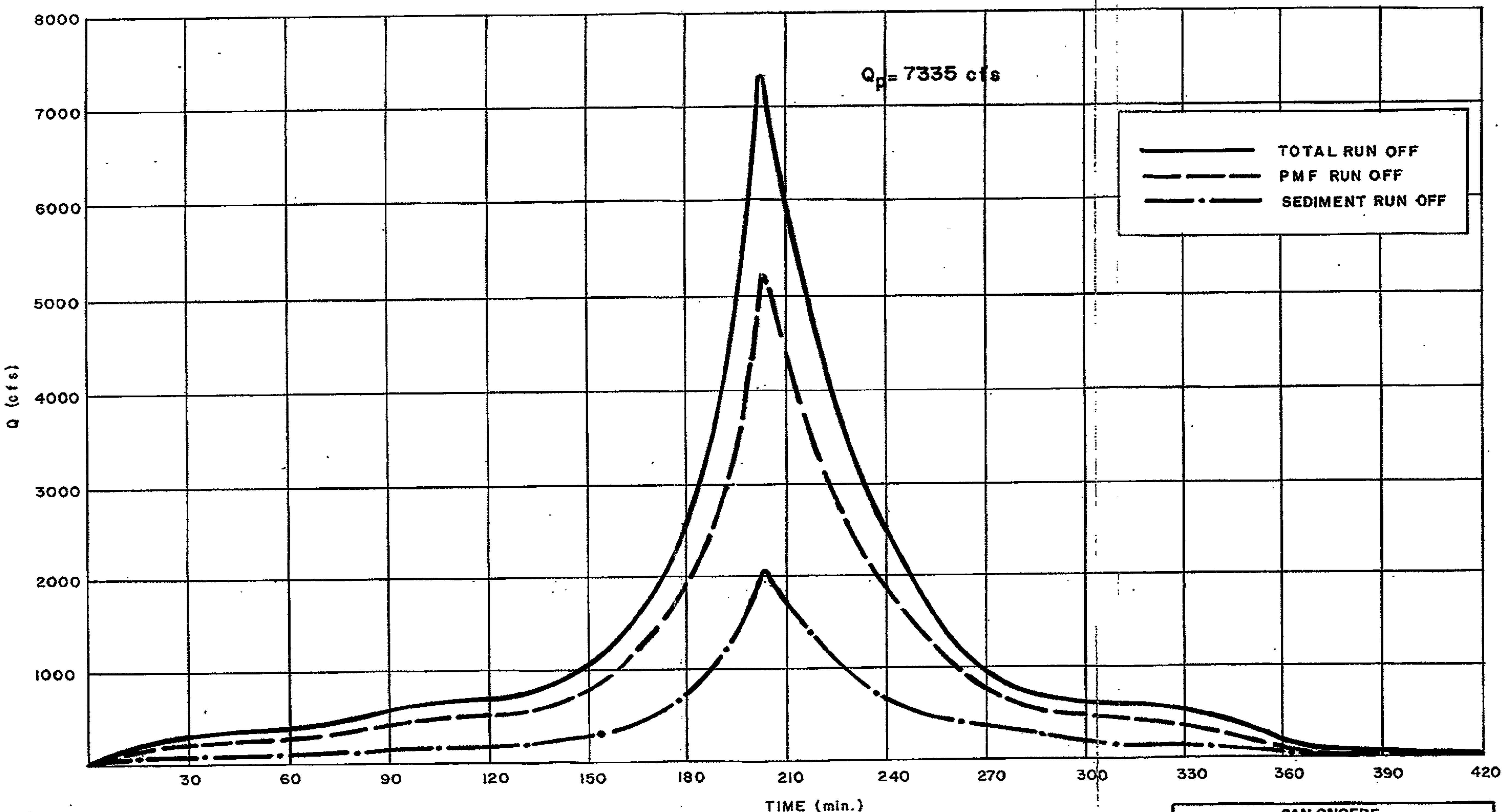

SAN ONOFRE
NUCLEAR GENERATING STATION
Units 2 & 3

PMF HYDROGRAPH
FOOTHILL DRAINAGE BASIN
COMPOSITE HYDROGRAPH

Figure 2.4-17

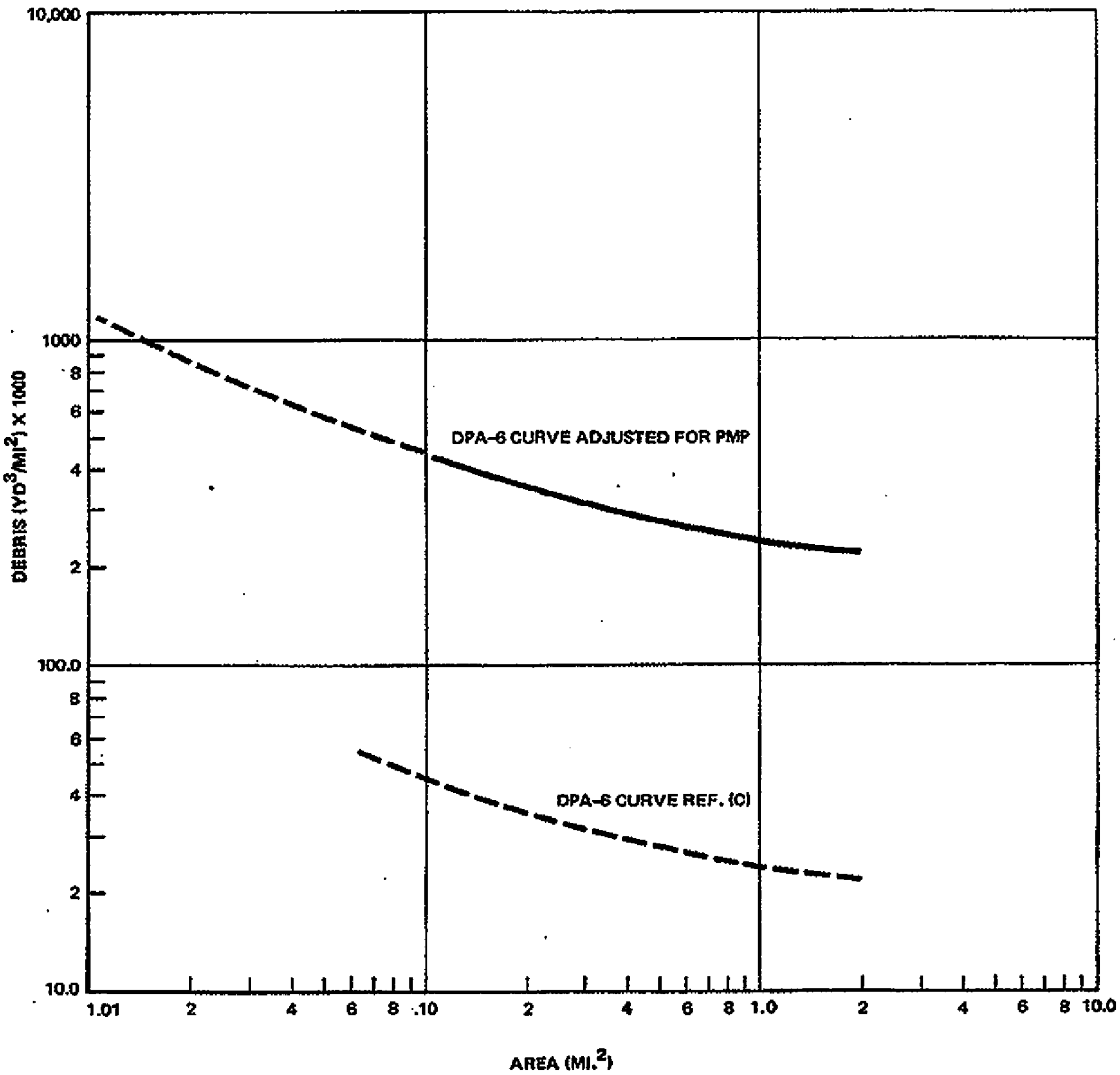

SAN ONOFRE NUCLEAR GENERATING STATION Units 2 & 3
DEBRIS PRODUCTION CURVE FOOTHILL DRAINAGE BASIN
Figure 2.4-18

SAN ONOFRE
NUCLEAR GENERATING STATION
Units 2 & 3

SAN ONOFRE CREEK
CROSS-SECTION LOCATIONS

Figure 2.4-19

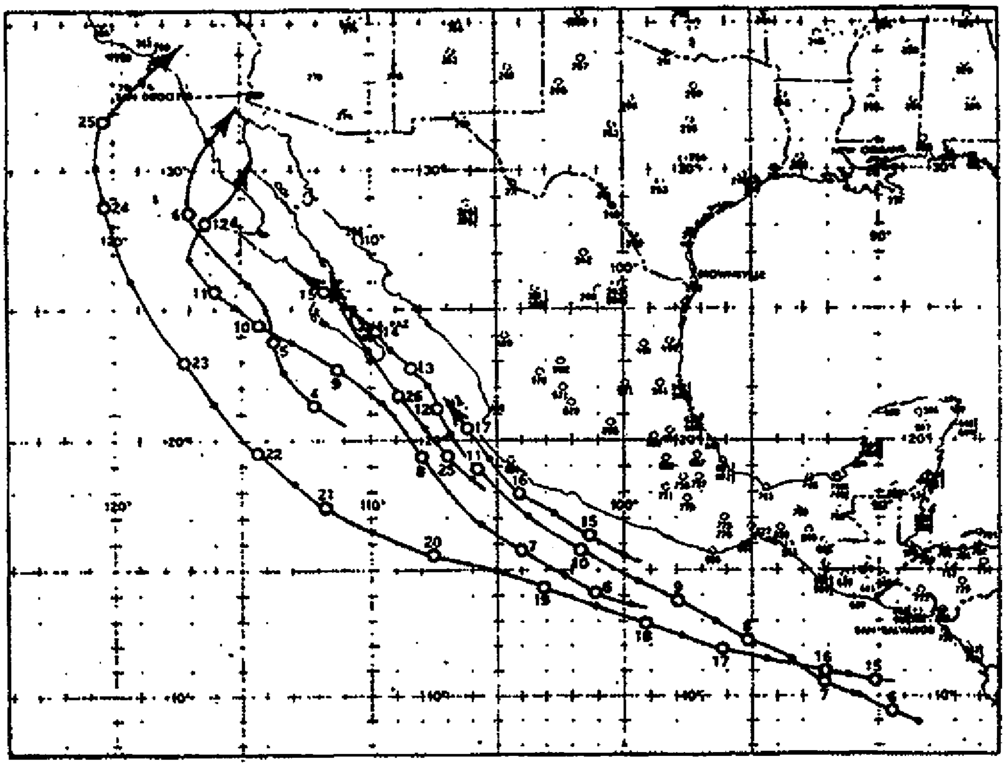

NOTE: NUMBERS ALONG CYCLONE TRACKS DENOTE CALENDAR DATE OF STORM.

SAN ONOFRE
NUCLEAR GENERATING STATION
Units 2 & 3

TRACKS OF TROPICAL CYCLONES ALONG THE WEST COAST OF MEXICO DURING SEPTEMBER 1939

Figure 2.4-23

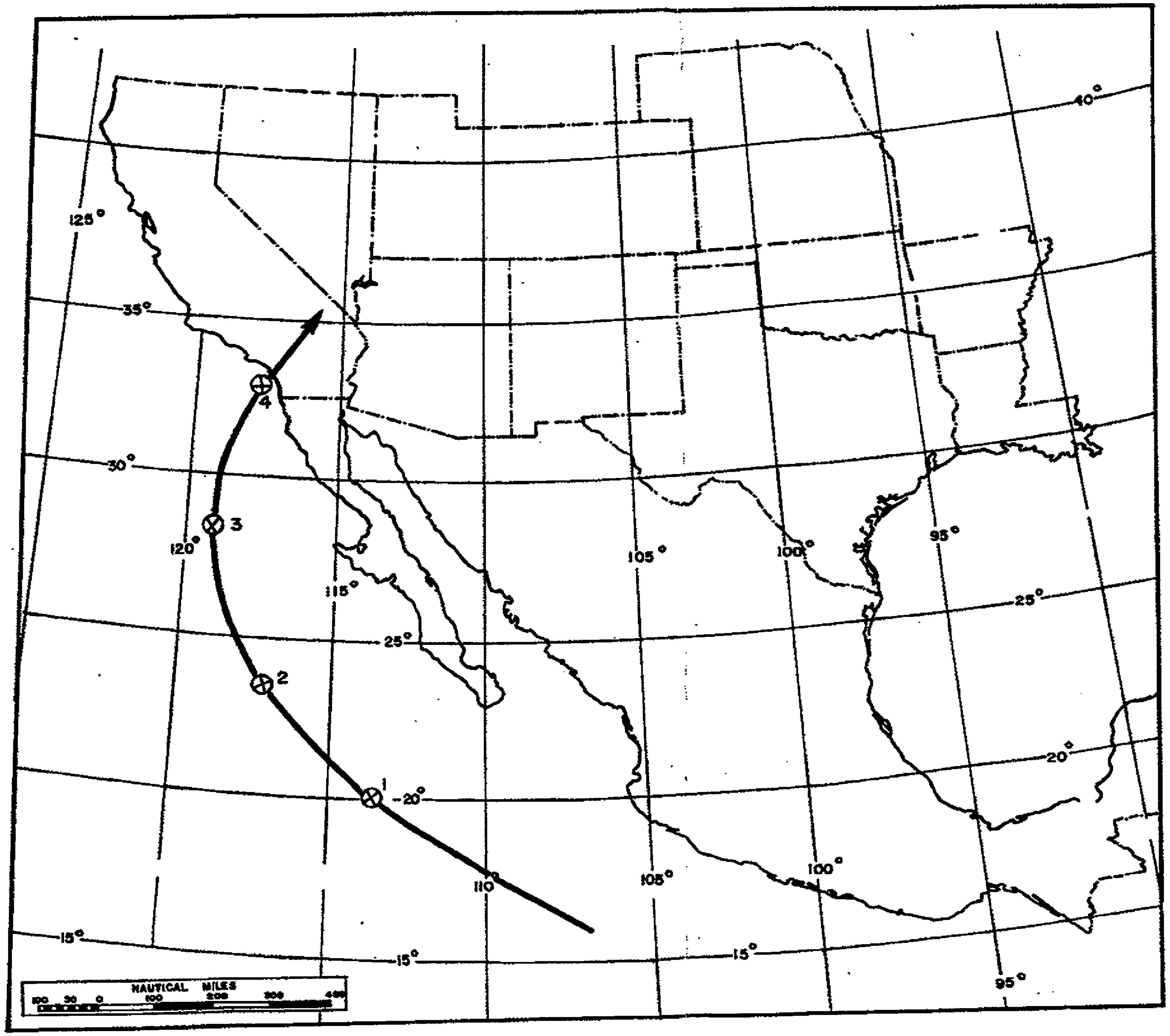

SAN ONOFRE
NUCLEAR GENERATING STATION
Units 2 & 3

TRACK OF THE HYPOTHETICAL HURRICANE THAT CAUSES THE MAXIMUM SURGE AT THE SAN ONOFRE SITE

Figure 2.4-24

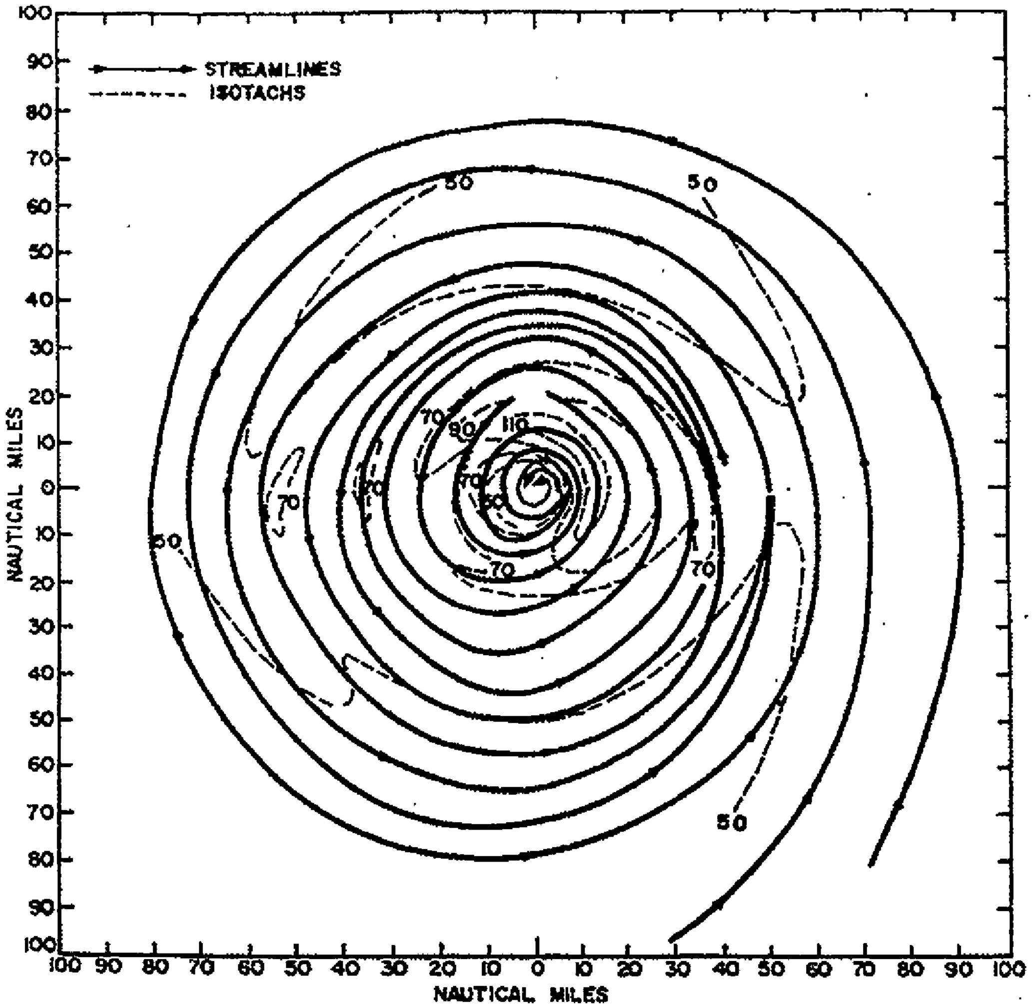

SAN ONOFRE NUCLEAR GENERATING STATION, UNITS 2 & 3

MAXIMUM PROBABLE WIND FIELD (KNOTS) OF HYPOTHETICAL HURRICANE AT POSITIONS 1, 2, AND 3 SHOWN IN FIGURE 2.4-24

Figure: 2.4–25

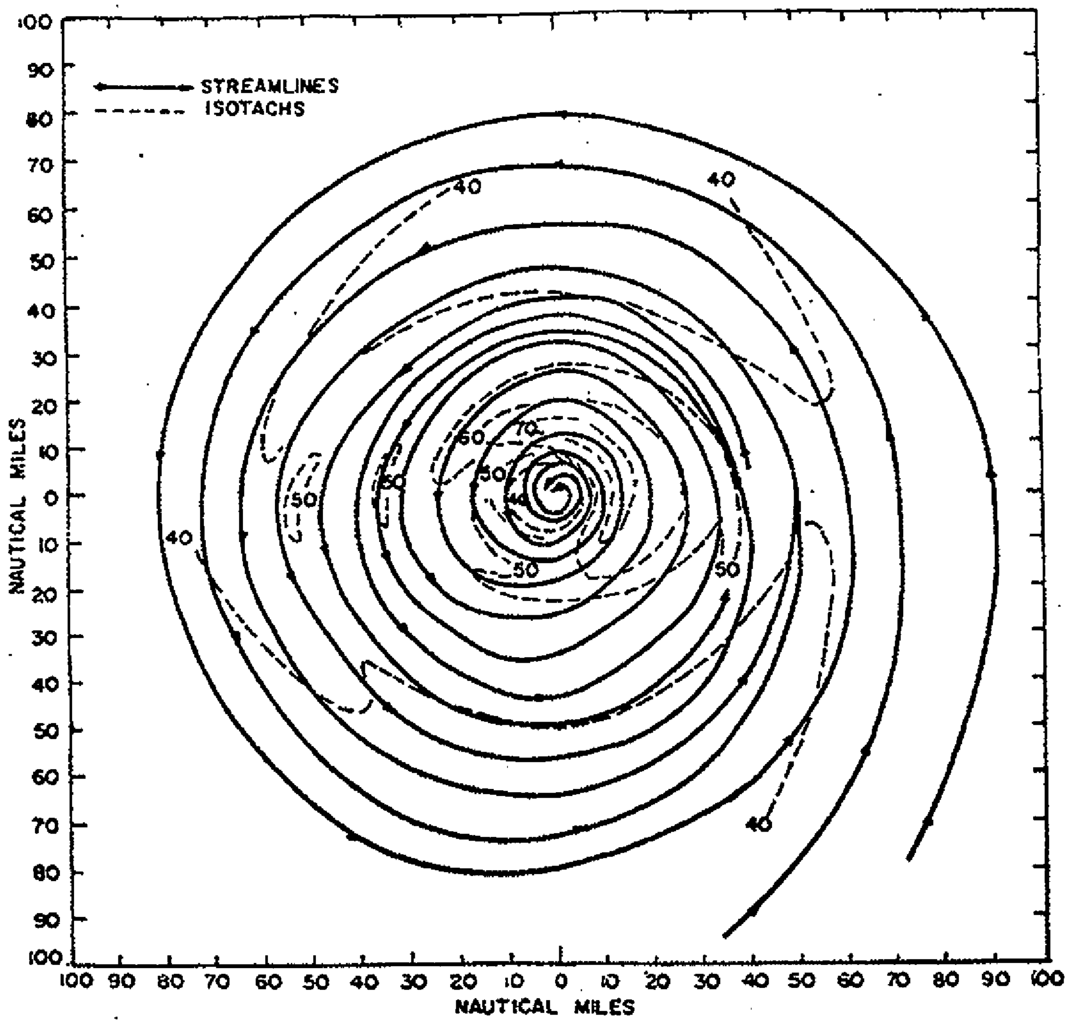

SAN ONOFRE NUCLEAR GENERATING STATION, UNITS 2 & 3

MAXIMUM PROBABLE WIND FIELD (KNOTS) OF HYPOTHETICAL HURRICANE AT POSITION 4 SHOWN IN FIGURE 2.4-24

Figure: 2.4-26

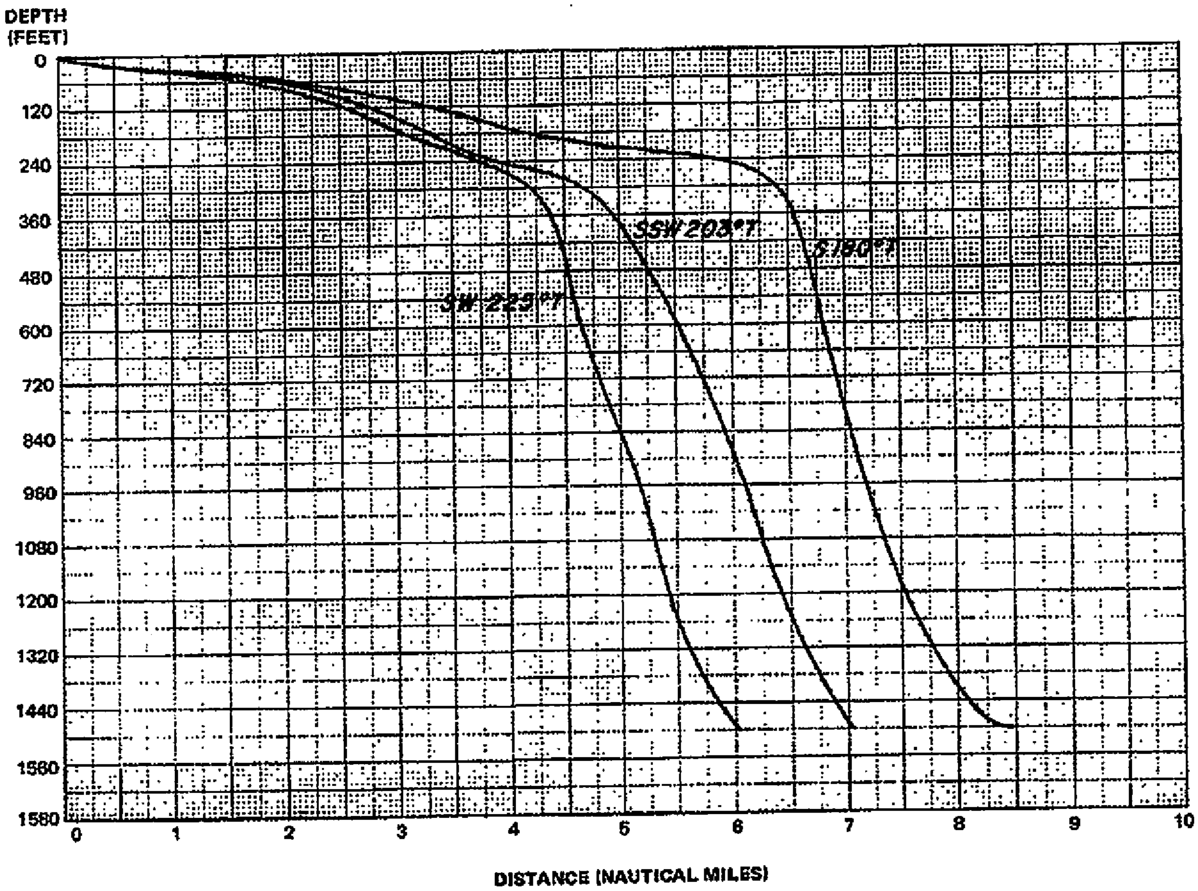

SAN ONOFRE NUCLEAR GENERATING STATION Units 2 & 3
BATHYMETRIC SECTIONS SEAWARD FROM SAN ONOFRE ALONG SELECTED AZIMUTH HEADINGS (Sheet 1 of 2)
Figure 2.4-27

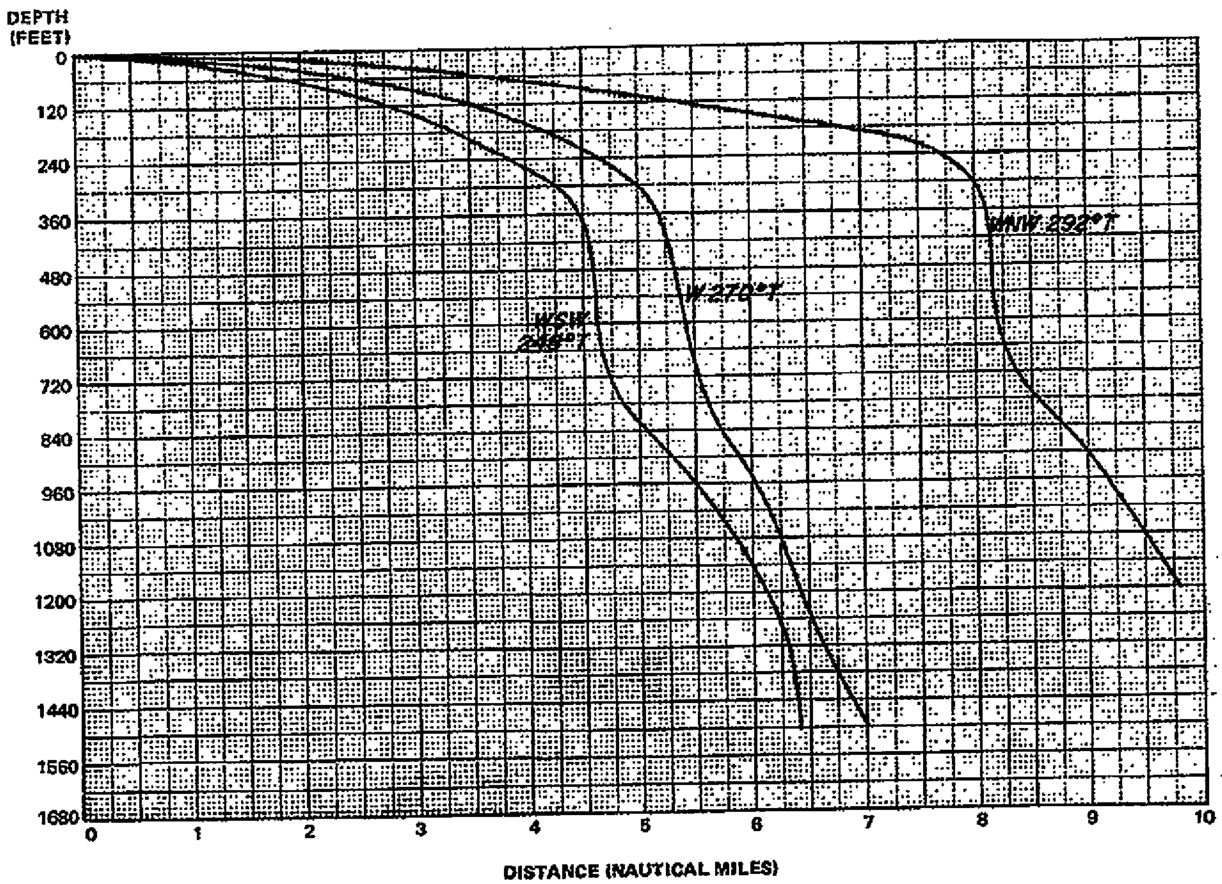

SAN ONOFRE
NUCLEAR GENERATING STATION
Units 2 & 3

BATHYMETRIC SECTIONS
SEAWARD FROM SAN ONOFRE
ALONG SELECTED AZIMUTH HEADINGS
(Sheet 2 of 2)

Figure 2.4-27

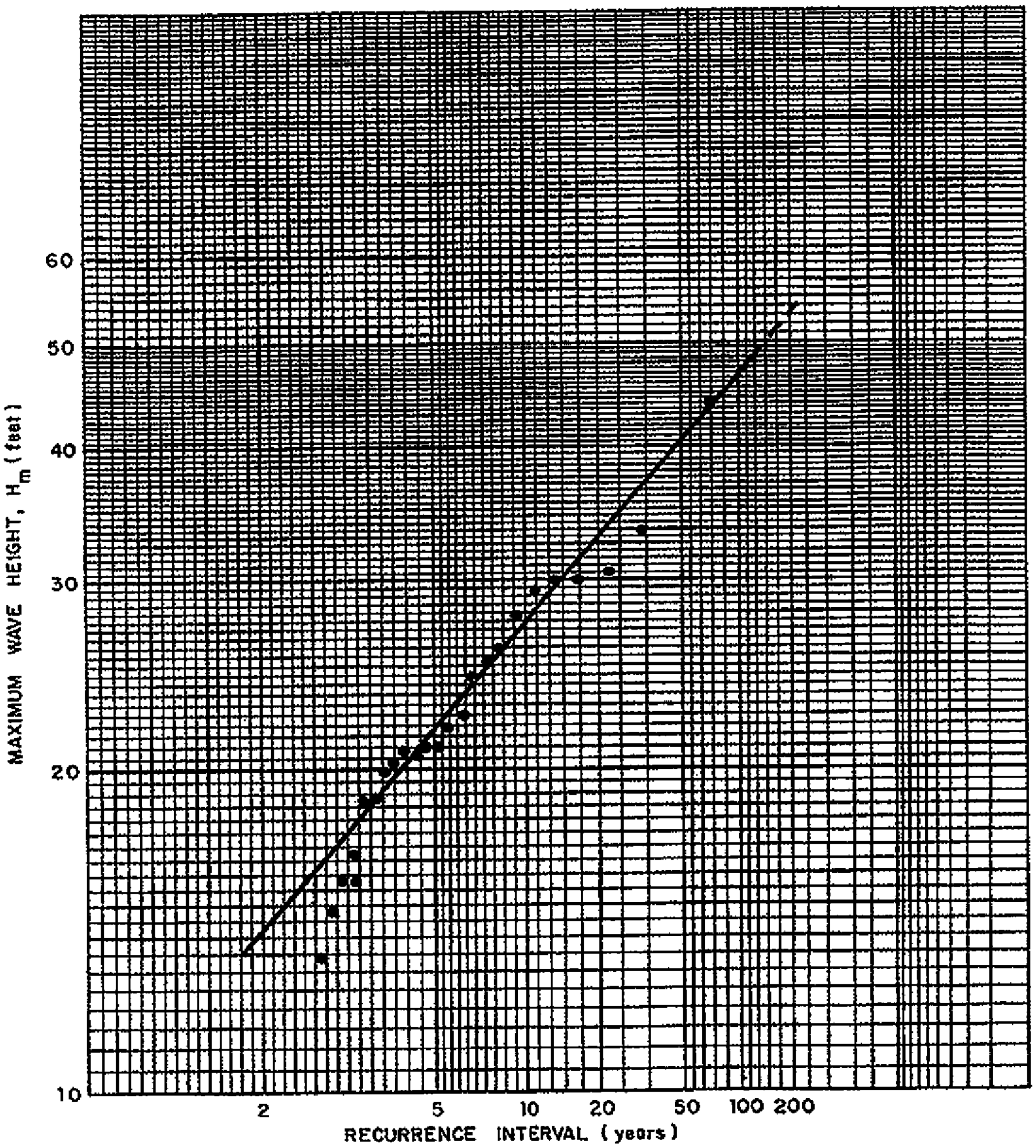

SAN ONOFRE NUCLEAR GENERATING STATION Units 2 & 3

HINDCASTED EXTREME EVENT HIGHEST INDIVIDUAL WAVE RECURRENCE INTERVAL

Figure 2.4-28

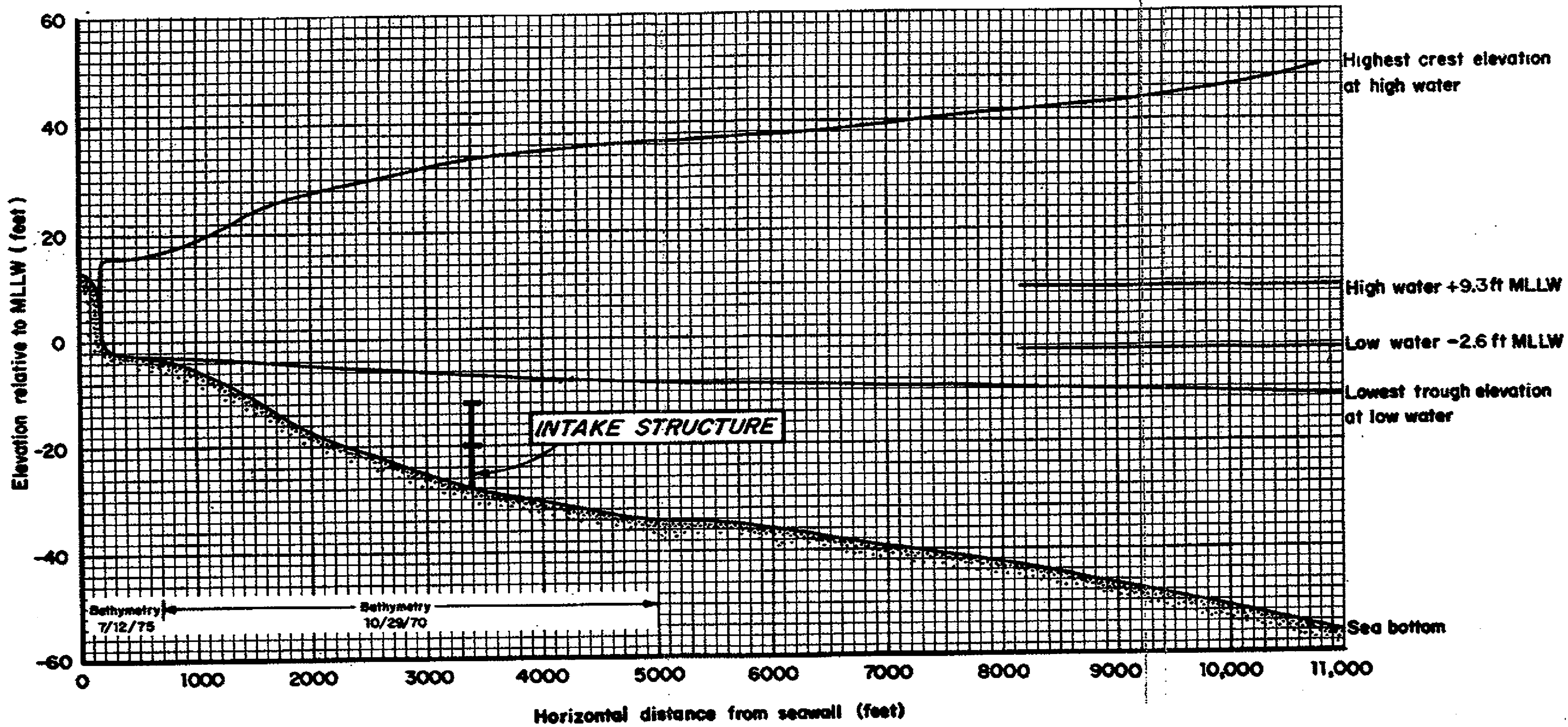

SAN ONOFRE
NUCLEAR GENERATING STATION
Units 2 & 3

HIGHEST STORM WAVE CREST ELEVATIONS AND LOWEST STORM WAVE TROUGH ELEVATIONS AT EXTREME STILL WATER LEVELS, EXCLUDING TSUNAMI

Figure 2.4-29

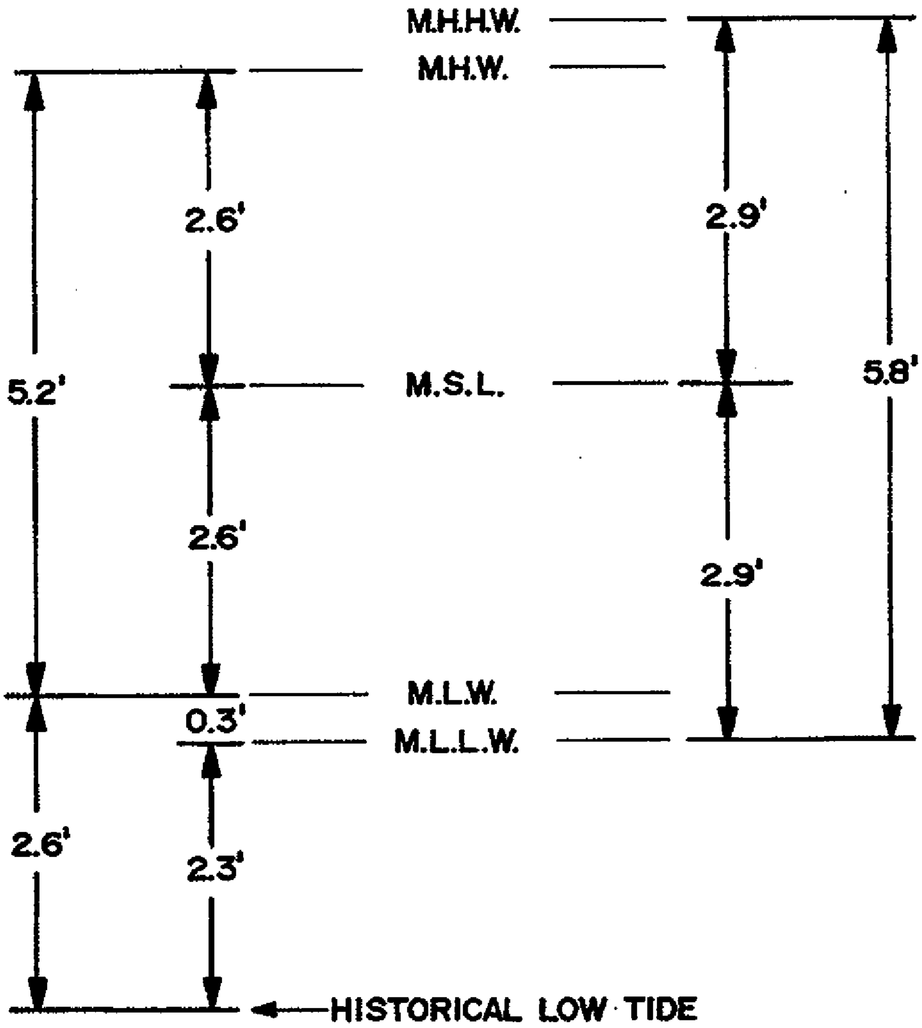

M.H.H.W. – MEAN HIGHER HIGH WATER

M.H.W. – MEAN HIGH WATER

M.S.L. – MEAN SEA LEVEL

M.L.W. – MEAN LOW WATER

M.L.L.W. – MEAN LOWER LOW WATER

SAN ONOFRE NUCLEAR GENERATING STATION Units 2 & 3
REPRESENTATION OF HISTORICAL LOW TIDE
Figure 2.4-30

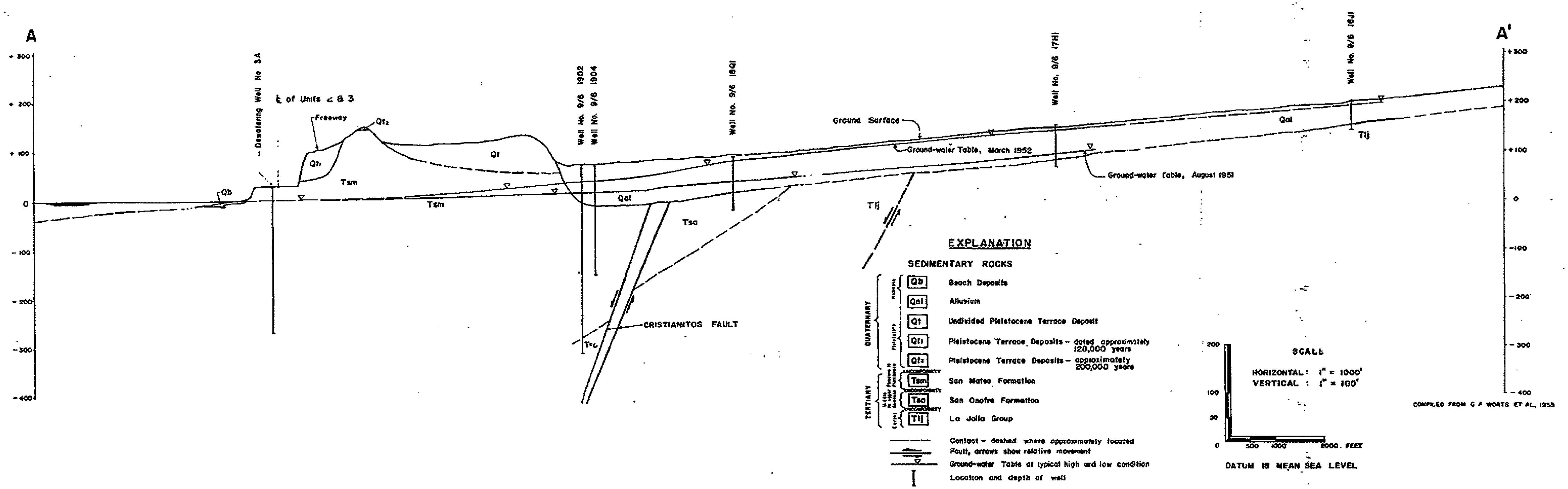

SAN ONOFRE
NUCLEAR GENERATING STATION
Units 2 & 3

CROSS-SECTION OF SAN ONOFRE GROUNDWATER BASIN SHOWING TYPICAL HIGH AND LOW CONDITIONS

Figure 2.4-32

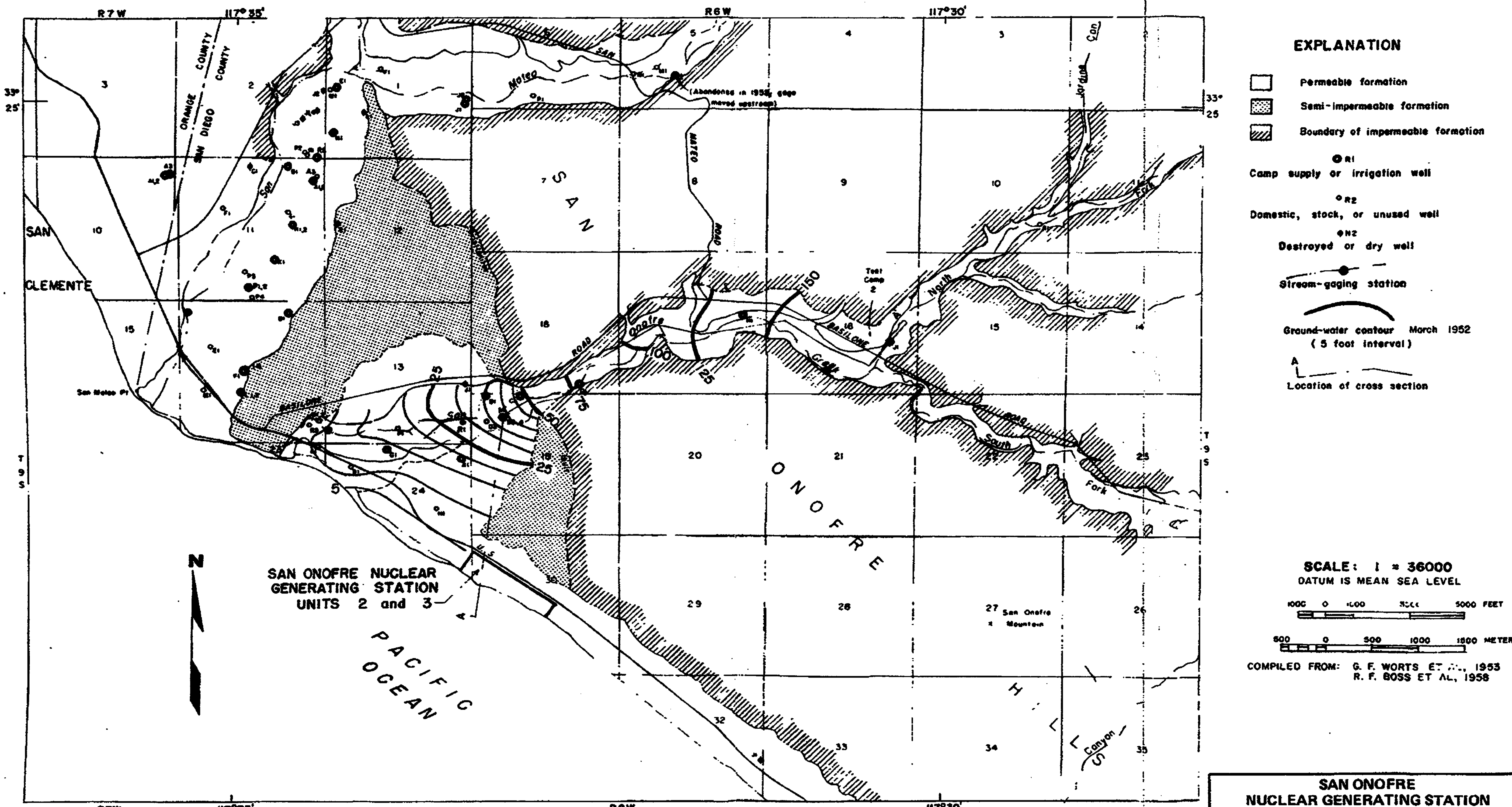

SAN ONOFRE
NUCLEAR GENERATING STATION
Units 2 & 3

GROUNDWATER CONTOUR MAP
SAN ONOFRE VALLEY BASIN
TYPICAL HIGH-WATER CONDITION

Figure 2.4-33

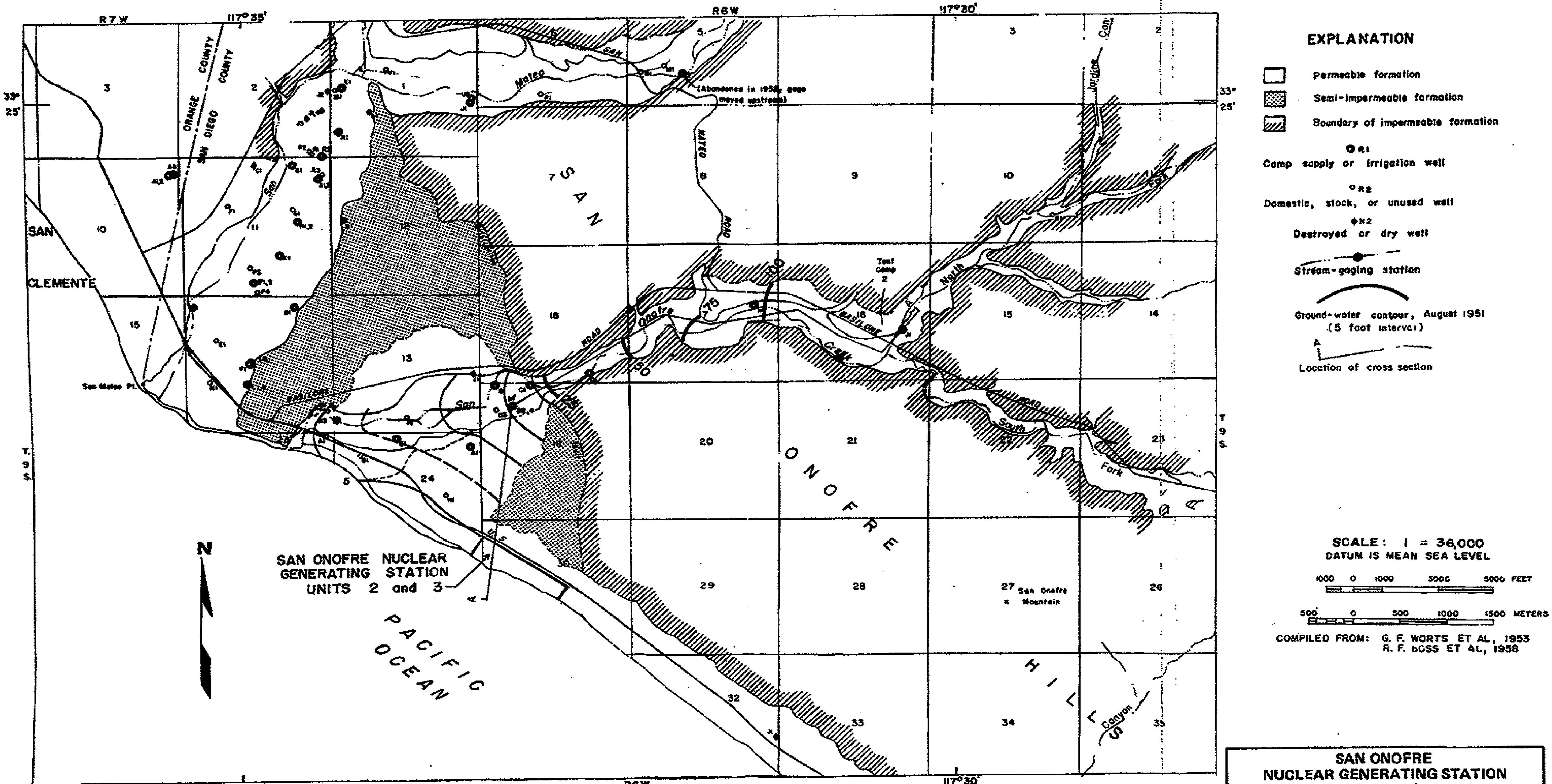

SAN ONOFRE NUCLEAR GENERATING STATION
Units 2 & 3

GROUNDWATER CONTOUR MAP
SAN ONOFRE VALLEY BASIN
TYPICAL LOW-WATER CONDITION

Figure 2.4-34

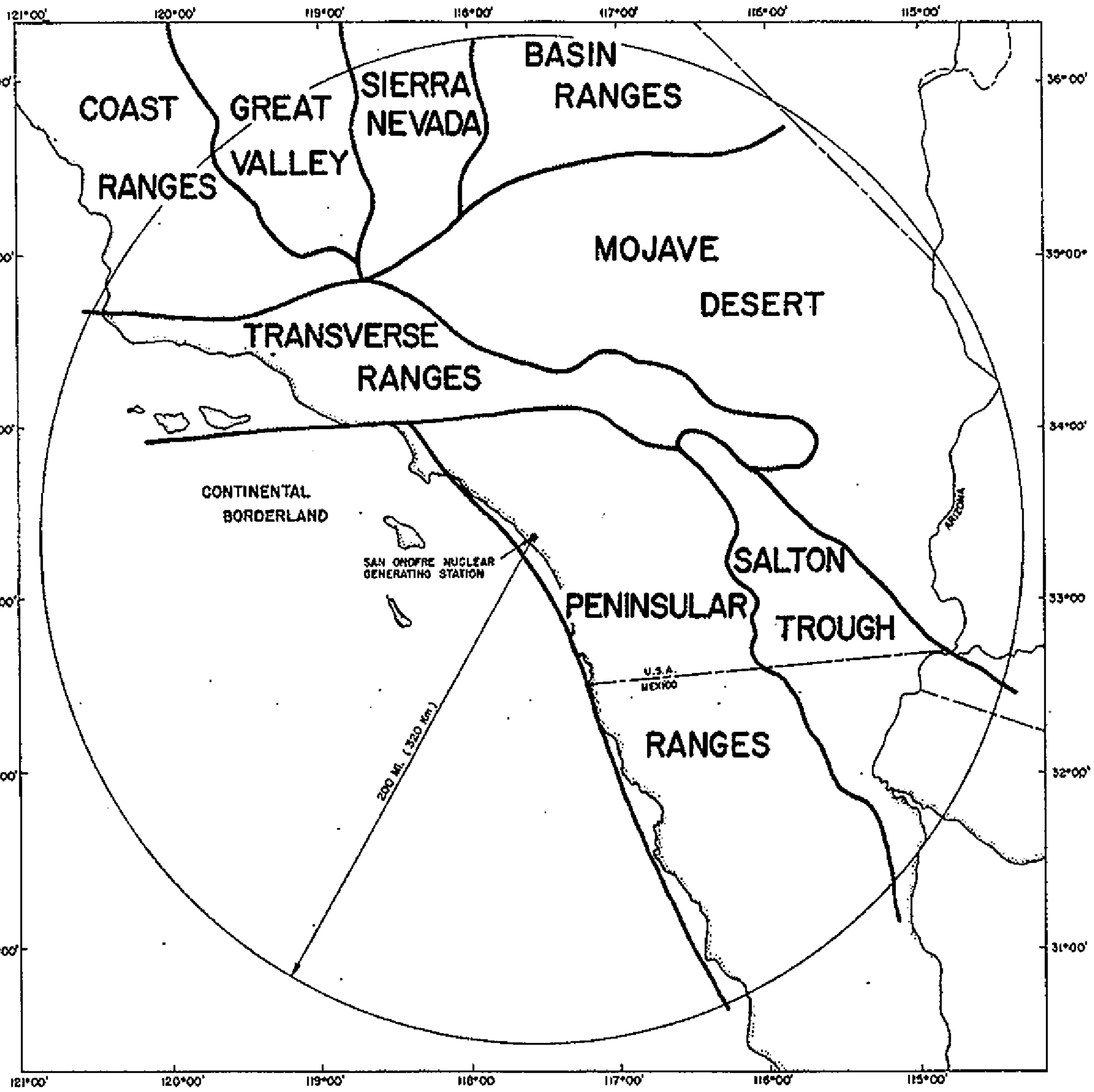

SAN ONOFRE NUCLEAR GENERATING STATION Units 2 & 3
NATURAL GEOMORPHIC PROVINCES
Figure 2.5-1

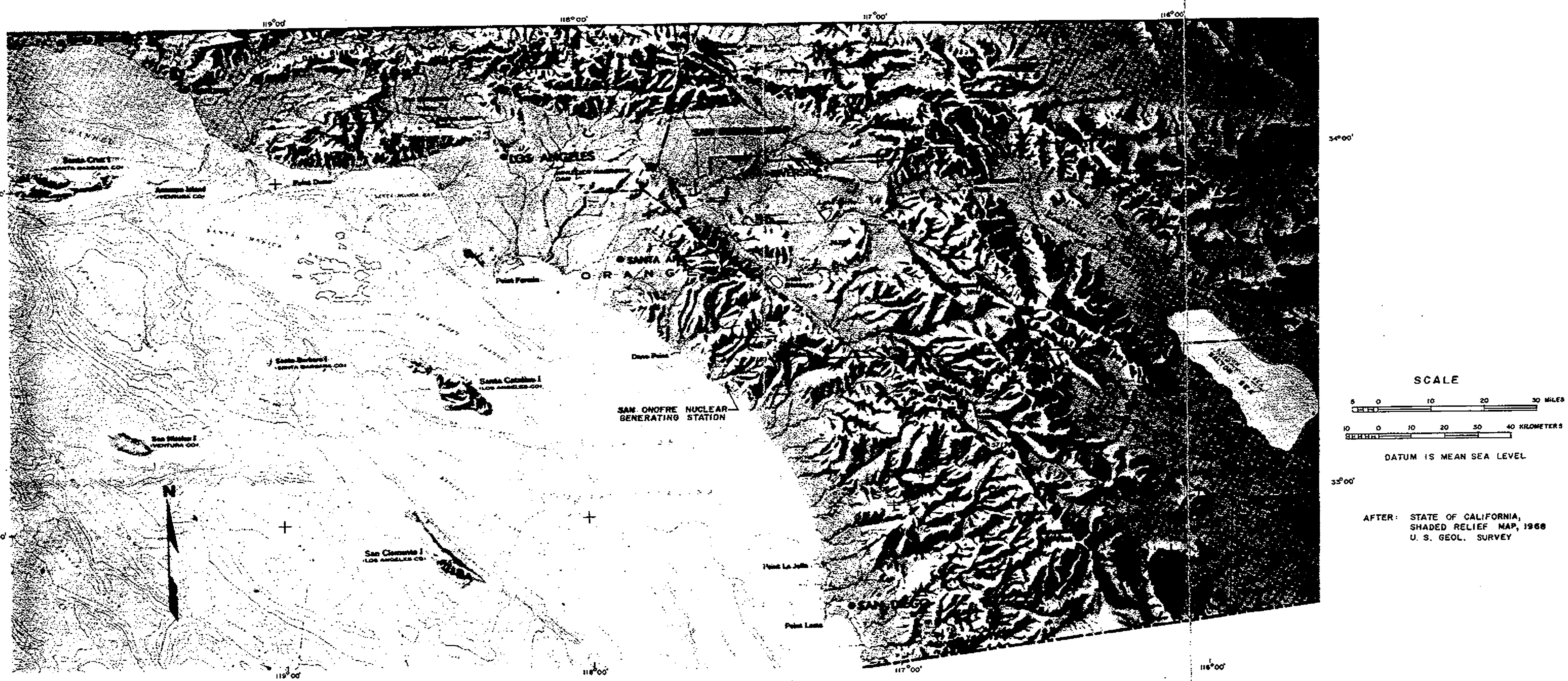

SAN ONOFRE
NUCLEAR GENERATING STATION
Units 2 & 3

REGIONAL PHYSIOGRAPHIC MAP

Figure 2.5-2

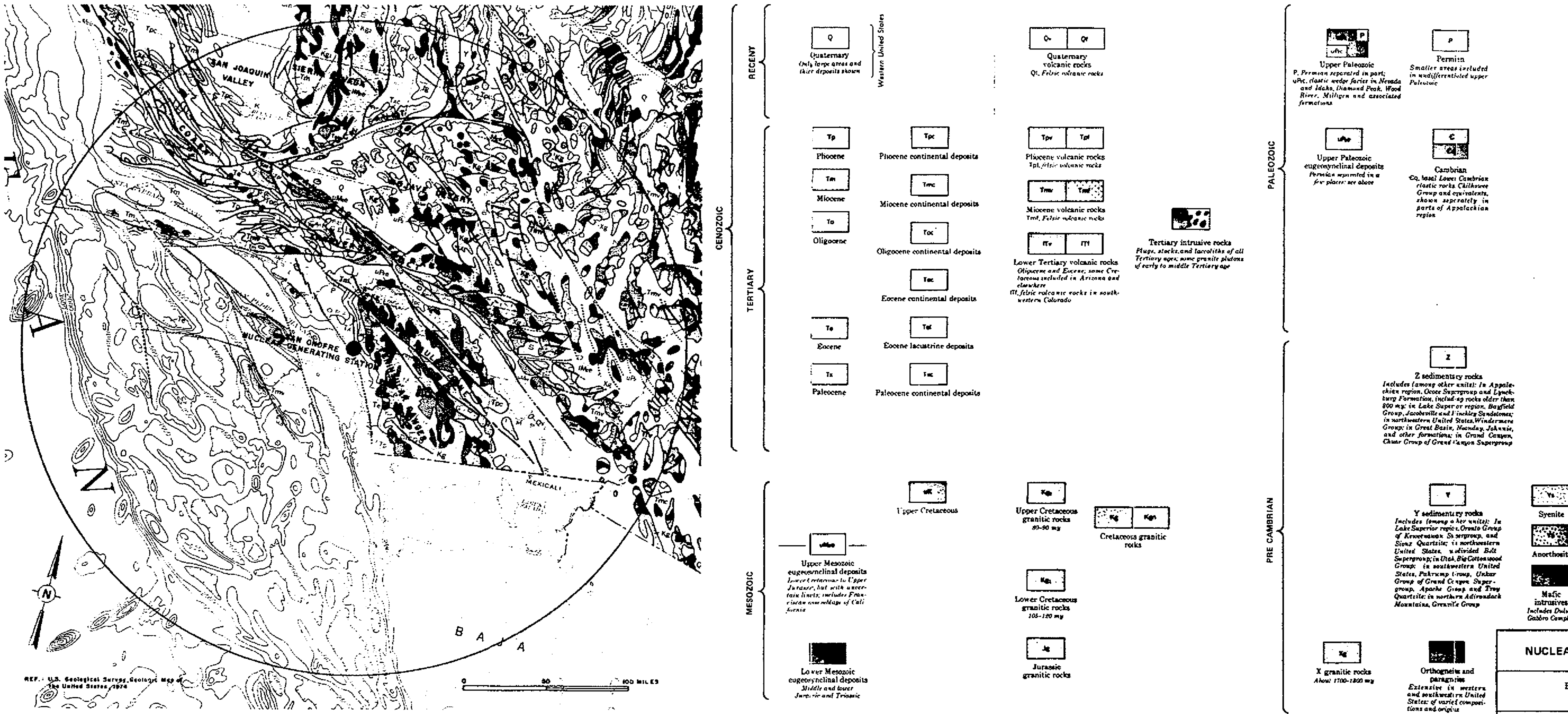

SAN ONOFRE
NUCLEAR GENERATING STATION
Units 2 & 3

REGIONAL GEOLOGIC MAP

Figure 2.5-3

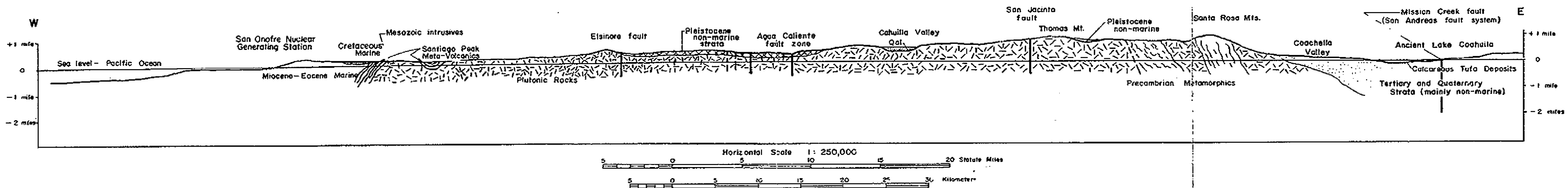

Note: For location of cross section see Regional Geologic Map Figure 2.5-2

Data compiled from Jenkins, 1965, Geologic Map of California - Santa Ana Sheet

SAN ONOFRE NUCLEAR GENERATING STATION Units 2 & 3

REGIONAL CROSS-SECTION PENINSULAR RANGES PROVINCE

Figure 2.5-4

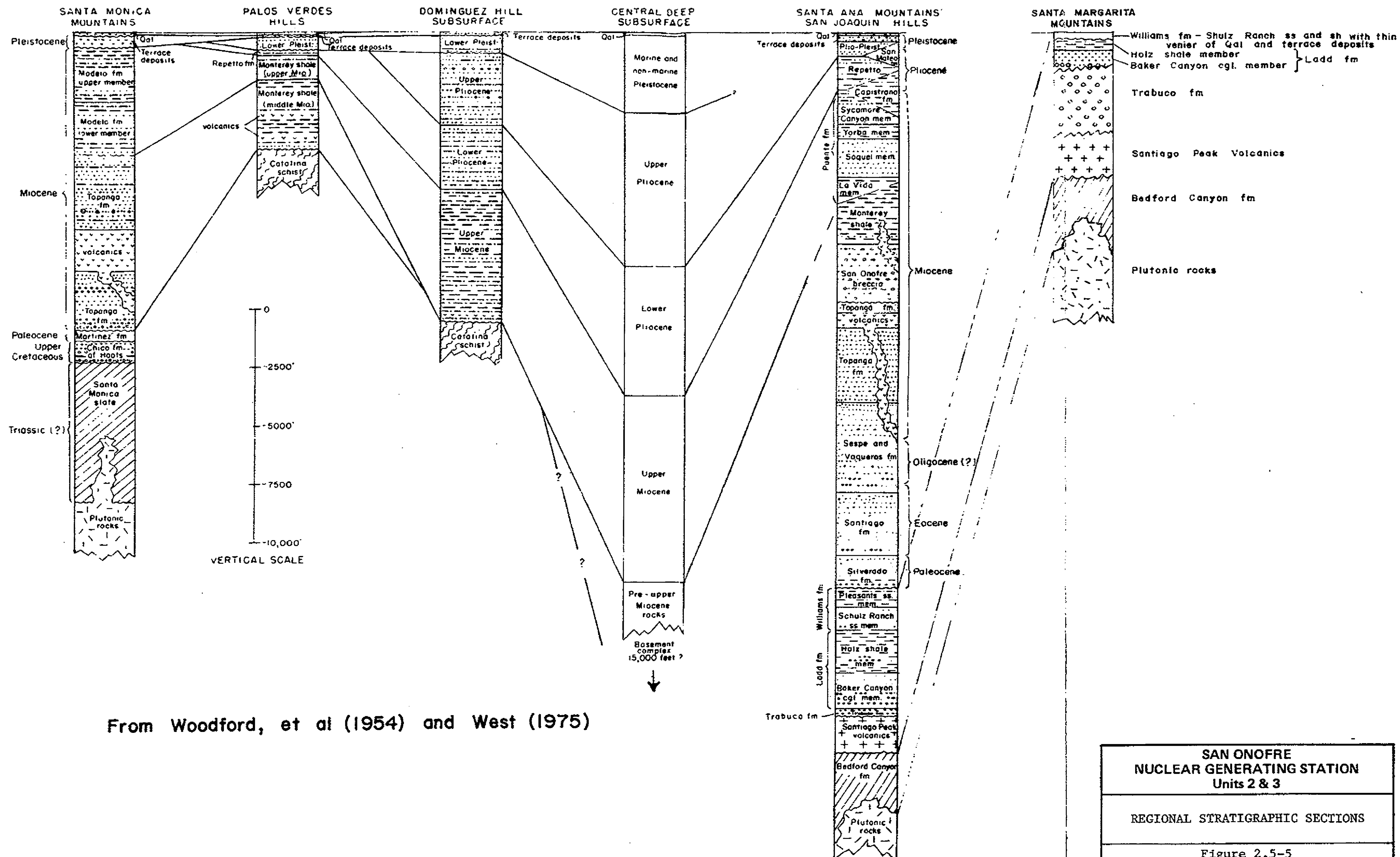

From Woodford, et al (1954) and West (1975)

SAN ONOFRE
NUCLEAR GENERATING STATION
Units 2 & 3

REGIONAL STRATIGRAPHIC SECTIONS

Figure 2.5-5

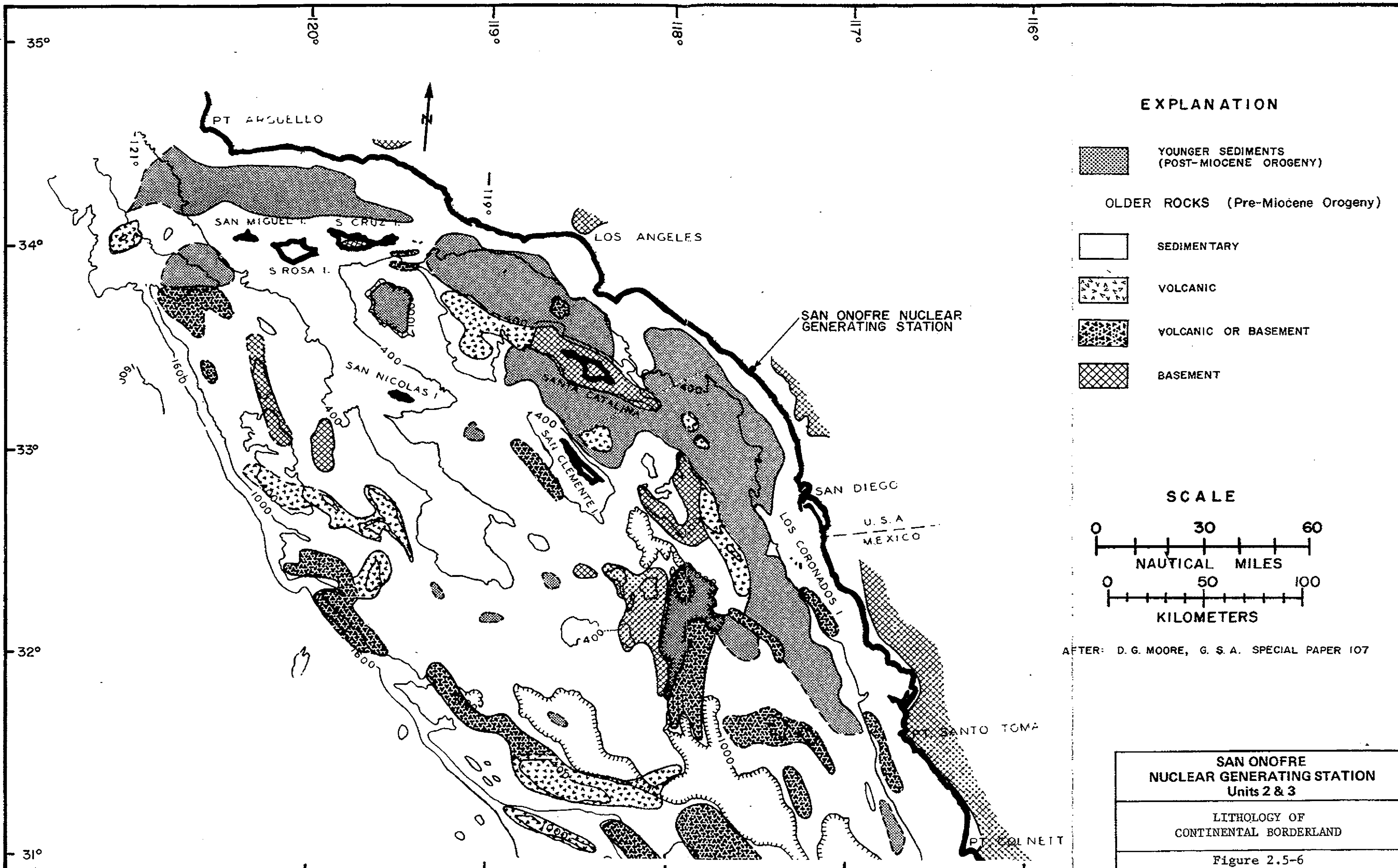

SAN ONOFRE
NUCLEAR GENERATING STATION
Units 2 & 3

LITHOLOGY OF
CONTINENTAL BORDERLAND

Figure 2.5-6

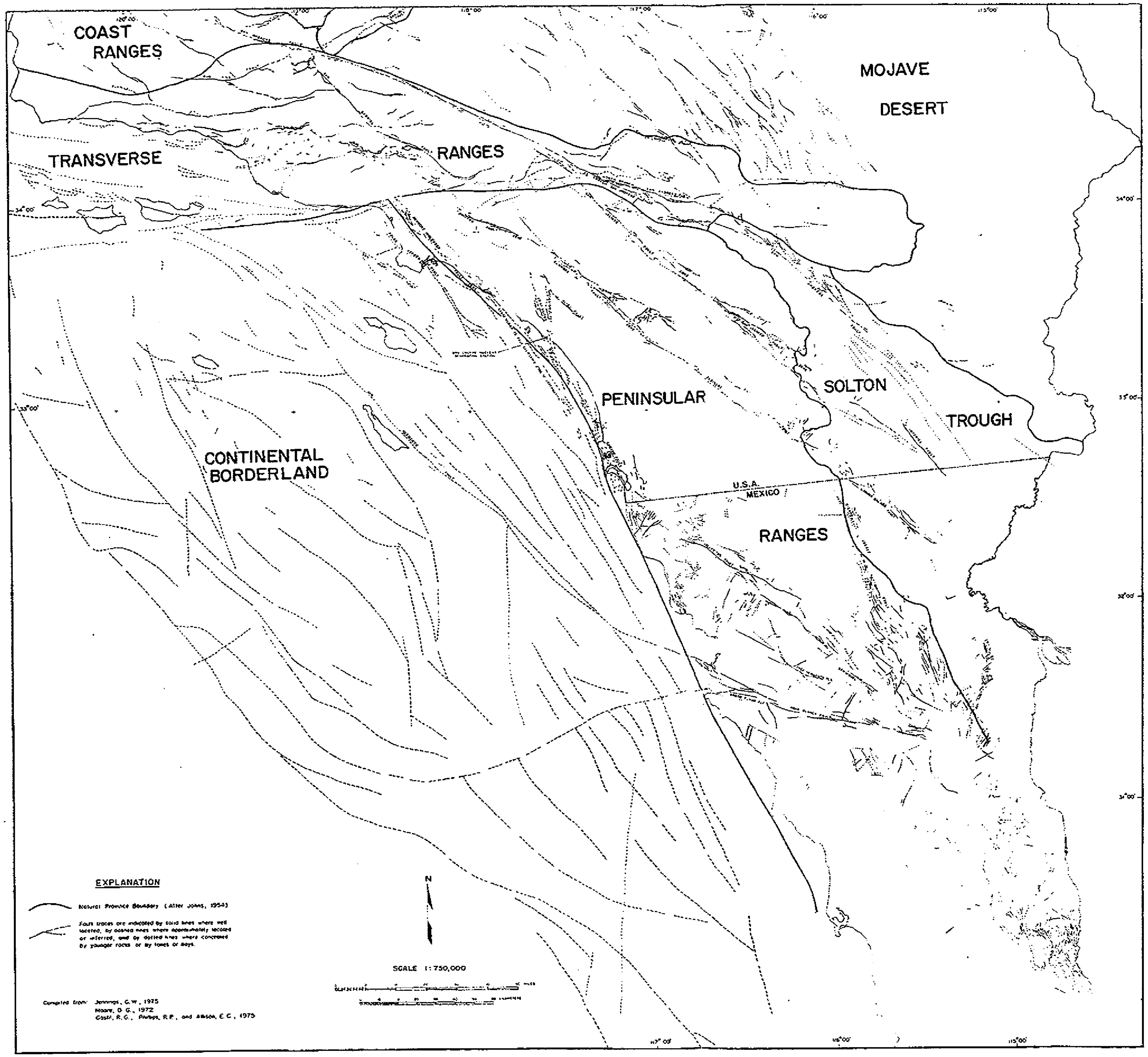

SAN ONOFRE
NUCLEAR GENERATING STATION
Units 2 & 3

REGIONAL FAULT MAP

Figure 2.5-7

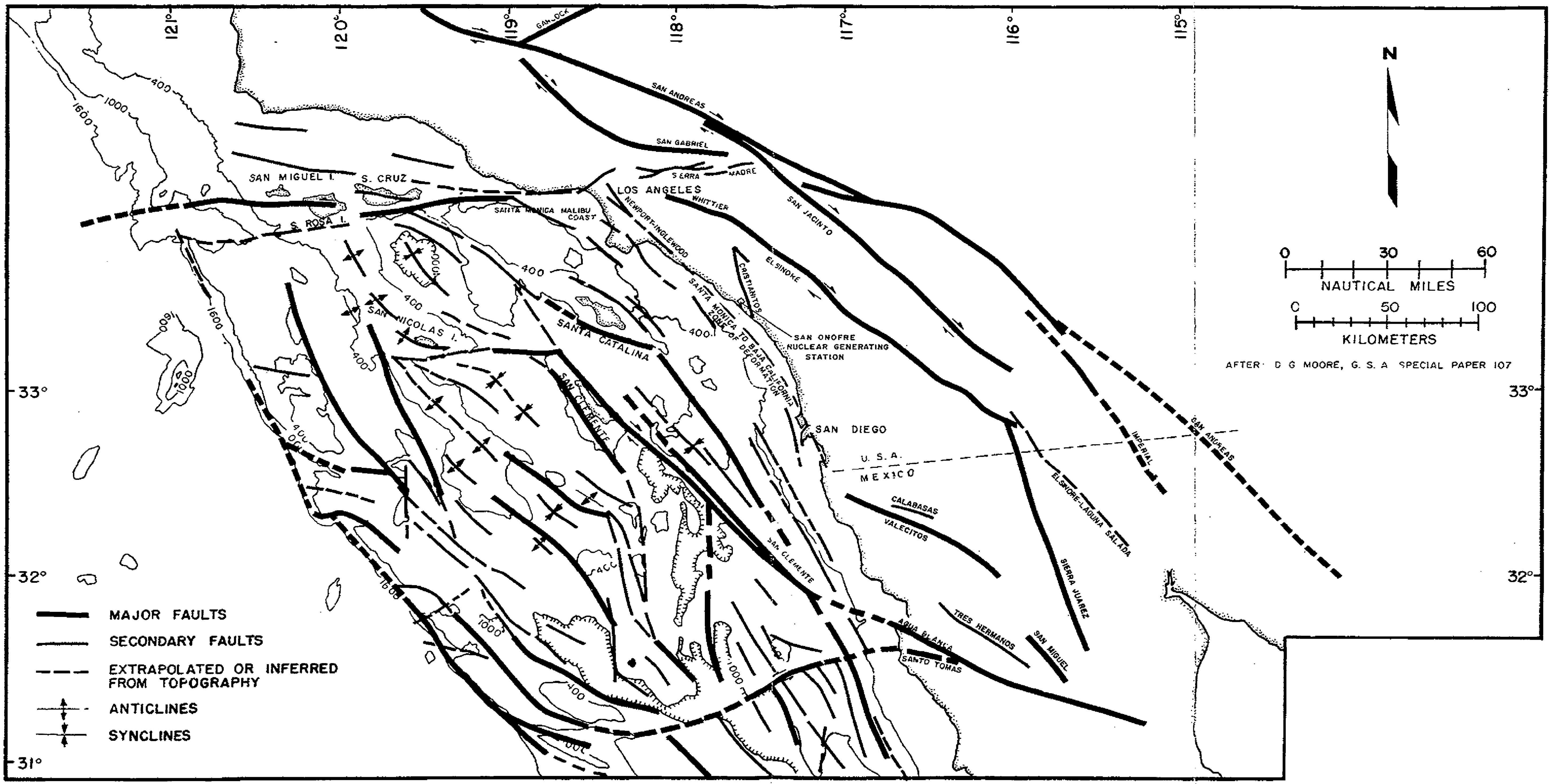

SAN ONOFRE NUCLEAR GENERATING STATION Units 2 & 3

STRUCTURE OF THE CONTINENTAL BORDERLAND AND ADJACENT REGIONS

Figure 2.5-8

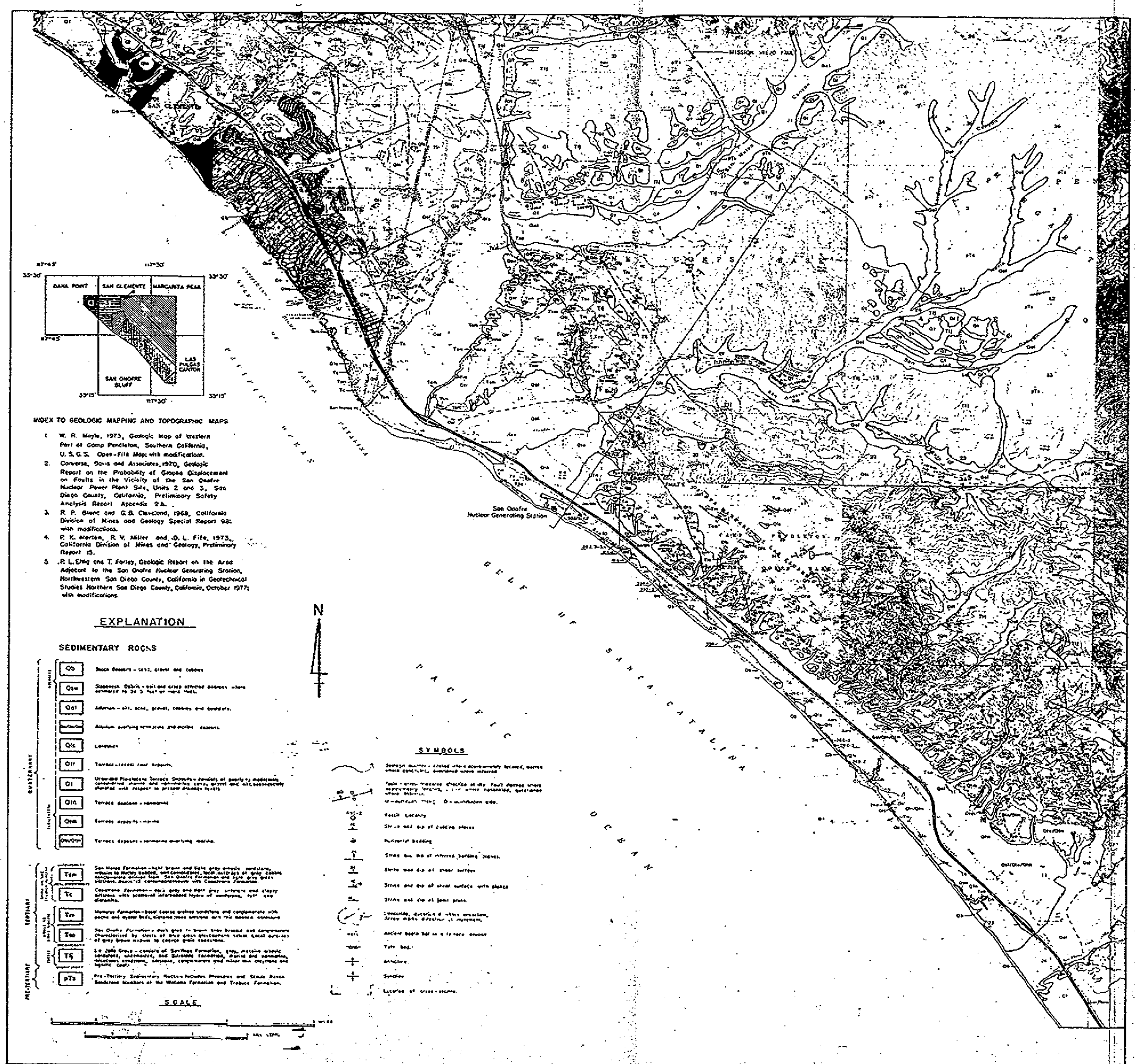

SAN ONOFRE
NUCLEAR GENERATING STATION
Units 2 & 3

SITE GEOLOGIC MAP

Figure 2.5-9

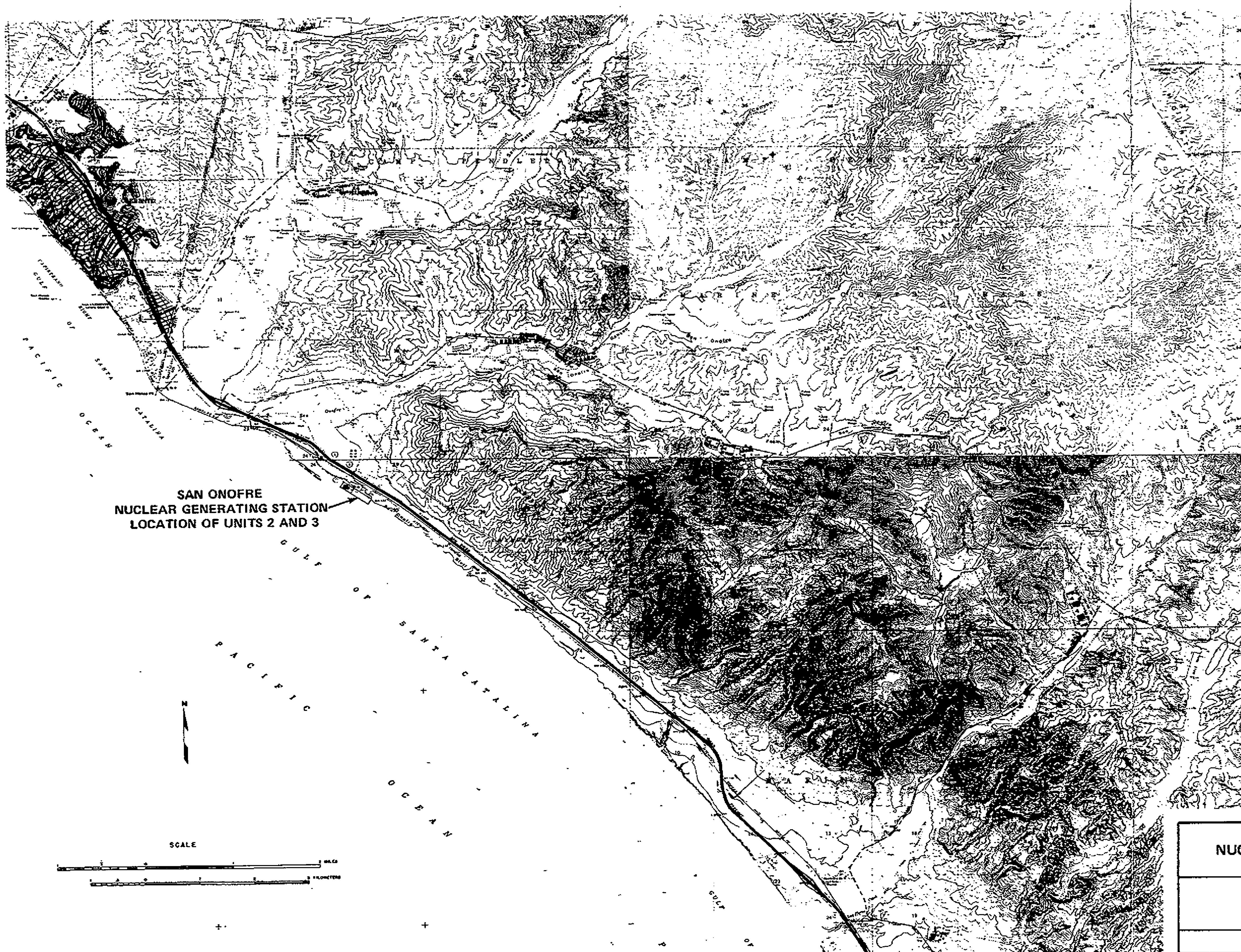

SAN ONOFRE
NUCLEAR GENERATING STATION
Units 2 & 3

SITE PHYSIOGRAPHIC MAP
(WITH LOCAL LAND FORMS)

Figure 2.5-10

COMPILED FROM:
J. C. WEST, 1975
C. J. STUART, 1975
H. R. LANG, 1972
P. K. MORTON, 1972

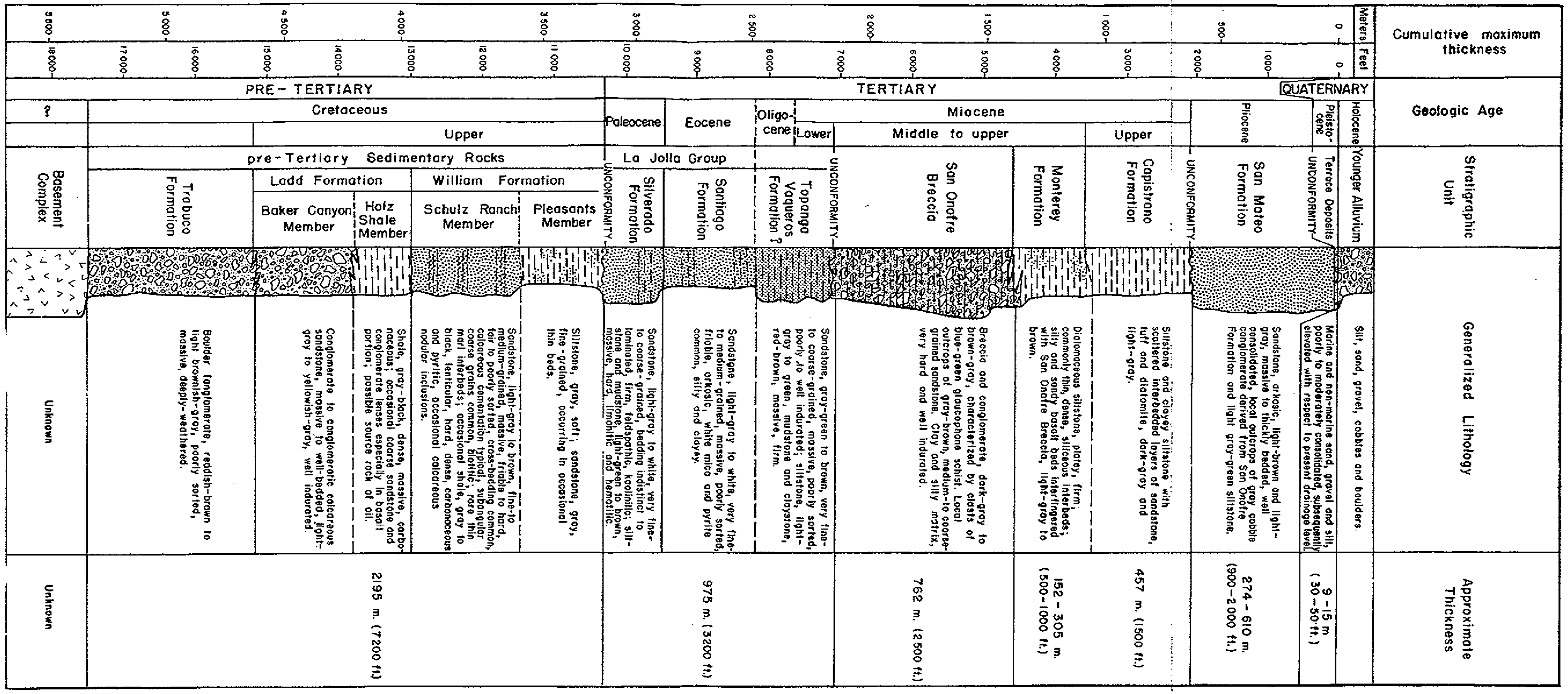

SAN ONOFRE
NUCLEAR GENERATING STATION
Units 2 & 3

COMPOSITE STRATIGRAPHIC SECTION
FOR THE SAN ONOFRE AREA

Figure 2.5-11

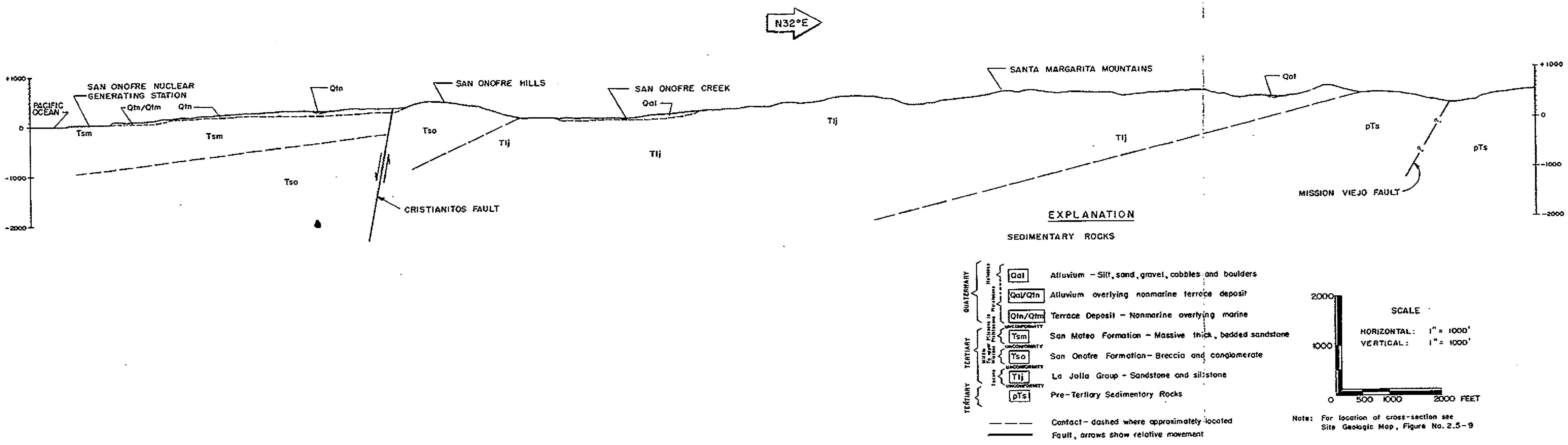

SAN ONOFRE
NUCLEAR GENERATING STATION
Units 2 & 3

SITE GEOLOGIC CROSS-SECTION

Figure 2.5-12

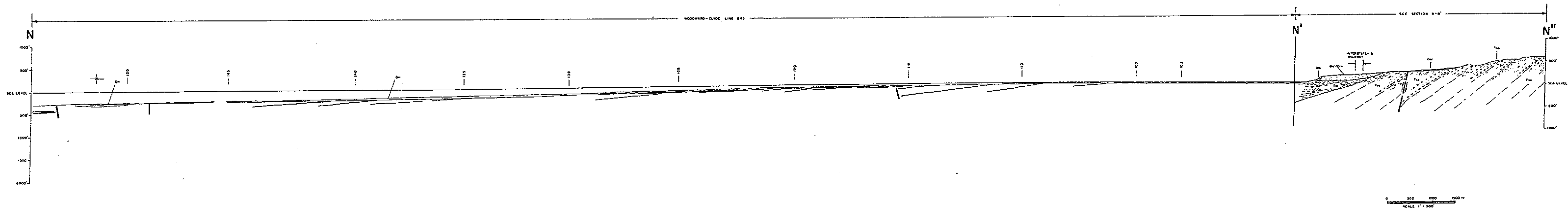

SAN ONOFRE
NUCLEAR GENERATING STATION
Units 2 & 3

COMPOSITE GEOLOGIC CROSS-SECTION
N-N'-N'' AUGUST 1980

Figure 2.5-13

Amended: April 2009 TL: E048000

Site File Copy

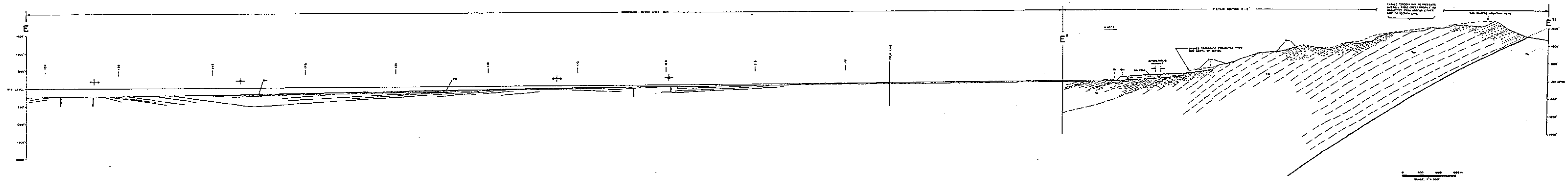

SAN ONOFRE
NUCLEAR GENERATING STATION
Units 2 & 3

COMPOSITE GEOLOGIC CROSS-SECTION
E-E'-E" AUGUST 1980

Figure 2.5-14

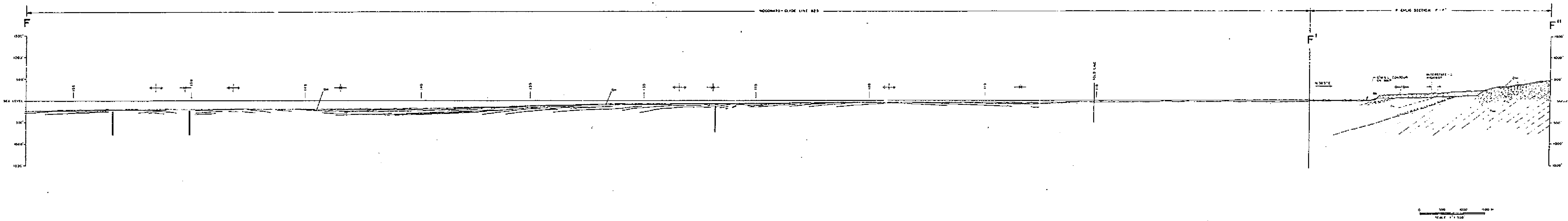

SAN ONOFRE
NUCLEAR GENERATING STATION
Units 2 & 3

COMPOSITE GEOLOGIC CROSS-SECTION
F-F'-F'' AUGUST 1980

Figure 2.5-15

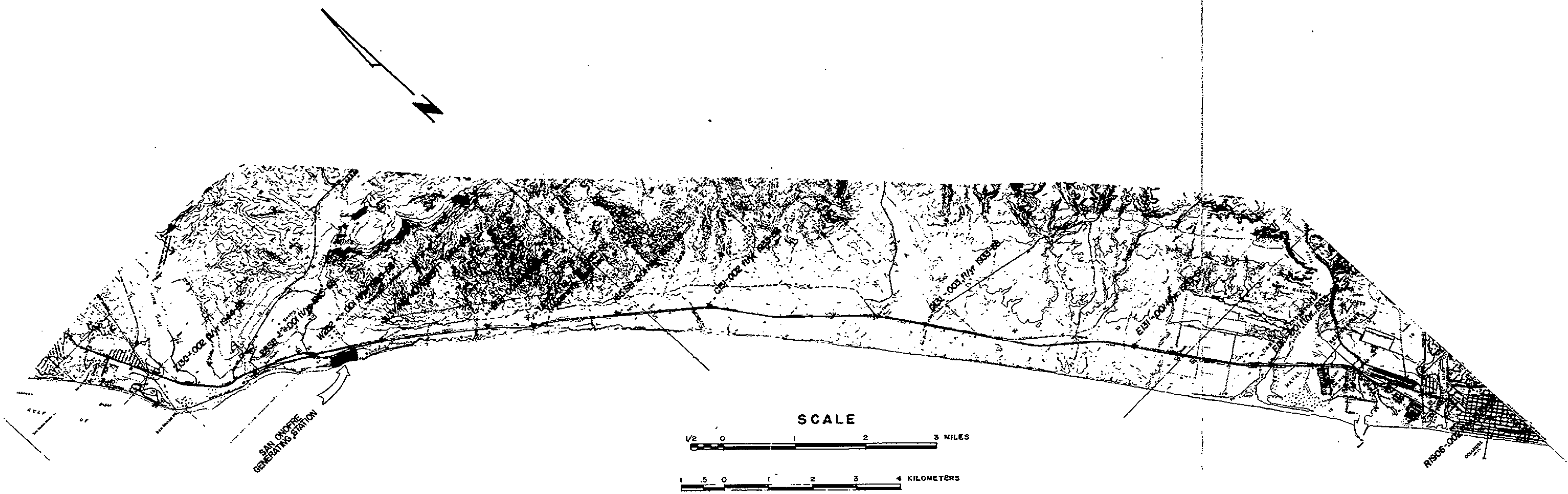

SAN ONOFRE
NUCLEAR GENERATING STATION
Units 2 & 3

SUBSIDENCE STUDY MAP

Figure 2.5-16

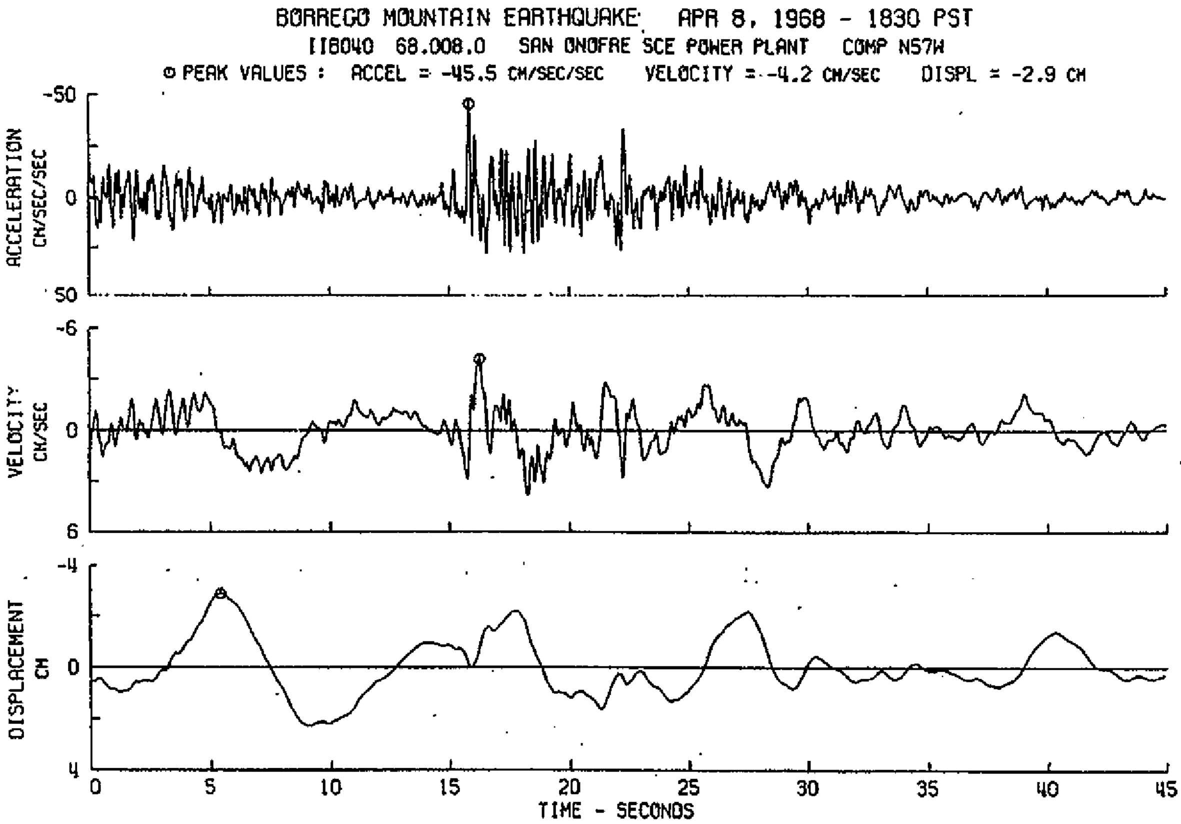

SAN ONOFRE NUCLEAR GENERATING STATION Units 2 & 3

CORRECTED ACCELEROGRAM
BORREGO MOUNTAIN EARTHQUAKE
(Sheet 1 of 3)

Figure 2.5-17

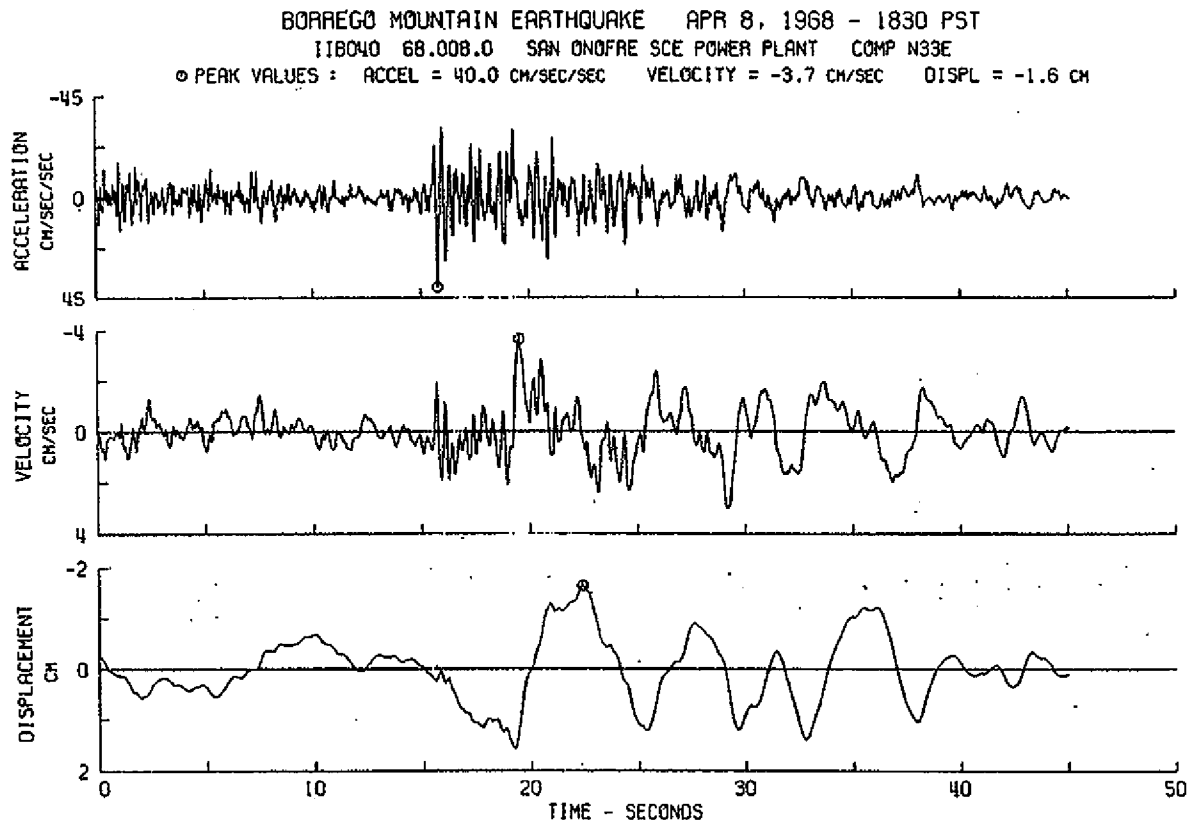

SAN ONOFRE NUCLEAR GENERATING STATION Units 2 & 3
CORRECTED ACCELEROGRAM BORREGO MOUNTAIN EARTHQUAKE (Sheet 2 of 3)
Figure 2.5-17

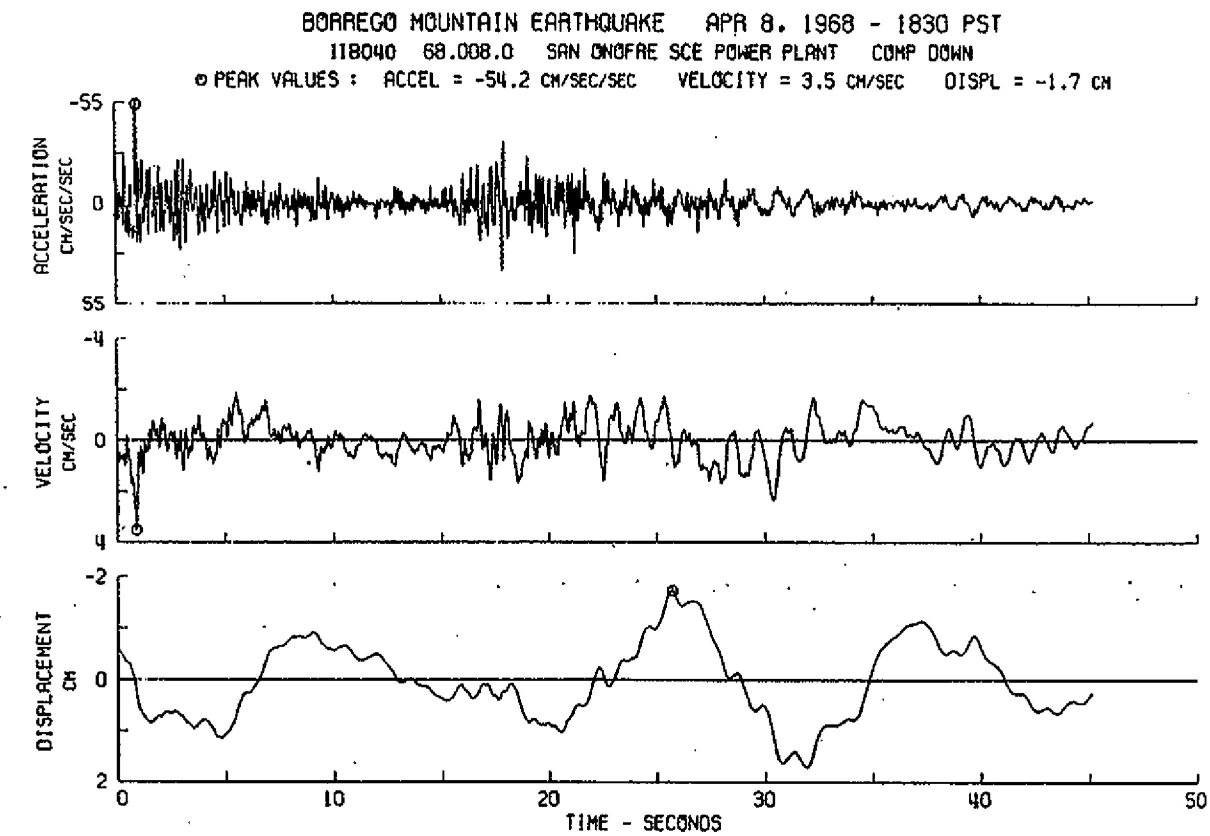

SAN ONOFRE NUCLEAR GENERATING STATION Units 2 & 3
CORRECTED ACCELEROGRAM BORREGO MOUNTAIN EARTHQUAKE (Sheet 3 of 3)
Figure 2.5-17

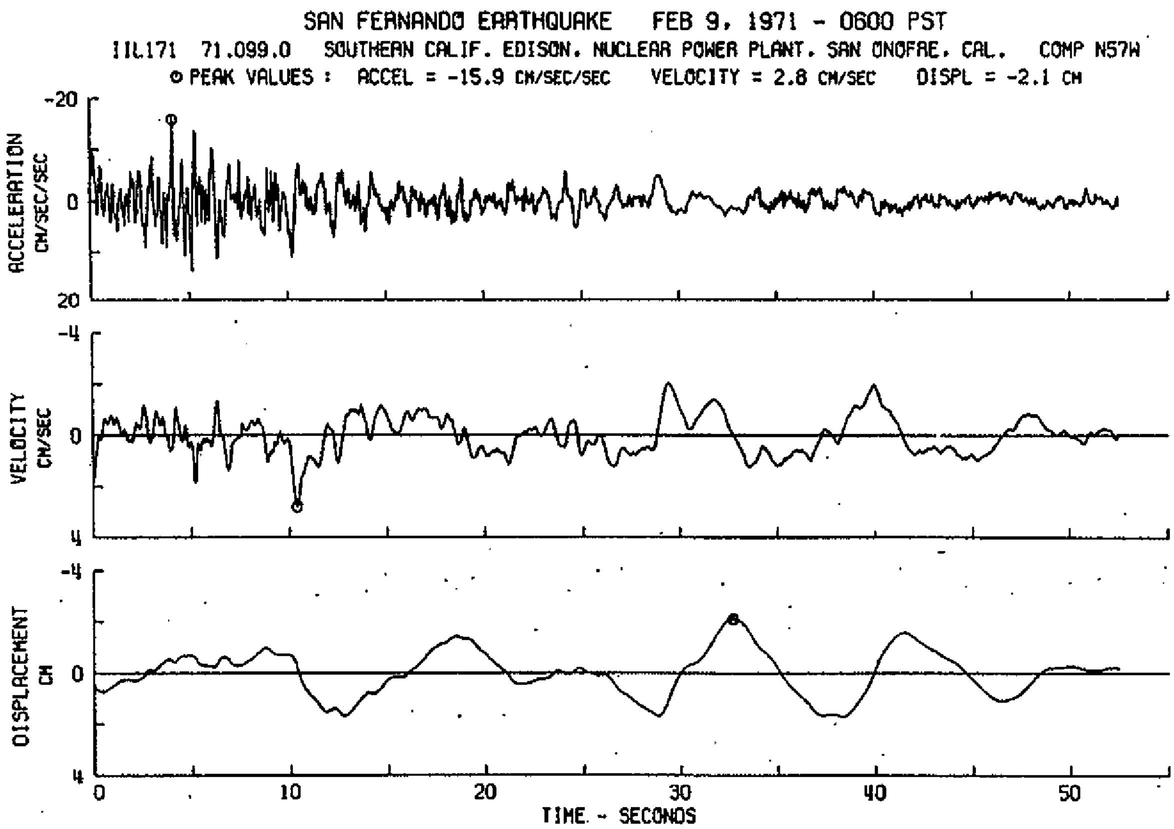

SAN ONOFRE NUCLEAR GENERATING STATION Units 2 & 3
CORRECTED ACCELEROGRAM SAN FERNANDO EARTHQUAKE (Sheet 1 of 3)
Figure 2.5-18

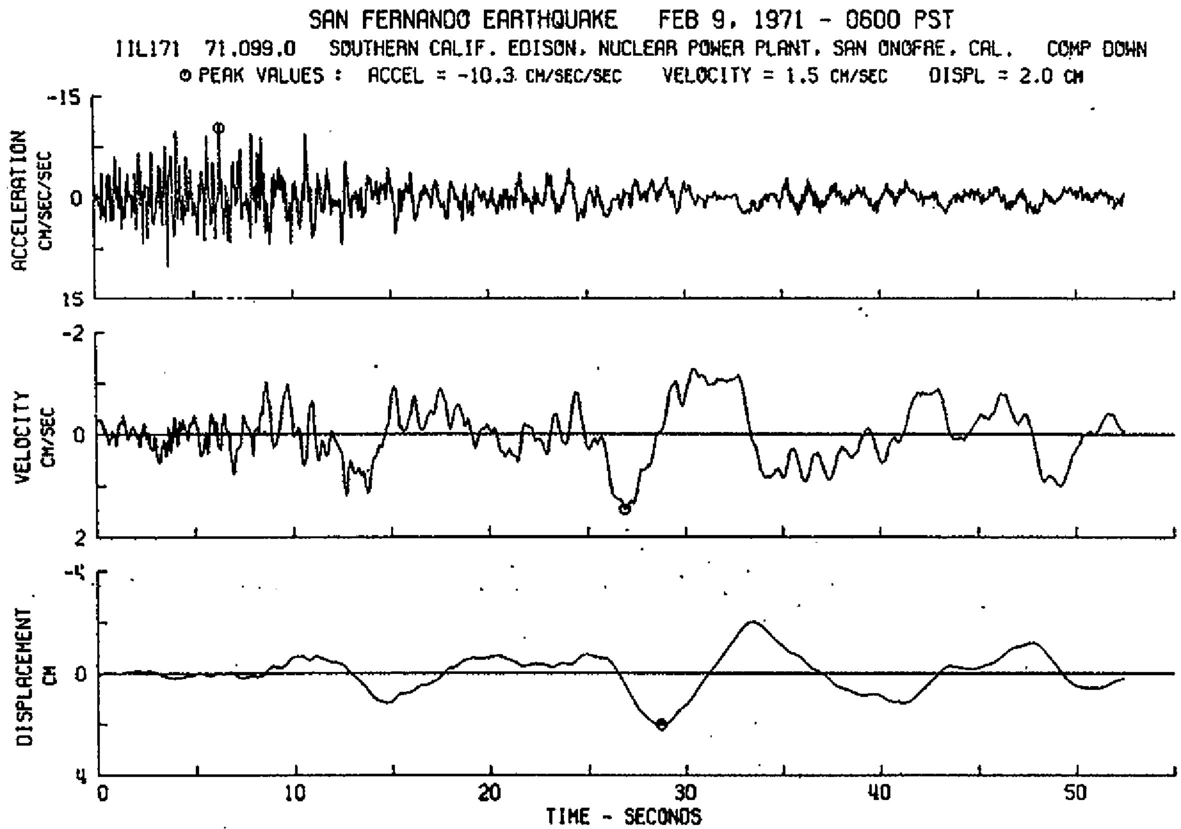

SAN ONOFRE NUCLEAR GENERATING STATION Units 2 & 3
CORRECTED ACCELEROGRAM SAN FERNANDO EARTHQUAKE (Sheet 2 of 3)
Figure 2.5-18

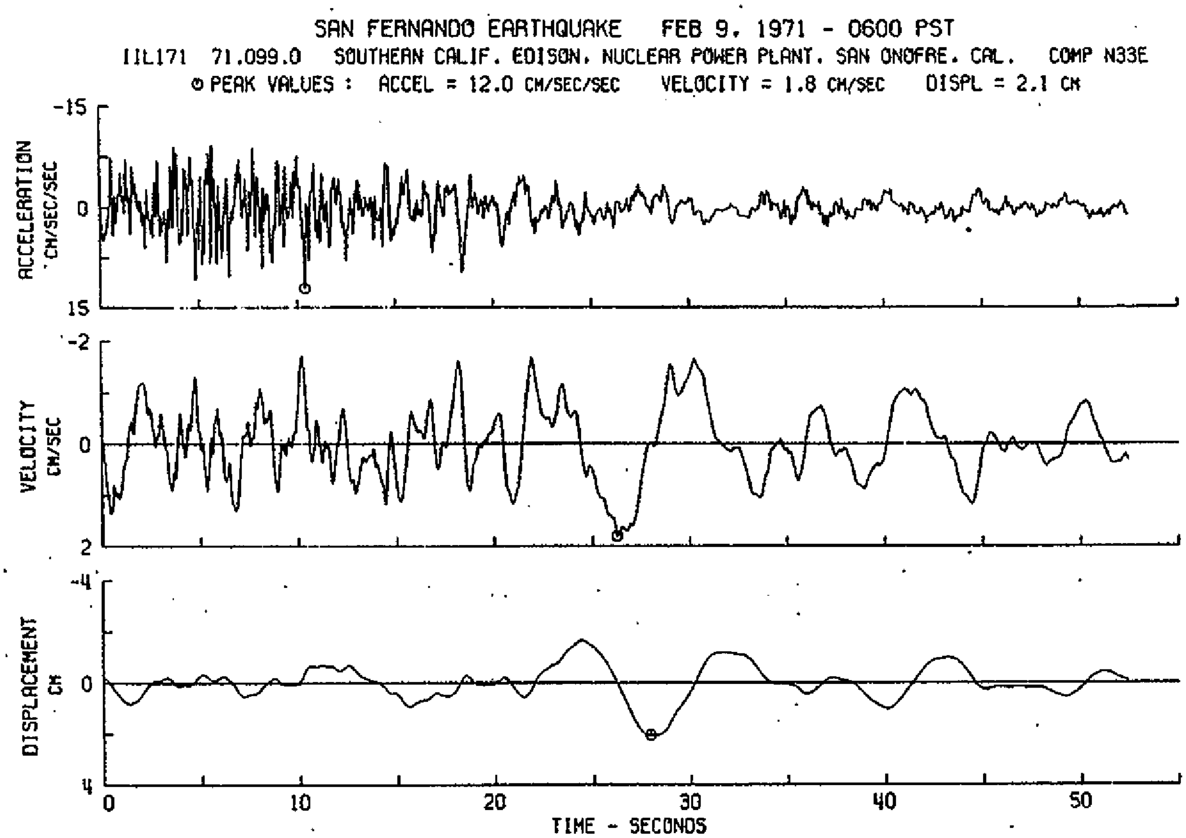

SAN ONOFRE
NUCLEAR GENERATING STATION
Units 2 & 3

CORRECTED ACCELEROGRAM
SAN FERNANDO EARTHQUAKE
(Sheet 3 of 3)

Figure 2.5-18

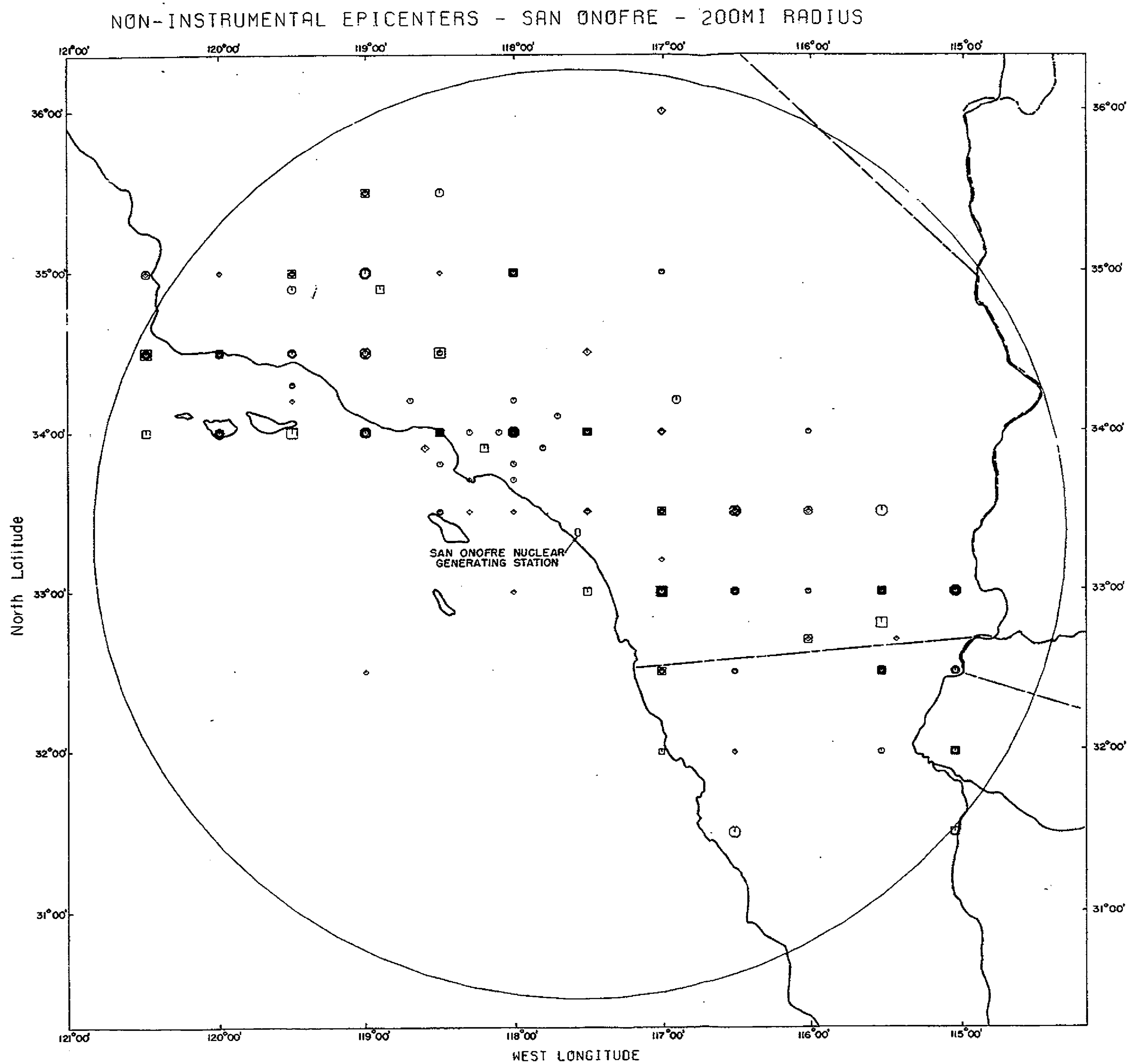

EXPLANATION

MAGNITUDES 0.0 TO 0.9	(	3)
MAGNITUDES 1.0 TO 1.9	(	145)
MAGNITUDES 2.0 TO 2.9	(	119)
MAGNITUDES 3.0 TO 3.9	(	45)
MAGNITUDES 4.0 TO 4.9	(	32)
MAGNITUDES 5.0 TO 5.9	(	20)
MAGNITUDES 6.0 TO 6.9	(	7)
MAGNITUDES 7.0 TO 7.9	(	8)
MAGNITUDES 8.0 TO 8.9	(	1)
MAGNITUDES 9.0 TO 9.9	(	0)
MAGNITUDES UNKNOWN	(	0)

C SAN ONOFRE

Compiled from: Wood, Heck and Eppley, (1961)
S. D. Townley and M. W. Allen (1939)
Heck, Bodle, Newman and others (1968)
Richter, (1958)

N

SCALE

0 40 80 MILES

0 50 100 KILOMETERS

SAN ONOFRE NUCLEAR GENERATING STATION Units 2 & 3

APPROXIMATE LOCATION OF NON-INSTRUMENTAL EARTHQUAKES, 320-KILOMETER RADIUS

Figure 2.5-19

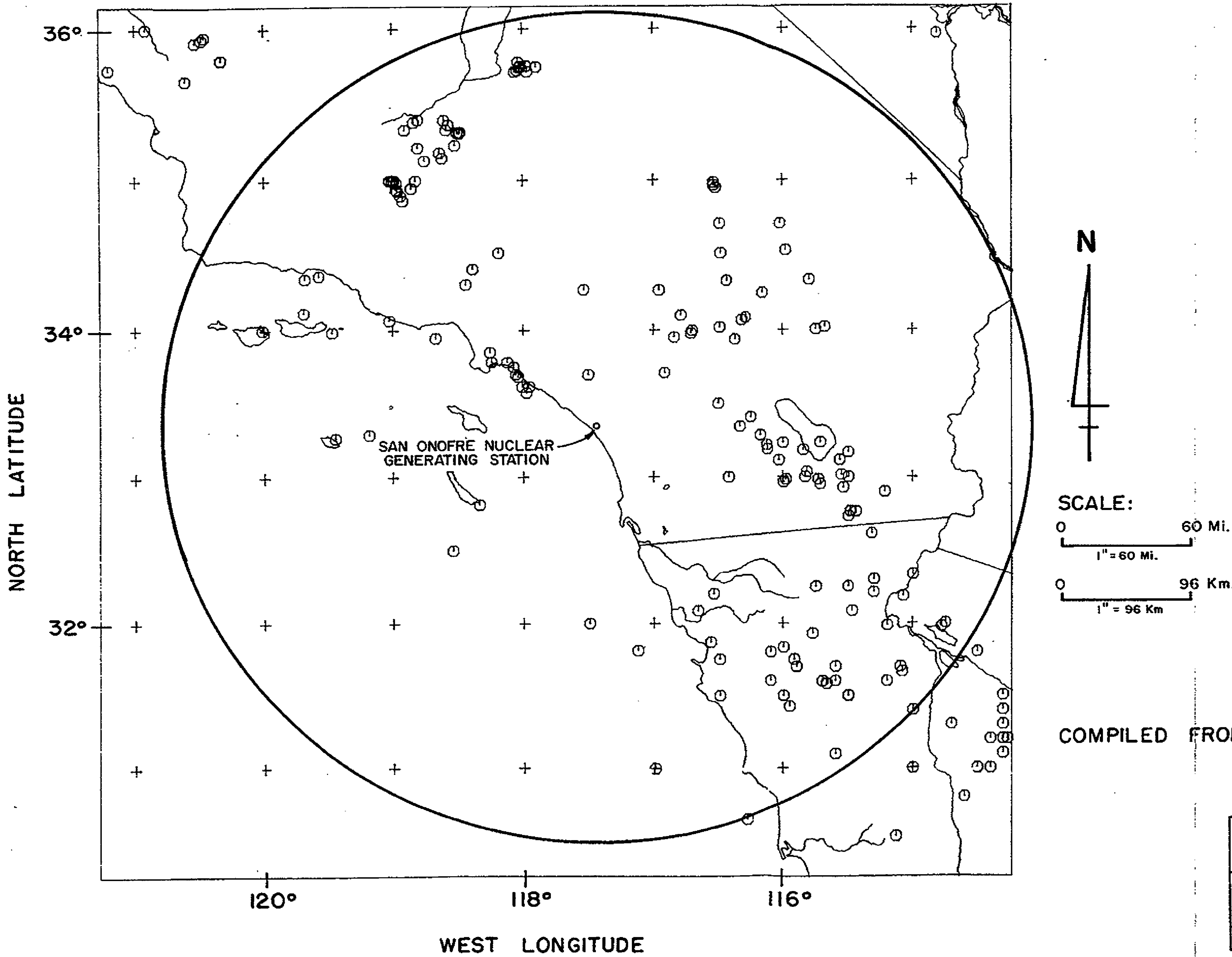

SAN ONOFRE
NUCLEAR GENERATING STATION
Units 2 & 3

PLOT OF INSTRUMENTAL
EPICENTERS M5.0 AND GREATER
320-KILOMETER RADIUS

Figure 2.5-20

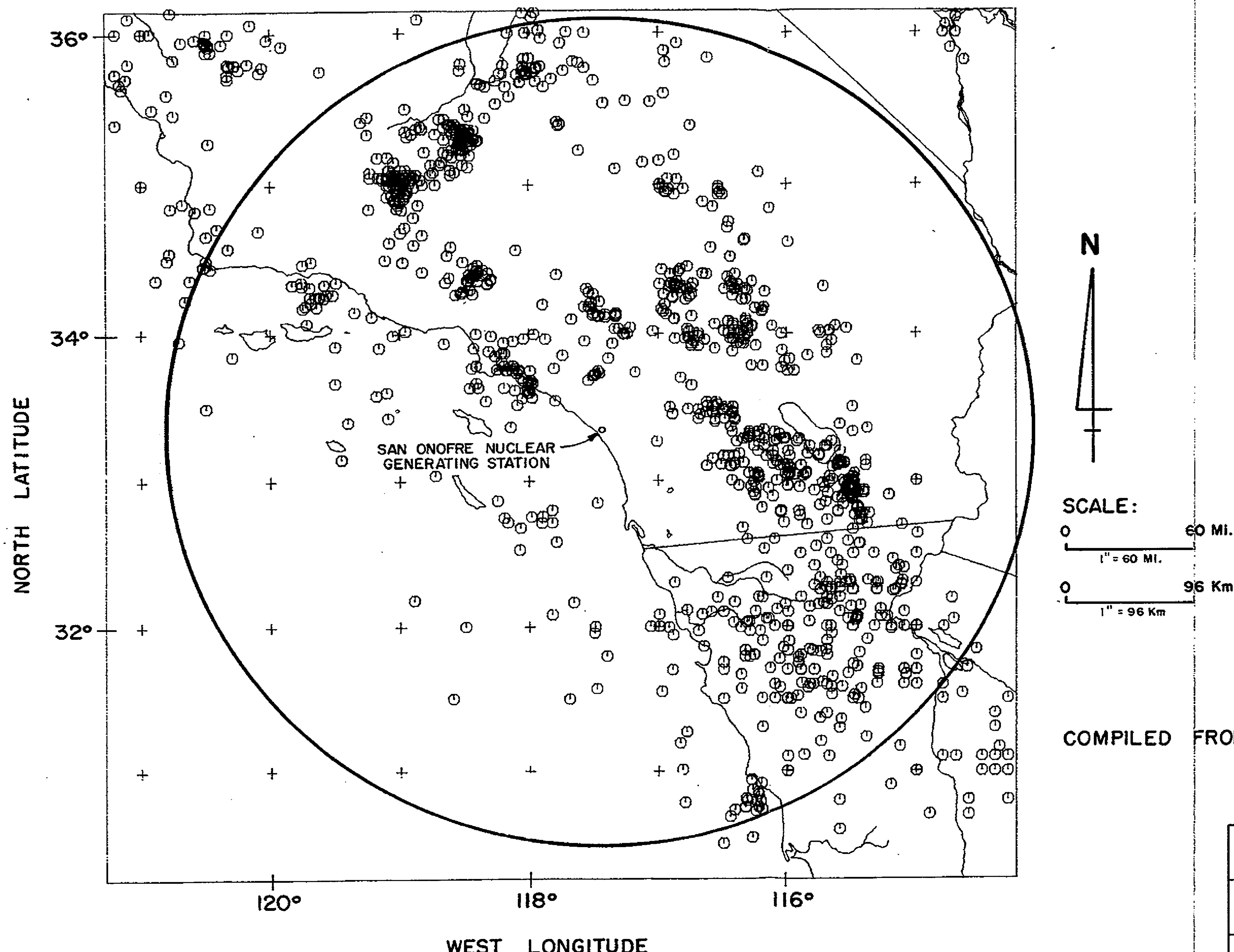

COMPILED FROM CIT CATALOG, 1932-1980

SAN ONOFRE NUCLEAR GENERATING STATION Units 2 & 3
PLOT OF INSTRUMENTAL EPICENTERS M4.0 TO M4.99 320-KILOMETER RADIUS
Figure 2.5-21

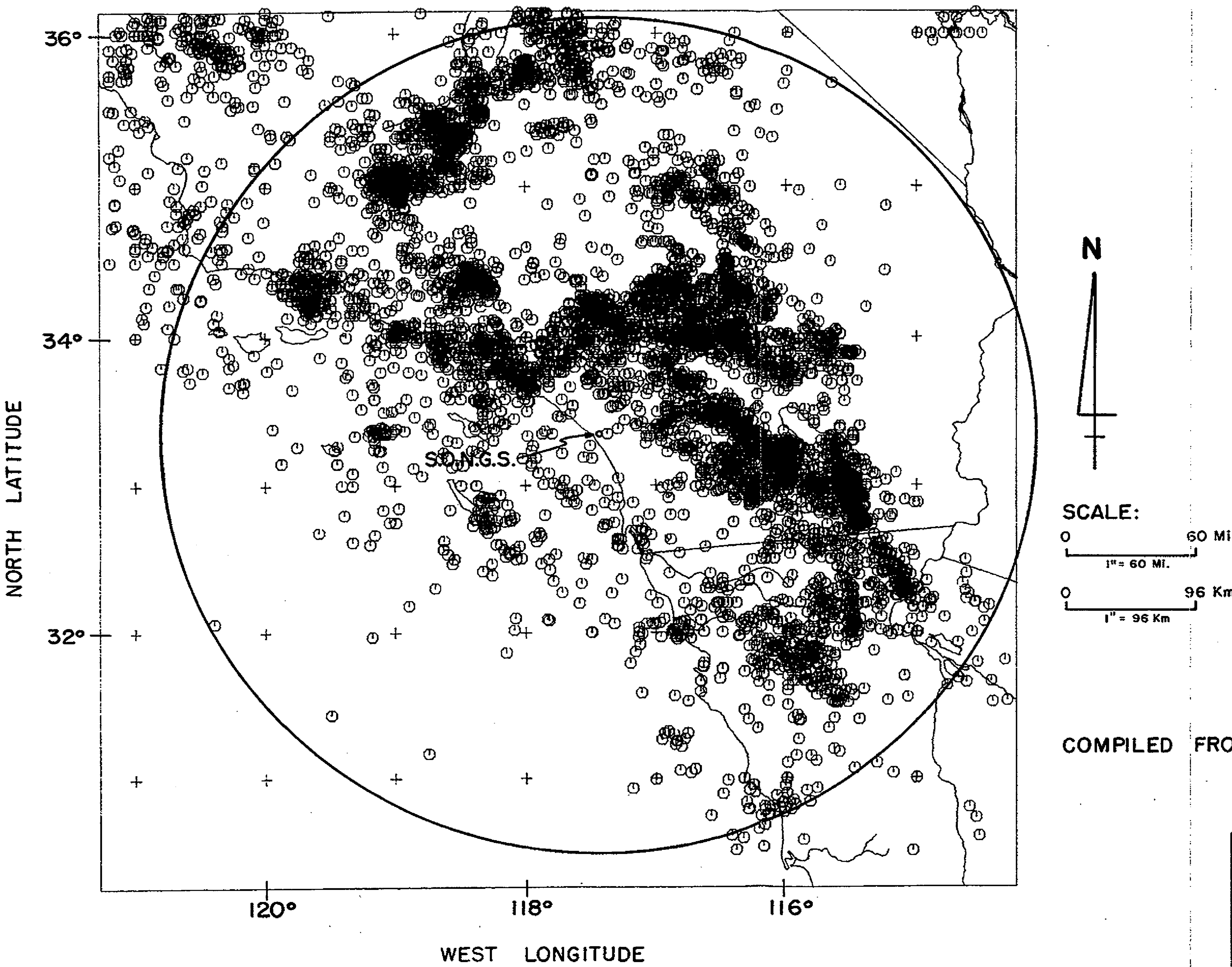

COMPILED FROM CIT CATALOG, 1932-1980

SAN ONOFRE NUCLEAR GENERATING STATION Units 2 & 3
PLOT OF INSTRUMENTAL EPICENTERS M3.0 TO M3.99 320-KILOMETER RADIUS
Figure 2.5-22

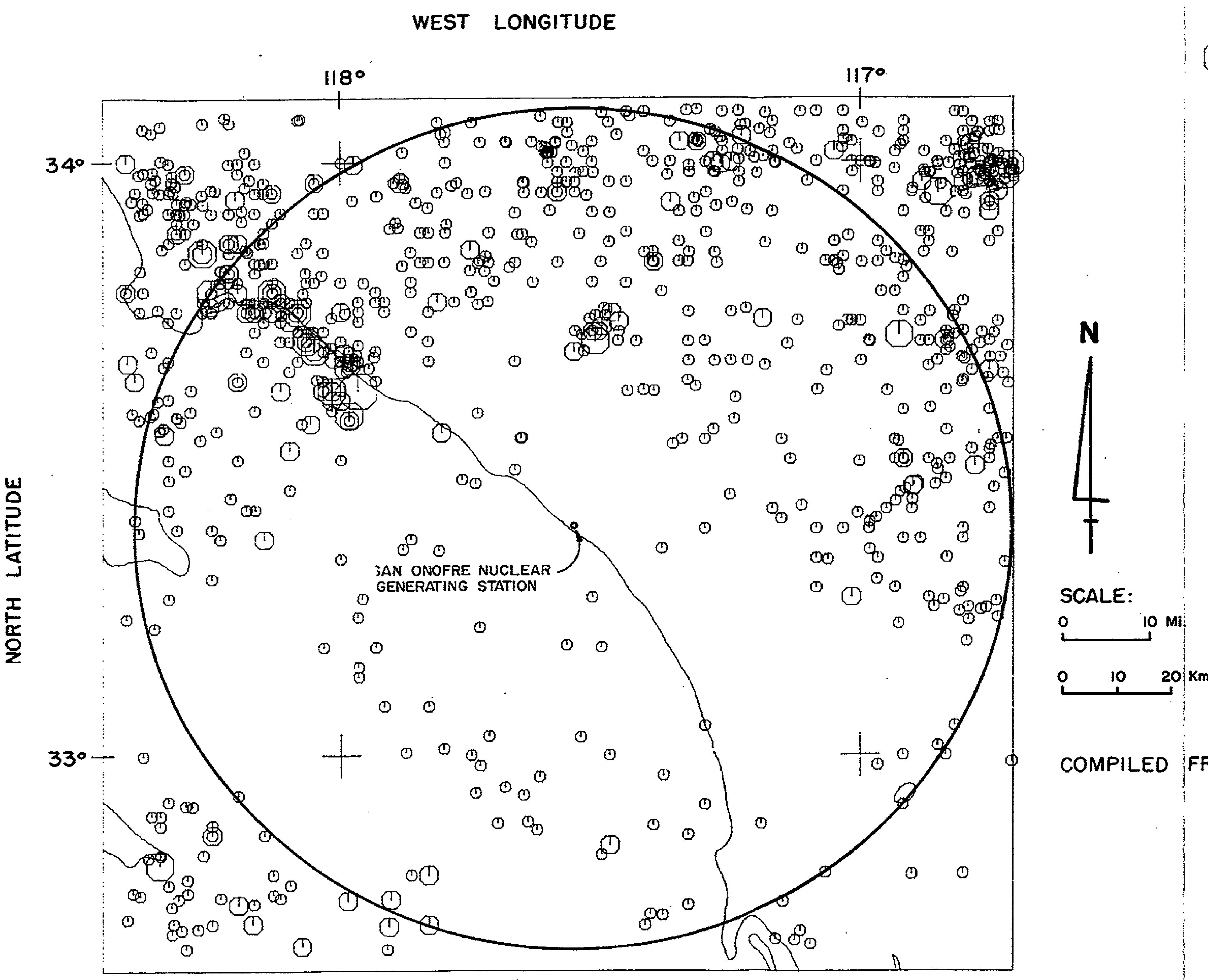

SAN ONOFRE NUCLEAR GENERATING STATION
Units 2 & 3

PLOT OF INSTRUMENTAL EPICENTERS M3.0 AND GREATER WITHIN 80-KILOMETER RADIUS

Figure 2.5-23

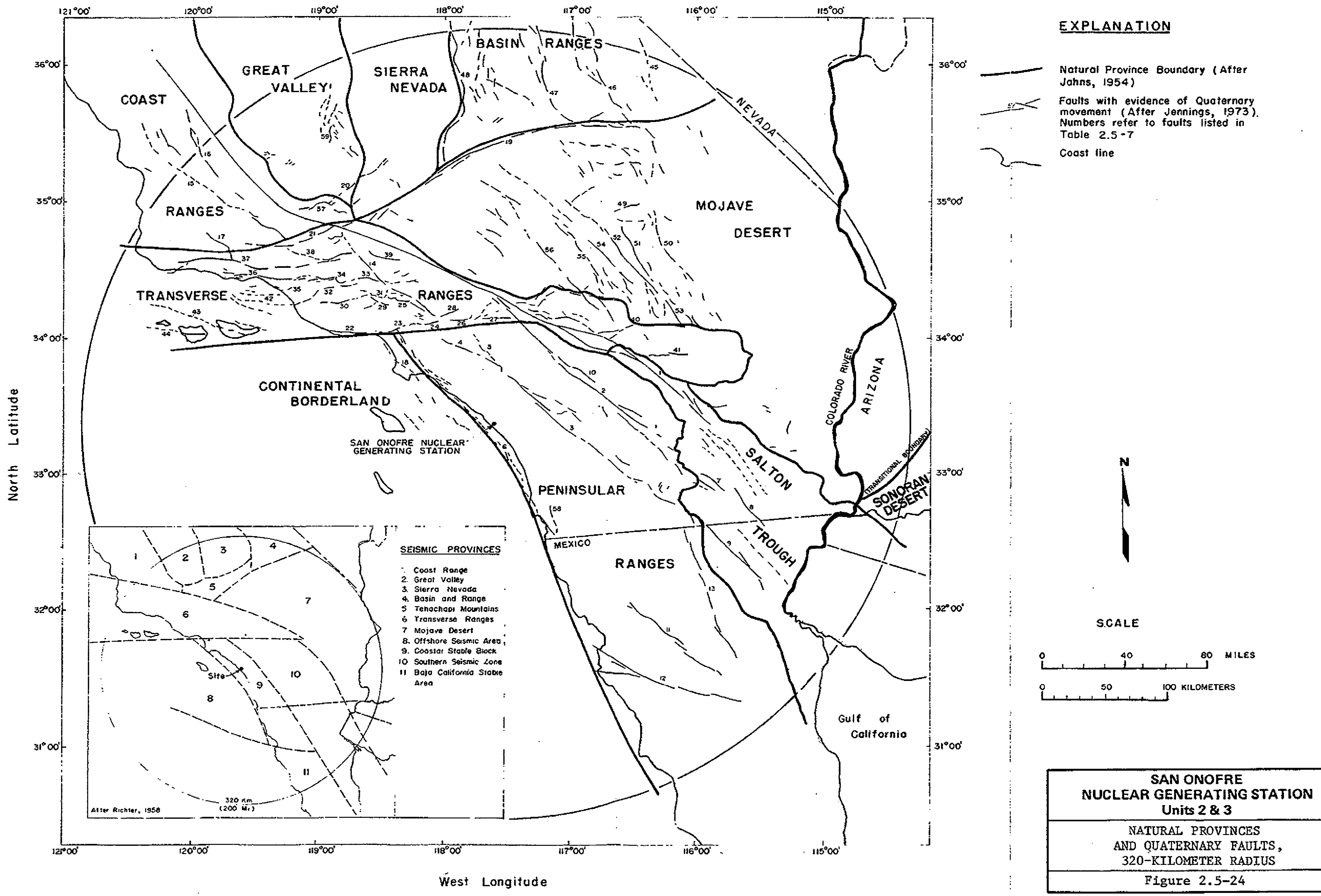

SAN ONOFRE NUCLEAR GENERATING STATION Units 2 & 3

NATURAL PROVINCES AND QUATERNARY FAULTS, 320-KILOMETER RADIUS

Figure 2.5-24

Site File Copy

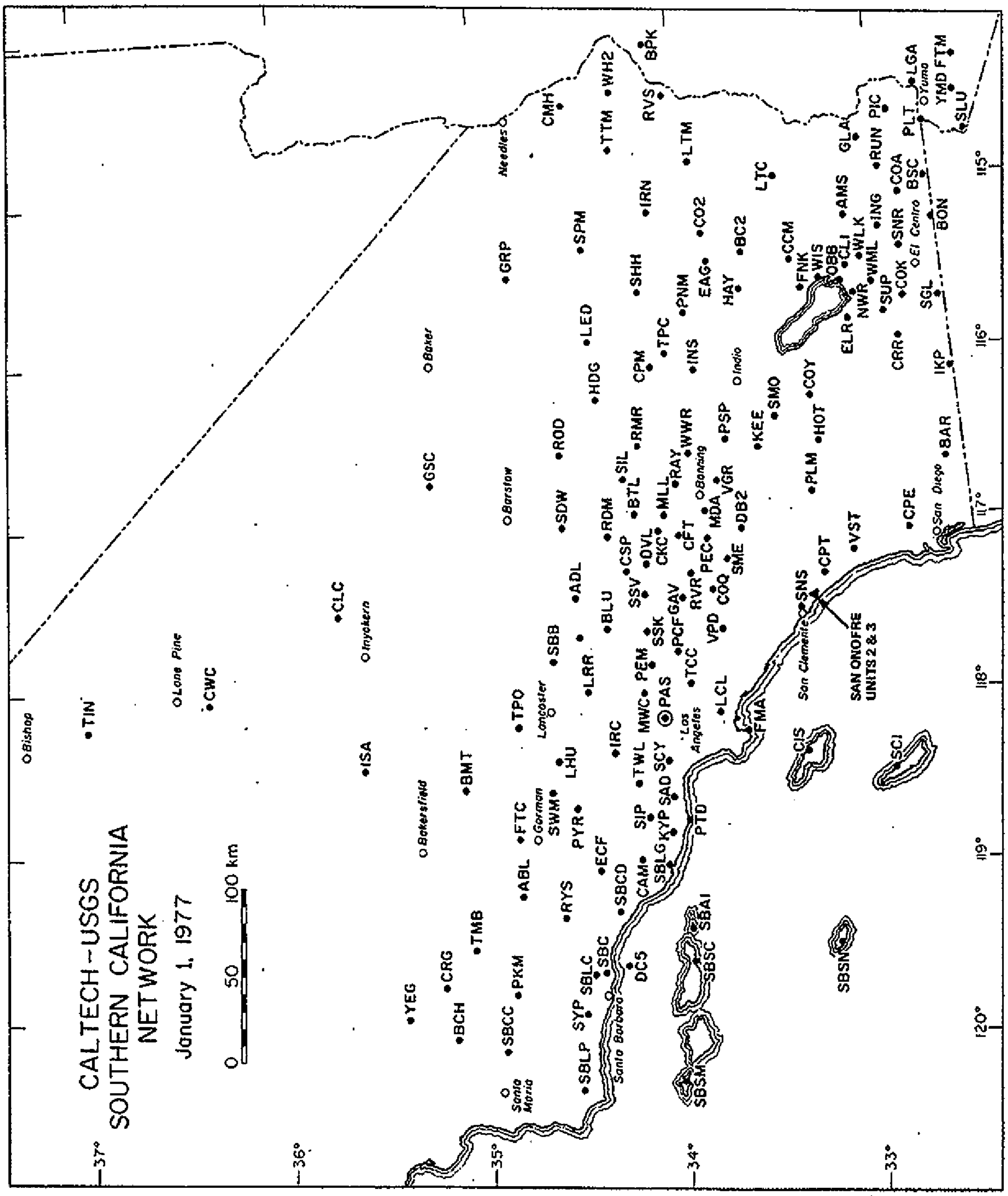

SAN ONOFRE
NUCLEAR GENERATING STATION
Units 2 & 3

CALTECH - USGS
SOUTHERN CALIFORNIA
SEISMOGRAPHIC STATION NETWORK

Figure 2.5-25

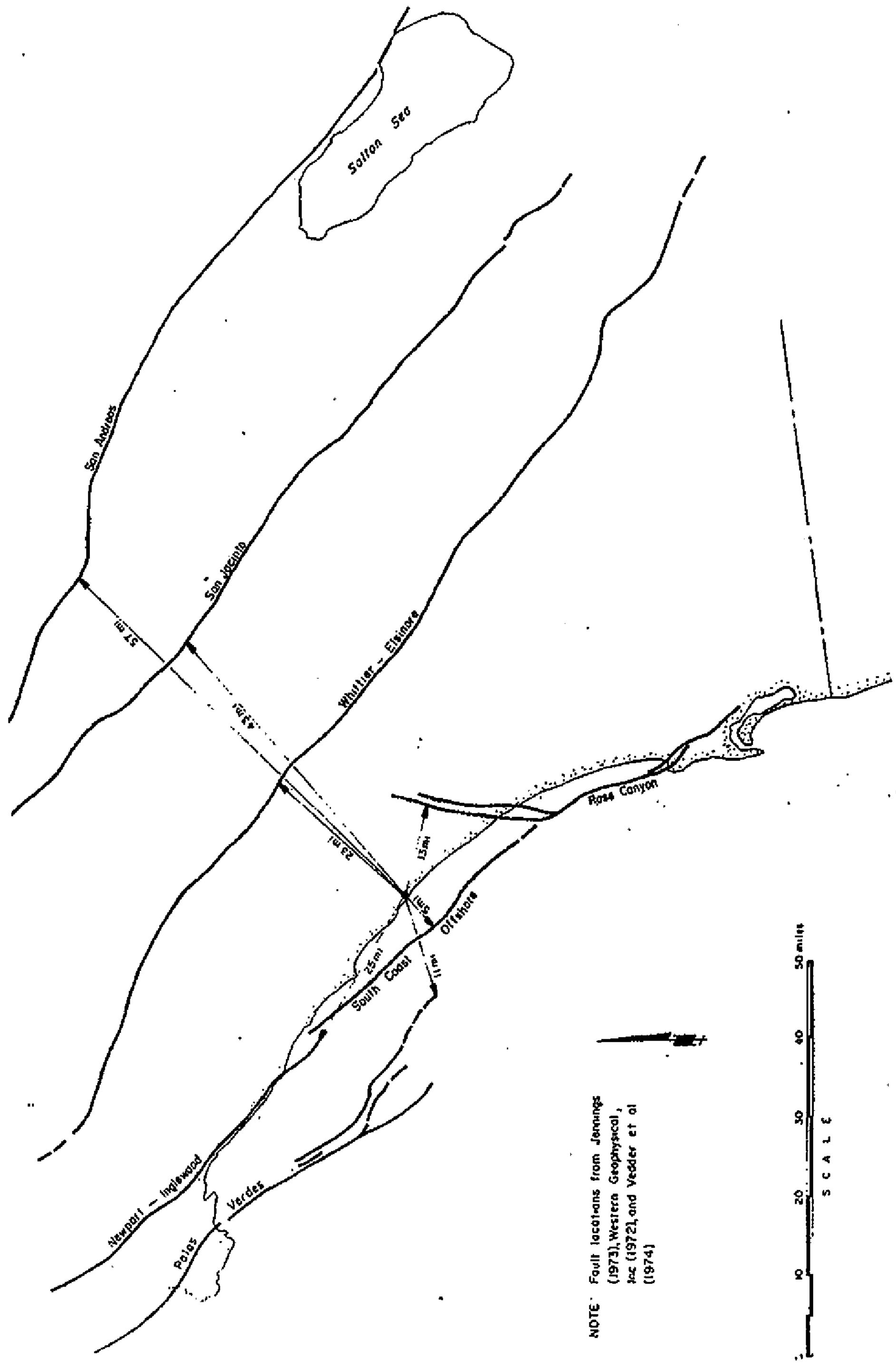

SAN ONOFRE NUCLEAR GENERATING STATION Units 2 & 3

FAULTS AND ZONES OF DEFORMATION CONSIDERED IN MAXIMUM EARTHQUAKE POTENTIAL EVALUATION

Figure 2.5-26

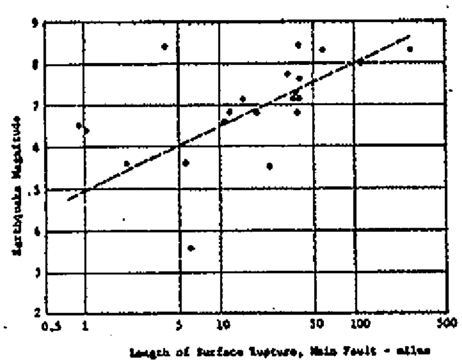

a) EARTHQUAKE MAGNITUDE vs LENGTH OF SURFACE RUPTURE (After Seed and Idriss, 19 9)

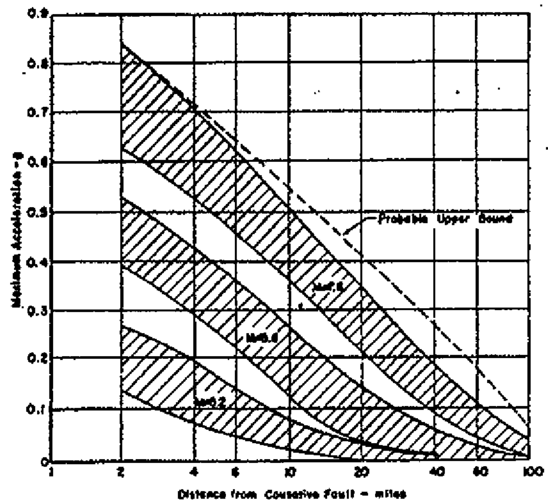

b) RANGES OF MAXIMUM ACCELERATION IN ROCK
(After Schnabel & Seed, 1972)

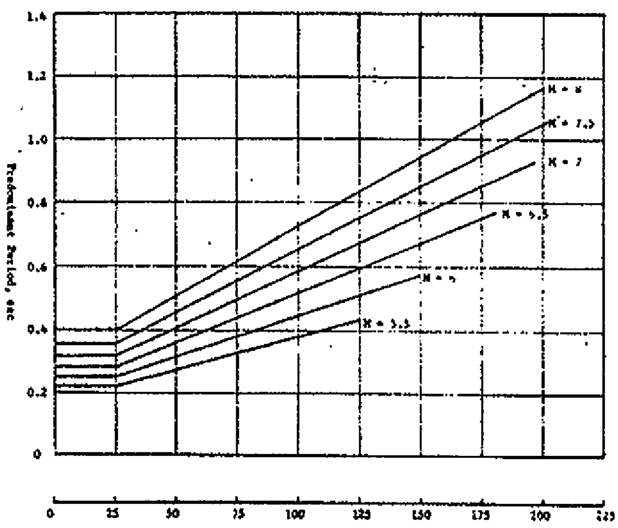

c) PREDOMINANT PERIODS FOR MAXIMUM ACCELERATION IN ROCK
(After Seed and Idriss, 1969)

SAN ONOFRE NUCLEAR GENERATING STATION Units 2 & 3
EMPIRICAL RELATIONSHIPS USED FOR EARTHQUAKE CHARACTERISTICS
Figure 2.5-27

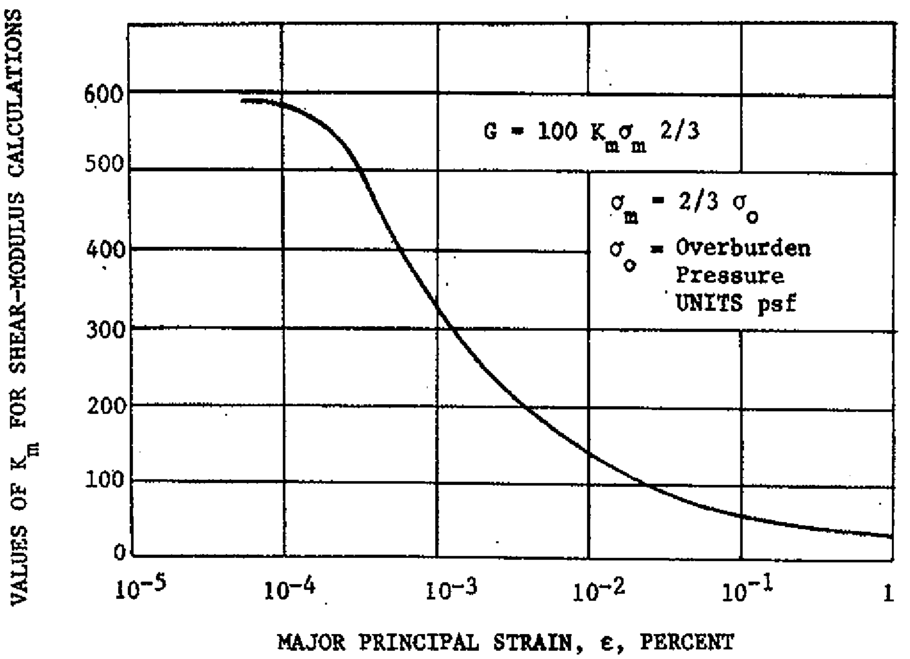

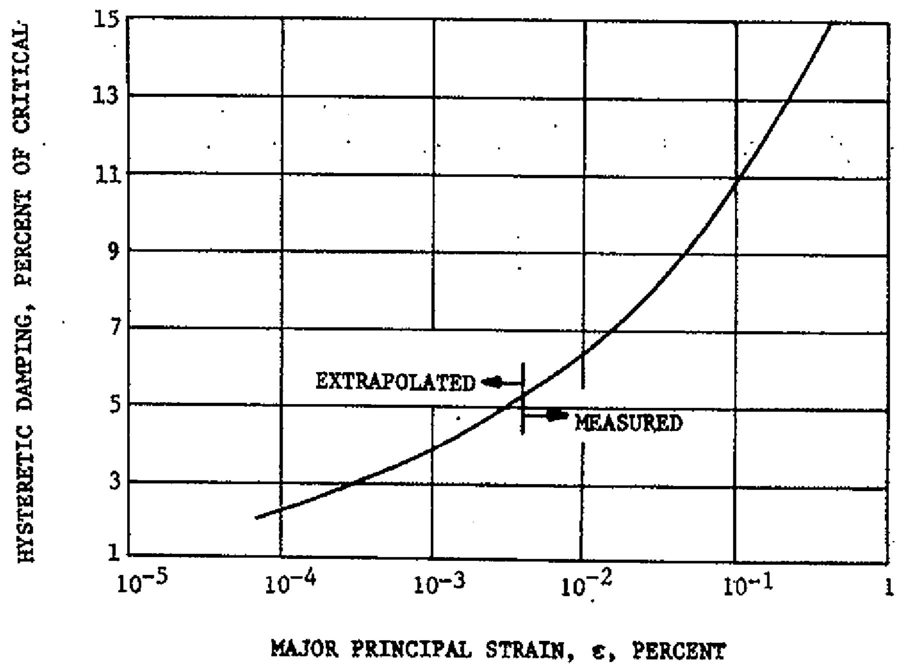

SAN ONOFRE NUCLEAR GENERATING STATION Units 2 & 3
VALUES OF ELASTIC PARAMETERS FOR USE IN FEASIBILITY STUDIES
Figure 2.5-31

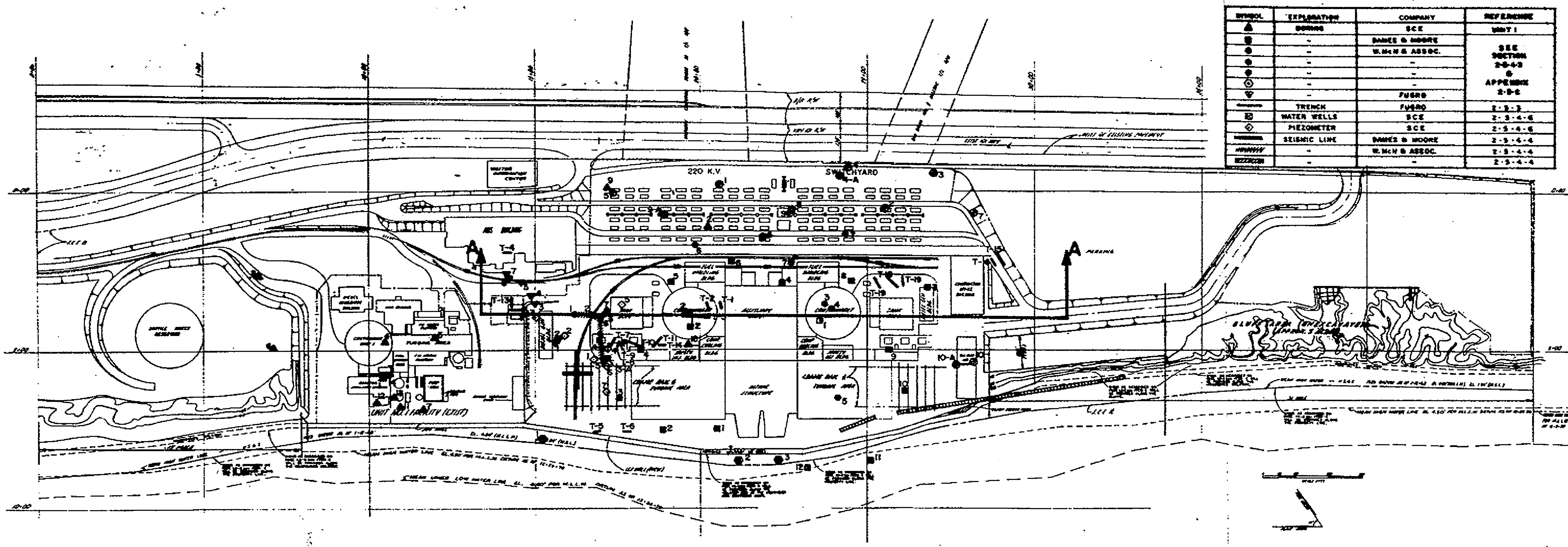

SAN ONOFRE
NUCLEAR GENERATING STATION
Units 2 & 3

PLOT PLAN

Figure 2.5-32

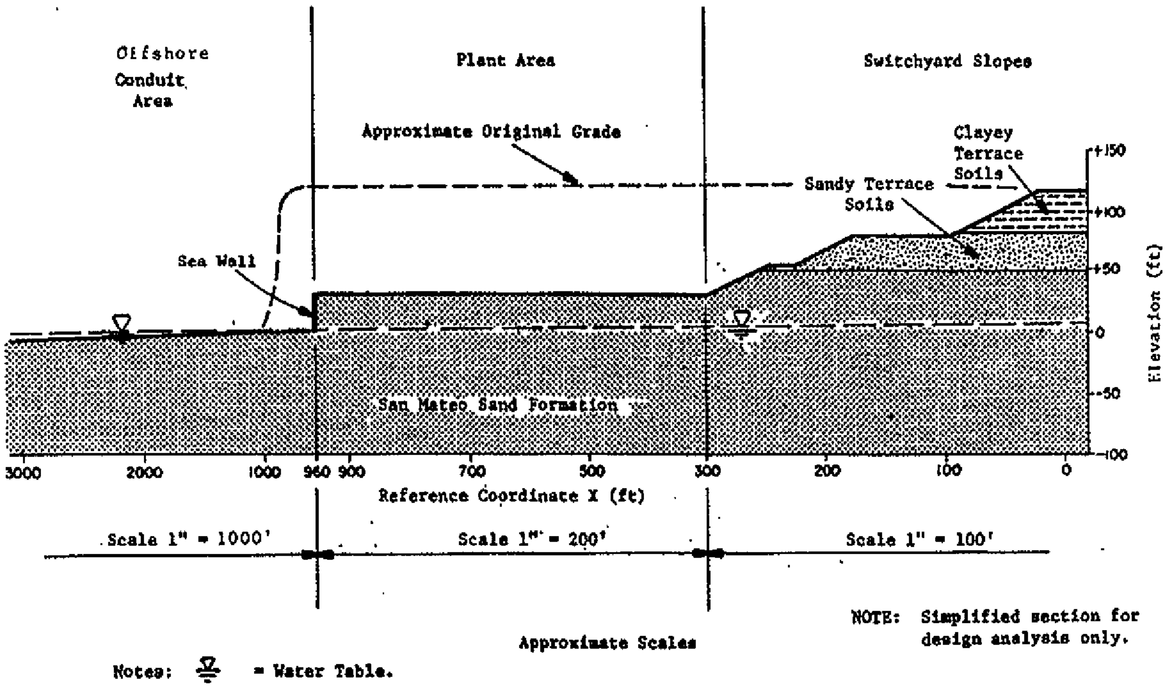

SAN ONOFRE
NUCLEAR GENERATING STATION
Units 2 & 3

COMPOSITE
CROSS-SECTION OF THE SITE

Figure 2.5-33

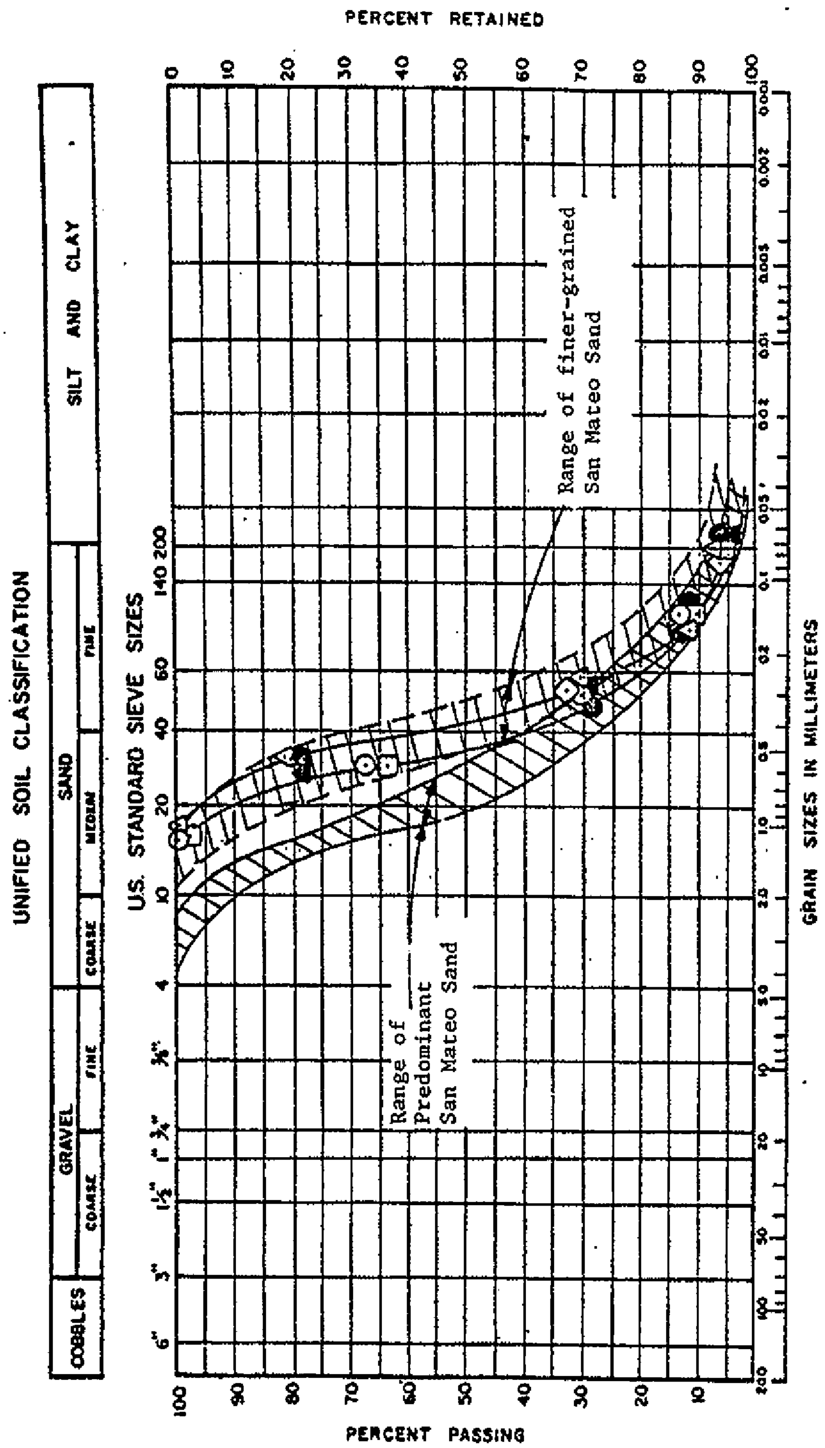

SAN ONOFRE
NUCLEAR GENERATING STATION
Units 2 & 3

GRAIN SIZE DISTRIBUTION CURVES
FOR SAN MATEO SAND

Figure 2.5-34

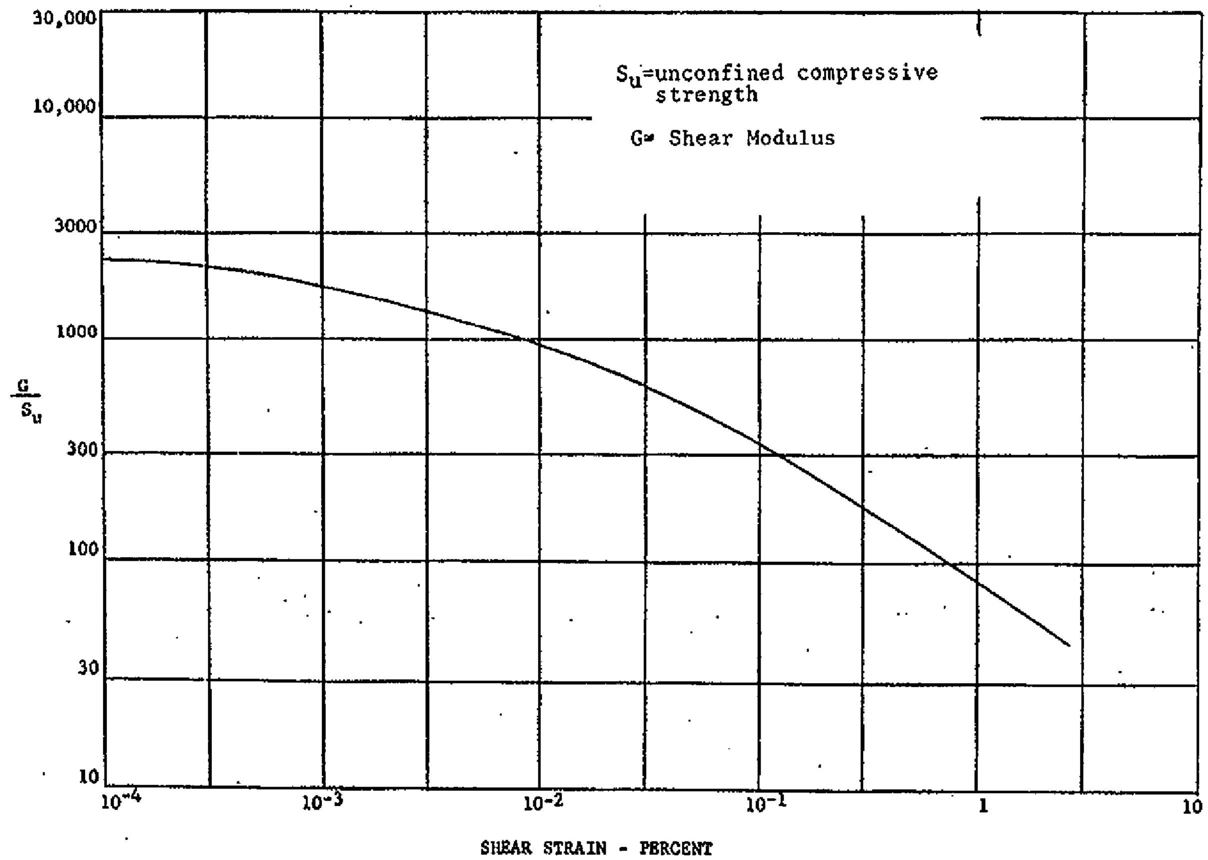

SAN ONOFRE
NUCLEAR GENERATING STATION
Units 2 & 3

VARIATION OF SHEAR MODULUS
WITH STRAIN FOR
CLAYEY TERRACE DEPOSIT SOILS

Figure 2.5-35

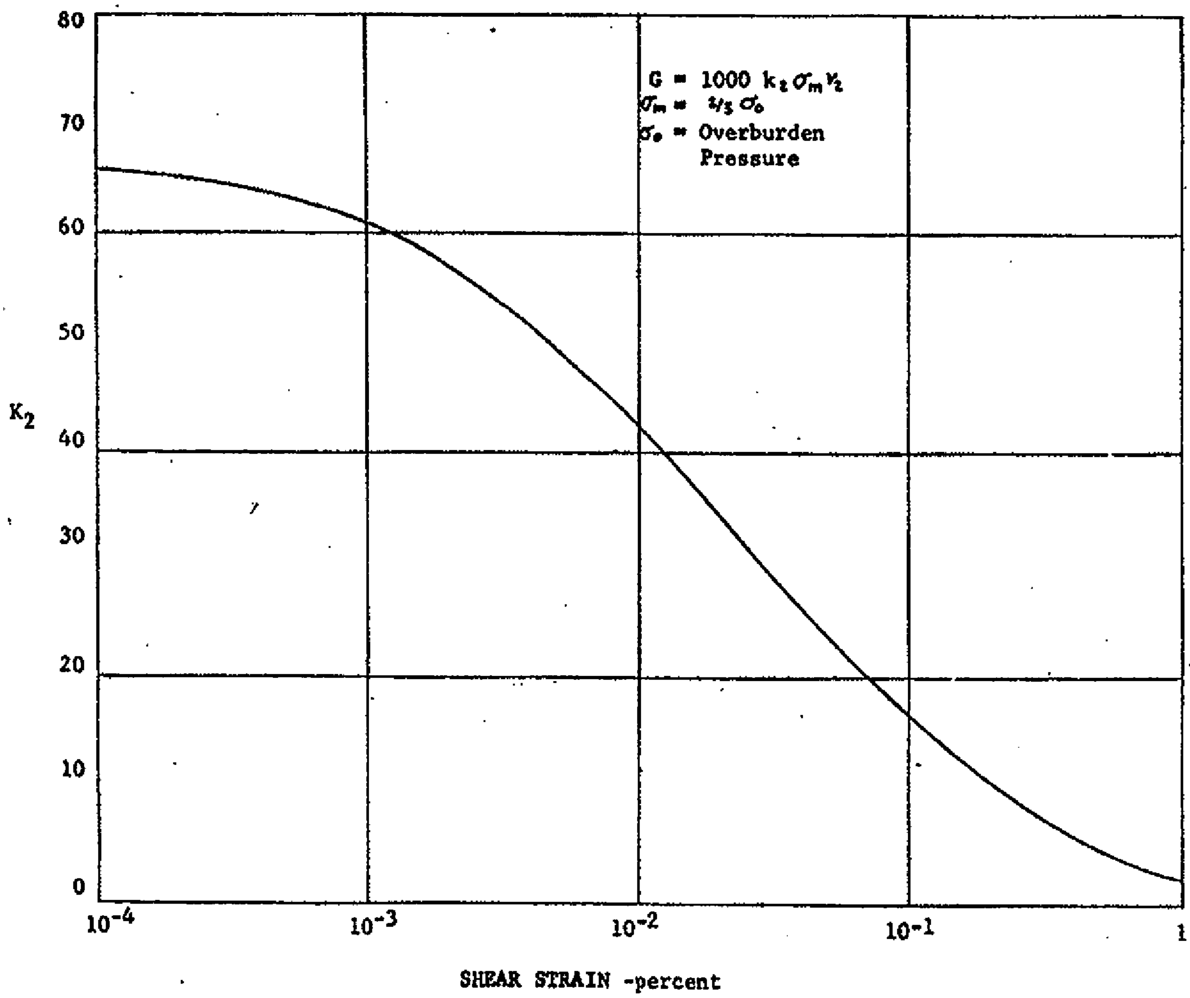

SAN ONOFRE NUCLEAR GENERATING STATION Units 2 & 3
VARIATION OF SHEAR MODULUS WITH STRAIN FOR TERRACE DEPOSIT SAND
Figure 2.5-36

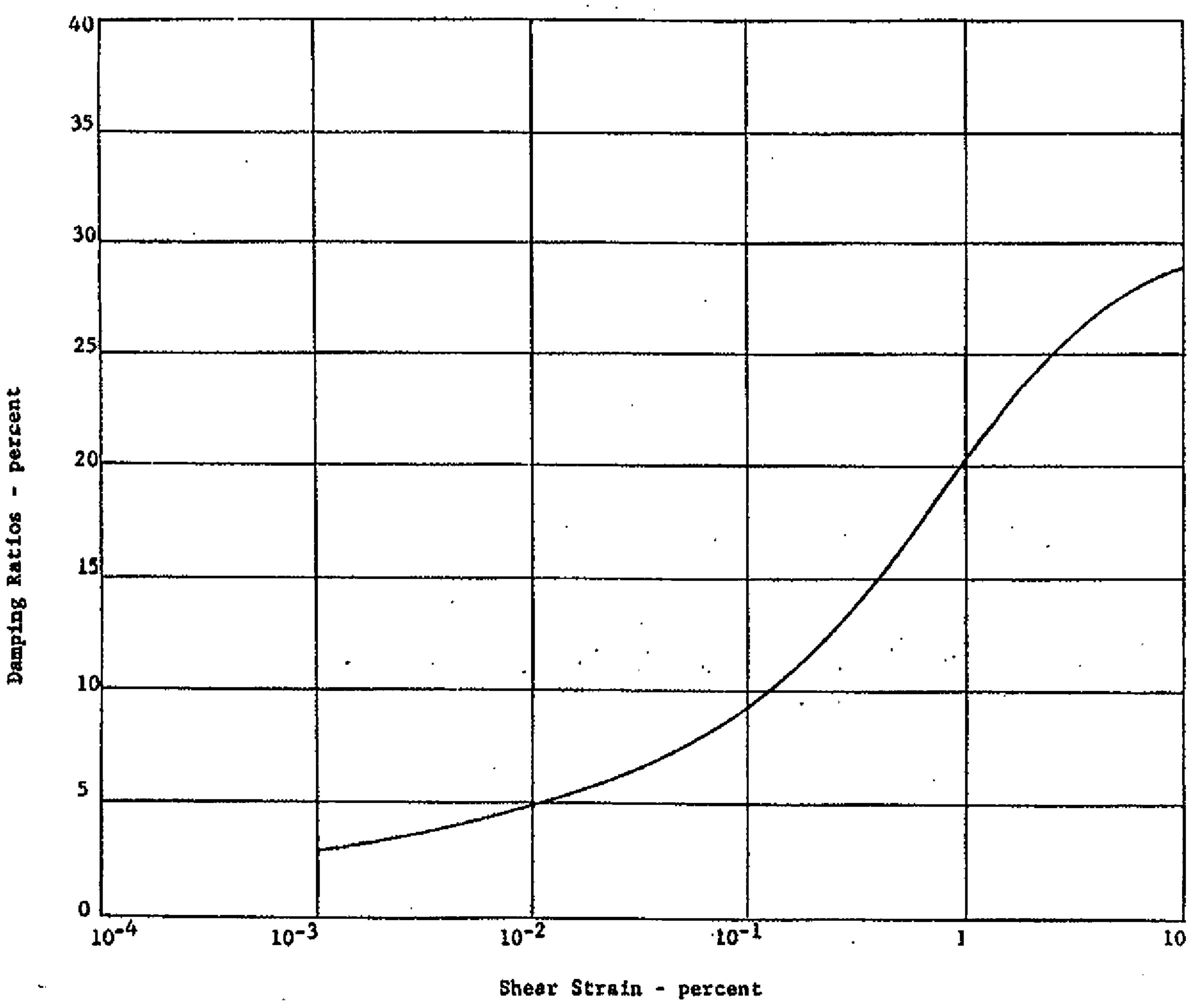

SAN ONOFRE
NUCLEAR GENERATING STATION
Units 2 & 3

VARIATION OF DAMPING RATIO
WITH STRAIN FOR
CLAYEY TERRACE DEPOSIT SOILS

Figure 2.5-37

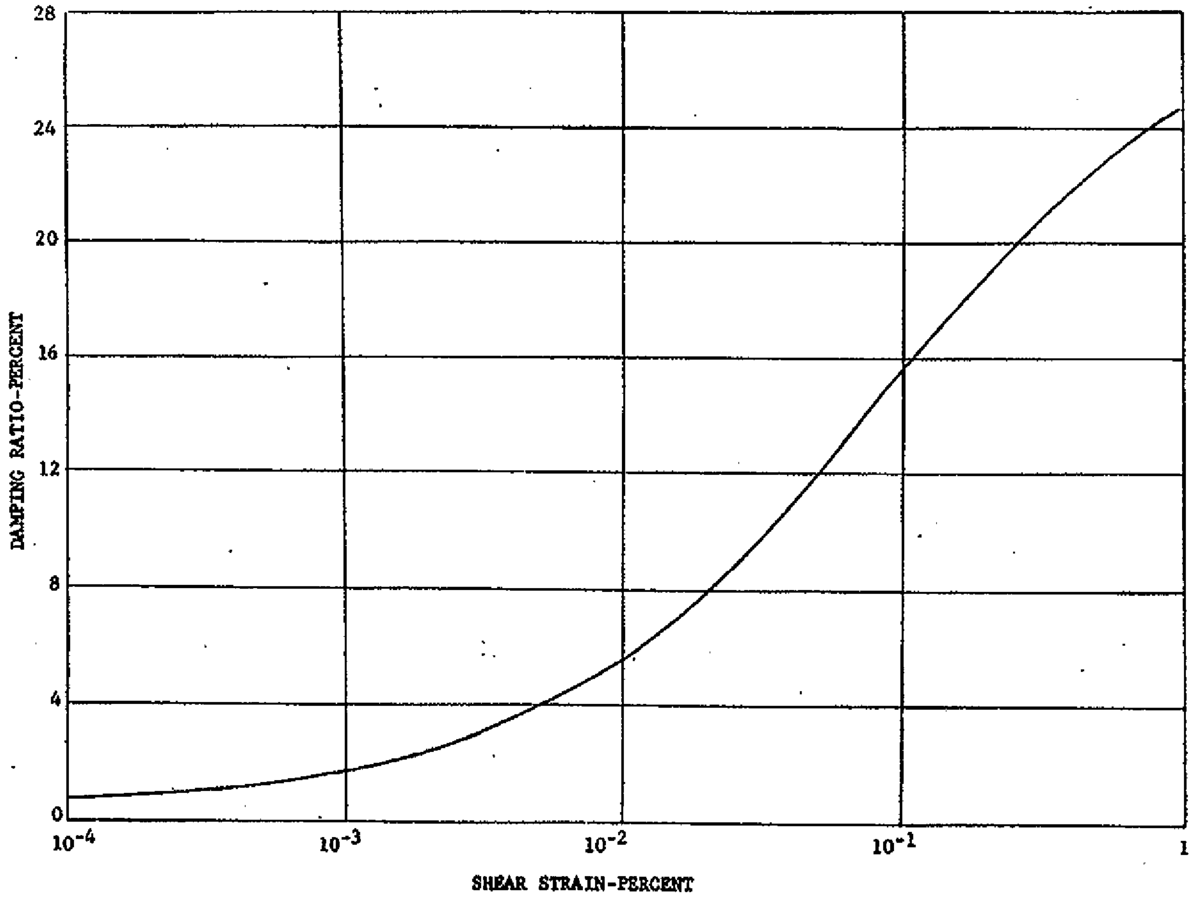

SAN ONOFRE
NUCLEAR GENERATING STATION
Units 2 & 3

VARIATION OF DAMPING RATIO
WITH STRAIN FOR
SANDY TERRACE DEPOSIT SOILS

Figure 2.5-38

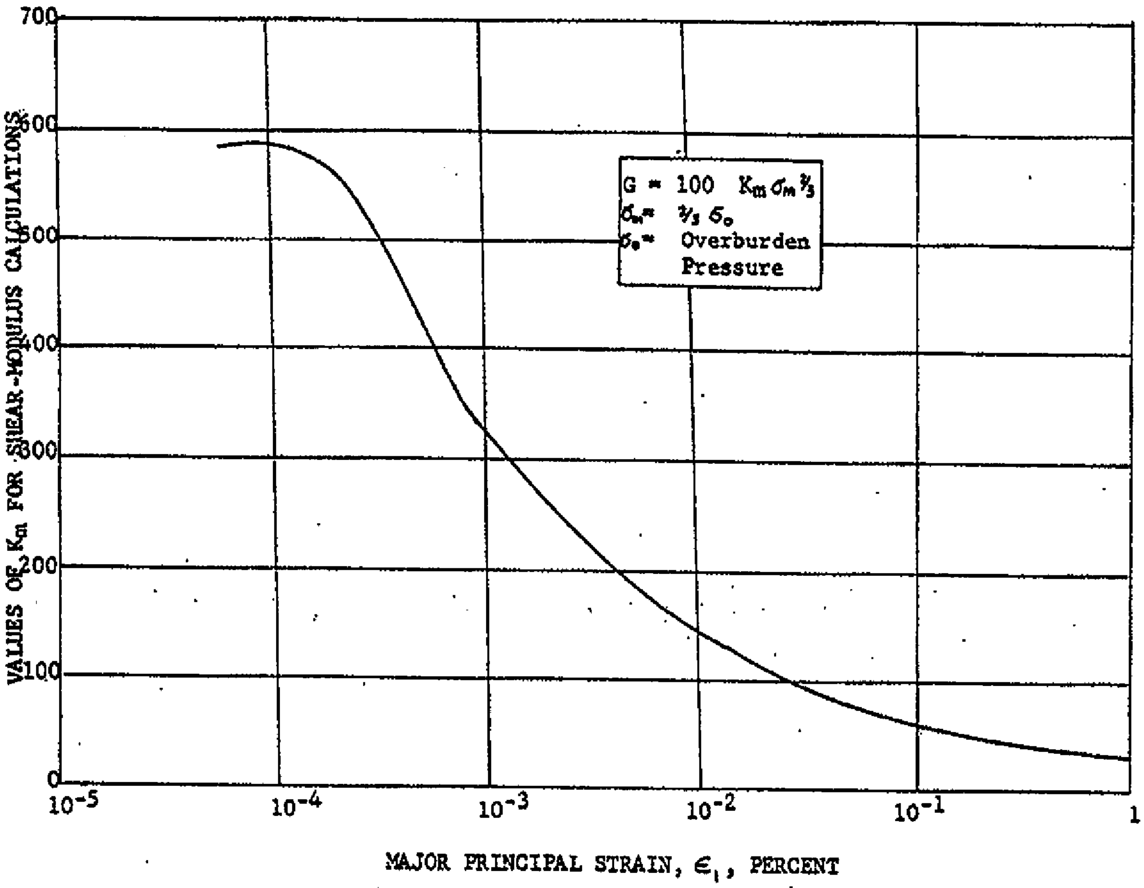

SAN ONOFRE
NUCLEAR GENERATING STATION
Units 2 & 3

VARIATION OF SHEAR MODULUS
WITH STRAIN FOR
SAN MATEO SAND

Figure 2.5-39

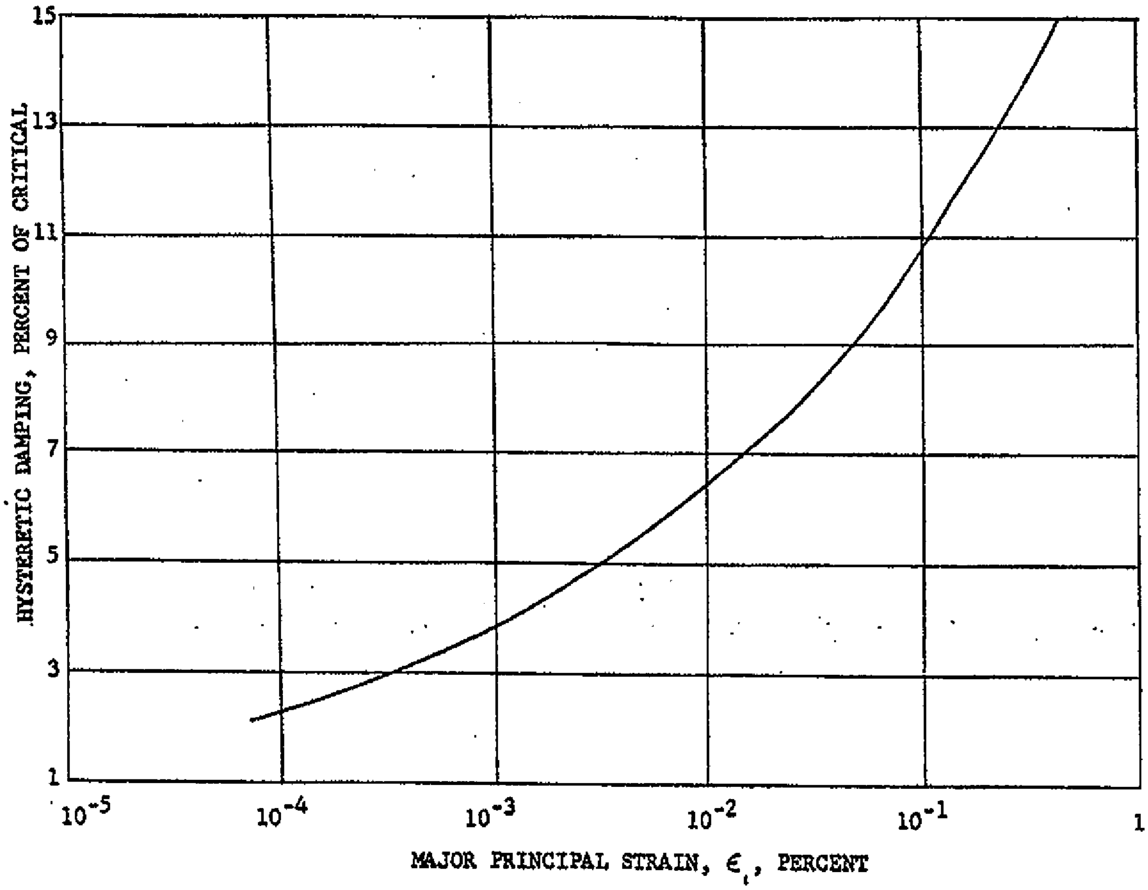

SAN ONOFRE
NUCLEAR GENERATING STATION
Units 2 & 3

VARIATION OF DAMPING RATIO
WITH STRAIN FOR
SAN MATEO SAND

Figure 2.5-40

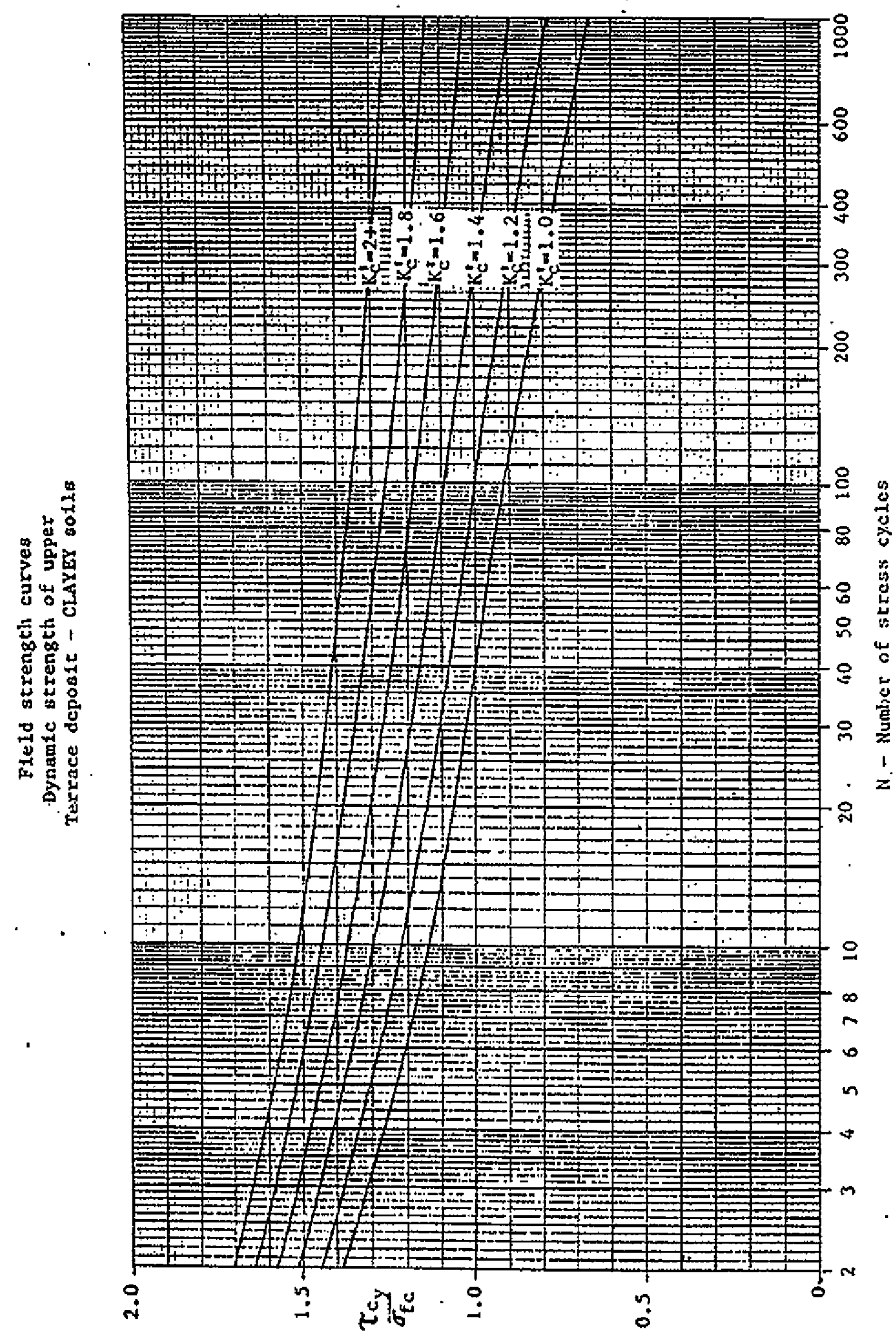

SAN ONOFRE
NUCLEAR GENERATING STATION
Units 2 & 3

DYNAMIC STRENGTH,
CLAYEY TERRACE SOILS

Figure 2.5-41

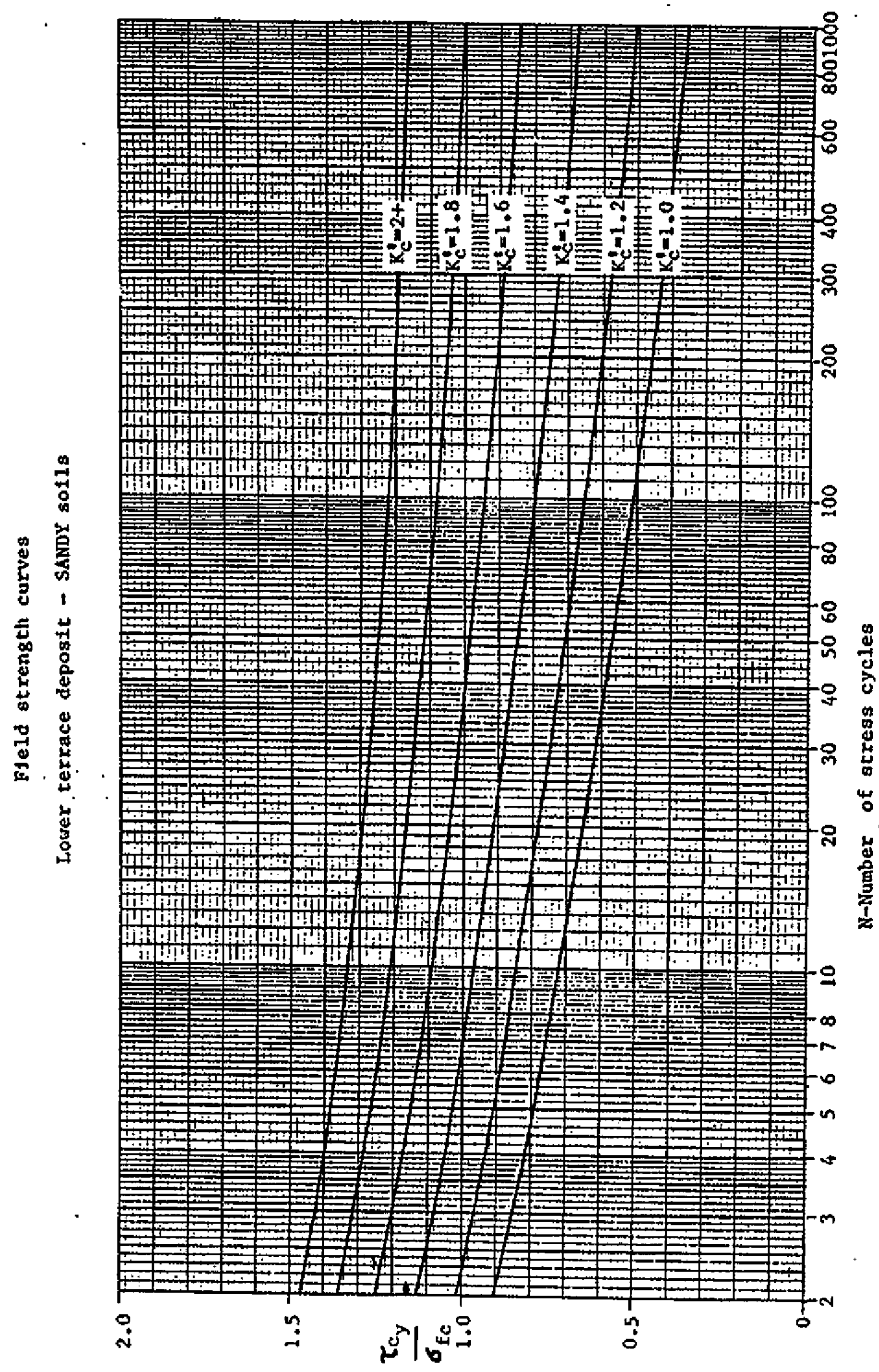

SAN ONOFRE
NUCLEAR GENERATING STATION
Units 2 & 3

DYNAMIC STRENGTH,
SANDY TERRACE SOILS

Figure 2.5-42

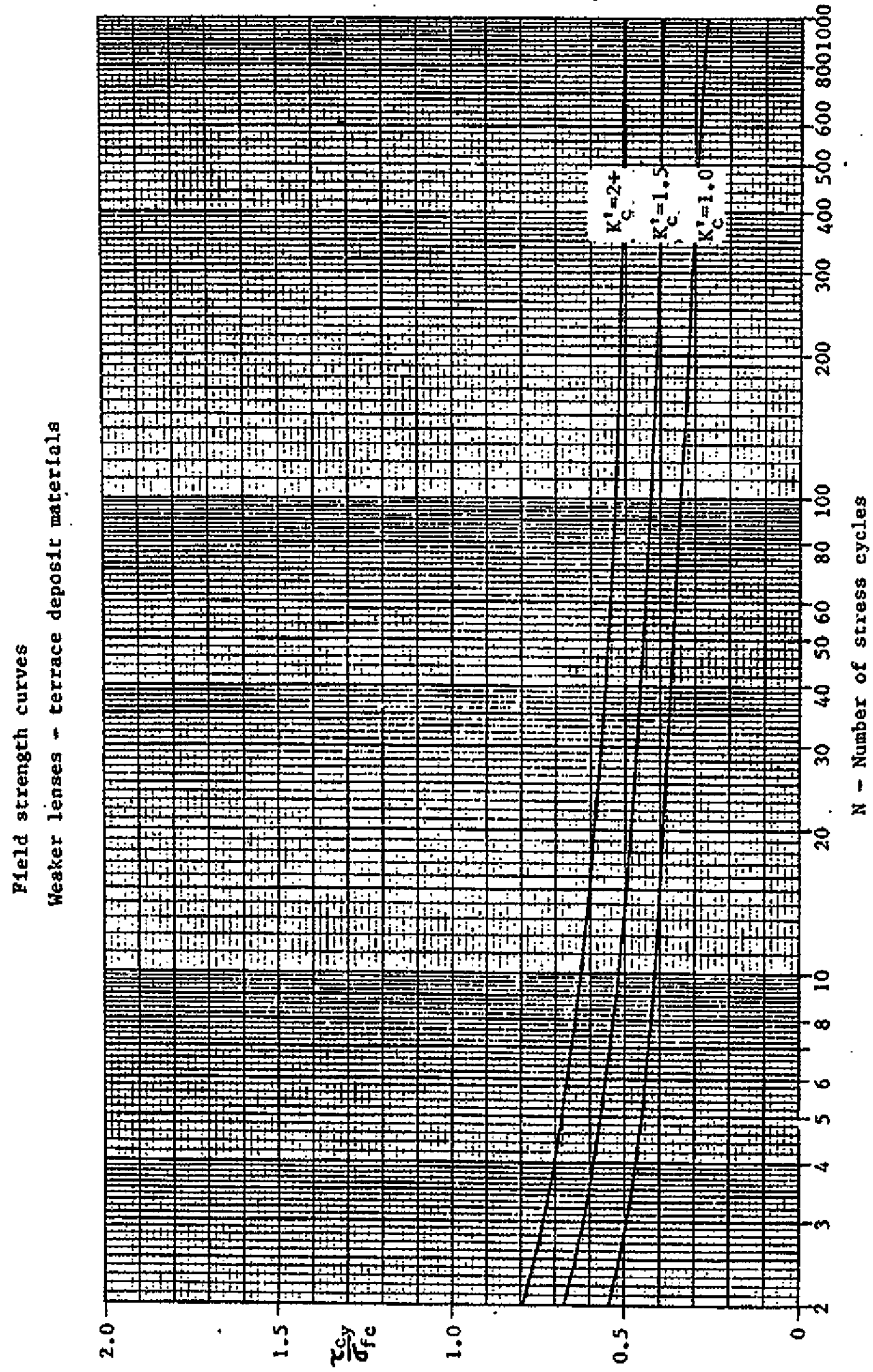

SAN ONOFRE
NUCLEAR GENERATING STATION
Units 2 & 3

DYNAMIC STRENGTH,
WEAKER SOIL LENSES,
TERRACE DEPOSITS

Figure 2.5-43

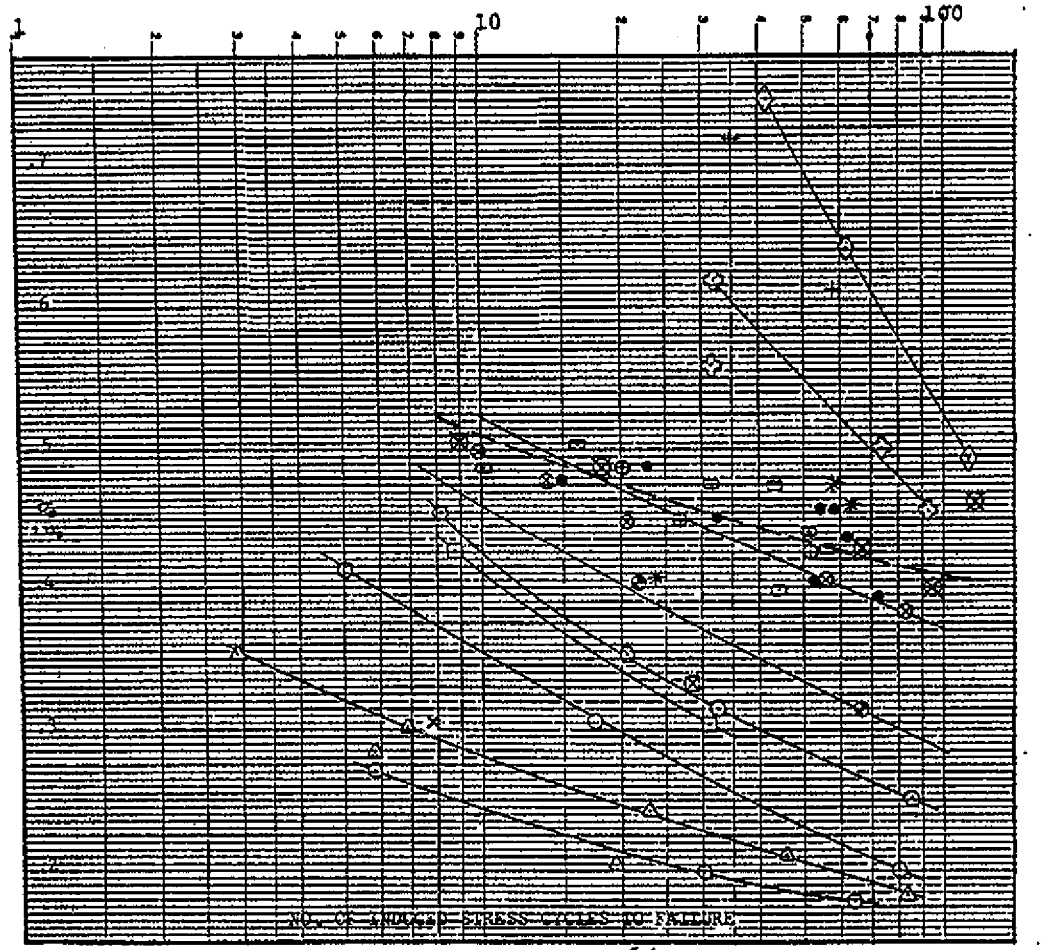

Symbol	Preparation	γ_d PCF	σ_3 PSF	σ_1/σ_3	Frequency
⊙	Remolded	112	4000	1	1 cps
⊙	Remolded	105	7500	1	1 cps
△	Remolded	105	4000	1	1 cps
×	Block	109	4000	1	1 cps
⊡	Block	109	4000	1	1 cps
⊗	Remolded	118	4000	1	1 cps
⊖	Remolded	118	4000	1	1 cps
*	Remolded	118	4000	1	4 cps
⊂⊃	Remolded	118	4000	1	2 cps
●	Remolded	118	4000	1	3 cps
◇	Remolded	118	4000	1.5	1 cps
✧	Remolded	118	4000	1.25	1 cps
+	Remolded	118	4000	1.5	3 cps
○	Remolded	109	4000	1	1 cps
⊠	Remolded	113	4000	1	1 cps
⊗	Remolded	115	4000	1	1 cps
⊠	Block (Finer-grained)	105-111	4000	1	1 cps

NOTES:

1. 10% PEAK TO PEAK AXIAL STRAIN WAS CONSIDERED FAILURE.
2. IT WAS NOT POSSIBLE TO OBTAIN IN-SITU SAMPLES OF SOIL WITH THE SAME DENSITY (γ_d = 120 TO 125 PCF) AS MEASURED IN THE FIELD. THEREFORE, SAMPLES WERE REMOLDED TO VARIOUS DENSITIES AND THE DATA ANALYZED AS DESCRIBED IN APPENDIX 2.5A.
3. REMOLDED SAMPLES WERE PREPARED BY KNEADING COMPACTION USING THE HARVARD MINIATURE COMPACTOR.
4. INTERPRETED FIELD STRENGTH CURVES DEVELOPED FROM THESE DATA ARE GIVEN ON FIGURES 2.5-46 AND 2.5-47

SAN ONOFRE
NUCLEAR GENERATING STATION
Units 2 & 3

LABORATORY TEST RESULTS,
SAN MATEO SAND

Figure 2.5-44

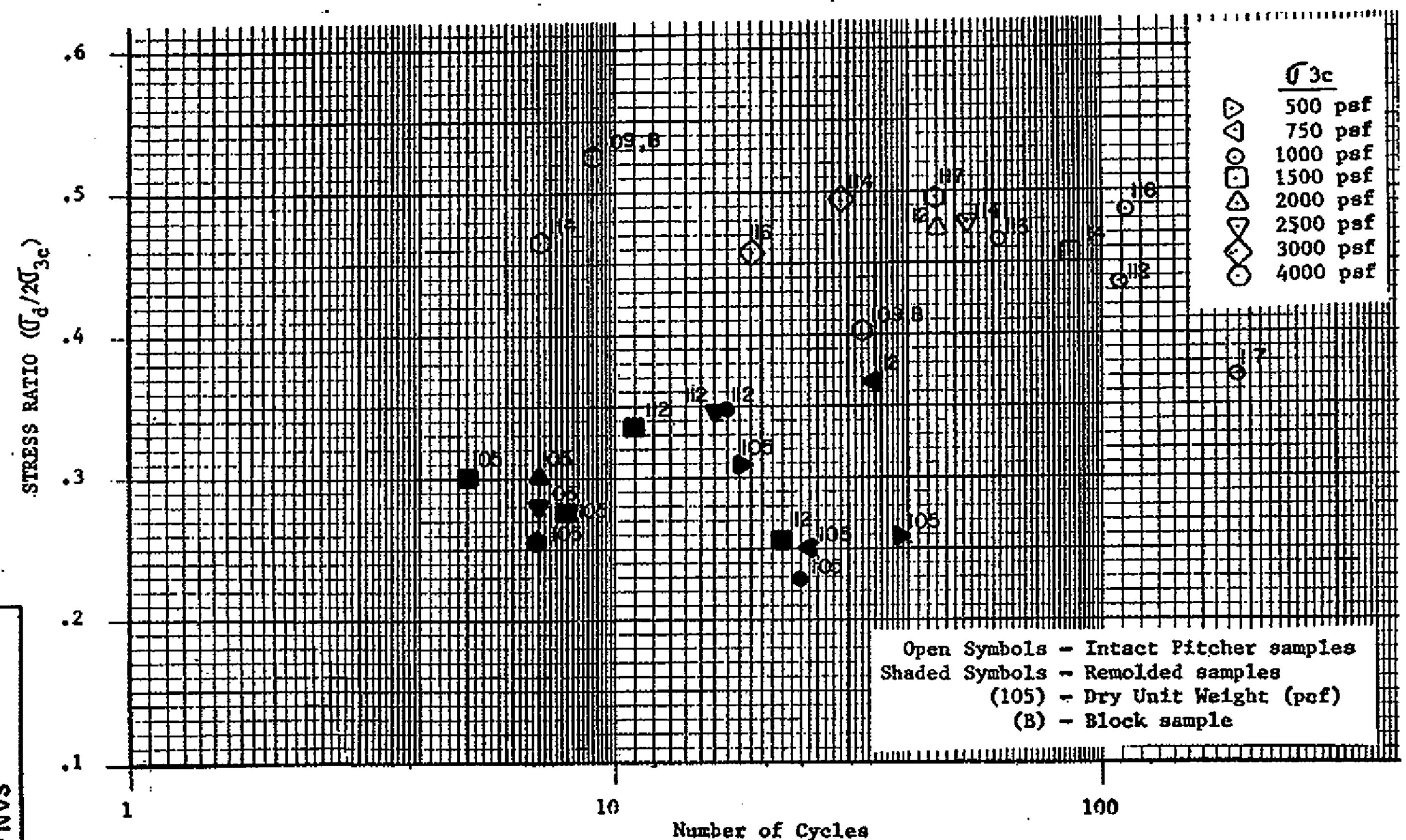

NOTES:

1. 10% PEAK TO PEAK STRAIN WAS CONSIDERED FAILURE.
2. IT WAS NOT POSSIBLE TO OBTAIN IN-SITU SAMPLES OF SOIL WITH THE SAME DENSITY (γ_d = 120 TO 125 PCF) AS MEASURED IN THE FIELD. THEREFORE, SAMPLES WERE REMOLDED TO VARIOUS DENSITIES AND THE DATA ANALYZED AS DESCRIBED IN APPENDIX 2.5A.
3. REMOLDED SAMPLES WERE PREPARED BY KNEADING COMPACTION USING THE HARVARD MINIATURE COMPACTOR.
4. INTERPRETED FIELD STRENGTH CURVES DEVELOPED FROM THESE DATA ARE GIVEN ON FIGURES 2.5-46 AND 2.5-47.

SAN ONOFRE
NUCLEAR GENERATING STATION
Units 2 & 3

DYNAMIC STRENGTH TEST RESULTS
FOR SAN MATEO SAND

Figure 2.5-45

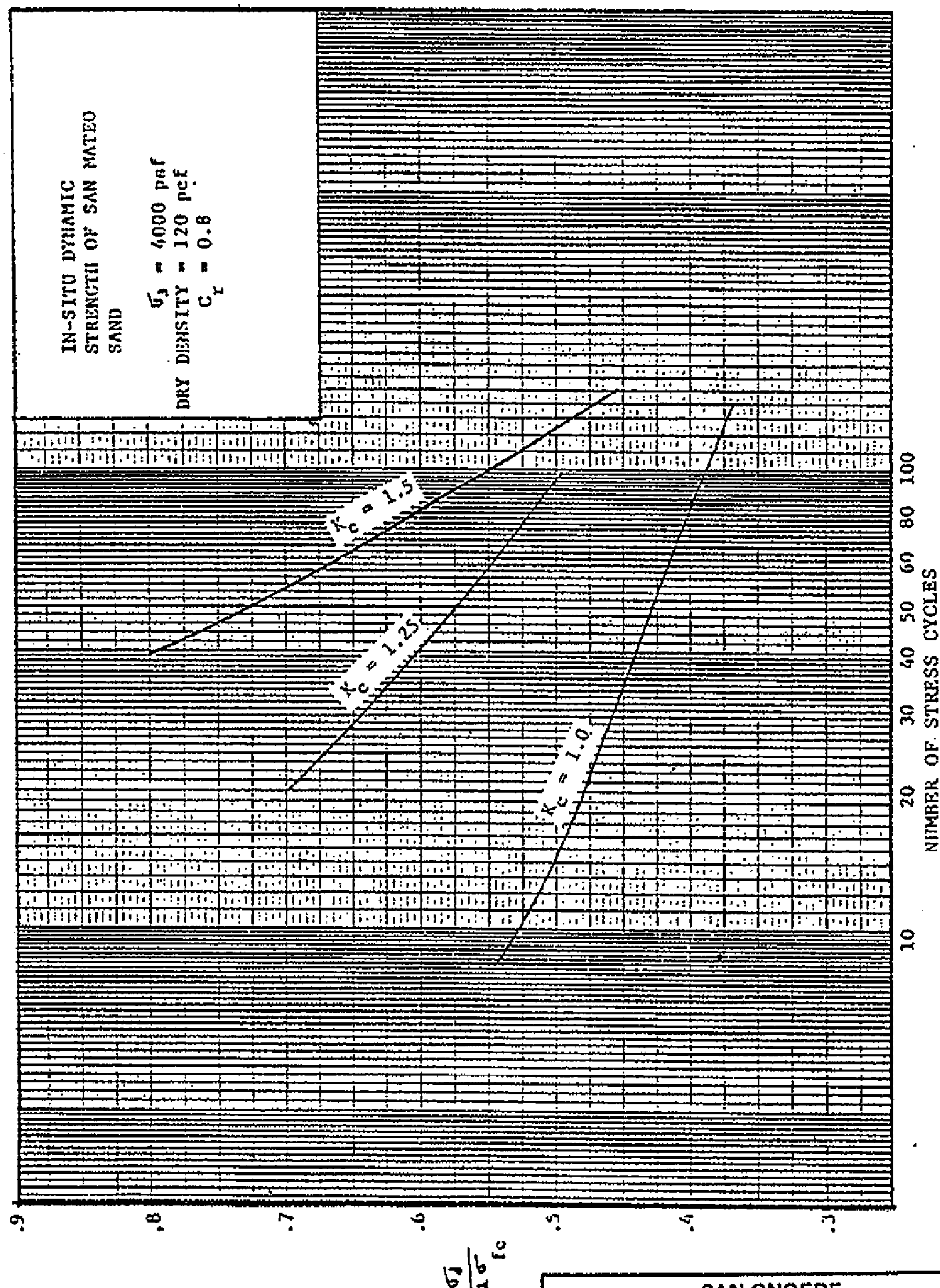

NOTE: THIS FIGURE IS UPDATED BY FIGURE 2.5-74.

SAN ONOFRE
NUCLEAR GENERATING STATION
Units 2 & 3

IN-SITU DYNAMIC STRENGTH OF ANISOTROPICALLY CONSOLIDATED SAN MATEO SAND

Figure 2.5-46

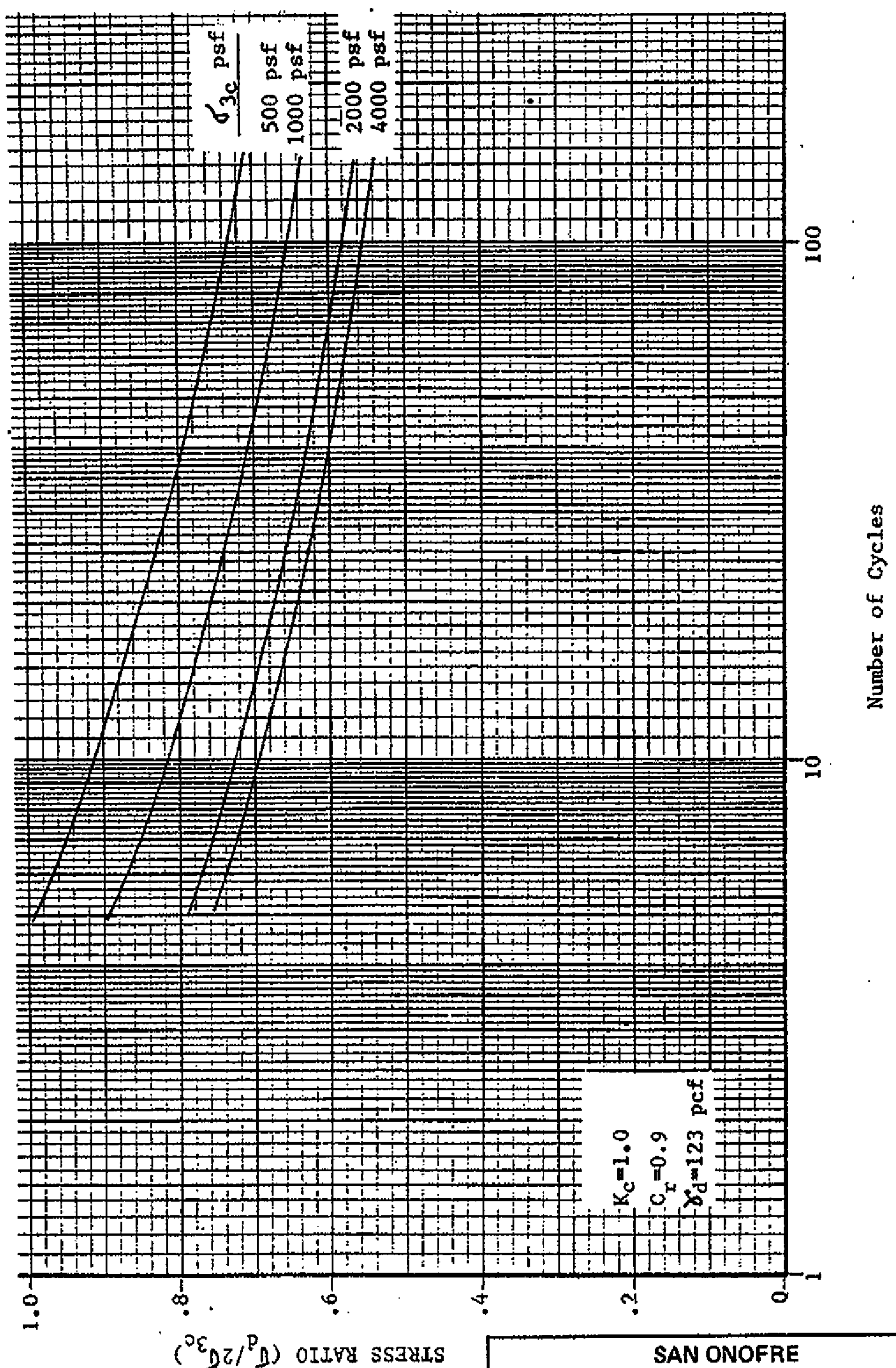

NOTE: THIS FIGURE IS UPDATED BY FIGURE 2.5-75.

SAN ONOFRE NUCLEAR GENERATING STATION Units 2 & 3

IN-SITU DYNAMIC STRENGTH OF SAN MATEO SAND

Figure 2.5-47

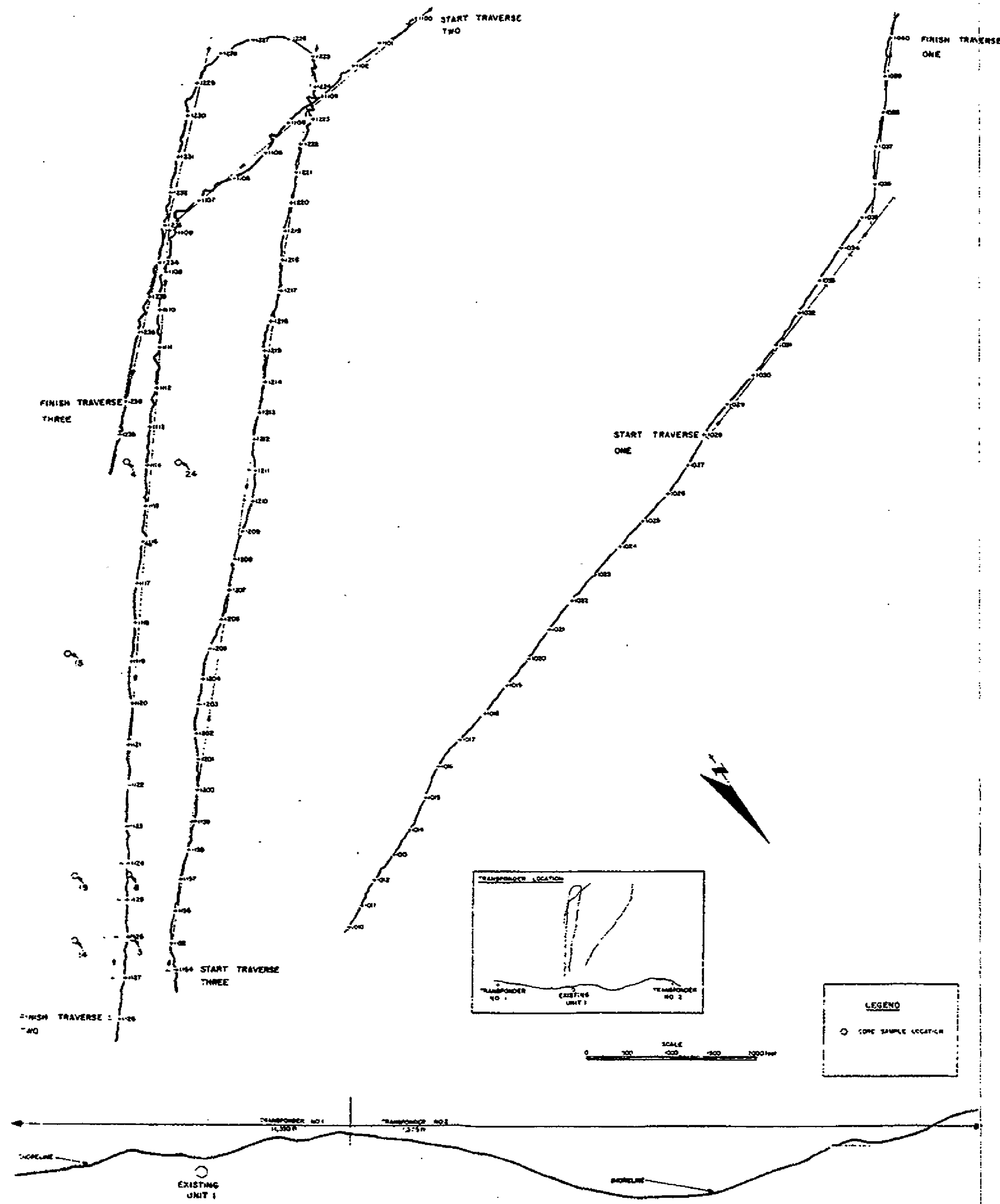

SAN ONOFRE NUCLEAR GENERATING STATION Units 2 & 3

TRAVERSE FOR BOOMER SURVEY AND LOCATIONS FOR VIBRACORE SAMPLING

Figure 2.5-48

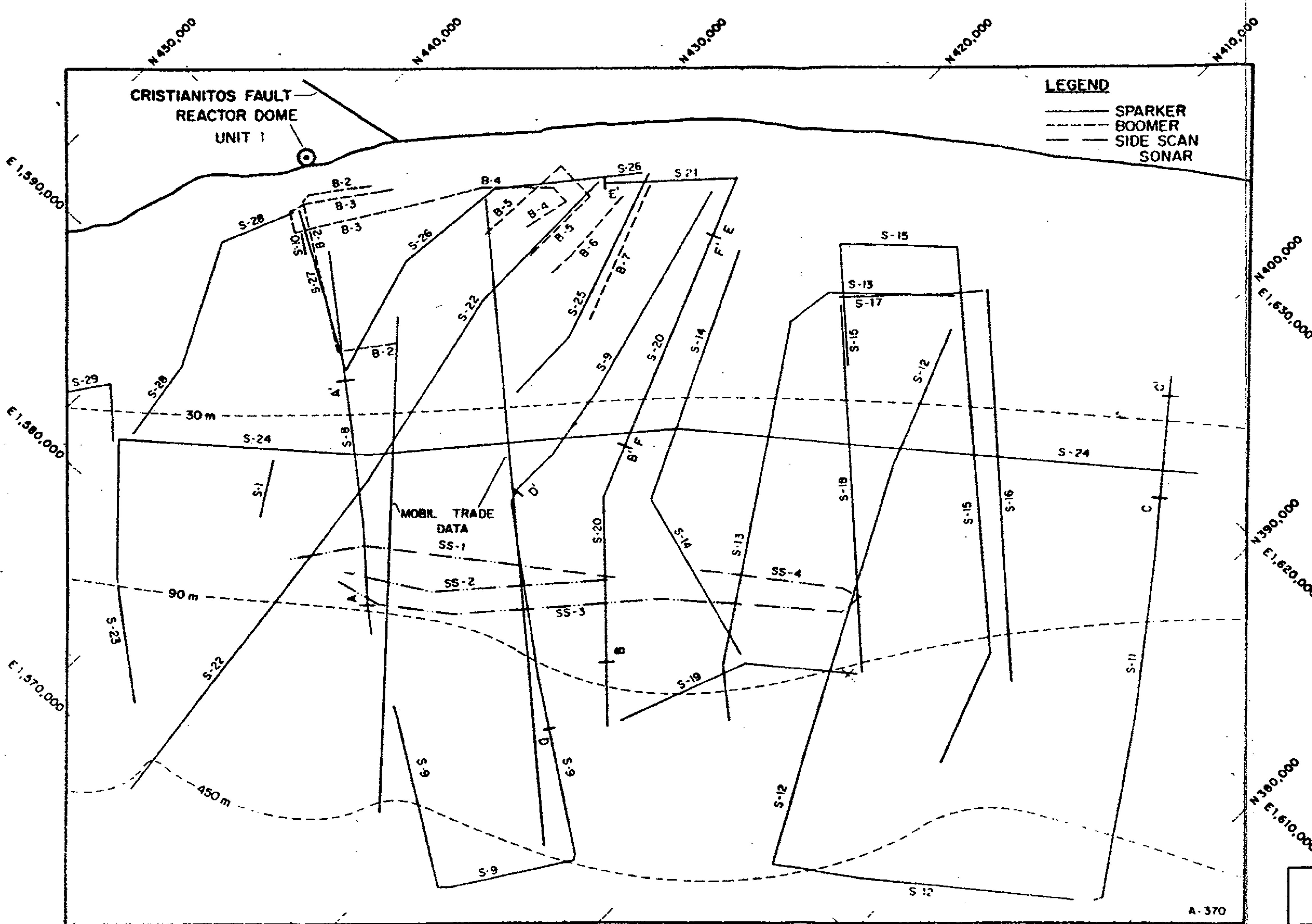

SAN ONOFRE
NUCLEAR GENERATING STATION
Units 2 & 3

SEISMIC PROFILE
AND SIDE SCAN SONAR TRACK
LINE CHART

Figure 2.5-49

Site File Copy

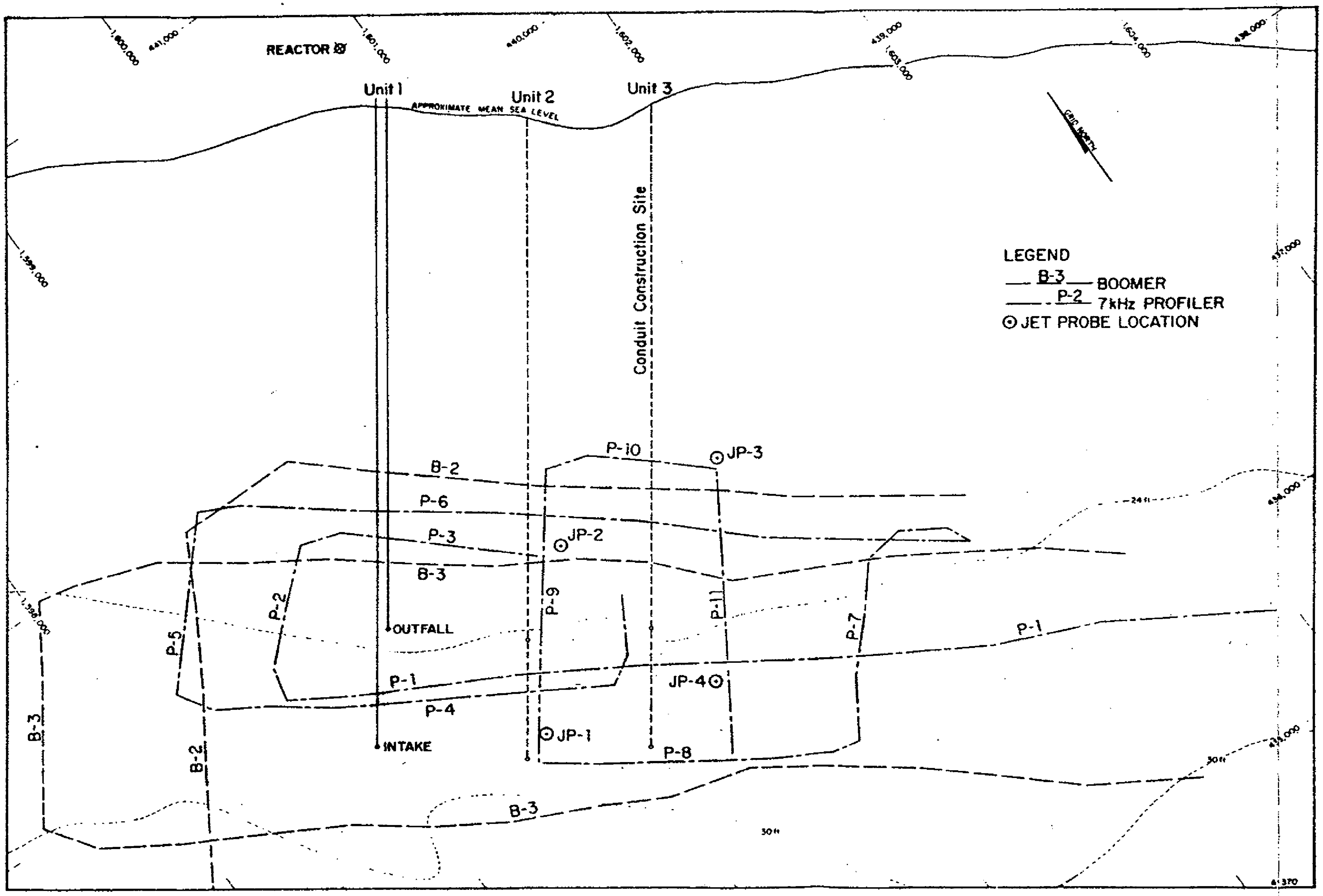

SAN ONOFRE
NUCLEAR GENERATING STATION
Units 2 & 3

HIGH-RESOLUTION PROFILE LINES AND JET PROBE LOCATIONS IN VICINITY OF COOLING WATER CONDUIT CONSTRUCTION SITES

Figure 2.5-50

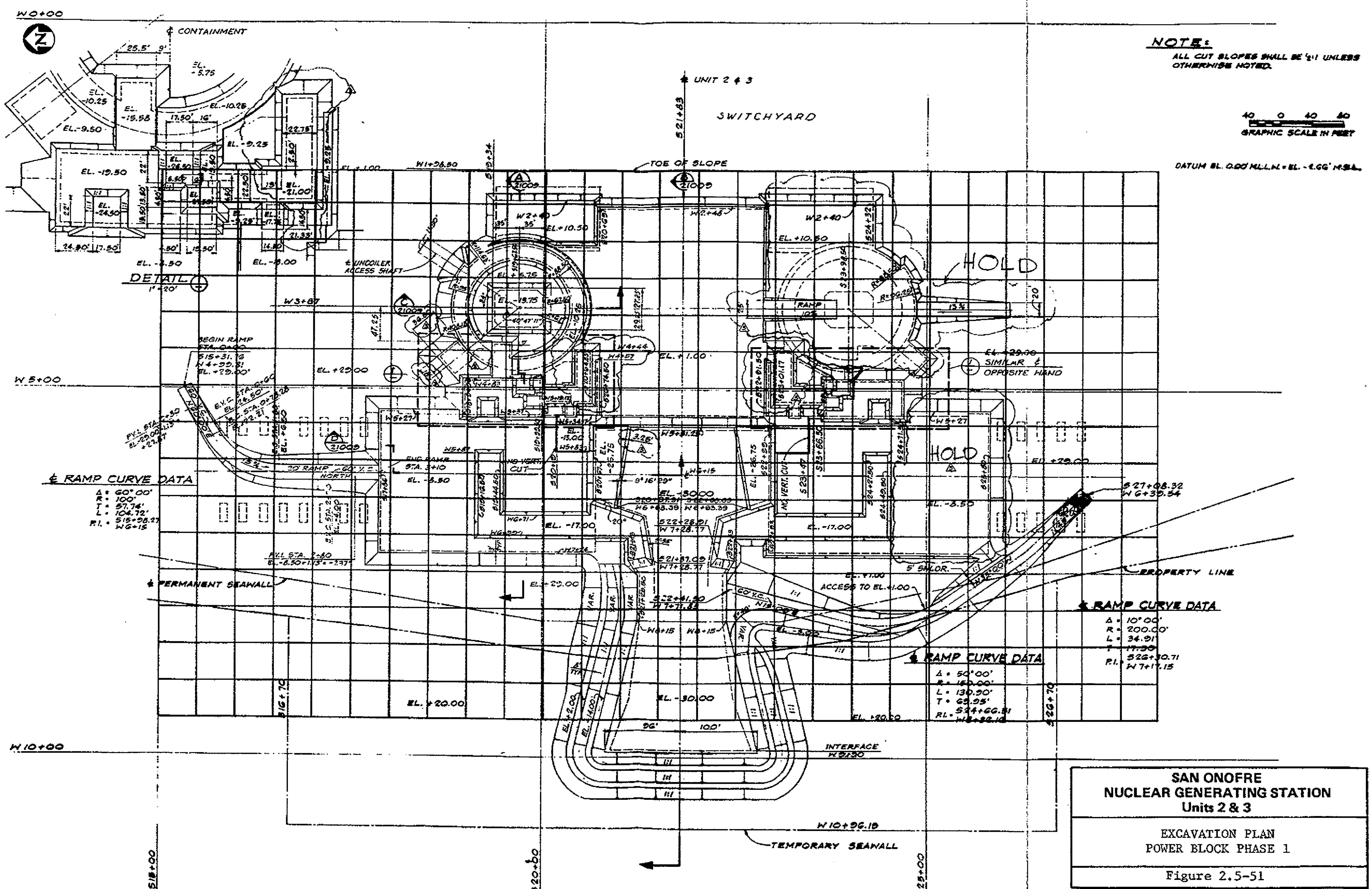

SAN ONOFRE
NUCLEAR GENERATING STATION
Units 2 & 3

EXCAVATION PLAN
POWER BLOCK PHASE 1

Figure 2.5-51

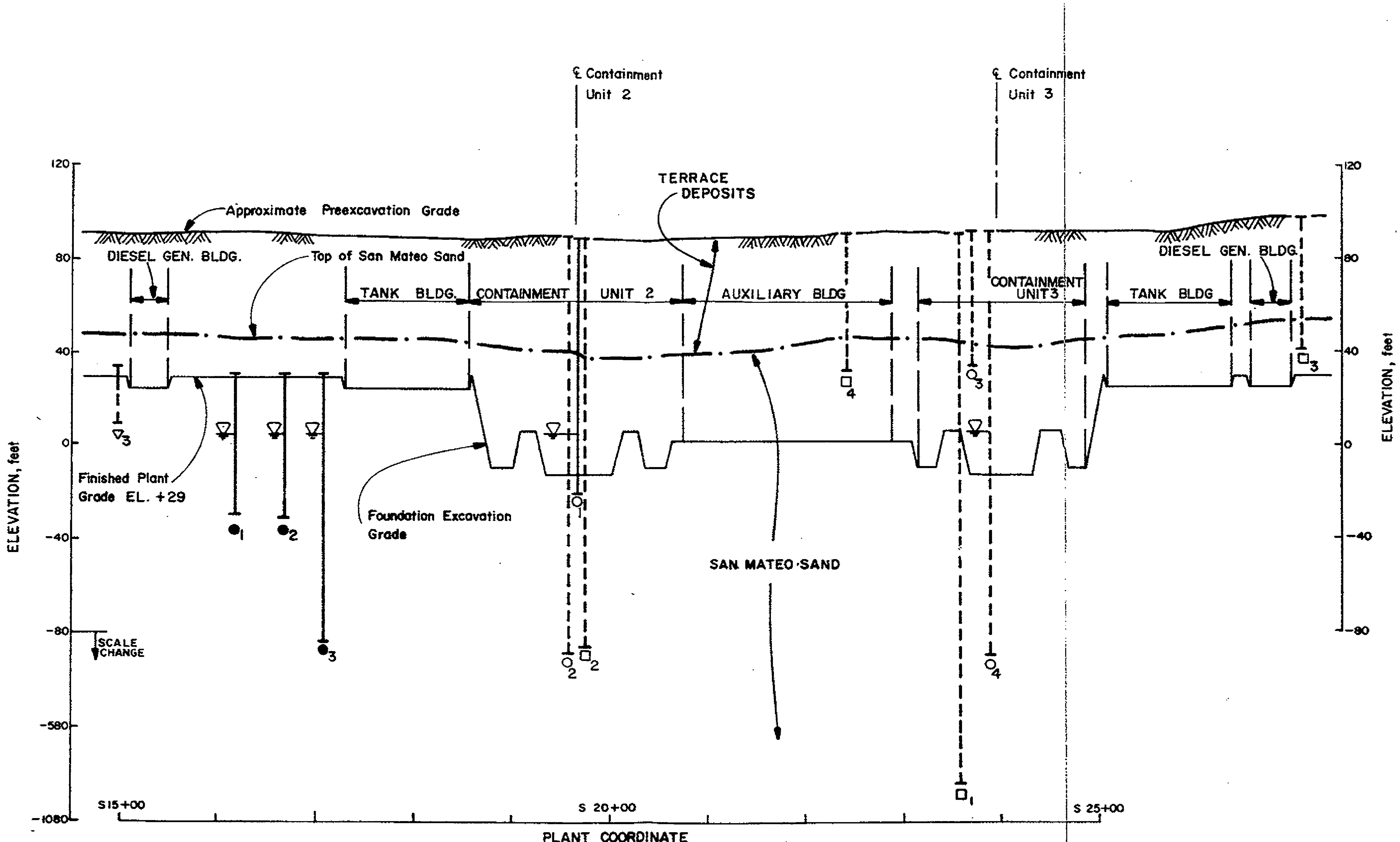

NOTES

1. See Fig. 2.5-40 for Section location.
2. Groundwater levels ▽ on borings are measured values at the time of investigation.
3. Borings shown as dashed(-----)lines are projected onto the section line.
4. Borings with top elevation below preexcavation grade were made after excavation.
5. Number and symbol below boring line refer to boring number and identification as shown on Plan, Fig. 2.5-36
6. Bottom elevations and locations of buildings other than Containments and Auxiliary Bldg. are subject to revision.

SAN ONOFRE NUCLEAR GENERATING STATION Units 2 & 3

GENERALIZED SOIL PROFILE (NORTH-SOUTH) SECTION A-A

Figure 2.5-52

SAN ONOFRE
NUCLEAR GENERATING STATION
Units 2 & 3

SITE ON FEBRUARY 11, 1974, ONE MONTH PRIOR TO START OF EXCAVATION

Figure 2.5-53

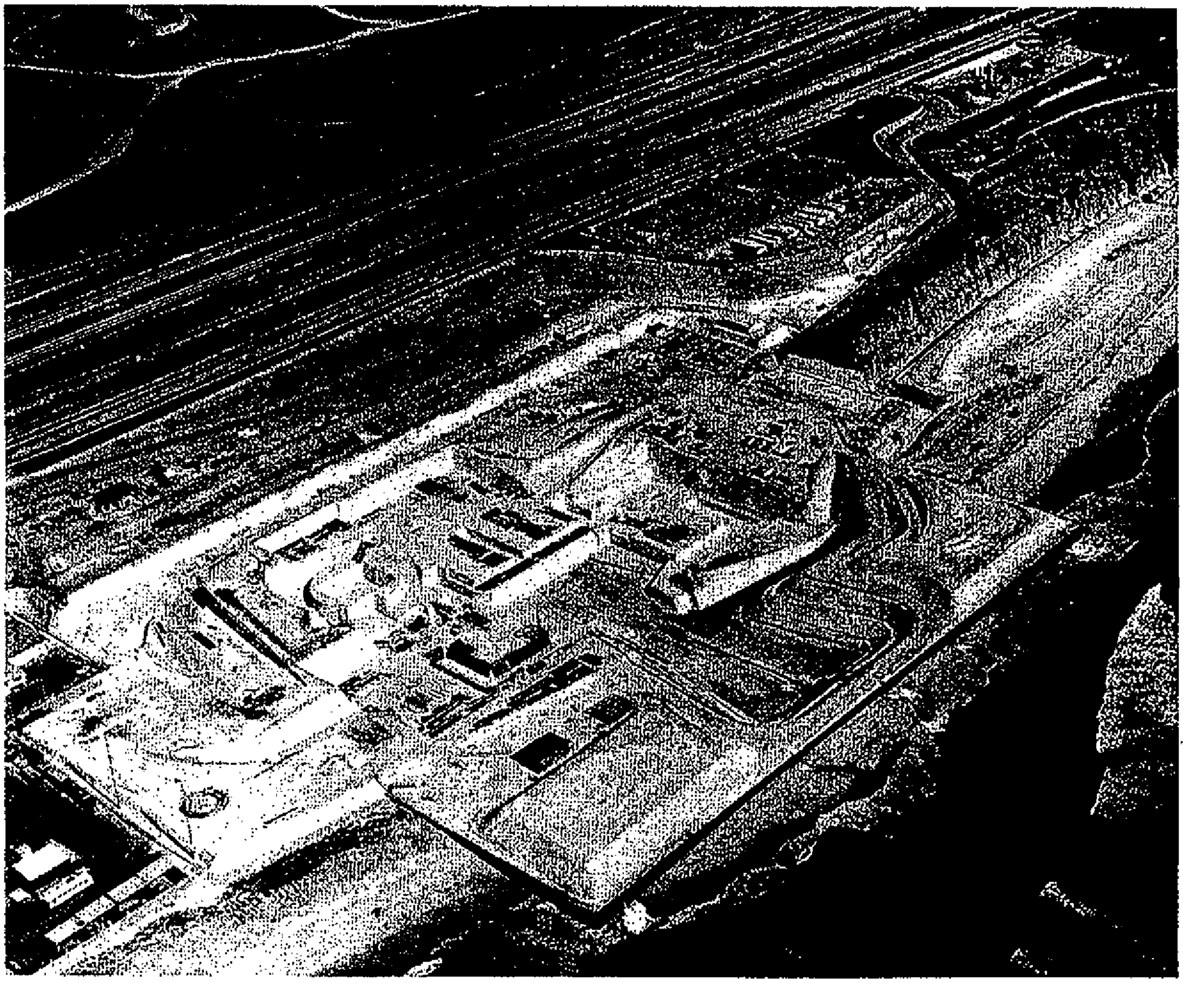

SAN ONOFRE
NUCLEAR GENERATING STATION
Units 2 & 3

SITE ON OCTOBER 15, 1974,
CUT TO FINISH SUBGRADE ELEVATION
(EXCEPT UNIT 3
CONTAINMENT AND TURBINE AREA)

Figure 2.5-54

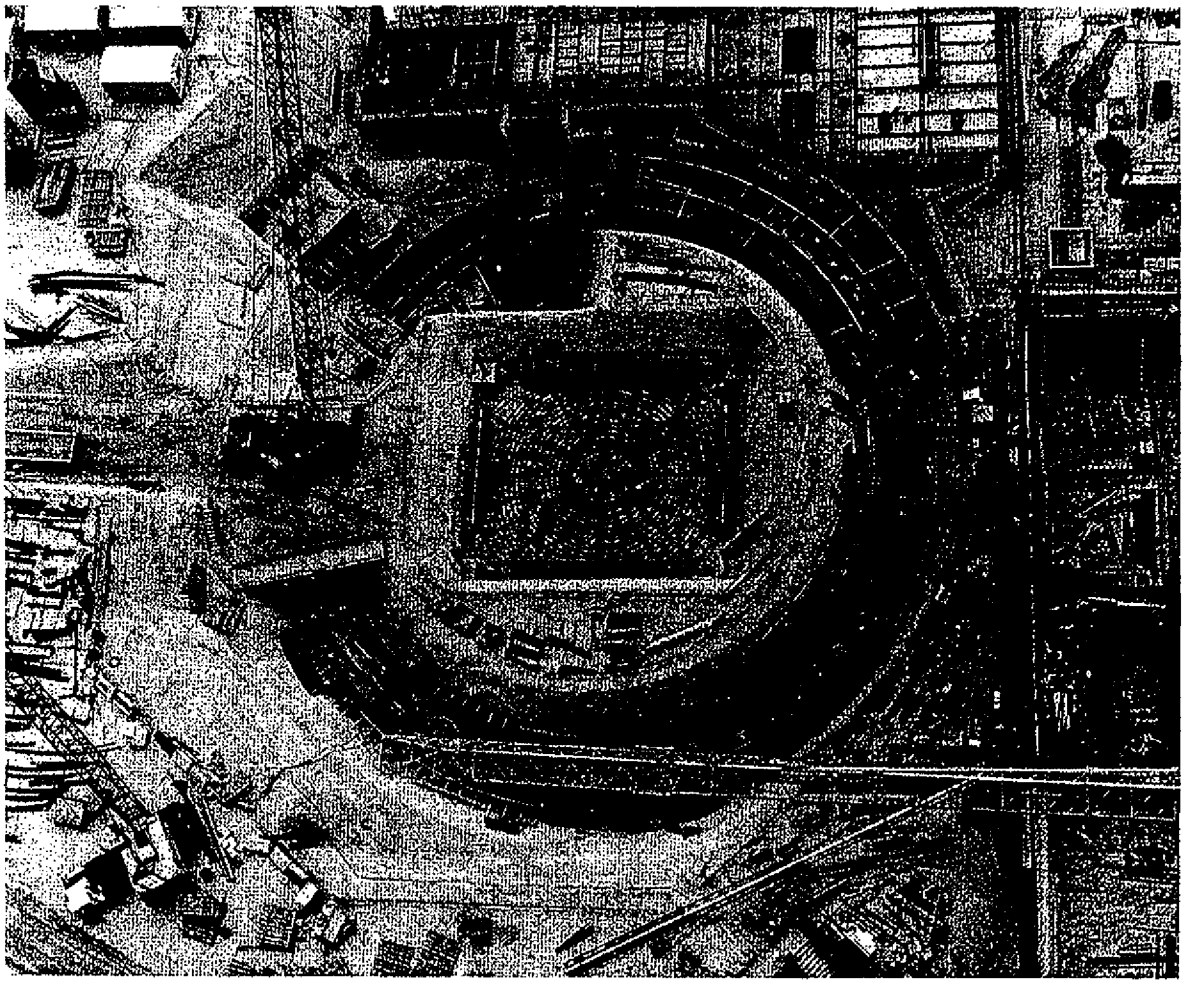

SAN ONOFRE
NUCLEAR GENERATING STATION
Units 2 & 3

SITE ON JULY 8, 1975,
UNIT 3 CONTAINMENT
STRUCTURE EXCAVATION

Figure 2.5-55

DEPTH IN FEET	DESCRIPTION	COMPRESSIONAL WAVE VELOCITY (FT./SEC.)	POISSON'S RATIO	SHEAR WAVE VELOCITY (FT./SEC.)	TOTAL UNIT WEIGHT (LBS./CU. FT)
0	TERRACE DEPOSITS - silt, sand, gravel & cobbles	1000 3100	(.44)	(330) (1000)	120
	SAN MATEO FORMATION - fine to coarse sandstone, some gravel & siltstone	* 6600	.44	2200	130
		7500	.42	2750	135
1000	CAPISTRANO FORMATION - thin bedded siltstone & shale	7000	.40	2800	131
2000	MONTEREY FORMATION - diatomaceous shale	7000	.35	3350	110
3000	SAN ONOFRE BRECCIA - conglomerate, sandstone & siltstone	11000	(.30)	(6000)	(140)
4000 5000	UNDIFFERENTIATED SEDIMENTS INCLUDING SANTIAGO FORMATION - siltstone, sandstone & shale	(9000)	(.28)	(5000)	(154)
11000	CRYSTALLINE BASEMENT - undifferentiated igneous & metamorphics	(16000)	(.20)	(10000)	(172)

* VALUES FOR UPPER 50' OF FORMATION

( ) INDICATES ESTIMATED VALUES

—•— APPROXIMATE FOUNDATION LEVEL

SAN ONOFRE NUCLEAR GENERATING STATION Units 2 & 3

STRATIGRAPHIC COLUMN SHOWING GEOPHYSICAL DATA

Figure 2.5-56

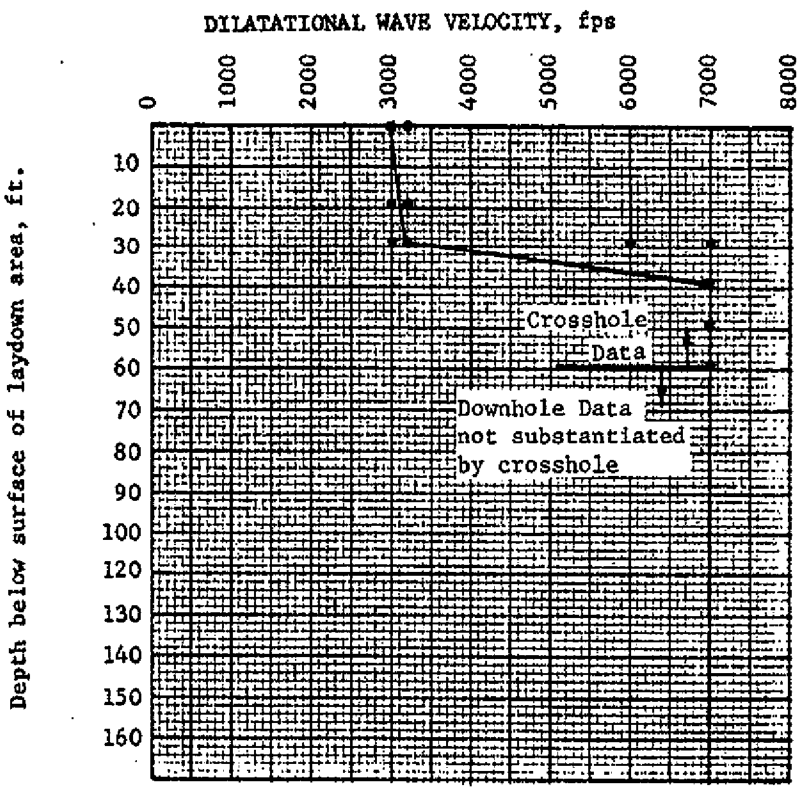

SAN ONOFRE
NUCLEAR GENERATING STATION
Units 2 & 3

DILATATIONAL WAVE VELOCITIES

Figure 2.5-57

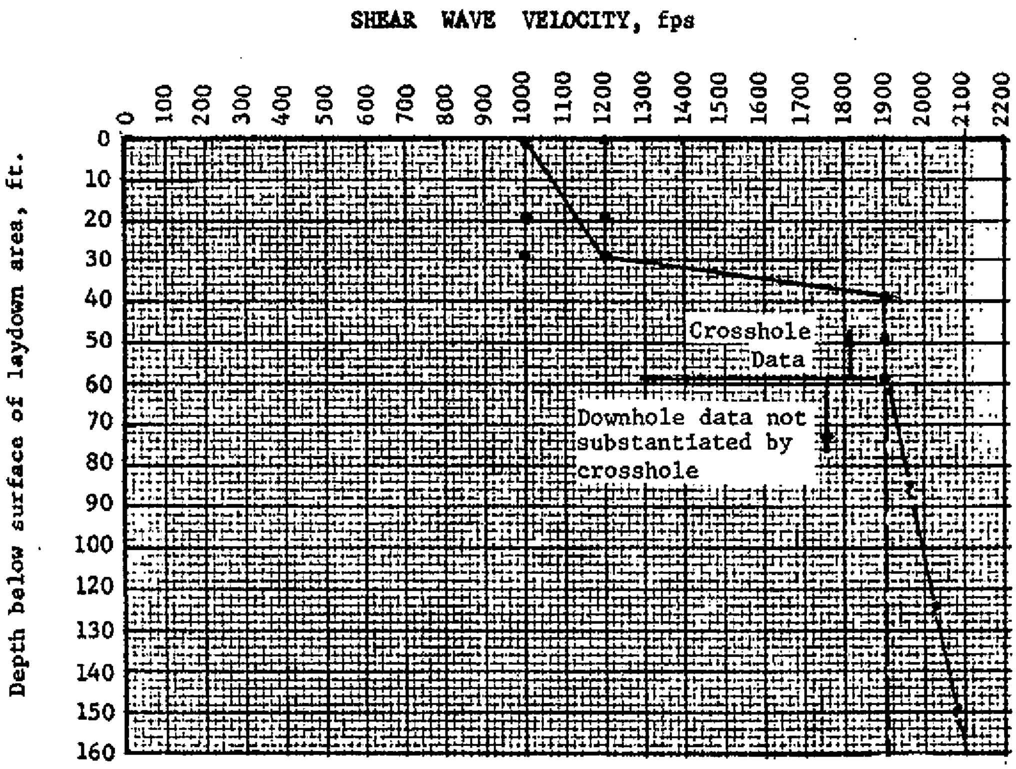

SAN ONOFRE
NUCLEAR GENERATING STATION
Units 2 & 3

SHEAR WAVE VELOCITIES

Figure 2.5-58

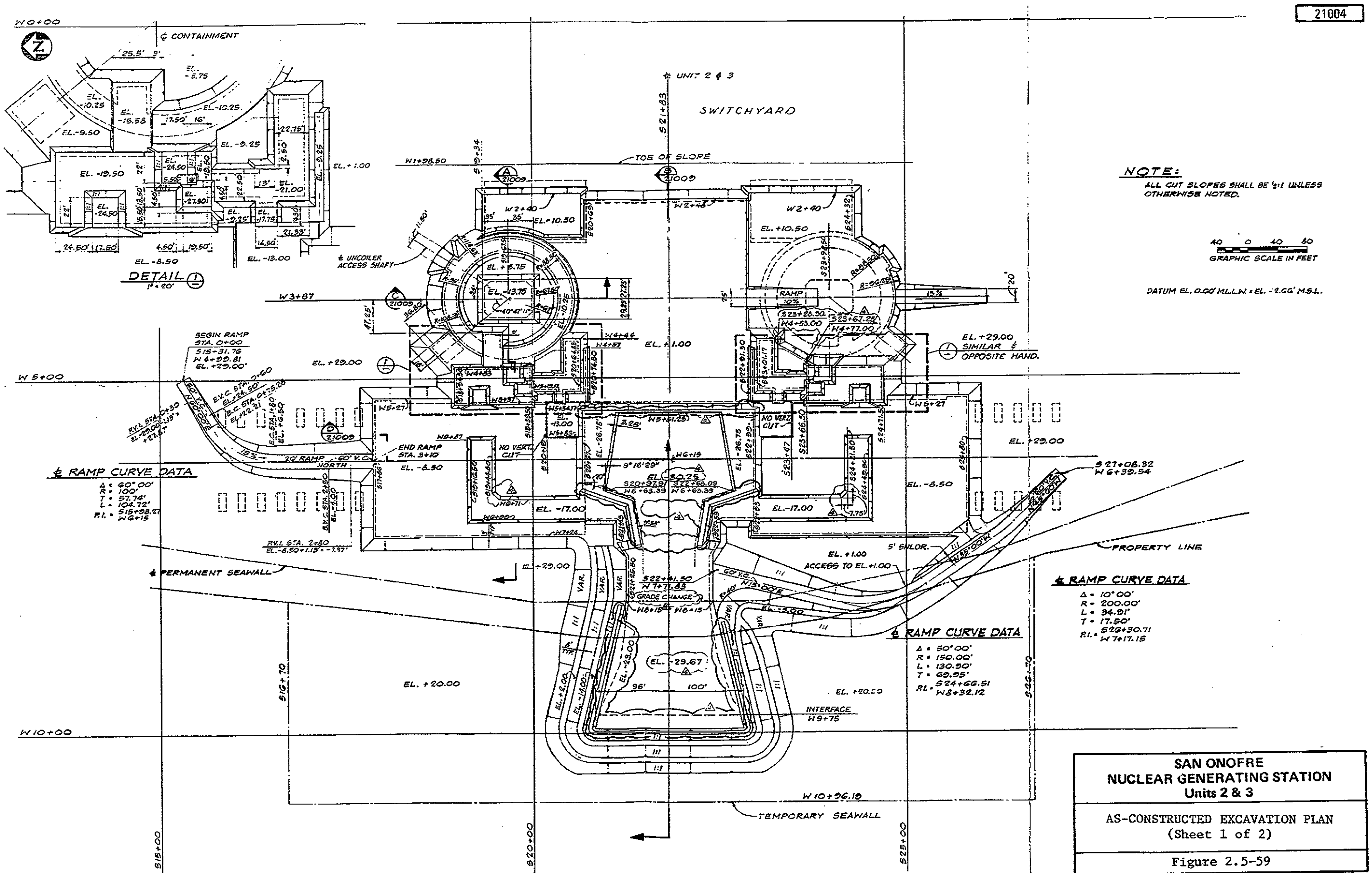

SAN ONOFRE
NUCLEAR GENERATING STATION
Units 2 & 3

AS-CONSTRUCTED EXCAVATION PLAN
(Sheet 1 of 2)

Figure 2.5-59

21005

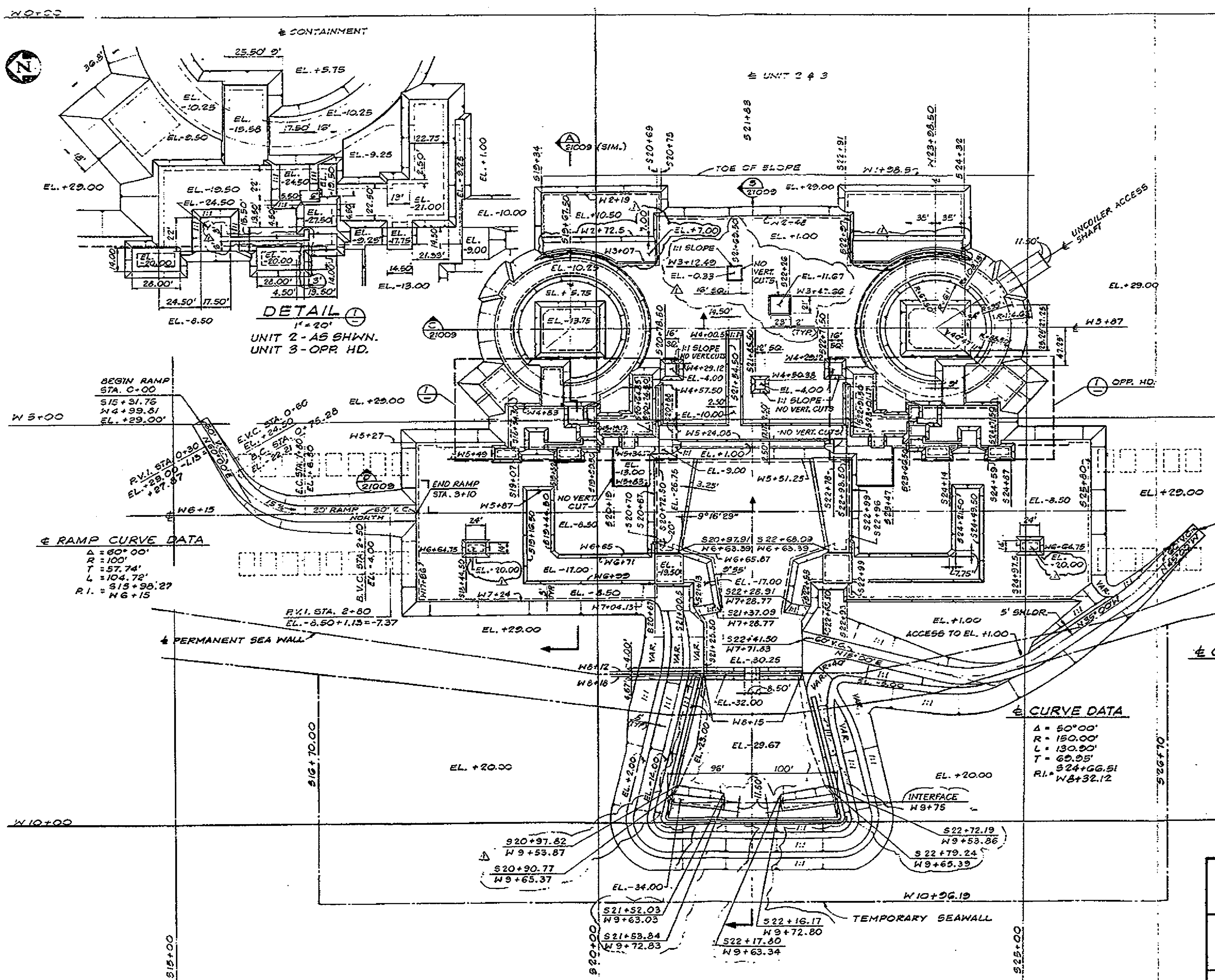

NOTES:

1. ALL CUT SLOPES ARE ½:1 UNLESS OTHERWISE NOTED.
2. THIS DRAWING IS NOT PART OF SITE PREPARATION. (SPEC. 5023-113).
3. THIS DRAWING SHOWS THE TOTAL EXCAVATION FOR THE POWER BLOCK

40 0 40 80
GRAPHIC SCALE IN FEET

DATUM EL. 0.00' M.L.L.W. = EL. -2.66' M.S.L.

SAN ONOFRE NUCLEAR GENERATING STATION Units 2 & 3

AS-CONSTRUCTED EXCAVATION PLAN (Sheet 2 of 2)

Figure 2.5-59

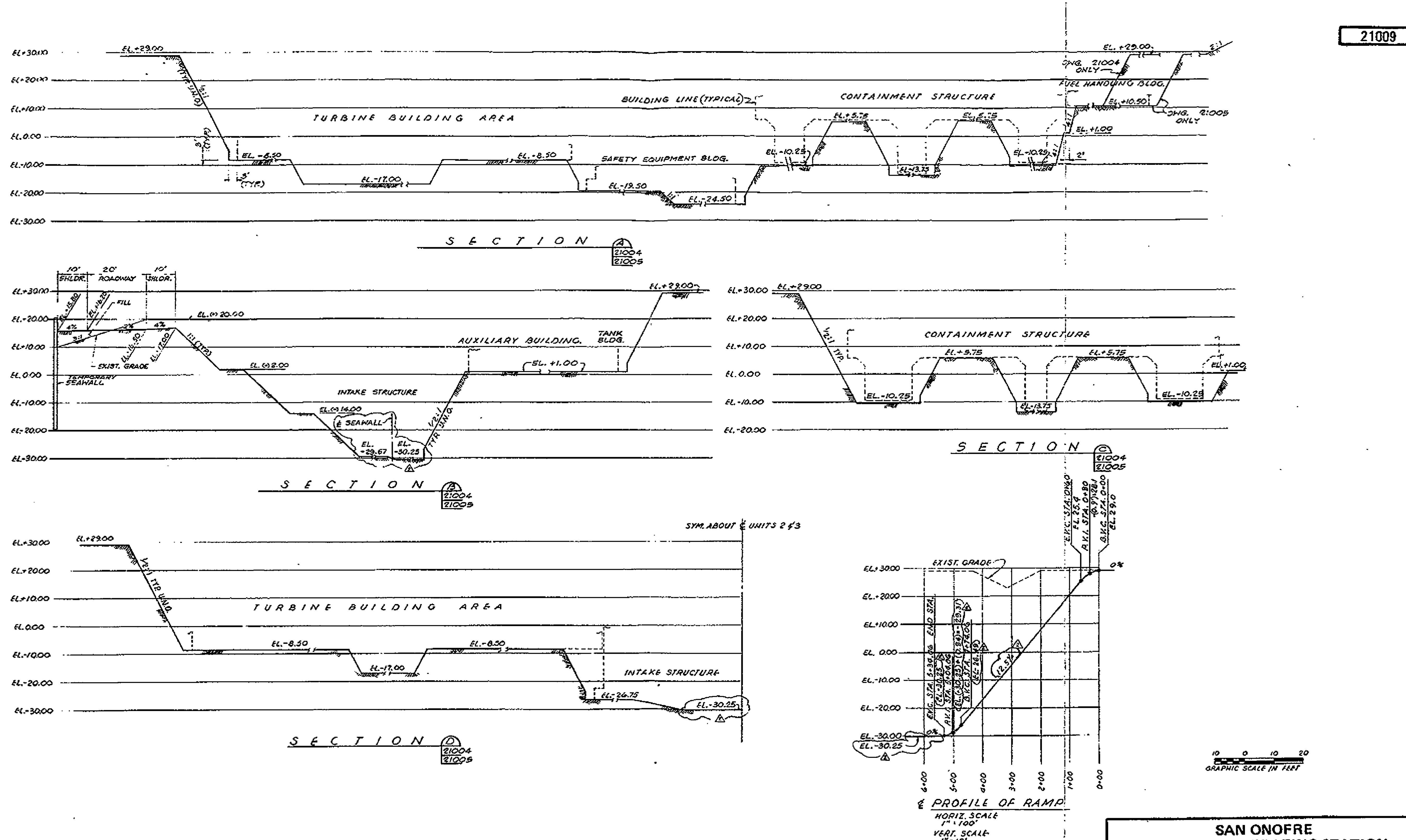

DATUM EL. 0.00' M.L.L.W. = EL. -2.66' M.S.L.

SAN ONOFRE NUCLEAR GENERATING STATION
Units 2 & 3

TYPICAL AS-CONSTRUCTED EXCAVATION CROSS-SECTIONS

Figure 2.5-60

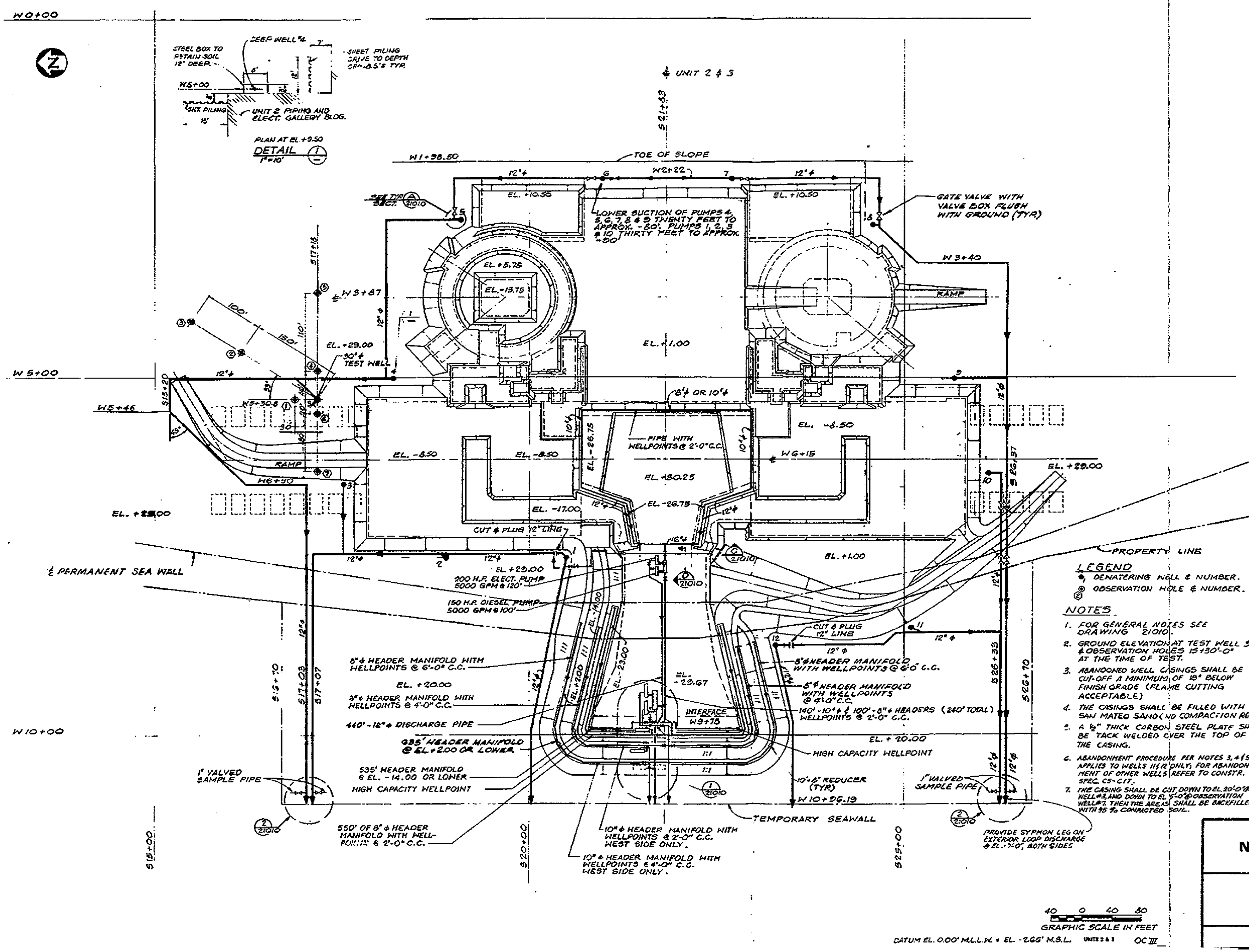

LEGEND

- DEWATERING WELL & NUMBER.
- OBSERVATION HOLE & NUMBER.

NOTES

1. FOR GENERAL NOTES SEE DRAWING 21010.
2. GROUND ELEVATION AT TEST WELL 3A & OBSERVATION HOLES IS +30'-0" AT THE TIME OF TEST.
3. ABANDONED WELL CASINGS SHALL BE CUT-OFF A MINIMUM OF 18" BELOW FINISH GRADE (FLAME CUTTING ACCEPTABLE)
4. THE CASINGS SHALL BE FILLED WITH SAN MATEO SAND (NO COMPACTION REQD)
5. A ½" THICK CARBON STEEL PLATE SHALL BE TACK WELDED OVER THE TOP OF THE CASING.
6. ABANDONMENT PROCEDURE PER NOTES 3, 4 & 5 APPLIES TO WELLS 11 & 12 ONLY; FOR ABANDONMENT OF OTHER WELLS REFER TO CONSTR. SPEC. CS-C17.
7. THE CASING SHALL BE CUT DOWN TO EL. 20'-0" @ WELL #3, AND DOWN TO EL. 5'-0" @ OBSERVATION WELL #7. THEN THE AREAS SHALL BE BACKFILLED WITH 95% COMPACTED SOIL.

WELL LOCATION CHART

WELL NO.	GR. ELEV.	COORDINATES SOUTH	COORDINATES WEST
1	20.00	20+30	7+82
2	DO.	18+90	7+52
3	DO.	17+55	6+30
4	DO.	18+80	—
5	DO.	19+11	2+86
6	DO.	20+94	2+22
7	DO.	22+72	2+22
8	DO.	24+55	2+86
9	DO.	25+66	5+01
10	DO.	26+12	6+35
11	20.00	25+10	8+50
12	DO.	23+50	8+75
TEST WELL 3A	30.00	17+18	5+30.8

OBSERVATION HOLE DATA

OBSERV. HOLE	TYPE CONSTR.	DEPTH OF HOLE (FT.)	PLANT COORD. SOUTH	PLANT COORD. WEST
1	A	200	16+88	5+30.8
2	B	250	1+92	4+46.6
3	B	50	15+08	3+94.8
4	A	200	17+18	4+90.8
5	B	100	17+18	9+80.8
6	B	250	17+18	5+50.8
7	B	100	17+18	6+30.8

SAN ONOFRE NUCLEAR GENERATING STATION Units 2 & 3

DEWATERING SYSTEM PLAN (Sheet 1 of 2)

Figure 2.5-61.

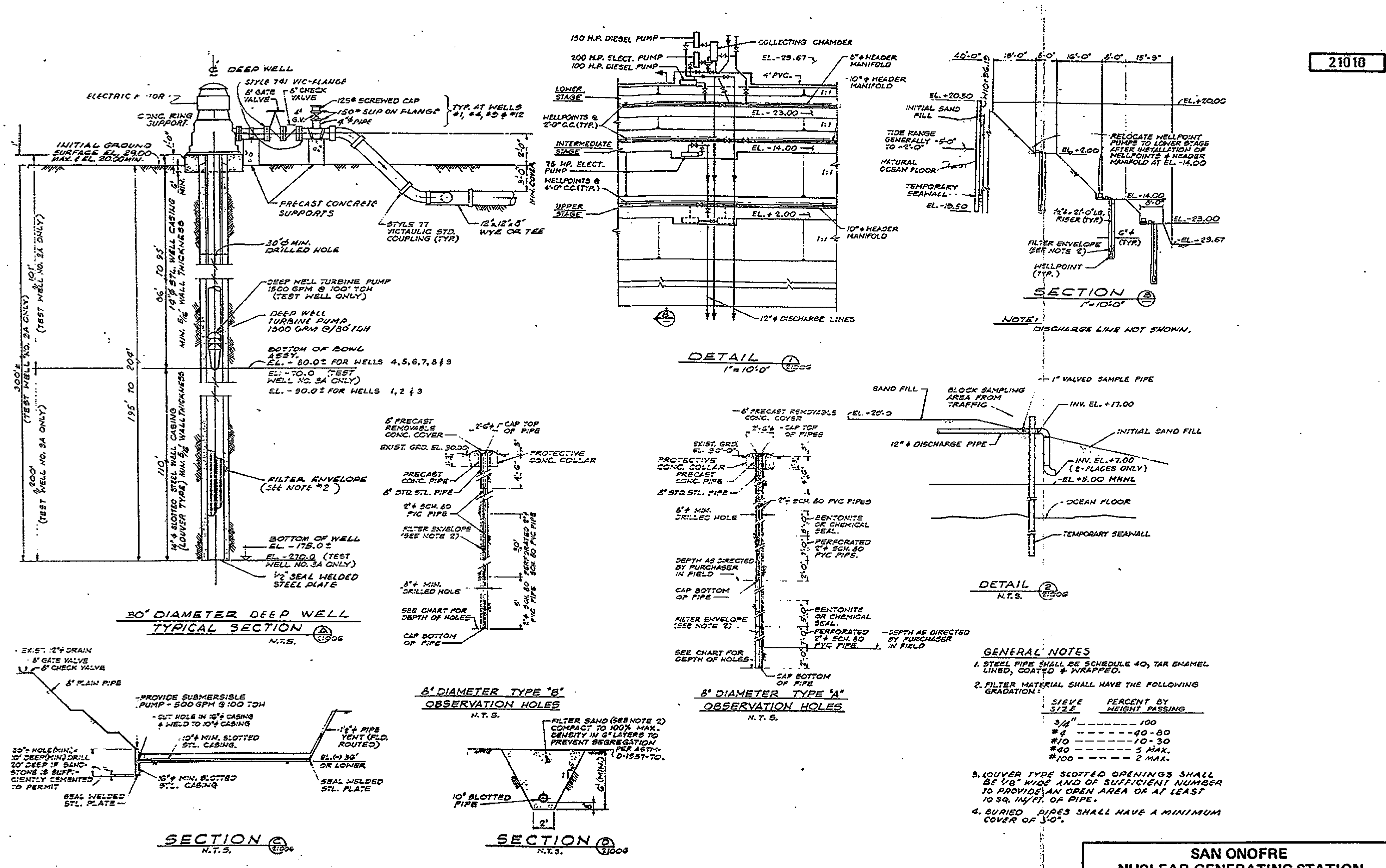

GENERAL NOTES

1. STEEL PIPE SHALL BE SCHEDULE 40, TAR ENAMEL LINED, COATED & WRAPPED.
2. FILTER MATERIAL SHALL HAVE THE FOLLOWING GRADATION:

SIEVE SIZE	PERCENT BY WEIGHT PASSING
3/4"	100
#4	40-80
#10	10-30
#40	5 MAX.
#100	2 MAX.

3. LOUVER TYPE SLOTTED OPENINGS SHALL BE 1/8" WIDE AND OF SUFFICIENT NUMBER TO PROVIDE AN OPEN AREA OF AT LEAST 10 SQ. IN/FT. OF PIPE.
4. BURIED PIPES SHALL HAVE A MINIMUM COVER OF 3'-0".

SAN ONOFRE
NUCLEAR GENERATING STATION
Units 2 & 3

DEWATERING SYSTEM PLAN
(Sheet 2 of 2)

Figure 2.5-61

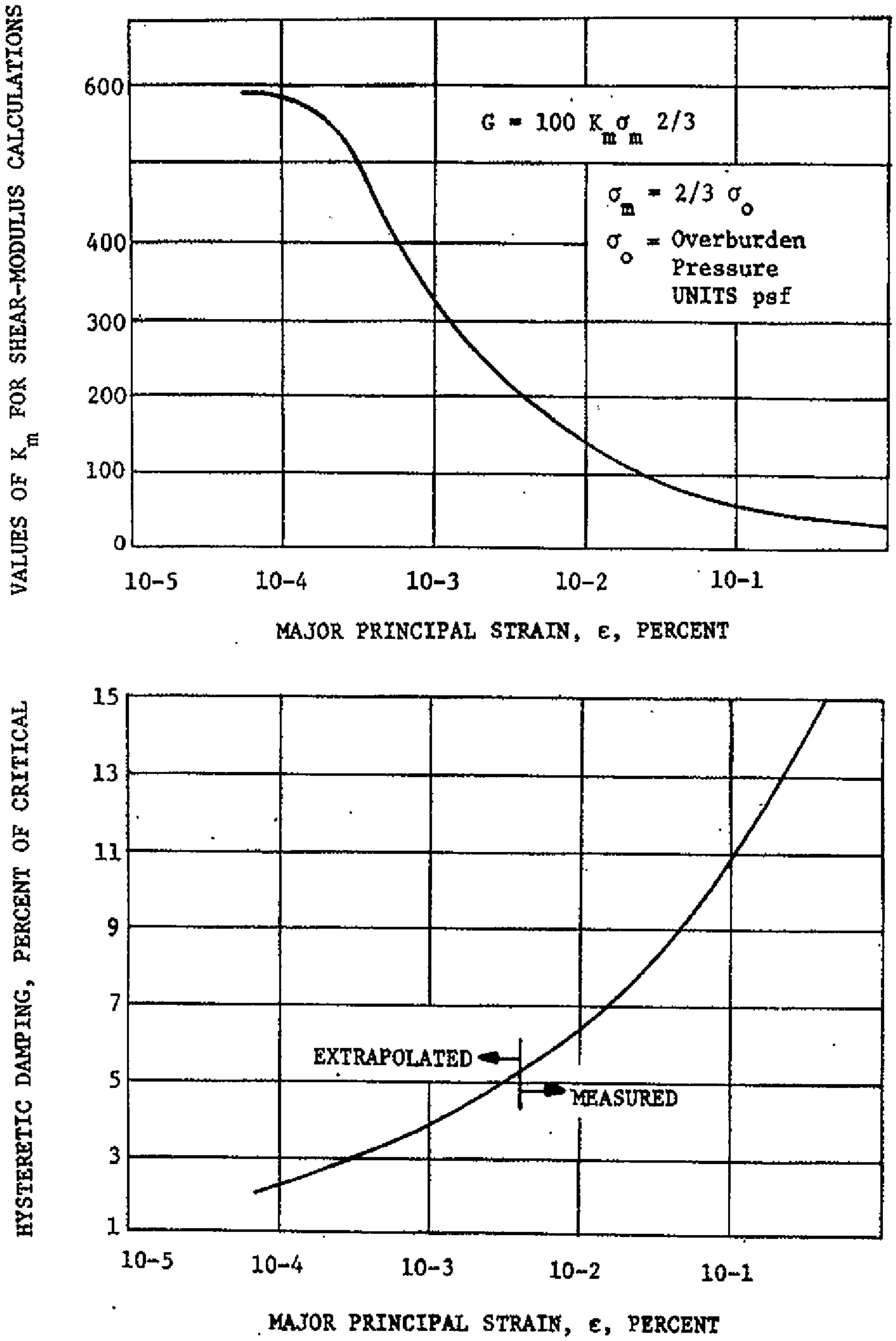

SAN ONOFRE
NUCLEAR GENERATING STATION
Units 2 & 3

MODULUS AND DAMPING vs. STRAIN
SAN MATEO FORMATION SAND

Figure 2.5-62

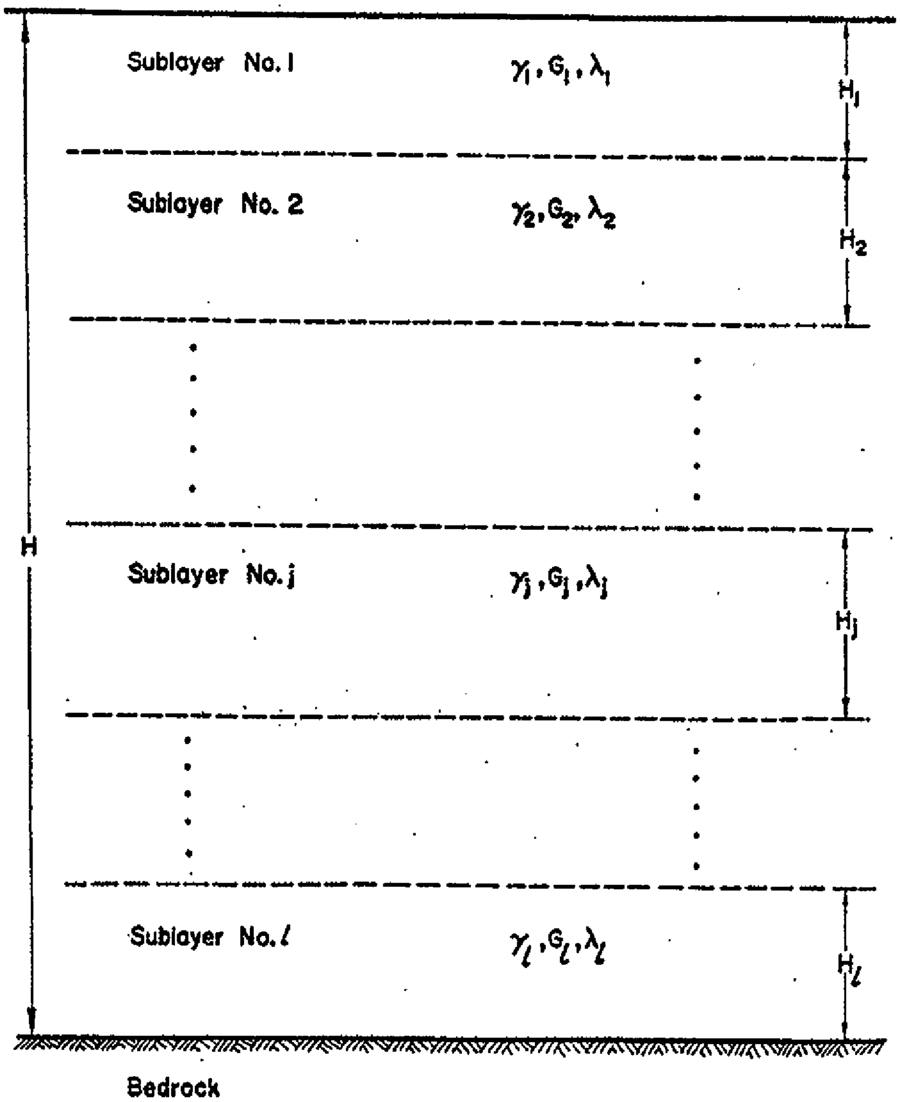

SAN ONOFRE
NUCLEAR GENERATING STATION
Units 2 & 3

HORIZONTAL SOIL DEPOSIT

Figure 2.5-63

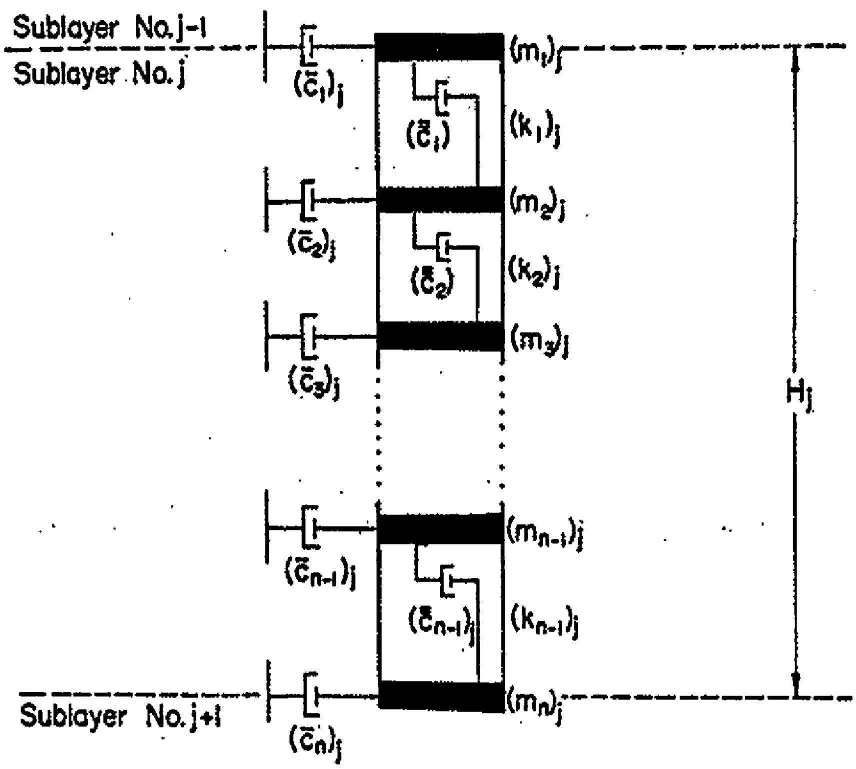

SAN ONOFRE
NUCLEAR GENERATING STATION
Units 2 & 3

LUMPED-MASS IDEALIZATION FOR SUBLAYER NO. j

Figure 2.5-64

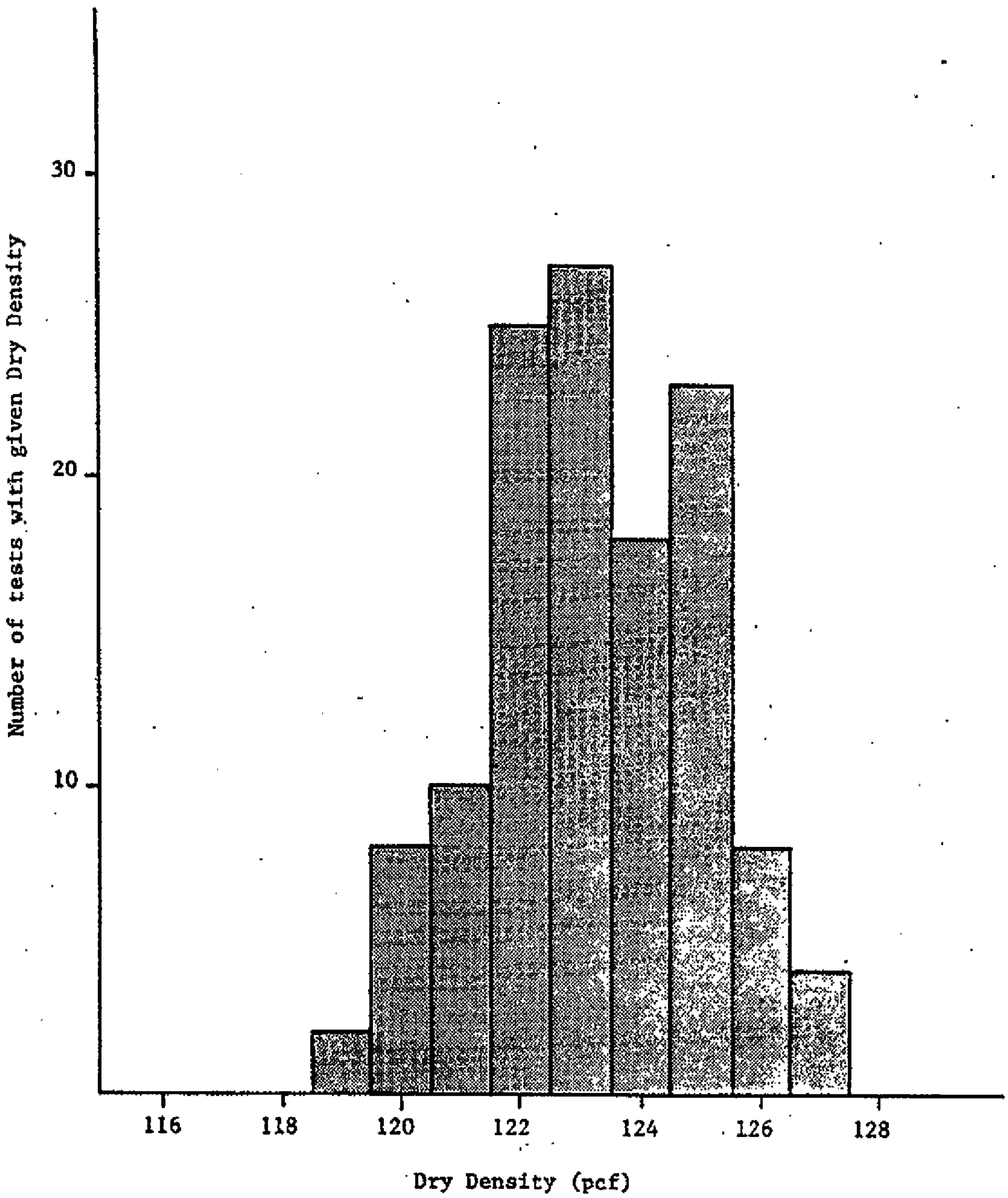

SAN ONOFRE
NUCLEAR GENERATING STATION
Units 2 & 3

RESULTS OF SAND CONE TESTS
ON IN-SITU SAN MATEO SAND

Figure 2.5-65

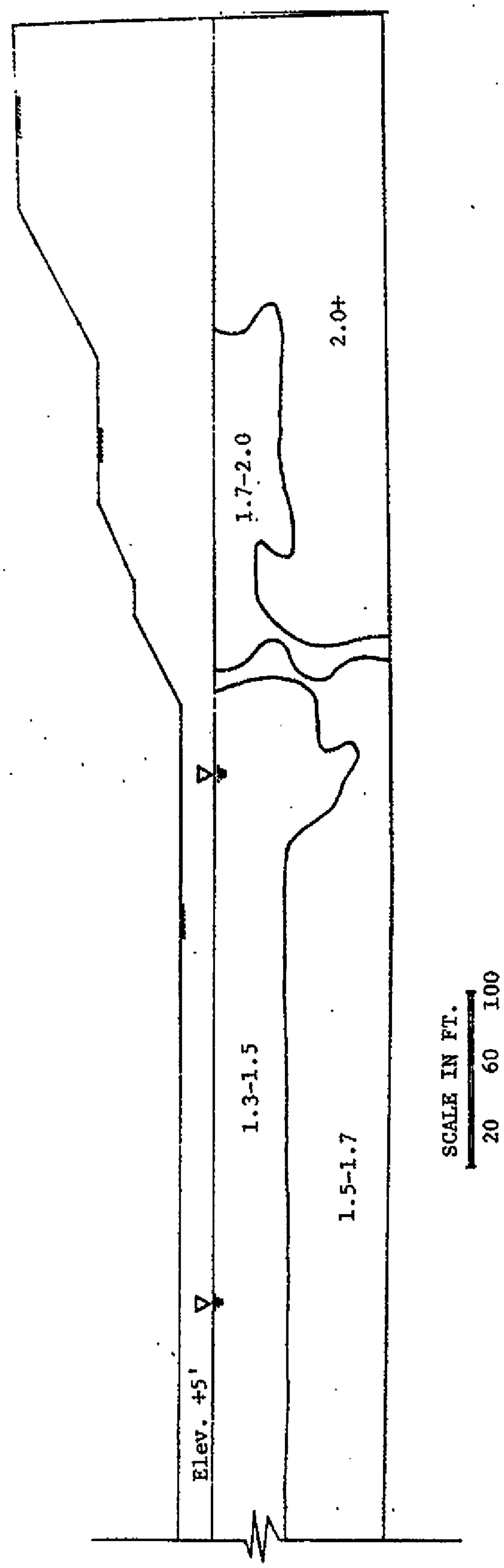

SAN ONOFRE
NUCLEAR GENERATING STATION
Units 2 & 3

ZONES OF EQUAL FACTOR-OF-SAFETY

Figure 2.5-66

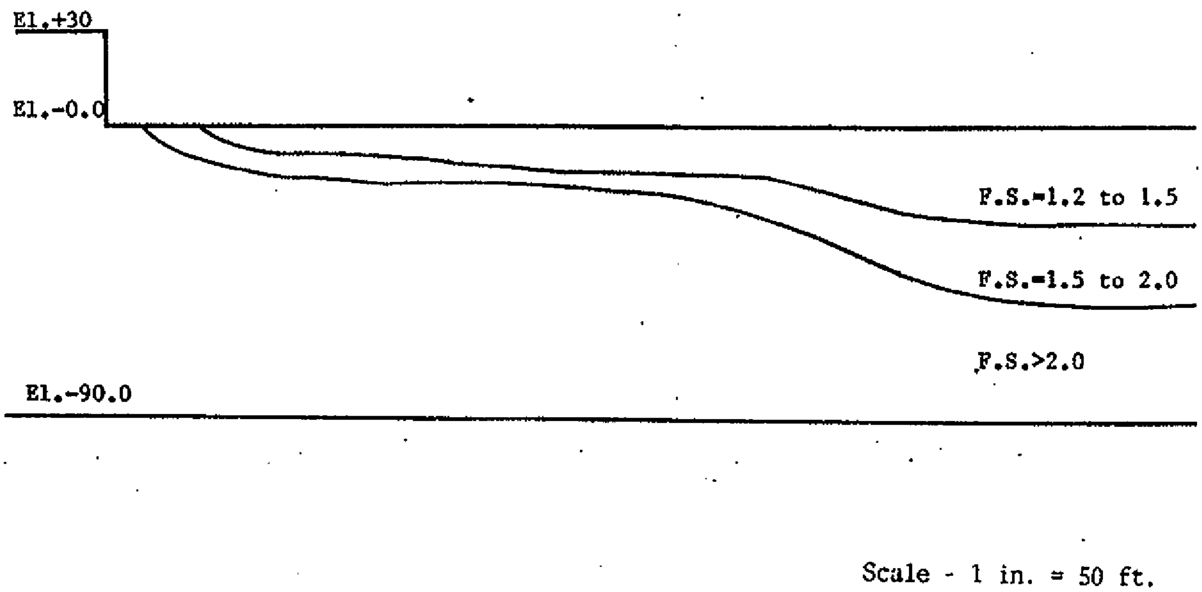

SAN ONOFRE
NUCLEAR GENERATING STATION
Units 2 & 3

ZONES OF FACTOR-OF-SAFETY

Figure 2.5-67

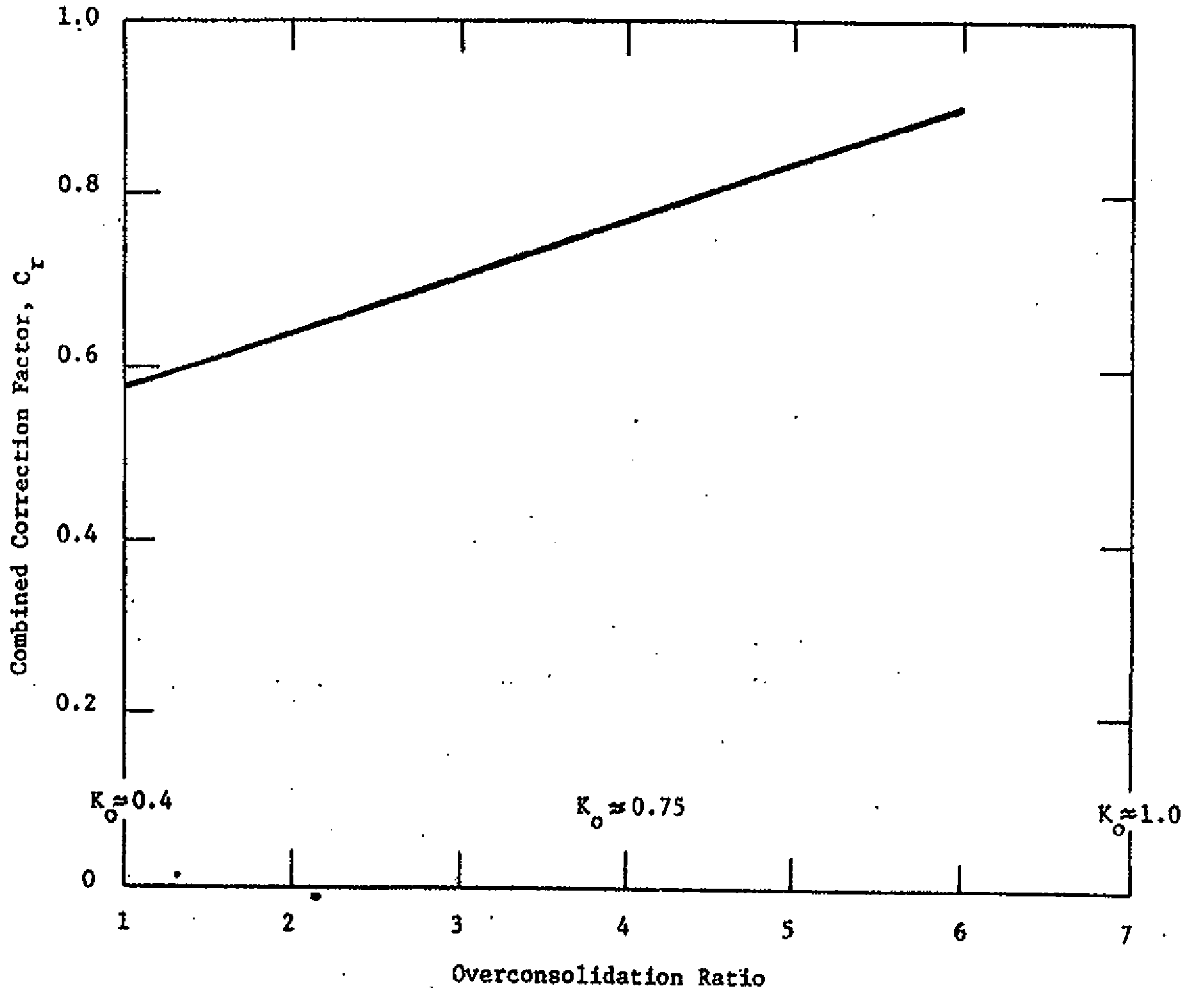

*(after Seed, Arango and Chan, 1975)

SAN ONOFRE
NUCLEAR GENERATING STATION
Units 2 & 3

COMBINED CORRECTION FACTOR FOR CYCLIC TRIAXIAL COMPRESSION TESTS ACCOUNTING FOR MULTIDIRECTIONAL SHAKING AND OVERCONSOLIDATION*

Figure 2.5-68

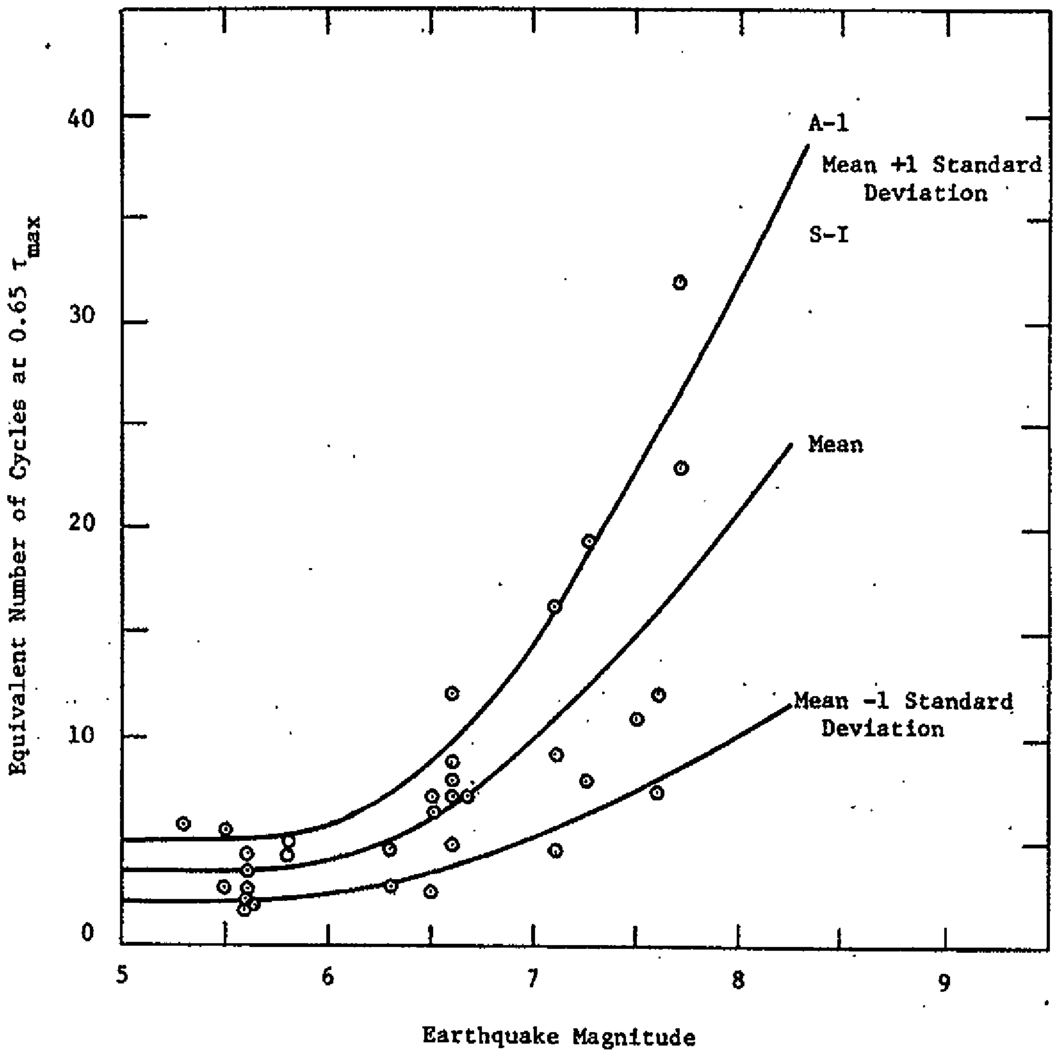

*(after Seed, Idriss, Makdisi and Banerjee, 1975)

SAN ONOFRE
NUCLEAR GENERATING STATION
Units 2 & 3

EQUIVALENT NUMBERS
OF UNIFORM STRESS CYCLES
BASED ON STRONGEST COMPONENTS
OF GROUND MOTION*

Figure 2.5-69

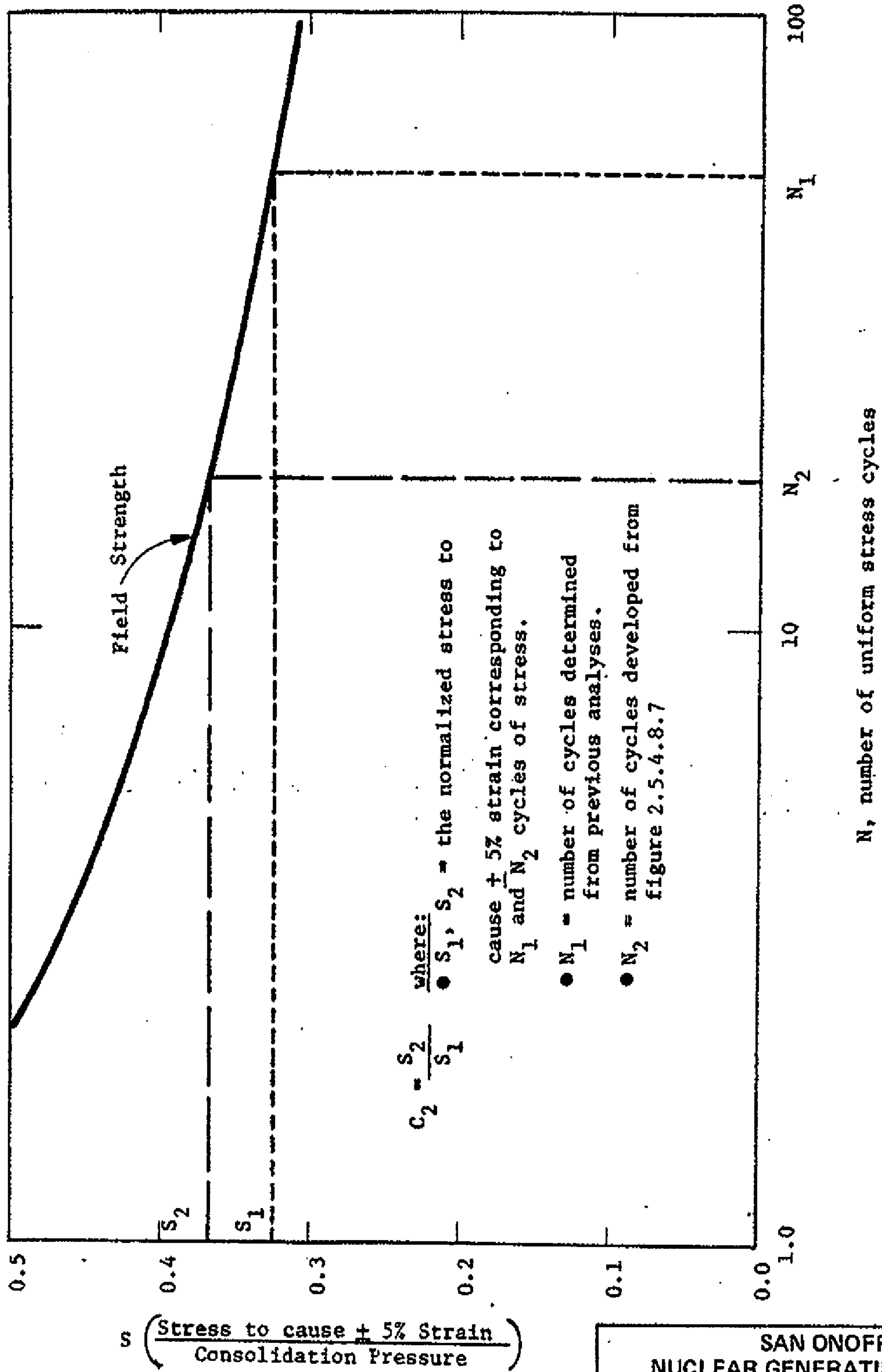

SAN ONOFRE
NUCLEAR GENERATING STATION
Units 2 & 3

SCHEMATIC DIAGRAM
OF THE DETERMINATION
OF CORRECTION FACTOR C_2

Figure 2.5-70

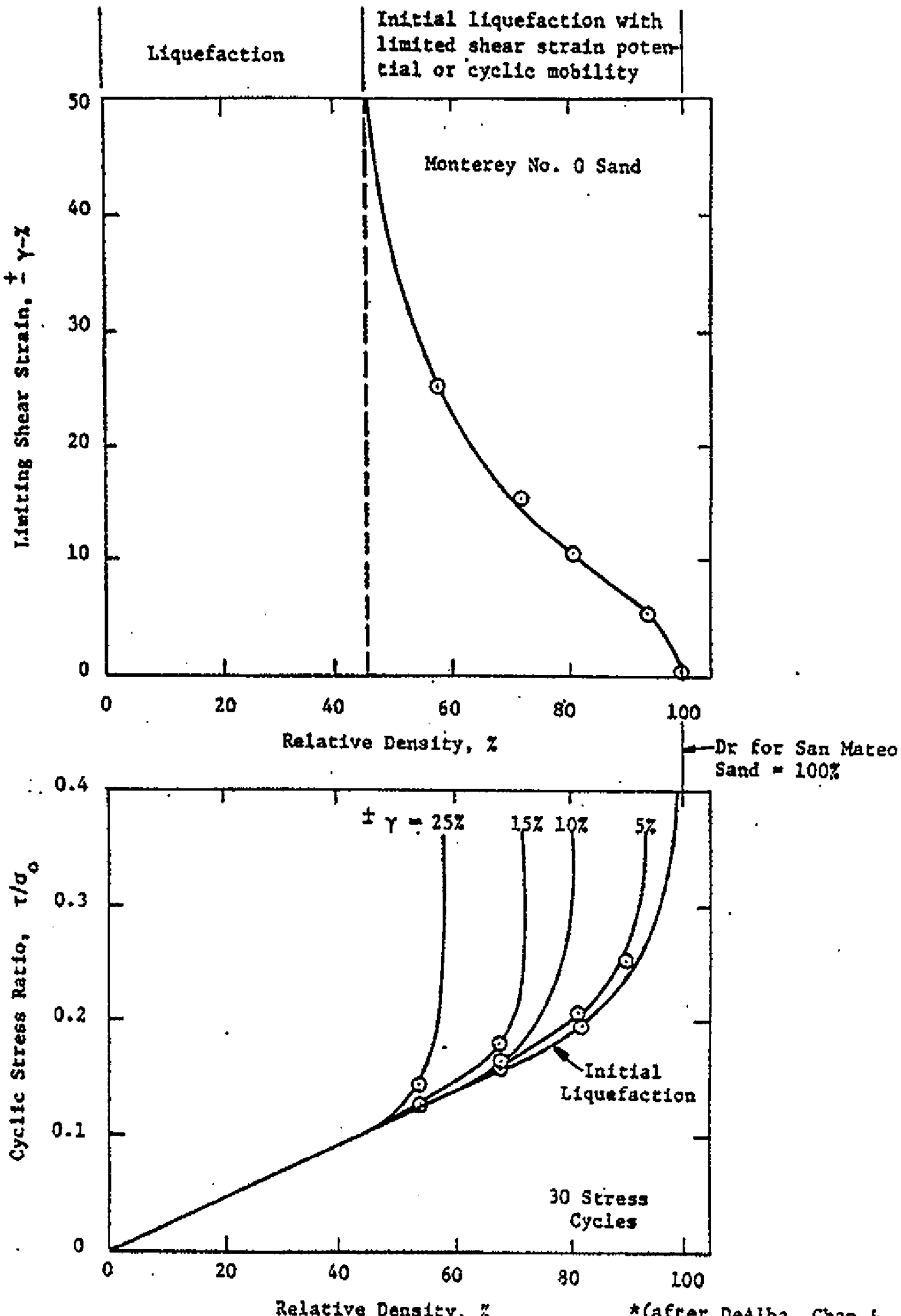

*(after DeAlba, Chan & Seed 1975)

SAN ONOFRE NUCLEAR GENERATING STATION Units 2 & 3
RELATIVE DENSITY - LIMITING SHEAR STRAIN RELATIONSHIPS FOR 30 STRESS CYCLES*
Figure 2.5-71

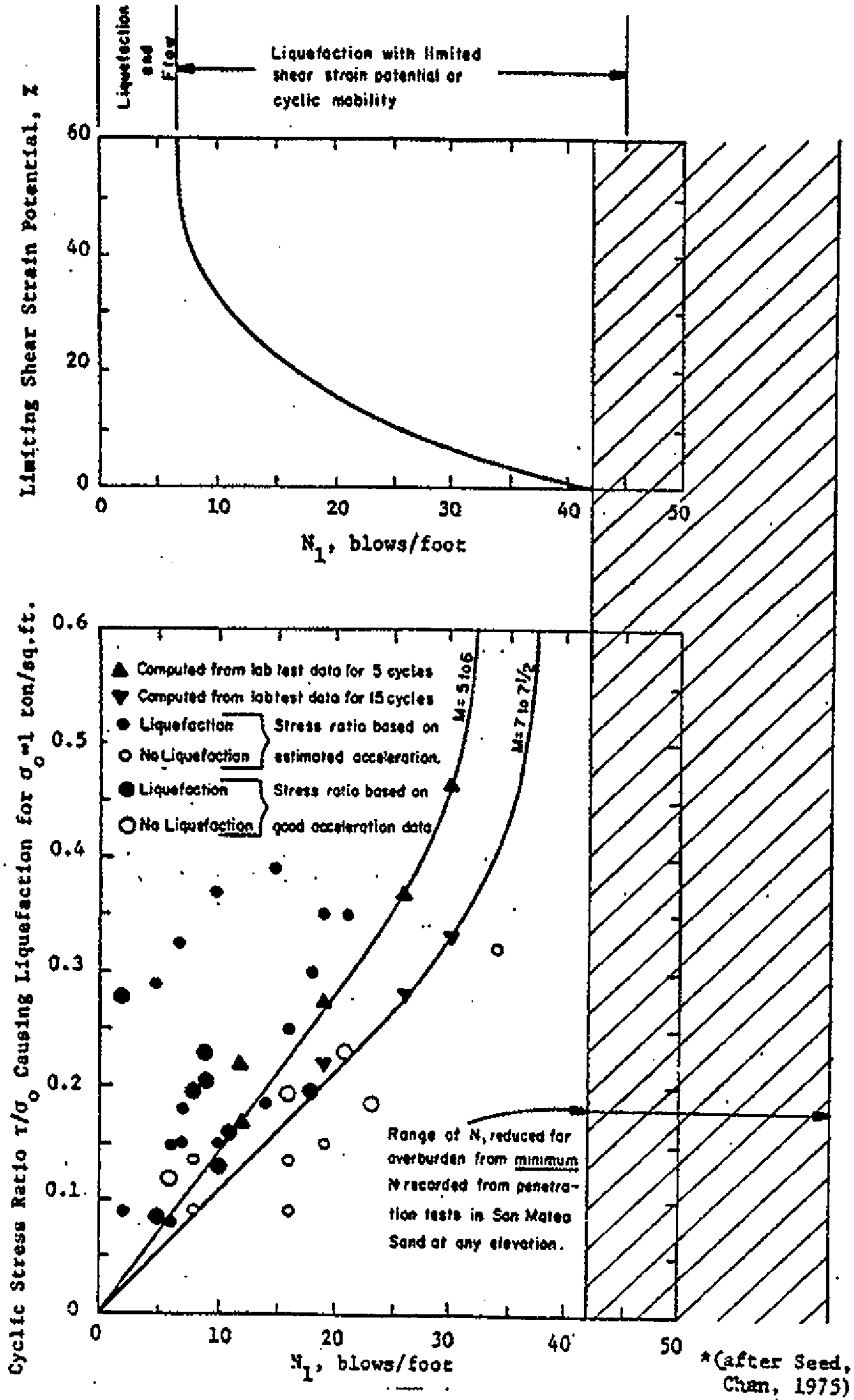

*(after Seed, Arango, and Chan, 1975)

SAN ONOFRE
NUCLEAR GENERATING STATION
Units 2 & 3

CORRELATION BETWEEN STRESS RATIO CAUSING VARIOUS DEGREES OF LIQUEFACTION IN THE FIELD AND IN THE LABORATORY AND PENETRATION RESISTANCE OF SAND

Figure 2.5-72

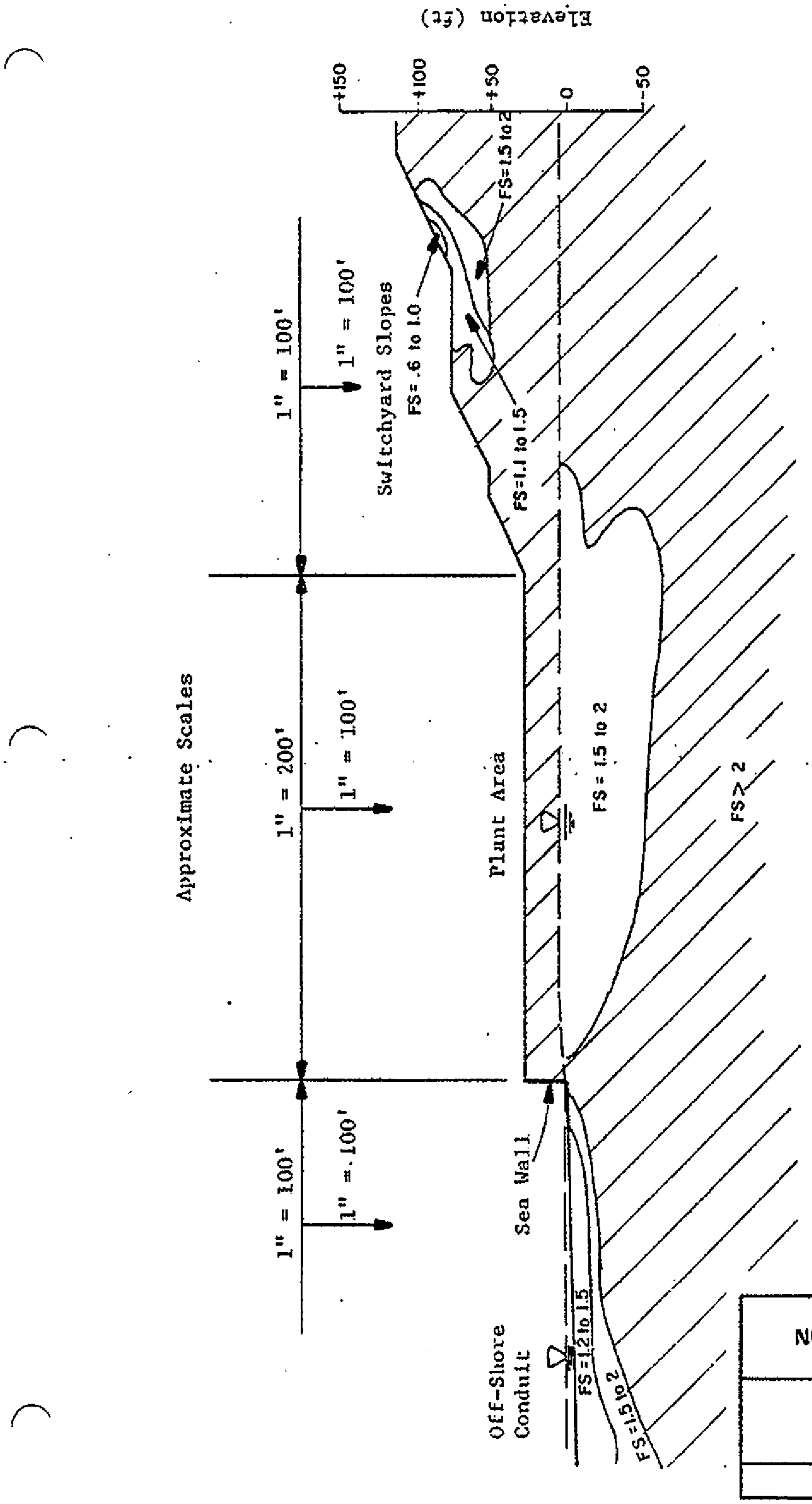

Notes:

1. F.S. defined as the ratio of the stress necessary to cause ± 5% strain to the induced stress.
2. ▽ = water table
3. Based on choice of worst conditions encountered for all analysis values.

SAN ONOFRE NUCLEAR GENERATING STATION Units 2 & 3

COMPOSITE SUMMARY OF F.S. TO DEVELOP ±5% STRAIN

Figure 2.5-73

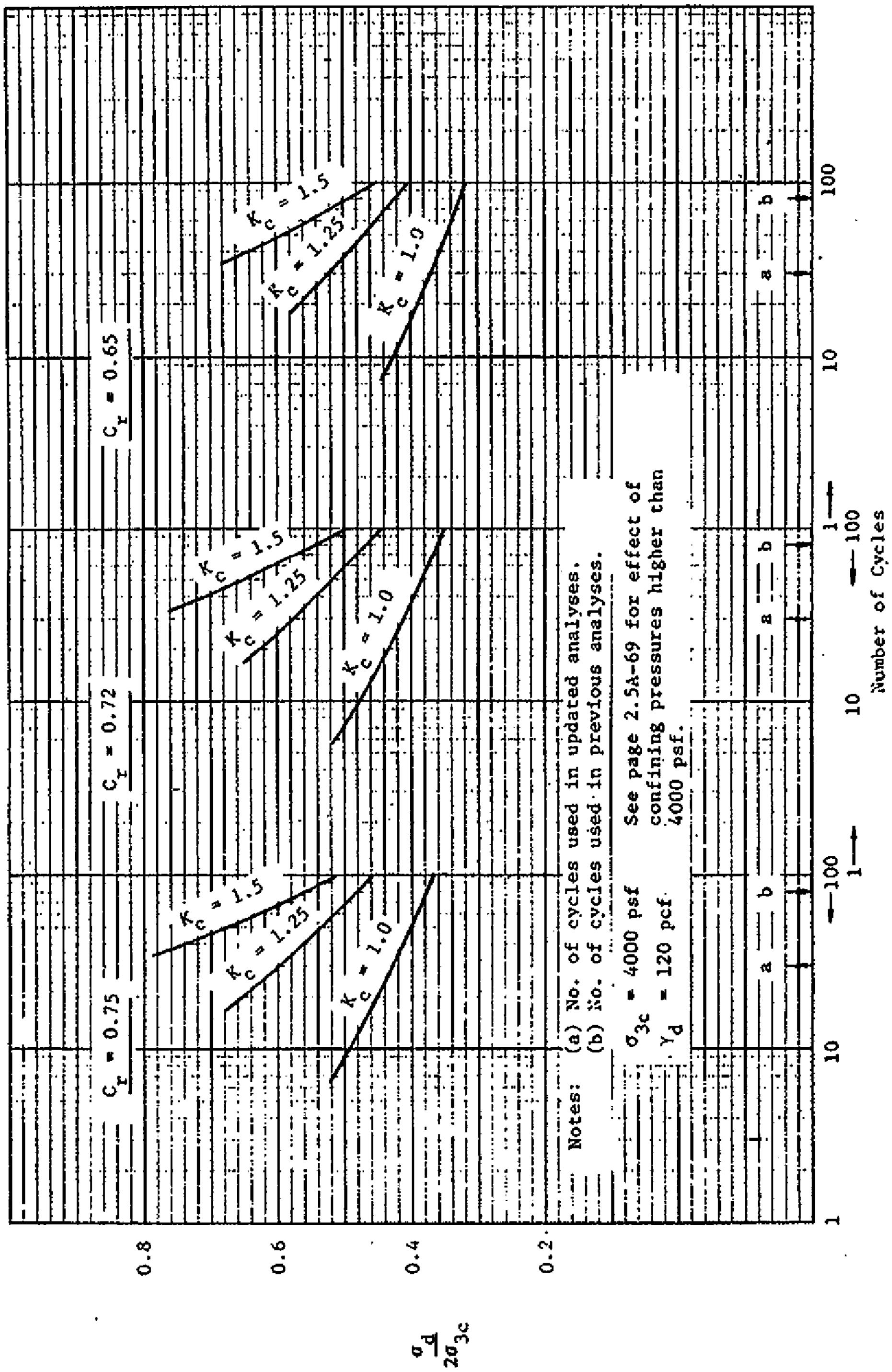

SAN ONOFRE
NUCLEAR GENERATING STATION
Units 2 & 3

FIELD DYNAMIC STRENGTH
OF SAN MATEO SAND
(PLANT AREA)

Figure 2.5-74

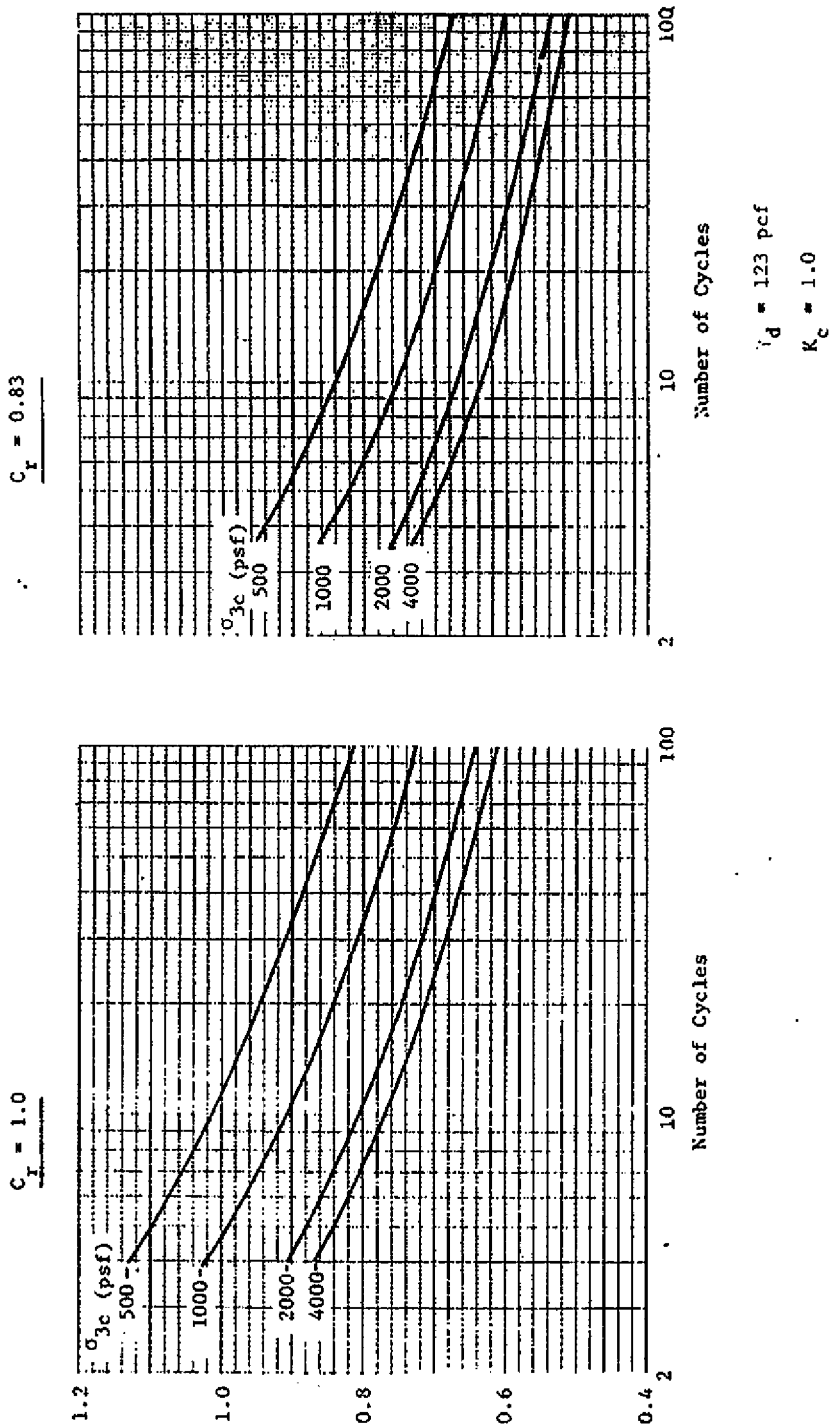

SAN ONOFRE
NUCLEAR GENERATING STATION
Units 2 & 3

FIELD DYNAMIC STRENGTH
OF SAN MATEO SAND
(OFFSHORE AREA)

Figure 2.5-75

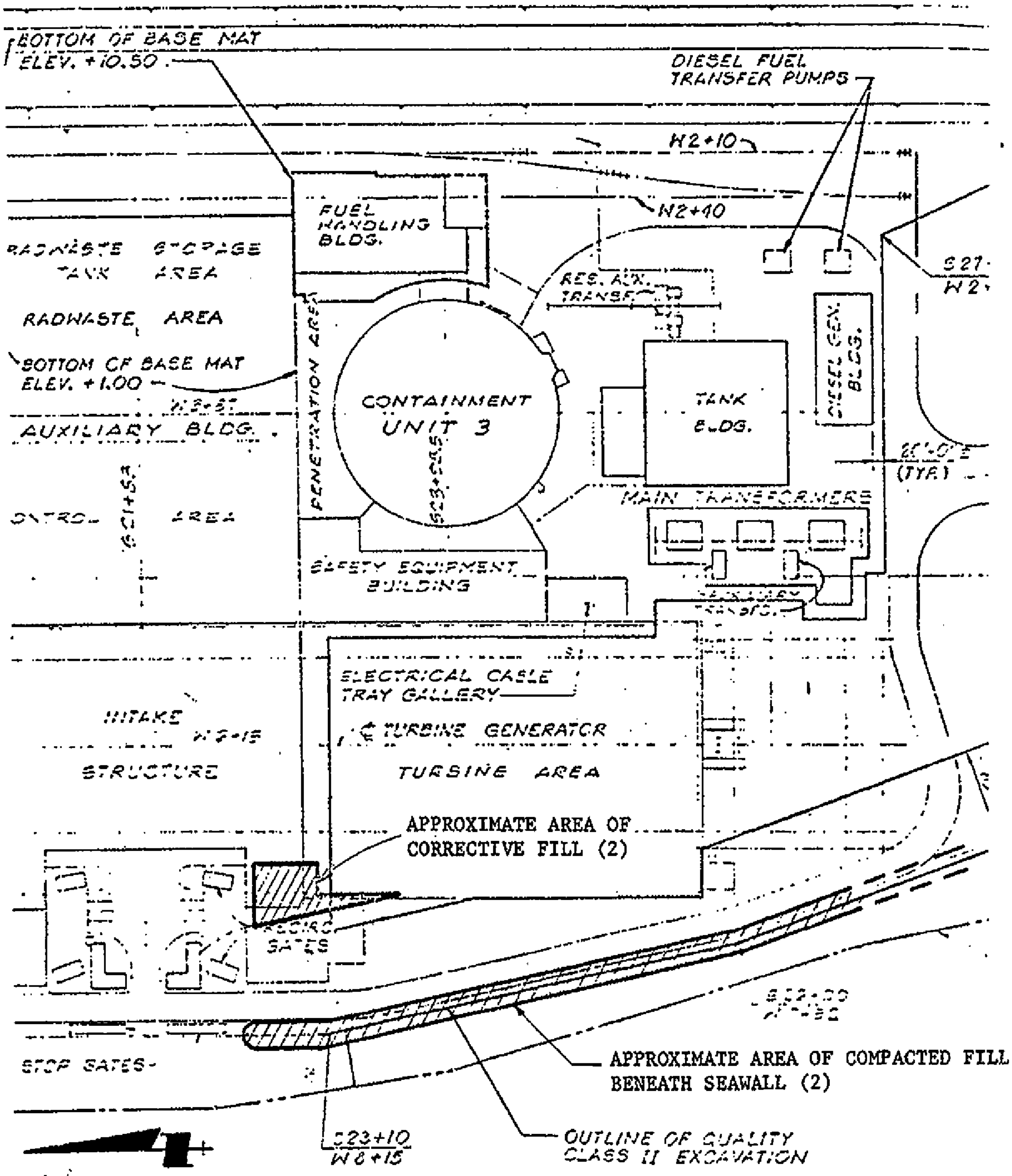

NOTES:

1. THIS PLAN IS A PORTION OF DRAWING NO. 21011-0, PREPARED BY BECHTEL CORP., DATED 19 AUG. 74. IT HAS BEEN XEROX-COPIED AND IS NOT TO AN EXACT SCALE.
2. AREAS SHOWN ARE BELOW ELEV. 5 FT. AND WERE COMPACTED TO AT LEAST 100% OF THE MAXIMUM DENSITY DETERMINED BY ASTM D-1557-70A

Approx. Scale 1" ≅ 100 ft

SAN ONOFRE NUCLEAR GENERATING STATION Units 2 & 3
LOCATION PLAN OF FILLS BENEATH STRUCTURES
Figure 2.5-76

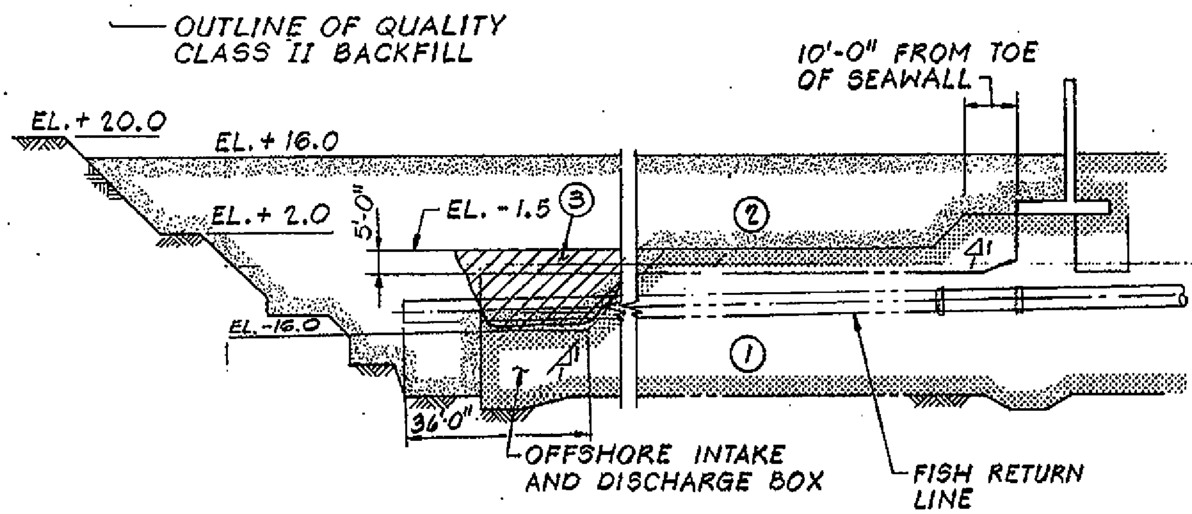

SECTION B
1" = 20'-0"

LEGEND

1 100% COMPACTION BELOW EL +5.00
95% COMPACTION ABOVE EL +5.00

2 BACKFILL – NO COMPACTION REQUIRED

3 THE BASE OF THE SEAWALL IS AT EL. +5 FT.

SAN ONOFRE NUCLEAR GENERATING STATION Units 2 & 3
ZONES OF FILL OUTSIDE PERMANENT SEAWALL
Figure 2.5-77

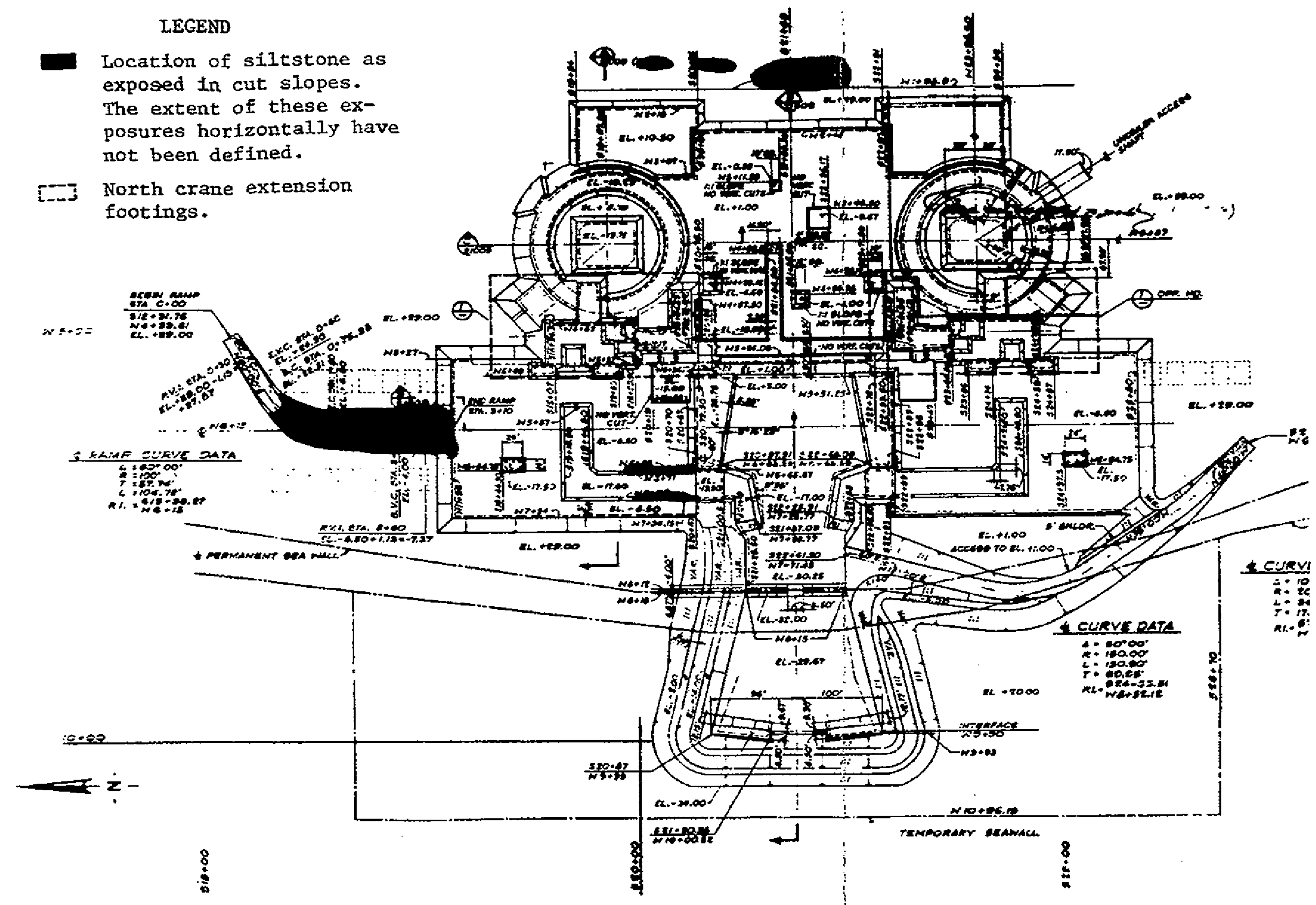

SAN ONOFRE
NUCLEAR GENERATING STATION
Units 2 & 3

SILTSTONE LOCATION PLAN

Figure 2.5-78

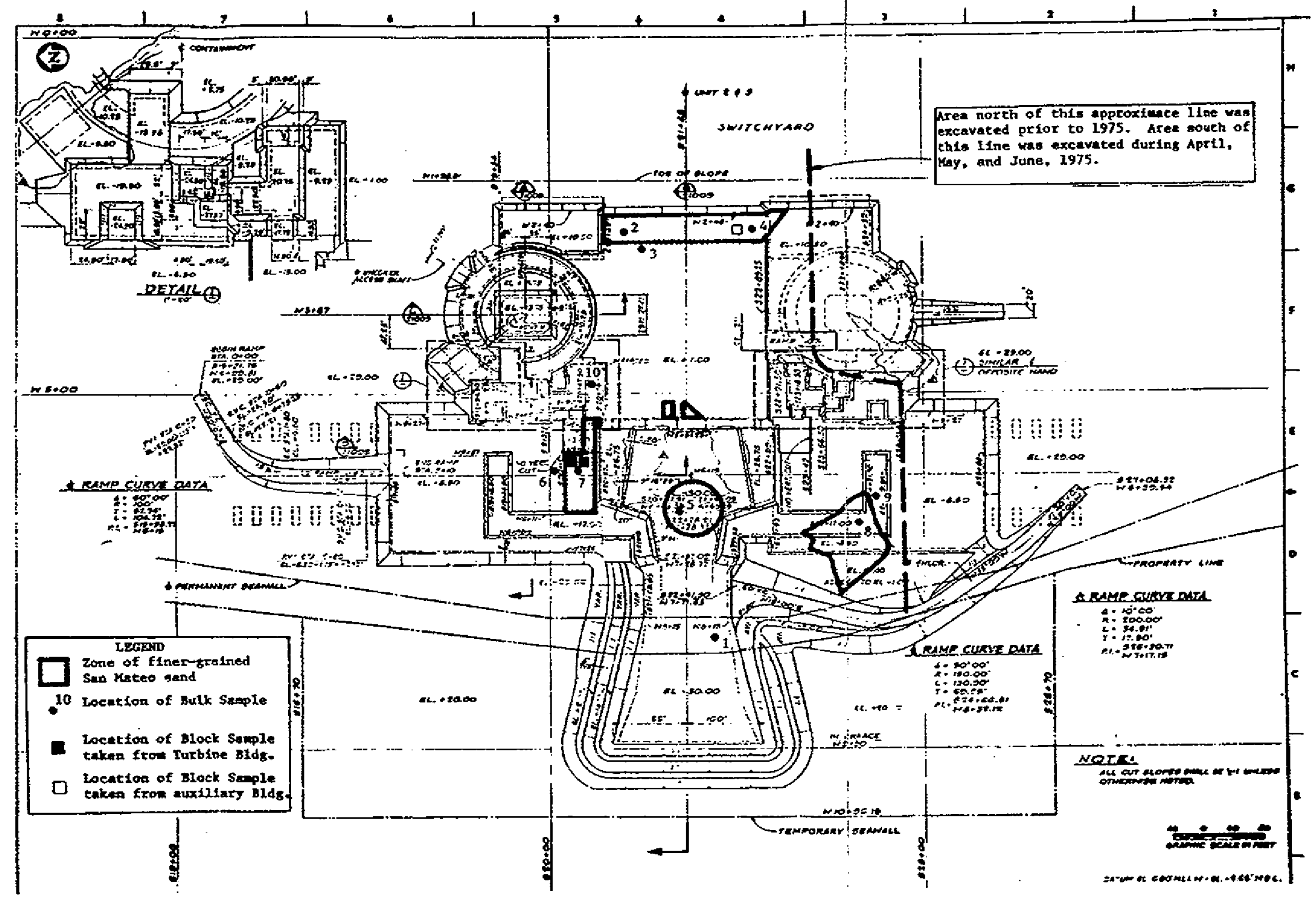

SAN ONOFRE NUCLEAR GENERATING STATION Units 2 & 3

FINER GRAINED SOIL LOCATION PLAN

Figure 2.5-79

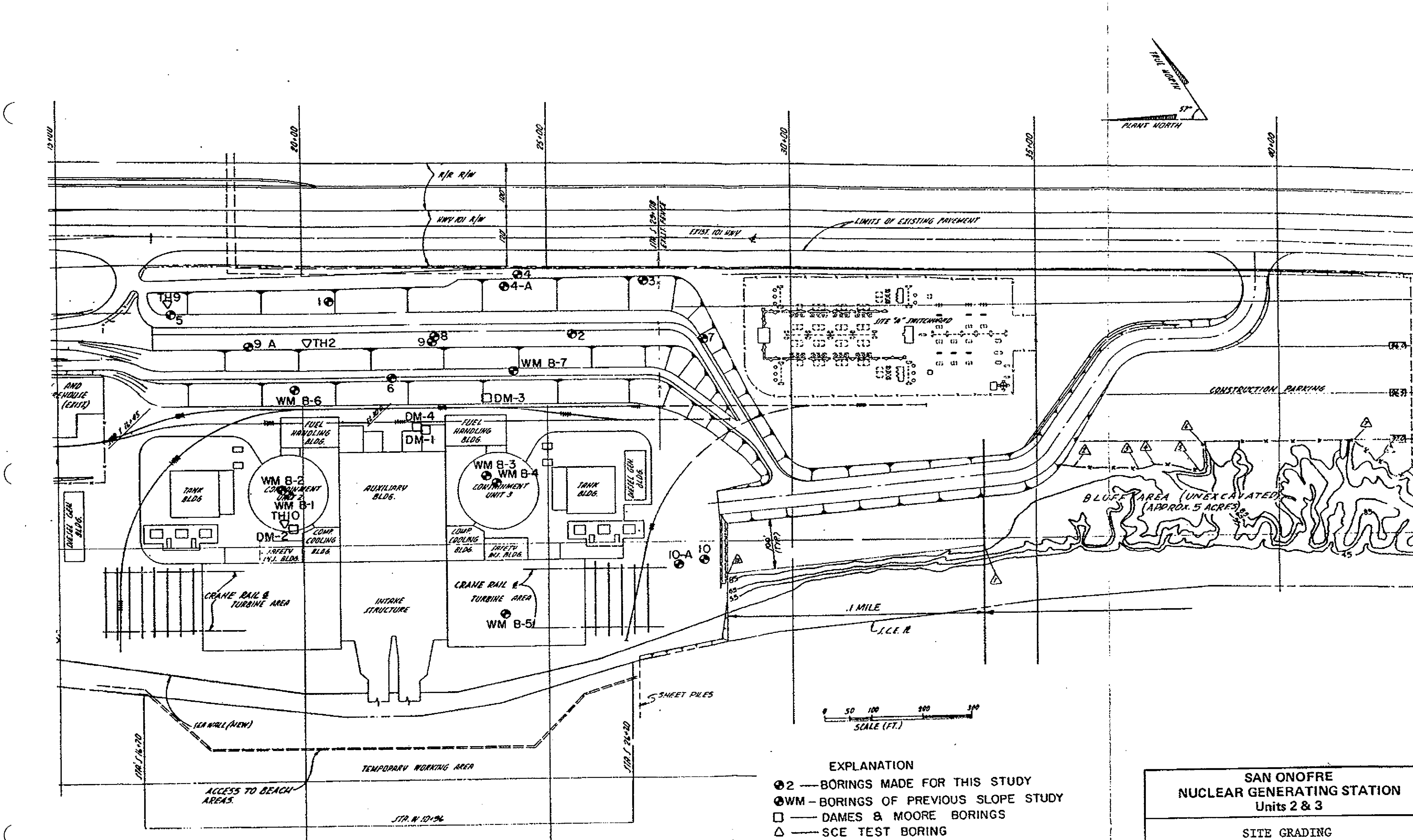

SAN ONOFRE
NUCLEAR GENERATING STATION
Units 2 & 3

SITE GRADING
AND ACCESS ROADS

Figure 2.5-80

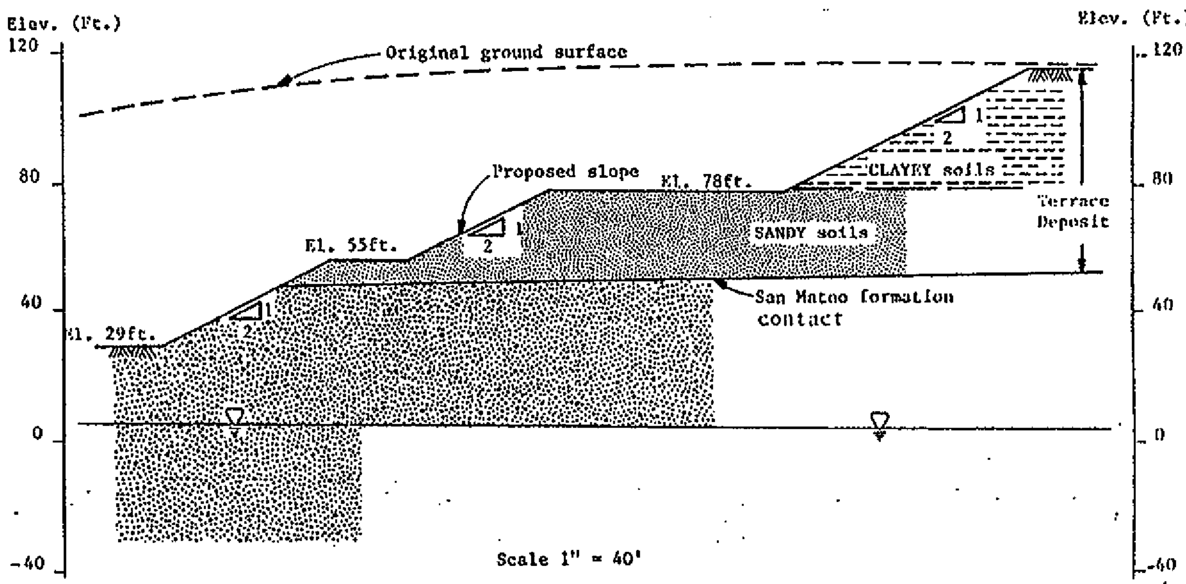

SAN ONOFRE
NUCLEAR GENERATING STATION
Units 2 & 3

SECTION OF PROPOSED
SWITCHYARD SLOPES

Figure 2.5-81

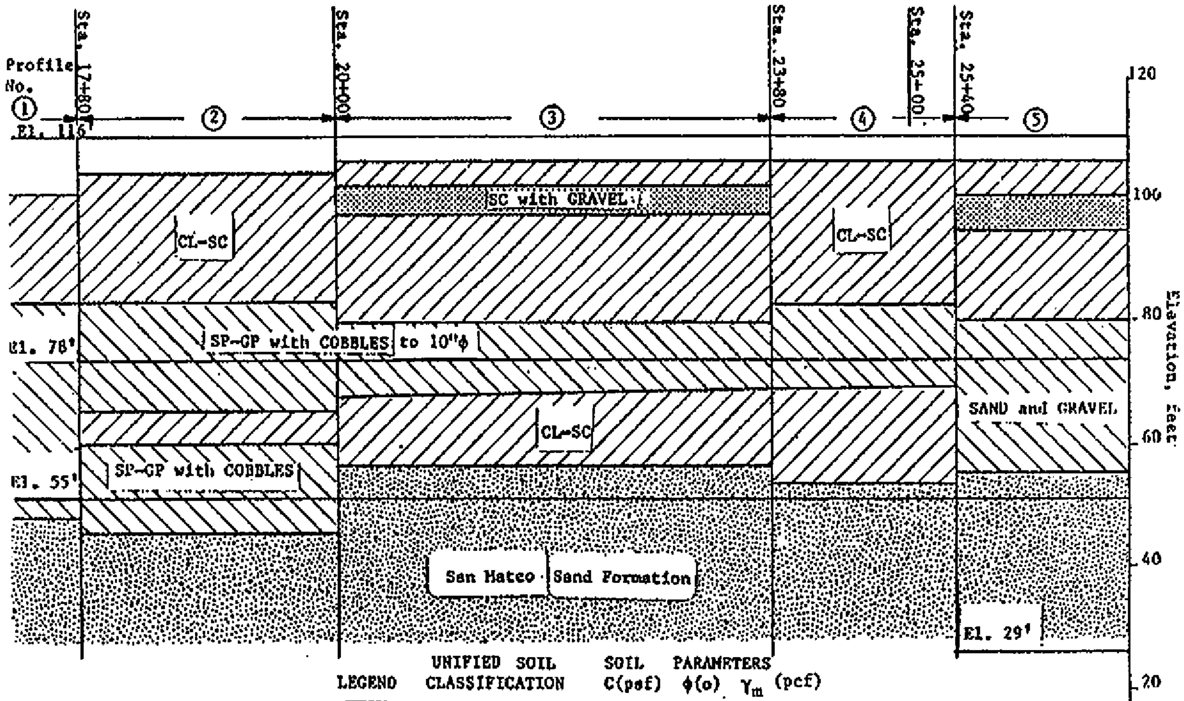

LEGEND	UNIFIED SOIL CLASSIFICATION	SOIL C(psf)	PARAMETERS ϕ(o)	γ_m (pcf)
	Fill	500	33	135
	CL-SC	2600	17	130
	SC with GRAVEL	1400	17	140
	SP-GP	200	38	132
	San Mateo SAND	800	41	126

Vertical Scale 1 in. = 20 ft
Horizontal Scale 1 in. = 100 ft

SAN ONOFRE
NUCLEAR GENERATING STATION
Units 2 & 3

IDEALIZED SWITCHYARD PROFILE

Figure 2.5-82

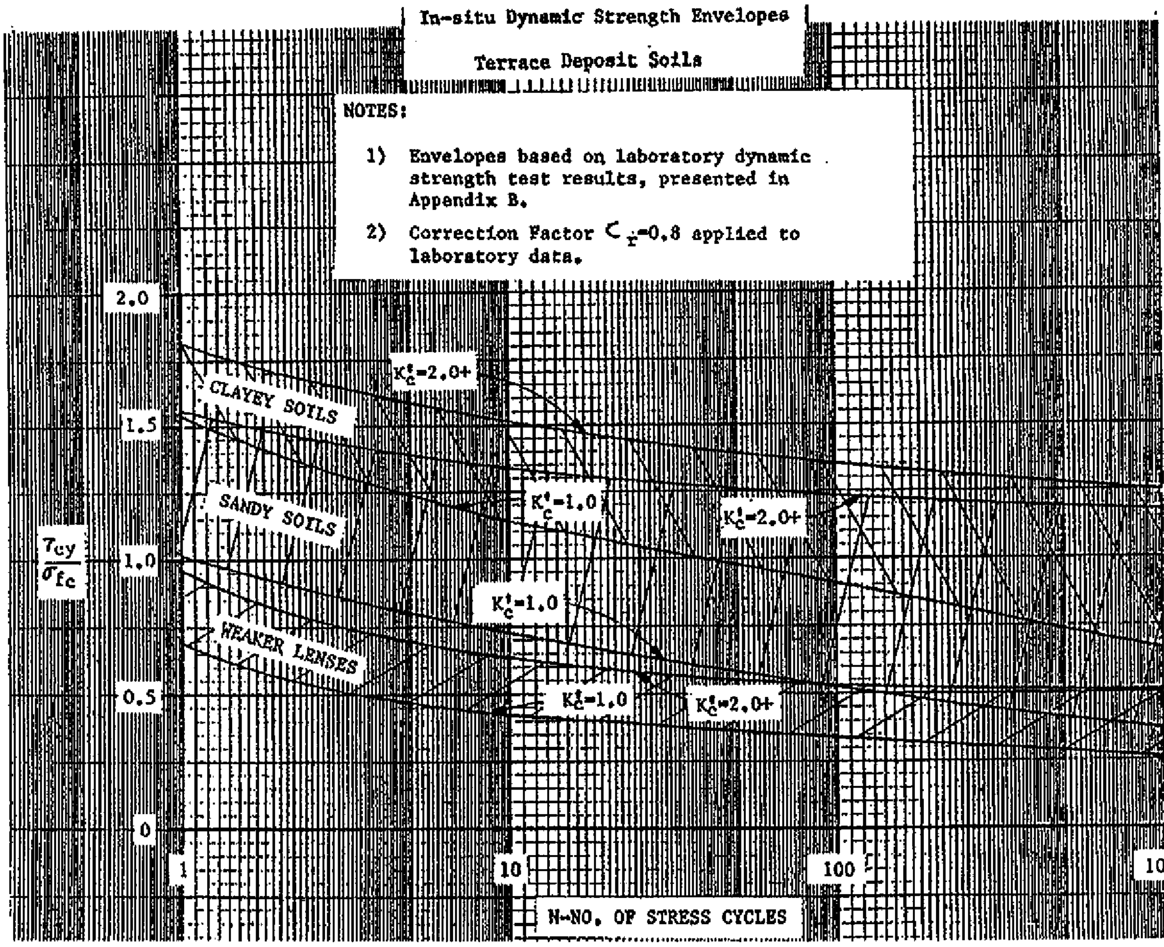

SAN ONOFRE
NUCLEAR GENERATING STATION
Units 2 & 3

IN-SITU DYNAMIC STRENGTH ENVELOPES - TERRACE DEPOSIT SOILS

Figure 2.5-83

RESULTS OF SWITCHYARD SLOPE STABILITY EVALUATION
(Schematic
Scale 1"=40')

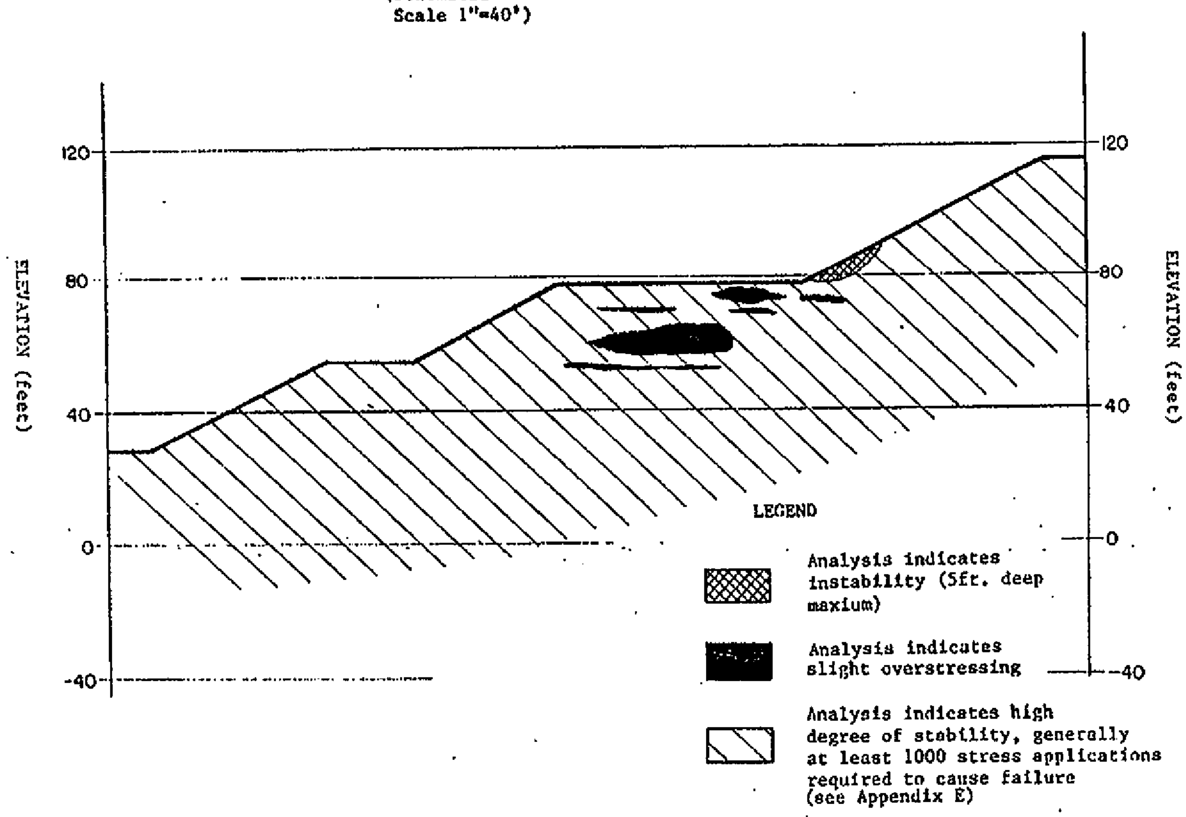

SAN ONOFRE NUCLEAR GENERATING STATION Units 2 & 3

RESULTS OF STABILITY EVALUATION

Figure 2.5-84

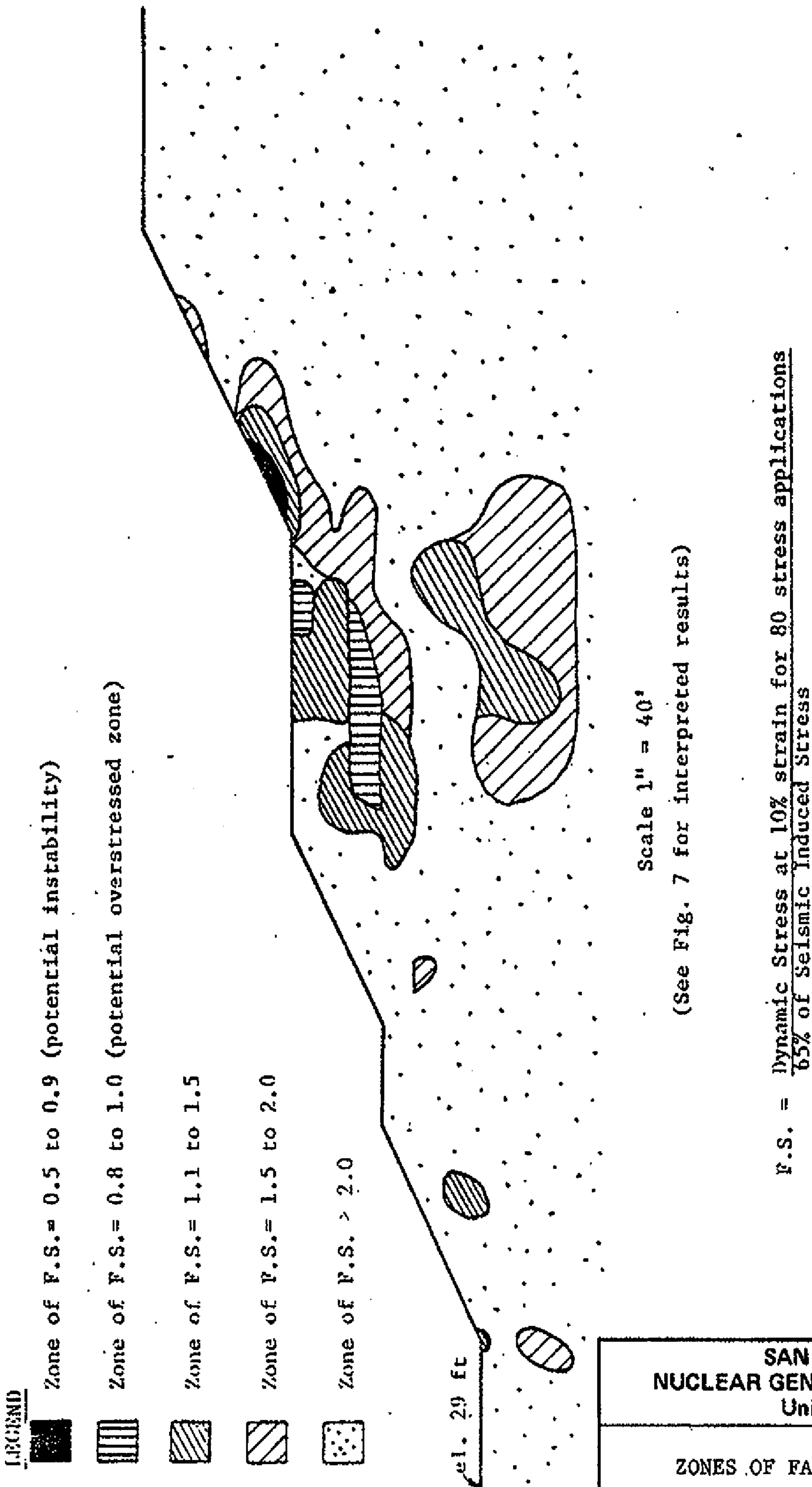

SAN ONOFRE
NUCLEAR GENERATING STATION
Units 2 & 3

ZONES OF FACTOR-OF-SAFETY

Figure 2.5-85

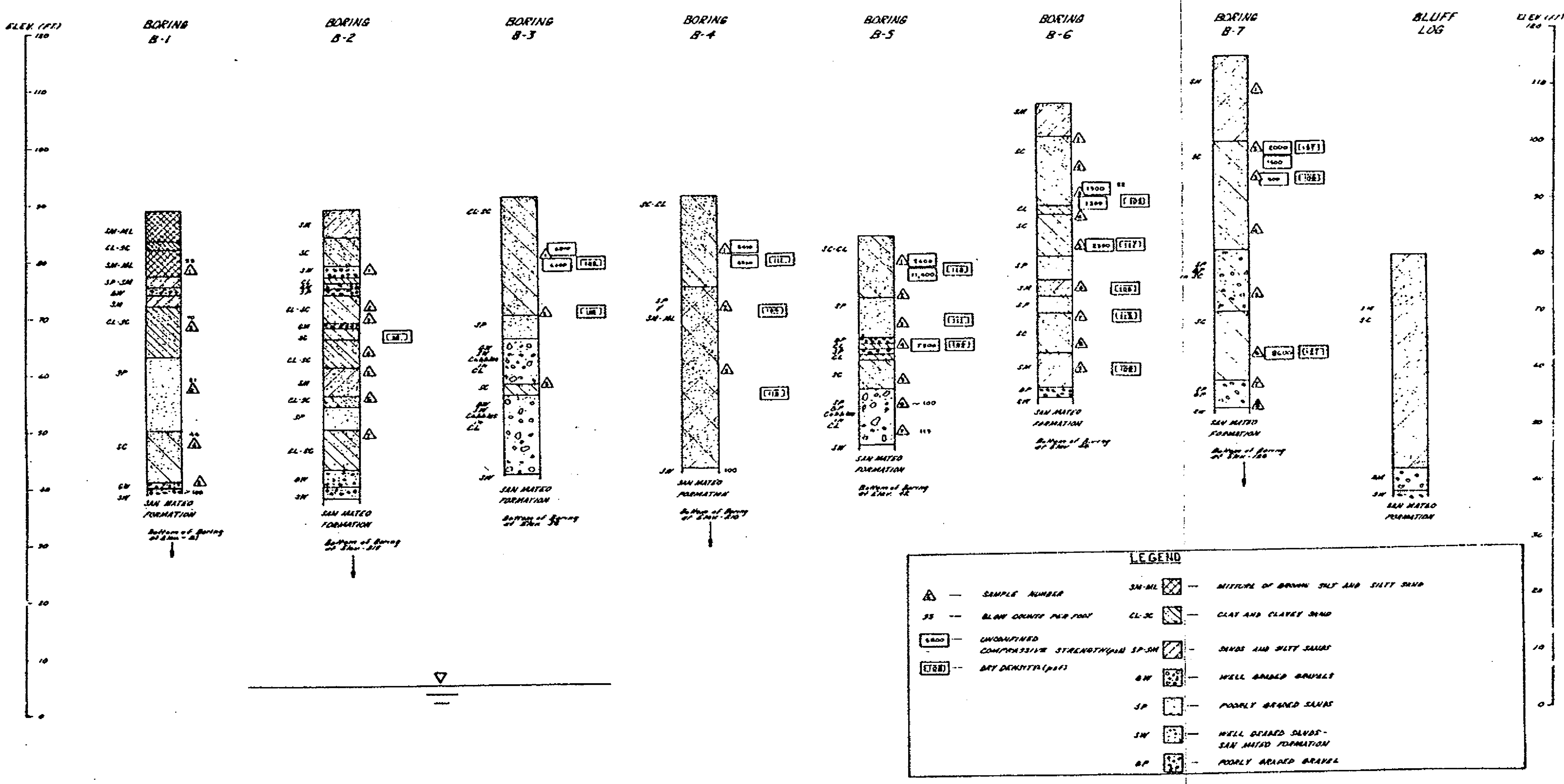

SAN ONOFRE
NUCLEAR GENERATING STATION
Units 2 & 3

BORING LOG SUMMARY

Figure 2.5-86

DATE OF BORING 19 Mar.74 WATER DEPTH ________ DATE MEASURED ________ SAMPLES California and Shelby Tube

TYPE OF DRILL RIG Cont. Flight Auger HOLE DIAMETER 6" WEIGHT OF HAMMER 140 lbs. FALLING 30"

DEPTH, FT.	SAMPLES	BLOWS / FOOT	GROUND WATER	DESCRIPTION	UNC. COMP. STRENGTH, ksf	MOISTURE CONTENT, %	DRY DENSITY pcf	OTHER TESTS
SURFACE ELEVATION: 102'								
				Medium stiff, moist, dark brown SANDY CLAY (CL) (Fill)				
	SK 1							
	M1	62		Very dense, moist, CLAYEY SAND (SC) with GRAVEL		12.3	119	SG
				Increasing CLAY content				
10	M2	56				7.4	121	SG MA
	M3	78				12.6	125	SG
	SK 2			Very dense, damp, brown SILTY SAND (SM) with GRAVEL				
20	M4	73				4.9	121	SG
				Dense, damp, light brown GRAVELLY SAND (SW)				
	M5	34				7.2	125	SG
	ST 1			Dense, moist, reddish brown SILTY SAND (SM)		17.	111	MA CT
30	M6	76		Dense to very dense, damp, light brown GRAVELLY SAND (SW)		2.9	105	SG
				Lens of SILTY SAND (SM)				
				With COBBLES to 6"				
	M7	40				6.4	125	SG
				Lens of SANDY SILT (ML)				
40	M8	40				10.6	[illegible]	SG
	ST 2							
				Dense, damp, brown GRAVELLY SAND (SW) with COBBLES to 5" (Unable to sample due to COBBLES)				
50				Dense, damp, yellow SAND (SW) SAN MATEO FORMATION				
60				Bottom of boring at 57½ ft. depth (elev. 44.5ft.)				
				No water observed in boring				
70								
80								

SAN ONOFRE
NUCLEAR GENERATING STATION
Units 2 & 3

LOG OF BORING 1

Figure 2.5-87

DATE OF BORING 21 Mar.74 WATER DEPTH ________ DATE MEASURED ________ SAMPLES Mod. Calif. & Shelby Tube

TYPE OF DRILL RIG Cont. Flight Auger HOLE DIAMETER 6" WEIGHT OF HAMMER 140 lbs. FALLING 30"

SURFACE ELEVATION: 112'

DEPTH, FT.	SAMPLES	BLOWS / FOOT	GROUND WATER	DESCRIPTION	UNC. COMP. STRENGTH, ksf	MOISTURE CONTENT, %	DRY DENSITY pcf	OTHER TESTS
	SK 1			Medium dense, moist, brown SILTY SAND (SM) (FILL)				
	SK 2			Medium stiff, moist, dark brown SANDY CLAY (CL)				
				Grading SILTY				
	M1	66		Medium dense to dense, moist, light brown SILTY SAND (SM) with some GRAVEL		11.8	114	SG
10	SK 3			Grading dark brown				
	M1	23				3.4	120	SG MA
	ST 1			With COBBLES				
	M3	44				7.4	131	SG
20	M4	61				7.8	121	
				Grading very dense		6.8	134	SG
	M5	93				6.9	140	SG
				Dense, moist, reddish brown SILTY SAND (SM)				
30	M6	76				3.4	109	SG
				Very dense, damp, brown GRAVELLY SAND (SW) with COBBLES to 4"				
	M7	94		Lens of SILTY SAND (SM)		2.5	113	SG
40	M8	66				4.3	127	SG
	M9	92/9"						
				Very dense, damp, tan SILTY SAND (SM)				
50	ST 2			Very dense, moist, tan GRAVELLY SAND (SW) with COBBLES				
	M 10	90/10"				3.6	110	SG MA
				Caving in COBBLES				
60								
				Bottom of boring at 60½ ft. depth (elev. 51.5ft.)				
				No water observed in boring				
70								
80								

SAN ONOFRE
NUCLEAR GENERATING STATION
Units 2 & 3

LOG OF BORING 2

Figure 2.5-88

DATE OF BORING 22 Mar.74 WATER DEPTH ________ DATE MEASURED ________ SAMPLES Mod. Calif. & Shelby Tube

TYPE OF DRILL RIG Cont. Flight Auger HOLE DIAMETER 6" WEIGHT OF HAMMER 140 lbs. FALLING 30"

SURFACE ELEVATION: 112'

DEPTH, FT.	SAMPLES	BLOWS / FOOT	GROUND WATER	DESCRIPTION	UNC. COMP. STRENGTH, ksf	MOISTURE CONTENT, %	DRY DENSITY pcf	OTHER TESTS
	SK 1			Dense, moist, dark brown CLAYEY SAND (SC)				
	M1	36				4.8	113	SG
				Dense, moist, light brown SILTY SAND (SM)				
	SK 2			Grades to CLAYEY SAND (SC)				
10	M2	60				11.8	129	SG
	SK 3			Stiff, moist, dark brown SANDY CLAY (CL)				
	M3	46		Grading lighter brown with GRAVEL to 3/4"		8.5	132	SG
	SK 4							
20	M4	38				8.0	129	SG
	M5	55				7.6	132	SG
				Very dense, moist, brown SILTY SAND (SM) with some GRAVEL				
30	M6	74		Reddish brown		3.4	103	SG
	SK 5			Very dense, damp, gray GRAVELLY SAND (SW)				
	M7	28		Dense, moist, reddish brown CLAYEY SAND (SC) with GRAVEL to 1"	7.75	15.9	119	SG
	ST 1							
40	M8	95		Very dense, damp, gray SAND (SP)		2.5	103	SG
	M9	94/10"		Very dense, damp, yellow SAND (SW) SAN MATEO FORMATION		1.7	102	SG
50	M 10	100/8"				2.7	105	SG
				Could not sample due to cave-in of GRAVELLY material above				
60								
	SK 6							
70				Bottom of boring at 70 ft. depth (elev. 42ft.)				
				No water observed in boring				
80								

SAN ONOFRE
NUCLEAR GENERATING STATION
Units 2 & 3

LOG OF BORING 3

Figure 2.5-89

DATE OF BORING 25 Mar.74 WATER DEPTH ______ DATE MEASURED ______ SAMPLES Modified California

TYPE OF DRILL RIG Cont. Flight Auger HOLE DIAMETER 6" WEIGHT OF HAMMER 140 lbs. FALLING 30"

SURFACE ELEVATION: 112'

DEPTH, FT.	SAMPLES	BLOWS / FOOT	GROUND WATER	DESCRIPTION	UNC. COMP. STRENGTH, ksf	MOISTURE CONTENT, %	DRY DENSITY pcf	OTHER TESTS
				Stiff, damp, brown SILTY CLAY (CL) with GRAVEL				
				Grading SANDY				
10	M1	25		Medium dense, damp, brown SILTY SAND (SM) with GRAVEL to ½"		8.2	109	SG
	M2	26		Stiff, damp, brown CLAYEY SAND (SC)	5.7	14.8	120	SG
20	M3	53		Very stiff, damp, brown SANDY CLAY (CL)	14.5	13.2	124	SG
	M4	62				17.6	114	SG
30	M5	74/10"				6.2	129	SG
				Very dense, damp, gray GRAVELLY SAND (SP)				
	M6	54		Dense		4.5	108	SG
40	M7	86/10"		Very dense, damp, tan SILTY SAND (SM)		2.4	124	SG
	M8	96/10"		GRAVEL lens		2.9	113	SG
50	M9	98/8"				2.1	108	SG
				Bottom of boring at 51½ ft. depth (elev. 60.5ft.)				
				No water observed in boring				
60								
70								
80								

SAN ONOFRE
NUCLEAR GENERATING STATION
Units 2 & 3

LOG OF BORING 4

Figure 2.5-90

DATE OF BORING 27 Mar.74 WATER DEPTH ________ DATE MEASURED ________ SAMPLES Mod. Calif. & Shelby Tube

TYPE OF DRILL RIG Cont. Flight Auger HOLE DIAMETER: 6" WEIGHT OF HAMMER 140 lbs. FALLING 30"

SURFACE ELEVATION: 112'

DEPTH, FT.	SAMPLES	BLOWS / FOOT	GROUND WATER	DESCRIPTION	UNC COMP. STRENGTH, ksf	MOISTURE CONTENT, %	DRY DENSITY pcf	OTHER TESTS
				Medium dense, damp, tan-gray GRAVELLY SAND (SW) (Fill)				
				Stiff, damp, brown SANDY CLAY (CL)				
10								
	ST1							
	ST2							
				GRAVEL lens				
	ST3			Dense, damp, brown CLAYEY SAND (SC)		7.9	111	MA CT SG
20								
	ST4					9.7	118	CT
				Dense, damp, brown-gray CLAYEY SAND (SC) with GRAVEL GRAVEL to 2½"				
30								
	ST5			Dense, damp, gray-brown GRAVELLY SAND (SW)				
40								
	ST6			Dense, damp, tan SAND (SP) with GRAVEL		12	102	CT MA SG
				Grades to very dense, damp, gray-brown SILTY SAND (SM)				
50	M1	50/2"						
				COBBLES to 5"				
	M2	50/4"				3.4	121	SG
60	ST 7							
				Grading tan				
	M3	100/9"				14.5	104	SG
70	M4	50/4"				10.1	110	SG
				Very dense, damp, yellow tan SAND (SW) SAN MATEO FORMATION				
	M5	50/4"				3.3	111	SG
80				Bottom of boring at 80 ft. depth (elev. 32ft.) No water observed in boring				

SAN ONOFRE
NUCLEAR GENERATING STATION
Units 2 & 3

LOG OF BORING 4A

Figure 2.5-91

DATE OF BORING 26 Mar.74 WATER DEPTH ______ DATE MEASURED ______ SAMPLES Modified California

TYPE OF DRILL RIG Cont. Flight Auger HOLE DIAMETER 6" WEIGHT OF HAMMER 140 lbs. FALLING 30"

DEPTH, FT.	SAMPLES	BLOWS / FOOT	GROUND WATER	DESCRIPTION	UNC. COMP. STRENGTH, ksf	MOISTURE CONTENT, %	DRY DENSITY pcf	OTHER TESTS
SURFACE ELEVATION: 103"								
				Medium stiff, dry, brown SILTY CLAY (CL)				
10								
				GRAVEL to 1½"				
20	M1	50/2"		Very dense, damp, tan-brown CLAYEY SAND (SC)				SG
				GRAVEL to 3"				
	M2	95/9"		Very dense, damp, tan SAND (SM-SP) with GRAVEL		4.3	125	SG
30	M3	56						SG
	M4	50/3"				4.3	120	SG
40	M5	56		Dense, damp, brown CLAYEY SAND (SC) with GRAVEL		6.4	129	SG
	M6	NR						
				Grading with less GRAVEL				
50	M7	50/3"						
	M8	50/4"		Very dense, damp, yellow SAND (SW) SAN MATEO FORMATION		2.9	118	SG
	M9	50/3"		Sample disturbed		2.1	108	SG
60	M 10	50/2"						
	M 11	50/3"				2.2	124	SG
				Bottom of boring at 66½ ft. depth (elev. 36.5ft.) No water observed in boring				
70								
80								

SAN ONOFRE
NUCLEAR GENERATING STATION
Units 2 & 3

LOG OF BORING 5

Figure 2.5-92

DATE OF BORING 29 Mar.74 WATER DEPTH ______ DATE MEASURED ______ SAMPLES Mod. Calif. & Shelby Tube

TYPE OF DRILL RIG Conc. Flight Auger HOLE DIAMETER 6" WEIGHT OF HAMMER 140 lbs. FALLING 30"

SURFACE ELEVATION: 107'

DEPTH, FT.	SAMPLES	BLOWS / FOOT	GROUND WATER	DESCRIPTION	UNC. COMP. STRENGTH, ksf	MOISTURE CONTENT, %	DRY DENSITY pcf	OTHER TESTS
				Stiff, damp, brown SANDY CLAY (CL) (Fill)				
	M1	54		Dense, damp, brown CLAYEY SAND (SC)				
10	ST 1			Dense, moist, brown GRAVELLY SAND (SW)				
				Dense, damp, brown CLAYEY SAND (SC)				
	M2	49			12.3	11.7	134	SG
20	ST 2							
	M3	75/9"		GRAVEL to 2"		2.7	116	SG
30	ST 3							
	M4	56		Dense, damp, tan SAND (SP)		2.9	110	SG
40	ST 4			Dense, damp, brown GRAVELLY SAND (SP-SW)				
				Dense, damp, tan SILTY fine-grained SAND (SM)				
	M5	50		Dense, damp, tan GRAVELLY SAND (SW)		16.7	113	SG
50	M6	NR 50/2"						
	M7	NR		Very dense, damp, yellow SAND (SW) SAN MATEO FORMATION				
60				Bottom of boring at 56 ft. depth (elev. 51ft.) No water observed in boring				
70								
80								

SAN ONOFRE
NUCLEAR GENERATING STATION
Units 2 & 3

LOG OF BORING 6

Figure 2.5-93

DATE OF BORING 29 Mar.74 WATER DEPTH ________ DATE MEASURED ________ SAMPLES Mod. Calif. & Shelby Tube

TYPE OF DRILL RIG Cont. Flight Auger HOLE DIAMETER 6" WEIGHT OF HAMMER 140 lbs. FALLING 30"

DEPTH, FT.	SAMPLES	BLOWS / FOOT	GROUND WATER	DESCRIPTION	UNC. COMP. STRENGTH, ksf	MOISTURE CONTENT, %	DRY DENSITY pcf	OTHER TESTS
SURFACE ELEVATION: 116'								
				Stiff, damp, dark brown SANDY CLAY (CL) (Fill)				
	M1	50		Very dense, damp, brown CLAYEY fine-grained SAND (SC)		2.8	122	SG
10	ST 1							
	M2	60				9.5	127	SG
20	ST 2					11.0	122	CT MA SG
	M3	74		Hard CLAY		8.3	138	MA SG
30	ST 3							
	M4	96 10"		Dense, damp, gray GRAVELLY SAND (SW-SP)		2.0	114	SG
40	ST 4			GRAVEL content decreasing				
	M5	74		Very dense, dry, tan fine-grained SAND (SP)		1.4	103	SG
50	ST 5			Grading with coarse-grained SAND GRAVEL				
	M6	50 3"				2.4	99	SG
60	ST 6							
	M7	50 3"		Very dense, damp, tan SAND (SW) SAN MATEO FORMATION				
				Bottom of boring at 66 ft. depth (elev. 50ft.) No water observed in boring				
70								
80								

SAN ONOFRE NUCLEAR GENERATING STATION Units 2 & 3

LOG OF BORING 7

Figure 2.5-94

DATE OF BORING 25 Mar. 74	WATER DEPTH	DATE MEASURED	SAMPLES 2" Modified California
TYPE OF DRILL RIG Cont. Flight Auger	HOLE DIAMETER 6"	WEIGHT OF HAMMER 140 lbs.	FALLING 30"

DEPTH, FT.	SAMPLES	BLOWS / FOOT	GROUND WATER	DESCRIPTION	UNC. COMP. STRENGTH, ksf	MOISTURE CONTENT, %	DRY DENSITY pcf	OTHER TESTS
SURFACE ELEVATION: 104'								
				Stiff, damp, brown SANDY CLAY (CL)				
10								
	M 1	61				12.4	130	SG
20	M 2	43			7.4	15.9	119	SG
	M 3	50/5"	NR	Dense, damp, tan GRAVELLY SAND (SP-SM)				
30	M 4	42				2.0	95	MA SG
	M 5	44		CLAY lens		15.7	114	SG
				Stiff, moist, brown SANDY CLAY (CL)				
40	M 6	40			12.0	16.3	118	SG
				Very dense, damp, tan SILTY SAND (SM)				
	M 7	50/2"						
50	M 8	50/5"				4.6	113	SG
				SAN MATEO FORMATION				
	M 9	50/3"		Very dense, damp, white SAND (SW) ~~SAN MATEO FORMATION~~				
				Bottom of boring at 36½ ft. depth (elev. 47.5±ft.)				
60				No water observed in boring				
70								
80								

SAN ONOFRE NUCLEAR GENERATING STATION Units 2 & 3

LOG OF BORING 8

Figure 2.5-95

DATE OF BORING 29 Mar.74 WATER DEPTH NONE DATE MEASURED ______ SAMPLES Pitcher Barrel

TYPE OF DRILL RIG Rotary Auger & Mud HOLE DIAMETER 6" WEIGHT OF HAMMER ______ FALLING ______

SURFACE ELEVATION: 104'

DEPTH, FT.	SAMPLES	BLOWS/FOOT	GROUND WATER	DESCRIPTION	UNC. COMP. STRENGTH, ksf	MOISTURE CONTENT, %	DRY DENSITY pcf	OTHER TESTS
	SK 1			Fill, COBBLES, concrete and CLAY				
	P1			Very stiff, damp, dark brown SANDY CLAY (CL) to CLAYEY SAND (SC)				
10	P2							
				Brown SAND (SW)		13.8	118	CT MA SG
	P3							
	P4					15.8	122	CT SG MA
	P5							
20						15.2	118	CT
	P6					9.4	127	CT SG MA
	P7							
	SK 2			Dense, damp, tan GRAVELLY SAND (SP-SW)		11.5	116	CT SG MA
30								
	SK 3							
				No GRAVEL				
	SK 4							
40	P8			No GRAVEL				
	P9							
	P10							
50	SK 4			Dense, damp, tan SANDY GRAVEL (GP)				
	P11			Very dense, damp, light yellow SAND (SW) SAN MATEO FORMATION				
60				Bottom of boring at 59ft. depth (elev. 45ft.) No water observed in boring				
70								
80								

SAN ONOFRE
NUCLEAR GENERATING STATION
Units 2 & 3

LOG OF BORING 9

Figure 2.5-96

DATE OF BORING 29 Mar.74 WATER DEPTH ________ DATE MEASURED ________ SAMPLES Pitcher Barrel

TYPE OF DRILL RIG Rotary with Mud HOLE DIAMETER 6" WEIGHT OF HAMMER ________ FALLING ________

SURFACE ELEVATION: 98'

DEPTH, FT.	SAMPLES	BLOWS / FOOT	GROUND WATER	DESCRIPTION	UNC. COMP. STRENGTH, ksf	MOISTURE CONTENT, %	DRY DENSITY pcf	OTHER TESTS
				Asphalt Concrete				
				Stiff, damp, brown SILTY CLAY (CL) with GRAVEL (FILL)				
	P1			SILTY SAND (SM)				
	P2							
10	P3			Dense, moist, dark brown SANDY SILT (ML) with organic root material				
	P4			Very dense, damp, gray CLAYEY SAND (SC)				CT
				Grading brown		10.8	127	SG MA
	P5			Very stiff, damp, light brown SANDY CLAY (CL)		11.7	127	CT SG
20	P6					8.0	127	MA CT
	P7							MA
	SK1					20.5	127	SG CT MA SG
				Dense, damp, gray GRAVELLY SAND (SP-SW)				
	SK2							
30				No GRAVEL				
	P8			Dense, damp, brown SAND (SC) with GRAVEL and SOBBLES				
	SK3							
40	P9							
	P10							
	P11			Lens of CLAY (CL)				
	SK4			Very dense, damp, brown SANDY GRAVEL (GP)				
50	P12			Very dense, damp, yellow SAND (SW) SAN MATEO FORMATION				
				Bottom of boring at 51½ ft. depth (elev. 46.5ft.)				
				No water observed in boring				
60								
70								
80								

SAN ONOFRE
NUCLEAR GENERATING STATION
Units 2 & 3

LOG OF BORING 9A

Figure 2.5-97

DATE OF BORING 28 Mar.74 WATER DEPTH ________ DATE MEASURED ________ SAMPLES Pitcher Barrel

TYPE OF DRILL RIG Rotary & Mud HOLE DIAMETER 6" WEIGHT OF HAMMER ________ FALLING ________

DEPTH, FT.	SAMPLES	BLOWS / FOOT	GROUND WATER	DESCRIPTION	UNC. COMP. STRENGTH, ksf	MOISTURE CONTENT, %	DRY DENSITY pcf	OTHER TESTS
SURFACE ELEVATION: 94'								
0				Very dense, damp, dark brown, SILTY SAND (SM)				
10	P1					12.1	118	CT MA SG
	P2					14.4	121	CT MA SG
	P3							
	P4							
20	SK 1			Very dense, damp, brown GRAVELLY SAND (SP-SW)				
30				COBBLES to 4"				
				Refusal on COBBLES				
40				Bottom of boring at 38 ft. depth (elev. 56ft.) No water observed in boring				
50								
60								
70								
80								

SAN ONOFRE
NUCLEAR GENERATING STATION
Units 2 & 3

LOG OF BORING 10

Figure 2.5-98

DATE OF BORING 2 Apr. 74 WATER DEPTH ________ DATE MEASURED ________ SAMPLES Mod. Calif. & Shelby Tube

TYPE OF DRILL RIG Cont. Flight Auger HOLE DIAMETER 8" WEIGHT OF HAMMER 140 lbs. FALLING 30"

DEPTH, FT.	SAMPLES	BLOWS / FOOT	GROUND WATER	DESCRIPTION	UNC. COMP. STRENGTH, ksf	MOISTURE CONTENT, %	DRY DENSITY pcf	OTHER TESTS
SURFACE ELEVATION: 94'								
				Medium dense, moist, dark brown SILTY SAND (SM)				
				Dense				
	M1	39			2.8			MA
10	ST 1			Hard, damp, brown SANDY CLAY (CL)		13.3	119	CT MA SG
	M2	56		Dense, damp, tan SILTY SAND (SM-SP)		4.0	112	SG MA
20	ST 2	NR		With GRAVEL				
	M3	30				1.9	111	SG
	M4	44				2.8	120	SG
30	M5	50/3"		Grading very dense		3.5	124	SG MA
				Grading with COBBLES, caving				
				Bottom of boring at 35 ft. depth (elev. 59ft.) No water observed in boring				
40								
50								
60								
70								
80								

SAN ONOFRE
NUCLEAR GENERATING STATION
Units 2 & 3

LOG OF BORING 10A

Figure 2.5-99